

**The biology and characterization of NOD-like receptors in
goldfish (*Carassius auratus* L.) macrophages exposed to bacterial
pathogens**

by

Jiasong Xie

A thesis submitted in partial fulfillment of the requirements for the degree of

Doctor of Philosophy

in

Physiology, Cell and Developmental Biology

Department of Biological Sciences
University of Alberta

© Jiasong Xie, 2016

ABSTRACT

The recognition of pathogen-associated molecular patterns (PAMPs) by pattern recognition receptors (PRRs) is important for the initiation of the host defense against pathogens. NOD-like receptors (NLRs) are a family of PRRs that primarily detect the cytosolic PAMPs of the pathogens. The NLRs have been well studied in mammals, but are relatively less known in fish. The objective of my thesis was to identify and functionally characterize NLRs and their signaling molecules of goldfish macrophages in response to bacterial pathogens.

The NOD1, NOD2 and NLRX1 of goldfish macrophages were functionally characterized. Treatment of macrophages with LPS, Poly I:C, muramyl dipeptide (MDP), peptidoglycan (PGN), heat-killed *Aeromonas salmonicida* or *Mycobacterium marinum* differentially altered the expression of the NOD-like receptors. These results indicated that goldfish NLRs were functionally highly conserved and that they played a pivotal role in recognition of fish pathogens such as *A. salmonicida* and *M. marinum*. The association between the NOD1/NOD2 receptors and the key adaptor protein (RIP2) of their signaling pathway was examined. Treatment of goldfish macrophages with LPS, PGN, MDP, Poly I:C, heat-killed and live *M. marinum*, and heat-killed *A. salmonicida* differentially changed the expression of RIP2 at both mRNA and protein levels. RIP2 was found to associate with NOD1 and NOD2 receptors in eukaryotic cells, and RIP2 over-expression resulted in the activation of the NF- κ B. RIP2 was shown to play a central role in the production of pro-inflammatory cytokines TNF α -2 and IL-1 β 1 by goldfish macrophages exposed to *M. marinum*.

I identified and functionally characterized, for the first time, an NLRP inflammasome-like molecule (= NLRP3rel), and its adaptor protein (ASC) of bony fish macrophages. Treatment of goldfish macrophages with nigericin, an inducer of inflammasome pathway, up-regulated the expression of both NLRP3rel and ASC at mRNA and protein levels. Confocal microscopy and co-immunoprecipitation assays results indicated that goldfish NLRP3rel associated with ASC in eukaryotic cells. In addition, the results indicated that ASC associated with caspase-1 and RIP2, and ASC over-expression did not cause the activation of NF- κ B, but down-regulated RIP2 ability to activate NF- κ B. These results indicate that the goldfish NLRP3rel molecule has a similar inflammasome signaling pathway to that of mammals. An inflammasome signaling pathway downstream molecule, HMGB1, was also functionally characterized after exposure to bacteria. My results indicated that goldfish HMGB1, was a critical regulatory cytokine of inflammatory and antimicrobial responses of the goldfish. The results of my dissertation highlight the importance of NLRs in antimicrobial responses of bony fish.

PREFACE

This thesis is the original work by Jiasong Xie and conducted under the supervision of Dr. Miodrag Belosevic. The research project, of which this thesis is a part, received ethics approval from the University of Alberta Research Ethics Board, project entitled “Innate Immunity in Bony Fish”, protocol # AUP00000069. The animals in this study were kept in the research facility according to guidelines set by Canadian Council of Animal Care (CCAC).

Portions of Chapter 4, 5, 7 and 8 of this thesis have been published. The published manuscripts are: (1) Xie, J., Hodgkinson, J.W., Katzenback, B.A., Kovacevic, N., and Belosevic, M., 2013. Characterization of three Nod-like receptors and their role in antimicrobial responses of goldfish (*Carassius auratus* L.) macrophages to *Aeromonas salmonicida* and *Mycobacterium marinum*. *Developmental and Comparative Immunology*, 39: 180-187; (2) Xie, J., Hodgkinson, J.W., Li, C., Kovacevic, N., and Belosevic, M., 2014. Identification and functional characterization of the goldfish (*Carassius auratus* L.) high mobility group box 1 (HMGB1) chromatin-binding protein. *Developmental and Comparative immunology*, 44: 245-253; (3) Xie, J., and Belosevic, M., 2015. Functional characterization of receptor-interacting serine/threonine kinase 2 (RIP2) of the goldfish (*Carassius auratus* L.). *Developmental and Comparative Immunology*, 48: 76-85; (4) Xie, J., and Belosevic, M., 2016. Functional characterization of apoptosis-associated spec-like protein (ASC) of the goldfish (*Carassius auratus* L.). *Developmental and Comparative Immunology*, 65: 201-210; The manuscripts in preparation are: (1) Review of the cytosolic NOD-like receptors of teleosts (Chapter II of

the thesis); and (2) Characterization of NLRP3-related molecule of the goldfish (*Carassius auratus* L.) (Chapter VI of the thesis);

The research presented in this thesis represents the first comprehensive analysis of the biology and characterization of NOD-like receptors in goldfish macrophages exposed to bacterial pathogens. It is also the first comprehensive analysis of the molecular characterization of NOD1, NOD2, NLRX1 and NLRP3rel, as well as relevant signaling molecules RIP2, ASC and HMGB1 in teleosts. I was responsible for data collection, analysis and writing of the manuscripts. Hodgkinson, J.W. assisted in *M. marinum* infection and collection of goldfish tissue samples, Li, C., Katzenback, B.A., and Kovacevic, N. assisted in the treatment studies of goldfish macrophages for use in quantitative PCR analyses. Belosevic, M. was the supervisory author and involved in discussion of concepts and writing of the manuscripts.

ACKNOWLEDGEMENTS

I am grateful for a number of individuals whom have taken the journey with me for these five years. It is therefore a pleasant task to express my gratitude to all those who contributed in many ways throughout the duration of this thesis.

First and foremost, I would like to express my deepest gratitude to my supervisor, Dr. Miodrag (Mike) Belosevic. He has provided me an opportunity to study in Canada and undertake this research in his laboratory, as well as with important advice, helpful suggestions and constant encouragement during the course of this thesis. I appreciate him standing by me and supporting me throughout this endeavor. His contribution in my life has not only stimulated me to become a good researcher, but encouraged me to follow a path that I would enjoy. His dedication and enthusiasm for science has been inspirational.

I would like to thank the members of my committee, Dr. John Chang and Dr. James Stafford for their input and guidance during the course of this thesis. Your comments, suggestions and encouragements had a paramount effect and are greatly appreciated. I would also like to thank my candidacy and defense examining members, Dr. Ted Allison, Dr. Byeong Hwa Jeon, Dr. Warren Gallin and Dr. Kris Chadee for their time. Dr. Daniel Barreda and Dr. Patrick Hanington were the best teachers and Dr. Allen Shostak has been an excellent source of constructive criticism.

To my past and present fellow lab mates Dr. Erick Garcia-Garcia, Dr. Junqing Ge, Dr. Zengfu Song, Dr. Ayo Oladiran, Dr. Fumihiko Katakura, Dr. Arvinder Singh, Dr. Barbara Katzenback, Jordan Hodgkinson, Mariel Hagen, Nikolina Kovacevic, Mark

McAllister, Chad Fibke as well as colleagues Dr. Benjamin Montgomery, Dr. Aja Reiger, Wing Fuk Chan, Herman Cortes, Dustin Lillico, Myron Zwozdesky, Lena Jones, Ningyu Zhang, Yanna Xiao and Chenjie Fei, as well as many others, all of you have made the lab a fun place to work.

To the Biological Sciences Aquatics Facility, I would like to thank you for maintaining our experimental fish. Likewise, I would like to thank Bio Store and MBSU team for ordering the lab supplies and reagents.

This thesis would not have been possible without the endless patience, support and help from my family. Most of all, I must thank my beautiful, loving, and patient wife, Chao Li, for her constant support. It was she who stayed with me for all hours of the day and night working in the lab.

To all those who have not been mentioned, your help and encouragement has not gone unnoticed, and I thank you all for your support.

TABLE OF CONTENTS

	Page
CHAPTER I: GENERAL INTRODUCTION	1
1.1. INTRODUCTION	1
1.2. OBJECTIVES OF THE THESIS	3
1.3. OUTLINE OF THE THESIS	4
1.4. SIGNIFICANCE OF RESEARCH	5
CHAPTER II LITERATURE REVIEW - CYTOSOLIC NLRs and their signaling pathways	6
2.1. INTRODUCTION	6
2.2. DISCOVERY OF NLRs IN MAMMALS AND TELEOSTS	6
2.3. CLASSIFICATION OF NLRs IN MAMMALS AND TELEOSTS	8
2.4. MAMMALIAN NON-INFLAMMASOME NLRs	9
2.4.1. Mammalian NOD1 and NOD2	9
2.4.2. Mammalian NOD1 and NOD2 signaling pathways	11
2.4.3. Mammalian NOD1/NOD2 signaling adaptor, RIP2	13
2.4.4. The roles of NOD1, NOD2 and RIP2 in bony fish	14
2.4.5. NLRC3 and NLRC5 in mammals and teleosts	16
2.4.6. NLRX1 in mammals and teleosts	18
2.4.7. Signaling pathways of mammalian NLR-associated inflammasomes	19
2.4.7.1. General introduction of mammalian NLR-associated inflammasomes	19
2.4.7.2. Canonical (classic) and non-canonical (alternate) inflammasomes	20
2.4.7.3. NLRP1 inflammasome	21
2.4.7.4. NLRP3 inflammasome	22
2.4.7.5. NLRC4 inflammasome	24
2.4.7.6. Other emerging inflammasomes: NLRP6, and NLRP12	26
2.4.7.7. Non-canonical inflammasomes	27
2.4.7.8. Teleost inflammasomes	28
2.4.7.9. Apoptosis associated speck-like protein (ASC) of mammals and teleosts	30
2.4.7.10. Caspase-1 in mammals and teleosts	32
2.4.7.11. Caspase-11 in mammals and teleosts	34
2.4.7.12. High mobility group box protein 1 (HMGB1) in mammals and teleosts	35
2.4.7.13. IL-1 β and IL-18, in mammals and teleosts	38
2.4.7.13.1. IL-1 β in mammals and teleosts	38
2.4.7.13.2. IL-18 in mammals and teleosts	41
2.4.7.14. Pyroptosis in mammals and teleosts	43
2.5. SUMMARY	46
CHAPTER III: MATERIALS AND METHODS	53
3.1. ANIMALS AND FISH CELL CULTURES	53
3.1.1. Fish	53
3.1.2. Fish serum	53
3.1.3. Fish primary cell culture medium	54
3.1.4. Isolation of goldfish kidney leukocytes	54
3.1.4.1. Primary kidney macrophage (PKM) cultures	54
3.1.4.2. Primary kidney neutrophils	55
3.1.5. Establishment of primary kidney macrophages cultures	55
3.1.6. Collection of cell conditioned medium (CCM)	56

3.1.7. Isolation of goldfish spleen leukocytes (splenocytes)	56
3.1.8. Isolation of goldfish peripheral blood leukocytes	57
3.1.9. Fluorescence-activated cell sorting (FACS) of goldfish monocytes and macrophages	57
3.1.10. Cultivation of mammalian cell line	58
3.2. PATHOGENS AND FISH INFECTION.....	58
3.2.1. <i>Aeromonas salmonicida</i> A449	58
3.2.2. <i>Mycobacterium marinum</i>	59
3.2.3. Fish infection.....	59
3.3. IDENTIFICATION OF GOLDFISH NOD-LIKE RECEPTORS AND INFLAMMATORY GENES	60
3.3.1. Primers.....	60
3.3.2. RNA isolation	60
3.3.3. cDNA synthesis	61
3.3.4. RT-PCR.....	61
3.3.5. Cloning into pJET1.2/blunt cloning vector	62
3.4. DNA SEQUENCING AND <i>IN SILICO</i> ANALYSES.....	63
3.4.1. General approach	63
3.4.2. DNA sequencing and <i>in silico</i> analyses of goldfish NOD1, NOD2 and NLRX1	63
3.4.3. DNA sequencing and <i>in silico</i> analyses of goldfish RIP2	64
3.4.4. DNA sequencing and <i>in silico</i> analyses of goldfish HMGB1	65
3.5. QUANTITATIVE EXPRESSION ANALYSIS OF GOLDFISH IMMUNE GENES.....	65
3.5.1. Primers.....	65
3.5.2. Quantitative PCR thermocycling conditions and analyses	66
3.5.3. Quantitative PCR analysis of NOD1, NOD2 and NLRX1 expression in normal goldfish tissues	66
3.5.4. Quantitative PCR analysis of NOD1, NOD2 and NLRX1 expression in goldfish immune cell populations.....	67
3.5.5. Quantitative PCR analysis of NOD1, NOD2 and NLRX1 expression in activated goldfish macrophages	67
3.5.6. Quantitative PCR analysis of RIP2 expression in normal goldfish tissues	68
3.5.7. Quantitative PCR analysis of RIP2 expression in goldfish immune cell populations..	68
3.5.8. Quantitative PCR analysis of RIP2 in activated goldfish macrophages.....	69
3.5.9. Quantitative PCR analysis of NLRP3rel expression in normal goldfish tissues	69
3.5.10. Quantitative PCR analysis of NLRP3rel expression in goldfish immune cell populations	70
3.5.11. Quantitative PCR analysis of NLRP3rel expression in activated goldfish macrophages	70
3.5.12. Quantitative PCR analysis of ASC expression in normal goldfish tissues	71
3.5.13. Quantitative PCR analysis of ASC expression in goldfish immune cell populations. .	71
3.5.14. Quantitative PCR analysis of ASC in activated goldfish macrophages.....	71
3.5.15. Quantitative PCR analysis of HMGB1 expression in normal goldfish tissues	72
3.5.16. Quantitative PCR analysis of HMGB1 expression in goldfish immune cell populations	72
3.5.17. Quantitative PCR analysis of rgHMGB1 induced IL-1 β 1 and TNF α -2 gene expression in macrophages.....	73
3.6. PROKARYOTIC EXPRESSION OF GOLDFISH RECOMBINANT PROTEINS	73
3.6.1. Cloning of goldfish genes into prokaryotic expression vectors	73
3.6.2. Recombinant goldfish protein expression studies	74
3.6.3. Scale up production of goldfish recombinant proteins	75

3.7. ASSESSMENT OF rgHMGB1 ABILITY TO PRIME THE GOLDFISH MACROPHAGES RESPIRATORY BURST RESPONSE	76
3.8. NITRITE OXIDE ASSAY	77
3.8.1. Generation of nitrite standard curve.....	77
3.8.2. Assessment of rgHMGB1 ability to elicit goldfish macrophages nitric oxide production	77
3.9. PRODUCTION OF POLYCLONAL ANTIBODIES TO RECOMBINANT PROTEINS.....	78
3.10. TRANSFECTIONS AND DUAL-LUCIFERASE REPORTER ASSAY	78
3.10.1. Assessment of the ability of RIP2 to activate NF- κ B.....	78
3.10.2. Assessment of the ability of ASC to activate NF- κ B.....	79
3.10.3. Assessment of the ability of HMGB1 to activate NF- κ B	80
3.11. CO-IMMUNOPRECIPITATION (CO-IP) ANALYSES.....	81
3.11.1. Co-IP analysis of goldfish RIP2 and NOD1/NOD2	81
3.11.2. Co-IP analysis of goldfish NLRP3rel and ASC	82
3.11.3. Co-IP analysis of goldfish ASC and caspase-1/RIP2	83
3.12. CONFOCAL MICROSCOPY	83
3.12.1 Co-localization analysis of goldfish NLRP3rel and ASC	84
3.12.2 Co-localization/aggregation analysis of goldfish ASC	84
3.13. LDH RELEASE ASSAY	85
3.14. WESTERN BLOT ANALYSES	85
3.14.1. Western blot analysis of recombinant protein expression	86
3.14.2. Validation of specificity of polyclonal anti-RIP2 antibody and RIP2 inhibitors.....	86
3.14.3. Evaluation of the involvement of RIP2 in pro-inflammatory cytokine production in response to heat-killed <i>M. marinum</i>	87
3.14.4. Western blot analysis of NLRP3rel in activated goldfish macrophages	88
3.14.5. Assessment of the role of NLRP3rel in cytokine processing of nigericin-activated macrophages	89
3.14.6. Western blot analysis of ASC expression in activated goldfish macrophages.....	89
3.14.7. <i>In vitro</i> cross-linking studies of rgfASC.....	90
3.14.8. Western blot analysis of HMGB1 in activated goldfish macrophages.....	90
3.14.9. Assessment of the ability of rgHMGB1 to induce IL-1 β 1 and TNF α -2 production in macrophages	91
3.15. DENSITOMETRIC AND STATISTICAL ANALYSES	92
 CHAPTER IV: CHARACTERIZATION OF THREE NOD-LIKE RECEPTORS AND THEIR ROLE IN ANTIMICROBIAL RESPONSES OF GOLDFISH (<i>Carassius auratus</i> L.) MACROPHAGES TO <i>Aeromonas salmonicida</i> and <i>Mycobacterium marinum</i> ¹	 103
4.1. INTRODUCTION	103
4.2. RESULTS.....	105
4.2.1. Sequence analysis of goldfish NOD1, NOD2 and NLRX1	105
4.2.2. Phylogenetic analysis and classification of gfNOD1, gfNOD2 and gfNLRX1 genes...	106
4.2.3. Analysis of NOD1, NOD2 and NLRX1 expression in goldfish tissues.....	106
4.2.4. Analysis of NOD1, NOD2 and NLRX1 expression in non-stimulated goldfish immune cell populations.....	106
4.2.5. Analysis of goldfish NLR expression in macrophages treated with LPS, Poly I:C, MDP and PGN	107
4.2.6. Analysis of goldfish NOD-like receptors expression in macrophages treated with heat-killed <i>A. salmonicida</i> and <i>M. marinum</i>	107

4.3. DISCUSSION.....	108
CHAPTER V: CHARACTERIZATION OF RECEPTOR-INTERACTING SERINE/THREONINE KINASE 2 (RIP2) OF THE GOLDFISH (<i>Carassius auratus</i> L.)¹	
5.1. INTRODUCTION	125
5.2. RESULTS.....	127
5.2.1. Sequence analysis and characterization of recombinant goldfish RIP2 (gfRIP2)	127
5.2.2. Analysis of RIP2 expression in normal goldfish tissues.....	127
5.2.3. Analysis of RIP2 expression in non-stimulated goldfish immune cell populations ..	128
5.2.4. Recombinant gfRIP2 expression, purification and antibody characterization	128
5.2.5. Confirmation of the specificity of anti-RIP2 antibody and RIP2 inhibitors.....	128
5.2.6. Analysis of gfRIP2 expression in macrophages treated with LPS, PGN, MDP and Poly I:C.....	129
5.2.7. Analysis of gfRIP2 expression in macrophages treated with heat-killed <i>A. salmonicida</i> and heated-killed or live <i>M. marinum</i>	129
5.2.8. GfRIP2 associates with NOD1 and NOD2.....	130
5.2.9. Goldfish rgRIP2 promotes NF- κ B transcriptional activity	131
5.2.10. GfRIP2 regulates the production of TNF α -2, IL-1 β 1 and HMGB1.....	131
5.3. DISCUSSION.....	132
CHAPTER VI: CHARACTERIZATION OF NLRP3-RELATED MOLECULE OF THE GOLDFISH (<i>Carassius auratus</i> L.)	
6.1. INTRODUCTION	147
6.2. RESULTS.....	148
6.2.1. Sequence analysis and characterization of NLRP3rel molecule	148
6.2.2. Analysis of NLRP3rel expression in normal goldfish tissues and non-stimulated goldfish immune cell populations.....	149
6.2.3. Analysis of gfNLRP3rel expression in macrophages treated with bacteria and chemical stimuli	150
6.2.4. Recombinant CT-NLRP3rel expression, purification and antibody characterization	150
6.2.5. GfNLRP3rel associates with gfASC	151
6.2.6. LDH release in goldfish macrophages in response to nigericin	152
6.2.7. gfNLRP3rel and caspase-1 control the IL-1 β 1 and HMGB1 production in nigericin-activated macrophages.....	152
6.3. DISCUSSION.....	153
CHAPTER VII: CHARACTERIZATION OF APOPTOSIS-ASSOCIATED SPECK-LIKE (ASC) MOLECULE OF THE GOLDFISH (<i>Carassius auratus</i> L.)¹	
7.1. INTRODUCTION	173
7.2. RESULTS.....	175
7.2.1. Sequence analysis and characterization of gfASC	175
7.2.2. Analysis of ASC expression in normal goldfish tissues.....	176
7.2.3. Analysis of ASC expression in non-stimulated goldfish immune cell populations ...	176
7.2.4. Analysis of gfASC expression in macrophages treated with bacteria and chemical stimuli	177
7.2.5. Recombinant gfASC expression, purification and antibody characterization	177
7.2.6. Co-localization analysis of rgfASC.....	178
7.2.7. Oligomerization of goldfish rgASC	178
7.2.8. RgfASC associates with RIP2 and caspase-1	179

7.2.9. RgfASC cooperates with RIP2, but not caspase-1, to regulate NF- κ B activity	179
CHAPTER VIII: CHARACTERIZATION OF THE GOLDFISH (<i>Carassius auratus</i> L.) HIGH MOBILITY GROUP BOX 1 (HMGB1) CHROMATIN-BINDING PROTEIN ¹	199
8.1. INTRODUCTION	199
8.2. RESULTS.....	200
8.2.1. Sequence analysis of goldfish HMGB1.....	200
8.2.2. Analysis of HMGB1 expression in normal goldfish tissues	201
8.2.3. Analysis of HMGB1 expression in goldfish immune cell populations.....	202
8.2.4. Analysis of HMGB1 expression in <i>M. marinum</i> infected goldfish tissues.....	202
8.2.5. Recombinant goldfish HMGB1 expression, purification and antibody characterization	202
8.2.6. Recombinant HMGB1 induces respiratory burst response of goldfish macrophages	203
8.2.7. Recombinant HMGB1 induces nitric oxide responses of goldfish macrophages	203
8.2.8. Expression of goldfish HMGB1 gene and protein in macrophages treated with heat-killed <i>M. marinum</i> and <i>A. salmonicida</i>	204
8.2.9. Analysis of goldfish macrophage TNF α -2 and IL-1 β 1 production after treatment of macrophages with rgHMGB1.....	204
8.2.10. Goldfish rgHMGB1 promotes NF- κ B transcriptional activity.....	205
8.3. DISCUSSION.....	205
CHAPTER IX: GENERAL DISCUSSION.....	222
9.1. OVERVIEW OF FINDINGS.....	222
9.2. THE ROLE OF CYTOSOLIC NOD-LIKE RECEPTORS IN THE REGULATION OF THE INNATE IMMUNITY IN TELEOSTS.....	227
9.3. FUTURE DIRECTIONS	233
9.3.1. Understanding the cross-talk between NOD-like receptors and inflammasome pathways.....	233
9.3.2. Pyroptosis	234
9.3.3. Using siRNA or CRISPR to mutate target genes to study NLR signaling pathways ...	236
9.3.4. Functional assessment of PRY/SPRY domain, and other NLR family members and associated signaling molecules, in teleosts	236
9.3.5. Using the goldfish spleen transcriptome database as a valuable resource to study anti-mycobacterial responses in teleosts	237
9.4. SUMMARY	238
REFERENCES	242
Appendix A: <i>DE NOVO</i> ASSEMBLY, TRANSCRIPTOME SEQUENCING AND DIFFERENTIAL EXPRESSION ANALYSIS OF THE IMMUNE-RELATED GENES DURING THE ACUTE PHASE OF INFECTION WITH <i>Mycobacterium marinum</i> IN THE GOLDFISH (<i>Carassius auratus</i> L.) ..	280
Paired-end sequencing and <i>de novo</i> assembly.....	280
Functional annotation by searching public databases	281
Functional classification by GO and COG.....	282
Functional classification by KEGG	283
Analysis of DEGs and immune related DEGs	284
GO and KEGG pathway enrichment analysis of DEGs	284
Appendix B. Goldfish spleen transcriptome KEGG analysis.....	302

Appendix C. The data of all the differentially expressed genes	307
Appendix D. KEGG enrichment analysis of all the DEGs	336
Appendix E. List of immune relevant signaling pathway and involved DEGs in these pathways	342

LIST OF TABLES

		Page
Table 2.1.	Summarized NLRs and their recognized PAMPs in human and mouse	47
Table 2.2.	Summarized NLRs and their recognized PAMPs in teleosts	48
Table 3.1.	Composition of incomplete NMGFL-15 medium	94
Table 3.2.	Composition of nucleic acid precursor solution	95
Table 3.3.	Composition of 10 X Hanks Balanced Salt Solution (HBSS)	95
Table 3.4.	Vector specific primers	96
Table 3.5.	RT-PCR and RACE PCR primers	97
Table 3.6.	Quantitative PCR primers for goldfish genes	98
Table 3.7.	Recombinant protein expression primers	99
Table 3.8.	Primers used in transcriptome gene expression validation	100
Table 3.9.	Recombinant proteins	101
Table 5.1.	Percent identity of goldfish RIP2 and other organisms (aa)	137
Table 6.1.	Percent identity between goldfish NLRP3rel and NLRC3, NLRP3 and NLRP12 homologous of other organisms (aa)	158
Table 7.1.	Percent identity between goldfish ASC and that of other organisms (aa)	186
Table 8.1.	Percent identity of HMGB1 in different organisms (aa)	210
Table A1.	Statistics of goldfish spleen transcriptome assembly	286
Table A2.	Alignment statistics result with reference gene for all the second round of sequencing of goldfish spleen transcriptome obtained from PBS-sham injected (SI) and <i>M. marinum</i> -infected (MI) fish	287
Table A3.	Top 20 KEGG pathway enrichment analysis of all differentially expressed genes	288

LIST OF FIGURES

		Page
Figure 2.1.	The NLR subfamilies and their domains in mammals	49
Figure 2.2.	Schematic representation of NOD1 and NOD2 signaling pathways	50
Figure 2.3.	Schematic representation of canonical and non-canonical inflammasome pathways	51
Figure 2.4.	Schematic representation of priming (first) and activation (second) signals of the NLRP3 inflammasome	52
Figure 3.1.	The nitrite standard curve of nitrite oxide assay	102
Figure 4.1.	Goldfish NOD1 full-length cDNA showing ORF, untranslated regions (UTR) and various domains	112
Figure 4.2.	Goldfish NOD2 full-length cDNA showing ORF, untranslated regions (UTR) and various domains	113
Figure 4.3.	Goldfish NLRX1 full-length cDNA showing ORF, untranslated regions (UTR) and various domains	114
Figure 4.4.	Schematic representation of domain organizations of gfNOD1 (A), gfNOD2 (B) and gfNLRX1 (C)	115
Figure 4.5.	Phylogenetic analysis of goldfish NOD1, NOD2 and NLRX1	116
Figure 4.6.	Expression analysis of NOD1, NOD2 and NLRX1 in tissues obtained from normal goldfish	117
Figure 4.7.	Expression analyses of goldfish NOD1, NOD2 and NLRX1 in different immune cell populations obtained from normal goldfish	118
Figure 4.8.	Time-dependent expression analysis of goldfish NOD1 (A and B), NOD2 (C and D) and NLRX1 (E and F) in macrophages treated with either PBS, Poly I:C or PGN (A, C and E), or either PBS, LPS or MDP (B, D and F)	121
Figure 5.1.	Nucleotide and predicted aa sequence of goldfish RIP2 cDNA	138
Figure 5.2.	Phylogenetic analysis of goldfish RIP2	139
Figure 5.3.	Quantitative analysis of goldfish RIP2 expression in different tissues and immune cell populations obtained from normal goldfish	140
Figure 5.4.	Validation of anti-human RIP2 antibody and RIP2 inhibitors in goldfish	141
Figure 5.5.	Quantitative expression and Western blot analysis of goldfish RIP2 in macrophages treated with different stimuli	142

Figure 5.6.	Goldfish RIP2 associates with NOD1 and NOD2 in HEK293 cells	143
Figure 5.7.	Goldfish recombinant RIP2 protein promotes NF- κ B transcriptional activation	144
Figure 5.8.	Evaluation of the expression of TNF α -2, IL-1 β 1 and HMGB1 in macrophages treated with either PBS, SB203580, or heat-killed <i>M. marinum</i> for 12 h and then treated SB203580 for 2 h or untreated	145
Figure 6.1.	Nucleotide and predicted aa sequence of goldfish NLRP3rel cDNA	160
Figure 6.2.	Phylogenetic analysis of goldfish NLRP3rel and other mammalian and teleost NLRC3, NLRP3, NLRP12 and their homologues	162
Figure 6.3.	Quantitative analysis of goldfish NLRP3rel expression in different tissues and immune cell populations obtained from normal goldfish	163
Figure 6.4.	Quantitative expression and Western blot analysis of goldfish NLRP3rel in macrophages treated with different stimuli	164
Figure 6.5.	SDS-PAGE and Western blot analysis of recombinant CT-NLRP3rel	165
Figure 6.6.	Mass spectrometry analysis of SUMO-CT-NLRP3rel protein	166
Figure 6.7.	Confocal microscopy analysis of goldfish NLRP3rel and ASC in HEK293 cells	169
Figure 6.8.	Goldfish NLRP3rel associates with ASC in HEK293 cells	170
Figure 6.9.	Evaluation of LDH release in goldfish macrophages treated with nigericin for 12 h with or without a pre-treatment of pan-caspase inhibitor (Q-VD-OPH) for 3 h	171
Figure 6.10.	Western blot and quantitative densitometry analysis of Caspase-1, HMGB1 and IL-1 β 1 in goldfish macrophages treated with either PBS, DMSO or nigericin for 12 h with or without pre-treatment of 100 μ M Q-VD-OPH for 3 h	172
Figure 7.1.	Nucleotide and predicted aa sequence of goldfish ASC cDNA	187
Figure 7.2.	Phylogenetic analysis of goldfish ASC	188
Figure 7.3.	Quantitative analysis of goldfish ASC expression in different tissues obtained from normal goldfish	189
Figure 7.4.	Quantitative analysis of goldfish ASC expression in different immune cell populations obtained from normal goldfish	190
Figure 7.5.	Quantitative expression and Western blot analysis of goldfish	

	ASC in macrophages treated with different stimuli	192
Figure 7.6.	SDS-PAGE and Western blot analysis of recombinant ASC	193
Figure 7.7.	Mass spectrometry analysis of SUMO-ASC protein	194
Figure 7.8.	Co-localization analysis of goldfish ASC in HEK293 cells	195
Figure 7.9.	Oligomerization analysis of goldfish ASC in HEK293 cells	196
Figure 7.10.	Goldfish ASC associates with RIP2 (A) and caspase-1 (B) in HEK293 cells	197
Figure 7.11.	Goldfish recombinant ASC protein incorporates with RIP2, but not caspase-1, to regulate NF- κ B transcriptional activation	198
Figure 8.1.	Nucleotide and predicted aa sequence of goldfish HMGB1 cDNA	211
Figure 8.2.	Phylogenetic analysis of goldfish HMGB1	212
Figure 8.3.	Quantitative analysis of goldfish HMGB1 expression in tissues obtained from normal fish	213
Figure 8.4.	Quantitative analysis of goldfish HMGB1 in different immune cell populations of normal fish	214
Figure 8.5.	Quantitative analysis of goldfish HMGB1 expression kidney and spleen from day-7 <i>M. marinum</i> infected goldfish	215
Figure 8.6.	SDS-PAGE and Western blot analysis of recombinant HMGB1	216
Figure 8.7.	Recombinant goldfish HMGB1 (rgHMGB1) primes goldfish monocytes for enhanced respiratory burst response (production of reactive oxygen intermediates; ROI)	217
Figure 8.8.	Recombinant goldfish HMGB1 enhances nitric oxide response (production of reactive nitrogen intermediates; RNI) of goldfish macrophages	218
Figure 8.9.	Western blot and quantitative expression analysis of goldfish HMGB1 in macrophages treated with heat-killed <i>M. marinum</i> (A, C & E) or <i>A. salmonicida</i> (B, D & F) for 12 h	219
Figure 8.10.	Dose-dependent Western blot and quantitative expression analysis of goldfish TNF α -2 (A & C) and IL-1 β 1 (B & D) in macrophages treated with rgHMGB1	220
Figure 8.11.	Goldfish HMGB1 protein promotes NF- κ B transcriptional activation	221
Figure 9.1.	Schematic representation of the NOD-like receptors signaling cascades in teleosts	240
Figure 9.2.	Schematic representation of the NOD-like receptors signaling cascades in vertebrates	241

Figure A1.	Length distribution of the assembled unigenes in the goldfish transcriptome database	289
Figure A2.	Classification of the raw reads for second round sequencing	290
Figure A3.	The number of unigenes from goldfish transcriptome database annotated using six public databases	291
Figure A4.	Characteristics of similarity search of unigenes against NR database	292
Figure A5.	Gene ontology classifications of assembled goldfish transcriptome database unigenes	295
Figure A6.	Histogram presentation of clusters of orthologous groups (COG) classification	296
Figure A7.	Differentially expressed genes (DEGs) between sham-injected and <i>M. marinum</i> -injected goldfish	297
Figure A8.	Gene ontology functional classification of differentially expressed genes (DEGs)	300
Figure A9.	Scatter plot of KEGG pathway enrichment of top 20 statistics	301

LIST OF ABBREVIATIONS

α:	alpha
ASC	apoptosis-associated speck-like protein
β:	beta
Ab:	antibody
ANOVA:	analysis of variance
ATP:	adenosine triphosphate
BCA:	bicinchoninic acid
CCM:	cell conditioned medium
cDNA:	complementary deoxyribonucleic acid
cfu:	colony forming units
CLRs:	C-type lectin receptors
CT-NLRP3:	C-terminal region of goldfish NLRP3
DAMPs:	danger associated molecular patterns
DAPI:	4', 6-diamidino-2-phenylindole
DEG:	differentially expressed genes
DMSO:	dimethyl sulfoxide
DsRed-NLRP3:	pDsRed-Monomer-C-NLRP3
EDTA:	ethylenediaminetetraacetic acid
EF-1α:	elongation factor 1 alpha
EST:	expression sequence tag
FACS:	fast performance liquid chromatography
FBS:	fetal bovine serum
FCA:	freund's complete adjuvant
FIA:	freund's incomplete adjuvant
GBP:	guanylate-binding protein
GFP:	green fluorescent protein
GFP-empty:	pcDNA3.1-NT-GFP-empty
GFP-ASC:	pcDNA3.1-NT-GFP-ASC
HBSS:	hank's balanced salt solution
HEK:	human embryonic kidney
His-empty:	pcDNA3.1/V5-His TOPO TA expression vector
His-ASC:	pcDNA3.1/V5-His-ASC
HMGB1:	high mobility group box 1 protein
HRP:	horseradish peroxidase
ICE:	interleukin-1 β converting enzyme (caspase-1)
IFN:	interferon
Ig:	immunoglobulin domain
IL:	interleukin
IL-1β:	interleukin 1 beta
IPTG:	isopropyl β -D-thiogalactoside
IRF:	interferon regulatory factor

IVDKM:	<i>in vitro</i> derived kidney macrophages
Jak:	janus activated kinase
kDa:	kilodaltans
LB:	Luria-Bertani
LDH:	Lactate dehydrogenase
LPS:	lipopolysaccharide
LRR:	leucine-rich repeats
MAPKs:	mitogen-activated protein kinases
mRNA:	messenger ribonucleic acid
MW:	molecular weight
N/A:	not applicable
NBT:	nitro blue tetrazolium
NF-κB:	nuclear factor- κ B
NLR:	nucleotide-binding domain leucine-rich repeat containing receptors
O.D.:	optical density
PAMPs:	pathogen-associated molecular patterns
PBS:	phosphate buffered saline
PCR:	polymerase chain reaction
PGN:	peptidoglycan
PKM:	primary kidney macrophages
PMA:	phorbol myristate acetate
Poly I:C:	polyinosinic:polycytidylic acid
PRR:	pattern recognition receptor
P/S:	penicillin/streptomycin
Q-PCR:	quantitative real-time PCR
RACE:	rapid amplification of cDNA ends
PBCs:	red blood cells
Rg:	recombinant goldfish
RIG:	retinoic acid inducible gene
RLRs:	retinoid acid-inducible gene-I (RIG-I)-like receptors
RNA:	ribonucleic acid
RNI:	reactive nitrogen intermediates
ROI:	reactive oxygen intermediates
RT-PCR:	reverse transcriptase polymerase chain reaction
SDS-PAGE:	sodium dodecyl sulfate polyacrylamide gel electrophoresis
Stat:	signal transducer and activator of transcription
TGF:	transforming growth factor
TIR:	toll/interleukin-1 receptor (TIR) domain
TLRs:	toll-like receptors
TMS:	tricaine methane sulfonate
TNF:	tumor necrosis factor
UTR:	untranslated region

CHAPTER I: GENERAL INTRODUCTION

1.1. INTRODUCTION

The innate immune response is short-lasting immunity that represents the first line of defense against various microorganisms, whereby the conserved microbial structures known as pathogen-associated molecular patterns (PAMPs) are recognized by germ line-encoded pattern recognition receptors (PRRs), which exist as four major classes, including the Toll-like receptors (TLRs), the NOD-like receptors (NLRs), the retinoid acid-inducible gene-I (RIG-I)-like receptors (RLRs) and the C-type lectin receptors (CLRs). PAMPs include lipopolysaccharides (LPS), polyinosinic: polycytidylic acid (Poly: IC), lipopeptide, peptidoglycan (PGN), flagellin, double-stranded RNA (dsRNA), single-stranded RNA (ssRNA) and CpG DNA, among others. Damage-associated molecular patterns (DAMPs) are microbial or non-microbial insults that, upon stress or damage to the host cell, are released or modified and are capable of initiating an inflammatory response, such as DNA-binding proteins like high-mobility group protein 1 (HMGB1), heat-shock proteins (HSPs), extracellular ATP, and uric acid crystals (1). Recognition of these PAMPs or DAMPs by PRRs triggers the activation of signaling pathway components, such as nuclear factor- κ B (NF- κ B) and mitogen-activated protein kinases (MAPKs), resulting in the generation of pro-inflammatory cytokines [Type I and II interferons (IFN), interleukin 1 beta (IL-1 β), tumor necrosis factor alpha (TNF- α), interleukin-18 (IL-18) and interleukin-33 (IL-33)]. In turn these cytokines regulate pro-inflammatory and antimicrobial responses of phagocytes.

The TLRs are the best known group of the PRRs whose functions have been well characterized (2, 3). TLRs play a fundamental role in innate immune responses by sensing the molecular signatures of microbial pathogens through the recognition of structural components shared by many bacteria, viruses, fungi and protozoa (3–5). At present, at least 18 TLRs have been characterized and TLR14, TLR19, TLR20, TLR21, TLR22 and TLR23 were found to be non-mammalian TLRs (6), indicating the existence of unique PRRs in lower vertebrates.

Another important family of innate immune receptors, are the cytosolic receptors called NLRs, that recognize intracellular bacteria and protozoan parasites. In the early 2000s, NLRs and their subfamilies were discovered in humans and named by various groups as CATERPILLER (7, 8), NODs (9), NOD-LRR (10, 11), NACHT-LRR (12) and NOD-like receptor (13, 14). It is now recognized that NLRs are evolutionarily highly conserved and are present in animals from sea urchins to mammals (8, 15). Certain NLRs such as NACHT, LRR and PYD domain-containing protein 1 (NLRP1), NLRP3 & NLR family CARD domain-containing protein 4 (NLRC4), after pathogen recognition, form oligomerized protein complexes termed “inflammasomes” (16–18). Recently, NLRP3 has been identified as a crucial element in the adjuvant applications (19, 20).

From the evolutionary perspective, bony fish (teleosts) are at the transition point since they can generate both innate and adaptive immune responses. However, teleosts rely heavily on the innate immune system for defense against pathogens. In the aquatic environment, teleosts are more likely to be exposed to different PAMPs and DAMPs, highlighting a crucial role of PRRs in host defense and maintenance of homeostasis. To

date, different TLRs, NLRs and RLRs have been identified in teleosts. For example, more than 18 fish TLRs have been reported, including 8 mammalian TLR orthologues (TLR1-5, and 7-9) and 10 non-mammalian TLRs (TLR5, 14, 18-23, 25-26) (6, 16, 21), 3 RLRs containing retinoic acid inducible gene-I (RIG-I), melanoma differentiation-associated gene 5 (MDA5) and laboratory of genetics and physiology 2 (LGP2) (22–26). In addition, numerous NLRs (22, 27, 28) and C-type lectin receptors (CLRs) exist in teleosts (22, 29–32).

Research on the immune mechanisms of teleosts is important to understand the evolution of immune system in vertebrates. Although the NLRs have been well studied in mammals, the precise roles of these receptors in teleost host defense remain to be fully elucidated.

1.2. OBJECTIVES OF THE THESIS

The main objective of my thesis research was to identify and functionally characterize NLRs of goldfish macrophages in response to bacterial pathogens. The specific aims of my research were:

- 1) To characterize at the molecular and functional levels major goldfish macrophage NOD-like receptors; and
- 2) To examine whether the signaling pathways of NOD-like receptors in goldfish macrophages in response to bacterial pathogens are similar between fish and mammals.

The overall hypothesis of my thesis was that NLRs and inflammasome signaling pathways are generally conserved in fish and play an important role in mediating host defense.

1.3. OUTLINE OF THE THESIS

The thesis consists of 10 chapters. Chapter I is the general introduction of the thesis. Chapter II is literature review of NLRs that covers the discovery of the cytosolic pattern recognition receptors with a focus on the NLRs, their classification and signaling pathways in mammals and the research progresses of NLRs in teleosts. In Chapter III, detailed Materials and Methods used to perform the research are presented. The characterization of three NOD-like receptors (NOD1, NOD2 and NLRX1) and their role in antimicrobial responses of goldfish macrophages to *A. salmonicida* and *M. marinum*, are presented in chapter IV. In Chapter V, I present the results of functional characterization of receptor-interacting serine/threonine kinase 2 (RIP2), a downstream signaling molecule in the NOD1/NOD2 pathway of goldfish macrophages. The results of the functional characterization of NLRP3rel molecule and downstream adaptor molecule, apoptosis-associated spec-like protein (ASC), of goldfish macrophages are presented in chapters VI and VII. The identification and functional characterization of the goldfish high mobility group box 1 (HMGB1) chromatin-binding protein, an inflammasome pathway downstream molecule, are presented in chapter VIII. Lastly, a general discussion on the findings presented in this thesis, as well as the future research directions on teleost NLRs are detailed in chapter IX.

1.4. SIGNIFICANCE OF RESEARCH

NLRs have emerged as central regulators of immunity and inflammation during the past decade. The understanding of the molecular mechanisms of NLRs activation is essential for our understanding of the antimicrobial responses of macrophages in lower vertebrates such as teleosts. It is also well established that in aquaculture setting, due to stress and crowding conditions, there is a high prevalence of infectious diseases. Thus, the understanding of the host immune defense mechanisms may pave a way for therapeutic applications in controlling of fish infectious diseases.

CHAPTER II LITERATURE REVIEW - CYTOSOLIC NLRs AND THEIR SIGNALING PATHWAYS

2.1. INTRODUCTION

Depending on the subcellular localization and expression pattern, the major innate immune pattern recognition receptors (PRRs) can be broadly classified into two groups: (i) Transmembrane PRRs including TLRs and CLRs; and (ii) Cytosolic PRRs including NLRs and RLRs. Most of TLRs and all the CLRs are expressed on the plasma membrane for detection of the conserved PAMPs present on the cell surface of pathogens. By contrast, the cytosolic NLRs and RLRs are responsible for the recognition of cytosolic PAMPs of the pathogens. In this literature review, I mainly focus on the ligands and signaling pathways of the cytosolic NLRs in mammals and teleosts. For excellent reviews of TLRs, RIG-I and CLRs, please see reviews by Zhang et al. (2014) (33) and Rauta et al., (2014) (34), Aoki et al., (2013) (35) and Langevin et al. (2013) (36), and Zhu et al. (2013) (22) and Ng et al. (2015) (37), respectively. This literature review focuses on the NLRs of teleosts and mammals.

2.2. DISCOVERY OF NLRs IN MAMMALS AND TELEOSTS

The NLRs were originally discovered in plants as R-proteins, which share nucleotide binding site (NBS) and leucine rich repeat (LRR) domains, that recognized avirulence proteins delivered by pathogenic bacteria to trigger rapid activation of host

defense (38, 39). Later, a family of molecules (NLRs) that shared high structural similarity to the NBS-LRR molecules were characterized in mammals. The first identified mammalian NLR was human NOD1, also known as CARD4 by Bertin et al. (40) and Inohara et al. (41) in 1999. The NOD1/CARD4 have a typical NOD domain (also referred to as the NACHT domain), which is a critical structural feature of NLRs, that had been earlier identified in apoptotic protease activating factor 1 (APAF1) and its homologue CED-1 in *Caenorhabditis elegans* (42–44). Subsequently, NOD2/CARD15 was identified by searching for NOD1 homologues in the genomic databases (45), and at present there are 23 and 34 NLRs known to exist in humans and mice, respectively.

The first reported teleost NLRs were identified in the zebrafish genome (46). Three subfamilies of NLRs were present in zebrafish: the first resembled mammalian NODs, the second resembled mammalian NLRPs, and the third was reported to be a unique subfamily of genes having similarities to both mammalian NOD3 and NLRPs (27). Subsequently, fish NLRs were reported in grass carp (47), rainbow trout (48), channel catfish (28, 49), rohu (50, 51), orange-spotted grouper (52), goldfish (53), Japanese founder (54, 55), and miiuy croaker (56, 57). The results of these studies indicated the presence of inducible NLRs, and that teleost NLRs shared the conserved structural domains with their mammalian counterparts. To date, studies on most of teleost NLRs primarily focused on the examination of gene expression induced by different immune stimuli and/or fish pathogens.

2.3. CLASSIFICATION OF NLRs IN MAMMALS AND TELEOSTS

Structurally, NLR proteins were classified based on their tripartite domains: (i) a variable N-terminal protein-protein interaction domain that is defined by the either caspase recruitment domain (CARD), pyrin domain (PYD), or baculovirus inhibitor repeat (BIR); (ii) an intermediary nucleotide-binding oligomerization (NOD) domain that mediates nucleotide binding and self-oligomerization after activation; and (iii) a C-terminal leucine-rich repeat (LRR) that senses PAMPs to modulate NLR activity (Fig. 2.1). Depending on the type of effector domain featured at N-terminus, NLRs were subdivided into four subfamilies, NLRA, NLRB, NLRC and NLRP.

NLRA subfamily contains only CIITA, which is the only NLR with an acidic transactivation domain. BIR, CARD or PYD domain define the NLRB, NLRC and NLRP subfamilies, respectively. Compared to the NLRA and NLRB subfamilies, NLRC and NLRP have more members. In human, the NLRC subfamily has six members, NOD1, NOD2, NLRC3, NLRC4 (IPAF), NLRC5 and NLRX1. Among them, NLRX1 appears to be unique without a N-terminal domain and is localized in mitochondria (58, 59). NLRX1 was included in the NLRC subfamily because it featured a CARD-related "X" domain (60). Currently, the assignment of the amino-terminal effector domain of NLRX1 remains unclear, but the N-terminus of NLRX1 has been reported to include a mitochondrial-targeting sequence (61). In contrast to the NLRA subfamily, NLRP subfamily is more diverse containing 14 members, NLRP1 to NLRP14 (Fig. 2.1).

Generally, the recognition of PAMPs or DAMPs by NLRs results in activation of NF- κ B and/or MAP kinase signaling cascades, and/or the formation of inflammasomes

(62, 63). Several molecular mechanisms have been proposed to regulate inflammasome activation, including single PYD or CARD-containing proteins, indicating the importance of these domains in regulation of inflammatory responses.

Similar to mammals, teleost NLRs were classified to NLRA, NLRB, NLRC and NLRP subfamilies based on the predicted functional domains located at their N-terminus. For example, the reported NOD1 and NOD2 in grass carp (48), rohu (50, 51), goldfish (53) and miiuy croaker (56) share one CARD or two CARD domains. NLRC3 has one CARD domain at the N-terminus in catfish (49) and seabass (64). In contrast, teleost NLRC5 featured either no CARD domain in black rockfish (65) and Japanese pufferfish (57) or one CARD domain in catfish (49). There are no reported NLRPs in teleosts, but several computational approaches predicted NLRPs in the National Center for Biotechnology Information (NCBI) database. Due to the polymorphism of teleost NLRPs, the accuracy of these transcripts remains to be validated. The conserved NLR domains were described by Laing and colleagues (27), in which three subfamilies of NLRs shared CARD, PYD, and NACHT domains as well as LRR regions, suggesting that NLRs are structurally conserved throughout evolution.

2.4. MAMMALIAN NON-INFLAMMASOME NLRs

2.4.1. Mammalian NOD1 and NOD2

NOD1 and NOD2 were first identified as mammalian members of the CED4/APAF-1 family of apoptosis regulators (41, 45). Structurally, both NOD1 and NOD2 have a central NACHT domain and a C-terminal LRR domain, and NOD1 contains only

one N-terminal CARD domain, whereas NOD2 contains two CARD domains. CARD domain is primarily responsible for the recruitment of downstream adaptor proteins through homophilic and heterophilic protein interactions that are required to initiate inflammatory signaling cascades in response to PAMPs or DAMPs (10). Generally, NOD1 and NOD2 remain indolent with a folded LRR domain bound to NACHT domain in a dormant state, and upon activation, the LRR domain alters its conformation resulting in the NACHT oligomerization to form an active platform (66, 67). LRR domain contains multiple LRRs that consist of motifs with a length of 20-29 amino acids, whose function is to sense PAMPs or DAMPs.

To date, the ligands of NOD1 and NOD2 have been well characterized in mammals but not teleosts. NOD1 recognizes conserved structure of PGN that is widely found in almost all Gram-negative bacteria, and some Gram-positive bacteria, such as *B. subtilis* and *L. monocytogenes* (68, 69). Specifically, NOD1 detects the L-Ala- γ -D-Glu-*m*-diaminopimelic acid (iE-DAP) on most Gram-negative organisms including *P. aeruginosa* (70), *H. pylori* (71), entero-invasive *Escherichia coli* (72), *C. jejuni* (73), *S. flexneri* (74, 75) and *Streptococcus pneumoniae* (76), whereas most of the Gram-positive bacteria contain a lysine residue at the terminal position of their PGN, rendering their PGN incapable of signaling through NOD1 (Table 2.1). In contrast, the recognition of bacterial PGN by NOD2 is dependent on the presence of MDP that is present in the PGN of both Gram-positive and Gram-negative bacteria (Table 2.1) (77). These observations were confirmed by direct binding assays between NOD1 and iE-DAP using atomic force microscopy (AFM) and surface plasmon resonance (SPR). Additional studies

demonstrated the relationship between the status of RIP2 phosphorylation and affinity for NOD1, when iE-DAP was pre-bound to the LRR domain of NOD1 (78). Similarly, MDP was also confirmed as a specific ligand of NOD2 using surface plasmon resonance (79).

NOD2 has been reported to play a critical role in clearance of *L. monocytogenes* and *M. tuberculosis* (80–82). For example, a higher pulmonary bacterial burden was observed after *M. tuberculosis* infection in NOD2-deficient mice (83). Interestingly, NOD1 and NOD2 have been also implicated in the host defense against intracellular parasites, *Typanosoma cruzi* and *Toxoplasma gondii*, respectively (84, 85).

In mammals, NOD1 is widely expressed in most cell types with high expression reported in epithelial cells of the intestinal tract (86, 87), whereas the NOD2 expression is restricted to leukocytes, such as T cells (88), neutrophils (76), monocytes, macrophages (45), and dendritic cells (89), as well as keratinocytes, intestinal epithelial cells (90) and osteoblasts (91).

2.4.2. Mammalian NOD1 and NOD2 signaling pathways

Upon detection of their ligands, NOD1 and NOD2 homodimerize via their central NACHT domains and subsequently recruit receptor-interacting serine/threonine-protein kinase 2 (RIP2) through homotypic CARD-CARD interactions to initiate downstream signaling cascades (45, 74, 80, 92, 93). Recruited RIP2 is K63-polyubiquitinated within its kinase domain, and then mediates the recruitment and activation of the serine/threonine kinase TAK1 to further activate the I κ B kinase (IKK) complex and MAPK pathway. IKK-mediated phosphorylation of NF- κ B inhibitor I κ B α leads to its

polyubiquitination and degradation of IKK complex and I κ B proteins (41, 45, 92, 93), triggering NF- κ B to translocate into the nucleus, where it promotes the transcription of pro-inflammatory molecules including IL-1 β , CXCL5, CXCL8 and macrophage inflammatory protein-2 (71, 77). Recently, a few members of the inhibitors of apoptosis proteins (IAPs), including XIAP, cIAP1, and cIAP2 (all E3 ubiquitin ligases), were shown to initiate RIP2-dependent K63-linked polyubiquitination through direct interaction (Fig. 2.2) (94–96).

In addition, NOD1 and NOD2 were also shown to induce Type I IFN production via different molecular mechanisms (88, 97). Upon detection, NOD1 binding to its ligand activates RIP2, that then binds to TNF receptor-associated factor 3 (TRAF3), that leads to activation of TANK-binding kinase 1 (TBK1) and I κ B kinase ϵ (IKK ϵ), and eventual activation of IFN regulatory factor 7 (IRF7) (97). The produced Type I IFN mediated by IRF7 signals through the IFN-stimulated gene factor 3 (ISGF3), can induce the production of chemokine CXCL-10 (IP-10) and amplify the type I IFN response (98). NOD2 can also induce Type I IFN production via a different pathway. After recognition of the ssRNA viruses, NOD2 interacts with mitochondrial antiviral signaling molecule (MAVS) to promote IFN production by engaging with a RIP2-independent mitochondrial signaling complex that was observed in RIG-I signaling pathway (97). In this process, MAVS is a central adaptor molecule of this mitochondrial complex formed with NOD2 after its translocation to mitochondria, which is analogous to TRAF3 in NOD1-mediated Type I IFN production, through the activation of TBK1 and IKK- ϵ (Fig. 2.2) (97).

2.4.3. Mammalian NOD1/NOD2 signaling adaptor, RIP2

RIP2, also called RIPK2, CARD3, RICK, or CARDIAK, is a serine/threonine kinase, which contains a CARD-containing kinase, implicated in the induction of NF- κ B and MAPK activation with consequent production of several inflammatory mediators (99–101). RIP2 functions as a key signaling protein in host defense responses induced by activation of NOD1 and NOD2 via CARD-CARD interactions, and RIP2 deficiency has been shown in mammals to affect cellular signaling and cytokine responses triggered by NOD1 and NOD2 ligands (102). Previous observations suggested that the MAPK kinase family member, TAK1, provides the link between RIP2 and NF- κ B activation after NOD1 and NOD2 stimulation (Fig. 2.2) (93, 103). In addition to CARD-CARD interactions with NOD1 and NOD2, RIP2 has been shown to interact with apoptosis-associated speck-like protein (ASC), which is capable of inducing apoptosis and caspase-1 activation (104). ASC has been demonstrated to direct caspase-1 away from RIP2-mediated NF- κ B activation, and toward caspase-1-mediated processing of pro-IL-1 β . Alternatively, RIP2, has the ability to activate caspase-1 under inflammatory conditions and can serve as a stress-inducible upstream modulator of pro-caspase-1 apoptotic activation (105–107). Moreover, upon viral infection, RIP2 was shown to regulate the activation of inflammasomes by mediating mitophagy in a kinase-dependent manner (108). These observations clearly suggest that RIP2 not only mediates the NOD1 and NOD2 signaling pathway, but also participates in the regulation of inflammasome-associated pathways.

RIP2 can also associate with other signaling proteins (independently of CARD-containing molecules), including members of the tumor necrosis factor receptor (TNFR)

family (109), TNFR-associated factor (TNAF) (110), CD40 (111), toll-like receptor 2 (112), and the inhibitor of apoptosis proteins (IAP) family (cIAP-1 and cIAP-2) (99, 105). Recent report also suggests that TNAF3 is a RIP2 binding partner because it inhibited RIP2-induced NF- κ B activation (110). The precise function of RIP2 in immune signaling remains to be fully elucidated in mammals, and the activation of NF- κ B and MAPK signaling pathways through RIP2, are believed to be primarily associated with its capacity to activate the downstream molecules of the TNFR family, TLR family and NOD-like receptor family (92, 99, 100, 105, 109, 113).

2.4.4. The roles of NOD1, NOD2 and RIP2 in bony fish

To date, relatively few studies have identified and characterized the signaling pathways of NLRs in bony fish, although NOD1 and NOD2 have been identified in different bony fishes including zebrafish (27, 46), grass carp (47), Japanese flounder (54), olive flounder (55), rainbow trout (48), rohu (50, 51), catfish (28) and others (Table 2.2). The NOD1 and NOD2 in these fish were differentially expressed in all the tissues with notable differences in the expression between different fish genera and species. For example, NOD1 was highly expressed in the spleen of rohu (50) and kidney of olive flounder (55), while the highest mRNA levels of NOD2 were detected in the muscle (51) and the liver of rainbow trout (48). The injection of rohu with LPS, Poly I:C, *A. hydrophila*, *Edwardsiella tarda* or *S. flexneri* resulted in the up-regulation of NOD1 expression (50). Similarly, the expression of NOD2 was enhanced in response to PGN, LTA, Poly I:C, *A. hydrophila* and *E. tarda* (51). The NOD1 and NOD2 appear to also play an important role

in viral infections of fish (47, 48, 50–52, 55, 114). In goldfish, I found that the expression of goldfish NOD-like receptors (NOD1, NOD2 and NLRX1) were differentially induced by LPS, Poly I:C, MDP, PGN, *A. salmonicida* and *M. marinum*, suggesting that teleost NLRs might play a critical role in host defense against bacteria and viruses (53). Subsequently, NOD1 and NOD2 have also been characterized in other teleost species, such as mrigal (white) carp (115), pufferfish (116), miiuy croaker (56) and zebrafish (114). The results of these studies confirmed the involvement of NOD1 and NOD2 in recognition of fish pathogens.

As a highly versatile immune regulator, RIP2 has been shown to regulate both innate and acquired immunity in mammals (100, 102, 113). However, there are only a few studies in fish that examined the RIP2 mRNA levels after exposure of the host or host cells to defined stimuli. Swain and colleagues were first to report a correlated up-regulation of NOD1 and RIP2 expression in rohu after bacterial challenge (50). These findings suggested that RIP2 was a downstream molecule for NOD1 and NOD2 signaling pathways in teleosts. However, the proposed NOD1/NOD2-RIP2 interactions were based solely on the co-expression profiles upon stimulation by PAMPs, and not the actual association between these molecules. In this thesis, I functionally characterized a bony fish RIP2 (see Chapter V) and provided direct evidence that RIP2 was an essential component of the NOD1/NOD2 signaling pathways that eventually results in pro-inflammatory cytokine processing and secretion in a teleost (117).

2.4.5. NLRC3 and NLRC5 in mammals and teleosts

NLRC3 and NLRC5 share high structure similarity with one N-terminal CARD domain. Although NLRC5 is widely expressed in different tissues, it is particularly highly expressed in cells of myeloid and lymphoid lineages (118). Compared to other NLRs, NLRC3 and NLRC5 were relatively less studied, and are believed to be the negative regulators of the NF- κ B pathway. For example, NLRC3 was shown to down-regulate TLR4-dependent NF- κ B activation by interacting with TRAF6 (119, 120), as well as type I interferon signaling by interacting with the DNA sensor STING (121). Similarly, NLRC5 has been shown to act as a key negative regulator of inflammatory responses of immune cells. Overexpression studies in HEK293T cells showed that NLRC5 repressed the activation of NF- κ B, activator protein (AP-1) and type I IFN-dependent signaling pathways (118). Thus, NLRC5 negatively regulated both NF- κ B and type-1 interferon-dependent responses (122), while at the same time it promoted activation of inflammasomes (123).

The NLRC3 and NLRC5 have recently been shown to also regulate adaptive immunity. For example, NLRC3 was shown to be a negative regulator of T cell activation (120), and NLRC5 is believed to be involved in the regulation of MHC class I expression (118, 124). Meissner and colleagues described a crucial role for NLRC5 in the regulation of MHC class I transcription, where a nuclear localization signal (NLS) region was found to be present on NLRC5, and NLRC5 was shown to be able to shuttle between the cytoplasm and nucleus (125). Instead of interacting with DNA-binding motifs directly, NLRC5 associated with and activated the promoters of MHC class I genes, and induced

the transcription of MHC class I, as well as, related genes involved in MHC class I antigen presentation (125).

In teleosts, only a few studies examined the expression of NLRC3 in response to bacterial infections. As early as in 2009, Sha and co-workers investigated the expression profiles of NLRC3 in catfish, but no significant changes of the mRNA level of NLRC3 were observed upon challenge with *E. ictaluri* (49). Later, seabass NLRC3 was characterized and its mRNA levels were up-regulated following exposure to LPS and both Gram-negative and Gram-positive bacteria (Table 2.2) (54). These authors suggested that teleost NLRC3 may play a role in IL-1 β induction after LPS-stimulation (54). More recently, Li and colleagues (126) identified and characterized NLRC3 in Japanese flounder, and found that the NLRC3 expression was up-regulated following stimulation with extracellular ATP (Table 2.2). Similarly, seabass NLRC3 was demonstrated to be a pivotal cytosolic innate immune receptor that recognized a wide array of PAMPs (64). The available preliminary evidence suggests that teleost NLRC3 may be a cytosolic sensor of different PAMPs, akin to other NLRs. Similar to teleost NLRC3, NLRC5 expression was up-regulated in pufferfish exposed to *Lactobacillus paracasei*, LPS, nigericin or LPS+nigericin (57). Furthermore, exposure to LPS and Poly I:C were shown to up-regulate NLRC5 expression in black rockfish (65). Thus, mammalian NLRC3 and NLRC5 negatively regulate the innate immune responses by modulating NF- κ B, AP-1 and type I IFN-dependent signaling pathways. In contrast, they positively regulate the innate immune responses of teleosts induced by various PAMPs.

2.4.6. NLRX1 in mammals and teleosts

NLRX1 homologues are present in most vertebrates and are highly conserved (61). NLRX1 is the only NLR family member that specifically localizes in the mitochondria although this protein is expressed ubiquitously (59, 61). It is relatively well established that mitochondria serve as a major source of ROS production and released mitochondrial DNA triggers inflammasome activation (127). Mitochondria also contribute to antiviral responses through the involvement of viral RNA sensors, retinoic acid-inducible gene 1 (RIG-I) and melanoma differentiation-associated protein 5 (MDA5) (13, 14).

To date, the reported specific function(s) of NLRX1 are controversial. NLRX1 has been shown to act either as an antiviral response activator or as a negative immune regulator of TLRs and RLRs. When acting as an activator, like other NLRs, NLRX1 is a pro-inflammatory receptor that promotes the production of ROS via TNF- α activation and interaction with the matrix-facing protein ubiquinol-cytochrome C reductase core protein II (UQCRC2) (59, 128). The produced ROSs are directly microbicidal and also activate pro-inflammatory pathways, such as NF- κ B and c-Jun N-terminal kinases (JNK) (129). NLRX1 is also believed to be a direct sensor of byproducts of different mitochondrial metabolic processes. Allen and colleagues (130) and Xia and co-workers (131) reported a more general role for NLRX1 as a negative regulator of TRAF6-dependent NF- κ B signaling. Moore and co-workers (61) showed that the depletion of NLRX1 using small interference RNA (siRNA) promoted virally-induced type I interferon (IFN) production, and proposed that NLRX1 appeared to be a negative modulator of

antiviral signaling induced by RLR and TLR pathways, through a direct binding with MAVS and TRAF6-IKK, respectively (130, 131). Hong and colleagues (132) demonstrated direct interaction between the C-terminal fragment of NLRX1 and RNA ligands, and suggested that this interaction played a key role in NLRX1-mediated ROS activation.

In teleosts, NLRX1 was first described in catfish (49). Infection with *E. ictaluri* caused an up-regulation in splenic NLRX1 mRNA levels. In this thesis, I present findings that showed that Gram-negative (LPS, PGN) and Gram-positive bacterial components (MDP) induced the expression of NLRX1 in goldfish macrophages (Chapter IV and Table 2.2). Surprisingly, the viral mimic component (Poly I:C) did not affect NLRX1 mRNA levels. This observation differs from the findings of Li and colleagues (133), that reported that both bacterial (*Vibrio anguillarum*) and Poly I:C induced higher NLRX1 expression in miiuy croaker. Interestingly, an inflammasome-inducing agent, nigericin, was shown to stimulate NLRX1 expression in Japanese pufferfish, however, the NLRX1 signaling cascades remain to be fully elucidated in teleosts.

2.4.7. Signaling pathways of mammalian NLR-associated inflammasomes

2.4.7.1. General introduction of mammalian NLR-associated inflammasomes

Inflammasome was originally extracted from human THP-1 monocytic cells and was found as a protein complexes containing NLRP1, caspase-1, caspase-5, ASC and CARDINAL (134). In response to invading pathogens, PAMPs and DAMPs, certain NLRs such as NLRP1, NLRP3, NLRC4 and others can form oligomerized multiprotein aggregates termed “inflammasomes” (16–18).

NLRs have been found to be expressed in various cell populations, although different NLRPs differ in their sites of expression. For example, NLRP1 is ubiquitously expressed in leukocytes, especially in T lymphocytes, Langerhans cells, stomach, gut, lungs and brain (135). NLRP3 is present in various leukocytes, and epithelial-type cells in particular, whereas NLRC4 is located in brain and some macrophage-rich tissues, such as spleen, lungs and liver (135, 136).

At present, NLRP3 is the best known and most comprehensively studied inflammasome component that is generated following exposure to diverse stimuli including nigericin, ATP, silica dioxide, etc. Once activated, NLRP3s oligomerize through their NACHT domains to recruit ASC, through PYD-PYD interaction, which results in the subsequent recruitment with procaspase-1 to the inflammasome complexes via CARD-CARD interaction. By contrast, NLRP1 and NLRC4 inflammasomes are primarily activated by anthrax lethal toxin and flagellin, respectively (Fig. 2.3).

2.4.7.2. Canonical (classic) and non-canonical (alternate) inflammasomes

Depending on the downstream activated caspases, the inflammasomes can be divided into canonical and non-canonical inflammasomes. Canonical inflammasomes, including NLRP1, NLRP3, and NLRC4, recruit and cleave procaspase-1 in response to a range of microbial stimuli and endogenous danger signals (Fig. 2.3). Caspase-1 activation promotes the secretion of IL-1 β and IL-18 and pyroptosis (“inflammatory apoptosis”). Whereas activated non-canonical inflammasomes convert procaspase-11 into active

caspase-11. Caspase-11 activation mediates pyroptotic cell death in response to cytosolic bacteria (Fig. 2.3).

2.4.7.3. NLRP1 inflammasome

NLRP1 inflammasome was first characterized as a caspase-activating complex in 2002 (134). Similar to other NLRs, NLRP1 contains a PYD, a central NACHT and a short LRR domain.

Humans have only a single NLRP1 gene, whereas mice have three tandem NLRP1 paralogues (NLRP1a-c), which makes it very difficult to generate NLRP1-deficient mice as a triple knock-out is required (137). A big difference between human NLRP1 and its murine NLRP1 orthologues is that the latter do not have a PYD domain at the N-terminus (137). Among the NLRP1 paralogues in mouse, NLRP1b is highly polymorphic between mouse strains. For example, macrophages from 129S1 mice produce functional NLRP1b but lack the other two isoforms (137, 138). In contrast, C57BL/6 mice express NLRP1a and NLRP1c but have mutations in NLRP1b that render the Nlrp1b protein nonfunctional. The function(s) of NLRP1c are not known at present, but genetic data support its role in inflammasome signaling for NLRP1a and NLRP1b.

Among these murine NLRP1 paralogues, NLRP1b inflammasome is the best studied and is believed to be the lethal toxins (LeTx)-sensing protein (137). LeTx is a bipartite toxin composed of two subunits, protective antigen (PA) and lethal factor (LF). PA can bind to the receptor on the surface of cells and forms a membrane-inserted pore to assist in the delivery of LF into the host cell cytosol. The mechanism of activation of

NLRP1 by is controversial, however, it was suggested that NLRP1b physically interacted with cytosolic LF, and that LF metalloprotease was required for its recognition (139). It has also been shown that LeTx cleaves NLRP1b at N-terminal region (140, 141).

The NLRP1b has been shown to form two functionally different inflammasomes: one is an ASC-deficient complex that induces pyroptosis, the other is an ASC-containing complex for processing of IL-1 β and IL-18 (142). Macrophages from NLRP1b-deficient mice do not activate caspase-1, do not secrete IL-1 β and do not exhibit pyroptosis in response to LeTx (143). NLRP1b recruits caspase-1 directly via its CARD motif, although the bipartite PYD-CARD adaptor protein ASC may stabilize these interactions. Indeed, ASC is critical for NLRP1b-induced caspase-1 auto-processing but dispensable for LeTx-induced pyroptosis and IL-1 β secretion (144).

2.4.7.4. NLRP3 inflammasome

The NLRP3 inflammasomes are NLRP3-ASC-caspase-1 multiprotein complexes formed through the homotypic interactions of PYD-PYD domains of NLRP3 and ASC, and CARD-CARD domains of ASC and caspase-1. It is believed that rather than binding with NLRP3 directly, NLRP3 inducers activate one or more downstream cellular events that lead to its activation (17, 145–147). In terms of PAMPs activation, the canonical NLRP3 inflammasome is activated by bacterial, viral and fungal pathogens, pore-forming toxins, endogenous ligands and crystalline substances such as silica, and alum (148). It is generally accepted that the following events occur during NLRP3 activation: (i) potassium efflux (149); (ii) production of mitochondrial reactive oxygen species (ROS)

(150); (iii) cytosolic release of lysosomal cathepsins (151); (iv) release of mitochondrial DNA or the mitochondrial phospholipid cardiolipin (150, 152–154); and (v) translocation of NLRP3 to mitochondria. In addition, dsRNA-activated protein kinase, PKR, may also play a role in NLRP3 activation, but this remains controversial.

It is well accepted that the formation of NLRP3 inflammasome requires two signals. The first signal is provided by microbial or endogenous molecules that primes the activation of TLR-Myd88-IRAK-NF- κ B pathway to synthesize pro-IL-1 β and pro-IL-18 and to upregulate the transcription of NLRP3 (155, 156). The second signal promotes NLRP3 to undergo homotypic oligomerization and assemble inflammasome upon activation (Fig. 2.4). In this process, the activation of NLRP3 can be induced by exogenous ATP, nigericin, silica, and pore-forming bacterial toxins, all of which promote efflux of potassium (149, 157–159). During the first signal, the induction of NLRP3 does not contribute directly to NLRP3 inflammasome assembly (Fig. 2.4). Instead, the assembly of the NLRP3 inflammasome occurs when the second signal is provided by an NLRP3 activator (148). It seems like NLRP3 deubiquitination is required for inflammasome assembly and activation (160–162), and that the K63-specific deubiquitinase BRCC3 may act as a critical regulator of NLRP3 activity by promoting its deubiquitination (162). However, whether this promotes NLRP3 re-localization or conformational changes to assemble NLRP3 inflammasome is not known. In addition, the mechanism of how E3 ubiquitin ligase modifies NLRP3 in the basal state is also unclear.

2.4.7.5. NLRC4 inflammasome

Structurally, NLRC4 forms inflammasome and lacks a PYD domain, which is required for interaction with ASC that leads to cytokine processing. Instead, NLRC4 directly binds to caspase-1 via homotypic CARD-CARD interactions to induce pyroptosis (163). Interestingly, NLRC4 has also been shown to recruit ASC, via an unknown mechanism, to promote cytokine processing rather than induction of pyroptosis (142). It is clear that ASC can amplify NLRC4 inflammasome activity because it is critical for NLRC4-induced caspase-1 auto-processing and secretion of mature IL-1 β and IL-18 (142, 144, 164).

Previously, NLRC4 inflammasome was also known as IPAF inflammasome, that was assembled after exposure to intracellular flagellin from Gram-negative bacteria, such as *S. typhimurium*, *S. flexneri*, *P. aeruginosa* and *L. pneumophila* (164–168). The flagellin is believed to contain a species-conserved amino acid motif at its C-terminus that is specifically recognized by NLRC4 (169, 170). Supporting this postulate is the evidence that genetically engineered *S. tryphimurium* strain that persistently expressed flagellin was cleared by wild-type mice, but not by NLRC4-deficient mice (170). On the other hand, flagella-deficient *Shigella* strain can also trigger NLRC4-dependent caspase-1 activation, resulting in IL-1 β processing and secretion (166). These observations suggest that other virulence factors can also activate NLRC4 inflammasome. Indeed, these virulence factors are basal body PrJ-like proteins that are homologous to segments of flagellin (170).

Recent studies suggested that NLRC4 inflammasome was a trimeric complex containing NAIP, the ligand and NLRC4. Instead of the old concept where the NLRC4 was the sensor of the ligand (171–175), NAIPs appear to be the real sensors of the ligands. NAIPs belong to the NLRB subfamily, which contain NACHT, LRR and BIR domains. Upon detection of the ligand(s), NAIPs oligomerize with NLRC4 to form the NAIP/NLRC4 inflammasome. In mice, four NAIP members have been identified, NAIP1, 2, 5 and 6, whereas only one NAIP exists in humans. Human NAIP and mouse NAIP1 are believed to be homologous and both recognize Type III secretion system (T3SS) needle proteins (173). NAIP2 detects T3SS rod protein (including PrJ-like protein). NAIP5 and NAIP6 are found to bind flagellin (169, 172, 173). Furthermore, the interaction between NAIP2 and PrJ-like proteins was shown to induce NLRC4 inflammasome activation (172, 173). Alternatively, protein kinase C (PKC)-dependent phosphorylation, which is an upstream regulator of NLRP3 inflammasome, has also been shown to be able to regulate NLRC4 inflammasome activation (176). Serine-533 of NLRC4 has been shown to be phosphorylated by PKC in response to *Salmonella*, suggesting NLRC4 inflammasome assembly may require modification at the protein level (176). Thus, NAIP/NLRC4 can form distinct inflammasomes for diverse functions: (i) an ASC-deficient complex to induce caspase-1 for pyroptosis; and (ii) an ASC-dependent canonical pathway for cytokine processing.

2.4.7.6. Other emerging inflammasomes: NLRP6, and NLRP12

Similar to NLRP3, NLRP6 and NLRP12 can form ASC-caspase-1 inflammasome complexes. The first evidence regarding NLRP6 inflammasomes was the increased caspase-1 cleavage observed when NLRP6 and ASC were co-expressed (177). Evidence from other studies also support the protective role of NLRP6 in intestinal inflammation and tumorigenesis, since NLRP6-deficient mice are highly susceptible to chemically-induced colitis and colitis-associated tumorigenesis (178–180). In addition, NLRP6-deficient mice have reduced IL-18 production, expanded *Bacteroidetes* and TM7 microbiota population, and higher incidence for spontaneous and induced colitis (179), similar to what has been observed for the ASC-, caspase-1- and caspase-11-deficient mice (179). NLRP6 has also been shown to negatively regulate innate immunity and host defense against bacterial pathogens by attenuating NF- κ B- and MAPK-dependent cytokine and chemokine production (181). Thus, NLRP6 can form inflammasome, and also function as a negative regulator of inflammatory responses.

The NLRP12 was the first NLR shown to associate with ASC in transfected cells (182), and NLRP12 was defined as an inflammasome molecule due to its co-localization with ASC and caspase-1, NF- κ B activation and induction of IL-1 β and IL-18 production (177, 182). However, the role of NLRP12 in innate immunity remains unclear, although both inflammatory and anti-inflammatory functions have been attributed to NLRP12. Zaki and colleagues (183) and Allen and co-workers (184) showed that NLRP12-deficient mice exhibit increased NF- κ B activation and strong extracellular regulated kinase (ERK) induction in chemically-induced colitis and colitis-associated tumorigenesis models. It

was reported that *Yersinia pestis* infection induces NLRP12 inflammasome activation leading to production of IL-18 for the clearance of the infection, since NLRP12-deficient mice were more susceptible to *Y. pestis* infection (185). Given the evidence that NLRP12 and NLRP3 inflammasome complexes were present in monocytes of malaria patients, NLRP12 was also believed to play a pivotal role in IL-1 β production and hypersensitivity to secondary bacterial infections during malaria (186). Collectively, these studies suggest that NLRP12 inflammasome is important in innate immune responses against pathogens, although the specific ligand(s) of NLRP12 remain to be identified.

2.4.7.7. Non-canonical inflammasomes

Normally, the recognition of microbial products such as bacterial flagellin and DNA in the cytosol leads to the assembly of canonical inflammasomes and the recruitment of caspase-1, triggering its autocatalytic activity. However, instead of activating caspase-1, caspase-11 is activated in the non-canonical inflammasome pathway, which is different to all known inflammasomes including NLRP1, NLRP3 and NLRC4 (187–189). Recently, caspase-11 was found to be a direct receptor for cytosolic LPS and can form an alternative multiprotein platform following LPS recognition (190). The caspase-11 platform was first identified in insect cells, in which caspase-11 exists as a monomer, and upon exposure to LPS it oligomerizes. Subsequent biochemical studies confirmed that caspase-11 binds LPS directly, which in turn leads to its activation and the multiprotein platform formation. In addition, results from experiments utilizing the site

directed mutagenesis approach revealed that positively charged lysine residue motifs in the CARD domain of caspase-11 serve as the binding sites for LPS (190).

In general, caspases are not known to be able to bind directly to PAMPs and the recruitment of caspases to an upstream molecular scaffold is widely believed to be a prerequisite for their activation. It appears that caspase-11 is an exception to this rule. However, it is still unknown whether this caspase-11 complex contains additional proteins. Interestingly, there are no caspase-11 transcripts in humans, while in mice caspase 4 and caspase 5 appear to be functionally similar to caspase-11, since they directly bind LPS and trigger pyroptotic cell death (190).

2.4.7.8. Teleost inflammasomes

To date, there are limited reports on the inflammasomes of teleost fish, although NLRP isoforms are present in the (NCBI) database, such as NLRP3 (Accession number: XM_017212365.1), NLRP3X1 (XP_017206752.1), NLRP12 (XP_009299711.1), NLRP12-like (XO_009289652.1) and their homologues in zebrafish. In addition, there are several other NLRs in teleosts as well as the inflammasome signaling downstream proteins, ASC and caspase-1 in teleosts (22, 27, 28, 46, 53, 56, 126, 133) and HMGB1 protein (191–194), suggesting that inflammasome signaling pathway may be conserved in lower vertebrates.

Inflammasomes are multi-protein complexes generated in response to pathogens and other danger signals. Three typical NLR-associated inflammasome molecules have been well characterized in mammals, including NLRP1, NLRP3 and

NLRC4 (195). Despite the growing evidence of an expanded family of NLR receptors in lower vertebrates (196), and the suggestion that inflammasome and caspase-1 triggered seabream macrophage cell death (197), no study has specifically identified functional inflammasome molecules in teleost. Using conventional cloning methods, I made several attempts to clone NLRP3 in goldfish without success. The main reason for the difficulty in obtaining full-length sequences of genes encoding inflammasomes in goldfish was that NLRP subfamily members in teleosts are highly polymorphic. High NLRs polymorphism is present in various organisms including *Arabidopsis* spp. (198), zebrafish (27), mouse (199, 200) and humans (201–203). Using the high-throughput sequencing and transcriptome assembly, I successfully identified a NLRP3rel molecule of the goldfish (Appendix A). To our knowledge, this is the first discovery and confirmation of NLRP3rel molecule in a teleost, although previous reports suggested the presence of this NLRP subfamily in zebrafish (27).

The NLRP3rel molecule was identified and functionally characterized in nigericin-activated goldfish macrophages (see Chapter VI). Goldfish NLRP3rel was differentially expressed in goldfish immune cell populations with highest mRNA levels present in PBLs and macrophages. I generated a recombinant form of the molecule [functional domain containing PRY/SPRY domains (aa 851-1025, C-terminus), that has been denoted as rgfNLRP3rel] and an anti-CT-NLRP3rel antibody. Treatment of goldfish primary kidney macrophages *in vitro* with nigericin, an inducer of inflammasome pathway, up-regulated the expression of NLRP3rel at both mRNA and protein levels. Confocal microscopy and co-immunoprecipitation assays indicated that goldfish rgfNLRP3rel molecule associated

with the ASC in HEK293 cells. Nigericin activation of macrophages also induced caspase-1-dependent HMGB1 and IL-1 β production.

2.4.7.9. Apoptosis associated speck-like protein (ASC) of mammals and teleosts

ASC has gained a great attention as a PYD and CARD domain containing molecule, and as such it plays a central role in transduction of the signaling after inflammasome activation in mammals (144, 204). It was first identified as a target of methylation-induced silencing (TMS)-1, as the methylation mediated silencing of TMS-1 conferred a survival advantage by allowing cells to escape from apoptosis (205). The ability of ASC to regulate apoptosis has been shown to be primarily associated with the CARD via homologous CARD-CARD domain interaction (206).

The main functions of ASC as an adaptor molecule are: (i) to bridge NLRs and caspase-1 to form inflammasomes; (ii) to form pyroptosome; (iii) to elicit “cytokine-like” functions; and (iv) to interact with other CARD-containing molecules to regulate cytosolic PRR functions.

As a bridging molecule of inflammasomes, particularly NLRP3, ASC binds to NLRP3 via its PYD domain, forming the NLRP3/ASC complex which in turn binds to caspase-1 via its CARD domain. Binding of caspase-1 to the NLRP3/ASC complex causes caspase-1 activation and processing of caspase-1 substrates, including IL-1 β or IL-18, to initiate pro-inflammatory cytokine production and eventual cytokine-mediated regulation of inflammatory responses (207). ASC gene deletion in macrophages has

been shown to impair their ability to form inflammasomes and activate caspase-1 in response to DAMPs, indicating a crucial role for ASC in this process (164, 208, 209).

ASC has also been shown to self-oligomerize to pyroptosome, which is a supramolecular assembly formed in response to inflammatory stimuli. The pyroptosome rapidly recruits and activates caspase-1 to induce pyroptosis and release of pro-inflammatory cytokines, in particular, HMGB1 (210).

After pyroptosis, the ASC specks have “cytokine-like” function because they are present in the extracellular space after pyroptosis, and shown to promote maturation of IL-1 β (211). In addition, phagocytosis of extracellular ASC specks by macrophages, induced lysosomal damage, increased nucleation of soluble ASC and induction of IL-1 β production (211).

ASC also regulates the function of other PRRs because it interacts with other PYD or CARD domain molecules, such as RIP2 (104, 212). In mammals, it has been demonstrated that ASC not only up-regulates NF- κ B activation upon co-transfection with other PYD family proteins like cytopyrin and PYPAF7 (182, 213), but also down-regulates NF- κ B signaling by modifying RIP2 interaction with procaspase-1 upon LPS activation (104). Interestingly, an ASC-RIP2 axis has been proposed to be involved in the generation of prostaglandin E₂ (PGE₂) in patients diagnosed with chronic adult periodontitis (214).

To date, there are few reports regarding the role of ASC in teleosts. Sun and colleagues (215), characterized ASC in mandarin fish and found that ASC formed a speck in the transfected HEK293T cells, further transfection analyses indicated that

overexpression of ASC inhibited NF- κ B activity with or without stimulation in eukaryotic cells. ASC was also cloned and characterized in Japanese flounder: the expression of ASC was shown to be up-regulated by *E. tarda* infection, and by exposure to LPS, poly I:C, zymosan and extracellular ATP (216). The overexpressed ASC formed speck-like aggregations in the cytoplasm of the Japanese flounder FG-9703 cells. I also examined the functions of goldfish ASC, and report that it played a role as an adaptor molecule in the NLRP3-related inflammasome signaling pathway, and that it exhibited a regulatory role for the NOD-1/NOD-2 pathway, by modifying the RIP2 functions (see Chapter VII). Together, the above studies suggest that ASC may be multifunctional and of central importance in inflammatory responses of teleosts.

2.4.7.10. Caspase-1 in mammals and teleosts

Caspase-1 is a prototypic protein that belongs to a family of inflammatory caspases, that all have a CARD domain. Caspase-1 was originally characterized as IL-1 β -converting enzyme (ICE) that cleaves the IL-1 β precursor to active IL-1 β to mediate inflammation (206, 217, 218). After stimulation by myriad microbial and endogenous signals, the procaspase-1 can be self-activated by proteolytic cleavage into the enzymatically active heterodimer consisting of two 10- and 20-kilodalton subunits (12). Active caspase-1 was found to be an essential regulator of inflammatory responses for its role in generation and activation of IL-18 and IL-33 (219). For example, caspase-1-knockout mice cannot activate pro-IL-1 β , pro-IL-18 and pro-IL-33, and cells isolated from these mice appear to be sensitive to most apoptotic inducers (220, 221). Following the

discovery of inflammasomes, caspase-1 has been demonstrated to be an essential component for the inflammasome assembly (12, 134).

Depending on the stimulus, the activation of caspase-1 can either promote cytokine release or cause cell death. It is well documented that various microbial agents induce caspase-1 activation, including *S. typhimurium*, *Legionella pneumophila*, *Francisella tularensis*, *Bacillus anthracis*, Myxoma virus, etc (137, 222–226). Different mechanisms have been proposed to elucidate the role of caspase-1 in host response to the pathogens, and, not surprisingly, the NLR family of proteins features prominently in described mechanism of host defense.

In teleost, the function of caspase-1 has been reasonably well studied. As early as in 2003, Masumoto and colleagues (227) identified two caspase-1 isoforms in zebrafish and demonstrated that overexpression of these isoforms induced apoptosis in mammalian cells. However, only one of the identified isoforms, caspy, oligomerized with zebrafish ASC to enhance caspy-dependent apoptosis (227). Ten years after, a few caspase-1 molecules and their ability to process IL-1 β were investigated in zebrafish, seabass and seabream (197, 228, 229). In zebrafish, infection of primary leukocytes with *F. noatunensis* induced caspase-1-like activity that resulted in IL-1 β processing. In addition, both zebrafish caspase orthologues, caspase A and caspase B, were shown to cleave IL-1 β . These findings were similar to the cleaved IL-1 β observed in seabream, whose IL-1 β was processed after caspase-1 activation (230). The activated caspase-1 was found to be auto-processed to two active heterodimers, p24/p10 and p20/p10, which are similar to those observed in humans. But the seabass caspase-1 has a

different, but phylogenetically conserved, ICE cleavage site that was similar to that of bird but not mammalian caspase-1 (228). The available results suggest that activated teleost caspase-1 can cleave the pro-IL-1 β and process IL-1 β for inflammatory responses, akin to caspase-1 of higher organisms.

2.4.7.11. Caspase-11 in mammals and teleosts

Caspase 1 and 11 belong to a family of aspartate-specific cysteine proteases conserved through evolution. In mammals, caspase-11 and caspase-1 mRNA are transcribed from the same chromosomal locus, and both of them have been traditionally classified as “inflammatory caspases”. Like caspases 8, 9, and 10, which initiate apoptotic cell death, caspase 1 and 11 have large pro-domains that mediate interactions with other proteins.

Caspase-11 has very low mRNA expression in normal murine tissues. However, following LPS stimulation, the expression of caspase-11 is significantly up-regulated in tissues including the thymus, lung, spleen, and kidney (231). The elevated expression profiles of caspase-11 were also observed in monocytes and macrophages (232). In mice, caspase-11 activation is required for NLRP3 inflammasome activation in response to infection by Gram-negative bacteria, which has been termed as non-canonical NLRP3 inflammasome activation (187). In contrast, Gram-positive pathogens do not activate caspase-11 (146).

It is generally accepted that both caspase-1 and caspase-11 induce pyroptosis, but only caspase-1 processes IL-1 β and IL-18. In contrast, activation of caspase-11 is

triggered by acylated lipid A, a component of the LPS found in many Gram-negative bacteria (188, 233). Indeed, TLR4-deficient mice, treated first with a TLR3 agonist to induce expression of caspase-11, were susceptible to a lethal dose of LPS, whereas the majority of caspase-11-deficient mice survived this regimen (188, 233), suggesting that intracellular LPS and/or acylated lipid A can activate caspase-11 in macrophages lacking the LPS receptor TLR4. Recently, a direct interaction between intracellular LPS and the CARD domain of caspase-11 (and human caspases-4 and -5) has been demonstrated (190). Collectively, these findings suggest that caspase-11 has the capacity to recognize cytosolic LPS directly, thereby initiating the non-canonical inflammasome pathway. There are no direct homologues of caspase-11 in humans, however, caspases-4 and caspase-5 are considered to be functional orthologues to mouse caspase-11, and this is believed to have arisen following a gene duplication event (12).

To date, caspase-4, caspase-5 and caspase-11 have not been identified in teleosts. In my research, I have searched the NCBI database, as well as the goldfish transcriptome database, but failed to obtain the sequence information of these molecules.

2.4.7.12. High mobility group box protein 1 (HMGB1) in mammals and teleosts

HMGB1 belongs to HMGB family, which consists of a group of non-histone chromosomal proteins that regulate DNA-dependent transcription, replication, recombination and DNA repair (234). Four subfamilies of HMGBs are known to exist including HMGB1, HMGB2, HMGB3 and HMGB4. These are small proteins (less than 30

kDa) that share high sequence identities and similar biochemical properties (235–238). Structurally, all of the HMGB proteins possess two HMG boxes located at the N-terminus (Box A and Box B), a middle region, while a C-terminal acidic tail is present in HMGB1, HMGB2, and HMGB3, but not HMGB4 (235–237). HMG boxes contain three α -helices that fold DNA into a typical wedge shape (239–242). The C-terminus acidic tail can also regulate the binding capacity of HMG boxes to DNA. During the resting status, the acidic tail interacts with basic stretches in the HMG boxes and shields them from other interactions that might occur before HMGB1 binds DNA, and upon activation, the intramolecular interaction between the acidic tail and HMG boxes is disrupted generating HMG boxes in open conformation for DNA binding (238–240, 242).

The HMGB1 has been linked to properly functioning innate and adaptive immunity (243). As a nuclear protein, HMGB1 was first discovered and named because of its quick migration during electrophoresis (244). The sequences of HMGB1 proteins have been highly conserved throughout evolution in mammals (>99%), implying the tight evolutionary conservation of this protein. HMGB1 is abundantly expressed in mammals, with higher expression level in lymphoid tissues and testis, and a less extent in brain and liver (245). The importance of HMGB1 in maintenance of homeostasis, as well as responses to pathogens, is indicated by the fact that HMGB1-knock-out mice die a few hours after birth with severe organ disorders (246).

HMGB1 is highly conserved through evolution and is primarily found in the nucleus where it functions as a non-histone chromatin-binding protein (247). With the capacity to bind the damaged DNA, HMGB1 is a universal sentinel for DNA-induced

innate immune responses and dendritic cell-mediated adaptive immune responses (243, 248).

One of the unique functional aspects of HMGB1, compared to other HMGBs, is that it can act as an inflammatory cytokine (249). The HMGB1 is also present in the cytoplasm and can be secreted to extracellular space upon inflammasome and caspase activation (148, 250, 251). Extracellular HMGB1 triggers inflammatory responses through TLR2 and TLR4, and exhibits chemoattractant activity by interacting with the receptor for advanced glycation end-products (RAGE) (252). The activation of HMGB1 leads to the activation of NF- κ B and MAP kinases (253). It has been demonstrated that blockade of either RAGE or TLR4 causes a reduced nitric oxide response and an overall decrease in inflammatory responses of mammals (254, 255). These observations suggest that HMGB1 acts as a pro-inflammatory cytokine in mammals.

The mammalian HMGB1 contains two folded DNA binding motifs called box A and box B and an acidic C-terminus tail. Box A acts as an HMGB1 antagonist, whereas box B exerts the cytokine-like inducing functions. Interestingly, HMGB1 was identified as a product of pyroptosis and a delayed cytokine-like mediator released by activated monocytes, macrophages, neutrophils, and dendritic cells following infection (256, 257). As such, inflammasome-induced HMGB1 release can be used as a biomarker for pyroptosis (258).

In teleost, HMGB1 has been characterized in zebrafish (191, 259, 260), grass carp (192), goldfish (194) and humphead snapper (193). Structurally all of the teleost HMGB1s contain HMG box A and HMG box B, and a highly acidic C-terminal region. Two

HMGB1 genes have been characterized in grass carp and their expression was up-regulated after GCRV infection and other viral PAMPs (192). In addition, HMGB1 has been demonstrated to function as a cytokine during bacterial infections and was shown to promote the innate immunity by activating macrophages of red drum (261). Interestingly, studies in zebrafish showed that HMGB1 is required for brain development (259) and contributes to the regeneration processes after spinal cord injury (260), demonstrating the multifaceted functional roles for HMGB1 in biological processes of teleosts. I have reported on the cloning and comprehensive expression and functional analysis of the goldfish HMGB1 (194). The tissue and immune cell population expression of goldfish HMGB1 was found to be highest in the brain and splenocytes. A recombinant form of goldfish HMGB1 (rgHMGB1) was generated and shown to prime goldfish monocytes and macrophages for enhanced respiratory burst and nitric oxide responses, respectively. Western blot and quantitative qPCR analysis indicated that goldfish HMGB1 participated in the antimicrobial responses against *M. marinum* and *A. salmonicida*. Cai and colleagues (2014) recently confirmed my observations that HMGB1 plays a major role in host defense against pathogens in teleosts (193).

2.4.7.13. IL-1 β and IL-18, in mammals and teleosts

2.4.7.13.1. IL-1 β in mammals and teleosts

Both IL-1 β and IL-18 belong to IL-1 family of cytokines that plays a major role in inflammation, host responses to pathogens and in autoimmune diseases (262, 263).

IL-1 β is a pro-inflammatory cytokine secreted by activated macrophages and monocytes. It promotes local and systemic responses to infection, injury, and immunological challenges and plays a central role in controlling the acute and chronic inflammation (263). Unlike other cytokine promoters, IL-1 β regulatory regions are distributed over several thousand base pairs upstream from the transcriptional start site. In addition to cAMP response element, there are NF- κ B-like and activating protein-1 (AP-1) sites. IL-1 β gene regulation and its role in different diseases has been comprehensively reviewed by Dinarello (264, 265), and is not addressed in this review.

The IL-1 β production is regulated via different pathways: inflammasome-dependent or inflammasome-independent. IL-1 β is produced as a dormant cytoplasmic precursor (proIL-1 β , p35) that can be cleaved by caspase-1 to generate a smaller bioactive form (p17). Although pro-caspase-1 is abundant in hematopoietic cells, activation of caspase-1 requires cleavage by the inflammasomes. Thus, the key requirement in this process is the formation of macromolecular complexes (particularly the NLRP3-inflammasome) (266). However, not all IL-1 β -mediated inflammation is exclusively due to NLRP3 or caspase-1 activity. For example, mice deficient in caspase-1 develop the same IL-1 β -mediated disease as do wild-type mice (264, 265).

In humans, the primary sources of IL-1 β are macrophages, skin dendritic cells, B lymphocytes, NK cells and brain microglia, generated in response to activated complement components, other cytokines (such as TNF- α) and IL-1 itself (265). In contrast, fibroblasts and epithelial cells do not produce IL-1 β , and circulating blood

monocytes or bone marrow aspirates from healthy humans do not constitutively express IL-1 β .

To date, IL-1 β has been characterized in many teleost species, including rainbow trout (267, 268), salmon (269), catfish (270), seabass (271–274), Atlantic cod (275, 276), Japanese flounder (277) and Atlantic halibut (278). The inflammasome mediated IL-1 β production has been proposed by Angosto and colleagues (2012) who demonstrated the release of mature IL-1 β from isolated seabream leukocytes upon infection with *S. typhimurium* or *L. monocytogenes* lysteriolysin treatment (197). Mature IL-1 β was generated from seabream macrophages after infection with *S. typhimurium* or stimulated with hypotonic solution while the production of IL-1 β was blocked by the caspase-1 inhibitor YVAD (197). These results suggest that seabream caspase-1 plays an important role in the generation of IL-1 β . Despite the fact that the typical ICE cutting site present in mammalian IL-1 β , this is not a feature of teleost IL-1 β molecules. Growing evidence indicates that teleost IL-1 β is produced as a precursor that is subsequently cleaved to be active (268, 271). For example, the seabass IL-1 β was cleaved *in vitro* following incubation with caspase-1 into a 18 kDa isoform. The caspase-1-mediated IL-1 β processing in seabream leukocytes occurred after 4 h, which is significantly longer than IL-1 β processing in other animals, and the processing of IL-1 β was blocked by pan-caspase inhibitor, Ac-YVAD-CHO. Similarly, zebrafish IL-1 β processing was caspase-1 dependent in a mixed leukocyte population exposed to fish pathogen *Francisella*, and was inhibited by the caspase-1 inhibitor YVAD (229, 279). Thus, IL-1 β is an evolutionarily conserved, pro-inflammatory cytokine that is generated upon exposure to pathogens.

2.4.7.13.2. IL-18 in mammals and teleosts

IL-18 was initially identified as an IFN- γ -inducing factor in sera from mice infected with bacterium *Propionibacterium acnes* and after *in vitro* challenge of naïve spleen cells with LPS (280). IL-18 is mainly produced by Kupffer cells (liver macrophages) as a 192 amino acids precursor, that is cleaved to produce a 157 aa mature protein (281). A short time after the discovery of murine IL-18, human IL-18 was cloned using murine IL-18 cDNA as a probe and expressed in *E. coli* (282), and shown to induce IFN- γ in peripheral blood mononuclear cells (PBMCs). The IL-18 gene is located on chromosome 9 in mouse and on chromosome 11 in humans (283–286).

Pro-IL-18 is constitutively expressed in endothelial cells, keratinocytes and intestinal epithelial cells throughout the gastrointestinal tract. The inactive IL-18 precursor remains in the intracellular compartment of mesenchymal cells, whereas macrophages and dendritic cells secrete active IL-18. As with the processing of IL-1 β , following cleavage by active caspase-1, IL-18 is secreted by the phagocytes, although as much as 80% of the pro-IL-18 remains unprocessed inside the cells. Mice deficient in caspase-1 do not secrete IL-18 after endotoxin (LPS) exposure, and this deficiency is believed to be the result of failed IL-18 processing (287, 288). It is also known that IL-18 production may be caspase-1 independent, as the Fas ligand stimulation results in release of biologically active IL-18 in caspase-1-deficient murine macrophages (289).

Similar to IL-1 β , IL-18 is also a pro-inflammatory cytokine, that induces cell adhesion, synthesis of nitric oxide and production of chemokines. For example, blocking

IL-18 generation reduced metastasis in mouse because of decreased production of vascular cell adhesion molecule-1 (290). Unlike other pro-inflammatory cytokines, IL-18 does not induce fever and the formation of acute phase proteins (291, 292). However, IL-18 is involved in promoting the production of interferon- γ (IFN- γ) in T helper type 1 (Th1) cells, natural killer cells and cytotoxic T lymphocytes, enhancing the development of T helper type 2 (Th2) cells (293). For example, IL-18 induces IL-4 production in the absence of IL-12. In transgenic mice overexpressing IL-18, serum levels of IgE, IgG1, IL-4 and IFN- γ are significantly increased (294). Thus, high IL-18 production participates in the polarization of Th1 and Th2 responses in hosts.

In teleost, IL-18 has been identified in a few fish species, including rainbow trout, medaka, pufferfish and seabream. The first report showing the existence of IL-18 was described by Huising and colleagues (295) through the analysis of pufferfish genome. Zou and co-workers (296) characterized IL-18 in rainbow trout and found that the gene organization of trout and pufferfish IL-18 was similar to that of mammalian IL-18.

Unlike IL-1 β , sequence analysis of IL-18 revealed that there is a putative ICE cleavage site at Asp³² in trout and Asp³¹ in pufferfish. Surprisingly, treatment of primary kidney cells with LPS, poly I:C and trout recombinant IL-1 β did not affect the mRNA levels of IL-18. However, two IL-18 transcripts had different expression patterns in a fibroblast cell line in response to LPS and recombinant IL-1 β , suggesting that the quantitative balance of two IL-18 transcripts may influence IL-18 expression and processing. To date, there are no reports on the involvement of IL-18 in the

inflammasome pathways and IL-18 appears not to be present in other teleost genomes (goldfish, zebrafish and carp).

2.4.7.14. Pyroptosis in mammals and teleosts

Programmed cell death (PCD) is essential for the tissue homeostasis and elimination of damaged cells and plays crucial roles in cell fate (297). Apoptosis, necrosis and pyroptosis are the three main forms of PCD with distinct morphological characteristics and biochemical mechanisms (297, 298). Apoptosis was first defined based on a distinct sequence of morphologic features by electron microscopy in 1972 (299). The mechanisms of apoptosis were first investigated using the development of the nematode *C. elegans* (300). From the total generated 1,090 somatic cells to form the adult worm, 131 of them underwent apoptosis at particular stages during the development process.

Apoptosis occurs not only during the development and aging as a homeostatic mechanism to maintain and renew cells in tissues, but also during ongoing immune response or when cells are damaged by pathogens or noxious agents (301). Apoptosis is characterized by specific morphological and biochemical changes of dying cells, including cell shrinkage, nuclear condensation and fragmentation, dynamic membrane blebbing and loss of adhesion to neighbor cells or to the extracellular matrix (302). In contrast, necrosis involves cell swelling, organelle dysfunction and cell lysis (303–305). Necrosis has also been considered as the “accidental” and “unregulated” cell death (306, 307). When cells undergo necrosis, the integrity of the cell membrane is disrupted so

that the intracellular materials are released to the extracellular milieu, leading to inflammatory responses by immune cells (306, 307).

Pyroptosis was originally described in *S. flexneri*-infected macrophages in 1992 (308) and after infection with *Salmonella* spp. (309, 310). Initially, this type of cell death was first considered to be apoptosis because of the characteristic nuclear condensation, DNA fragmentation, and caspase dependence. In 2001, pyroptosis (also referred to as “inflammatory” apoptosis) was recognized as a distinct cell death process. “Pyro” means fire or fever, implying the inflammatory feature of this form of cell death, and “ptosis” means falling, which is similar to other forms of programmed cell death (311). At present, pyroptosis is considered as a hallmark of inflammasome-induced caspase-1-dependent processes (312–314).

Apoptosis and pyroptosis can be distinguished as follows: (i) the cell size; pyroptotic cell death accompanies the plasma membrane pore forming, water influx and cell swelling, so cell dying by pyroptosis increase significantly in size (315–317); (ii) caspase-1 activity; the apoptotic cell death is initiated by caspase-3/8/9, while pyroptosis is caspase-1-dependent; (iii) the integrity of plasma membrane; during the apoptosis, the cell membrane remains intact, unlike pyroptosis that features a rapid loss of cell integrity; and (iv) the nuclear integrity; during apoptosis, caspase-mediated proteolysis of ICAD releases caspase-activated DNase (CAD) that cleaves DNA nucleosomes, resulting in characteristic oligonucleosomal DNA fragments of approximately 180 bp (317). In contrast, during pyroptosis, the caspase-1-activated

nuclease does not produce the oligonucleosomal DNA fragmentation pattern so that the nuclear integrity is maintained (224, 318).

Although pyroptosis and necrosis share similar morphological events, they can be differentiated as follows: (i) caspase activation: pyroptotic cells result from caspase-1 activation, whereas necrosis requires no caspase activation; and (ii) condensed chromatin; one of features of pyroptosis is chromatin condensation, that does not occur during necrosis.

In teleosts, Angosto and colleagues (2012) were first to demonstrate pyroptosis in seabream macrophages exposed to *Salmonella* spp. (197). Recently, Varela and colleagues (319) reported possible pyroptosis of zebrafish larval macrophages exposed to hemorrhagic virus, however, these authors did not document classical morphological changes associated with pyroptotic cell death. In addition to the classical morphological changes, to confirm pyroptotic cell death, one must examine the caspase-1 activation and release of pyrogenic interleukins, such as IL-1 β and IL-18, into the extracellular milieu (17, 320). Given that pyroptosis is also considered as one of the hallmarks of inflammasome-induced caspase-1 dependent processes (312, 313), and features rapid plasma membrane rupture and release of pro-inflammatory intracellular contents (321), documenting inflammasome formation as well as HMGB1 release would confirm that cells were undergoing pyroptotic cell death.

2.5. SUMMARY

One of the main goals of my thesis research was to further the understanding of NLRs biology in fish. NLRs have emerged as central regulators of immunity and inflammation during the past decade. The understanding of the molecular mechanisms of NLRs activation is essential for our understanding of the antimicrobial responses of macrophages in both higher and lower vertebrates such as teleosts. Initial studies of NLRs functions were done in mammalian systems, and NLRs were only recently examined in teleost model systems. The loss of key NLRs (i.e. NLRC4) and downstream signalling molecule (caspase-11), as well as the polymorphism of NLRPs due to whole genome duplication events suggest that although NLRs are evolutionarily conserved in vertebrates, the recognition and signalling cascades involved in host defence differ between mammals and teleosts.

Table 2.1. Summarized NLRs and their recognized PAMPs in human and mouse

NLR subfamily	Human	Mouse	Other names	Recognized PAMPs or pathogens	References
NLRA	CIITA	CIITA	NLRA; MHC2TA; C2TA; NLRA; MHC2TA	N/A	(322, 323)
NLRB	NAIP	NAIP1-7	NLRB1; BIRC1; CLR5.1 BIRC1a-g	Flagellin from <i>Legionella</i>	(324) (200, 224, 226)
NLRC	NOD1	NOD1	NLRC1; CARD4; CLR7.1	IE-DAP	(40, 41)
	NOD2	NOD2	NLRC2, CARD15	MDP	(10, 77, 90)
	NLRC3	NLRC3	NOD3; CLR16.2	N/A	(8, 325)
	NLRC4	NLRC4	CARD12; CLAN; CLR2.1; IPAF	Flagellin from <i>Salmonella</i> , <i>Legionella</i> , <i>Listeria</i> , <i>Pseudomonas</i>	(173, 326–330)
	NLRC5		NOD27; CLR16.1	N/A	(10, 124, 323, 331–333)
	NLRX1	NOD9; CLR11.3		N/A	(8, 61, 323, 334)
NLRP	NLRP1(NALP1, DEFCAP, NAC, CARD7)		NLRP1; DEFCAP; NAC; CARD7; CLR17.1	MDP, Lethal Toxin	(134, 141, 335)
		NLRP1a,b,c	NALP1a,b,c	Lethal toxin	(137, 138, 141, 336)
	NLRP2		NALP2; PYPAF2; NBS1; PAN1; CLR19.9	N/A	(8, 337–339)
		NLRP2	PYPAF2; NBS1; PAN1;	N/A	(340–342)
	NLRP3		CIAS1; PYPAF1; Cryopyrin; NALP3; CLR1.1	Bacterial or viral RNA; uric acid, crystals, LPS, LTA; MDP; Nigericin	(213, 331, 332, 343)
		NLRP3	CIAS1; PYPAF1; Cryopyrin; NALP3; MMIG1;	Bacterial or viral RNA; uric acid, crystals, LPS, LTA; MDP; Nigericin	(344–347)
	NLRP4		NALP4; PYPAF4; PAN2; RNH2; CLR19.5;	N/A	(348–352)
		NLRP4a-g	NALP4a-g;	N/A	(351, 353)
	NLRP5		NALP5; PYPAF8; MATER; PAN11; CLR19.8;	N/A	(354–357)
		NLRP5	Master; Op1; NALP5; PYPAF5; PANS; CLR11.4	N/A	(177, 356, 358)
	NLRP6-14	NLRP6-14	NALP6-14	N/A	(8, 177, 179, 354, 359–362)

Table 2.2. Summarized NLRs and their recognized PAMPs in teleosts

NLR subfamily	NLRs	Fish species	Recognized PAMPs or fish pathogens	References	
NLRA	CIITA	Catfish	<i>E. tarda</i> , <i>S. iniae</i> , catfish virus	(363)	
NLRB	NAIP	Zebrafish	N/A	(27)	
NLRC	NOD1	Zebrafish	iE-DAP, <i>S. enterica</i>	(364, 365)	
		Goldfish	LPS, PGN, Poly I:C, <i>A. salmonicida</i>	(53)	
		Catfish		(49)	
		Miiuy croaker	Poly I:C, LPS,	(56)	
		Oliver flounder	<i>E. tarda</i> , <i>S. iniae</i> , VHSV	(55)	
		Orange-spotted grouper	LPS, <i>V. alginolyticus</i>	(52)	
		Grass carp	LPS, PGN, Poly I:C, GCRV	(47)	
		Mrigal carp	IE-DAP, <i>S. uberis</i> , <i>A. hydrophila</i>	(115)	
		Rohu	<i>E. tarda</i> , <i>S. iniae</i> , VHSV	(50)	
		Rainbow trout	IE-DAP	(366)	
		NOD2	Zebrafish	MDP, <i>E. tarda</i> , SVCV	(114)
		Goldfish	LPS, MDP, PGN, Poly I:C, <i>A. salmonicida</i> , <i>M. marinum</i>	(53)	
		Catfish	N/A	(49)	
		Miiuy croaker	Poly I:C, <i>S. aureus</i> , <i>V. anguillarum</i>	(56)	
Pufferfish	NOD2	Pufferfish	LPS, Nigericin, Nigericin+LPS	(116)	
		Rohu	PGN, LTA, <i>A. hydrophila</i> , <i>E. tarda</i> , Poly I:C	(51)	
		Grass carp	LPS, PGN, Poly I:C, GCRV	(47)	
		Mrigal carp	MDP, <i>S. uberis</i> , <i>A. hydrophila</i>	(50)	
		NLRC3	Japanese flounder	LPS, <i>E. tarda</i>	(126)
		NLRC4	N/A	N/A	N/A
NLRC5	NLRC5	Black rockfish	LPS, poly I:C	(65)	
		Pufferfish	Lpp, LPS, nigericin, Nigericin+LPS	(116)	
NLRX1	NLRX1	Goldfish	<i>A. salmonicida</i> , <i>M. marinum</i>	(53)	
		Pufferfish	LPS, Nigericin+LPS	(116)	
		Miiuy croaker	<i>V. anguillarum</i> , poly I:C	(133)	
NLRP	NLRP3rel	Goldfish	Nigericin, ATP	Chapter VI	
		NLRPL1	Zebrafish	<i>E. tarda</i> , <i>F. columnare</i> , SVCV	(367)
		NLRPL2	Zebrafish	<i>E. tarda</i> , <i>F. columnare</i> , SVCV	(367)

Abbreviations: SVCV = Spring viremia of carp virus; GCRV = Grass carp reovirus; VHSV = Viral hemorrhagic septicemia virus; Lpp = *Lactobacillus paracasei* spp. *paracasei*; N/A = Not applicable

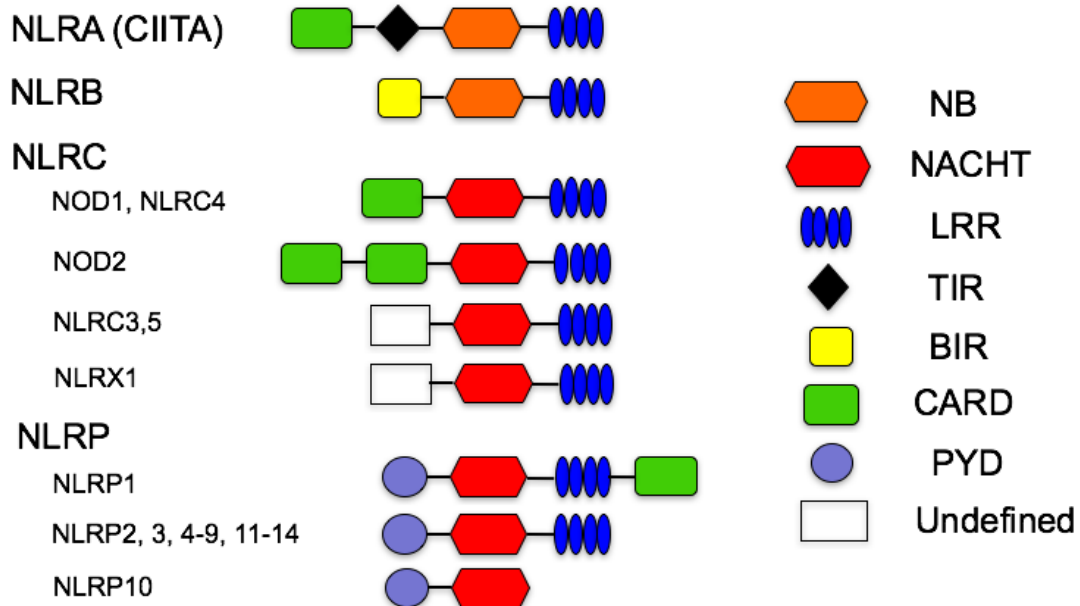


Figure 2.1. The NLR subfamilies and their domains in mammals.

NB and NACHT, nucleotide binding domains; LRR, leucine rich repeats; TIR, Toll interleukin-1; BIR, baculoviral inhibition of apoptosis protein repeat; CARD, caspase recruitment domain; PYD, pyrin domain [After Elinav et al., 2011 (179) and Robertson et al., 2012 (368)].

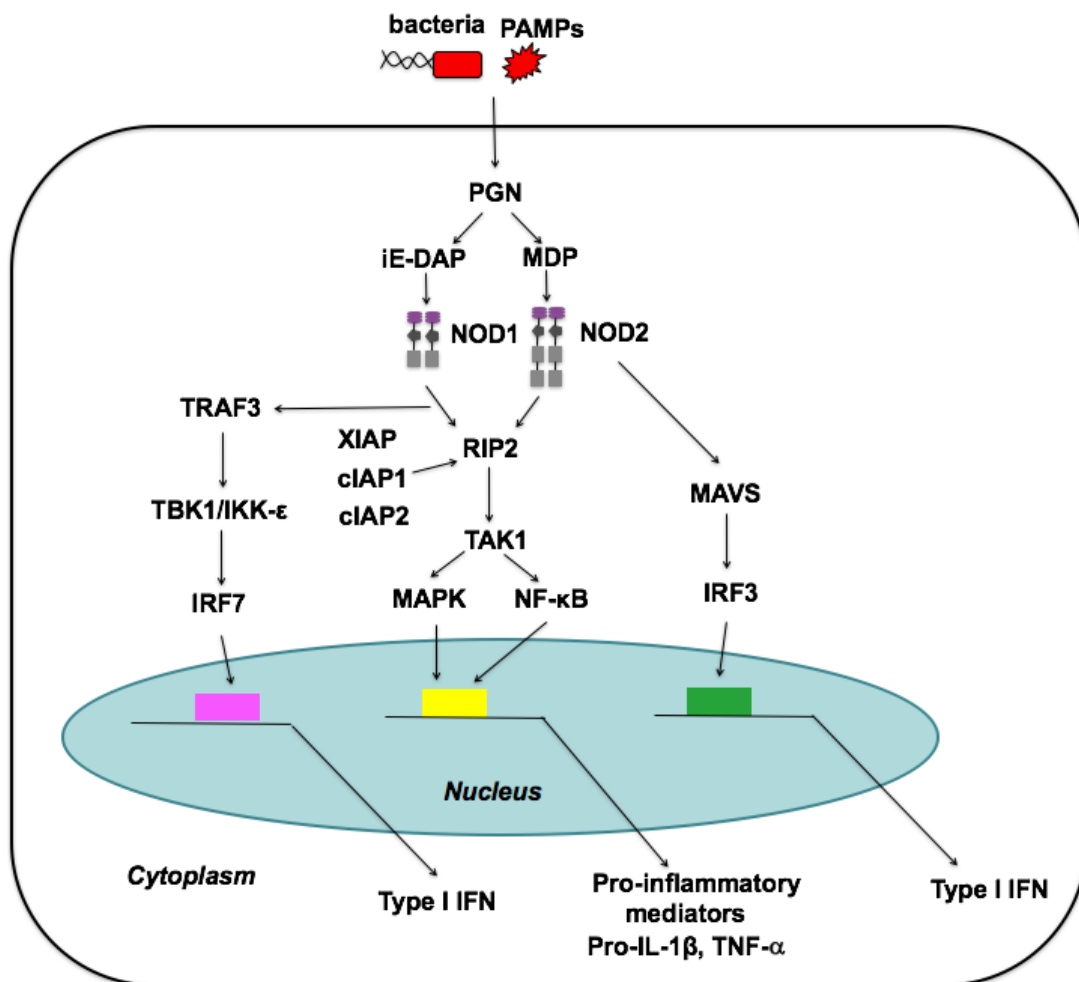


Figure 2.2. Schematic representation of NOD1 and NOD2 signaling pathways.

NOD1 and NOD2 can be activated by its specific ligand iE-DAP or MDP via two distinct signaling pathways. The shared pathway is the activation of NOD1/NOD2, which triggers pro-inflammatory cytokines production, such as TNF- α and IL-1 β , through the consecutive activation of RIP2, TAK1 and MAPK or NF- κ B. NOD1 activation can also promote Type I IFN production in a RIP2-independent way through the activation of TRAF3, TBK1/IKK- ϵ and IRF7. NOD2 also induces Type I IFN production through MAVS by engaging a RIP2-independent mitochondrial signaling complex through IRF3. Modified from Saxena and Yeretssian, 2014 (369) and Motta et al., 2015 (370).

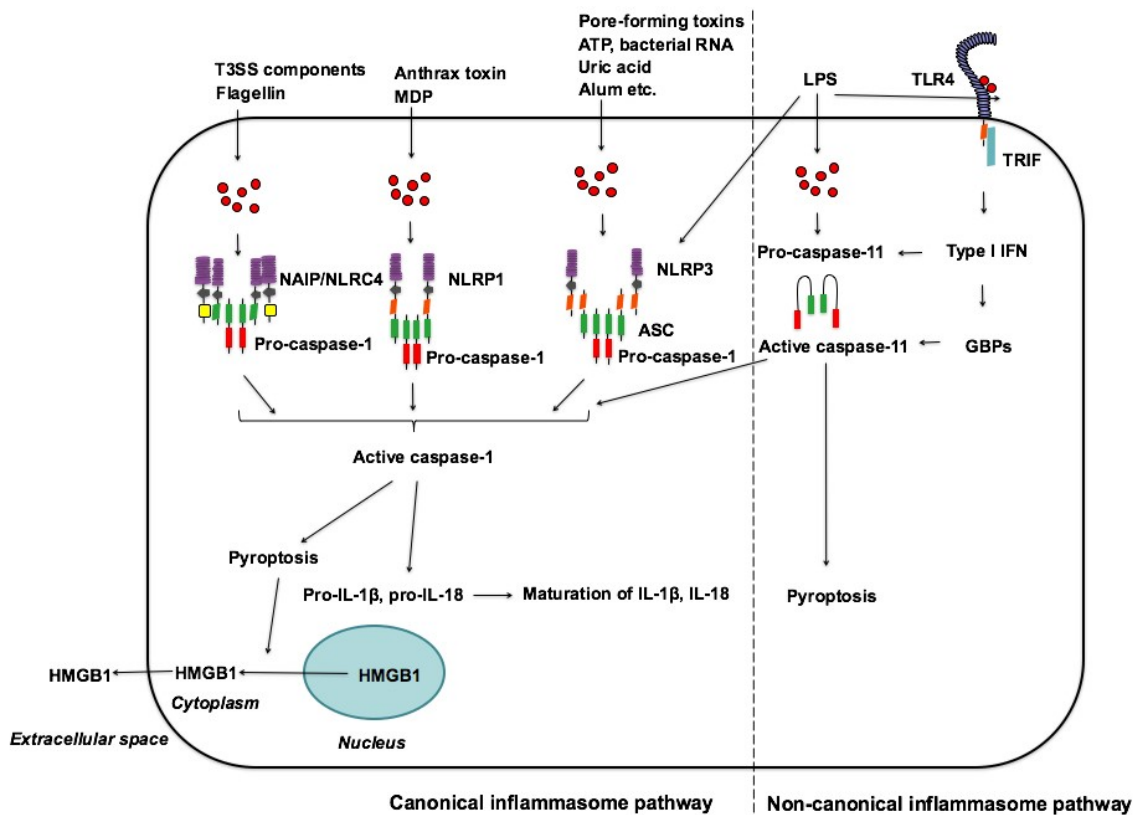


Figure 2.3. Schematic representation of canonical and non-canonical inflammasome pathways.

Canonical inflammasomes contain sensors, NLRP1, NLRP3 and NAIP/NLRC4. NAIP/NLRC4 is activated by bacterial flagellin or T3SS components, NLRP1 is activated by anthrax lethal toxin. NLRP3 is activated by a wide variety of signals including pore-forming toxins, ATP, uric acid, and alum. Once activated the receptors form an inflammasome complex with or without the adaptor, ASC, and recruit procaspase-1, which is subsequently cleaved into active caspase-1. Caspase-1 cleaves pro-IL-1 β and pro-IL-18 into their active forms as well as induces pyroptosis. Non-canonical inflammasome can be activated by cytosolic lipopolysaccharide (LPS). Gram-negative bacterial infections lead to the activation of TLR4-TRIF-type I IFN pathway, as well as assembly of NLRP3 inflammasome. Type I IFN induces the expression caspase-11. Caspase-11 oligomerize upon binding with cytosolic LPS from bacteria, and this activated caspase-11 controls NLRP3 inflammasome-dependent cleavage of caspase-1 though an unknown mechanism. Modified from Latz et al., 2013 (371), Yang et al., 2015 (189) and Vanaja et al., 2015 (147).

Abbreviation: ASC, apoptosis-associated speck-like protein containing a CARD; IL, interleukin; GBP, guanylate-binding protein.

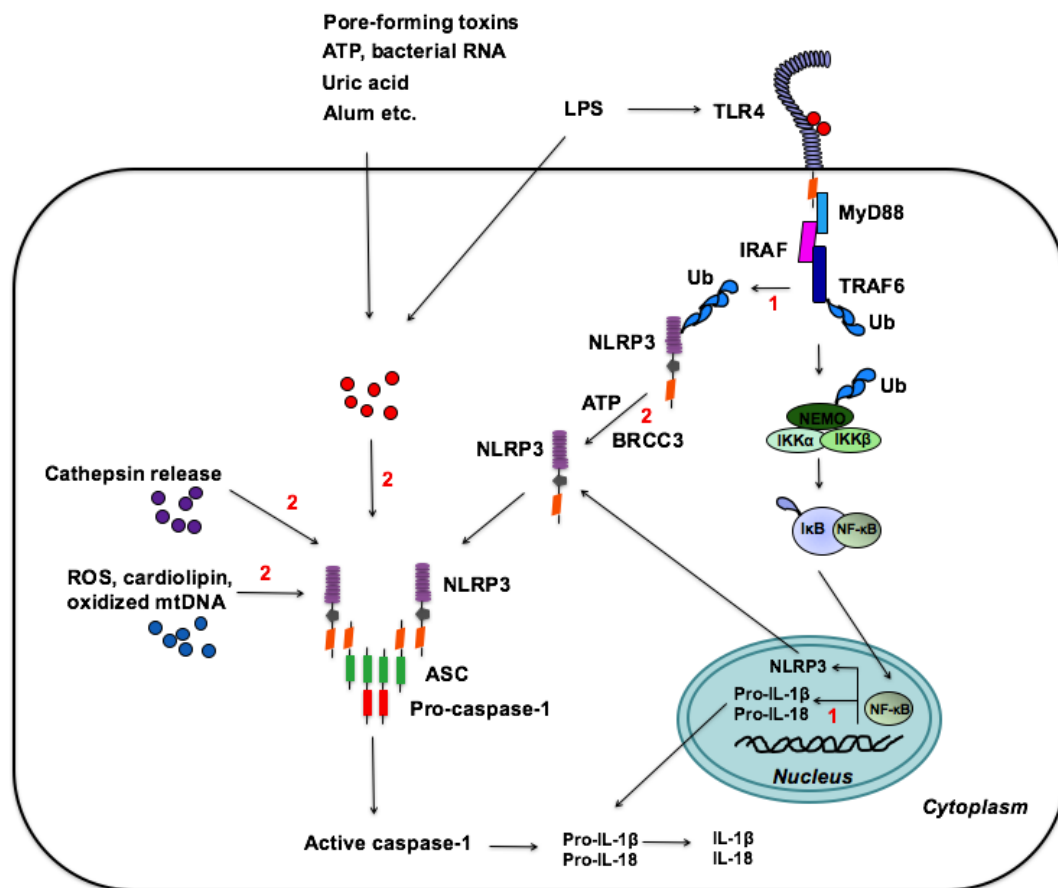


Figure 2.4. Schematic representation of priming (first) and activation (second) signals of the NLRP3 inflammasome.

NLRP3 activation requires two signals. The first signal is the binding of the TLR4 ligand LPS to its receptor. This triggers NF- κ B-mediated upregulation of NLRP3, pro-IL-1 β and pro-IL-18. Alternatively, TLR4 may provide signal through its adaptor molecules MyD88 and IRAK. BRCC3-mediated K63-deubiquitination of NLRP3 is required for NLRP3 inflammasome assembly and activation by extracellular ATP and other NLRP3-activating stimuli. These agents together with cytosolic release of lysosomal cathepsins, cytosolic release of mitochondria-derived factors such as reactive oxygen species (ROS), cardiolipin, and oxidized mitochondrial DNA (mtDNA) provide a second signal to facilitate the NLRP3 oligomerization and inflammasome assembly. Modified from Franchi et al., 2012 (372), Lamkanfi and Dixit, 2014 (17) and Ozaki et al., 2015 (373).

CHAPTER III: MATERIALS AND METHODS

3.1. ANIMALS AND FISH CELL CULTURES

3.1.1. Fish

Goldfish (*Carassius auratus* L.) were purchased from Aquatic Imports (Calgary, AB) and kept in the Aquatic Facility of the Department of Biological Sciences, University of Alberta. Fish were maintained at 17°C using a flow-through water system and a simulated natural photoperiod. Fish were fed to satiation daily with trout pellets, and acclimated to this environment for at least three weeks prior to use in experiments. All fish ranged from 10 to 15 cm in length. Prior to handling, fish were sedated using a TMS (tricaine methane sulfonate, Syndel Laboratories) solution of 40-50 mg/L in water. The animals in the aquatic facility were maintained according to the guidelines of the Canadian Council of Animal Care (CCAC-Canada).

3.1.2. Fish serum

Fish serum was obtained by bleeding common carp (*Cyprinus carpio*). Carp were anaesthetized with TMS (Syndel Laboratories) and bled from the caudal vein using 3 mL syringes and 23 Gauge needles every 4 to 8 weeks. Blood was pooled and allowed to clot overnight at 4°C. The next day blood was centrifuged for 25 minutes at 1,000 x *g* at 4°C. Serum was collected, heat inactivated at 56°C for 30 minutes, sterilized by filtration using a 0.22 µm filter, and frozen at -20°C until use in the experiments. Carp serum was

used for the cultivation of goldfish primary kidney macrophage (PKM) cultures and primary kidney neutrophil cultures.

3.1.3. Fish primary cell culture medium

The culture medium used for cultivation of goldfish primary kidney macrophages and primary kidney neutrophils, NMGFL-15, was described previously (374, 375). The composition of incomplete NMGFL-15 medium, the nucleic acid precursor solution and Hank's Balanced Salt Solution (HBSS) are shown in Table 3.1-3.3. Complete NMGFL-15 medium contained 10% heat-inactivated newborn calf serum, 5% heat-inactivated carp serum, 100 U/mL penicillin/100µg/mL streptomycin (P/S) (Gibco), 100 µg/mL gentamicin (Gibco).

3.1.4. Isolation of goldfish kidney leukocytes

3.1.4.1. Primary kidney macrophage (PKM) cultures

The procedures for the isolation and cultivation of PKM have been described previously (376, 377). Briefly, fish were anesthetized using TMS, the kidneys were aseptically removed and placed in ice-cold NMGFL-15. The kidneys were gently passed through sterile stainless steel screens using medium containing antibiotics (100 U/mL penicillin, 100 µg/mL streptomycin) and heparin (50 U/mL). The resulting cell suspension was layered over 51% Percoll (51 mL Percoll, 10 mL 10 X HBSS, 39 mL NMGFL-15 medium) and centrifuged at 400 x *g* for 25 minutes at 4°C. Cells at the 51% Percoll/medium interface were transferred to a new sterile 15 mL tube containing 10 mL

of incomplete NMGFL-15 medium. The cell suspension was then centrifuged for 10 minutes at 230 x *g*. This washing step was repeated twice before the cells were re-suspended in complete NMGFL-15 medium. The number of viable leukocytes was determined using trypan blue exclusion method. The cell viability was always greater than 95%.

3.1.4.2. Primary kidney neutrophils

The isolation of goldfish kidney leukocytes was performed as previously described (374, 377, 378), with the following minor modifications. Briefly, the kidney cell suspension was layered on 51% Percoll, centrifuged at 400 x *g* at 4°C for 25 minutes and cells at the 51% Percoll/medium interface removed. All remaining Percoll was removed, leaving behind the red blood cell/neutrophil pellet. The red blood cells were lysed using ACK lysing buffer (Gibco). The cells were washed twice using incomplete medium (400 x *g* for 10 minutes) and re-suspended in the complete medium (medium supplemented with serum). The contaminating monocytes/macrophages were removed by allowing the monocytes/macrophages to adhere to the bottom of culture flasks, and non-adherent neutrophils harvested prior to use in the experiments.

3.1.5. Establishment of primary kidney macrophages cultures

Goldfish macrophage cultures were established by seeding freshly isolated kidney leukocytes from individual fish (18-20 x 10⁶ cells/fish) into 75 cm² tissue culture flasks containing 15 mL of complete medium and 5 mL of cell-conditioned medium (CCM)

from previous cultures. The PKM cultures consisted of heterogeneous populations of cells including early progenitors, monocytes and mature macrophages as determined by flow cytometry, morphology, cytochemistry and function. Less aged cultures (3-4 days) consisted predominantly of monocytes, while older cultures (6-8 days) were predominately mature macrophages (376, 377).

3.1.6. Collection of cell conditioned medium (CCM)

Goldfish PKM cultures aged 6-8 days were centrifuge at 230 x *g* for 10 minutes at 4°C and the resulting CCMs from individual cultures were pooled, filter sterilized using a 0.22 µm filter, and stored at 4°C until use.

3.1.7. Isolation of goldfish spleen leukocytes (splenocytes)

Spleens from individual fish were aseptically removed, passed through #50 stainless steel mesh screens and re-suspended in incomplete NMGFL-15 medium containing 100 U/mL penicillin/100 µg/mL streptomycin. The cell suspensions were then layered over 51% Percoll and centrifuged at 400 x *g* at 4°C for 25 minutes. The cells at the 51% Percoll-medium interface were carefully removed, washed twice in NMGFL-15 medium (230 x *g* for 10 minutes) and re-suspended in complete NMGFL-15 prior to use in the experiments.

3.1.8. Isolation of goldfish peripheral blood leukocytes

Individual fish were bled from the caudal vein using a 1 mL heparin-coated syringe to prevent clotting, and approximately 2 mL of whole blood obtained from individual fish was diluted in 10 mL of incomplete NMGFL-15 medium containing 100 U/mL penicillin, 100 µg/mL streptomycin and heparin (50 U/mL). The cells were layered over a density gradient of 60% Percoll, and centrifuged at 400 x *g* at 4°C for 25 minutes. The buffy coat was removed and any residual red blood cells were lysed. The PBL suspensions were washed twice in incomplete medium (400 x *g* for 10 minutes) and re-suspended in the complete NMGFL-15 medium prior to use in the experiments.

3.1.9. Fluorescence-activated cell sorting (FACS) of goldfish monocytes and macrophages

PKMs were cultured for 3-4 days for the isolation of monocytes, or 6-8 days for the isolation of macrophages. Following the cultivation time indicated, PKMs were harvested, centrifuged at 230 x *g* for 10 minutes, and adjusted to a concentration of $\sim 2 \times 10^6$ cells/mL. Monocytes and macrophages were sorted based on their size and internal complexity using standard gates (R3 and R2, respectively) on an FACS Aria flow cytometer located in the flow cytometry facility of the Department of Medical Microbiology and Immunology, University of Alberta (379). Cells were sorted into 15 mL tubes contain complete NMGFL-15 medium. Tubes containing sorted cells were centrifuged at 230 x *g* at 4°C for 10 minutes and re-suspended in complete NMGFL-15, to desired number of cells/mL before used in the experiments.

3.1.10. Cultivation of mammalian cell line

HEK293 cells were maintained in DMEM supplemented with 10% FBS, 1% P/S, 1% non-essential amino acids, 10 Mm HEPES and 44 mM sodium bicarbonate at 37°C with 5% CO₂. Approximately every 3-4 days, when cells became confluent, cells were rinsed with incomplete DMEM, and treated with 0.25% trypsin/0.03% EDTA to detach cells from culture vessels. Trypsin was neutralized by the addition of complete DMEM medium. Cells were passed at a 1:10 dilution.

3.2. PATHOGENS AND FISH INFECTION

3.2.1. *Aeromonas salmonicida* A449

A. salmonicida A449 was a kind gift from Dr. Jessica Boyd (NRC Institute, Halifax, Canada) and is a virulent strain that possesses an A layer and is auto-aggregating as previously described (378). Glycerol stocks of *A. salmonicida* A449 stored at -80°C were used to streak Tryptic Soy Agar (TSA) + 20 µg/mL chloramphenicol (Sigma) plates and the plates incubated at 18°C for 72 h. A single colony was used to inoculate 5 mL of tryptic soy broth (TSB) + 20 µg/mL chloramphenicol that was grown for 24 h at 18°C with shaking. A 1:100 dilution of the stationary phase culture was used to inoculate 100 mL of TSB + chloramphenicol and cultured at 18°C until mid-log phase. Bacteria were harvested and washed twice in sterile 1 X PBS. Due to the auto-aggregating nature of the bacteria, a sample of bacteria was serially diluted in TSB containing 1% SDS prior to plating on TSA + chloramphenicol plates which mitigated clumping and allowed for the

enumeration of individual colony forming units (CFUs). Plates were incubated for 48 h at 18°C and colonies counted. *A. salmonicida* A449 was heat-killed by incubating at 60°C for 45 minutes in a circulating water bath. Following heat killing, a sample of the bacteria was plated on TSB + chloramphenicol plates to ensure bacteria were non-viable. Heat killed *A. salmonicida* A449 was stored at -20°C until used.

3.2.2. *Mycobacterium marinum*

The *M. marinum* strain ATCC 927 (fish isolate) was a kind gift from Dr. Lourens Robberts, School of Public Health, University of Alberta. Bacteria were generated as previously described (380). Briefly, *M. marinum* was grown with shaking at 30°C as a dispersed culture in 7H9 broth (Difco, USA) supplemented with 0.5% glycerol and 10% albumin-dextrose complex for 7-10 days. The number of colony forming units (cfu)/mL was determined by plating on Middlebrook 7H10 agar (Difco). Before use in the experiments, bacterial cultures were dispersed by 10-15 passages through a 25-gauge needle. When required, enumerated bacterial cultures were heat-killed by incubation in an 80°C water bath for 30 minutes. Heat killing efficiency (loss of bacterial viability) was confirmed by plating heat killed *M. marinum* on Middlebrook 7H10 agar (Difco), and failure of bacteria to grow after 5 days of incubation.

3.2.3. Fish infection

M. marinum were grown at 30°C as a dispersed culture in 7H9 broth (Difco, USA) supplemented with 0.5% glycerol, 0.05% Tween 80 and 10% albumin-dextrose complex

for 7-10 days. The number of colony forming unites (cfu)/mL was determined as above described (section 3.2.2). Before use in the experiments, bacterial cultures were dispersed by 10-15 passages though a 25-gauge needle. Fish were infected by intraperitoneal injection with 10^7 cfu of *M. marinum* diluted in 1X PBS as previously described (381) and from each of three PBS-injected (Sham-injected; SI) and *M. marinum*-infected (MI) fish, spleen tissues were collected 24 h after infection for RNA-seq analysis.

3.3. IDENTIFICATION OF GOLDFISH NOD-LIKE RECEPTORS AND INFLAMMATORY GENES

3.3.1. Primers

Primers used in this thesis for vector specific sequencing are shown in Table 3.4. The primers used in homology-based PCR, RACE-PCR, RT-PCR are shown in Table 3.5.

3.3.2. RNA isolation

RNA was isolated from goldfish tissues or cells using TRIzol (Gibco) according to the manufacturer's instructions. Briefly, tissues or cells were placed in an RNase free Eppendorf tube, lysed in 1 mL of TRIzol reagent and homogenized by continually filling and expelling the tissue or cell sequentially through a 1 mL syringe fitted with a 18 G, 21 G and finally 25 G needle. Following homogenization, the TRIzol mixture was allowed to sit at room temperature for 5 minutes prior to the addition of 200 μ L of chloroform. The process of mixing and centrifuging was repeated. The aqueous layer was transferred to a new 1.5 mL Eppendorf tube containing 500 μ L of isopropanol. Tubes were inverted 10

times and samples were centrifuged at 10,000 x *g* at 4 °C for 10 minutes to pellet the RNA. Supernatants were aspirated, and the RNA pellet washed twice with 1 mL of 75% reagent grade ethanol followed by centrifugation at 10,000 x *g* at 4 °C for 5 minutes. Ethanol was aspirated and pellets allowed to air-dry for 5-10 minutes. Nuclease-free water was used to re-suspend the RNA pellet. The nucleic acid concentration was quantified using a Nanodrop apparatus at an absorbance of 230 nm, 260 nm and 280 nm to determine phenolic and protein contamination.

3.3.3. cDNA synthesis

cDNA synthesis from RNA was performed using the Superscript II or III cDNA synthesis kit (Invitrogen) according to manufacturer's specifications. RNA levels were quantified using a Nanodrop apparatus and normalized prior to cDNA synthesis. For all cDNA synthesis procedures, Oligo dT was used as the primer.

3.3.4. RT-PCR

Target mRNA transcripts were amplified by adding 1 µL of cDNA template to 18.15 µL of nuclease free water, 2.5 µL of 10 x PCR buffer (without MgCl₂), 0.75 µL of 50 mM MgCl₂, 0.5 µL of 10 mM dNTP Mix, 2.0 µL of 20 µM primer solution, 0.1 µL of 5 U/µL Taq DNA polymerase. PCR reactions were amplified in an Eppendorf Mastercycler Gradient thermocycler. The general thermocycling program consisted of an initial denaturation step of 94°C for 5 minutes; followed by 30-33 cycles of 94°C for 30

seconds; 55°C ± 10°C for 30 seconds; 72°C for 3 minutes, and a final extension of 72°C for 10 minutes.

For colony PCR, the PCR mixture was set up in a similar manner as described above. However, instead of cDNA template, a single colony was picked and swirled into 12.5 µL of reaction mixture. The thermocycling program for pJET1.2 forward and reverse sequencing primers is as follows: an initial denaturation step of 94°C for 5 minutes; followed by 30-33 cycles of 94°C for 30 seconds; 51°C for 30 seconds; 72°C for 3 minutes, and a final extension of 72°C for 10 minutes. For T7 forward and BGH reverse primers, the annealing temperature was set to 55°C. PCR products were run on a 1% agarose gel, stained with ethidium bromide, and visualized under UV light.

3.3.5. Cloning into pJET1.2/blunt cloning vector

Bands of interest were excised from gels and purified using the Gel Extraction Kit (Qiagen) according to manufacturer's protocol. All bands were eluted in 30 µL of elution buffer provided with kit. Three microliters of the purified PCR product was transferred to a 0.6 mL tube on ice. To the reaction mixture, 0.5 µL of pJET1.2/blunt cloning vector, 0.5 µL of T4 DNA ligase and 5 µL of 2 x reaction buffer were added and gently mixed by swirling the pipette tip in the mixture. The tube was placed at room temperature for 5-10 minutes. For larger inserts (> 1500 bp), the incubation time was extended to 20-30 minutes. During the final five minutes of incubation, One Shot Top 10 or NEB 10-beta *E. coli* competent cells, stored frozen at -80°C, were placed on ice and allowed to thaw. The entire 2.5 µL ligated products was added and transferred to the competent cells, mixed

by gently swirling the pipette tip in the solution, and incubated for 20 minutes on ice. Cells were heat-shocked at 42°C for 30 seconds and allowed to recover for 2 minutes on ice. Three hundred microliters of SOC or LB medium was added, and cells incubated at 37°C for 1 h with shaking at 250 rpm. Cells were then plated on LB agar plates containing 100 µg/mL ampicillin and incubated overnight at 37°C. The next day, the presence of inserts was assessed by colony PCR.

3.4. DNA SEQUENCING AND *IN SILICO* ANALYSES

3.4.1. General approach

Generated amplicons were gel purified using the QIA Gel Extraction kit (Qiagen) and cloned into pJET1.2/blunt cloning vector (Thermo Scientific). Positive colonies were identified by colony PCR using the vector specific pJET1.2 forward and reverse sequencing primers. The constructed plasmids were extracted from positive colonies using QIAspin Miniprep Kit (Qiagen) and sequenced using an ET terminator cycle sequencing dye and a PE Applied Biosystems 377 automatic sequencer. Single pass sequences were analyzed using 4peaks software (<http://mekentoj.com/4peaks/>) and sequences aligned and analyzed using BLAST programs (<http://blast.ncbi.nlm.nih.gov/Blast.cgi>).

3.4.2. DNA sequencing and *in silico* analyses of goldfish NOD1, NOD2 and NLRX1

The sequences for goldfish NOD1, NOD2 and NLRX1 were identified using homology-based PCR using primers (IDT) designed against the NOD1 genes of grass carp

(Accession No. FJ937972.1) and zebrafish (Accession No. XM_002665060.2), NOD2 gene of rohu (Accession No. JF923468.1) and zebrafish (Accession No. XM_692832.4) and NLRX1 gene of catfish (Accession No. FJ004848.1) and zebrafish (Accession No. XM_680389.5), respectively. From these initial fragments, RACE PCR (Clontech) was performed to obtain the full open reading frame for NOD1, NOD2 and NLRX1 according to manufacturer's specifications.

Protein sequences, secretion signals, transmembrane domains, molecular weight and isoelectric point were predicted using programs from the ExPASy website (<http://ca.expasy.org/>) and the conserved domains program on Pfam (pfam.xfam.org). Phylogenetic analysis of NOD1, NOD2 and NLRX1 was done by the neighbor-joining method of the MEGA 4 program and bootstrapped 10,000 times (382). The goldfish NOD1 (JX965184), NOD2 (JX965186) and NLRX1 (JX965186) mRNA sequences have been submitted to GenBank.

3.4.3. DNA sequencing and *in silico* analyses of goldfish RIP2

The sequences for goldfish RIP2 were identified using homology based PCR using primers (IDT) designed against RIP2 gene of zebrafish (Accession number: NM_194411.2) and Nile tilapia (Accession number: XM_003438043.2). From this initial fragment, RACE PCR (Clontech) was performed to obtain the full open reading frame for RIP2 according to manufacturer's specifications.

Protein sequences, secretion signals, transmembrane domains, molecular weight and isoelectric point were predicted using programs from the ExPASy website

(<http://ca.expasy.org/>) and the conserved domains program on Pfam (pfam.xfam.org).

Phylogenetic analysis of goldfish RIP2 was done by the neighbor-joining method of the MEGA 5.1 program and bootstrapped 10,000 times (382). The goldfish RIP2 (KJ636470) mRNA sequence has been submitted to GenBank.

3.4.4. DNA sequencing and *in silico* analyses of goldfish HMGB1

The sequences for goldfish HMGB1 were identified using homology-based PCR using primers (IDT) designed against the HMGB1 gene of zebrafish (Accession number: BC067193.1) and Blunt snout bream (Accession number: FJ785329.1). From this initial fragment, RACE PCR (Clontech) was performed to obtain the full open reading frame for RIP2 according to manufacturer's specifications.

Protein sequences, secretion signals, transmembrane domains, molecular weight and isoelectric point were predicted using programs from the ExPASy website (<http://ca.expasy.org/>) and the conserved domains program on Pfam (pfam.xfam.org). Phylogenetic analysis of goldfish HMGB1 was done by the neighbor-joining method of the MEGA 5.1 program and bootstrapped 10,000 times (382). The goldfish HMGB1 (KF638272) mRNA sequence has been submitted to GenBank.

3.5. QUANTITATIVE EXPRESSION ANALYSIS OF GOLDFISH IMMUNE GENES

3.5.1. Primers

All Q-PCR primers used in this thesis were designed with the Primer Express software (Applied Biosystems) and are shown in Table 3.6. Primers for Q-PCR were

validated by running primers with 1:2 serial dilutions of cDNA and creating a standard curve, which was utilized in the determination of the R^2 value, y-intercept, and efficiency of the primer set using the 7500 Fast software. All primer sets were chosen with an R^2 value of 0.95 or higher, a y-intercept value of -3.0 to -3.2, and an efficiency of 90% or higher. Melt curves were analyzed to ensure a single melting peak, and Q-PCR products were run on a gel, excised, and sequenced to ensure the correct amplicons were being amplified.

3.5.2. Quantitative PCR thermocycling conditions and analyses

All quantitative expression of goldfish genes was performed using SYBR green reagents and an Applied Biosciences 7500 Fast Real Time Machine. Elongation factor 1 alpha (EF-1 α) was employed as an endogenous control. Thermocycling conditions were 95°C for 10 minutes followed by 40 cycles of 95°C for 15 seconds and 60°C for 1 minute. A melting curve step was added to the end of this protocol. Data were analyzed using the 7500 fast software (Applied Biosciences) and is represented as the average of the samples with standard error shown. Fold difference of gene expression was determined using $\Delta\Delta C_t$ method ($2^{-(\Delta C_t, \text{experimental sample} - \Delta C_t, \text{reference sample})}$). $\Delta C_t = C_t$ (target gene) – C_t (endogenous control).

3.5.3. Quantitative PCR analysis of NOD1, NOD2 and NLRX1 expression in normal goldfish tissues

Goldfish heart, kidney, liver, muscle, spleen, brain, gill and intestine were harvested from five individual fish ($n = 5$), and their RNA isolated using TRIzol, and reverse transcribed into cDNA using Superscript III cDNA synthesis kit. The RQ values were normalized against the expression seen in the lowest tissue group for NLRs (liver).

3.5.4. Quantitative PCR analysis of NOD1, NOD2 and NLRX1 expression in goldfish immune cell populations

PKM cultures from four individual fish ($n = 4$) were used for this experiments. Monocytes and macrophages were sorted using a FACS flow cytometer using a previously described protocol (376). RNA was isolated from the cell populations immediately after sorting using TRIzol and RNA was reverse transcribed into cDNA using Superscript III cDNA synthesis kit. The RQ values were normalized against the lowest observed expression of NLRs (macrophage).

3.5.5. Quantitative PCR analysis of NOD1, NOD2 and NLRX1 expression in activated goldfish macrophages

Primary macrophage cultures were derived from four individual fish ($n = 4$) and cells from 6 to 8-day old cultures were treated with either PBS, LPS (25 $\mu\text{g}/\text{mL}$, Sigma L2630), Poly I:C (50 $\mu\text{g}/\text{mL}$, Sigma P9582), PGN (10 $\mu\text{g}/\text{mL}$, Sigma 79682), MDP (Muramyl dipeptide) (5 $\mu\text{g}/\text{mL}$, Sigma A9519), heat-killed *A. salmonicida* (2×10^6 cfu/mL) or heat-killed or viable *M. marinum* (2×10^6 cfu/mL). Each treatment group consisted of 1×10^6 cells in a final volume of 500 μL of complete medium. Immediately following the

indicated incubation times, the total RNA was isolated from the cells using the TRIzol and reverse transcribed into cDNA using the Superscript III cDNA synthesis kit according to manufacturer's directions. Expression analysis of goldfish NOD1, NOD2 and NLRX1 was performed relative to EF-1 α , using the ddCT value of PBS at 3 h to standardize the expression of the three NLRs. The RQ values were normalized against values from the PBS groups for baseline expression (3 h). The primer sequences for these genes are listed in Table 3.6.

3.5.6. Quantitative PCR analysis of RIP2 expression in normal goldfish tissues

Goldfish heart, kidney, liver, muscle, spleen, brain, gill and Intestine were harvested from four individual fish (n = 4), and their RNA isolated using TRIzol and reverse transcribed into cDNA using Superscript III cDNA synthesis kit. The RQ values were normalized against the expression seen in the lowest tissue group for RIP2 (liver).

3.5.7. Quantitative PCR analysis of RIP2 expression in goldfish immune cell populations

PKM cultures from four individual fish (n = 4) were used for this experiments. Monocytes and macrophages were sorted using a FACS flow cytometer using a previously described protocol (376). RNA was isolated from the cell populations immediately after sorting using TRIzol and RNA was reverse transcribed into cDNA using Superscript III cDNA synthesis kit. The RQ values were normalized against the lowest observed expression of RIP2 (macrophage).

3.5.8. Quantitative PCR analysis of RIP2 in activated goldfish macrophages

The analysis of RIP2 in goldfish macrophages after activation using different stimuli was done as previously described (53). Briefly, macrophage cultures were derived from four individual fish ($n = 4$) and cells from 6 to 8-day old cultures were either treated with either PBS, lipopolysaccharide (LPS; 25 $\mu\text{g}/\text{mL}$, Sigma 79682), peptidoglycan (PGN; 10 $\mu\text{g}/\text{mL}$, Sigma A9519), muramyl dipeptide (MDP; 5 $\mu\text{g}/\text{mL}$), Poly I:C (25 $\mu\text{g}/\text{mL}$, Sigma P9582), heat-killed *A. salmonicida* (2×10^6 cfu/mL) or heat-killed or live *M. marinum* (2×10^6 cfu/mL). Each treatment group consisted of 1×10^6 cells in the final volume of 500 μL of complete medium. After 6 or 12 h of treatment, the total RNA was isolated from the cells using the TRIzol and reverse transcribed into cDNA using the Superscript III cDNA synthesis kit. Expression analysis of gfRIP2 was performed relative to EF-1 α , using ddCT value of PBS at 6 h to standardize the expression of the RIP2. The RQ values were normalized against PBS for baseline expression (6 h). The primer sequences for these genes are listed in Table 3.6.

3.5.9. Quantitative PCR analysis of NLRP3rel expression in normal goldfish tissues

Goldfish heart, kidney, liver, muscle, spleen, brain, gill and intestine were harvested from four individual fish ($n = 4$) and RNA isolated using TRIzol, and reverse transcribed into cDNA using Superscript III cDNA synthesis kit. The RQ values were normalized against the expression seen in the lowest tissue group for NLRP3rel (muscle).

3.5.10. Quantitative PCR analysis of NLRP3rel expression in goldfish immune cell populations

PKM cultures from four individual fish ($n = 4$) were used for this experiment. Monocytes and macrophages were sorted using a FACS flow cytometer using a previously described protocols (376). RNA was isolated from the cell populations immediately after sorting using TRIzol and RNA was reverse transcribed into cDNA using Superscript III cDNA synthesis kit. The RQ values were normalized against the lowest observed expression of NLRP3rel (monocytes).

3.5.11. Quantitative PCR analysis of NLRP3rel expression in activated goldfish macrophages

The analysis of NLRP3rel in goldfish macrophages after activation using different stimuli was done as previously described (53, 117). Briefly, macrophage cultures were derived from four individual fish ($n = 4$) and cells from 6 to 8-day old cultures were treated with either controls received either PBS or dimethyl sulfoxide (DMSO) (final concentration of DMSO was less than 0.1%), nigericin (20 μ M), LPS (25 μ g/mL), ATP (4 mM), heat-killed *A. salmonicida* (1×10^7 cfu/mL), heat-killed or live *M. marinum* (1×10^7 cfu/mL). Each treatment group consisted of 1×10^6 cells in a final volume of 500 μ L of complete medium. After 6 and 12 h of treatment, the total RNA was isolated from the cells using the TRIzol reagent and reverse transcribed into cDNA using the Superscript III cDNA synthesis kit (Life technologies). Expression of gfNLRP3rel was performed relative to EF-1 α , using the ddCT value of PBS at 6 h to standardize the expression of the

NLRP3rel. The RQ values were normalized against PBS for baseline expression (6 h). The primer sequences for these genes are listed in Table 3.6.

3.5.12. Quantitative PCR analysis of ASC expression in normal goldfish tissues

Goldfish heart, kidney, liver, muscle, spleen, brain, gill and intestine were harvested from four individual fish (n = 4) and their RNA isolated using TRIzol and reverse transcribed into cDNA using Superscript III cDNA synthesis kit. The RQ values were normalized against the expression seen in the lowest tissue group for NLRP3rel (muscle).

3.5.13. Quantitative PCR analysis of ASC expression in goldfish immune cell populations

PKM cultures from four individual fish (n = 4) were used for this experiments. Monocytes and macrophages were sorted using a FACS flow cytometer using a previously described protocol (376). RNA was isolated from the cell populations immediately after sorting using TRIzol and RNA was reverse transcribed into cDNA using Superscript III cDNA synthesis kit. The RQ values were normalized against the lowest observed expression of NLRP3rel (monocytes).

3.5.14. Quantitative PCR analysis of ASC in activated goldfish macrophages

The analysis of ASC in goldfish macrophages after activation using different stimuli was done as previously described (53, 117). Briefly, macrophage cultures were

derived from four individual fish ($n = 4$) and cells from 6 to 8-day old cultures were either treated with either controls received either PBS or DMSO (final concentrations of DMSO was less than 0.1%), nigericin ($20 \mu\text{M}$), LPS ($25 \mu\text{g/mL}$), ATP (4 mM), heat-killed *A. salmonicida* ($1 \times 10^7 \text{ cfu/mL}$), heat-killed or live *M. marinum* ($1 \times 10^7 \text{ cfu/mL}$). Each treatment group consisted of 1×10^6 cells in a final volume of $500 \mu\text{L}$ of complete medium. After 6 and 12 h of treatment, the total RNA was isolated from the cells using the TRIzol reagent and reverse transcribed into cDNA using the Superscript III cDNA synthesis kit (Life technologies). Expression of goldfish ASC (gfASC) was performed relative to EF-1 α , using the ddCT value of PBS at 6 h to standardize the expression of the ASC. The RQ values were normalized against PBS for baseline expression (6 h). The primer sequences for these genes are listed in Table 3.6.

3.5.15. Quantitative PCR analysis of HMGB1 expression in normal goldfish tissues

Goldfish heart, kidney, liver, muscle, spleen, brain, gill and intestine were harvested from five individual fish ($n = 5$) and their RNA isolated using TRIzol and reverse transcribed into cDNA using Superscript III cDNA synthesis kit. The RQ values were normalized against the expression seen in the lowest tissue group for HMGB1 (liver).

3.5.16. Quantitative PCR analysis of HMGB1 expression in goldfish immune cell populations

PKM cultures from five individual fish ($n = 5$) were used for this experiment. Monocytes and macrophages were sorted using a FACS flow cytometer using a

previously described protocol (376). RNA was isolated from the cell populations immediately after sorting using TRIzol and RNA was reverse transcribed into cDNA using Superscript III cDNA synthesis kit. The RQ values were normalized against the lowest observed expression of HMGB1 (macrophage).

3.5.17. Quantitative PCR analysis of rgHMGB1 induced IL-1 β 1 and TNF α -2 gene expression in macrophages

Primary macrophage cultures were derived from three individual fish (n = 3) and cells from 6 and 8-day old cultures were incubated with medium alone (control) or treated with 5 ng, 20 ng and 100 ng rgHMGB1 for 12 h before they were lysed with 50 μ L of RIPA buffer. Each treatment group consisted of 1×10^6 cells in a final volume of 500 μ L of complete medium. The IL-1 β 1 and TNF α -2 gene expressions for different experimental groups were determined using quantitative PCR.

3.6. PROKARYOTIC EXPRESSION OF GOLDFISH RECOMBINANT PROTEINS

3.6.1. Cloning of goldfish genes into prokaryotic expression vectors

The production of the recombinant goldfish proteins (rgRIP2, rgCT-NLRP3rel, rgASC and rgHMGB1) characterized in this thesis has been described previously (117, 194). Briefly, PCR fragment encoding the full sequence of gfRIP2 ORF was amplified with gene-specific primers introduced with *EcoR* I and *Xho* I at their 5'-end (Table 3.6). The PCR product was digested completely by restriction enzymes *EcoR* I and *Xho* I (Invitrogen), and then linked to the *EcoR* I/*Xho* I digested pET-32a (+) vector (Novagen).

PCR fragment encoding the C-terminal region of goldfish NLRP3rel (CT-NLRP3rel) (851-1025 aa, having PRY and SPRY functional domains, C-terminus) was amplified with gene-specific primers introduced with *Sac* I and *Not* I at their 5'-end (Table 3.7). The PCR product was digested by restriction enzyme *Sac* I and *Not* I (Invitrogen), and then ligated to the *Sac* I/*Not* I digested pET-28a (+) vector (Novagen). PCR fragment encoding the full sequence of goldfish ASC ORF was amplified with gene-specific primers designed to meet the requirements of the pET-SUMO expression vector (Invitrogen). PCR fragment encoding the full sequence of goldfish HMGB1 ORF was amplified with gene-specific primers introduced with *EcoR* I and *Not* I at their 5'-end (Table 3.7). The PCR product was digested completely by restriction enzymes *EcoR* I and *Not* I (Invitrogen), and then linked to the *EcoR* I/*Not* I digested pET-28a (+) vector (Novagen).

3.6.2. Recombinant goldfish protein expression studies

Preliminary pilot expression studies were performed where bacterial cultures expressing the desired recombinant were grown for 1 hour, induced with 1 mM IPTG and sampled every subsequent 30 minutes to determine the optimal induction and protein expression times for each respective recombinant protein. Following the sampling period, bacterial lysate supernatants and pelleted bacterial fractions were resolved by SDS-PAGE and visualized by western blotting against the His tags on the recombinant proteins. By assaying lysates and pelleted bacterial fractions, I was able to determine the optimal induction time and whether the respective recombinants were being retained in bacterial inclusion bodies and would require denaturing conditions

during lysis. The list of optimal induction conditions determined from these preliminary studies can be found in Table 3.9.

3.6.3. Scale up production of goldfish recombinant proteins

Following the above preliminary expression studies, *E. coli* were scaled up overnight and grown for 2 hours, and then induced in the presence of 0.1 mM IPTG for respective optimal times (as indicated in Table 3.9), pelleted, and kept frozen at -20°C overnight. The following day, the bacteria were lysed (2.5 mL of 10 X FastBreak cell lysis reagent (Promega) in 22.5 mL denaturing wash buffer (100 mM Hepes, 10 mM imidazole, 7.5 M urea, pH 7.5) and incubated with MagneHis Ni-particles (Promega). A PolyATtract System 1000 magnet (Promega) was used to retain the Ni-particles bound to the recombinant HMGB1, the supernatants were discarded and the beads were washed three times under denaturing conditions using the denaturing washing buffer described above. The recombinant protein was eluted from the beads using 500 mM imidazole. The protein was subsequently renatured in 10 volumes of renaturation buffer (4mM reduced glutathione, 2 mM oxidized glutathione, 50 mM sodium borate, 5 mM EDTA, pH 8.5) overnight, while being dialyzed in 1 X PBS. The protein was concentrated using dialysis tubing placed in polyethylene glycol flakes for 4-5 h, and further dialyzed overnight against PBS to reduce traces of imidazole and urea. The recombinant protein was passed through a ProteoSpin™ Endotoxin removal column (Norgen) as per the manufacturer's directions. The protein concentration was determined using a Micro BCA Protein Assay Kit (Thermo Scientific) and the presence of the recombinant protein

verified by Western blot and the identity of the protein confirmed using mass spectrometry.

3.7. ASSESSMENT OF rgHMGB1 ABILITY TO PRIME THE GOLDFISH MACROPHAGES

RESPIRATORY BURST RESPONSE

Respiratory burst assays were performed as previously described (383). Briefly, four- to five-day-old PKMs were seeded into 96-well plates at a density of 3×10^5 cells per well and incubated in culture medium alone (control) or treated with the following: rgTNF α -2 (250 ng/mL), or rgHMGB1 (5, 20, 100 or 250 ng/mL). The cell cultures were incubated for 18 h at 20°C after which NBT (2 mg/mL, Sigma) and PMA (final conc. 100 ng/mL, Sigma) in PBS was added to the cultures and incubate at room temperature for an additional 30 minutes. The plates were then centrifuged at $400 \times g$ at 4°C for 10 minutes, the supernatants aspirated and cells in the pellet fixed with absolute methanol. Non-reduced NBT was removed by washing with methanol and reduced NBT was dissolved with 2 M KOH. DMSO was added to induce the colorimetric response and the plates were read at 630 nm. Reading from cells alone (no PMA) was subtracted from treatment group values to factor in background NBT reduction. Experiments were done using PKMs from three individual fish (n = 3).

3.8. NITRITE OXIDE ASSAY

3.8.1. Generation of nitrite standard curve

Seventy five microliters of sodium nitrite, diluted in PBS to different concentration (0, 1.56, 3.13, 6.25, 12.5, 25, 50, 100, 150, 200 and 250 μM), was seeded into 96-well plates in triplicates. 100 μl of 1% (w/v) sulphanilamide in 2.5% (v/v) phosphoric acid with 100 μl of 0.1% (w/v) *N*-naphthyl-ethylenediamine in 2.5% (v/v) phosphoric acid were subsequently added. The absorbance was measured at 540 nm for the standard curve generation.

3.8.2. Assessment of rgHMGB1 ability to elicit goldfish macrophages nitric oxide production

Nitric oxide assays were performed as performed as previously described (383). Briefly, macrophages were isolated from individual goldfish kidneys ($n = 3$) were cultured for 6 to 8 days, and then seeded into individual wells of 96-well plates at a density of 3×10^5 cells per well. These were then incubated in culture medium alone (control) or treated with the following: heat-killed *A. salmonicida*, rgTNF α -2 (250 ng/mL), or rgHMGB1 (5, 20, 100 or 250 ng/mL) and incubated at 20°C for 72 h. Nitrite production was determined using the Griess reaction. Nitrite levels were determined colorimetrically at 540 nm with the generated nitrite standard curve (Fig. 3.1).

3.9. PRODUCTION OF POLYCLONAL ANTIBODIES TO RECOMBINANT PROTEINS

Two hundred and fifty µg of purified recombinant goldfish HMGB1, CT-NLRP3rel and ASC was used to immunize rabbits mixed with 750 µL of Freund's Complete Adjuvant (FCA). Booster injections were performed every 4 weeks for 12 weeks using the same quantity of recombinant proteins in mixed with Freund's incomplete adjuvant (FIA). The polyclonal anti-HMGB1, anti-CT-NLRP3rel and anti-ASC IgG antibodies were purified from 100 µL of rabbit serum using a Melon Gel IgG Purification kit (Thermo Scientific) according to the manufacturer's protocol. Briefly, the resin was washed twice with Melon Gel buffer and incubated with diluted serum for 5 minutes to allow for the binding of serum proteins. Antibodies were then spun through the resin and stored at -20°C in aliquots.

3.10. TRANSFECTIONS AND DUAL-LUCIFERASE REPORTER ASSAY

3.10.1. Assessment of the ability of RIP2 to activate NF-κB

Dual-luciferase reporter assays were performed as previously described (194). Briefly, HEK 293 cells were grown at 37°C in the presence of 5% CO₂ in complete DMEM supplemented with 10% fetal bovine serum (FBS). HEK 293 cells in 24-well plates (2 x 10⁵ cells/well) were co-transfected with a total of 200 ng pcDNA3.1/V5-His empty or pcDNA3.1/V5-His-RIP2 or pcDNA3.1/V5-His-LBP (LPS binding protein), including 20 ng of pRL-TK vector (Promega) and 200 ng of pNF-κB-Luc (Stratagene), using polyethylenimine (PEI) reagent (Polysciences). Firefly and renilla luciferase activities were measured using Dual-Luciferase Reporter Assay System (Promega) according to the manufacturer's

instruction. Briefly, at 24 h post-transfection, HEK293 cells in 24-well plates were washed with 500 μ L 1 X PBS twice, then lysed with 100 μ L 1 X passive lysis buffer at room temperature for 15 minutes. Twenty μ L of cell lysate was transferred to a 1.5 mL eppendorf tube and 100 μ L Luciferase assay reagent II and 1 X stop & glo reagent were added in sequence, then firefly and renilla luciferase activities were measured using a GloMax 20/20 Luminometer (Promega), respectively.

3.10.2. Assessment of the ability of ASC to activate NF- κ B

Dual-luciferase reporter assays were done as previously described (117, 194) with the following modifications. Briefly, HEK293 cells in 24-well plates (1×10^5 /well) were co-transfected with a total of either 200 ng pcDNA3.1/V5-His-empty (His-empty), pcDNA3.1/V5-His-ASC (His-ASC), pcDNA3.1/V5-His-caspase-1 (His-caspase-1), pcDNA3.1/V5-His-RIP2 (His-RIP2), His-empty and His-RIP2, His-ASC and His-RIP2, His-ASC and His-caspase-1, His-ASC and His-RIP2 and His-caspase-1, His-empty and His-RIP2 and His-caspase-1, or His-RIP2 and His-caspase-1 including 20 ng of pRL-TK vector (Promega) and 200 ng of pNF- κ B-Luc (Stratagene), using Turbofect transfection reagent (Thermo Fisher scientific). Firefly and renilla luciferase activities were measured using a Dual-Luciferase Reporter Assay System according to the manufacturer's instructions (Promega).

3.10.3. Assessment of the ability of HMGB1 to activate NF- κ B

The goldfish HMGB1 ORF region was amplified using gene specific primers (Table 3.7) and cloned into the pcDNA3.1/V5-His TOPO TA expression vector (Invitrogen) according to manufacturer's protocols. Constructs were screened and confirmed by DNA sequencing with vector specific primers T7 and BGH (Table 3.4). HEK293 cells were grown at 37°C in the presence of 5% CO₂ in complete DMEM supplemented with 10% fetal bovine serum (FBS). HEK 293 cells in 24-well plates (2 x 10⁵ cells/well) were co-transfected with a total of 200 ng pcDNA3.1/V5-His empty or pcDNA3.1/V5-His-HMGB1 or pcDNA3.1/V5-His-LBP (LPS binding protein), including 20 ng of pRL-TK vector (Promega) and 200 ng of pNF- κ B-Luc (Stratagene), using polyethylenimine (PEI) reagent (Polysciences). Firefly and renilla luciferase activities were measured using a Dual-Luciferase Reporter Assay System (Promega) according to the manufacturer's instruction. Briefly, at 24 h post-transfection, HEK293 cells in 24-well plates were washed with 500 μ L 1 X PBS twice, then lysed with 100 μ L 1 X passive lysis buffer at room temperature for 15 minutes. Twenty μ L of cell lysate was transferred to a 1.5 mL eppendorf tube and 100 μ L Luciferase assay reagent II and 1X stop & glo reagent were added in sequence, then firefly and renilla luciferase activities were measured by GloMax 20/20 Luminometer (Promega), respectively.

3.11. CO-IMMUNOPRECIPITATION (CO-IP) ANALYSES

3.11.1. Co-IP analysis of goldfish RIP2 and NOD1/NOD2

Goldfish NOD1 and NOD2 ORF regions were amplified using gene specific primers (Table 3.7) and cloned into the pcDNA3.1/NT-GFP-TOPO expression vector (Invitrogen), while gfRIP2 ORF was amplified and cloned into pcDNA3.1/V5-His TOPO expression vector (Invitrogen) with gene specific primers (Table 3.7). Constructs were screened and confirmed by DNA sequencing with vector specific primers GFP Forward or T7 promoter and BGH Reverse (Table 3.4). Co-IP assay was performed as described by Montgomery and co-workers previously with following modifications (384). Briefly, HEK 293 cells ($\sim 1 \times 10^6$) were co-transfected with pcDNA3.1/NT-GFP-empty or pcDNA3.1/NT-GFP-NOD1/NOD2 and pcDNA3.1/V5-His-RIP2 expression plasmids and harvested after 48 h for IP. Cells were lysed by incubating them for 10 minutes in 500 μ L of ice-cold IP buffer (50 mM Tris-HCl, 150 mM NaCl, 1% Triton X-100, supplemented with complete mini EDTA-free protease inhibitor and phosphatase inhibitor cocktail tablets; Roche) and incubated overnight at 4°C on a rotary mixer with 1 μ g of either anti-GFP polyclonal antibody (Thermo Scientific) or anti-His monoclonal antibody (Sigma), respectively. Fifty μ L of pre-washed (with IP buffer) protein G Sepharose beads (GE Healthcare) were then added to the samples and incubated for a further 2 h at 4 °C on a rotary mixer. Beads were washed three times with 1 mL of IP buffer, subjected to SDS-PAGE, and then electrotransferred to nitrocellulose membranes. The blots were incubated for 2 h at room temperature in blocking buffer (5% skim milk in 1 X TBST) and then overnight at 4°C with anti-GFP or anti-His antibody. Detection was performed using the ECL Western

Blot Substrate kit (Thermo Scientific) after incubation with anti-mouse IgG or anti-rabbit IgG antibody (Bio-Rad).

3.11.2. Co-IP analysis of goldfish NLRP3rel and ASC

Co-IP assays were performed as described previously (117) with the following modifications. Briefly, HEK293 cells in 24-well plates (1×10^5 cells/well) were co-transfected with 1 μ g pcDNA3.1/V5-His TOPO TA expression vector (His-empty) or pcDNA3.1/V5-His-ASC (His-ASC) and GFP-NLRP3rel expression plasmids and harvested after 48 h for IP analysis. Cells were lysed by incubating them for 10 minutes in 500 μ L of ice-cold NP40 cell lysis buffer (Invitrogen) supplemented with protease inhibitor cocktail (Calbiochem). Fifty microliters of pre-washed beads (wash buffer: PBS with 0.02% Tween-20; Dynabeads protein A (Invitrogen)) were first cross-linked to anti-His or anti-GFP antibody using the cross-linker bis [sulfosuccinimidyl] substrate (BS³) (Thermo Fisher Scientific) according to the manufacturer's protocol. The antibody cross-linked beads were then washed and incubated with the lysed proteins overnight at 4°C on a rotary mixer. Beads were washed, three times, with 500 μ L of wash buffer, and eluted in 30 μ L of elution buffer (50 mM Glycine, pH=2.8) before being subjected to SDS-PAGE analysis and then electrotransferred to nitrocellulose membranes (Bio-Rad). The blots were incubated for 2 h at room temperature in blocking buffer (5% skim milk in 1 X TBST) and then overnight at 4°C with anti-His and/or anti-GFP antibody. Detection was performed using ECL Western Blot Substrate kit (Thermo Fisher Scientific) after incubation with anti-mouse IgG or anti-rabbit IgG antibody (Bio-Rad).

3.11.3. Co-IP analysis of goldfish ASC and caspase-1/RIP2

Co-IP assays were performed as described previously (117) but with the following modifications. Briefly, HEK293 cells in 24-well plates (1×10^5 cells/well) were co-transfected with 1 μ g of either His-empty or His-ASC and GFP-RIP2 or GFP-caspase-1 expression plasmids and harvested after 48 h for co-IP analysis. Cells were lysed by incubating them for 10 minutes in 500 μ L of ice-cold NP40 cell lysis buffer (Invitrogen) supplemented with protease inhibitor cocktail (Calbiochem). Fifty microliters of pre-washed beads (wash buffer: PBS with 0.02% Tween-20; Dynabeads protein A (Invitrogen)), were first cross-linked to anti-His or anti-GFP antibody using the cross-linker BS³ (Thermo Fisher Scientific) according to the manufacturer's protocol. The antibody cross-linked beads were then washed and incubated with the lysed proteins overnight at 4°C on a rotary mixer. Beads were washed, three times, with 500 μ L of wash buffer, and eluted in 30 μ L of elution buffer (50 mM Glycine, pH=2.8) before being subjected to SDS-PAGE and electrotransfer to nitrocellulose membranes (Bio-Rad). The blots were incubated for 2 h at room temperature in blocking buffer (5% skim milk in 1 X TBST), and then overnight at 4 °C with anti-His and/or anti-GFP antibody. Detection was performed using the ECL Western Blot Substrate kit (Thermo Fisher Scientific) after incubation with anti-mouse IgG or anti-rabbit IgG antibody (Bio-Rad).

3.12. CONFOCAL MICROSCOPY

3.12.1 Co-localization analysis of goldfish NLRP3rel and ASC

HEK 293 cells were seeded on sterilized coverslips (Neuvitro) in 24-well plates at a density of 1×10^5 /well. After 24 h, cells were co-transfected with 1 μ g of either pcDNA3.1-NT-GFP-empty (GFP-empty) or pcDNA3.1-NT-GFP-ASC (GFP-ASC) and pDsRed-Monomer-C-NLRP3rel (DsRed-NLRP3rel) using Turbofect transfection reagent (Thermo Fisher Scientific). At 48 h hours after transfection, cells were washed twice with PBS before being fixed in 4% paraformaldehyde (PFA) for 15 minutes at room temperature. Subsequently, cells were mounted on slides using Fluoroshield mounting media containing 4', 6-diamidino-2-phenylindole (DAPI; Sigma), and viewed using a Laser Scanning Confocal Microscope (Zeiss LSM 710, objective 40 \times 1.3 oil plan-Apochromat) at the Cross Cancer Institute Cell Imaging Facility, Edmonton, Alberta. Quantification of "ring" structures was performed by visualizing 100 co-transfected cells in three separate experiments.

3.12.2 Co-localization/aggregation analysis of goldfish ASC

HEK 293 cells were seeded on sterilized coverslips (Neuvitro) in 24-well plates at a density of 1×10^5 /well. After 24h, cells were co-transfected with 1 μ g of either pcDNA3.1-NT-GFP-empty (GFP-empty) or pcDNA3.1-NT-GFP-ASC (GFP-ASC) and pDsRed-Monomer-C-ASC (DsRed-ASC) using Turbofect transfection reagent (Thermo Fisher Scientific). At 48 h after transfection, cells were washed twice with PBS and fixed using 4% paraformaldehyde (PFA) for 15 minutes at room temperature. The cells were mounted on slides using Fluoroshield mounting media containing DAPI (Sigma), and viewed using

a Laser Scanning Confocal Microscope (Zeiss LSM 710, objective 40 × 1.3 oil plan-Apochromat) at the Cross Cancer Institute Cell Imaging Facility, Edmonton, Alberta.

3.13. LDH RELEASE ASSAY

Lactate dehydrogenase (LDH) release was measured using the Pierce LDH Cytotoxicity assay kit (Thermo scientific). Briefly, cells from 6 to 8-day old cultures were seeded into individual wells of 96-well plates at a density of $1 \times 10^5/100 \mu\text{L}$ per well. These were pretreated with 100 μM of a pan-caspase inhibitor (Q-VD-OPH, SM Biochemicals) for 3 h or left untreated, and then incubated in culture medium alone (control) or treated with 10 μL of the following: DMSO (1:10 diluted with complete media), 20 μM nigericin (final concentration) and incubated at 20°C incubator for 12 h. The plates were then centrifuged at 230 x *g* at 4°C for 10 minutes, 50 μL of supernatants were transferred into a new 96-well plate and 50 μL of reaction buffer was added to each well for an additional 30 minutes. Subsequently, 50 μL stop reagent was added before the absorbance was measured at 490 nm and 680 nm in sequence. To determine LDH activity, the absorbance at 680 nm was subtracted by that at 490 nm first, then the % cytotoxicity was calculated using the following formula: % LDH release = (Compound-treated LDH activity – Spontaneous LDH activity)/(Maximum LDH activity – Spontaneous LDH activity) x 100. Water- and lysis buffer-induced LDH activities were considered as spontaneous and maximum LDH activity, respectively.

3.14. WESTERN BLOT ANALYSES

3.14.1. Western blot analysis of recombinant protein expression

Following the production and isolation of all the recombinant goldfish proteins described above, equal amount of 2 × Laemmli sample buffer was added to the protein samples and the 15 µL of protein samples mixture loaded in gel lanes and SDS-PAGE performed at 120 V for 10 minutes followed by at 140 V for 50 minutes. Separated proteins were then transferred onto 0.2 µm nitrocellulose membranes (Bio-Rad) at 135 V for 45 minutes. Membrane were blocked for 1 h at room temperature with 5% skim milk in TBST and probed overnight at 4°C with primary antibody [anti-His (1:5000) or purified rabbit anti-recombinant protein IgG (1:3000)]. The following day, the membranes were washed, incubated for 1 h with HRP-conjugated goat anti-mouse or rabbit IgG antibody (Bio-Rad) for 1 h at room temperature, and developed using ECL (Thermo Scientific) on X-ray film (Eastman Kodak Co.).

3.14.2. Validation of specificity of polyclonal anti-RIP2 antibody and RIP2 inhibitors

Identical recombinant pET-32a-RIP2 (rgRIP2) protein samples were loaded on opposite halves of a single gel. After transfer, membranes were split and blocked as described above. Membranes were incubated for 2 h at room temperature with either anti-His mAb (diluted 1:5000 in 1 × TBST, Sigma), or anti-human RIP2 rabbit polyclonal antibody (diluted 1:3000 in 1 × TBST, Abcam ab85265) that has been predicted to recognize zebrafish, mouse, rat, chicken, cow and human RIP2. Membranes were subsequently washed three times with 1 × TBST, before incubation with anti-mouse IgG or anti-rabbit IgG (diluted 1:5000 in 1 × TBST, Bio-Rad) for 1 h at room temperature,

respectively. After another set of washes, detection was performed as above described (Section 3.14.1).

Three RIP2 inhibitors, SB203580 (Santa Cruz Biotechnology), gefitinib and erlotinib (LC Laboratories), that have been shown to inhibit RIP2 activity in mammals (385–389), were tested to determine whether they inhibited goldfish RIP2. The reagents were dissolved in DMSO in accordance with the manufacturer's instructions. In general, aliquots of stock solutions were stored at -20°C and final concentrations were achieved by diluting stock reagents in complete medium. In all instances, final concentrations of DMSO were less than 0.1% and had no effect on macrophage viability. Cells isolated from individual goldfish kidney that had been cultured for 6-8 days were seeded into individual wells of 24-well plates at a density of 1×10^6 cells per well in a final volume of 500 μ L of complete medium. These were then incubated in approximately 0.1% DMSO diluted in culture medium alone (control) or treated with the following: SB203580 (5 μ M or 10 μ M), gefitinib and erlotinib (0.1 μ M or 0.5 μ M). After 12 h of treatment, cells were washed three times with PBS and lysed using 100 μ L of ice-cold IP buffer and then subjected to Western blot analysis as above described (Section 3.14.1).

3.14.3. Evaluation of the involvement of RIP2 in pro-inflammatory cytokine production in response to heat-killed *M. marinum*

The anti-TNF α -2 and anti-IL-1 β 1 antibodies were generated as previously described (194, 390). Heat-killed *M. marinum* was prepared as described in section 3.2.2. Primary macrophage cultures were pooled from macrophage cultures established from

four individual fish ($n = 4$) and cells from 6 to 8 day old cultures were incubated with PBS (control), SB203580, or with heat-killed *M. marinum* (2×10^6 cfu/mL) for 12 h before treatment with 10 μ M SB203580 for 2 h. The same experimental design with an additional inflammasome-related protein [high mobility group box1 (HMGB1)] was employed for the Q-PCR analysis. Each treatment group consisted of 1×10^6 cells in a final volume of 500 μ L of complete medium. After treatment, cells were washed three times with PBS and lysed with 100 μ L of ice cold IP buffer and then subjected to Western blot analysis as described above (Section 3.14.1).

3.14.4. Western blot analysis of NLRP3rel in activated goldfish macrophages

The analysis of NLRP3rel in goldfish macrophages after activation using different stimuli was done as previously described (53, 117). Briefly, macrophage cultures were derived from three individual fish ($n = 3$) and cells from 6 to 8-day old cultures were either treated with either controls received either PBS or DMSO (final concentration of DMSO was less than 0.1%), nigericin (20 μ M), LPS (25 μ g/mL), ATP (4 mM), heat-killed *A. salmonicida* (1×10^7 cfu/mL), heat-killed or live *M. marinum* (1×10^7 cfu/mL). Each treatment group consisted of 1×10^6 cells in the final volume of 500 μ L of complete medium. After 6 and 12 h of treatment, the treated macrophages were washed three times with PBS and lysed with 100 μ L of NP-40 buffer and then subjected to Western blot analysis using anti-CT-NLRP3rel antibody or anti- β -actin antibody. β -actin was used as a loading control.

3.14.5. Assessment of the role of NLRP3rel in cytokine processing of nigericin-activated macrophages

The anti-HMGB1 and anti-IL-1 β 1 antibodies were generated as previously reported (194). The anti-caspase-1 antibody was also generated against the recombinant SUMO-caspase-1 and its specificity was confirmed by Western blot. Primary macrophage cultures were pooled from macrophage cultures established from three individual fish (n = 3) and cells from 6 to 8 day old cultures were incubated with culture medium alone or pre-incubated with 100 μ M Q-VD-OPH for 3 h before being treated with either 0.1% DMSO, 20 μ M nigericin for another 12 h. Each treatment group consisted of 1×10^6 cells in a final volume of 500 μ L of complete medium. After treatment, cells were washed three times with PBS and lysed with 100 μ L of NP-40 buffer and then subjected to western blot analysis using anti-CT-NLRP3rel antibody or anti- β -actin antibody. β -actin was used as a loading control.

3.14.6. Western blot analysis of ASC expression in activated goldfish macrophages

The analysis of ASC in goldfish macrophages after activation using different stimuli was done as previously described (53, 117). Briefly, macrophage cultures were derived from three individual fish (n = 3) and cells from 6 to 8-day old cultures were either treated with either controls received either PBS or DMSO (final concentration of DMSO was less than 0.1%), nigericin (20 μ M), ATP (4 mM), LPS (25 μ g/mL), heat-killed *A. salmonicida* [1×10^7 colony forming units (cfu)/mL] or heat-killed or live *M. marinum* (1×10^7 cfu/mL). Each treatment group consisted of 1×10^6 cells in a final volume of 500 μ L

of complete medium. After 6 or 12 h of treatment, the treated macrophages were washed three times with PBS and lysed with 100 μ L of NP-40 buffer and then subjected to western blot analysis using anti-ASC antibody or anti- β -actin antibody. β -actin was used as a loading control.

3.14.7. *In vitro* cross-linking studies of rgfASC

In vitro cross-linking assays were performed as previously described (391). Briefly, HEK293 cells were grown at 37°C in the presence of 5% CO₂ in complete DMEM supplemented with 10% fetal bovine serum (FBS). HEK293 cells at a density of 1 x 10⁵ cells/well were transfected with 1 μ g of either pcDNA3.1/V5-His TOPO TA expression vector (His empty) or pcDNA3.1/V5-His-ASC (His-ASC). After 48h, cells were washed twice with PBS before being incubated in conjugation buffer (20 mM HEPES) and then cross-linked for 30 minutes using 5 mM disuccinimidyl suberate (DSS, final concentration, Thermo Fisher Scientific). The cross-linking reactions were terminated by the treatment with a final concentration of 50 mM Tris for 15 minutes. The reactions were resolved under reducing conditions by SDS-PAGE and visualized by Western blot using anti-His and anti-ASC IgG antibody. Western blots were developed using ECL (Thermo Fisher Scientific) on BioMax XAR Film (Sigma).

3.14.8. Western blot analysis of HMGB1 in activated goldfish macrophages

Heat-killed *M. marinum* and *A. salmonicida* was prepared as previously described (380, 392). Primary macrophage cultures were derived from three individual

fish ($n = 3$) and cells from 6 to 8-old cultures were incubated with medium alone (control) or treated with heat-killed *M. marinum* (2×10^6 cfu/mL) or *A. salmonicida* (2×10^6 cfu/mL). Each treatment group consisted of 1×10^6 cells in a final volume of 500 μ L of complete medium. After 12 h, cells were washed three times with PBS and lysed with 50 μ L of radioimmunoprecipitation assay (RIPA) buffer (1 mM sodium vanadate, 1 mM p-nitrophenyl-phosphate, 2 mM phenylmethylsulfonyl fluoride (PMSF), 50 μ g/mL of aprotinin A, 25 μ g/mL of leupeptin, and 25 μ g/mL of pepstatin). Fifty microliters of $2 \times$ Laemmli sample buffer was added and the 20 μ L of protein samples loaded in gel lanes and SDS-PAGE performed at 120 V for 10 minutes followed by 140 V for 50 minutes. Separated proteins were then transferred onto 0.2 μ m nitrocellulose membranes (Bio-Rad) at 135 V for 45 minutes. Membrane were blocked for 1 h at room temperature with 5% skim milk in TBST and probed overnight at 4°C with primary antibody (purified rabbit anti-HMGB1 IgG; 1:3000) and anti-actin-beta (NT) zebrafish polyclonal IgG (1:1000, AnaSpec Inc.). The following day the membranes were washed, and incubated for 1 h with HRP-conjugated goat anti-rabbit IgG antibody (Bio-Rad) for 1 h at room temperature, and developed using ECL (Thermo Scientific) on X-ray film (Eastman Kodak Co.).

3.14.9. Assessment of the ability of rgHMGB1 to induce IL-1 β 1 and TNF α -2 production in macrophages

Primary macrophage cultures were derived from three individual fish ($n = 3$) and cells from 6 and 8-day old cultures were incubated with medium alone (control) or

treated with 5 ng, 20 ng and 100 ng rgHMGB1 for 12 h before lysed with 50 μ L of RIPA buffer. Each treatment group consisted of 1×10^6 cells in the final volume of 500 μ L of complete medium. Twenty microliters of 2 \times Laemmli sample buffer was added and loaded in SDS-PAGE for Western blotting as described in Section 3.14.1. The IL-1 β and TNF α -2 proteins were detected using polyclonal anti-IL-1 β and anti-TNF α -2 IgG antibodies. At the same time, gene expressions for the different experimental groups were determined using quantitative PCR.

3.15. DENSITOMETRIC AND STATISTICAL ANALYSES

The X-ray films developed from ECL were scanned onto a computer in colour using a flat-bed Canoscan 4400F scanner and protein density quantified using the analysis of gels option in image J software (<http://rsbweb.nih.gov/ij>). The involved images being converted into grayscale. Each band of interest was selected using the rectangular selection tool. Subsequently, a profile plot was created for each selected area and a straight line was drawn at the base of each peak. Finally, using the wand tracing tool to select each peak, the size could be expressed as a percentage of the total size of all the measured peaks. The percentage value of the protein of interest was divided by the loading control (β -actin) percentage to get a relative intensity. Significance was determined by Student's *t* test using StatPlus software.

Data from quantitative PCR, reactive oxygen and nitric oxide production assays were analyzed using StatPlus software one-way analysis of variance (ANOVA). Post hoc

tests used were Dunnett's or Tukey's test. Probability level of $P < 0.05$ was considered significant.

Table 3.1. Composition of incomplete NMGFL-15 medium

Reagent	Amount
HEPES	3.5 g
KH ₂ PO ₄	0.344 g
K ₂ HPO ₄	0.285 g
NaOH	0.375 g
NaHCO ₃	0.17 g
10 × Hank's Balanced Salt Solution	40 mL
MEM amino acid solution (50 ×)	12.5 mL
MEM non-essential amino acid solution (100 ×)	12.5 mL
MEM sodium pyruvate solution (100 Mm/100 ×)	12.5 mL
MEM vitamin solution	10 mL
Nucleic acid preparation solution	10 mL
2-Mercaptoethanol solution	3.5 µL
GFL-15 medium*	500 mL
L-glutamine	0.2922 g
Insulin	0.005 g
Milli-Q water	Fill to 1 L

pH to 7.4 and filter sterilized using a 0.2 µm filter. Stored at 4°C.

*GFL-15 medium is made by mixing equal volumes of Leibowitz's L-15 medium with Delbecco's Modified Eagle Medium (DMEM) with phenol red. GFL-15 medium is filtered using a 0.2 µm filter and stored at 4°C.

Table 3.2. Composition of nucleic acid precursor solution

Reagent	Amount
Adenosine	0.67 g
Cytidine	0.061 g
Hypoxanthine	0.034 g
Thymidine	0.061 g
Uridine	0.061 g
Milli-Q water	100 mL
Do not filter, store at 4°C.	

Table 3.3. Composition of 10 X Hanks Balanced Salt Solution (HBSS)

Reagent	Amount
KCl	2 g
KH ₂ PO ₄	0.3 g
NaCl	40 g
Na ₂ HPO ₄ -7H ₂ O	0.45 g
D-glucose	5 g
Phenol Red	0.05 g
Milli-Q water	Up to 500 mL
Filter sterilized with a 0.2 µm filter, store at 4°C.	

Table 3.4. Vector specific primers

Primer name	Vector	Sequence 5'-3'
pJET1.2 Forward	pJET1.2/blunt	C G A C T C A C T A T A G G G A G A G C G G C
pJET1.2 Reverse	pJET1.2/blunt	A A G A A C A T C G A T T T T C C A T G G C A G
SUMO Forward	pET-SUMO	A G A T T C T T G T A C G A C G G T A T T A G
T7 Reverse	pET-SUMO	T A G T T A T T G C T C A G C G G T G G
T7 Promoter	pET-28a, pET-32a	T A A T A C G A C T C A C T A T A G G G
T7 Terminator	pET-28a, pET-32a	G C T A G T T A T T G C T C A G C G G
T7	pcDNA3.1/V5-His, pcDNA3.1/NT-GFP	T A A T A C G A C T C A C T A T A G G G
BGH Reverse	pcDNA3.1/V5-His, pcDNA3.1/NT-GFP	T A G A A G G C A C A G T C G A G G

Table 3.5. RT-PCR and RACE PCR primers

Gene	Primers	Sequence (5' to 3')	Application
NOD1	F*	CACTCAGTTCATCACGTCCTAC	RT-PCR
	R	TGGAGAGTCTCGTGGAGGAACTC	RT-PCR
	R	CAGCGGCGTCTCCTCGCTCTTC	5'-RACE
	F	ATTACGGCGTGAAGCAACTGAGACC	3'-RACE
NOD2	F	TGATAAAGGAGAAGATGCATGCAG	RT-PCR
	R	GTTGTAGCTTAGGCCTTCTGCCAG	RT-PCR
	R	AGAGCTTCGCAGCTTCTTCTGGTA	5'-RACE
	F	CTGCGCTGGCGTATGTGCTAAA	3'-RACE
NLRX1	F	CAAAATGTGGCGATTTGGAAGG	RT-PCR
	R	ACATCAGTACGAAACACTGCCAG	RT-PCR
	R	GGATGATGCTCCAGGATAAGTGGC	5'-RACE
	F	CTGGCATCCCATTCTGAGCGTTAT	3'-RACE
RIP2	F	ACCAGCACATTACCGGTGATCCC	RT-PCR
	R	TGAGACACGCCTCGGTCATCTGG	RT-PCR
	R	ACACGGTCCCGAAGCCGCCTTTACT	5'-RACE
	F	ACGGCGCAGCATGTGTCCGACCTCA	3'-RACE
HMGB1	F	CCTCTTACGCATACTTTGTCCAG	RT-PCR
	R	GGTTAAATGCTTTATAGACAACA	RT-PCR
	R	CGTCGTCATCCTCGTCCTCATCT	5'-RACE
	F	AGGACATTGCTGCCTATCGTTC	3'-RACE

*F = forward; R = reverse

Table 3.6. Quantitative PCR primers for goldfish genes

Gene	Primers	Sequence (5' to 3')	Application
NOD1	F*	CCAGAAGGCAGCTGAAAACC	Real-time PCR
	R	TCTCCTTAAAGGCGCTGAACA	Real-time PCR
NOD2	F	GTTAGAGGATGTGGTGGGTCCAT	Real-time PCR
	R	CCTGCCTCCCCAGAGACAA	Real-time PCR
NLRX1	F	TGGTTCAGTCACCTTCCTCAAGA	Real-time PCR
	R	TGGCTGCACATGCATAGTTTC	Real-time PCR
RIP2	F	GCCACCAATCCCATGCA	Real-time PCR
	R	CTGTGTCGGGTCGAGATCCT	Real-time PCR
NLRP3rel	F	CAGAAGACGCTCTCGTAAGGTACA	Real-time PCR
	R	TCAGCTCCCAGTATGCCAATT	Real-time PCR
ASC	F	GAGCCGCGCATTTCGAA	Real-time PCR
	R	CCGGCGAGATCTATAGAATCTTCA	Real-time PCR
HMGB1	F	CAAAACATCAGCTGAGGATAAGCA	Real-time PCR
	R	AATGTCCTTCTCATACTTCTCCTTAAGC	Real-time PCR
TNF α -2	F	TCATTCCTTACGACGGCATT	Real-time PCR
	R	CAGTCACGTCAGCCTTGCAG	Real-time PCR
IL-1 β 1	F	GCGCTGCTCAACTTCATCTTG	Real-time PCR
	R	GTGACACATTAAGCGGCTTCAC	Real-time PCR
EF-1 α	F	CCGTTGAGATGCACCATGAGT	Real-time PCR
	R	TTGACAGACACGTTCTTCACGTT	Real-time PCR

*F = Forward; R = Reverse

Table 3.7. Recombinant protein expression primers

Gene	Primers	Sequence (5' to 3')	Application		
NOD1	F*	ATGGGCTCTTACAAGAGTGAGGG	pcDNA3.1/NT-GFP expression		
	R	TCAGTGGAAGCGAAGCCG			
NOD2	F	AACTCGAGATGACTGCTCACCAGTTGATCC	pcDNA3.1/NT-GFP expression		
	R	CGGGATCCCGTTGCTCTAGATACTGAAGTAACGTC			
RIP2	F	ATAGAATTCATGGAGCACGCCGGC	pET-32a expression		
	R	ACACTCGAGTCAGAAGAGTCGTGTGTTGTTAAAGG			
	F	GCAATGGAGCACGCCGGCTG		pcDNA3.1/V5-His expression	
	R	GAAGAGTCGTGTGTTGTTAAAGGAGTTGG			
NLRP3 rel	F	GTAGAGCTCCTCACCTTTGACCCTCAGACG	pET-28a expression		
	R	TAGCGGCCGCTTATAAACGGACTGAGCTGTCTGG			
	F	GCCATGGCACAGCAAGACGACATT		pcDNA3.1/V5-His expression	
	R	TAGTGATGCTTGCCTTAAACGGAC			
	F	ATGGCACAGCAAGACGACATT		pcDNA3.1/NT-GFP expression	
	R	TTATAGTGATGCTTGCCTTAAACGG			
	F	AAGGCCTCTGTGACGCCGCCATGGCACAGCAAGACGACATT		pDsRed-Monomer-C expression	
	R	AGAATTCGCAAGCTTTTATAGTGATGCTTGCCTTAAACGG			
	ASC	F		ATGGCGAAATCTATTAAGGATCACC	pET-SUMO expression
		R		TCAGTGACTCTCCAGGTCTTCC	
F		GCCATGGCGAAATCTATTAAGGATCACC	pcDNA3.1/V5-His expression		
R		GTGACTCTCCAGGTCTTCCATC			
F		ATGGCGAAATCTATTAAGGATCACC	pcDNA3.1/NT-GFP expression		
R		TCAGTGACTCTCCAGGTCTTCC			
F		AAGGCCTCTGTGACGCCGCCATGGCGAAATCTATTAAGGATCACC	pDsRed-Monomer-C expression		
R		AGAATTCGCAAGCTTTTCAGTGACTCTCCAGGTCTTCC			

*F = Forward; R = Reverse

Table 3.8. Primers used in transcriptome gene expression validation

Gene	Primers	Sequence (5' to 3')
TLR	F*	AAGCAGAGCGGTTTCGACATT
	R	AAGCAGAGCGGTTTCGACATT
NLRP3-iso1	F	CGGCGGGTTCGATTTCG
	R	GAGTGATGTCACCAGCACAGATC
NLRP3-iso2	F	TGAGGAAGATCTGCAGCATAGTG
	R	CCAGAAGAATGCAGATGAACATTT
NLRP3-iso3	F	TGATGAAAACACACCCGAAAACGT
	R	GCGTGAAGGATTTCCCTCTTC
NLRP3-isoX1	F	GGAAGCCAAACTCTTTCATCTCA
	R	CCAGTACTTGCTCTGATGTCAACA
C type lectin	F	CGTCTATGGGTGGCCATCTG
	R	CTTTCAAGTGCCTGGTATTGTTG
TNAF5	F	CGGCCAACATCTGATGCTAA
	R	TCGCCGTGGGATATGAATCT
IL-1 β 1	F	GCGCTGCTCAACTTCATCTTG
	R	GTGACACATTAAGCGGCTTCAC
IL-1R2	F	TTGGTGCTCGTTTGGTGATC
	R	GTGGACTGAGCTTGCTGGTTT
TGF- β	F	GGCGATCGGGCTCGATAT
	R	CGATCGGACAAGTCCTTGGA
IL-6 M17	F	ATCGCAGCGCATCTTGAGT
	R	TCTTCATGTGCGGCAGAAAC
Fbox	F	TCACGGACCGCACACTGA
	R	GGCTGGGCGATGTCAAGT
GCSF	F	GGGCTGGGCTCTGTCTCTAA
	R	GATGCGCACTGACGTCTCA
TCR	F	CCCGATCATGGAGCAGCTAT
	R	GTGGATGTTTGGGATGTAGTTGAC
CD2	F	AAGGCACCCGGAAGAATGA
	R	TTTGTGGCTTGATGTTCTCGTT
CD82	F	CCGAGAATGTGGCGATAAACA
	R	TGGATTCATTTGTGCAGGAACA
CXCF1	F	TGTATGCTTTGCTGGCTTTCA
	R	TGGCACTCACAGGTCTTTGGA
CC7-1	F	TGGAAGCAGTGCCAGTCA
	R	GGCTGGTTTTTCCCATGGTT
MycB	F	CCAGGACGTCGGA CTCTGA
	R	GCCGCTCGAGAACGTTATG
CREB	F	AAGAACGTCCTCAACCACATGA
	R	GAGCCACTTGGCAGGATTTG
Fibrinogen	F	GAACGTAATGTGAGGCCAACTG

	R	TGGTGGACTGGGTCAACTCTT
IFITM1	F	CCCAATGGCACGGTCTTATG
	R	TGGCGGCAGCAATGTTT
GCSFR	F	GGGCTGGGCTCTGTCTCTAA
	R	GATGCGCACTGACGTCTCA
STAT1	F	CGTTGCCTTTGGTCGCTACT
	R	TGGTCTTCATTTATCCCTCCTACAT
CSF3	F	CAGGCAGGATTTGACACATCA
	R	TGACCAGATCATGCGAATGC
EF-1 α	F	CCGTTGAGATGCACCATGAGT
	R	TTGACAGACACGTTCTTCACGTT

*F = Forward; R = Reverse

Table 3.9. Recombinant proteins

Protein	Induction time	Lysis conditions
rgRIP2	3.5 h	denaturing
rgCT-NLRP3rel	3.5 h	denaturing
rgASC	3.5 h	denaturing
rgHMGB1	3 h	denaturing

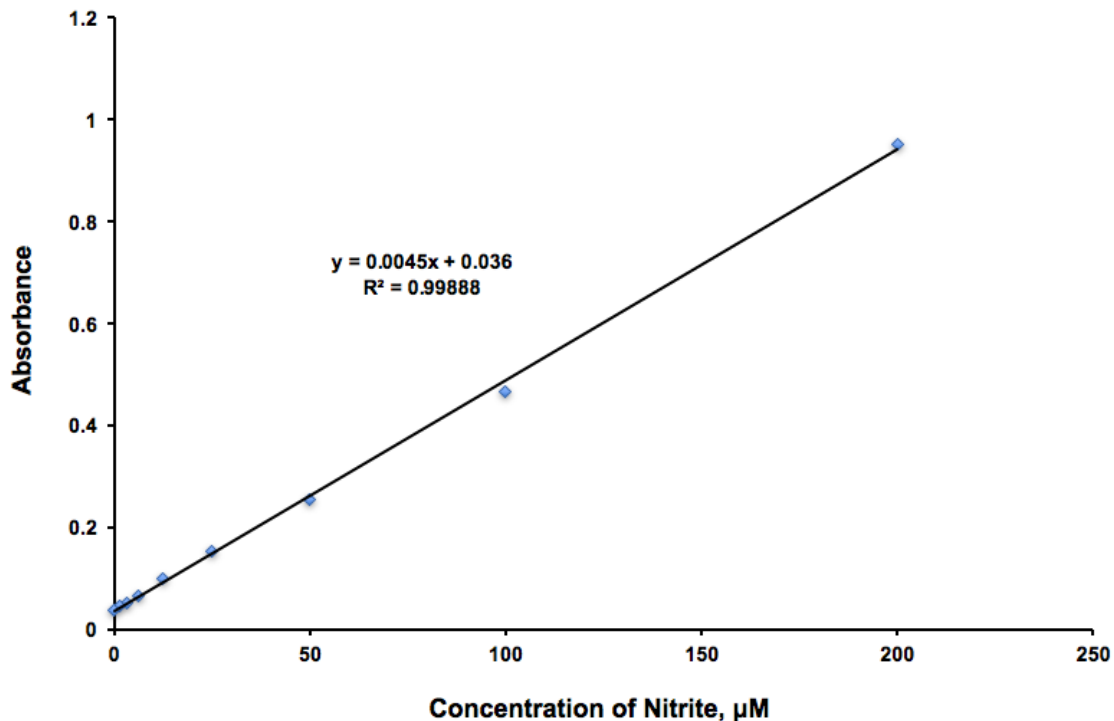


Figure 3.1. The nitrite standard curve of nitrite oxide assay.

Seventy five microliters of sodium nitrite diluted in PBS with different concentration (0, 1.56, 3.13, 6.25, 12.5, 25, 50, 100, 150, 200 and 250 μM) was seeded into 96-well plates in triplicates. 100 μl of 1% (w/v) sulphanilamide in 2.5% (v/v) phosphoric acid with 100 μl of 0.1% (w/v) N-naphthyl-ethylenediamine in 2.5% (v/v) phosphoric acid were subsequently added. The absorbance was measured at 540 nm for the standard curve generation.

CHAPTER IV: CHARACTERIZATION OF THREE NOD-LIKE RECEPTORS AND THEIR ROLE IN ANTIMICROBIAL RESPONSES OF GOLDFISH (*Carassius auratus* L.) MACROPHAGES TO *Aeromonas salmonicida* and *Mycobacterium marinum*¹

4.1. INTRODUCTION

As described in Chapter II, the conserved microbial structures known as PAMPs are recognized by germ line-encoded PRRs, which exist as four major classes, including the TLRs, NLRs, RLRs and CLRs. The TLRs are the best known group of the innate immune receptors whose function has been reasonably well characterized in different infectious diseases. TLRs play a fundamental role in innate immune responses by sensing the molecular signatures of microbial pathogens that recognize structural components shared by many bacteria, viruses and fungi (4). Structurally, TLRs are type I membrane proteins characterized by an extracellular domain composed of leucine rich repeats (LRR) that are responsible for recognition of PAMPs, and a cytoplasmic domain known as the TIR domain homologous to the cytoplasmic region of the IL-1 receptor, which is required for the activation of defense responses against an invading organism (465). To date, 10 members of TLRs have been identified in humans, and 13 in mice. A number of studies

¹ A version of this chapter has been published: Xie, J., Hodgkinson, J. W., Katzenback, B. A., Kovacevic, N., Belosevic, M. 2013. Characterization of three NOD-like receptors and their role in antimicrobial responses of goldfish (*Carassius auratus* L.) macrophages to *Aeromonas salmonicida* and *Mycobacterium marinum*. Developmental and Comparative Immunology 39: 180-187.

have identified their respective ligands that include LPS (TLR4), lipoproteins (TLR2), flagellin (TLR5), non-methylated CpG motifs of DNA (TLR9), double-stranded RNA (TLR3), and single-stranded RNA (TLR7 and TLR8) (4, 466). After recognition of microbial pathogens, TLRs trigger intracellular signaling pathways that result in the induction of Type I interferons (IFN) and chemokines, as well as other signaling pathways that play a role in the generation of antimicrobial responses against different pathogens (467). In contrast, NLRs and RLRs are intracellular cytosolic sensors (4, 465), which are not very well characterized, especially in lower vertebrates.

The NLRs, appear to be primarily involved in bacterial recognition. To date, several NOD-like receptors have been identified in different bony fishes including olive flounder (55), trout (48), rohu (50, 51), grass carp (47) and catfish (28). The NOD1 and NOD2 in these fish were differentially expressed in all the tissues with notable differences in the expression of these receptors in different fish. For example, NOD1 was highly expressed in the spleen of rohu (50) and kidney of olive flounder (55), while the highest mRNA levels of NOD2 were detected in muscle (51) and liver (48) of trout. The injection of rohu with LPS, Poly I:C, *Aeromonas hydrophila*, *Edwardsiella tarda* or *Shigella flexneri* resulted in the up-regulation of NOD1 expression (50). Similarly, the expression of NOD2 was enhanced in response to PGN, LTA, Poly I:C, *A. hydrophila* and *E. tarda* (51). The NLRs appear to play an important role in viral infections of fish (47) which is perhaps not surprising since NOD1, NOD2 and NLRX1 of grass carp shared high identity based on the phylogenetic analysis (28, 47, 48, 50, 51, 55, 115). To date, relatively few studies have identified and characterized the ligands of NLRs in bony fish.

In this chapter, I report on the cloning and characterization of goldfish NOD1, NOD2 and NLRX1. Comprehensive Q-PCR analysis revealed that these three NLRs were differentially expressed in tissues and different immune cell populations. Treatment of macrophages with different chemical stimuli or exposure to *A. salmonicida* or *M. marinum* increased the expression of these NLRs.

4.2. RESULTS

4.2.1. Sequence analysis of goldfish NOD1, NOD2 and NLRX1

The complete open reading frames (ORFs) and the untranslated regions of the goldfish NOD1, NOD2 and NLRX1 cDNA transcripts were obtained. Cloned goldfish NOD1 (gfNOD1), gfNOD2 and gfNLRX1 transcripts were 3234 bp, 3129 bp and 4900 bp with their ORFs encoding 937aa, 982aa and 1008aa, respectively (Figs. 4.1 to 4.3).

Conserved domains of NLRs predicted by Pfam showed that NOD1 has one CARD domain (12-86aa), one NACHT domain (187-356aa) and six LRRs (739-766aa, 767-794aa, 795-822aa, 823-850aa, 851-878aa and 879-906aa) (Figs. 4.1 and 4.4). The NOD2 has two CARD domains (6-82aa and 115-185aa), one NACHT domain (272-440aa) and LRR 6 (730-758aa, 759-786aa, 840-867aa, 868-895aa, 896-923aa and 924-951aa) (Figs. 4.2 and 4.4). NLRX1 has one NACHT domain (180-339aa) and four Leucine Rich repeats (LRR 4) (746-773aa, 800-827aa, 828-855aa and 856-883aa) but no CARD domains (Figs. 4.3 and 4.4). The nucleotide sequences of gfNOD1, gfNOD2 and gfNLRX1 have been submitted to the Genbank nucleotide database under accession no. JX965184, JX965185 and JX965186, respectively.

4.2.2. Phylogenetic analysis and classification of gfNOD1, gfNOD2 and gfNLRX1 genes

To further confirm the identities of the three NOD-like receptors of the goldfish, an unrooted phylogenetic tree was constructed using the gfNOD1, gfNOD2 and gfNLRX1 and all known NLR molecules from fish and select NLRs from higher vertebrates (Fig. 4.5).

The inferred phylogeny of the three goldfish NLRs showed two distinct clusters, the gfNOD1 & gfNOD2 and the gfNLRX1. For all the NOD1, NOD2 and NLRX1, goldfish branched closely to the fish groups, suggesting that NOD1, NOD2 and NLRX1 are highly conserved in bony fish (Fig. 4.5).

4.2.3. Analysis of NOD1, NOD2 and NLRX1 expression in goldfish tissues

Quantitative expression analysis of the goldfish NOD1, NOD2 and NLRX1 in the tissues of normal fish was performed using the liver as a reference tissue. The overall expression patterns of all the three NLRs were relatively similar with highest mRNA levels observed in the spleen, heart and kidney, and lower mRNA levels measured in liver, brain and gill (Fig. 4.6).

4.2.4. Analysis of NOD1, NOD2 and NLRX1 expression in non-stimulated goldfish immune cell populations

The expression of goldfish NLRs was assessed in different goldfish immune cell populations. The cell populations examined included kidney-derived neutrophils, splenocytes, monocytes and mature macrophages. The expression of NOD1 and NOD2

mRNA levels were highest in neutrophils and lowest in splenocytes. In contrast, NLRX1 was highly expressed in splenocytes (Fig. 4.7).

4.2.5. Analysis of goldfish NLR expression in macrophages treated with LPS, Poly I:C, MDP and PGN

To investigate the expression of the gfNOD1, gfNOD2 and gfNLRX1 to their potential ligands, mRNA levels of gfNOD1, gfNOD2 and gfNLRX1 were quantified in goldfish macrophages after treatment with either PBS, LPS, Poly I:C, MDP and PGN at different time points: 3h, 6h, 12h and 24h. As shown in Fig. 4.8, the expressions of the three receptors were up-regulated after LPS and PGN treatment. The mRNA levels of both gfNOD1 and gfNOD2 were significantly up-regulated after treatment with Poly I:C but not those of gfNLRX1. However, substantial increase at the mRNA levels were observed for gfNOD2 and gfNLRX1 in response to MDP at 6h and 12h for gfNOD2, and at 24h for gfNLRX1 (Fig. 4.8).

4.2.6. Analysis of goldfish NOD-like receptors expression in macrophages treated with heat-killed *A. salmonicida* and *M. marinum*

To examine whether gfNOD1, gfNOD2 and gfNLRX1 were modulated in response to bacterial infection, expressions of the gfNOD1, gfNOD2 and gfNLRX1 were determined in goldfish macrophages at 6h and 12h after exposure to 2×10^6 cfu/mL of heat-killed *A. salmonicida*, or heat-killed or viable *M. marinum*. The mRNA levels of gfNOD1, gfNOD2 and gfNLRX1 significantly increased after exposure of macrophages to

heat-killed *A. salmonicida* (Fig. 4.9). The mRNA levels of gfNOD1 and gfNOD2 were up-regulated at 6h and 12h and that of NLRX1 at 12h after exposure to *A. salmonicida* (Fig. 4.9). Notably, there was a significant difference observed at 6h and 12h treatment with heat-killed *A. salmonicida* for all of these three receptors (Fig. 4.9).

After exposure of macrophages to either heat-killed or viable *M. marinum*, significant up-regulation of gfNOD2 and gfNLRX1 mRNA levels were observed at 6h and 12h. However, there were no significant changes in the expression of gfNOD1 after exposure of macrophages to either heat-killed or viable *M. marinum* treatment (Fig. 4.9). There were no differences in the mRNA levels of gfNOD2 and gfNLRX1 when macrophages were treated with heat-killed or viable *M. marinum*.

4.3. DISCUSSION

The germ line-encoded innate immune receptors (PRRs), recognize microbial structures known as PAMPs. The four major classes of PRRs, including the TLRs, the NLRs, the RLRs and the CLRs. The NLRs, appear to be primarily involved in bacterial recognition.

In this chapter, I reported on the characterization and expression analysis of the NLRs in tissues and macrophages treated with various ligands and those exposed to heat-killed bacteria *A. salmonicida* and *M. marinum*. Structurally, the goldfish NOD-like receptors possess all of the characteristic domains of the NLR family (468). NOD1 and NOD2 recognize their indirect and direct ligands by the LRRs and then recruit RICK through CARD interactions (45, 469). In humans, both NOD1 and NOD2 utilize RICK as a downstream mediator of NF- κ B activation. Unlike NOD1, NOD 2 has two CARD domains

in the N terminus, and both are required for association with RICK and NF- κ B activation in mammals (45). Unlike mammals, but similar to that reported for catfish (28), goldfish NLRX1 has a NACHT domain and C-terminal LRR domains but no CARD domains. Moreover, all of these three NOD-like receptors shared high identity with their counterparts in teleost fish (28).

NOD1 and NOD2 are widely distributed in various mammalian tissues (467, 470) and in fish (28, 47–51, 55). Similar to other reports on teleost NLRs, goldfish NOD1 and NOD2 mRNA levels were the highest in the spleen, suggesting that NOD1 and NOD2 are the important intracellular cytosolic sensors for the initiation of innate immune responses against infectious agents (47, 50, 51). Furthermore, goldfish NOD1 and NOD2 expression in different immune cell populations, and in particular neutrophils, was similar to what has been observed for other teleosts (48–51, 55). My results confirm the findings of Sha and co-workers (49), in that the NLRX1 was broadly expressed in teleost tissues. However, gfNLRX1 mRNA levels were the highest in the spleen of goldfish, whereas NLRX1 expression was reported to be the highest in the muscle of catfish (471).

NOD1 and NOD2 sense bacterial molecules produced during the synthesis or degradation of PGN. NOD1 senses the dipeptide γ -D-glutamyl-meso-diaminopimelic acid (iE-DAP), a naturally occurring PGN degradation product (68, 77), that is produced by most Gram-negative and certain Gram-positive bacteria (472), while NOD2 recognizes muramyl dipeptide (MDP) produced by all bacteria (69, 77). Bacterial lipopolysaccharide (LPS) has been shown to induce the NOD1 and NOD2 gene expression in immune, epithelial and endothelial cells (473–475). Enhanced NOD1 and NOD2 signaling by Poly

I:C has also been reported in mice (476). I used different immuostimulants to assess whether they induced the expression of NLRs of goldfish macrophages. My results showed that the induction of NOD1, NOD2 and NLRX1 genes in goldfish was conserved in that LPS and PGN induced an increased expression of NOD1 and NOD2; This is consistent to what has been reported by others (48, 477). Interestingly, I observed that gfNLRX1 (like NOD2) expression was up-regulated by MDP and also by PGN (like NOD1 and NOD2), suggesting that NLRX1 may also participate in fish defense against bacterial infections. In contrast, NLRX1 expression was not induced by Poly I:C, which is different from human NLRX1 (61).

When the HEK cells were transfected with either NOD1 or NOD2 and stimulated with *M. tuberculosis* cell wall preparations, there was a dose-dependent increase in the mRNA levels of both genes, especially NOD2 (77). Brooks and colleagues (478), found that NOD2 plays a role in controlling the growth of *M. tuberculosis* in human macrophages as well as in regulating the nature of inflammatory response. Moreover, Coulombe and co-workers (83) reported that N-glycolyl MDP has a greater NOD2-stimulating activity than N-acetyl MDP. My observations support these findings because goldfish PKM treated with heat-killed *M. marinum* significantly increased the expression of gfNOD2, suggesting that NOD2 may play a pivotal role in sensing of mycobacteria in fish, as well as in mammals. In contrast, gfNOD1 was not significantly up-regulated after exposure of macrophages to mycobacteria. The goldfish NLR expression after exposure to *A. salmonicida* was similar to that reported for tissues of catfish exposed to *E. tarda*, *A. hydrophila*, *Streptococcus iniae* and catfish hemorrhage reovirus (CCRV) (471).

In summary, I cloned and characterized the gfNOD1, gfNOD2 and gfNLRX1 in goldfish and analyzed their expression in response to different ligands and *A. salmonicida* and *M. marinum*, and demonstrated that these three NOD-like receptors are generally conserved in teleost fish.

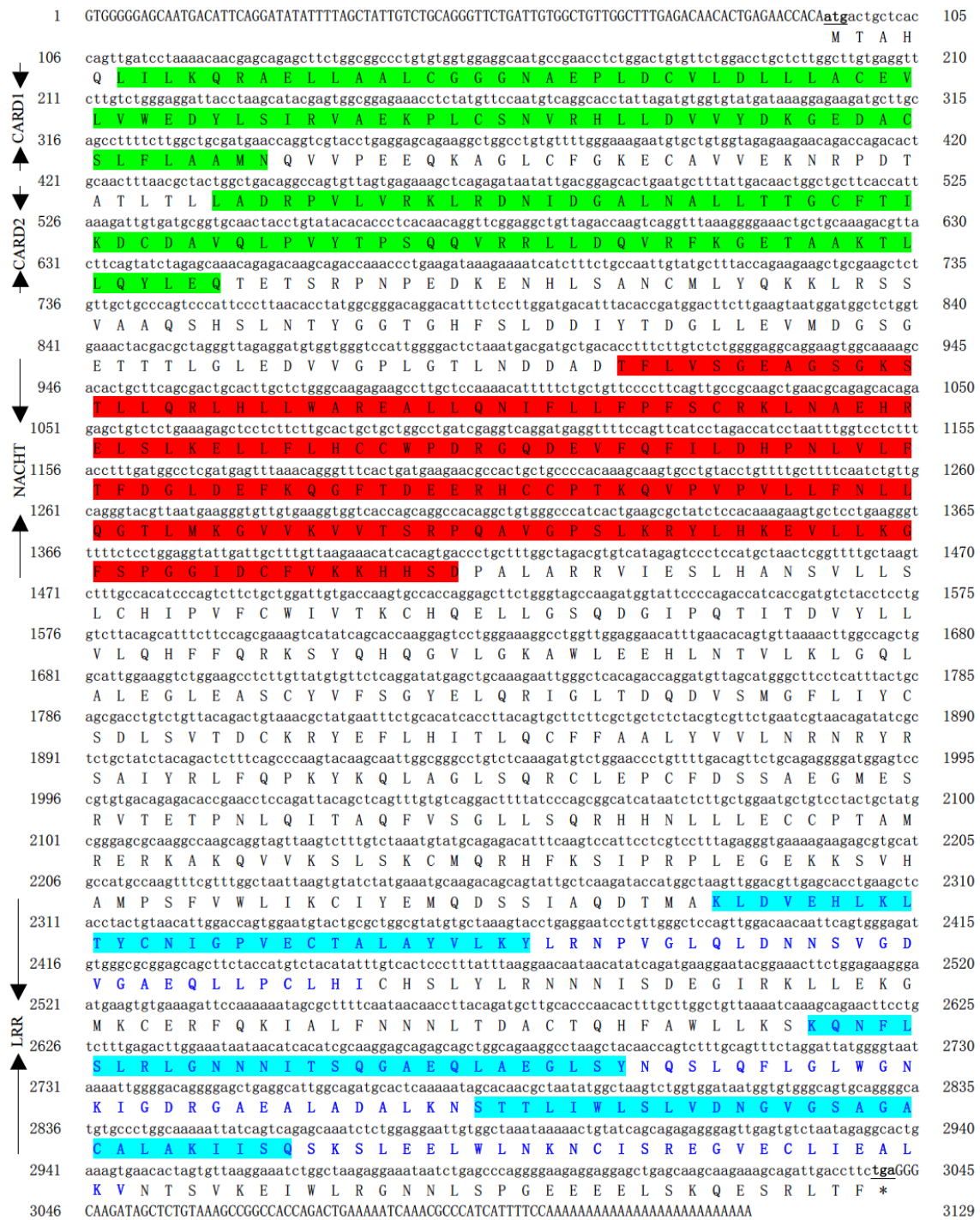


Figure 4.2. Goldfish NOD2 full-length cDNA showing ORF, untranslated regions (UTR) and various domains.

UTR at 5' and 3' were shown in upper case and ORF in lower case, start and stop codon were underlined. The CARDs were marked with green color. The NACHT domains were shown with the dark red color. Alternative LRR domains were indicated with the turquoise and blue & bold words.

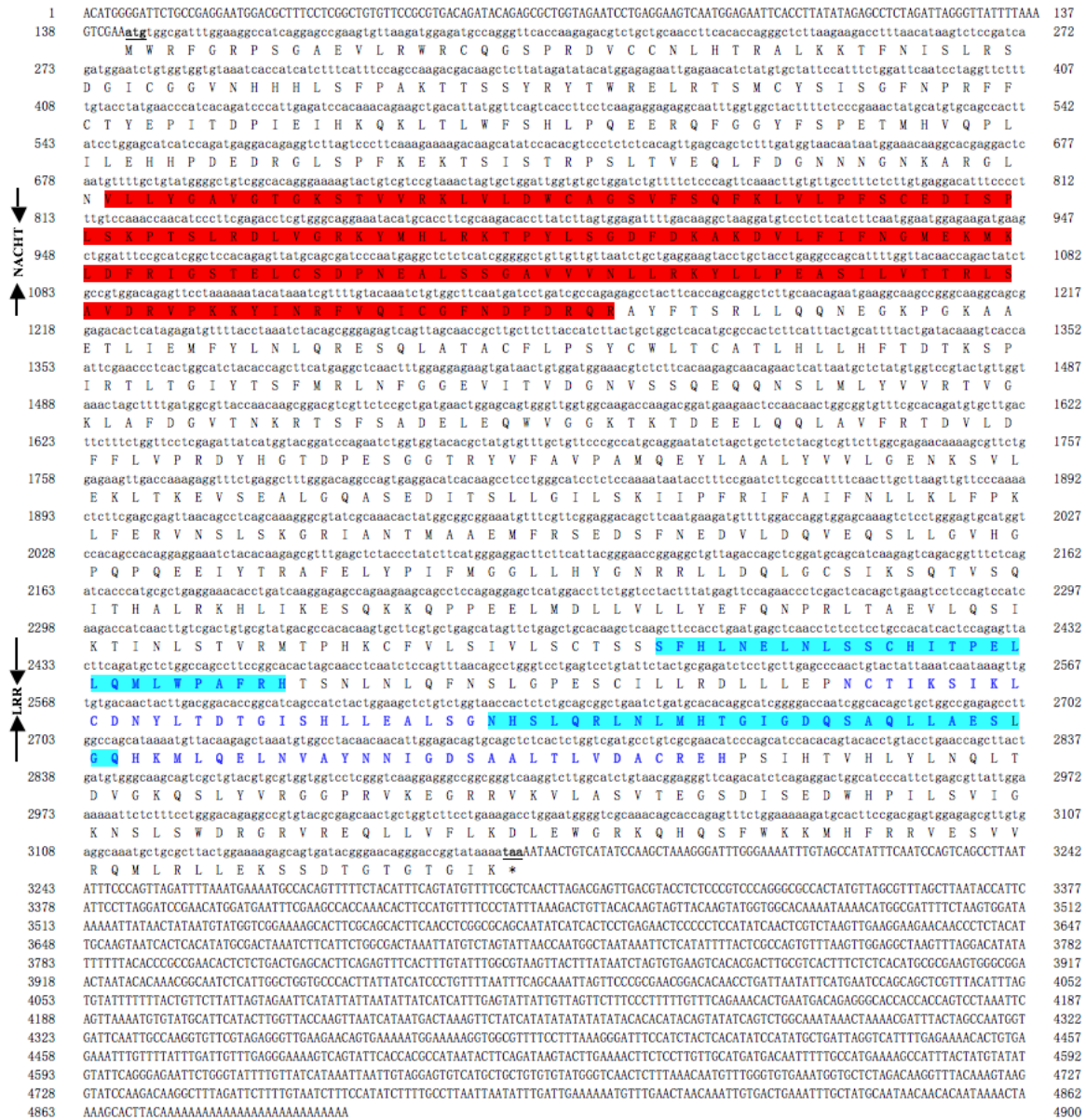


Figure 4.3. Goldfish NLRX1 full-length cDNA showing ORF, untranslated regions (UTR) and various domains.

UTR at 5' and 3' were shown in upper case and ORF in lower case, start and stop codon were underlined. The NACTH domains were shown with the dark red color. Alternative LRR domains were indicated with the turquoise color and blue & bold words.

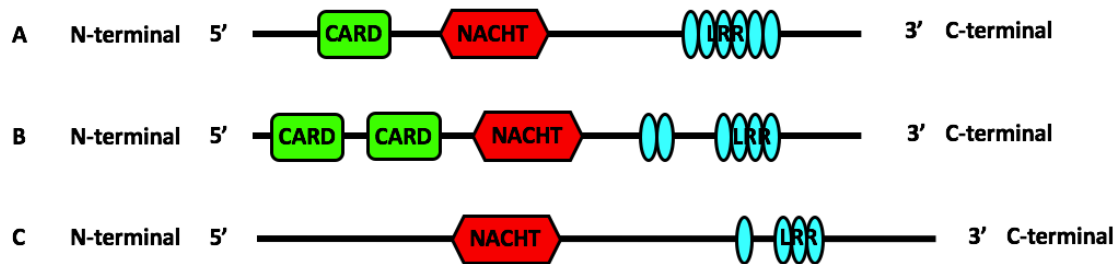


Figure 4.4. Schematic representation of domain organizations of gfNOD1 (A), gfNOD2 (B) and gfNLRX1 (C).

The CARDS are marked in green color, the NACHT domains are indicated in dark red and LRR domains are marked in turquoise color.

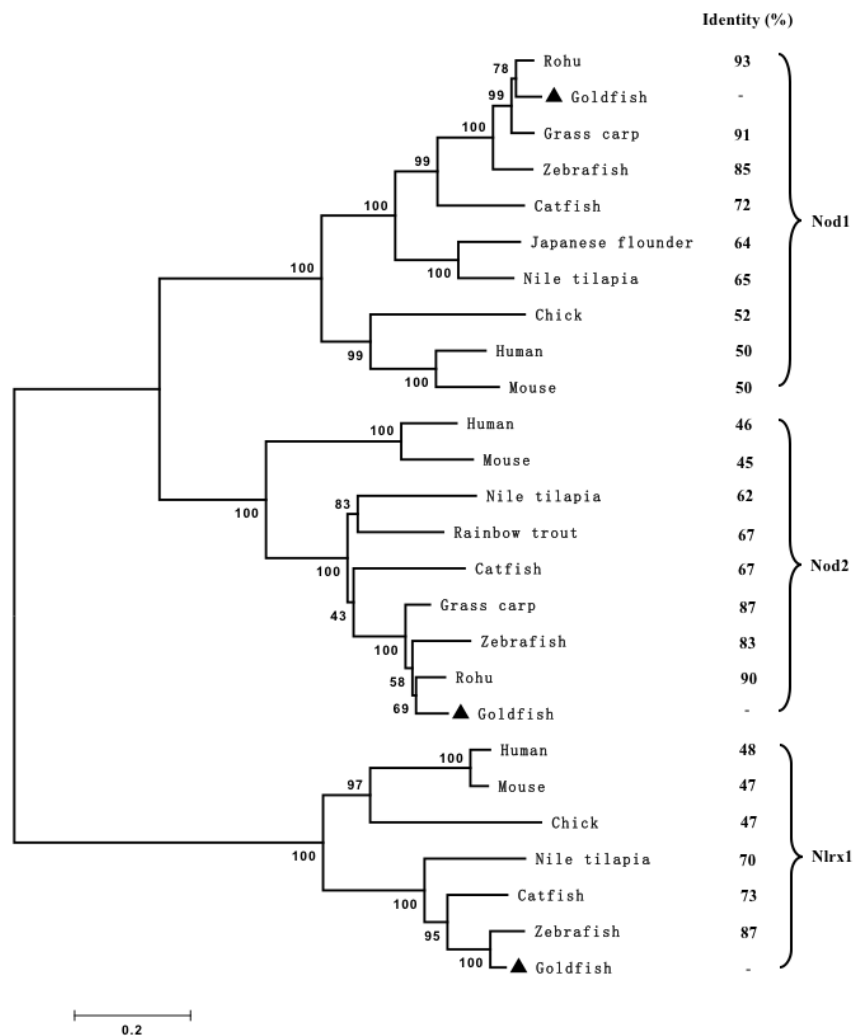


Figure 4.5. Phylogenetic analysis of goldfish NOD1, NOD2 and NLRX1.

NOD1, NOD2 and NLRX1 amino acid sequences were aligned by using CLUSTAL-W program with DNA-STAR and unrooted phylogenetic tree was generated using the neighbor-joining method of the MEGA 4 program. The tree was bootstrapped 10,000 times. The full length of NOD1, NOD2 and NLRX1 amino acids sequences used were: NOD1: Rohu AFE61355.1, Grass carp ACX71752.1, Zebrafish XP_002665106.2, Catfish NP_001186996.1, Japanese flounder AFD29894.1, Nile tilapia XP_003446247.1, Chick XP_418777.2, Human AAD28350.1, Mouse NP_766317.1. NOD2: Human NP_071445.1, Mouse AAN52477.1, Nile tilapia XP_003437591.1, Rainbow trout NP_001188484.1, Catfish ACM45225.1, Grass carp ACX71753.1, Zebrafish XP_697924.3, Rohu AEG89706.1. NLRX1: Human AAI10891.1, Mouse NP_848507.2, Chick XP_003642640.1, Nile tilapia XP_003460219.1, Catfish NP_001186993.1, Zebrafish XP_685481.4.

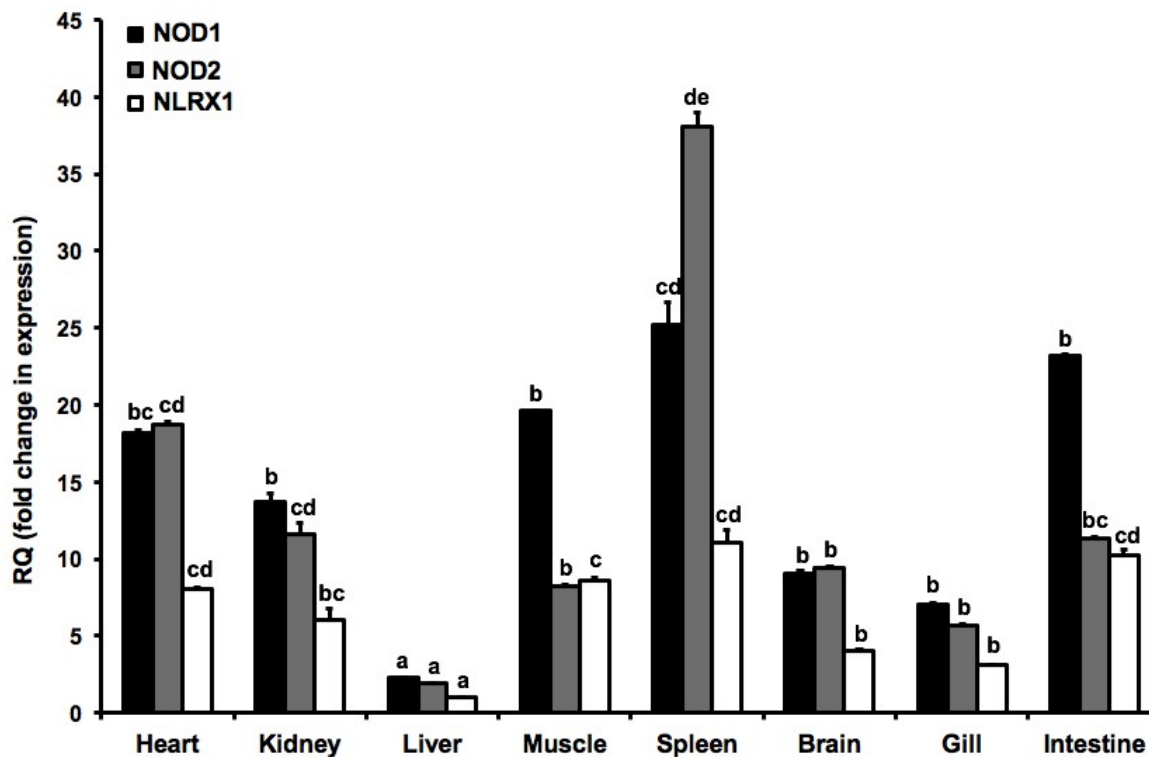


Figure 4.6. Expression analysis of NOD1, NOD2 and NLRX1 in tissues obtained from normal goldfish.

Analysis of the relative tissue expression was done using tissues from five fish ($n = 5$). The expression of NOD1, NOD2 and NLRX1 was relative to endogenous control gene, EF-1 α . All results were normalized to lowest expression measured (liver). Statistical analysis was performed using one-way ANOVA and differences between groups using Dunnett's post hoc test. Different letters above each bar denote significantly different ($P < 0.05$), and the same letter indicates no statistical differences between groups (H=Heart, K=Kidney, L=Liver, M=Muscle, S=Spleen, B=Brain, G=Gill, I=Intestine).

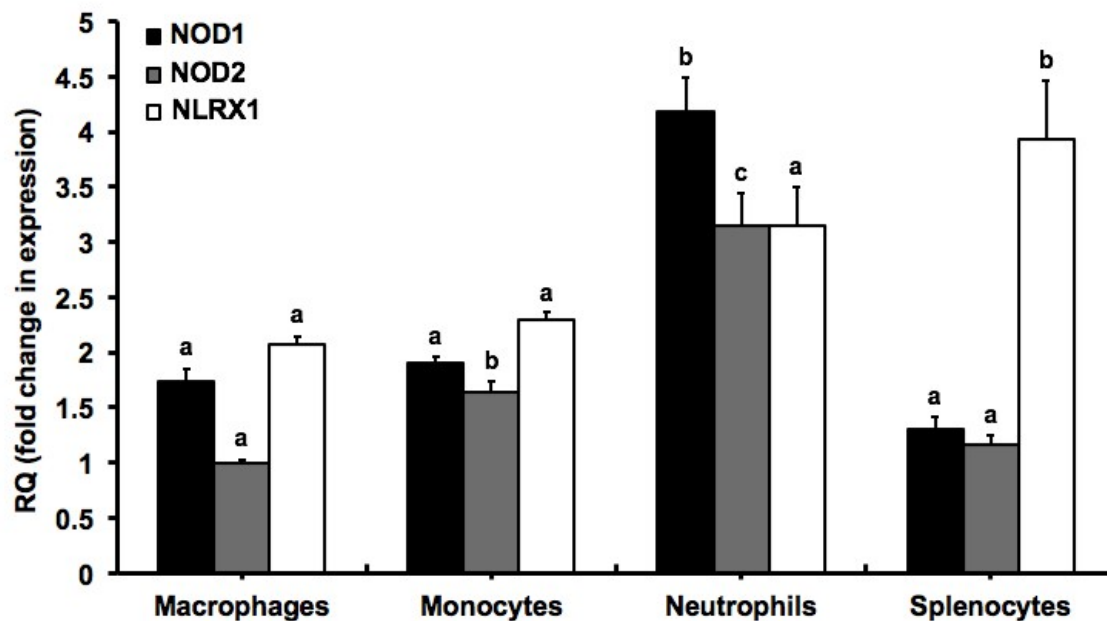
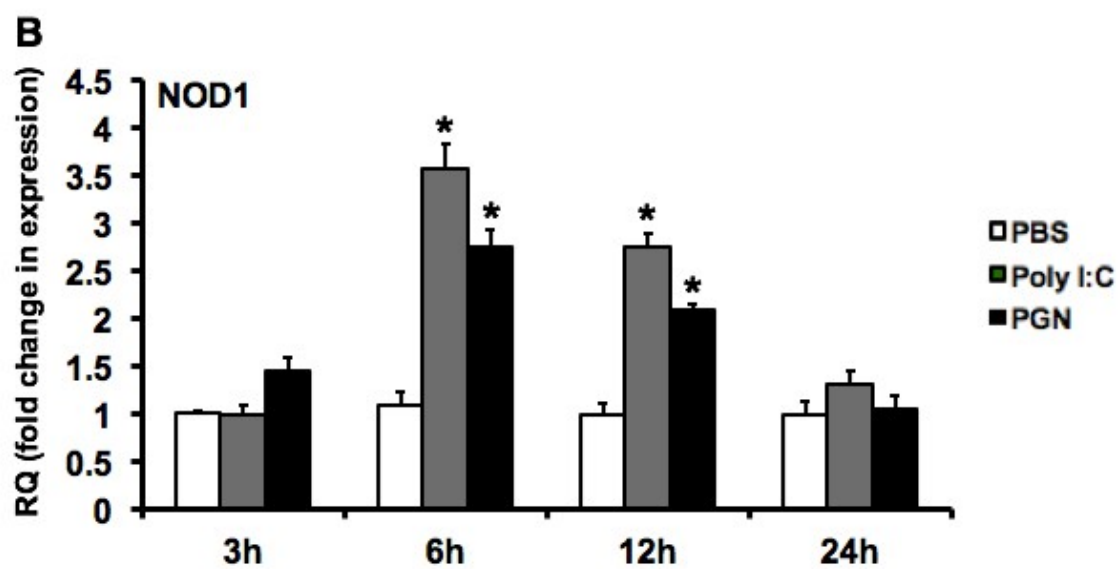
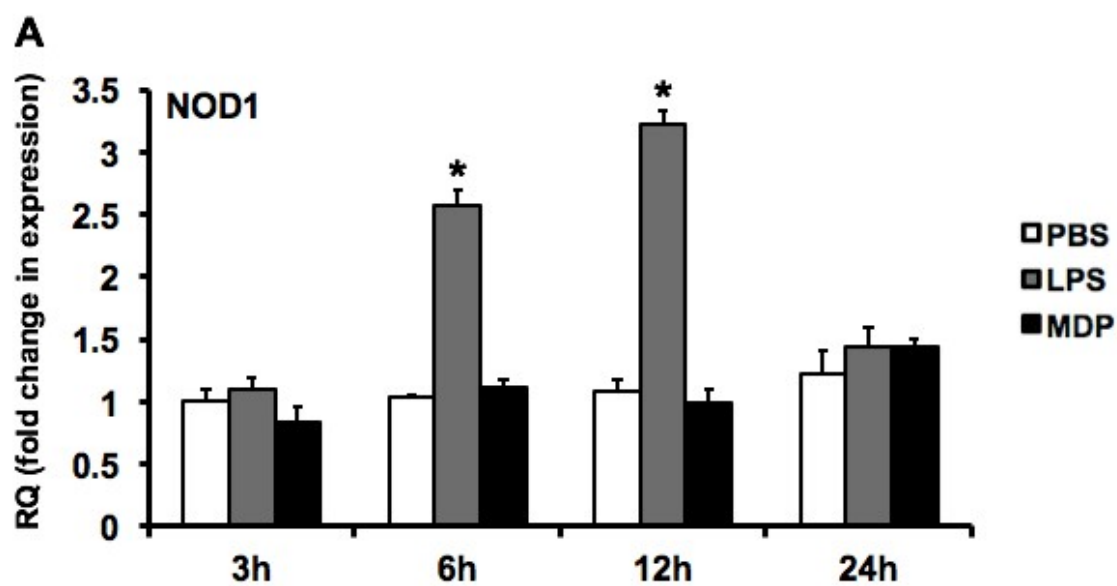
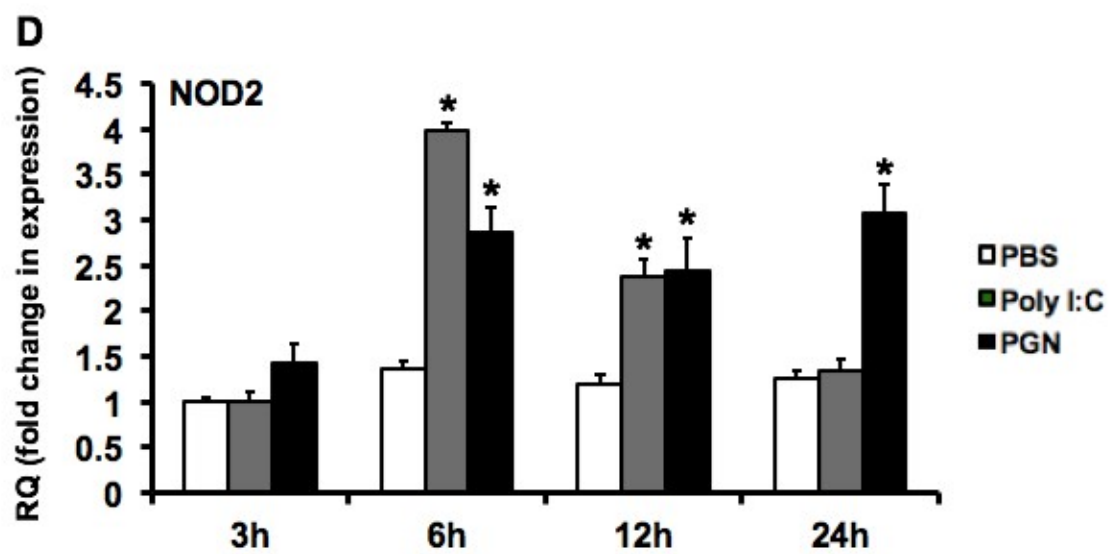
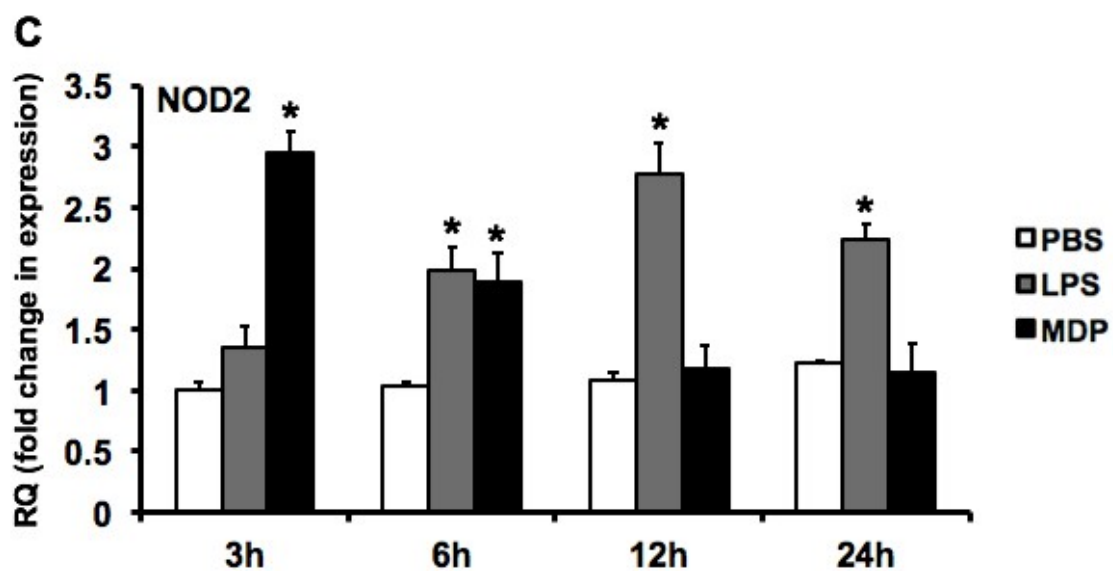


Figure 4.7. Expression analyses of goldfish NOD1, NOD2 and NLRX1 in different immune cell populations obtained from normal goldfish.

Cell cultures were established from four fish ($n = 4$) and the expression normalized against to the lowest expression in cells (macrophages). The expression of goldfish NOD1, NOD2 and NLRX1 was relative to endogenous control gene, elongation factor-1 alpha (EF-1 α). Statistical analysis was done using one-way ANOVA and differences between groups using Dunnett's post hoc test.





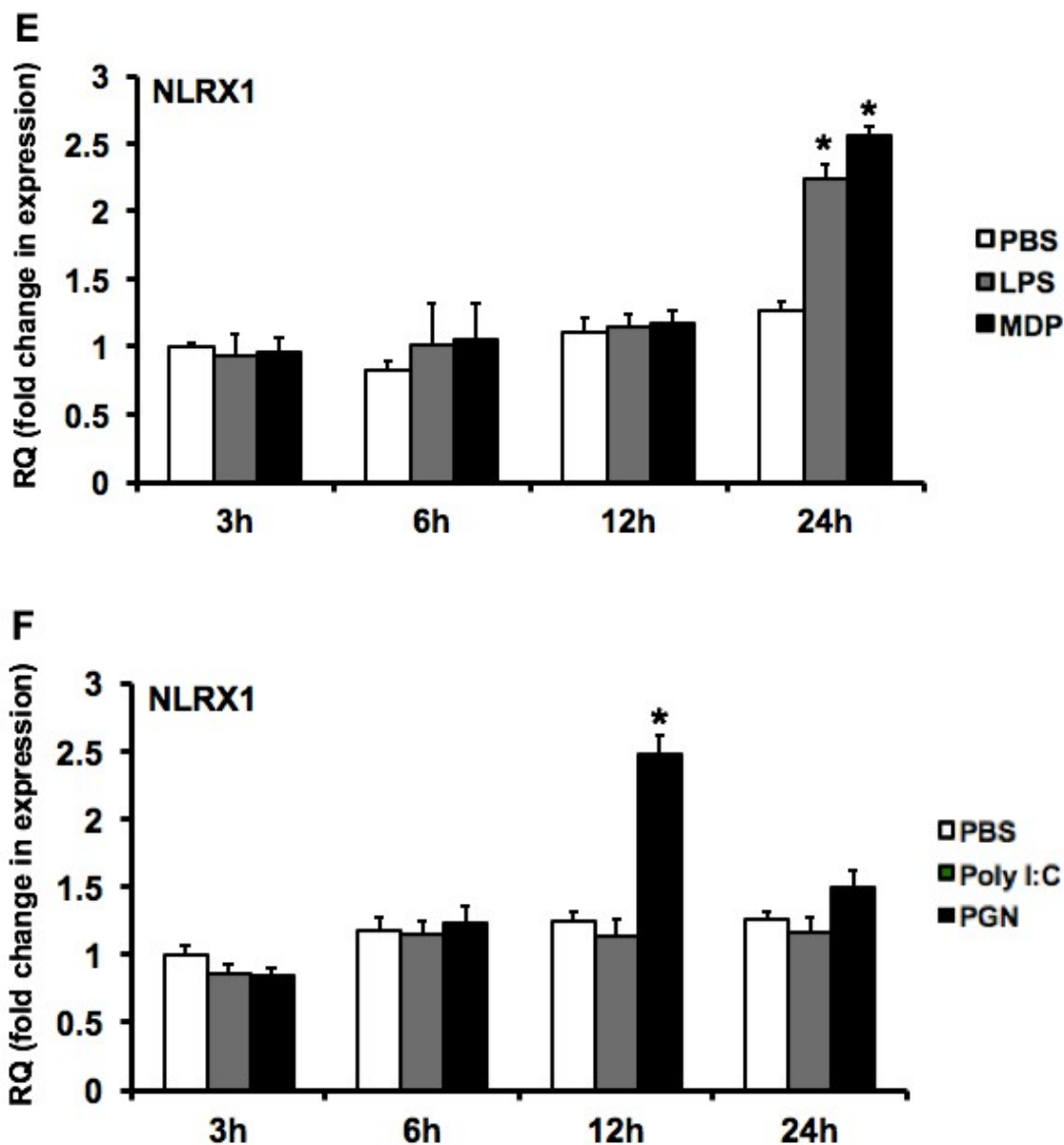
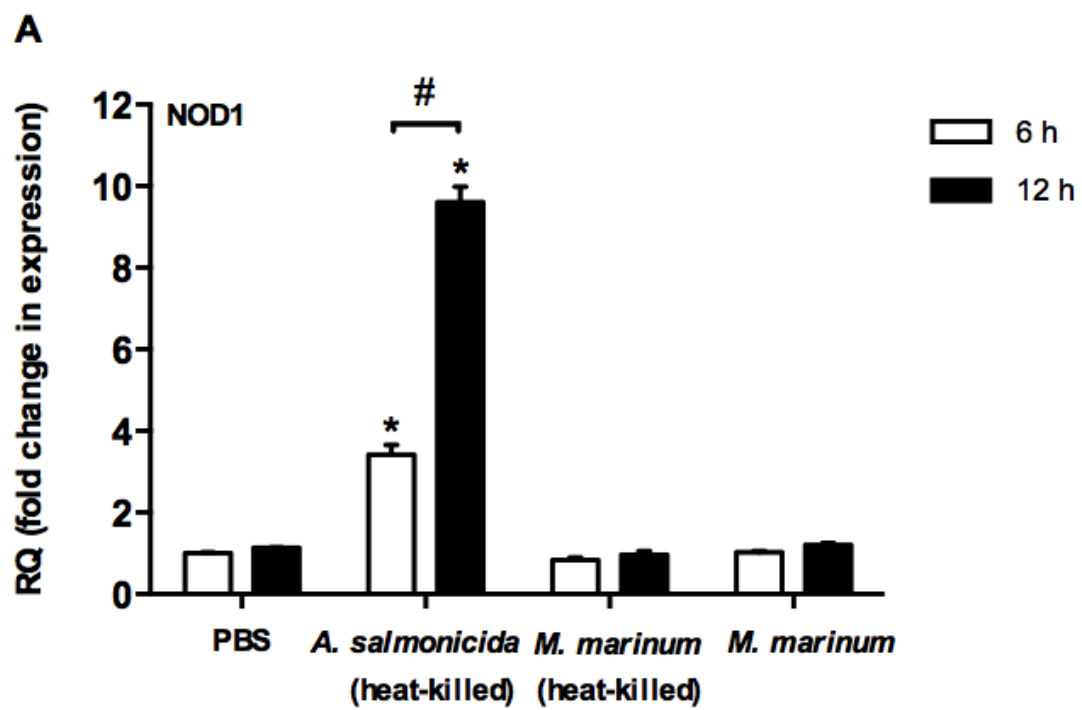
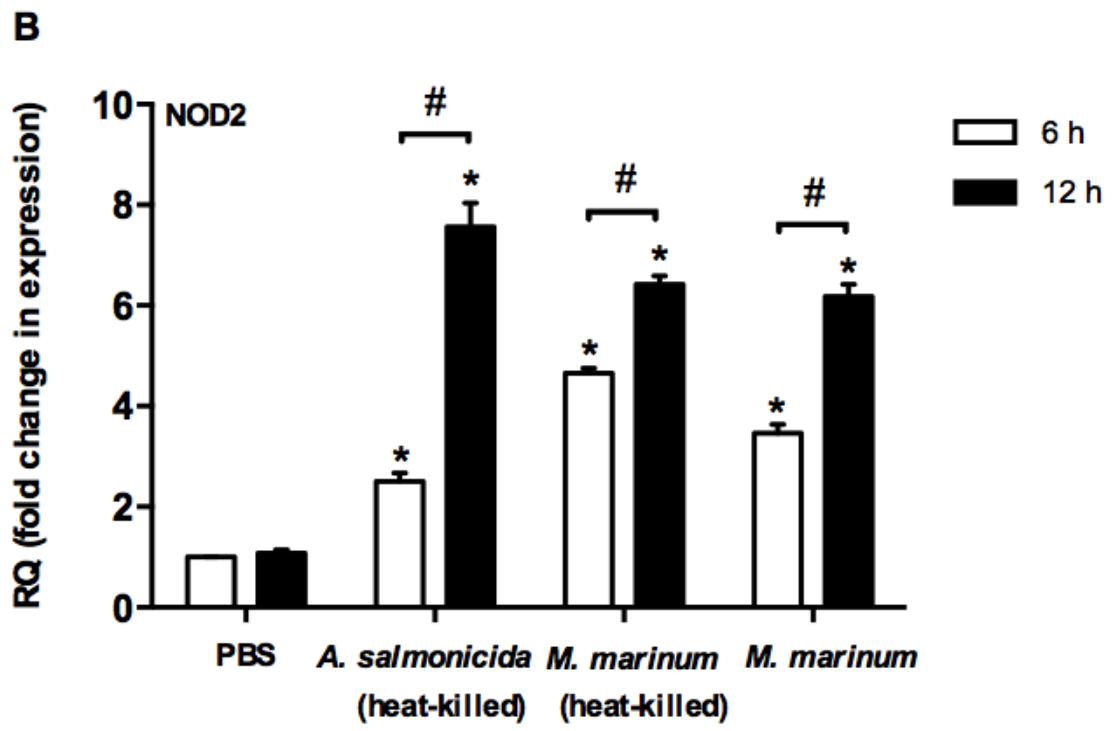


Figure 4.8. Time-dependent expression analysis of goldfish NOD1 (A and B), NOD2 (C and D) and NLRX1 (E and F) in macrophages treated with either PBS, Poly I:C or PGN (A, C and E), or either PBS, LPS or MDP (B, D and F).

The expression of goldfish NOD1, NOD2 and NLRX1 was relative to the endogenous control gene, elongation factor-1 alpha (EF-1 α). The expression values were normalized against those observed for NOD1, NOD2 and NLRX1 at the 3h time point of the PBS-treated control. The results are mean \pm SEM of primary macrophage cultures established from four individual fish ($n = 4$). (*) denotes significantly different ($P < 0.05$) from the PBS-treated control.





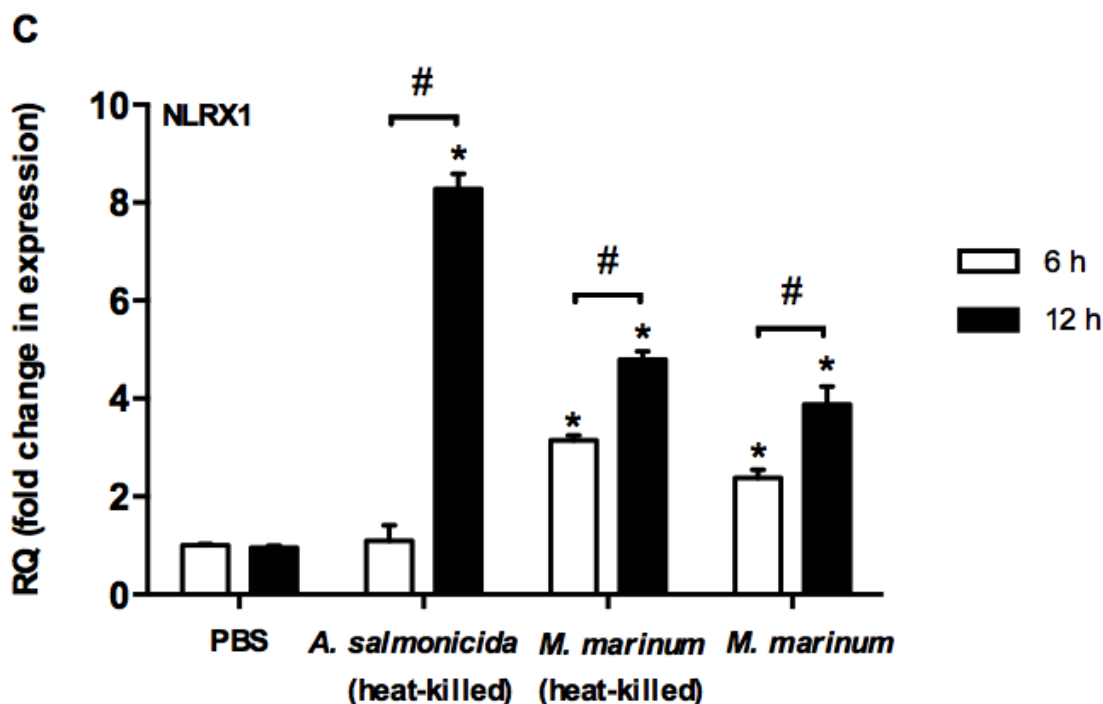


Figure 4.9. Time-dependent modulation of gfNOD1 (A), gfNOD2 (B) and gfNLRX1 (C) expression in macrophages treated with heat-killed *A. salmonicida* or heat-killed or viable *M. marinum*.

The expression of goldfish NOD1, NOD2 and NLRX1 was examined relative to the endogenous control gene, elongation factor 1 alpha (EF-1 α). The expression values were normalized against those observed for NOD1, NOD2 and NLRX1 at the 6h time point of the PBS-treated control. The results are mean \pm SEM of primary macrophage cultures established from four individual fish ($n = 4$). (*) denotes significantly different ($P < 0.05$) from the PBS-treated control and Tukey's post-hoc analysis. The pound sign (#) denotes the significant difference at $P < 0.05$ between 6 h and 12 h treated groups.

CHAPTER V: CHARACTERIZATION OF RECEPTOR-INTERACTING SERINE/THREONINE KINASE 2 (RIP2) OF THE GOLDFISH (*Carassius auratus* L.)¹

5.1. INTRODUCTION

As described in Chapter II, RIP2 functions as a key signaling protein in host defense responses induced by activation of the cytosolic pattern recognition receptors (PRR) NOD1 and NOD2 via CARD-CARD interactions (92, 100, 101), and the deficiency of RIP2 affects cellular signaling and cytokine responses triggered by NOD1 and NOD2 ligands (102). In addition to CARD-CARD binding with NOD1 and NOD2, RIP2 has been shown to interact with apoptosis-associated speck-like protein (ASC), which is capable of inducing apoptosis and caspase-1 activation (104). ASC has been demonstrated to direct caspase-1 away from RIP2-mediated NF- κ B activation, and toward caspase-1-mediated processing of pro-IL-1 β by interfering with the RIP2-caspase-1 interaction (104). Alternatively, RIP2, as a CARD-containing protein, has the ability to activate caspase-1 under inflammatory conditions and can serve as a stress-inducible upstream modulator of pro-caspase-1 apoptotic activation (105–107). Moreover, upon viral infection, RIP2 was shown to regulate the activation of inflammasomes by mediating mitophagy in a kinase-dependent manner (108). These observations clearly suggest that RIP2 does not

¹ A version of this chapter has been published: Xie, J., Belosevic, M. 2015. Functional characterization of receptor-interacting serine/threonine kinase 2 (RIP2) of the goldfish (*Carassius auratus* L.). Developmental and comparative Immunology 48: 76-85

only mediate the NOD1 and NOD2 signaling pathway, but also participates in the inflammasome-associated pathways for the maintenance of homeostasis.

In addition to the CARD-CARD interactions, RIP2 can also associate with other signaling proteins (independently of CARD), including members of the tumor necrosis factor receptor (TNFR) family (109), TNFR-associated factor (TNAF) (479), CD40 (111), toll-like receptor 2 (112), and the inhibitor of apoptosis protein (IAP) family (cIAP-1 and cIAP-2) (99, 105). Recent report also suggests that TNAF3 is a RIP2 binding partner because it inhibited RIP2-induced NF- κ B activation (110). Currently, the precise function of RIP2 in immune signaling remains to be fully elucidated, and the activation of NF- κ B and MAPK signaling pathways though RIP2 is primarily associated with its capacity to activate the downstream molecules of the TNFR family, TLR family and NOD-like receptor family (92, 99, 100, 105, 109, 113).

As a highly versatile immune regulator, RIP2 has been proved to be capable of regulating both innate and acquired immunity in mammals (100, 102, 113). However, there is no published information on the functional role of RIP2 in teleosts. In chapter IV, I reported on the role of goldfish NOD1 and NOD2 in response to different immune stimuli (53), and in this chapter, I report on the characterization and functional assessment of the involvement of RIP2 in pro-inflammatory and antimicrobial responses of goldfish macrophages.

5.2. RESULTS

5.2.1. Sequence analysis and characterization of recombinant goldfish RIP2 (gfRIP2)

The gfRIP2 cDNA was cloned by PCR amplification and consisted of 2763 bp with a 1752 bp ORF encoding a polypeptide of 583 aa (Acc. No. KJ636470), a 5' un-translated region (UTR) of 413 bp and a 3' UTR of 598 bp (Fig. 5.1). The predicted molecular mass and isoelectronic point are 65.7 kDa and 6.05, respectively. No signal peptide was predicted. Sequence analysis of the UTR regions revealed the presence of RNA instability regions (ATTTA) in both 5' and 3' UTR, with one in the 5' and two in the 3' regions (Fig. 5.1). The predicted amino acid sequences of the gfRIP2 contained a protein kinase domain (27-292 aa) and a CARD domain (470-554 aa).

Phylogenetic analysis of the cloned gfRIP2 demonstrated closest relationship to the zebrafish RIP2 (Fig. 5.2). The RIP2 proteins of the above two fish species branched independently of the RIP2s of the other fish species including fugu, medaka and tilapia (Fig. 5.2 and Table 5.1). All known fish RIP2 proteins branched independently from the RIP2 protein sequences of higher vertebrates with the exception of the frog (Fig. 5.2).

5.2.2. Analysis of RIP2 expression in normal goldfish tissues

Quantitative expression analysis of gfRIP2 in tissues of normal fish indicated that the highest mRNA levels of RIP2 were in the spleen, followed by brain, intestine, gill, and kidney (Fig. 5.3A). Lower mRNA levels were observed in the heart and muscle, and the lowest RIP2 mRNA levels were in the liver (Fig. 5.3A).

5.2.3. Analysis of RIP2 expression in non-stimulated goldfish immune cell populations

The expression of RIP2 was determined in different goldfish cell populations. The cell population assessed included peripheral blood leukocytes, kidney-derived neutrophils, splenocytes, and kidney-derived monocytes and mature macrophages. Monocytes had the highest RIP2 mRNA levels, followed by splenocytes, neutrophils and PBL, while the RIP2 expression was lowest in mature macrophages (Fig. 5.3B).

5.2.4. Recombinant gfRIP2 expression, purification and antibody characterization

To examine the activity and function of gfRIP2, I expressed the rgRIP2 in *E. coli* and purified it using the MagneHis protein purification system. A single faint band with the molecular weight of 86.1 kDa (including the size of 20.4 kDa of a thioredoxin protein, a six-histidine tag, a thrombin recognition site and a T7 tag at the N-terminus) was indicated by SDS-PAGE analysis (Fig. 5.4A). The presence of the recombinant protein was confirmed by Western blot analysis using an anti-His antibody (Fig. 5.4A).

5.2.5. Confirmation of the specificity of anti-RIP2 antibody and RIP2 inhibitors

To further explore the function of RIP2 of goldfish, I used a commercial anti-RIP2 antibody that recognizes highly conserved peptide of RIP2. This antibody recognizes RIP2 from a number of different organisms including zebrafish. As shown in Fig. 5.4A (lanes 3 and 4), both anti-His antibody and anti-RIP2 antibody recognized recombinant RIP2 protein, indicating that the commercial anti-RIP2 antibody is also specific for gfRIP2 (Fig. 5.4A).

To examine the signaling pathway of goldfish RIP2, I tested the specificity of three RIP2 inhibitors. As shown in Fig. 5.4B, SB203580 at concentrations of 5 and 10 μ M significantly inhibited RIP2, whereas gefitinib and erlotinib did not (Fig. 5.4B).

5.2.6. Analysis of gfRIP2 expression in macrophages treated with LPS, PGN, MDP and Poly I:C

I measured the expression of the RIP2 in macrophages treated with different NOD1/NOD2 ligands. The mRNA levels of gfRIP2 were determined using Q-PCR after treatment with either PBS, LPS, PGN, MDP and Poly I:C, for 6 h and 12 h. As shown in Fig. 5.5A, the expression of RIP2 was up-regulated after LPS and MDP treatment at 6 h. A significant increase in the RIP2 mRNA levels in goldfish macrophages were observed after treatment with all NOD1/NOD2 ligands at 12 h (Figs. 5.5A and 5.5B). In addition, Western blot analysis indicated that treatment of macrophages with the NLR ligands, increased RIP2 protein levels with exception of Poly I:C (Figs. 5.5C and 5.5D).

5.2.7. Analysis of gfRIP2 expression in macrophages treated with heat-killed *A. salmonicida* and heated-killed or live *M. marinum*

To examine whether gfRIP2 was involved in response to bacterial challenge, expression of RIP2 was determined in goldfish macrophages at 6 h and 12 h after exposure to 2×10^6 cfu/mL of heat-killed *A. salmonicida* or heat-killed or live *M. marinum*. The mRNA and protein levels of RIP2 were up-regulated at 12 h after

exposure to *A. salmonicida* and *M. marinum*. Notably, the exposure of macrophages to heat-killed *A. salmonicida* induced a robust increase in RIP2 mRNA levels (Fig. 5.5B).

5.2.8. GfRIP2 associates with NOD1 and NOD2

To examine the association between RIP2 and NOD1 and NOD2, we co-expressed either pcDNA3.1/NT-GFP-empty (control), pcDNA3.1/NT-GFP-NOD1 or pcDNA3.1/NT-GFP-NOD2 and pcDNA3.1/V5-His-RIP2 in HEK293 cells and performed co-immunoprecipitation (co-IP) assays. I firstly evaluated the transfection efficiency and recombinant proteins expression in eukaryotic cells using a Western blot assay. Following the transfection in HEK 293 cells, the expression of GFP, GFP-NOD1, GFP-NOD2, His-RIP2 was determined by anti-GFP antibody or anti-His antibody. As shown in Fig. 5.6A, all of the GFP-tagged proteins and His-tagged RIP2 were expressed in HEK293 cells, indicating appropriate transfection efficiency. I then performed the co-IP assays from the cells co-transfected with different groups of plasmids. The results showed that the pcDNA3.1/V5-His-RIP2 was co-precipitated with anti-GFP antibody when co-transfected with either pcDNA3.1/NT-GFP-NOD1 or -NOD2, and that pcDNA3.1/NT-GFP-NOD1 and -NOD2 were also co-precipitated with anti-His antibody when co-transfected with pcDNA3.1/V5-His-RIP2 (Fig. 5.6B). In contrast, the pcDNA3.1/NT-GFP-empty and pcDNA3.1/V5-His-RIP2 co-transfected HEK293 cells did not show any precipitated immune complex (Fig. 5.6B). These results show that the RIP2 associated with goldfish NOD1 and NOD2.

5.2.9. Goldfish rgRIP2 promotes NF- κ B transcriptional activity

In mammals, RIP2 has been identified as a mediator that eventually activates NF- κ B through the NLR pathway (92, 100, 101). To evaluate if the RIP2 protein was involved in the NF- κ B pathway, HEK293 cells were transfected with the pcDNA3.1/V5-His-RIP2 and pNF- κ B-Luc expression plasmids. The results showed that compared to the pcDNA3.1/V5-His empty vector, transfection with the RIP2 expression plasmid induced a significant increase in pNF- κ B-Luc expression ($P < 0.05$) (Fig. 5.7).

5.2.10. GfRIP2 regulates the production of TNF α -2, IL-1 β 1 and HMGB1

We previously reported that exposure of goldfish macrophages to *M. marinum* up-regulated the expression of pro-inflammatory cytokines TNF α -2, IL-1 β 1 and HMGB1 (194, 480). To examine the role of RIP2 in the regulation of macrophage pro-inflammatory responses, I measured the mRNA and protein levels of TNF α -2 and IL-1 β 1 in macrophages exposed to heat-killed *M. marinum*, those exposed to *M. marinum* and treated with the RIP2 inhibitor SB203580, and non-treated macrophages. As shown in Fig. 5.8, the mRNA levels of TNF α -2 and IL-1 β 1 were significantly reduced after treatment of macrophages with the RIP2 inhibitor SB203580, suggesting a central role for RIP2 in the regulation TNF α -2 and IL-1 β 1 production by activated macrophages (Figs. 5.8A, B D and E). Given that HMGB1 is a pro-inflammatory cytokine whose production is dependent on inflammasome and caspase-1 activation (481), I also measured the mRNA levels of HMGB1 in response to *M. marinum* in the presence or absence of the RIP2 inhibitor SB203580 (Fig. 5.8C). The results showed that the expression of HMGB1 was

significantly inhibited by SB203580, suggesting that goldfish RIP2 activation also influences the inflammasome pathway, similar to what has been observed for mammals (481).

5.3. DISCUSSION

In this chapter, I report on the cloning, molecular characterization and functional analysis of gfRIP2. The gfRIP2 sequence shared the highest identity with the zebrafish RIP2 (Table 5.1) and had the functional domains present in mammals, including the protein kinase domain and the CARD domain. In mammals, the CARD domain plays major roles in regulating (i) caspase activation in the context of apoptosis, (ii) inflammation, and (iii) NF- κ B activation (482). In general, the two main function of CARD domain-containing molecules are NF- κ B activation and caspase regulation in context of the generation of innate and adaptive immune responses (483). In addition, the activation of RIP2 kinase activity is also central to cellular responses regulated by mitogen-activated protein kinases (MAPK) (387). The predicted presence of the protein kinase domain and CARD domain in the goldfish RIP2 indicate that similar RIP2-dependent signaling pathways are present in teleosts.

Phylogenetic analysis showed that gfRIP2 grouped closely with other teleost RIP2s, especially with zebrafish RIP2, and to a lesser extent with fugu, medaka and tilapia, suggesting that teleost RIP2 is evolutionally conserved.

My study is the first quantitative expression analysis of RIP2 gene in tissues and different immune cell populations in bony fish. The expression analysis of gfRIP2

indicated highest mRNA levels in the spleen, which is similar to what has been observed in humans (99). The RIP2 mRNA levels in other tissues examined (brain, intestine, gill, kidney, heart, muscle and liver) were significantly lower than those in the spleen. I also measured RIP2 mRNA levels in different cell populations isolated from normal goldfish, including splenocytes, PBLs, neutrophils and primary monocytes and macrophages of the goldfish. The highest RIP2 expression was observed in monocytes and to a lesser extent in splenocytes, neutrophils and PBL. In mammals, the primary producers of RIP2 are PBLs (99).

To functionally characterize RIP2 in goldfish, I have used two approaches. The first approach was to use an anti-human-RIP2 antibody raised against a highly conserved peptide sequence. The synthetic peptide sequence (C-KLKDNKQMGLQPYPE) used to immunize rabbits for the production of anti-human-RIP2 antibody had greater than 93% identity with the goldfish C-terminal peptide (C-KLQDNKQMGLQPYPE). This antibody was predicted to recognize zebrafish, mouse, rat, chicken, cow and human RIP2. The anti-human RIP2 antibody specifically recognized recombinant goldfish RIP2, and was used to examine RIP2 protein levels in activated goldfish macrophages.

The second approach was to employ specific RIP2 inhibitors. SB203580, which was initially identified as a MAPK p38 kinase inhibitor, had been shown to efficiently inhibit RIP2 activity (412, 413) (Hollenbach et al., 2004; Argast et al., 2005). In this chapter, I have demonstrated that at the protein level, the inhibitor SB203580 significantly inhibited gfRIP2 in macrophages, akin to what has been observed for Dengue virus (DENV)-infected HepG2 cells (388). The other two inhibitors tested,

gefitinib and erlotinib, did not inhibit gfRIP2 protein expression, although they have been shown by others to inhibit RIP2 tyrosine phosphorylation in mammals (389). Due to the lack of specific anti-RIP2 phosphorylation antibody, I was not able to validate the specificity of these two RIP2 inhibitors.

RIP2 was originally identified as a downstream adaptor molecule in the NOD1/NOD2 signaling pathway (100). Based on the high identity of the predicted function domains, protein kinase and CARD domains, I hypothesized that RIP2 plays a central role in the signaling upon NOD1 and NOD2 activation. Previously in Chapter IV, I have shown that various ligands and Gram-negative and Gram-positive bacteria activate NOD1 and NOD2 of the goldfish (53). Here, I report that RIP2 expression and protein levels increased after activation of NOD1 and NOD2 with different ligands and two fish pathogens, *A. salmonicida* and *M. marinum*. Treatment of goldfish macrophages with different ligands or exposure to pathogens increased the expression and protein levels of RIP2 at 12 h post-exposure. The mRNA and protein levels of RIP2 were shown to increase after exposure of mammalian cells to LPS (100, 414, 415), PGN (100) and MDP (416). The up-regulation of RIP2 expression at mRNA level suggests that RIP2 is a key modulator of bacterial-induced response after NOD1/NOD2 activation. The observed increase in mRNA levels of RIP2 in macrophages treated with Poly I:C was consistent with the reports that exposure of pigs to porcine reproductive and respiratory virus, as well as Denge virus-infected HepG2 cells, induced a 10-fold and 1.5-fold increase in the expression of RIP2, respectively (388, 417).

In contrast to *Aeromonas* spp.-induced infection in goldfish, RIP2 has been well studied in mycobacterial infections in mammals (416, 418), which is primarily mediated by NOD2-RIP2 pathway. Given that goldfish RIP2 mRNA and protein levels significantly increased after exposure of macrophages to *A. salmonicida* and *M. marinum*, and that both NOD1 and NOD2 are activated after exposure of cells to bacterial pathogens (53), the NOD1/NOD2-RIP2 pathway appears to play a critical role in the regulation of antimicrobial responses in teleosts.

It is well established that in mammals, RIP2 mediates the innate and adaptive immune response by binding to activated NOD1 and NOD2 via CARD-CARD interactions (92, 100–102). Accordingly, I have examined the associations of NOD1/NOD2 with RIP2 using co-IP assays in this thesis. The gfRIP2 was shown to interact with NOD1 and NOD2, supporting the role of RIP2 as an adaptor molecule critical for NOD-like receptor signaling pathway in teleosts. Furthermore, the activation of RIP2 after binding to NOD1 and NOD2 causes the down-stream activation of transcriptional factor NF- κ B and MAPK, that eventually results in the production of pro-inflammatory cytokines (100, 101). Using the dual-luciferase reporter assay, I proved that gfRIP2 enhanced the expression of luciferase reporter gene NF- κ B binding site, suggesting that gfRIP2 activated NF- κ B pathway.

The activation of NOD1/NOD2 results in the production and release of the pro-inflammatory cytokines, including TNF α , IL-1 β , IL-18 and others (419, 420). Previously our lab showed that *M. marinum* activated the NOD2 pathway (53, 380, 381). To examine the pro-inflammatory mediators involved in the “NOD2-RIP2” signaling, I

challenged the goldfish macrophage with *M. marinum* and evaluated the protein levels of RIP2, TNF α -2 and IL-1 β 1. My results are consistent with previous observations that TNF and IL-1 β are the key effector cytokines that control immune responses against mycobacterial infections (421, 422). Interestingly, macrophages exposed to heat-killed *M. marinum*, and then treated with the specific RIP2 inhibitor SB203580, displayed significantly reduced TNF α -2 and IL-1 β 1 protein levels, suggesting a critical role for RIP2 in the generation of pro-inflammatory responses of goldfish macrophages. The inhibition of RIP2 in heat-killed *M. marinum*-activated macrophages by SB203580 caused significant decreases in HMGB1 mRNA levels, suggesting a possible role for RIP2 in the regulation of the inflammasome pathway. The possible interactions between RIP2, inflammasome activation, caspase-1 function and pyroptosis are currently under investigation in our laboratory.

My findings in this chapter indicate that RIP2 may be a critical protein involved in the modulation of macrophage pro-inflammatory responses in bony fish. Further studies are needed to elucidate RIP2 roles in the regulation of caspase-1 function and the inflammasome machinery of bony fish macrophages.

Table 5.1. Percent identity of goldfish RIP2 and other organisms (aa)

Species	Identity (%)
Zebrafish	89
Tilapia	81
Medaka	68
Fugu	66
Frog	60
Mouse	52
Human	51
Chicken	50

```

1 ACATGGGGACTCATTACGCACCTGCGAAATATTTACCGAGCGGTGACCCACCACCACCACCACGCTTCGTAATCGATAAATGTCA
90 AACTGCTGTGATTTTATTGGTTTGGCGGTAATTTGCAAGTTTGGTTTATGGCATGATATAAAATGCGTTGTTCCGGATTGGGGCGGTGTC
180 TCCAAGCGCGATCCGTAGGAAACATTCCTTTCCAGGGATATTTTATTACATAAAATAGTAACGTTTATCCCTAACCGCCTGTCTCTT
270 GGTAGTGTGGATTAGACTGCATTACAACATGTGAGTTCGTATTGTCTCTATCTGTGAGGGTTTTAAGCTGTAGCAGCGCTTTCAGTT
360 CTCCTTCCACTGAAGCTGAACGGGCCCGTCTCGTCTCATAATATCCTCAAAatggagcagcggcgtgcgtcaacatctgcagtctc
M E H A G C V N I C S L
450 accgacaccttaccggtgatcccgtaaccggaactaacggacctgcactacatcagtaaaggcggcttcgggaccggtgttcaggcgcag
T S T L P V I P Y R K L T D L H Y I S K G G F G T V F R A Q
540 cacagcgactggcgcaccacggtggcgatcaagtgttgaactggattcaccggttgagagagggagagaaactgtttattgaaggaa
H S D W R T T V A I K C L K L D S P V G E R E R N C L L K E
630 gctgaggtgcttcacaaagctcgatttaaccacatcatccagatctttggggttgtaatgagcccaggttctctcgtcattgtgactgag
A E V L H K A R F N H I I Q I F G V C N E P E F F C I V T E
720 tacatgaccaacggatcactggacgagctcctgcagagaaagatgtaccacgagggtggcctggccattgaggtgcgtattctttac
Y M T N G S L D E L H E L H E M Y P A V A W P L R L R I L Y
810 gagatcgttttaggagttaactccttcacaacatgacaccacccttctgcaccatgacctaaaactcagaacatcctgatggatggg
E I A L G V N F L H N M T P P L L H H D L K T Q N I L M D G
900 gagtaccatgttaagatcgctgattttggcttatctaaatggcgccagctctcgatcactaaaggtccagctccaaactcggaaatc
E Y H V K I A D F G L S K W R Q L S I T K G S S S K P A E M
990 ggaggcacggtcatctatatgccacctgaggagtagaaccttccaaaaaccgagagctgatgtcaaatatgacatgtacagttacgcc
G G T V I Y M P P E E Y E P S K N R R A D V K Y D M Y S Y A
1080 atcatcgttgggaagtgccttcaagacggataaccatttgaagagccaccaatcccatgacagatcattcagttgcttcggaaatc
I I M W E V L S R R I P F E E A T N P M Q I M F S V L R G S
1170 cgaccgacacagcctggacagctctgccagcagaatctccagtcgagagacctcattaactcatgaccagcgggtggaccggccg
R P D T G L D S L P A E I P S R E T L I K L M T S G W T A A
1260 ccaaatgaacggccctccctctcaattgtcttattgacctggagccatgctgagaagatttgatgagattaattcttgaagcagtg
P N E R P S L L N C L I D L E P M L R R F D E I N F L E A V
1350 ttggaagtgaacgaacaagatataatgagccatcaagctgctgctcatcatctcaaaacaatgggaaactaatccaagaaaagattgtg
L E V K R T K Y M R P S S C C S S S Q T N G K L I Q E K I V
1440 aaggagcaaaacatcccttggccagacacagttccacatctggatcaggatcctgctcttcccacgaagcagaatatacccacggggc
K E Q N I P W P D N S S T S G S G S C S S H E A E I S H P G
1530 tgcctaacatcccaatccctctcaagtgctgctcagctgctcagctgctcagcagcagcagcagcagcagcagcagcagcagcagc
C L T I S N P S Q G V S A A Q A G P Q A S L I S L P L D P P
1620 aaactcttggtagcactgctctcagaacaacctcaacctgaataccagacggcgcagcagcagcagcagcagcagcagcagcagcagc
K P L V D H C S Q N N L N P E Y Q T A Q H V S D L N I P F N
1710 ccgcatgcatcacagagtgaaagtgaactgctcttccatacaacccctcagcgtgcagccacatccacaagatttgtcacagcattg
P H A S Q S E S D L P L P I Q P L T L Q P H P Q D F V T A L
1800 gacactcaaggtccggtagctcgtggtgctgcccgaaggaggatggtgctgagcagtgacggaggcgtgctcaatcagagttta
D T Q G P V A R W I A A R R E D V V R Q M T E A C L N Q S L
1890 gatgctctgttgcctgagctgctgagcgcgaggaactgaactgctgctgctgctgctgctgctgctgctgctgctgctgctgctgct
D A L L S R E L L M R E D Y E L V V N Q P T R T A K V R K L
1980 ctagacacttgcgagcggcacagcagagacttctgccgctggtggtgctgctgctgctgctgctgctgctgctgctgctgctgctgct
L D T C E R H S E D F C R V V V R K L Q D N K Q M G L Q P Y
2070 cccgagctcagcaccaccagcctccgctccacctataaccgccccagcacccttctctccaactcctttaaacaacacagcactc
P E L S T T S P P P P P Y T A P S T P F L S N S F N N T R L
2160 ttctggaCCTTCTCCAATCTCACTGCTCTTGAACAGAGCTCTGTGAGTCTTCTTTTCAGTTAAGGATGGTCCCTGTTCACATGCTCTTA
F *
2250 CGTTTGTGCTGCTTGGCCGAAACTTTGTGTGCTTGACAAAGTCTTTTGGCCCTGTGGTTAAGGTGTTGGTGCCTATGACACACAACCTT
2340 AATGGTTGCAATCAAGACCGATTTCGGTCAATAGCCACTTGGCTTGTTTGACTTCTGAGCTAAATCCTTGATGACAGGGACGCCA
2430 ATTTAAGCAGTACAGTGGTTTGACATCGCCATGTTTAAACCTTTATTCAGTCATCAAAGAATCTGGTTGATGCTACTTGGAAAGCAG
2520 TGAACGCATAAGCAATCAATCTATCTTGTCAATTTGCACCTTCCATGCCAGCGGATTTAGTAAATAGAAGACTTGAGGTAAGTTAT
2610 AAAGACACACCTTCTGTAAATGCCACGAAACATCCAGATTACTGCACAGTTGCATGTCTGGACTTGATGAAAGCTCATGTGAATCAGCAG
2700 TTTTGTCTCTCTTTATAAACAGTTTTTTTCCAAAAAATAAAAAAAAAAAAAAAAAA

```

Figure 5.1. Nucleotide and predicted aa sequence of goldfish RIP2 cDNA.

The start and stop codons are boxed, the protein kinase domain is highlighted in light grey, the Caspase recruitment domain is highlighted in dark grey. The peptide region (KLQDNKQMG LQPYPE) for antibody validation is in bold. The RNA instability motifs are underlined (ATTTA).

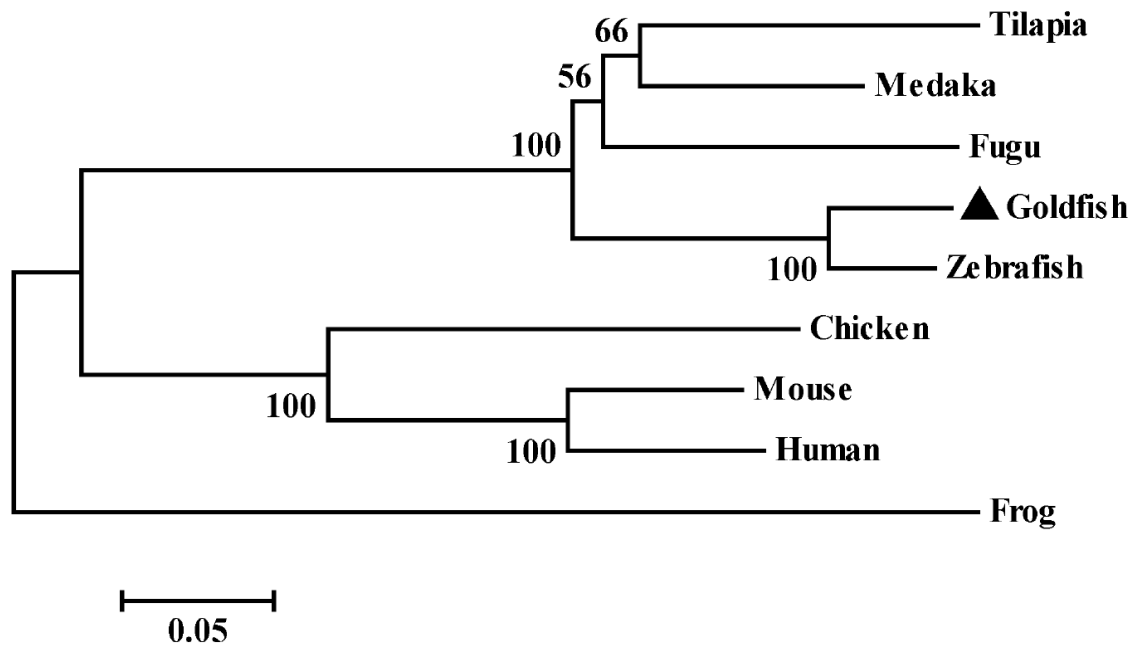


Figure 5.2. Phylogenetic analysis of goldfish RIP2.

RIP2 amino acid sequences were aligned by using CLUSTAL-W program and unrooted phylogenetic tree was constructed using the neighbor-joining method of the MEGA 5.1 program. The tree was bootstrapped 10,000 times. The full length of RIP2 amino acids sequences used were: Zebrafish NP_919392.2, Medaka XP_004078988.1, Tilapia XP_004078988.1, Fugu XP_003975835.1, Chicken NP_001026114.1, Mouse NP_620402.1, Human NP_003812.1, Frog XP_002939201.1.

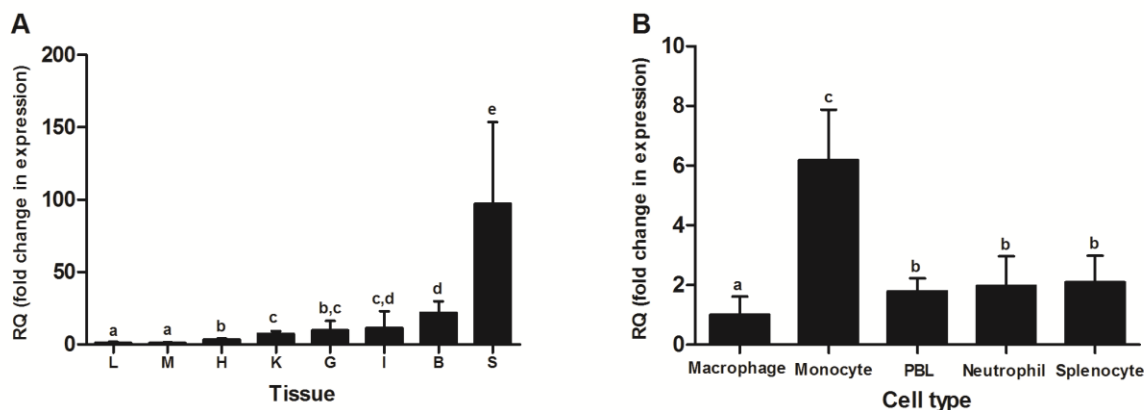


Figure 5.3. Quantitative analysis of goldfish RIP2 expression in different tissues and immune cell populations obtained from normal goldfish.

(A) Goldfish RIP2 tissue distribution analysis. The expression of goldfish RIP2 was measured relative to endogenous control gene, elongation factor 1 alpha (EF-1 α). Relative tissue expression from four individual fish are shown (n = 4). qPCR was done in triplicate for each tissue. All results were normalized against the liver RIP2 mRNA levels. (B) Goldfish RIP2 expression in different immune cell populations. Cell cultures were established from four fish (n = 4). qPCR was done in triplicate for each immune cell population. All results were normalized against the macrophage RIP2 mRNA levels. Statistical analysis was performed using one-way ANOVA followed by Dunnett's post-hoc test. Different letters above each bar denote statistically different ($P < 0.05$), and the same letter indicates no statistical differences between groups (L = liver, M = muscle, H = heart, G = gill, K = kidney, I = intestine, S = spleen, B = brain).

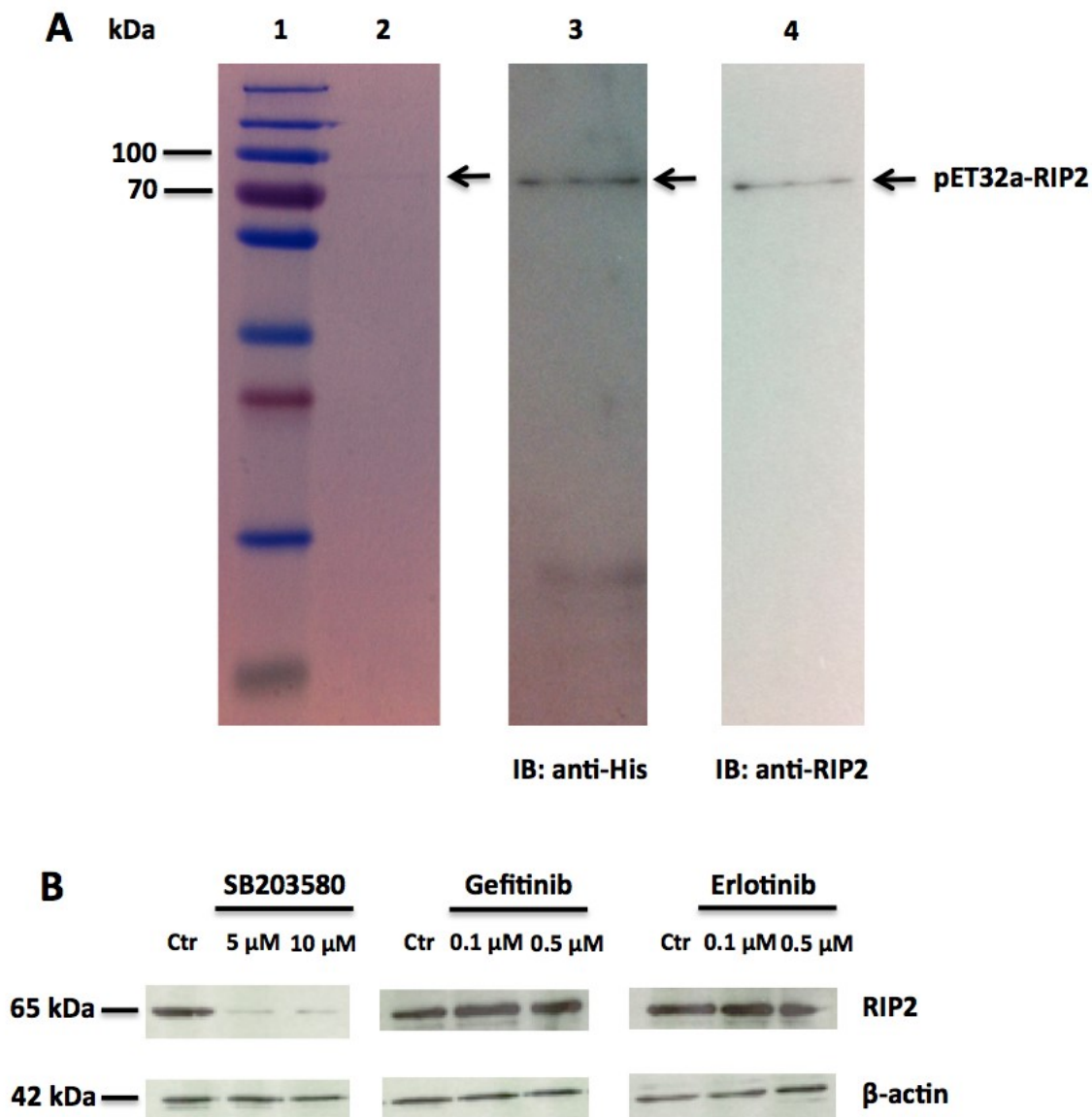


Figure 5.4. Validation of anti-human RIP2 antibody and RIP2 inhibitors in goldfish. (A) SDS-PAGE and Western blot analysis of recombinant RIP2. Lane 1: protein ladder; Lane 2: SDS-PAGE analysis of Coomassie brilliant blue stained of purified recombinant RIP2; Lane 3: Western blot analysis of purified recombinant RIP2 using anti-His antibody; Lane 4: Western blot analysis of purified recombinant RIP2 using anti-human RIP2 antibody (IB = immunoblotting). (B) The expression of RIP2 in goldfish macrophages in presence of SB203580 (5 μ M or 10 μ M), gefitinib and erlotinib (0.1 μ M or 0.5 μ M) was determined by Western blot analysis (Ctr = control). β -actin was loading control.

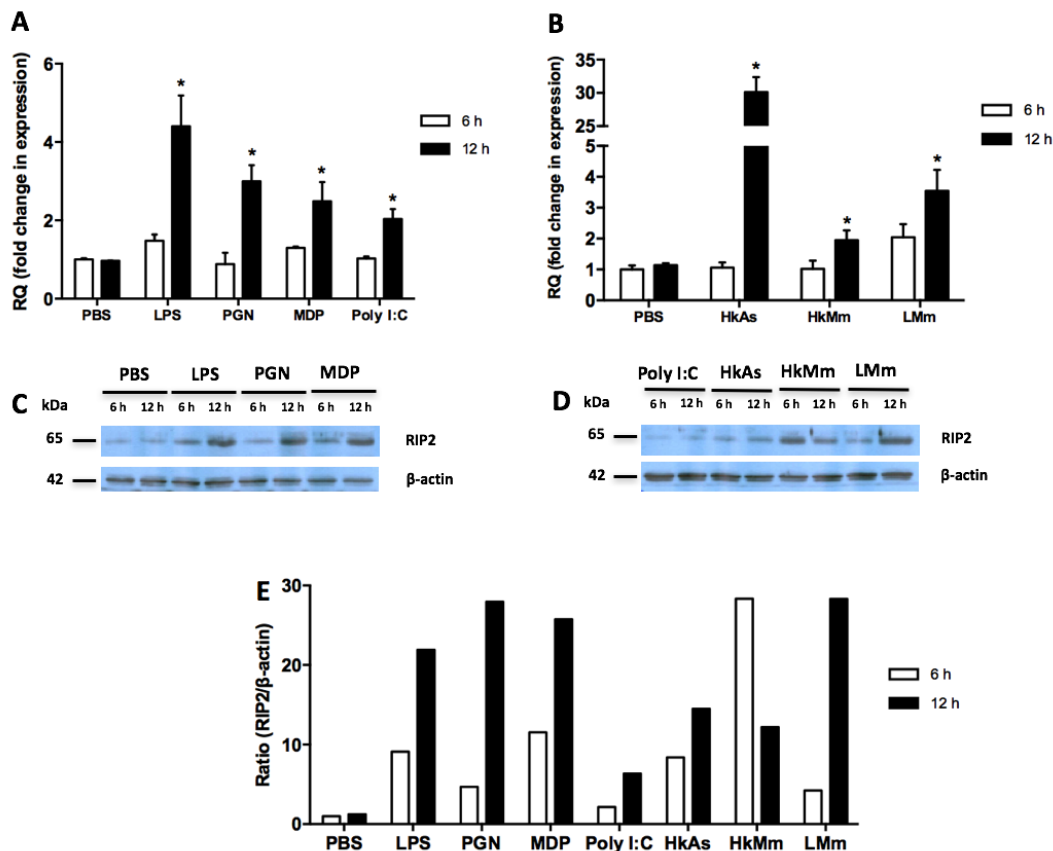


Figure 5.5. Quantitative expression and Western blot analysis of goldfish RIP2 in macrophages treated with different stimuli.

(A and B). Quantitative expression of goldfish RIP2 in macrophages treated with either PBS, or lipopolysaccharide (LPS), peptidoglycan (PGN), muramyl dipeptide (MDP), Poly I:C, heat-killed *A. salmonicida*, heat-killed or live *M. marinum*. The expression of RIP2 was examined relative to the endogenous control gene, elongation factor 1 alpha (EF-1 α). The expression values were normalized against those at the 6 h. The results are mean \pm S.E.M. of primary macrophage cultures established from four individual fish ($n = 4$). (*) Denotes significantly different ($P < 0.05$) compared to the 6 h or 12 h time point. (C and D) Western blot analysis of goldfish RIP2 in macrophages treated with either PBS, or LPS, PGN, MDP, Poly I:C, heat-killed *A. salmonicida*, heat-killed or live *M. marinum*. The treated macrophages were washed three times with PBS and lysed with 100 μ L of ice cold IP buffer and then subjected to Western blot analysis using anti-human RIP2 antibody or anti- β -actin antibody. β -actin was loading control. (E) Quantified ratios of RIP2 protein to β -actin in treated macrophages, compared to PBS at 6 h. The results are shown as the mean of pooled macrophages from cultures established from three individual fish ($n = 3$) (HkAs, heat-killed *A. salmonicida*; HkMm, heat-killed *M. marinum*; LMm, live *M. marinum*).

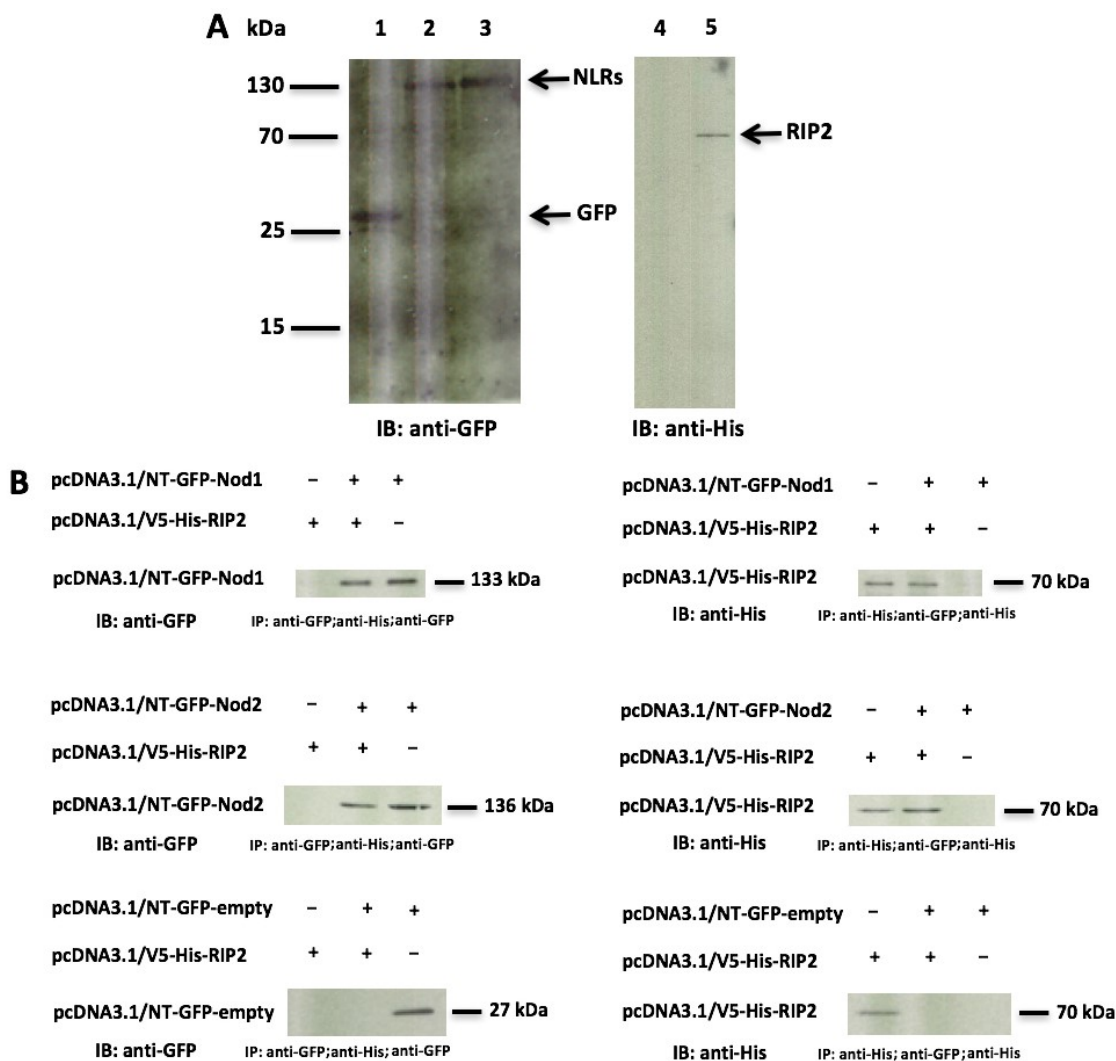


Figure 5.6. Goldfish RIP2 associates with NOD1 and NOD2 in HEK293 cells.

(A) Western blot analysis of pcDNA3.1/NT-GFP-empty, pcDNA3.1/NT-GFP-NOD1, pcDNA3.1/NT-GFP-NOD2 and pcDNA3.1/V5-His-RIP2 in HEK293 cells. Lane 1: Western blot analysis of pcDNA3.1/NT-GFP-empty using anti-GFP antibody; Lane 2: Western blot analysis of pcDNA3.1/NT-GFP-NOD1 using anti-GFP antibody; Lane 3: Western blot analysis of pcDNA3.1/NT-GFP-NOD2 using anti-GFP antibody; Lane 4: Western blot analysis of the lysate of untransfected HEK293 cells using anti-His antibody; Lane 5: Western blot analysis of pcDNA3.1/V5-His-RIP2 using anti-His antibody. NLR = NOD-like receptors. GFP = green fluorescence protein. (B) The total cell lysate was prepared from co-transfected cells and incubated with anti-His antibody or anti-GFP antibody. The precipitated immune complexes were subjected to Western blot analysis using either anti-GFP antibody or anti-His antibody (IP = immunoprecipitation; IB = immunoblotting).

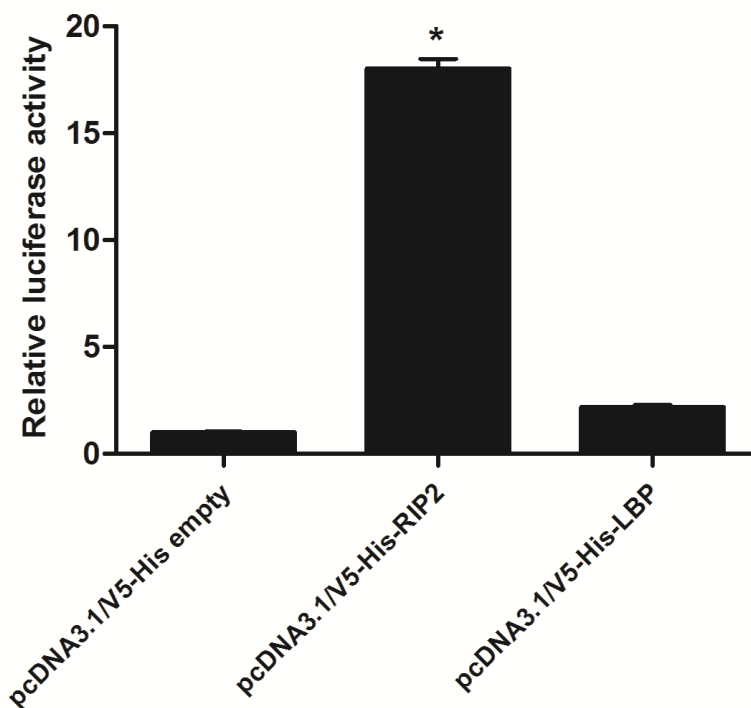


Figure 5.7. Goldfish recombinant RIP2 protein promotes NF- κ B transcriptional activation.

HEK293 cells were transfected with 200 ng of pNF- κ B-Luc, 20 ng of pRL-TK reporter vectors and either 200 ng of pcDNA3.1/V5-His empty vector or the same amount of pcDNA3.1/V5-His-RIP2 or pcDNA3.1/V5-His-LBP (negative control). At 24 h after transfection, cells were harvested and analyzed using the Dual Luciferase kit according to manufacturer's instructions. All values represent three independent experiments ($n = 3$). All results were normalized against the pcDNA3.1/V5-His empty luciferase value. The asterisk (*) indicates the significant difference at $P < 0.05$ compared to pcDNA3.1/V5-His empty for each group.

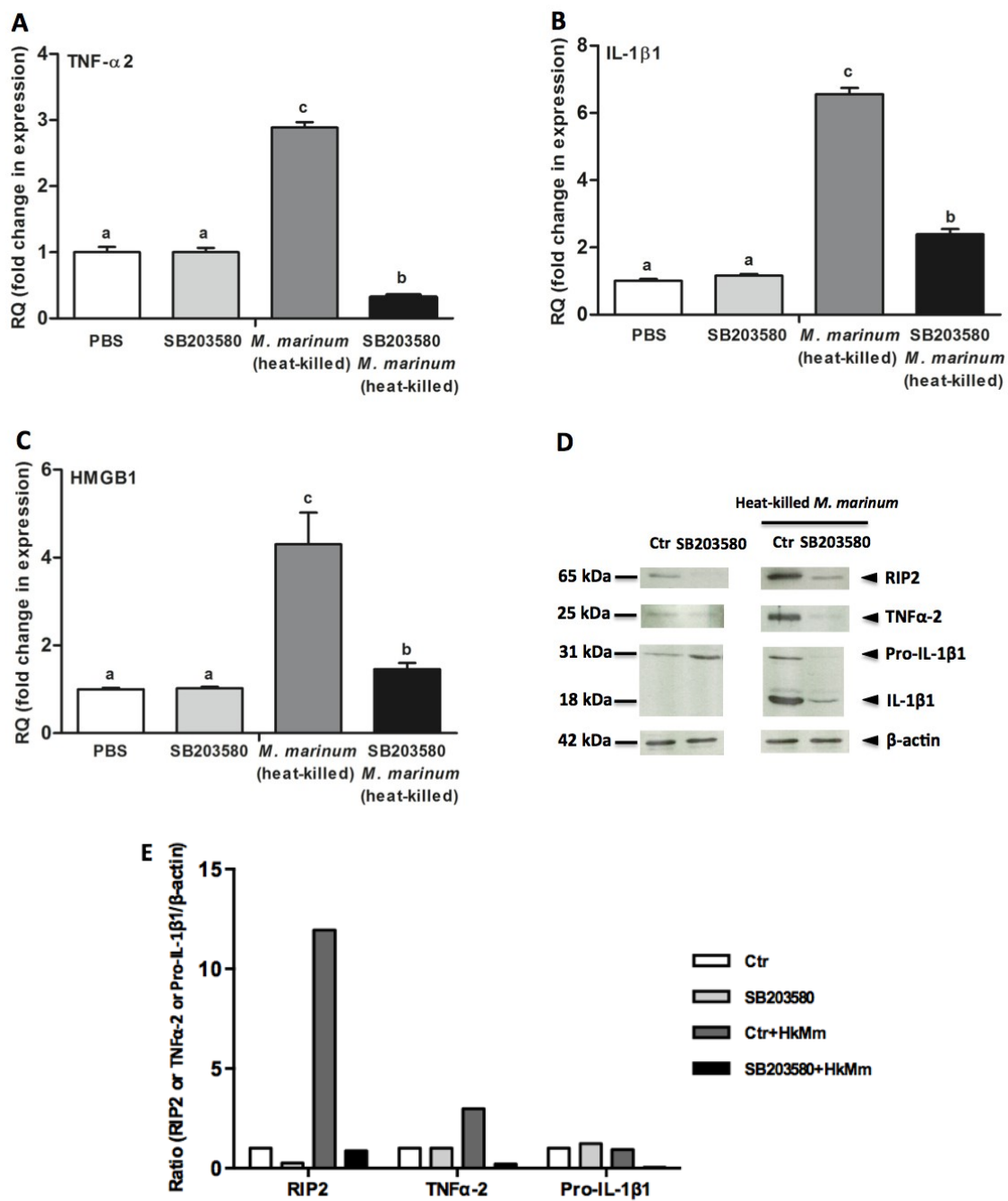


Figure 5.8. Evaluation of the expression of TNF α -2, IL-1 β 1 and HMGB1 in macrophages treated with either PBS, SB203580, or heat-killed *M. marinum* for 12 h and then treated SB203580 for 2 h or untreated cells.

(A, B and C) Quantitative expression of goldfish TNF α -2 and IL-1 β 1 in macrophages treated with either PBS, SB203580, or with heat-killed *M. marinum* for 12 h before treatment with SB203580 for 2 h. The expression of TNF α -2 (A), IL-1 β 1 (B) and HMGB1 (C) was examined relative to the endogenous control gene, elongation factor 1 alpha (EF-1 α). The expression values were normalized against PBS at the 12 h time point. The results are mean \pm S.E.M. of primary macrophage cultures established from four individual fish (n = 4). Different letters above each bar denote statistically different ($P < 0.05$), and the same letter indicates no statistical differences between groups. (D) Western blot analysis of RIP2, TNF α -2 and IL-1 β 1 in goldfish macrophages incubated with PBS, SB203580, or heat-killed *M. marinum* for 12 h before and then treated with SB203580 for 2 h or untreated. The cells were washed three times with PBS and lysed with 100 μ L of ice cold IP buffer and subjected to Western blot analysis using anti-human RIP2 antibody, anti-TNF α -2 antibody or anti-IL-1 β 1 antibody. β -actin was loading control. (E) Quantified ratios of RIP2 or TNF α -2 or IL-1 β 1 protein to β -actin in treated macrophages, compared to control group. The results are shown as the mean of pooled macrophages from cultures established from three individual fish (n = 3) (Ctr, control; HkMm, heat-killed *M. marinum*).

CHAPTER VI: CHARACTERIZATION OF NLRP3-RELATED MOLECULE OF THE GOLDFISH (*Carassius auratus* L.)

6.1. INTRODUCTION

The cytosolic receptors called NLRs recognize intracellular bacteria, fungi and protozoan parasites. The NLRs are evolutionarily highly conserved and are present in animals from sea urchins to mammals (8, 15, 53, 117). Certain NLRs such as NLRP1, NLRP3 & NLRC4 (in combination with NAIPs) after PAMPs recognition form large multiprotein complexes called inflammasomes, that in turn activate the downstream signaling molecule caspase-1 (12, 134). The recognition of a diverse range of microbial, stress and DAMPs by inflammasomes results in direct activation of caspase-1 through an adaptor molecule, ASC. Activated caspase-1 processes the cytosolic precursors of the related cytokines IL-1 β and IL-18, thus allowing secretion of the biologically active proteins (207, 219). The inflammasome signaling pathway also induces inflammatory cell death, known as pyroptosis (17, 134, 313). The results of recent studies indicate that during pyroptosis, there is a translocation of HMGB1 protein from the nucleus into the cell cytoplasm and eventual secretion of the HMGB1 by immune cells in response to a variety of exogenous and endogenous danger signals (251, 423). Genetic deletion of inflammasome components in mammals impairs HMGB1 release during endotoxemia or bacteriemia (251, 423).

To date, there are limited reports on the inflammasomes in teleost fish, although NACHT, LRR and PYD domains-containing protein (NLRP) isoforms of zebrafish are present in the National Center for Biotechnology Information (NCBI) database, such as NLRP3 (Accession number: XP_017212365.1), NLRP3X1 (XP_017206752.1), and NLRP12-like (XP_009299711.1). In addition, there are several other NLRs (22, 27, 28, 46, 53, 56, 57, 126), as well as the inflammasome signaling downstream proteins such as ASC and caspase-1 (126, 197, 215, 227, 229) and HMGB1 protein (191–194), suggesting that inflammasome signaling pathway probably exists in lower vertebrates and that it may play a critical role in host defense of teleosts.

In this chapter, I report on the functional characterization of an NLRP3-related molecule (NLRP3rel) of a bony fish. Goldfish NLRP3rel was highly expressed in spleen, intestine, PBLs and macrophages. NLRP3rel molecule was up-regulated in nigericin-activated primary kidney macrophages, and after treatment of cells with ATP. Results from confocal microscopy and co-immunoprecipitation assays suggested that goldfish NLRP3rel associated with ASC. Nigericin-activated macrophages exhibited significant LDH release and caspase-1-dependent IL-1 β and HMGB1 secretion, indicating that NLRP3 signaling pathway is highly conserved and functional in bony fish.

6.2. RESULTS

6.2.1. Sequence analysis and characterization of NLRP3rel molecule

I successfully assembled a complete NLRP3rel cDNA sequence from the goldfish transcriptomic database. The total goldfish NLRP3rel cDNA consisted of 3,851 bp with a

3,093 bp ORF encoding a polypeptide of 1,030 amino acids (aa). The predicted molecular weight and isoelectric point (*pI*) were 117.7 kDa and 7.96, respectively. No signal peptide was predicted. As shown in Fig. 6.1, the complete ORF and UTRs of goldfish NLRP3rel cDNA transcript were obtained. Sequence analysis of the ORF region revealed the presence of the fish-specific NACHT-associated domain (79-149 aa), NACHT domain (160-329 aa), PRY domain (851-897 aa), SPRY domain (900-1025 aa) and LRRs (683-704 aa and 743-762 aa) (Fig. 6.1). Phylogenetic analysis revealed goldfish NLRP3rel shared closest relationship with NLRP3-like of barbel. All the teleost NLRP3-like, NLRP12-like and most of the NLRC3-like molecules branched independently relative to the NLRC3s and NLRP3s of the other higher vertebrates, including mouse and human (Fig. 6.2). The aa identity between goldfish NLRP3rel and other teleosts and mammalian species is shown in Table 6.1.

6.2.2. Analysis of NLRP3rel expression in normal goldfish tissues and non-stimulated goldfish immune cell populations

Assessment of NLRP3rel expression in the tissues of normal goldfish indicated that the highest NLRP3rel mRNA transcript levels were found in goldfish spleen, followed by intestine, gill, brain and kidney. Relatively lower expression levels were observed in heart, liver and muscle (Fig. 6.3A).

I also examined the expression of NLRP3rel in different goldfish immune cell populations including PBLs, kidney-derived neutrophils, splenocytes, monocytes and mature macrophages. The PBLs had the highest NLRP3rel mRNA transcript levels,

followed by macrophages, splenocytes and neutrophils, while the NLRP3rel mRNA levels were lowest in monocytes (Fig. 6.3B).

6.2.3. Analysis of gfNLRP3rel expression in macrophages treated with bacteria and chemical stimuli

Mammalian NLRP3 inflammasome has been reported as the major inflammasome generated after exposure to a wide range of PAMPs, including pore-forming toxins (nigericin), extracellular ATP, LPS and others (424, 425). I examined whether goldfish NLRP3rel can be activated by nigericin, ATP and LPS. As shown in Fig. 6.4, the gfNLRP3rel mRNA levels were significantly up-regulated following treatment of macrophages with nigericin and ATP, but not LPS. However, LPS treatment up-regulated the protein levels of NLRP3rel in goldfish macrophages. There were no changes in the mRNA levels of gfNLRP3rel in macrophages exposed to heat-killed pathogens. In contrast, small but significant decreases in both mRNA and protein levels of gfNLRP3rel were observed when macrophages were exposed to live *M. marinum* (Fig. 6.4).

6.2.4. Recombinant CT-NLRP3rel expression, purification and antibody characterization

To explore the functional activities of gfNLRP3rel, I expressed the rgfCT-NLRP3rel (851-1025 aa, having PRY and SPRY functional domains, as well as most of the C-terminus) in *E. coli* and purified it using the magneHis protein purification system. A single band with the molecular weight of 24.6 kDa including a six-histidine tag, a

thrombin recognition site and a T7 tag at the N-terminus was indicated by SDS-PAGE analysis (Fig. 6.5). The presence of recombinant protein was further confirmed by mass spectrometry (Fig. 6.6) and Western blot using anti-His antibody and rabbit anti-CT-NLRP3rel IgG antibody (Fig. 6.5).

6.2.5. GfNLRP3rel associates with gfASC

To examine the possible association between gfNLRP3rel and its downstream signaling molecule ASC, I co-transfected either GFP-empty or GFP-ASC and DsRed-NLRP3rel into HEK293 cells. The DsRed-NLRP3rel signal was distributed throughout the cytosol of the HEK293 cells. Approximately 20 to 28% of co-transfected cells with DsRed-NLRP3rel and GFP-ASC (three independent experiments) showed “ring” structures, indicating that there was an association between these recombinant molecules (Fig. 6.7).

To further examine the association of gfNLRP3rel and gfASC, I co-expressed either His-empty (control) or His-ASC and GFP-NLRP3rel in HEK293 cells and performed co-IP assays. I first checked the transfection efficiency and recombinant proteins expression in eukaryotic cells using Western blot assay with either anti-His or anti-GFP antibody (Fig. 6.8). As illustrated in Fig. 6.8, the GFP-NLRP3rel was co-precipitated with anti-His antibody when cells were co-transfected with His-ASC, and that His-ASC was also co-precipitated with anti-GFP antibody when cells were co-transfected with GFP-NLRP3rel. In contrast, co-expression of His-empty and GFP-NLRP3rel protein in HEK293 cells did not produce any immune complexes. These results indicate NLRP3rel associated with goldfish ASC.

6.2.6. LDH release in goldfish macrophages in response to nigericin

LDH release is the hallmark of pyroptosis, which results from the inflammasome-induced caspase-1 activation (17, 320). I postulated that nigericin may induce caspase-1 activation, pyroptosis, and pro-inflammatory cytokine processing in goldfish macrophages. To test this, I treated goldfish macrophages with nigericin for 12 h and evaluated the LDH release and caspase-1 activation. Nigericin-induced significant LDH release, that was abrogated when cells were treated with the caspase-1 inhibitor Q-VD-OPH (Fig. 6.9). Treatment of macrophages with nigericin for 12 h induced caspase-1 activation and IL-1 β 1 production that was inhibited by the addition of Q-VD-OPH (Fig. 6.10). These results support the findings of several studies that showed that mammalian caspase-1 blockers inhibited zebrafish (229), sea bass (228), sea bream (197) and carp (426) caspase-1.

6.2.7. gfNLRP3rel and caspase-1 control the IL-1 β 1 and HMGB1 production in nigericin-activated macrophages

I examined the role of gfNLRP3rel and caspase-1 in cytokine processing and production. As shown in Fig. 6.9, nigericin induced the production of both IL-1 β 1 and HMGB1 in macrophages that was blocked by Q-VD-OPH (Fig. 6.10).

6.3. DISCUSSION

Due to the evolutionary differences between the immune system of plants, invertebrates, lower and higher vertebrates, it is not surprising that organisms that rely primarily on innate immunity for host defense, have highly polymorphic NLRs in order to recognize the plethora of different pathogens (427). For example, sea urchins have more than 200 NLR genes (428) and some plants have between 150 and 460 NLRs (*Arabidopsis* and rice, respectively) (429, 430) in contrast to only 22 NLRs in mammals, indicating that NLRs are significantly more polymorphic in invertebrates and lower vertebrates. The decrease in NLR polymorphism in higher vertebrates may have conferred an evolutionary advantage to higher vertebrates. For example, the association between the NLR polymorphism and autoimmune or inflammatory diseases has been well studied and includes Blau syndrome, Crohn's disease and early-onset sarcoidosis (11, 431, 432). The NLRP3 polymorphism has been linked to several disease conditions including the Muckle-Wells syndrome, chronic infantile neurologic cutaneous articular syndrome and familial cold inflammatory syndrome (433), as well as the susceptibility to food-induced anaphylaxis and aspirin-induced asthma (431).

Mammalian NLRs have been well documented as versatile cytosolic sentinels in pathogen recognition, pro-inflammatory cytokine processing, antigen presentation and pyroptosis. NLRs including NLRP1, NLRP3 and NLRC4, form multiprotein inflammasome complexes after recognition of PAMPs and DAMPs. For example, NLRP1 primarily detects toxins of Gram-negative bacteria (*Bacillus anthracis*), the protozoan parasite (*Toxoplasma gondii*), and muramyl dipeptide (MDP) (137, 434–436). The NAIP/NLRC4

detect cytosolic flagellin of Gram-negative bacteria, such as *Salmonella typhimurium*, *Shigella flexneri*, *Pseudomonas aeruginosa* and *Legionella pneumophila* (256–262). The NLRP3 is more of a “generalist” NLR, that recognizes a wide range PAMPs, including bacterial, viral, fungal and protozoan pathogens (425, 437, 438).

The information regarding the regulatory role of NLRP3 in lower vertebrates such as bony fish is limited. The first reported teleost NLRs were identified in zebrafish genome (46). In a comprehensive study, Laing and colleagues (27) identified multiple NLR gene orthologues in zebrafish, including five NLRAs, six NLRBs and several hundred NLRCs. The NLRs are very large molecules and typically have full nucleotide sequences of more than 3, 000 bp, and are highly polymorphic in bony fish, and are relatively difficult to clone. In preliminary experiments, several attempts to obtain a full length sequence of goldfish NLRP3rel using conventional rapid amplification of cDNA ends (RACE-PCR) methods were not successful. Using the goldfish transcriptome database generated in our laboratory, I obtained, for the first time a full sequence of teleost NLRP3rel. The gfNLRP3rel did not share very high aa sequence identity with all the predicted NLRP3s and NLRC3s except NLRP3-like of barbel (84%). Notably, most of the teleost NLRP3s and NLRC3s were computational predicted based on high throughput sequencing database; The only two confirmed NLRC3s were identified in olive flounder (ADX66441.1) and pufferfish (CAG12481.1). Phylogenetic analysis of goldfish NLRP3rel in comparison to NLRC3, NLRP3 and NLRP12 of other organisms revealed that this molecule is most likely an ortholog of NLRP3-like molecule in teleost as the gfNLRP3rel did not cluster with most of the teleost NLRC3s. Based on the polymorphic feature of NLRP and NLRC family

molecules in teleost, there is also a possibility that gfNLRP3rel could be an ortholog of NLRC3 or NLRC3-like molecule.

The goldfish NLRP3rel consists of 3,851 bp with a 1,030 aa ORF including a fish specific NACHT-associated domain, NACHT domain, PRY domain, SPRY domain and LRRs. Surprisingly, the goldfish NLRP3rel did not possess a PYD domain at the N-terminus. The mammalian NLRP subfamily is separated from other NLR subfamilies because it has a PYD domain. The PYD domain of mammalian NLRPs is important for the interaction with the downstream signaling adaptor molecule ASC. Since goldfish NLRP lacks the PYD domain, I postulated that the PYR and SPRY domains are the effector domains in goldfish. Supporting this postulate are the reports of Chae and co-workers (439) and Papin and co-workers (440), which indicated that PYD and SPRY and PYR are functionally similar in mammals. In non-activated cells, the NACHT and LRR domain are bound together rendering the NLRP3 inactive, and upon detection of PAMPs, the LRR domain changes its conformation causing the oligomerization of NACHT domain to form an active platform (425, 441). Subsequently the oligomerized NACHT recruits ASC via PYD-PYD interaction and further activates pro-caspase-1 through direct CARD-CARD bindings (425, 441). The activated caspase-1, cleaves pro-IL-1 β and pro-IL-18 to generate biological active IL-1 β and IL-18 (144, 164, 425).

To examine the regulation of NLRP3rel in goldfish macrophages, I examined the association of gfNLRP3rel and gfASC using a co-transfection approach and visualizing the association by confocal microscopy. I observed that gfNLRP3rel formed a “ring” structure around the co-expressed ASC, suggesting the gfNLRP3rel associated with

gfASC. Surprisingly, the gfNLRP3rel- and ASC-formed “ring” structure was phenotypically different from the inflammasome macromolecular complex “ring” structure in LPS-primed THP-1 cells, where the NLRP3 formed a smaller ring-like structure within the ASC ring, rather than surrounding ASC specks as observed in goldfish (442). These differences imply that the teleost NLRP3rel molecule and ASC inflammasome assembly may be different from the mammalian NLRP3 inflammasome assembly. The NLRP3rel and ASC association was further confirmed using co-IP. Given that the gfASC can also associate with gfcaspase-1, these results suggest that the NLRP3rel molecule participates in inflammasome formation in teleosts.

Nigericin is commonly used as an activator of mammalian NLRP3 inflammasome, caspase-1, and pro-inflammatory cytokine processing and production (149, 150). Nigericin causes the efflux of intracellular K⁺ that results in the induction of NLRP3 inflammasome assembly (361, 443, 444), and was shown to induce enhanced inflammatory responses in Japanese pufferfish (116). To examine the activators of NLRP3rel in goldfish, I treated goldfish primary kidney macrophages with nigericin, ATP, LPS, and two fish pathogens, heat-killed *A. salmonicida* and heat-killed or live *M. marinum*. I observed that gfNLRP3rel expression, like its mammalian counterpart, was induced by nigericin, ATP and LPS, but not by heat-killed Gram negative or Gram positive bacteria. Interestingly, gfNLRP3rel mRNA levels were down-regulated when macrophages were treated with live *M. marinum*. That live *M. marinum* did not activate the expression of goldfish macrophage NLRP3rel may be an evasion strategy by the mycobacteria to avoid being killed by activated macrophages. It has been shown that *M.*

tuberculosis has evolved mechanisms to interfere with NLRP3 inflammasome function in mammals (445), using the ESX-1 and ESX-5 secretion system to avoid host cell death and NLRP3 inflammasome activation (446–448).

The end result of the NLRP3 pathway is the release of pro-inflammatory cytokines, including IL-1 β and IL-18 (207), as well as pyroptosis that promotes the translocation of HMGB1 from nucleus into cytoplasm and its release into the extracellular milieu (251, 423). Consistent with what is known about the inflammasome activation in mammals, my results showed that IL-1 β and HMGB1 were produced after treatment of goldfish macrophages with nigericin, and that the caspase inhibitor blocked the nigericin-induced IL-1 β and HMGB1 production.

In this chapter, I identified and functionally characterized for the first time the gfNLRP3rel molecule in a lower vertebrate. I provided evidence that nigericin induced the expression of gfNLRP3rel in goldfish macrophages, and that gfNLRP3rel associated with downstream molecules of the inflammasome signaling pathway. Thus, my results suggest that the gfNLRP3rel molecule is functionally similar to the NLRP3 inflammasome of mammals. Further studies are required to fully elucidate the NLRP3rel inflammasome machinery in bony fish macrophages.

Table 6.1. Percent identity between goldfish NLRP3rel and NLRC3, NLRP3 and NLRP12 homologous of other organisms (aa)

Species	Identity (%)
Barbel NLRP3-like isoform X1	86%
Barbel NLRP3-like isoform X2	86%
Barbel NLRP3-like isoform X3	86%
Barbel NLRP3-like isoform X4	86%
Barbel NLRP3-like	84%
Barbel NLRP12-like	64%
Zebrafish NLRP12-like	62%
Barbel NLRC3-like	41%
Northern pike NLRC3-like	40%
Zebrafish NLRC3-like	40%
Atlantic salmon NLRP3-like	39.1%
Atlantic herring NLRP12-like	38%
Zebrafish NLRP3-like	37.7%
Salmon NLRP12-like isoform X2	37%
Mexican tetra NLRP12-like	37%
Herring NLRP3-like	36.7%
Olive flounder NLRC3	35%
Pufferfish NLRC3	31.3%
Atlantic salmon NLRP3 isoform X1	30.6%
Chick NLRC3 isoform X2	26.7%
Chick NLRC3 isoform X3	26.4%
Chick NLRC3 isoform X1	26.3%
Nile tilapia NLRC3	25.9%
Mouse NLRC3	25.8%
Human NLRP12	25.8%
Human NLRC3	25.7%
Mouse NLRP12	25.1%
Zebrafish NLRC3	24.7%
Mouse NLRP3	23.8%
Human NLRP3	23.5%
Chick NLRP3	17.8%

(Continued)

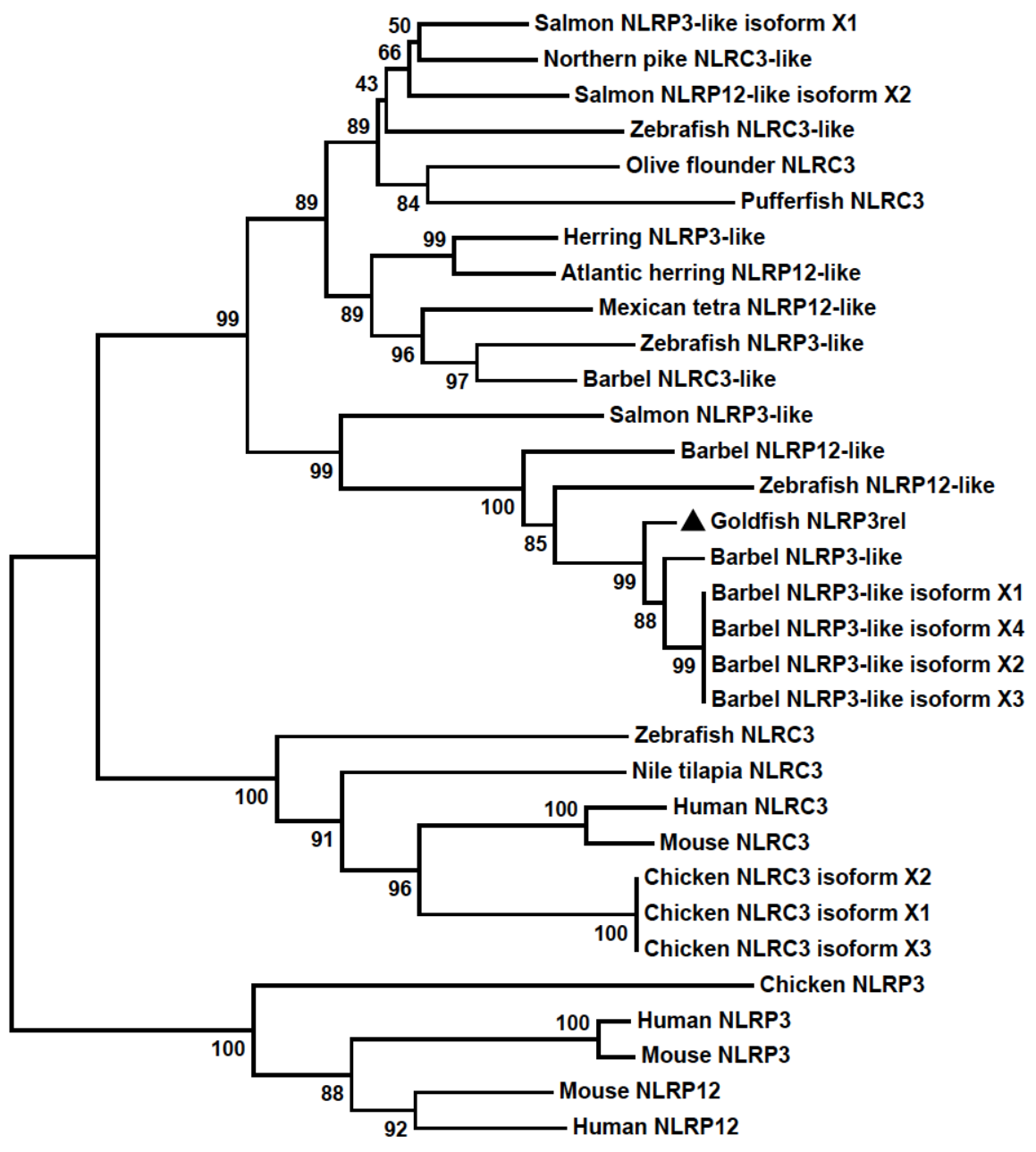
```

2422 aaactgaaaatcctggacctcagtgacaataatctagaggacgaaggagtaaaaatcctctctgctgggctgaggag
    K L K I L D L S D N N L E D E G V K I L S A G L R S
2500 gcaaagtgtcatcttgaagttctgaaactctcaggctgtcagattcaagaaggagtttgaagttgctgtcatctttg
    A K C H L E V L K L S G C Q I Q E G V L K L L S S L
2578 aaagaagtctgagagaactggacctgcagtataatgtcctcggaaagatcctggaaaagaaagtttgtgtgaaagtt
    K E S L R E L D L Q Y N V L G K I L E K K V C V K V
2656 cgtgtactgaaggataagttgcccttactgagaatttactgaggaggtctgcaaccacaaccaggactgtacaaa
    R V L K D K L P L L R I Y T G G V C N H K P G L Y K
2734 tatgtgtcatgtctcacctttgacctcagacggctaacgaatacctctgtctgagcgaggacaacactgtagctggt
    Y A V M L T F D P Q T A N E Y L C L S E D N T V A V
2812 cgtaagagagagaggcaacagtttctgctagtaataagatttgacaagtgcaaccaggtctgtgctgccagcgg
    R K R E R Q Q F P A S N E R F D K C N Q V L C C Q P
2890 ctgtcaggacgtgtcttctttacgggtggtgtgatcgggacaggggtgaacattggtgtggcctgtaagggaaatcaag
    L S G R C F F T V D V I G T G V N I G V A C K G I K
2968 aggaaaggtgcagatgacaccgtacgtctgggacgcaataagatgtcatgggtgtttatggttctcaaaaactgtatgt
    R K G A D D T V R L G R N K M S W C L C C S K T V C
3046 gtggctcatgacaaaataactgaatcactaactaaaccgcttcaaacagagtccaccagaaaactcgggtgtgttcatg
    V A H D K I T E S L T K P L Q T E S T R K L G V F M
3124 gaccgggaggctggttctgtttccttctataagttgagcccagactcagagcctgaactccttgcacatgtttgatgca
    D R E A G S V S F Y K L S P D S E P E L L H M F D A
3202 gagtttctcaggaccaggaactttatgctgcttccagttcaggaaccagacagctcagtcctggttaaggcaagca
    E F P Q D Q E L Y A A F S I Q E P D S S V R L R Q A
3280 tcactaCaacCTATACCTTTACAGTTACGGTTTGTGCTCCAGACATGAATGATGCCTCAAATTAGGAGAGTGTGATGT
    S L *
3358 TACAGTAAAAAACCCTGGCAGACCTACTGAAAGAAGCCTGCTGGGAAAAGCACCTGCTGTAGAAGATCAGCAAGTGTTC
3436 AACATGACTTCATCTTTATTATTGTGCGCTTTATAAACCCTAAACCACAGTACTATAGCATCTTTTGTCTCATATCA
3514 GTTAACATGTCTTTAGATTTTAATATCTCAGTGTAACCTGGTTTCATTTAATCGAAAATAGAGCTTTACTAATTTGGATC
3592 TGATGCAGTTTCTTTGTACTGGGCTGATTTTCAAACCTGCCATCCCAAACCTATACGACTTACTTTCTTCTGCGGGA
3670 CAATACAAGAAGATACTTTGAAGACACTTTTTTCTCTCTCTGTACAGTGGAAGTTAATAGGGTCCAATATTTTTGG
3748 CTCCCAACATTTCTGCAAAGTATTTTATTGTATGTTCCCTATAAATACCACCTGCTTATTTGAAACCTAAATGTTAAA
3826 TCACATTTCCGTAATCAAATTTTTTT

```

Figure 6.1. Nucleotide and predicted aa sequence of goldfish NLRP3rel cDNA.

The start and stop codons are boxed, fish-specific NACHT associated domain is highlighted in light grey, the NACHT domain is highlighted in dark grey, the leucine rich repeats are underlined, SPRY-associated domain is double underlined and the SPRY domain is wave underlined. The RNA instability motif is highlighted in bold (**ATTTA**).



0.1

Figure 6.2. Phylogenetic analysis of goldfish NLRP3rel and other mammalian and teleost NLRC3, NLRP3, NLRP12 and their homologues.

NLRP3rel amino acid sequences were aligned by using CLUSTAL-W program and unrooted phylogenetic tree was constructed using the neighbor-joining method of the MEGA 6.06 program. The tree was bootstrapped 10,000 times. The full length of NLRP3 or its homologous amino acid sequences used were: Zebrafish NLRP3-like XP_003200356.3, Atlantic salmon NLRP3-like XP_014057972.1, Herring NLRP3-like XP_012693427.1, Herring NLRP3-like isoform X1 XP_016326144.1, Herring NLRP3-like isoform X2 XP_016326146.1, Herring NLRP3-like isoform X3 XP_016326147.1, Herring NLRP3-like isoform X4 XP_016326148.1, Atlantic salmon NLRP3 isoform X1 XP_014013679.1, Chick NLRP3 AHY19021.1, Mouse NLRP3 NP_665826.1, Human NLRP3 AAI43360.1, Zebrafish NLRC3-like XP_017211127.1, Zebrafish NLRC3 XP_009295904.1, Barbel XP_016386998.1, Northern pike XP_012986783.1, Nile tilapia NLRC3 XP_003438651.1, Olive flounder NLRC3 ADX66441.1, Pufferfish NLRC3 CAG12481.1, Chick NLRC3 isoform X1 XP_015150161.1, Chick NLRC3 isoform X2 XP_015150162.1, Chick NLRC3 isoform X3 XP_015150163.1, Mouse NLRC3 Q5DU56.2, Human NLRC3 ACP40993.1, Salmon NLRP12-like isoform X2 XP_014000883.1, Atlantic herring NLRP12-like XP_012682165.1, Mexican tetra NLRP12-like XP_007235406.1, Barbel NLRP12-like XP_016420278.1, Zebrafish NLRP12-like XP_017213894.1, Mouse NLRP12 AAI16254.1, Human NLRP12 AAH28069.1.

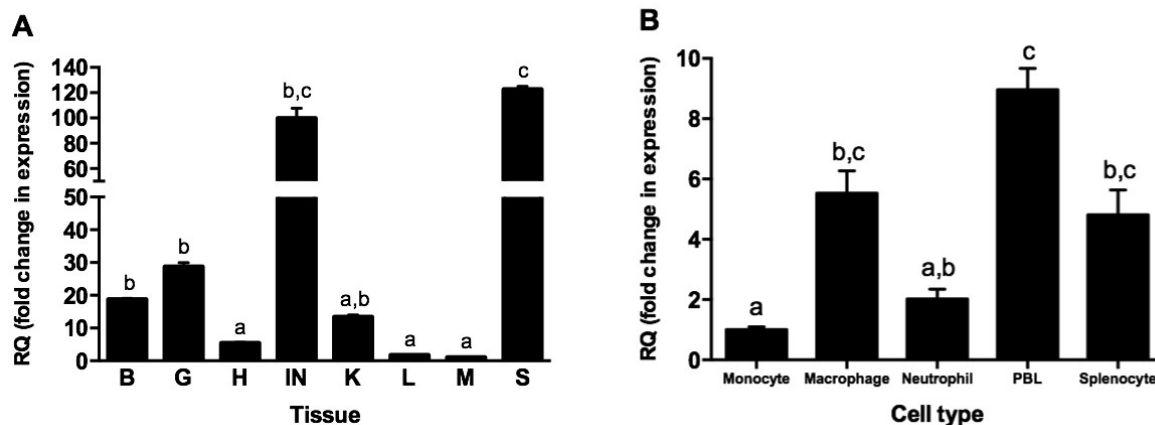


Figure 6.3. Quantitative analysis of goldfish NLRP3rel expression in different tissues and immune cell populations obtained from normal goldfish.

(A) Goldfish NLRP3rel tissue distribution analysis. The expression of goldfish NLRP3rel was measured relative to endogenous control gene, elongation factor 1 alpha (EF-1 α). Relative tissue expression was determined using tissues from four fish ($n = 4$), and Q-PCR was done in triplicate for each tissue. All results were normalized against the muscle NLRP3rel mRNA levels (L = liver, M = muscle, H = heart, G = gill, K = kidney, I = intestine, S = spleen, B = brain). (B) Goldfish NLRP3rel expression in different immune cell populations. Relative immune cell population expression was determined using cells from four fish ($n = 4$), and Q-PCR was done in triplicate for each immune cell population. All results were normalized against the monocyte NLRP3rel mRNA levels. Statistical analysis was performed using one-way ANOVA followed by Dunnett's post-hoc test. Different letters above each bar denote statistically different ($P < 0.05$), and the same letter indicates no statistical differences between groups.

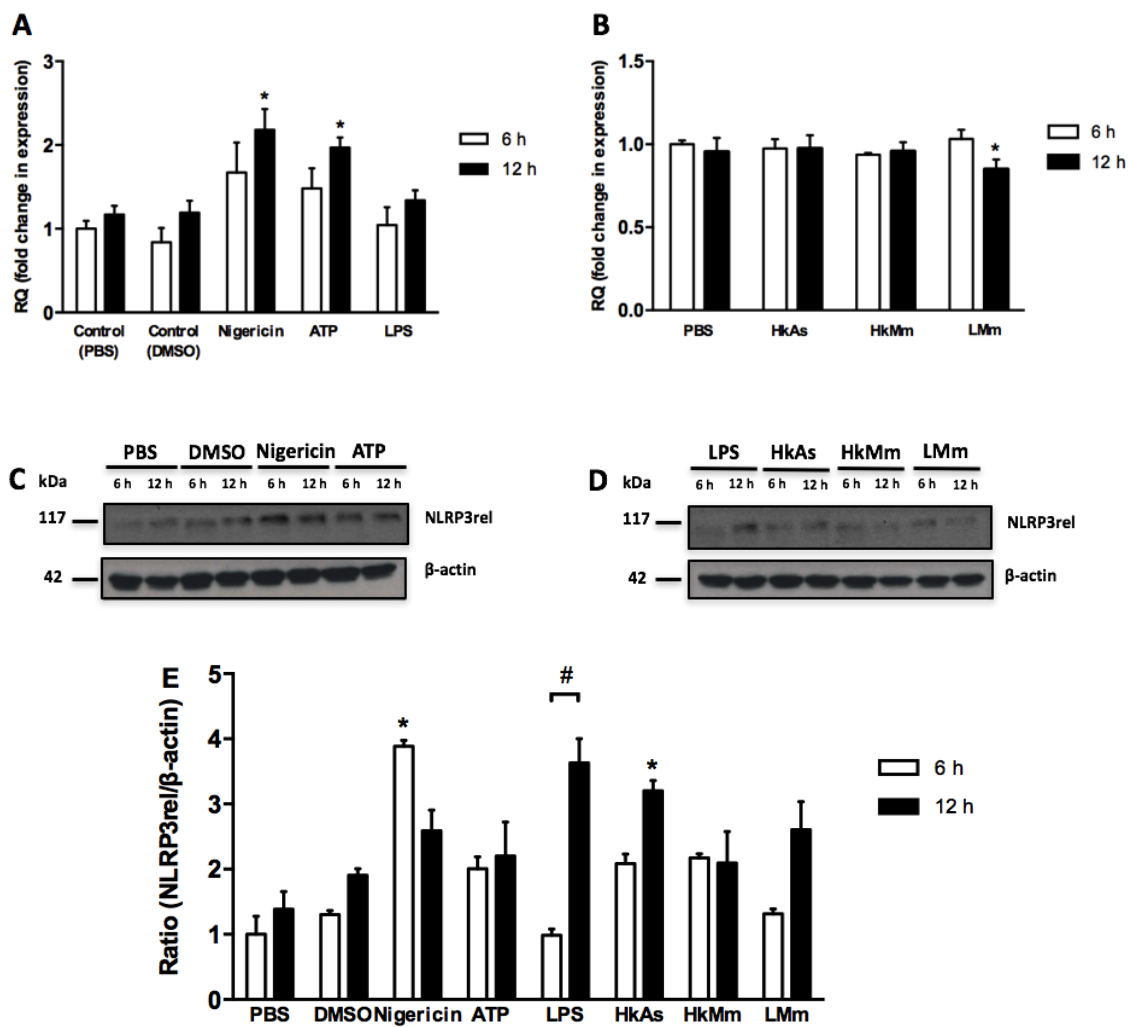


Figure 6.4. Quantitative expression and Western blot analysis of goldfish NLRP3rel in macrophages treated with different stimuli.

(A and B) Quantitative expression of goldfish NLRP3rel in macrophages treated with either PBS or DMSO (controls), nigericin, ATP, lipopolysaccharide (LPS), heat-killed *A. salmonicida*, heat-killed or live *M. marinum*. The expression of NLRP3rel was examined relative to the endogenous control gene, elongation factor 1 alpha (EF-1 α). The expression values were normalized against those of PBS at 6 h. The results are shown as the mean \pm SEM of macrophage from cultures established from four individual fish (n = 4). The asterisk (*) indicates the significant difference at $P < 0.05$ compared to the 6 h or 12 h time point. (C and D) Western blot analysis of goldfish NLRP3rel in macrophages treated with either PBS or DMSO (controls), nigericin, ATP, LPS, heat-killed *A. salmonicida*, heat-killed or live *M. marinum*. The treated macrophages were washed three times with PBS and lysed with 100 μ L of NP-40 buffer and then subjected to Western blot analysis using anti-CT-NLRP3rel antibody or anti- β -actin antibody. β -actin was used as a loading control. Results are from a representative experiment that was repeated three times showing similar results. (E) Quantified ratios of NLRP3rel protein to β -actin in treated macrophages, compared to PBS at 6 h. The results are shown as the mean \pm SEM of macrophage from cultures established from three individual fish (n = 3). The asterisk (*) indicates the significant difference at $P < 0.05$ compared to the PBS at 6 h or 12 h time point (HkAs, heat-killed *A. salmonicida*; HkMm, heat-killed *M. marinum*; LMm, live *M. marinum*). The pound sign (#) denotes the significant difference at $P < 0.05$ between 6 h and 12 h treated groups.

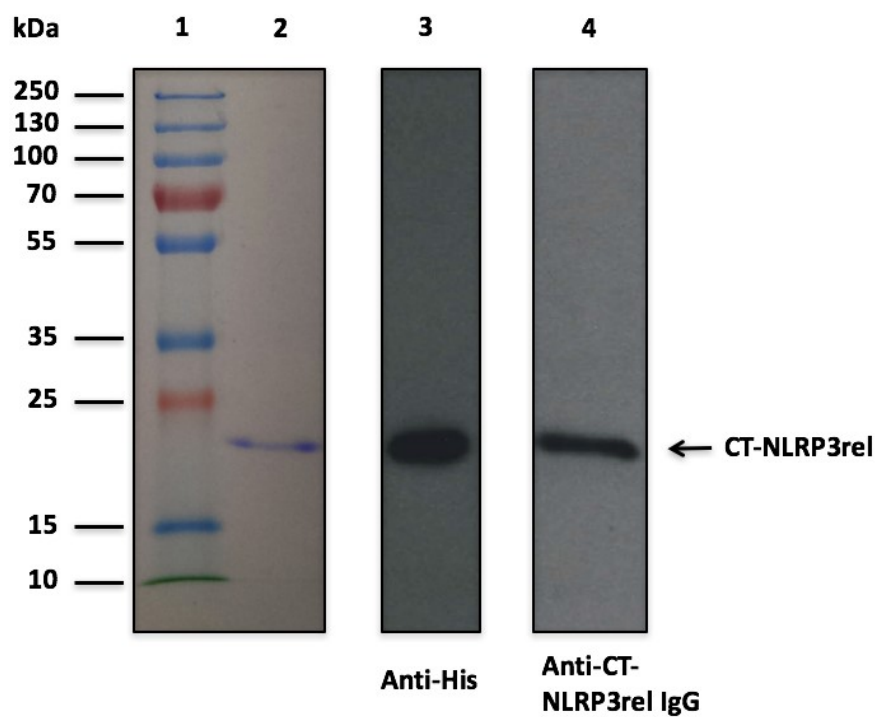


Figure 6.5. SDS-PAGE and Western blot analysis of recombinant CT-NLRP3rel.

Lane 1: protein ladder; Lane 2: SDS-PAGE analysis of Coomassie blue stained of purified recombinant CT-NLRP3rel; Lane 3 and 4: Western blot of purified recombinant CT-NLRP3rel using anti-His antibody and anti-CT-NLRP3rel IgG antibody, respectively.

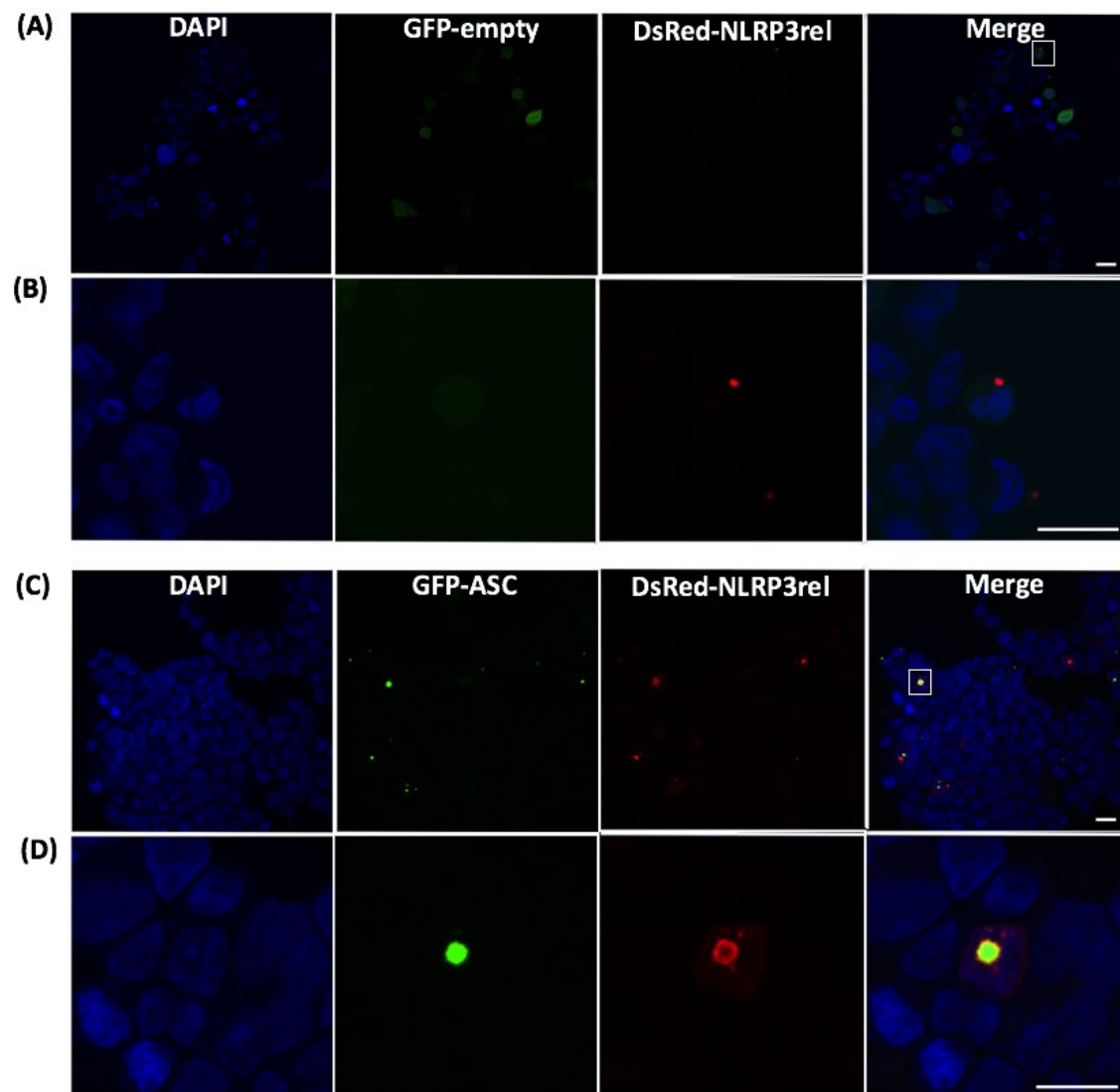
```

LTFDPQTANE YLCLSEDNTV AVRKR ERQQF PASNERFDKC NQVLCCQPLS
GRCFFTVDVI GTGVNIGVAC KGIKRRKGADD TVRLGRNKMS WCLCCSKTVC
VAHDKITESL TKPLQTESTR KLGVM DREA GSVSFYK LSP DSEPELLHMF
DAEFPQDQEL YAAFSIQEPD SSVRL

```

Figure 6.6. Mass spectrometry analysis of SUMO-CT-NLRP3rel protein.

86/175 amino acids (49% coverage) were achieved out of total 161 spectra. The purified SUMO-CT-NLRP3rel was fractionated with SDS-PAGE gel and then the excised gel digests were analyzed by nano LC/MS/MS with a Waters NanoAcquity HPLC system interfaced to a ThermoFisher Q Exactive. Peptides were loaded on a trapping column and eluted over a 75µm analytical column at 350nL/min; both columns were packed with Jupiter Proteo resin (Phenomenex). The mass spectrometer was operated in data-dependent mode, with MS and MS/MS performed in the Orbitrap at 70,000FWHM and 17,500 FWHM resolution, respectively. The fifteen most abundant ions were selected for MS/MS. Data were searched using a local copy of Mascot and the Mascot DAT files were parsed into the Scaffold software for validation, filtering and to create a non-redundant list per sample. Data were filtered using a minimum protein value of 90%, a minimum peptide value of 50% and requiring at least two unique peptides per protein. The highlighted area shows the sequences confirmed by MS/MS.



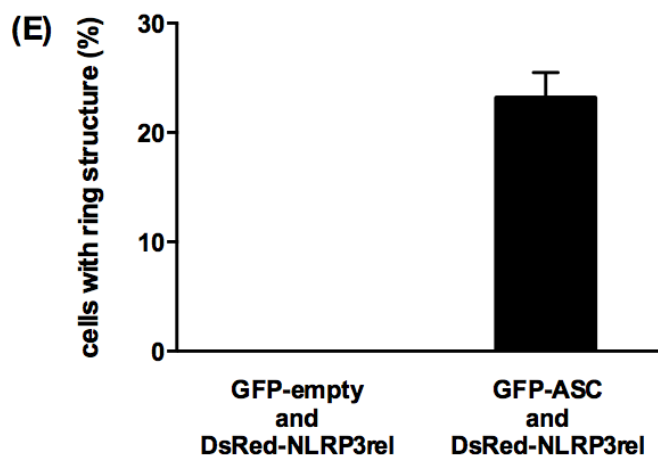


Figure 6.7. Confocal microscopy analysis of goldfish NLRP3rel and ASC in HEK293 cells. HEK293 cells (1×10^5 /well) were co-transfected with $1 \mu\text{g}$ of either GFP-empty or GFP-ASC and DsRed-NLRP3rel. After 48h, cells were washed twice with PBS before being fixed in 4% PFA for 15 min at room temperature. Cells were mounted on slides using Fluoroshield mounting media containing DAPI. Slides were viewed using a laser scanning confocal microscope. Green fluorescence, red fluorescence, and blue fluorescence were visualized in the same field (Merge). Cells were co-transfected with GFP-empty and DsRed-NLRP3rel as control (A and B). Non co-localized green and red signals were detected. The boxed area of Figure 6.7A was enlarged and shown as Figure 6.7B. Cells were co-transfected with GFP-ASC and DsRed-NLRP3rel and “ring” structures were detected (C and D). The boxed area of Figure 6.7C was enlarged and shown as Figure 6.7D. Quantification of “ring” structure per 100 co-transfected cells (E). Image and quantification results are depicted from a representative field taken after three independent experiments were performed. Scale bars equal $10 \mu\text{m}$.

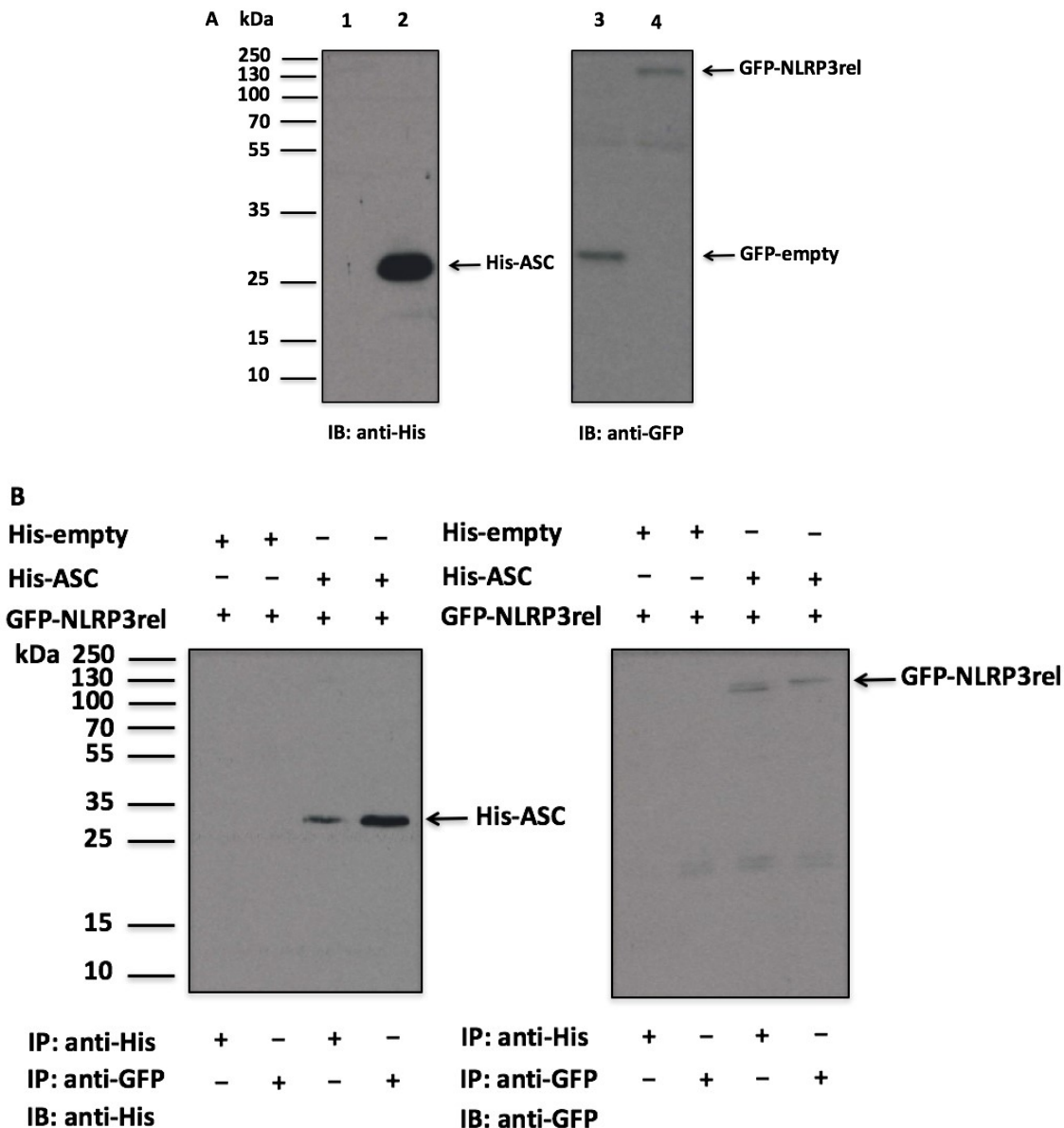


Figure 6.8. Goldfish NLRP3rel associates with ASC in HEK293 cells.

(A) Western blot analysis of His-empty, His-ASC, GFP-empty and GFP-NLRP3rel in HEK293 cells. Lane 1 and 2: Western blot analysis of His-empty and His-ASC using anti-His antibody, respectively. Lane 3 and 4, Western blot analysis of GFP-empty and GFP-NLRP3rel using anti-GFP antibody, respectively. (B) The total cell lysate was prepared from co-transfected cells and incubated with anti-His antibody or anti-GFP antibody. The precipitated immune complexes were subjected to western blot analysis using either anti-GFP antibody or anti-His antibody, respectively. Control samples are represented by cells co-transfected with His-empty and GFP-NLRP3rel. (IP = immunoprecipitation; IB = immunoblotting)

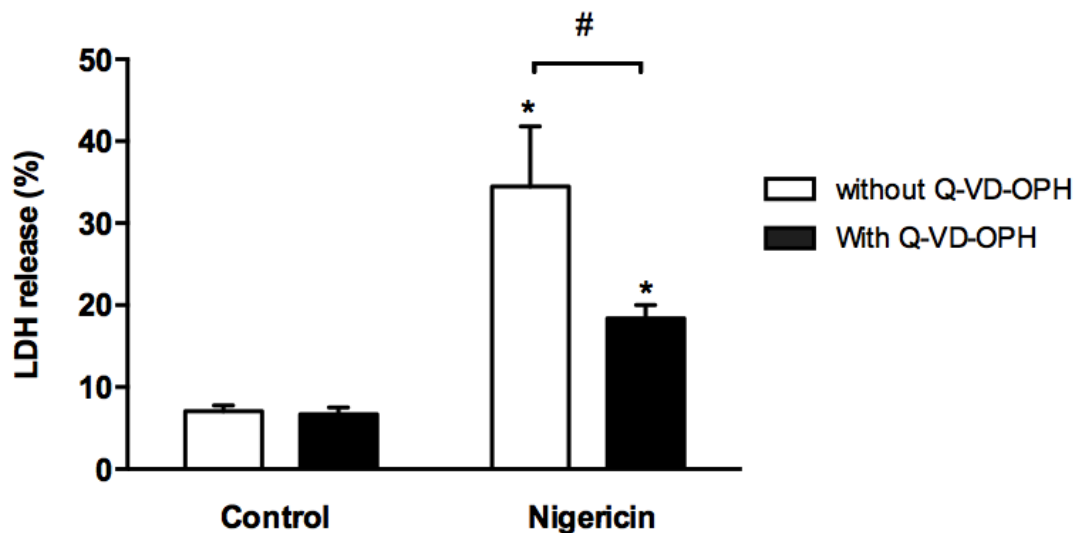


Figure 6.9. Evaluation of LDH release in goldfish macrophages treated with nigericin for 12 h with or without a pre-treatment of pan-caspase inhibitor (Q-VD-OPH) for 3 h. The induced LDH release was determined by LDH cytotoxicity assay kit. The results are mean \pm SEM of primary macrophage cultures established from four individual fish ($n = 4$). (*) denotes significantly different ($P < 0.05$) from the control group (untreated) and Tukey's post-hoc analysis. The pound sign (#) denotes the significant difference at $P < 0.05$ between with and without Q-VD-OPH treated groups.

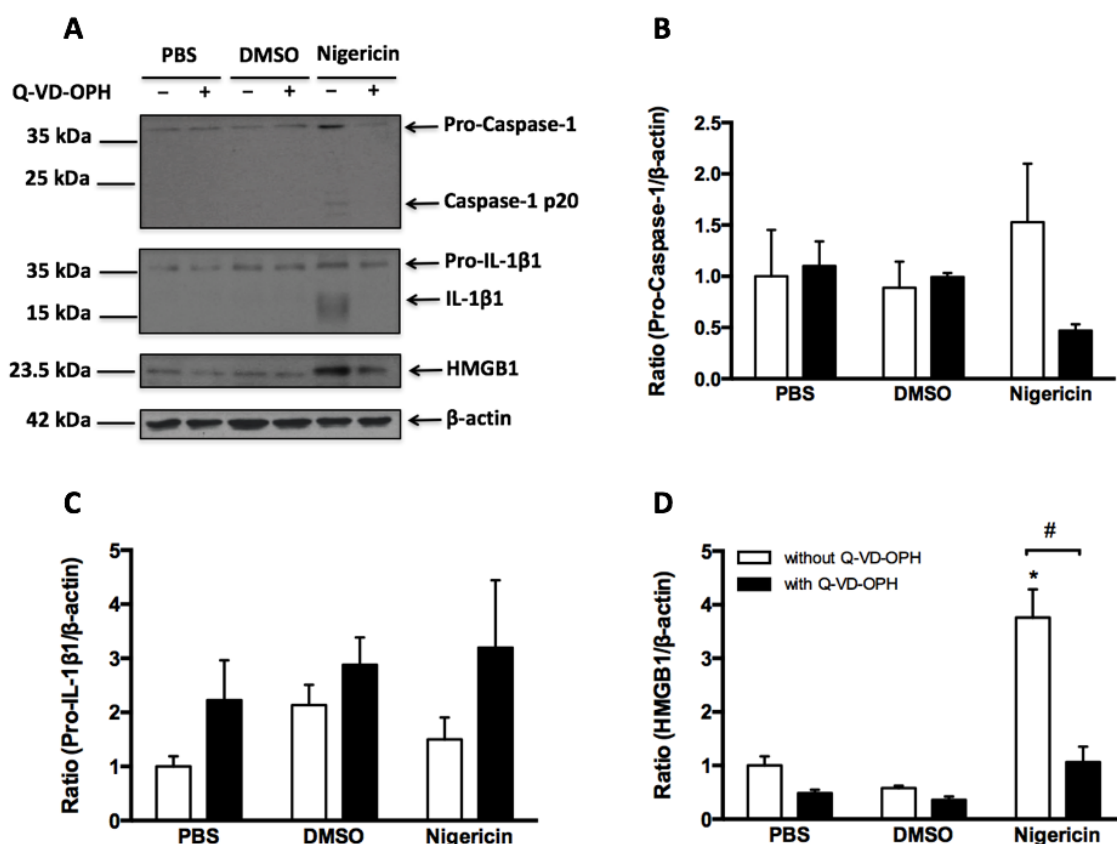


Figure 6.10. Western blot and quantitative densitometry analysis of Caspase-1, HMGB1 and IL-1 β 1 in goldfish macrophages treated with either PBS, DMSO or nigericin for 12 h with or without pre-treatment of 100 μ M Q-VD-OPH for 3 h. (A) Western blot analysis of goldfish Caspase-1, HMGB1 and IL-1 β 1 in macrophages treated with either PBS or DMSO (controls), nigericin. Each treatment group consisted of 1×10^6 cells in the final volume of 500 μ L of complete medium. After treatment, cells were washed three times with PBS and lysed with 100 μ L of NP-40 buffer and then subjected to western blot analysis using anti-caspase-1 antibody or anti-HMGB1 antibody or anti-IL-1 β 1 antibody. β -actin was used as a loading control. Results are from a representative experiment that was repeated three times showing similar results. (B, C and D) Quantified ratios of caspase-1 (B), Pro-IL-1 β 1 (C) and HMGB1 (D) protein to β -actin in treated macrophages, compared to the PBS without Q-VD-OPH treated group. The results are shown as the mean \pm SEM of macrophage from cultures established from three individual fish ($n = 3$). The asterisk (*) indicates the significant difference at $P < 0.05$ compared to the PBS without Q-VD-OPH treated group. The pound sign (#) denotes the significant difference at $P < 0.05$ between with and without Q-VD-OPH treated groups.

CHAPTER VII: CHARACTERIZATION OF APOPTOSIS-ASSOCIATED SPECK-LIKE (ASC) MOLECULE OF THE GOLDFISH (*Carassius auratus* L.)¹

7.1. INTRODUCTION

ASC was first identified as TMS-1, that confers a survival advantage by allowing cells to escape from apoptosis (205). The ability of ASC to regulate apoptosis has been shown to be primarily associated with the caspase recruitment domain (CARD), via homologous CARD-CARD domains interaction (206). As a CARD-and PYD-containing molecule, ASC was shown to function as an adaptor molecule that transduces the signaling after inflammasome activation in mammals (210, 449–451). The ASC has been cloned in zebrafish (*Danio rerio*) (452), mandarin fish (*Siniperca chuatsi*) (215) and Japanese flounder (*Paralichthys olivaceus*) (216). However, the functional roles of ASC in the NLR signaling pathways in bony fish remain to be elucidated.

Inflammasomes have been identified as a family of multi-protein complexes that are formed upon recognition of PAMPs and DAMPs. The recognition of a diverse range of microbial, stress and damage signals by inflammasomes results in direct activation of caspase-1 through ASC. Activated caspase-1 processes the cytosolic precursors of IL-1 β and IL-18, thus allowing for maturation and eventual secretion of the biologically active

¹ A version of this chapter has been published: Xie, J., Belosevic, M., 2016. Function characterization of apoptosis-associated spec-like protein (ASC) of the goldfish (*Carassius auratus* L.). Developmental and Comparative Immunology 65:201-210.

proteins. The inflammasome signaling pathway also induces inflammatory cell death, known as pyroptosis (17, 313, 453). The results of recent studies indicated that during pyroptosis, there was translocation of HMGB1 protein from the nucleus into the cell cytoplasm, and eventual secretion of the HMGB1 by immune cells in response to a variety of exogenous and endogenous danger signals (251, 423). Importantly, genetic deletion of inflammasome components in mammalian cells severely impaired HMGB1 release during endotoxemia or bacteriemia (251, 423). Although there are no specific reports on the functional characterization of inflammasomes in bony fish and the existence of teleost inflammasome remains controversial, a lot of automated computational predictions of NACHT, LRR and PYD domains-containing protein (NLRP) isoforms are present in the Genbank database, such as NLRP3 (XP_017212365.1), NLRP3X1 (XP_017206752.1), NLRP12 (XP_009299711.1), NLRP12-like (XP_009289652.1) and their homologues in zebrafish. In addition, the inflammasome downstream proteins have been identified in bony fish, including caspase-1 in zebrafish and seabream (197, 227, 229) and functional HMGB1 protein in the goldfish (see Chapter VIII) (194).

In addition to the inflammasome pathway, ASC is involved in NOD-like receptor signaling pathway, by interacting with another CARD domain molecule, RIP2 (104, 214). In mammals, it has been demonstrated that ASC up-regulated NF- κ B activation upon co-transfection with other PYD family proteins, such as cytopyrin and PYRAIN-containing Apaf-1-like proteins (PYPAF1-7) (177, 182, 213). ASC was shown to also down-regulate NF- κ B by modifying RIP2 interaction with pro-caspase-1 after LPS stimulation (104).

Moreover, an ASC-RIP2 axis has been proposed for the generation of PGE₂ in patients diagnosed with chronic adult periodontitis (214).

In Chapter V, I reported on the functional characterization of goldfish RIP2 and showed that it played a central role in the regulation of NOD1 and NOD2 pathways, by mediating the downstream molecules following the exposure of macrophages to Gram-positive and Gram-negative bacteria. Given that ASC appears to be a central molecule in the regulation of both the inflammasome and NOD1/NOD2 pathways in mammals, I examined its role in teleost fish by first elucidation the gfASC cDNA sequence followed by the quantification of its expression in tissues and immune cell populations obtained from normal goldfish, and after exposure of macrophages to bacterial pathogens. Subsequently the associations of the recombinant proteins, rgfASC and rgfRIP2 and rgfASC and caspase-1 of the goldfish, were also examined using cross-linking and co-immunoprecipitation assays and/or confocal microscopy.

7.2. RESULTS

7.2.1. Sequence analysis and characterization of gfASC

The gfASC cDNA was identified by transcriptomic analysis of goldfish spleen obtained from fish infected with *M. marinum*. It consisted of 869 bp with a 603 bp ORF encoding a polypeptide of 200 aa, a 5' untranslated region (UTR) of 57 bp and 3' UTR of 209 bp (Fig. 7.1). No signal peptide was predicted. Sequence analysis of the UTR regions revealed the presence of a RNA instability region (ATTTA) in the 3' UTR (Fig. 7.1). Pfam analysis indicated that the predicted protein contained a PYRIN domain (6-84 aa) and

CARD domain (116-199 aa) (Fig. 7.1). Theoretical isoelectric point (pI) and molecular mass of goldfish ASC was 5.61 and 22 kDa, respectively. Phylogenetic analysis revealed goldfish ASC shared the closest relationship to that of zebrafish among all the fish species analyzed. The ASC proteins of the fish species branched independently to the ASCs of the other higher vertebrates, including African clawed frog, mouse and human (Fig. 7.2). Surprisingly, goldfish ASC did not share very high amino acids identity with other teleost and mammalian species (Table 7.1).

7.2.2. Analysis of ASC expression in normal goldfish tissues

The expression levels of ASC in various tissues including brain, gill, heart, intestine, kidney, liver, muscle and spleen were investigated using Q-PCR. The results showed gfASC transcripts were ubiquitously expressed in all examined tissues and the highest and lowest expressions were detected in spleen and muscle, respectively (Fig. 7.3).

7.2.3. Analysis of ASC expression in non-stimulated goldfish immune cell populations

The expression level of ASC was determined in different goldfish immune cell populations (Fig. 7.4). The cell population examined included PBLs, kidney-derived neutrophils, splenocytes, and kidney-derived monocytes and mature macrophages. As shown in Fig. 7.4, the highest expression levels of ASC were in mature macrophages, lower mRNA levels were observed in PBLs, monocytes and splenocytes, while the lowest ASC mRNA levels were detected in the neutrophils.

7.2.4. Analysis of gfASC expression in macrophages treated with bacteria and chemical stimuli

ASC has been well documented as an adaptor molecule involved in inflammasome assembly, caspase activation and pro-inflammatory cytokine processing (207, 210, 211). Given that inflammasomes can be activated by a wide range of PAMPs and DAMPs (450), I examined whether gfASC was activated by the inflammasome activators, LPS, nigericin and ATP. As shown in Fig. 7.5A, the ASC mRNA levels were significantly up-regulated only when macrophages were treated with nigericin, and not by the other two reagents (Fig. 7.5A). Interestingly, there were no changes in the mRNA levels of gfASC in macrophages exposed to either heat-killed or live pathogens (Fig 7.5B). The gfASC protein level was also up-regulated when macrophages were treated with nigericin (Fig. 7.5C and E) and heat-killed *A. salmonicida* and *M. marinum* (Fig. 7.5D and E).

7.2.5. Recombinant gfASC expression, purification and antibody characterization

To examine the function of gfASC, I expressed the rgfASC in *E. coli* and purified it using the magneHis protein purification system. A single band with the molecular weight of approximately 40 kDa including a six-histidine tag and SUMO fusion protein at the N-terminus was indicated by SDS-PAGE analysis (Fig. 7.6). The recombinant protein identity was further confirmed by Western blot analysis using anti-His antibody, rabbit anti-rgfASC IgG and mass spectrometry (Figs. 7.6 and 7.7).

7.2.6. Co-localization analysis of rgfASC

In mammals, ASC was originally described as a speck-like molecule as it was observed as ASC foci under fluorescent microscope (454). To determine whether goldfish ASC formed specks, I transfected GFP-empty and GFP-gfASC into HEK293 cells; The aggregated ASC as foci structures similar to those reported in mammals were observed (Figs. 7.8A and 7.8B). In addition, expression of GFP-ASC and DsRed-ASC in HEK293 cells resulted in the oligomerization and co-localization of GFP-ASC and DsRed-ASC, indicating rgfASC can oligomerize and co-localize as a speck (Fig. 7.8B). No co-localized GFP-empty and DsRed-ASC specks were observed when the cells were co-transfected with the GFP-empty and DsRed-ASC (Fig. 7.8A). Trials to detect the oligomerized speck structure using anti-ASC-IgG and goat anti-Rabbit-IgG Cy5 conjugated antibodies in non-stimulated and stimulated goldfish macrophages were unsuccessful, as a strong non-specific signal was detected in goldfish macrophages.

7.2.7. Oligomerization of goldfish rgASC

I performed *in vitro* cross-linking studies to determine whether the rgfASC was capable of multimerization, which has been reported for mammalian ASC (210, 211, 451). The cells transfected with either His-empty or His-ASC were incubated in the absence or in the presence of the cross linker DSS, resolved by SDS-PAGE and visualized by Western blot analysis using anti-His or anti-rgfASC IgG antibodies. The results showed

that non cross-linked rgASC resolved as a monomer and the cross-linked rgASC appeared to be a multimer (Fig. 7.9).

7.2.8. RgfASC associates with RIP2 and caspase-1

The CARD domain-containing molecules RIP2 and caspase-1 have been reported to associate with ASC in mammals (104, 214). To investigate the associations between ASC and RIP2 and caspase-1, I performed co-IP assays after transfection of either His-empty (control) or His-ASC with GFP-RIP2 or GFP-caspase-1 in HEK293 cells. Following the transfection, the expression of His-ASC, GFP-empty, GFP-RIP2 and GFP-caspase-1 was determined by Western blot using anti-His or anti-GFP antibody. As shown in Fig. 7.10B, His-ASC was co-precipitated with anti-GFP antibody when co-transfected with either GFP-RIP2 or GFP-caspase-1 plasmid, while the His-empty and GFP-RIP2/caspase-1 co-transfected groups did not show precipitated complexes (Fig. 7.10B). These results indicate that rgfASC associated with RIP2 and caspase-1 *in vitro*. However, there was a non-specific band in the of Fig. 7.10B, that may be due to the non-specific bindings of anti-His antibody with degraded protein from HEK293 cells. A mass spectrometry analysis should be performed to identify this protein in future.

7.2.9. RgfASC cooperates with RIP2, but not caspase-1, to regulate NF- κ B activity

Goldfish RIP2 has been implicated in NF- κ B activation (117) (Chapter V). To further examine whether ASC protein was involved in the activation of NF- κ B and its relationship with RIP2/caspase-1, I transfected HEK293 cells with various plasmids as

indicated in section 3.10.2. Unlike the transfection with His-RIP2, transfection with either His-ASC or His-caspase-1 did not activate NF- κ B; However, the co-transfection with His-ASC and His-RIP2 downregulated RIP2-induced NF- κ B activity (Fig. 7.11). In contrast, co-transfection with caspase-1 has no effects on RIP2-induced NF- κ B activity (Fig. 7.11).

7.3. DISCUSSION

ASC is a pivotal molecule of the inflammasome signaling pathway in mammals (450). The PYD has been identified as a member of the death domain-fold family implicated in apoptosis and inflammation (453). Through the homotypic PYD-PYD domain interactions, PYD-containing molecules can regulate inflammatory signaling in myeloid cells (455, 456). In recent years, PYD-containing molecules have gained particular attention because of its role in controlling the delicate balance between survival and death through regulation of the NF- κ B and caspase activation, and especially in regulating the inflammasome signaling pathways (104). Taken together, and considering the functions of PYD and CARD, ASC proved to be a critical molecule in regulating NF- κ B, pro-inflammatory cytokine release and pyroptosis in mammals (210, 449–451). To date, a comprehensive functional characterization of the ASC has not been done in teleosts. The gfASC shared the highest identity with the zebrafish ASC and contained two typical functional domains, PYD and CARD. Relatively little is known regarding the function of PYD containing molecules in primitive vertebrates such as bony fish.

The expression pattern of ASC has been well examined in mammals, with the higher mRNA levels in the spleen and small intestine, and relatively lower mRNA levels in the brain and heart (452, 457). The pattern of ASC expression in goldfish tissues was similar to what has been reported for mammals, but is in contrast to the expression pattern of ASC reported for mandarin fish, where higher ASC mRNA levels were observed in the head kidney, spleen and hind kidney (215). The gfASC mRNA levels were also quantified in different immune cell populations of the goldfish. Among the immune cell populations examined, macrophages, PBLs and monocytes exhibited higher ASC mRNA levels than splenocytes and neutrophils. Higher ASC expression has also been observed in CD14-positive monocytes, PBLs and mucosal epithelial cells of mammals (452).

ASC was originally identified as a speck-like molecule that forms insoluble aggregates and enhances drug (etoposide)-induced apoptosis (452, 457). The ASC speck is indicative of initiation of pyroptosis, a pro-inflammatory cell death driven by caspase-1, and the ASC specks formation and pyroptosis are normally induced by variety of intracellular pathogens or by exposure to PAMPs or DAMPs (210, 424, 458, 459).

The caspase-1 activation is controlled by ASC via two distinct mechanisms: (i) the formation the multiprotein complexes called inflammasomes; and (ii) the oligomerization of ASC monomers into a cytosolic speck, called “pyroptosome” (210, 450). I report that goldfish ASC can form such oligomerized structures in appropriately stimulated kidney-derived macrophages. By co-transfecting GFP- and DsRed-ASC, I observed co-localized ASC complexes in HEK293 cells, indicating gfASC aggregate to

form the oligomerized structures in the goldfish. My findings are similar to those of Sun and colleagues (215) who reported the speck-like structures of mandarin fish ASC, using an overexpression system in eukaryotic cells. These observations are supported by cross-linking assay findings that indicated that goldfish recombinant ASC (rgfASC) aggregated to form multimer complexes *in vitro*. Surprisingly, we did not detect any dimeric ASC, instead most of the oligomerized ASC formed a multimeric structures. As there were no reports regarding the oligomerized ASC structures in teleost, we propose this might be an evolutionary difference between teleosts and mammals. Taken together, these findings suggest that the ASC-dependent formation of pyroptosome may be conserved in bony fish and presumably is responsible for the initiation of pyroptosis. Further studies are required to elucidate pyroptosis in immune cells, as well as the relationship of pyroptosome and pyroptosis in bony fish. However, since I performed the cross-linking studies in HEK293 cells in the presence of DSS, there is a possibility that the detected oligomerized ASC complex may involve other as yet non-identified proteins. In future, a mass spectrometry analysis should be used to confirm the oligomerized ASC.

Goldfish ASC expression was assessed in goldfish macrophages in response to different stimuli, including LPS, ATP, nigericin, and two fish pathogens, *A. salmonicida* and *M. marinum*. These stimuli are known inducers of mammalian inflammasomes and have been shown to be able to activate the canonical inflammasome pathway, which leads to ASC recruitment, caspase-1 activation, pyroptosis and pro-inflammatory cytokine processing (210, 450). Of the stimuli tested, nigericin was the best activator of

ASC in goldfish macrophages, inducing high ASC mRNA and protein levels. Nigericin, is an antibiotic derived from *Streptomyces hygroscopicus*, and has been shown to activate NLRP3 inflammasome in LPS-primed macrophages with features of caspase-1 activation, caspase-1 mediated pyroptosis and IL-1 β secretion (424).

After exposure of macrophages to different pathogens, only heat-killed *M. marinum* induced a strong up-regulation of ASC protein but not ASC mRNA. Interestingly, live *M. marinum* did not induce elevated ASC mRNA and protein levels. Our lab previously reported that the survival of *M. marinum* in goldfish macrophages was dependent on its ability to down-regulate the antimicrobial armamentarium of goldfish macrophages (380, 381). It is possible that live *M. marinum* suppresses the inflammasome signaling pathway by down-regulating ASC expression. This potential immune evasion mechanism would ensure the abolition of pyroptosis, allowing the relatively slow-growing mycobacteria to survive in their host cells. Based on my preliminary observations, the elevated ASC protein level may be related to the upstream inflammasome activation in goldfish macrophages, and suggest that teleosts may have a functional inflammasome pathway.

Upon inflammasome activation, ASC as an adaptor molecule regulates the conversion of pro-caspase-1 to generate active caspase-1, that then cleaves pro-IL-1 β and pro-IL-18 to generate the bioactive forms of the cytokines (142, 144, 164, 210, 450). To assess the possible associations between ASC and caspase-1, I performed co-IP assays and found that goldfish ASC and caspase-1 associated with each other, suggesting that ASC may function as an adaptor molecule in teleost inflammasome pathway. In addition

to playing a central role in the inflammasome pathway, ASC has been shown to interact with the NOD1/NOD2 signaling pathway through another CARD domain-containing molecule, RIP2 (460). This interaction is partially associated with caspase-1 through direct protein-protein bindings, which has been reported to affect both NOD1/NOD2 and inflammasome pathways (105, 460). Two mechanisms have been postulated for the physiological consequences of these interactions: (a) down-regulation of the NF- κ B activation by modifying RIP2; and (b) induction of caspase-1 activation for the processing of IL-1 β (104). Previously, I reported that recombinant goldfish RIP2 activated NF- κ B signaling pathway and associated with both NOD1 and NOD2 receptors, resulting in the production of pro-inflammatory mediators (117). It appears that that RIP2 mediated NF- κ B activation and the cross-talk with caspase-1 may also exist in teleosts. I demonstrated that ASC plays a central role in the communications between RIP2 and caspase-1, by binding to both RIP2 and caspase-1. Future studies are required to examine the physiological context of the demonstrated dual functionality of ASC in bony fish.

ASC has also been shown to induce NF- κ B activation in conjunction with cytopyrin and PYPAF7 (182, 213). This is similar to what has been reported in mandarin fish (215). Surprisingly, I found overexpressed gfASC did not activate NF- κ B in HEK293 cells. However, gfASC affected the gfRIP2 ability to activate NF- κ B, suggesting a possible inhibitory role of ASC in NF- κ B activation. That ASC down-regulated NF- κ B activity is consistent with the observations that overexpression of ASC in the presence of RIP2 and caspase-1 in HEK293 cells inhibited NF- κ B in mammals (104). These authors suggested

that the mechanism of ASC inhibition of RIP2-induced NF- κ B activation is through the competition of ASC and RIP2 for binding caspase-1 (104). I did not observe a caspase-1-mediated effect with regards to NF- κ B activation, suggesting that the mechanism of ASC inhibition of RIP2-induced NF- κ B activation may differ between mammals and fish.

My findings suggest that ASC may act as a regulator controlling NOD1/NOD2 signaling pathways (via associations with RIP2), inflammasome pathway (via associations with caspase-1), and pyroptosis (via ASC spec formation and pyroptosome formation). Further studies are required to elucidate the precise role of teleost ASC in inflammasome machinery and caspase-1 regulation of pro-inflammatory cytokine production in teleosts.

Table 7.1. Percent identity between goldfish ASC and that of other organisms (aa)

Species	Identity (%)
Zebrafish	53
Salmon	45
Rainbow trout	44
Northern pike	41
Spotted gar isoform X1	40
Spotted gar isoform X2	38
Mouse	35
African clawed frog	33
Human isoform A	34
Human isoform B	32

```

1 AGTACAGGGGATCCTCAGTACATCCTTGTCGAAGAGGCACAGCACTTTTAGAGAACatg
M
61 gcgaaatctattaaggatcacctgcaagatatttttgatgatcttggggcgggagatcaa
A K S I K D H L Q D I F D D L G A G D Q
121 agaaagtttaaagcaaattgtgcgaccggaagacagagccgcgcatcgaagagctgca
R K F K S K L C D R K T E P R I R R A A
181 gtcgaaaagggttgaagattctatagatctcgccggttgatggtgaccacttttacggag
V E K V E D S I D L A G L M V T T F T E
241 tctggtgctgttcctgtaacaatcgagattttacaggctattgggtgtaatgaacaagca
S G A V P V T I E I L Q A I G C N E Q A
301 gaggagctcatcactatcacaggaaaatcagctacacacgtttctccaacagcgccaaag
E E L I T I T G K S A T H V S P T A P K
361 gtttctttaccagccacaggccaagcgctccatctactgatcattcattgataagaat
V S L P A T G P S A P S T D H F I D K N
421 cggacgaagctgataagcagagtgcataatgtagactgcatcctagatgaacttcttcag
R T K L I S R V H N V D C I L D E L L Q
481 atgaaaatcatcacagaagaggataacgaaaccatccaagctgagaaaacctcaciaaag
M K I I T E E D N E T I Q A E K T S Q K
541 aagatgagaaatttattaatgggcccgattaatctgcaggcactaaagggaaagatgcc
K M R N L L M G P I K S A G T K G K D A
601 ttatacagtgctctcaagaaattgagccttgcttgatggaagacctggagagtcactga
L Y S A L K E I E P C L M E D L E S H *
661 AAAGCCATTTAAGAGTTTCTAATTGCTTGTTTAAATTGGTTTACAGGATACATGACAAAAG
721 CAAGAAATTTCTTTTTTTTAAATAACAGGAAACAAATGTTGTTTAAACATTTTAACTCGCC
781 ATCATTGAAATGTTGTTTCCCTACTTTTTTCTTCCAAAAGGACAATCTGTGACCAAAT
841 CAGGTGCATCCAAAATCTTGCTTGCCAAC

```

Figure 7.1. Nucleotide and predicted aa sequence of goldfish ASC cDNA.

The start and stop codons are boxed, the pyrin domain (PYD) is highlighted in light grey, the caspase recruitment domain (CARD) is highlighted in dark grey. The RNA instability motifs are underlined (ATTTA).

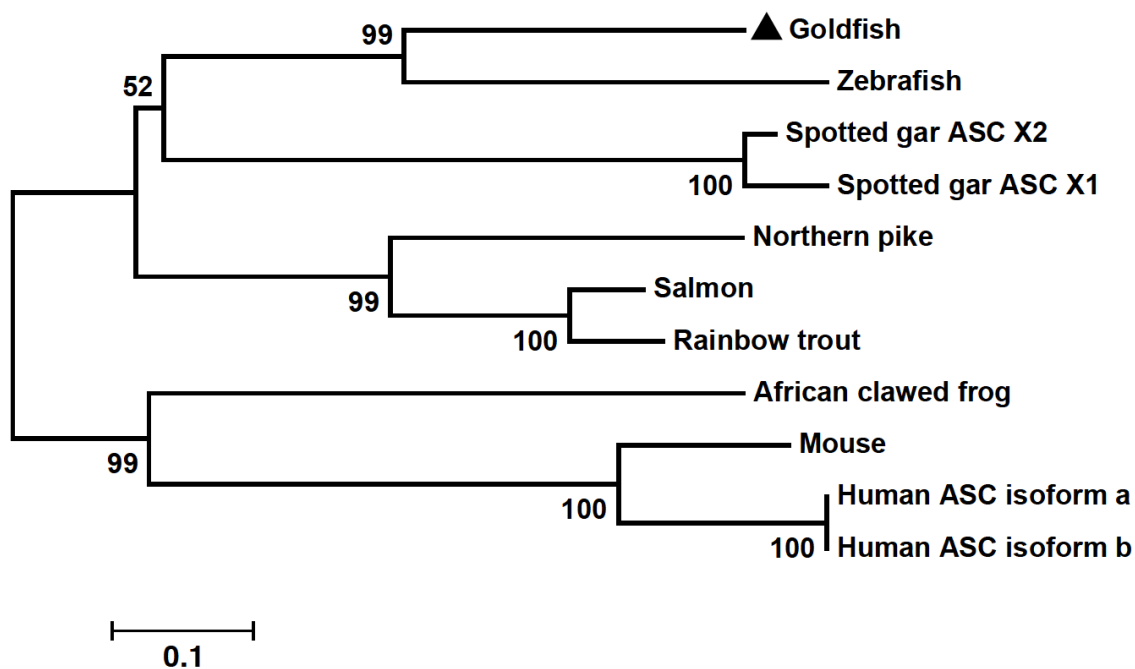


Figure 7.2. Phylogenetic analysis of goldfish ASC.

ASC amino acid sequences were aligned by using CLUSTAL-W program and unrooted phylogenetic tree was constructed using the neighbor-joining method of the MEGA 6.06 program. The tree was bootstrapped 10,000 times. The full length of ASC amino acids sequences used were: Zebrafish NP_571570.2, Salmon ACH70765.1, Rainbow trout ACO07786.1, Northern pike ACO13817.1, Spotted gar X1 XP_003451301.1, Spotted gar X2 XP_005456118.1, Mouse NP_075747.3, Human isoform a NP_037390.2, Human isoform b NP_660183.1, African clawed frog NP_001086388.1.

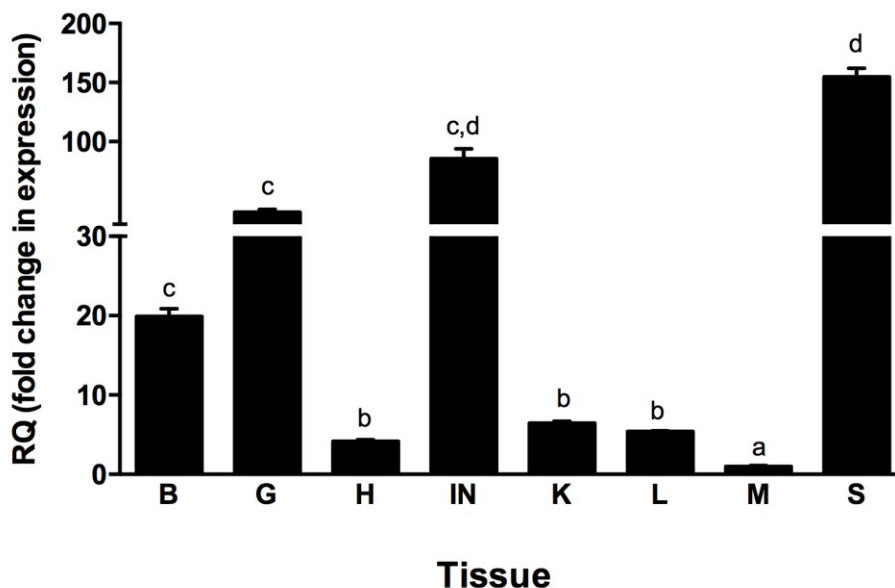


Figure 7.3. Quantitative analysis of goldfish ASC expression in different tissues obtained from normal goldfish.

The expression of goldfish ASC was measured relative to endogenous control gene, elongation factor 1 alpha (EF-1 α). Relative tissue expression from four individual fish (n = 4), Q-PCR was done in triplicate for each tissue. All results were normalized against the muscle ASC mRNA levels (L = liver, M = muscle, H = heart, G = gill, K = kidney, I = intestine, S = spleen, B = brain). Statistical analysis was performed using one-way ANOVA followed by Dunnett's post-hoc test. Different letters above each bar denote statistically different ($P < 0.05$), and the same letter indicates no statistical differences between groups.

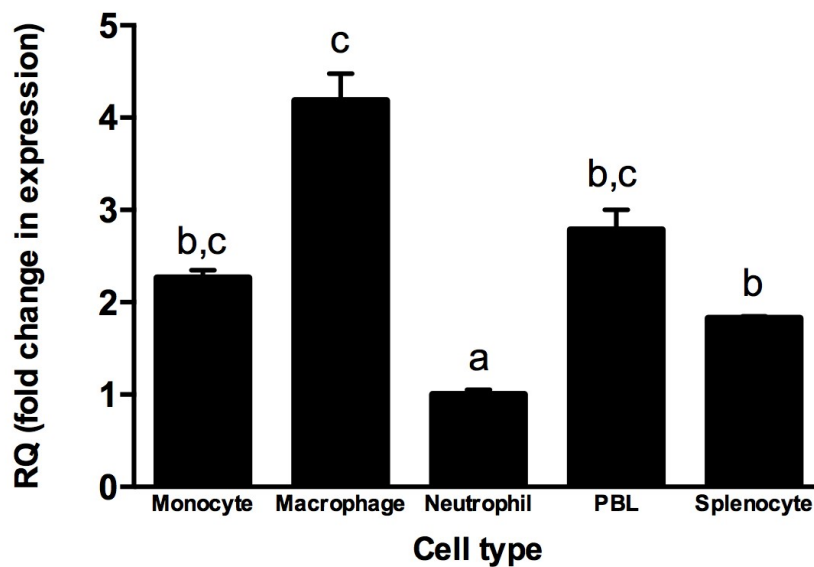


Figure 7.4. Quantitative analysis of goldfish ASC expression in different immune cell populations obtained from normal goldfish.

Cell cultures were established from four fish ($n = 4$), Q-PCR was done in triplicate for each immune cell population. All results were normalized against the neutrophils ASC mRNA levels. Statistical analysis was performed using one-way ANOVA followed by Dunnett's post-hoc test. Different letters above each bar denote statistically different ($P < 0.05$), and the same letter indicates no statistical differences between groups.

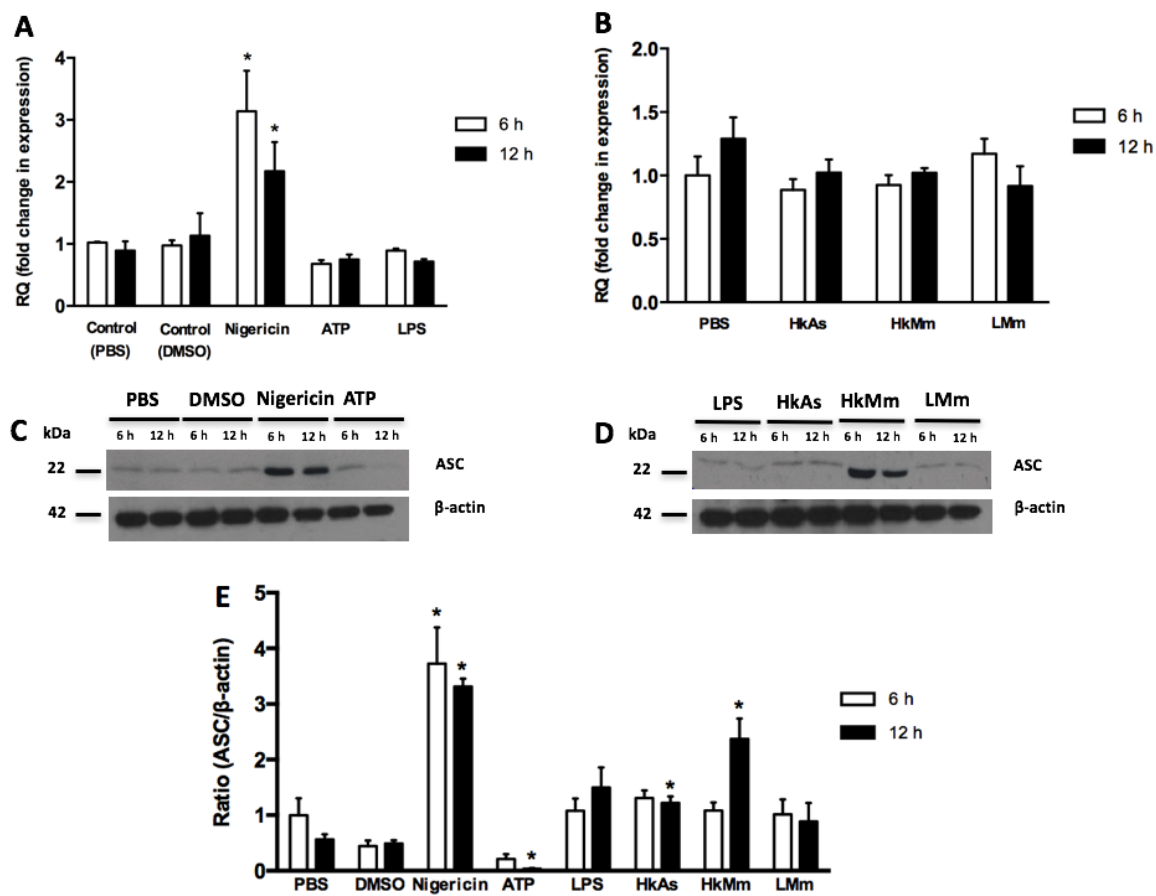


Figure 7.5. Quantitative expression and Western blot analysis of goldfish ASC in macrophages treated with different stimuli.

(A and B) Quantitative expression of goldfish ASC in macrophages treated with either PBS, or DMSO, Nigericin, ATP, lipopolysaccharide (LPS), heat-killed *A. salmonicida*, heat-killed or live *M. marinum*. The expression of ASC was examined relative to the endogenous control gene, elongation factor 1 alpha (EF-1 α). The expression values were normalized against those at the 6 h. The results are the mean \pm SEM of primary macrophage cultures established from four individual fish (n = 4). The asterisk (*) indicates the significant difference at $P < 0.05$ compared to the 6 h time point. (C and D) Western blot analysis of goldfish ASC in macrophages treated with either PBS, or DMSO, Nigericin, ATP, LPS, heat-killed *A. salmonicida*, heat-killed or live *M. marinum*. The treated macrophages were washed three times with PBS and lysed with 100 μ L of NP-40 buffer and then subjected to western blot analysis using anti-ASC antibody or anti- β -actin antibody. β -actin was used as a loading control. Results are from a representative experiment that was repeated three times showing similar results. (E) Quantified ratios of ASC protein to β -actin in treated macrophages, compared to PBS at 6 h. The results are shown as the mean \pm SEM of macrophage from cultures established from three individual fish (n = 3). The asterisk (*) indicates the significant difference at $P < 0.05$ compared to the PBS at 6 h or 12 h time point (HkAs, heat-killed *A. salmonicida*; HkMm, heat-killed *M. marinum*; LMm, live *M. marinum*).

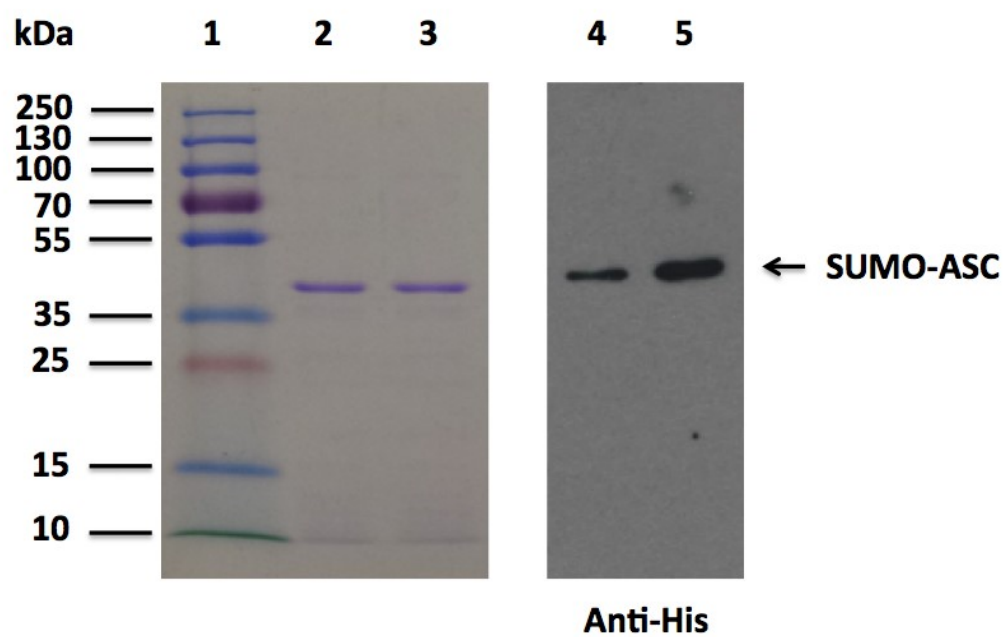


Figure 7.6. SDS-PAGE and Western blot analysis of recombinant ASC.

Lane 1: protein ladder; Lane 2: SDS-PAGE analysis of commassie blue stained of purified recombinant SUMO-ASC; Lane 3: Western blot of purified recombinant SUMO-ASC using anti-His antibody.

M	G	S	S	H	H	H	H	H	H	G	S	G	L	V	P	R	G	S	A	S	M	S	D	S	E	V	N	Q	E	A	K	P	E	V	K	P	E	V	K	P	E	T	H	I	N	L	K	V	S		
D	G	S	S	E	I	F	F	K	I	K	K	T	P	L	R	R	L	M	E	A	F	A	K	R	G	G	K	E	M	D	S	L	R	F	L	Y	D	G	I	R	I	Q	A	D	Q	T	P	E			
D	L	D	M	E	D	N	D	I	I	E	A	H	R	E	Q	I	G	G	M	A	K	S	I	K	D	H	L	Q	D	I	F	D	D	L	G	A	G	D	Q	R	K	F	K	S	K	L	C	D	R		
K	T	E	P	R	I	R	R	A	A	V	E	K	V	E	D	S	I	D	L	A	G	L	M	V	T	T	F	T	E	S	G	A	V	P	V	T	I	E	I	L	Q	A	I	G	C	N	E	Q	A		
E	E	L	I	T	I	T	G	K	S	A	T	H	V	S	P	T	A	P	K	V	S	L	P	A	T	G	P	S	A	P	S	T	D	H	F	I	D	K	N	R	T	K	L	I	S	R	V	H	N		
V	D	C	I	L	D	E	L	L	Q	M	K	I	I	T	E	E	D	N	E	T	I	Q	A	E	K	T	S	Q	K	M	R	N	L	L	M	G	P	I	K	S	A	G	T	K	G	K	D	A			
L	Y	S	A	L	K	E	I	E	P	C	L	M	E	D	L	E	S	H																																	

Figure 7.7. Mass spectrometry analysis of SUMO-ASC protein.

258/319 amino acids (81% coverage) were achieved out of total 230 spectra. The purified SUMO-ASC was fractionated with SDS-PAGE gel and then the excised gel digests were analyzed by nano LC/MS/MS with a Waters NanoAcquity HPLC system interfaced to a ThermoFisher Q Exactive. Peptides were loaded on a trapping column and eluted over a 75µm analytical column at 350nL/min; both columns were packed with Jupiter Proteo resin (Phenomenex). The mass spectrometer was operated in data-dependent mode, with MS and MS/MS performed in the Orbitrap at 70,000FWHM and 17,500 FWHM resolution, respectively. The fifteen most abundant ions were selected for MS/MS. Data were searched using a local copy of Mascot and the Mascot DAT files were parsed into the Scaffold software for validation, filtering and to create a non-redundant list per sample. Data were filtered using a minimum protein value of 90%, a minimum peptide value of 50% and requiring at least two unique peptides per protein. The highlighted area shows the sequences confirmed by MS/MS.

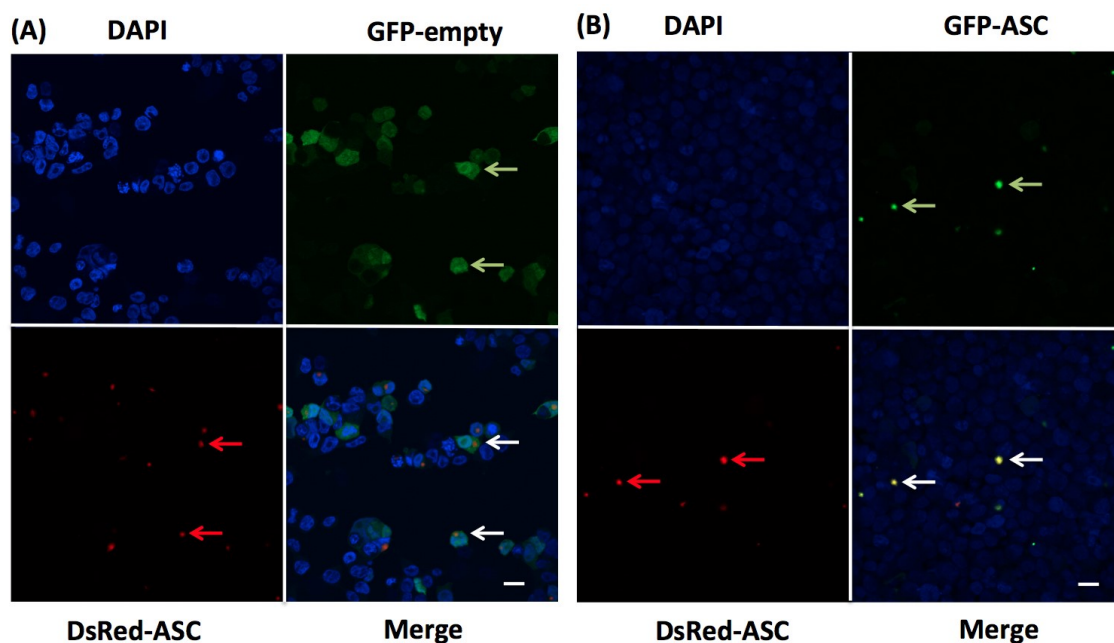


Figure 7.8. Co-localization analysis of goldfish ASC in HEK293 cells.

HEK293 cells (1×10^5 /well) were co-transfected with $1 \mu\text{g}$ of either GFP-empty or GFP-ASC and DsRed-ASC. After 48h, cells were washed twice with PBS before being fixed in 4% PFA for 15 min at room temperature. Subsequently cells were mounted on slides using Fluoroshield mounting media containing DAPI. Slides were then viewed with a Laser Scanning Confocal Microscope. Green fluorescence, red fluorescence, and blue fluorescence were visualized in the same field (Merge). (A) Cells were co-transfected with GFP-empty and DsRed-ASC as control. No co-localized green and red signals were detected (arrowheads). (B) Cells were co-transfected with GFP-ASC and DsRed-ASC and co-localized green and red signals were detected (arrowheads). Scale bars equal $10 \mu\text{m}$.

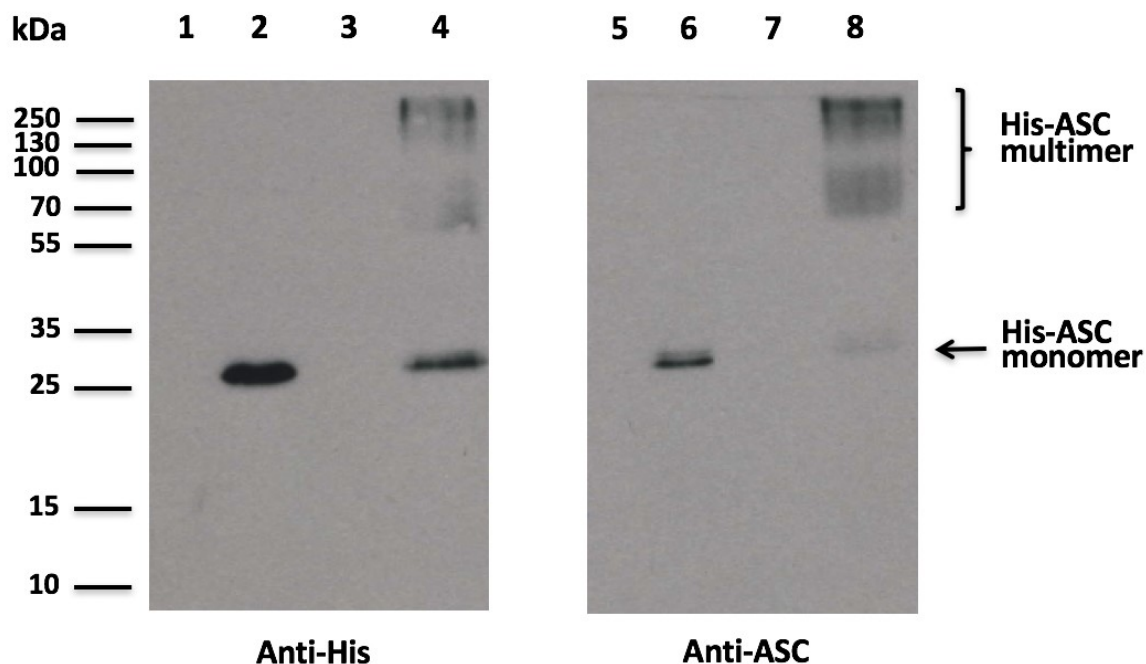


Figure 7.9. Oligomerization analysis of goldfish ASC in HEK293 cells.

1×10^5 HEK293 cells were transfected with $1 \mu\text{g}$ of either His-empty or His-ASC. After 48h, cells were washed twice with PBS before being incubated in conjugation buffer (20 mM Hepes) and cross-linked for 30 min using 5 mM DSS. The cross-linking reactions were terminated for 15 min by the addition of 50 mM Tris (Final concentration). The reactions were then resolved under reducing conditions by SDS-PAGE and visualized by Western blot using anti-His (Lane 1-4) or anti-ASC (Lane 5-8) antibodies. Lane 1 and 5: Protein lysate of cells transfected with His-empty; Lane 2 and 6: Protein lysate of cells transfected with His-ASC; Lane 3 and 7: Protein lysate of the cells transfected with His-empty cross-linked with DSS; Lane 4 and 8: Protein lysate of the cells transfected with His-ASC cross-linked with DSS;

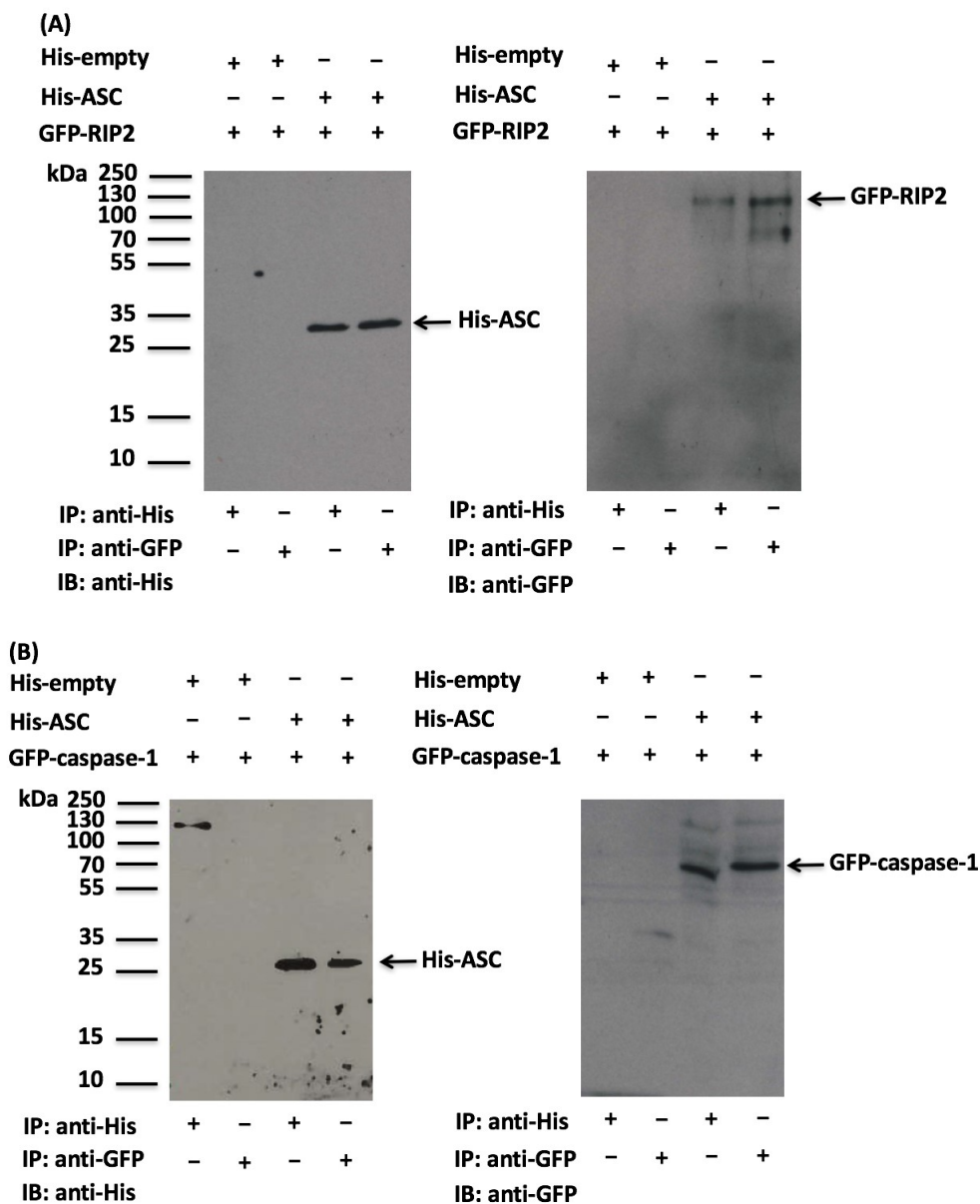


Figure 7.10. Goldfish ASC associates with RIP2 (A) and caspase-1 (B) in HEK293 cells. The total cell lysate was prepared from co-transfected cells and incubated with anti-His antibody or anti-GFP antibody. The precipitated immune complexes were subjected to western blot analysis using either anti-GFP antibody or anti-His antibody, respectively. Control samples are represented by cells co-transfected with pcDNA3.1/V5-His TOPO TA expression vector (His-empty) and either GFP-RIP2 or GFP-caspase-1. (IP = immunoprecipitation; IB = immunoblotting)

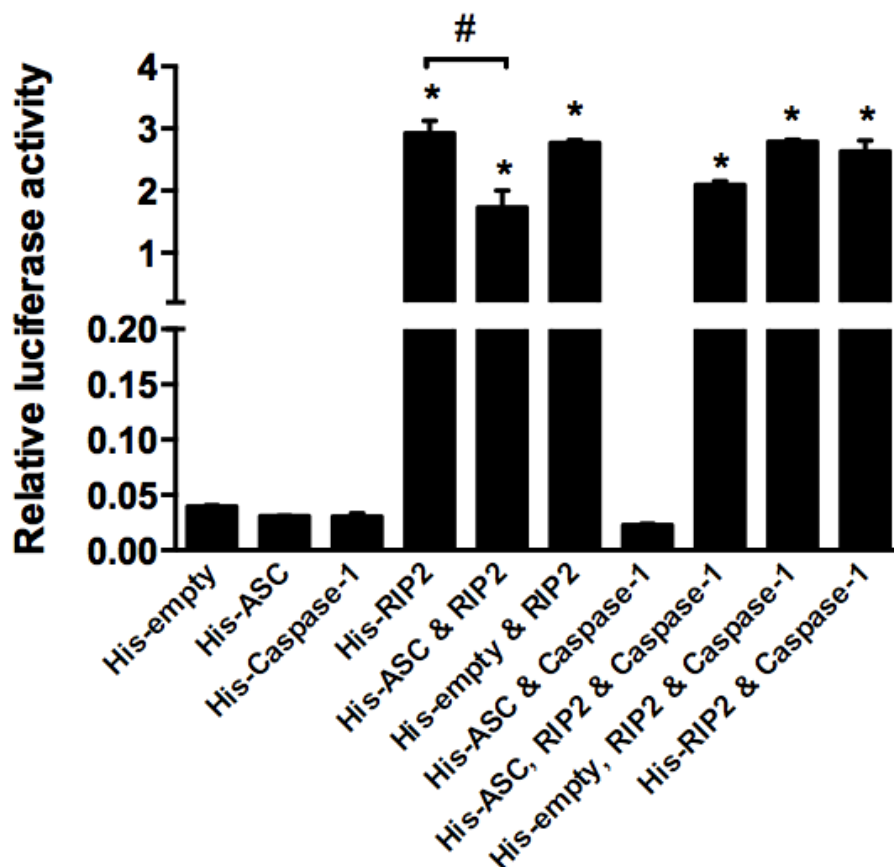


Figure 7.11. Goldfish recombinant ASC protein incorporates with RIP2, but not caspase-1, to regulate NF- κ B transcriptional activation.

HEK293 cells were transfected with 200 ng of pNF- κ B-Luc, 20 ng of pRL-TK reporter vectors and either 200 ng His-empty, His-ASC, His-caspase-1, His-RIP2, His-ASC and His-RIP2, His-empty and His-RIP2, His-ASC and His-caspase-1, His-ASC and His-RIP2 and His-caspase-1, His-empty and His-RIP2 and His-caspase-1, or His-RIP2 and His-caspase-1. At 24 h after transfection, cells were harvested and analyzed using the Dual Luciferase kit according to manufacturer's instructions. All values represent three independent experiments ($n = 3$). All results were normalized against the His-empty luciferase value. The asterisk (*) indicates the significant difference at $P < 0.05$ compared to His empty for each group. The pound sign (#) denotes the significant difference at $P < 0.05$ between His-RIP2 and His-ASC & RIP2 co-transfected groups.

CHAPTER VIII: CHARACTERIZATION OF THE GOLDFISH (*Carassius auratus* L.) HIGH MOBILITY GROUP BOX 1 (HMGB1) CHROMATIN-BINDING PROTEIN ¹

8.1. INTRODUCTION

Unlike most other classical pro-inflammatory cytokines, HMGB1 was identified as a late mediator of systemic inflammation (249) and was shown to be secreted by immunocompetent cells, including monocytes, macrophages, neutrophils, and dendritic cells following infection (256, 257). In mammals, HMGB1 is highly conserved through evolution (461, 462). Structurally, HMGB1 has two DNA-binding domains, termed A and B box, and a highly acidic C-terminal region. Primarily, HMGB1 localizes to the nucleus and functions as a non-histone chromatin-binding protein (247). HMGB1 is also present in the cytoplasm and can be secreted to extracellular space upon inflammasome and caspase activation, indicating that HMGB1 also functions outside the nucleus (148, 250, 251). Extracellular HMGB1 triggers inflammatory responses through TLR2 and TLR4 signaling pathways (252). It has been demonstrated that blockade of TLR4 causes the reduction of cytokine and nitric oxide production, and results in decreased inflammatory responses in mammals (254, 255). In addition, HMGB1 can also be secreted to

¹ A version of this chapter has been published: Xie, J., Hodgkinson, J.W., Li, C., Kovacevic, N., Belosevic, M., 2014. Identification and functional characterization of the goldfish (*Carassius auratus* L.) high mobility group box 1 (HMGB1) chromatin-binding protein. Developmental and Comparative Immunology 44: 245-253

extracellular environment by passive release from necrotic cells and has been shown to induce inflammation (463).

In teleost fish, two HMGB1 genes have been characterized in grass carp and their expression was up-regulated after GCRV infection or viral PAMP (192). HMGB1 has been demonstrated to function as a secreted cytokine in the case of bacterial infection and promotes the innate defense through the activation of macrophages in the red drum (261). Studies in zebrafish showed that HMGB1 was required for brain development (259) and that it contributed to the regeneration processes after spinal cord injury (260).

In this chapter, I report on the cloning and comprehensive expression and functional analysis of the goldfish HMGB1. The tissue and immune cell population expression of goldfish HMGB1 was found to be highest in the brain and splenocytes, respectively. RgHMGB1 was generated and shown to prime goldfish monocytes/macrophages for enhanced respiratory burst and nitric oxide responses. Western blot and quantitative qPCR analysis indicated that goldfish HMGB1 participated in the antimicrobial responses against *Mycobacterium marinum* and *Aeromonas salmonicida*. Treatment of goldfish macrophages with rgHMGB1 induced elevated expression of TNF α -2 and IL-1 β 1 at both mRNA and protein levels. Goldfish HMGB1 also enhanced NF- κ B transcriptional activity.

8.2. RESULTS

8.2.1. Sequence analysis of goldfish HMGB1

Goldfish HMGB1 cDNA was cloned by PCR amplification and consisted of 1321 bp with a 615 bp ORF encoding a polypeptide of 204 aa (Accession No. KF638272), a 5' UTR of 88 bp and a 3' UTR of 618 bp (Fig. 8.1). No signal peptide was predicted. Sequence analysis of the UTR regions revealed the presence of RNA instability regions (ATTTA) in the 5' UTR and 3' UTR (Fig. 8.1). Pfam analysis indicated that the predicted protein contained a HMG box A domain (5-77 aa) and B domain (94-162 aa) (Fig. 8.1). Theoretical pI and molecular weight of goldfish HMGB1 was 6.79 and 23.5 kDa, respectively. In addition, three conserved redox-sensitive cysteines and NLSs were also detected in the goldfish HMGB1 sequence. Phylogenetic analysis of goldfish HMGB1 demonstrated closest relationship to the Blunt snout bream HMGB1 (Fig. 8.2). HMGB1 proteins of the above fish species branched independently to the HMGB1s of the other fish species (Fig. 8.2). Fish HMGB1 proteins also share the high aa sequence identity except red drum (Table 8.1). All known fish HMGB1 proteins, other than for red drum, branched independently from the HMGB1 protein sequences of higher vertebrates (Fig. 8.2).

8.2.2. Analysis of HMGB1 expression in normal goldfish tissues

Quantitative expression analysis of goldfish HMGB1 in tissues of normal fish indicated that the highest mRNA levels of HMGB1 were in the brain, followed by spleen, intestine, kidney, and gill (Fig. 8.3). Lower expression levels were observed in heart and muscle, and the lowest HMGB1 mRNA levels were in the liver (Fig. 8.3).

8.2.3. Analysis of HMGB1 expression in goldfish immune cell populations

The expression of HMGB1 was determined in different goldfish cell populations. The cell populations assessed included peripheral blood leukocytes, kidney-derived neutrophils, splenocytes, monocytes and mature macrophages. Splenocytes had the highest HMGB1 mRNA levels, followed by PBL and neutrophils, while HMGB1 expression was lowest in monocytes and mature macrophages (Fig. 8.4).

8.2.4. Analysis of HMGB1 expression in *M. marinum* infected goldfish tissues

In order to understand the inflammatory role of HMGB1 in goldfish, I investigated the expression of HMGB1 in day-7 *M. marinum*-infected goldfish kidney and spleen. I observed a significantly elevated mRNA level of HMGB1 in kidney and spleen of *M. marinum*-infected compared to non-infected fish (Fig. 8.5).

8.2.5. Recombinant goldfish HMGB1 expression, purification and antibody characterization

With the aim to further examine the activity and function of goldfish HMGB1, I expressed the rgHMGB1 in *E. coli* and purified it using the MagneHis protein purification system. One single band with the molecular weight of 28.5 kDa including the size of 5 kDa of a six-histidine tag, a thrombin recognition site and a T7 tag at the N-terminus, was indicated by SDS-PAGE analysis (Fig. 8.6). The presence of the recombinant protein was confirmed by Western blot analysis using anti-His-tag antibody and rabbit anti-HMGB1 IgG. These results indicated that a consensus protein of 28.5 kDa was detected

(Fig. 8.6). In addition, the anti-HMGB1 IgG also detected a non-specific band in the purified preparation of recombinant HMGB1. This could be due to the non-specific binding between the generated anti-HMGB1 IgG and degraded bacterial products.

8.2.6. Recombinant HMGB1 induces respiratory burst response of goldfish

macrophages

To assess the ability of rgHMGB1 to activate primary goldfish macrophages (PKM), I measured the respiratory burst response of goldfish monocytes. Cells triggered with PMA, exhibited a significant concentration-dependent increase in the production of reactive oxygen intermediates when first primed with increasing amounts of rgHMGB1 (20, 100 or 250 ng/mL) when compared to PMA only stimulated cells (Fig. 8.7). At lower concentration (5 ng/mL) HMGB1 did not prime monocytes for respiratory burst response.

8.2.7. Recombinant HMGB1 induces nitric oxide responses of goldfish macrophages

The ability of rgHMGB1 to induce a nitric oxide response in goldfish macrophages was determined. Cells cultures from individual fish were either exposed to medium alone (negative control) or treated with rgTNF α -2 (positive control), or different amounts of rgHMGB1 (5, 20, 100 and 250 ng/mL). RgHMGB1 induced a significant nitric oxide response from macrophages in a dose-dependent manner (Fig. 8.8).

8.2.8. Expression of goldfish HMGB1 gene and protein in macrophages treated with heat-killed *M. marinum* and *A. salmonicida*

Since rgHMGB1 induced the respiratory burst and nitric oxide responses in macrophages, I examined whether the expression of HMGB1 gene and protein levels were modulated in response to bacterial challenge (Fig. 8.9). To examine this, the expression of HMGB1 was determined in goldfish macrophages at 0, 6, 12 and 24 h after exposure to 2×10^6 cfu/mL of heat-killed *M. marinum* or *A. salmonicida*. The mRNA and protein levels of goldfish HMGB1 increased after exposure of macrophages to heat-killed *M. marinum* at 6, 12 and 24 h (Fig. 8.9A and B) and *A. salmonicida* at 12 and 24 h (Figs. 8.9C and D).

8.2.9. Analysis of goldfish macrophage TNF α -2 and IL-1 β 1 production after treatment of macrophages with rgHMGB1

I examined the induction of TNF α -2 and IL-1 β 1 gene expression and protein levels in goldfish macrophage cultures treated with rgHMGB1 (Fig. 8.10). Macrophage treated with 20 and 100 ng/mL of rgHMGB1 exhibited an increased mRNA and protein levels of TNF α -2 (Figs. 8.10A, C and E) and IL-1 β 1 (Figs. 8.10B, D and F) at 12 h post treatment. The amount of IL-1 β 1 produced was approximately 3 times higher than that of TNF α -2 (Fig. 8.9). At both lowest (5 ng/mL) and highest (250 ng/mL) concentrations, rgHMGB1 did not affect the production of TNF α -2 and IL-1 β 1 (Fig. 8.10).

8.2.10. Goldfish rgHMGB1 promotes NF- κ B transcriptional activity

In mammals, HMGB1 has been identified as a mediator that activates NF- κ B (253). To determine whether the goldfish HMGB1 protein was involved in the NF- κ B pathway, HEK293 cells were transfected with goldfish HMGB1 expression plasmid and NF- κ B plasmid. The results showed that compared to the pcDNA3.1/V5-His empty vector, HMGB1 expression plasmid induced a significant increase in pNF- κ B-Luc expression ($P < 0.05$) (Fig. 8.11). These results indicated that goldfish HMGB1, like in mammals, is involved in the NF- κ B signaling pathway.

8.3. DISCUSSION

The innate immune system utilizes a limited number of PRRs to recognize evolutionary conserved structures on pathogens, such as PAMPs and DAMPs (464). PRRs located on the surface (TLRs) scout extracellular environment for the presence of microbes, and cytosolic PRRs such as NOD-like receptors and RIG-I-like receptors, among others (16, 465, 466), recognize intracellular bacteria (466) and protozoa (85, 467), or components of internalized microbes (16, 466). Certain cytosolic PRRs, such as NALP1 & NALP3, after pathogen recognition form oligomerized protein complexes termed “inflammasomes” (465, 466) that activate inflammatory caspases (*i.e.* caspase-1), and regulate cytokine maturation (IL-1 β and IL-18) and induce cell death known as pyroptosis (16, 134, 468), which has recently been reported to be an important pathway for active HMGB1 release. In addition, genetic deletion of inflammasome components severely impairs HMGB1 release during endotoxemia or bacteriemia (251, 423). These

studies clearly indicate that the major impetus for HMGB1 release is subsequent to inflammsome activation. Although the role of HMGB1 is relatively well characterized in mammals, little information is available on HMGB1 of lower vertebrates.

As an evolutionarily conserved nuclear protein, HMGB1 shares high identity with its mammalian counterpart and contains two folded helical DNA-binding motifs, called HMG A and B boxes, and an acidic tail. In teleost, all the identified HMGB1 sequences contained HMG A and B boxes as well as the acidic tail. In bony fish, these domains are believed to convey the bioactivity of extracellular HMGB1 while key lysine residues within the NLSs enable HMGB1 to promote inflammation (192).

HMGB1 is an abundant protein that is widely expressed in all mammalian tissues with high levels found in the thymus, lymphoid tissue, testis and neonatal liver (245). Among teleosts, grass carp HMGB1a was found to be higher expressed than HMGB1b, particularly in the gut and blood, and HMGB1b was more highly expressed in the skin and gill (192). In the present study, goldfish HMGB1 was ubiquitously distributed in all tissues with highest expression levels observed in the brain and spleen, followed by intestine, kidney and gill. These data are consistent with previously published studies suggesting that HMGB1 is a critical factor for zebrafish brain development (259) and neuroregeneration after spinal cord injury (260), which suggests that HMGB1 plays a critical role in brain development throughout evolution. I observed an elevated expression of HMGB1 in goldfish kidney and spleen one week post-infection with *M. marinum*. Our lab previously reported that the mRNA levels of pro-inflammatory

cytokines increased at day-7 post infection (381), which suggest that HMGB1 may play a pro-inflammatory during *M. marinum* infection.

There is relatively little information on the expression of HMGB1 in the immune cell populations of bony fish. In mammals, HMGB1 is released from necrotic cells and secreted by activated macrophages, natural killer cells, and mature dendritic cells, in response to infection and during inflammation (249). HMGB1 has also been reported to modulate mammalian neutrophil-associated NADPH oxidase activity and bacterial killing response (469), and the formation of neutrophil extracellular traps through interactions with TLR4 (470). In this study, high expression of HMGB1 was observed in goldfish splenocytes, PBL and neutrophils, and to a lesser extent in macrophages and monocytes. Zhao and co-workers (261) showed that red drum HMGB1 promoted innate defense through the activation of macrophages. The findings of this chapter, suggested multifunctional roles for HMGB1 in different teleost immune cell populations.

Although HMGB1 has been shown to be secreted during bacterial infections of fish, there is no information regarding the types of antimicrobial responses induced by HMGB1, with exception of the report that red drum HMGB1 can enhance the respiratory burst activities in head kidney macrophages (261). In order to gain a better understanding of the antimicrobial roles of HMGB1 in the goldfish, I measured the production of ROI in monocytes, and RNI in macrophages following treatment with rgHMGB1. Goldfish monocytes, macrophages and neutrophils are capable of the producing ROI, but on a per cell basis, neutrophils and monocytes are the most efficient producers of ROI. There is also evidence that as monocytes differentiate into mature

macrophages, they gradually lose the capacity to initiate this response (408, 471). Here I report that rgHMGB1 can induce the production of ROI by monocytes and RNI response of macrophage of the goldfish. These observations are in accord with previous reports that purified HMGB1 stimulates ROI and RNI production of rodent macrophages (472–474). Based on these findings, I next examined the expression profiles of HMGB1 after treatment of *M. marinum* or *A. salmonicida* in goldfish macrophages. Increased expressions at both gene and protein levels were observed 6, 12 and 24 h after treatment of *M. marinum*, and 12 and 24 h after treatment with *A. salmonicida*. Similar responses have also been reported in red rum head kidney macrophages treated with *Edwardsiella tarda* at 12 and 24 h (261), suggesting HMGB1 plays a critical role in the host defense against bacterial infection through the activation of macrophages.

The secreted HMGB1 also appears to have an important pro-inflammatory role, acting as a cytokine that can orchestrate a cascade of inflammatory responses (475). To investigate the role of HMGB1 in activation of pro-inflammatory cytokines production, I treated goldfish macrophages with rgHMGB1, and evaluated the mRNA and protein levels of TNF α -2 and IL-1 β 1. I observed an elevated expression of TNF α -2 and IL-1 β 1 at 12 h post treatment with rgHMGB1. In cultured human primary monocytes/macrophages, HMGB1 has been shown to stimulate the secretion of multiple pro-inflammatory cytokines, including TNF α , IL-1 α , IL-1 β , IL-6 and IL-8 (476).

The extracellular HMGB1 has been reported to engage a variety of receptors, including RAGE, TLR2, TLR4 and TLR9 (252, 253, 477). Amongst these receptors, RAGE has been reported to activate MAPKs, and both RAGE and Toll-like receptors activate

NF- κ B to promote the synthesis of pro-IL-1 β and pro-IL-18 (478–480). Using the dual-luciferase reporter assays, I demonstrated that goldfish HMGB1 significantly enhanced the expression of luciferase reporter genes for the NF- κ B binding site, suggesting that goldfish HMGB1 is involved in NF- κ B signaling pathway. My results indicate a conserved role for goldfish HMGB1 in the regulation of pro-inflammatory cytokine gene expression and production.

My findings indicate that HMGB1 may play a central role in mediation the inflammatory response of lower vertebrates such as bony fish. They also suggest that teleosts may possess inflammasome machinery, which remains to be fully elucidated.

Table 8.1. Percent identity of HMGB1 in different organisms (aa)

Species	Identity (%)
Blunt snout bream	94
Grass carp HMGB1a	94
Zebrafish HMGB1a	94
Catfish HMGB1	88
Atlantic salmon HMGB1	86
Ayu HMGB1	86
Rainbow smelt HMGB1	86
Zebrafish HMGB1b	86
Grass carp HMGB1b	84
Sablefish HMGB1	84
Chick HMGB1	83
Tropical clawed frog HMGB1	83
African clawed frog HMGB1	83
Rainbow trout HMGB1	81
Human HMGB1	81
Mouse HMGB1	81
Red drum HMGB1	77

```

1 ACATGGGGAGTACATTCACTATCCAGACAAGACAGCGGTTAAGTGTACAGCTTGTAGACATT
62 TCAAAGTCTAGGGATATTTAGGCAAAGAtggggaaggatccaacaaaaccaagaggcaaa
      M G K D P T K P R G K
122 atgtcgtccttagcgcatactttgtccagacctgcagagaggagcataagaagaacaccct
      M S S Y A Y F V Q T C R E E H K K K H P
182 gaggcgacgggtcaacttctctgagttttccaaaaagtgtccgagcgatggaagactatg
      E A T V N F S E F S K K C S E R W K T M
242 tcaggcaaagaaaaggggaagtttgaagacatggccaaacaagacaaggtccggttatgag
      S G K E K G K F E D M A K Q D K V R Y E
302 agggagatgaagaactacattccacccaaagggcagagaagaaaagaggtttaaaggacct
      R E M K N Y I P P K G E K K K R F K D P
362 aatgctcccaagagacccccgtccgccttcttcattttctgctccgaggtccgatccaag
      N A P K R P P S A F F I F C S E F R S K
422 gtgaaagaagagaccccctggctgtctattggagatgtggccaagagactgggtgagatg
      V K E E T P G L S I G D V A K R L G E M
482 tggacaacaaacatcagctgaggataagcagccatttgagaagaaggcagccaagcttaag
      W N K T S A E D K Q P F E K K A A K L K
542 gagaagtatgagaaggacattgctgcctatcgttctaaggcaaagtggtaggaggtgca
      E K Y E K D I A A Y R S K G K V V G G A
602 gccaaagccccttctaagccgggtcaaggttaatgatgatgacgacgacgatgatgaagat
      A K A P S K P V K V N D D D D D D D E D
662 gaggacgaggatgacgacgatgaagaagaggatgacgagTagATAAATAACATTTAGAGC
      E D E D D D E E D D E *
722 TTAGCTTTGTTGTCTATAAAGCATTTAACCCCTTGTATACTTTACTGATGCCATAAAAT
782 GGGTAAAAATAAAATAAAATAAAACCTGAAAGGGCAAAAAACAAAAATAACAATA
842 AGGCTGTGTATATGCTTTGTTTTTAACTGTACAGTTTCTTTTTTTTCCTTTTTTGTATA
902 GTTAACACTACAGAGGTGTCATCTGTGTTTCGTCCGAATGCCCAACCCTTAATTTAGTTTC
962 TTAGTTTAATTCCTTAAAGATGGTTCCAACACCACTATCCTCGCCTGGTACAGTAAAAAA
1022 AGAAAAGGTGGGGTTGTAAATTTGTCTTGAGGTCAGTGGAGTTTTAGATGTGTGCAGCGT
1082 ACAACCTAGTTTCATGTGAGGTTGTAGTTCATATCTCAATGTACTTTTGTGTTTACTT
1142 TTTTTTTTTCAGATCAAATATTATCATCATTAGTAAATCGCCGTATCAAAGTTATTTTACTG
1202 TATTTTGAATACCACTGTAATTGCAGAAATGATTTTAAAAAGTAATTGTTTTGTTCTGTA
1262 TGCTTCTGACATCAATAAACATTTTTTTTTTATAAAAAAAAAAAAAAAAAAAAAAAAAAAAA

```

Figure 8.1. Nucleotide and predicted aa sequence of goldfish HMGB1 cDNA.

The start and stop codons are boxed, the HMG box A and B is highlighted in light grey and dark grey, respectively. The acidic tail is dashed underlined. Three conserved redox-sensitive cysteines (C) were double underlined and italicized. Two nuclear localization signals were wave underlined. The polyadenylation signal (**AATAAA**) is bolded and the RNA instability motifs are underlined (ATTTA).

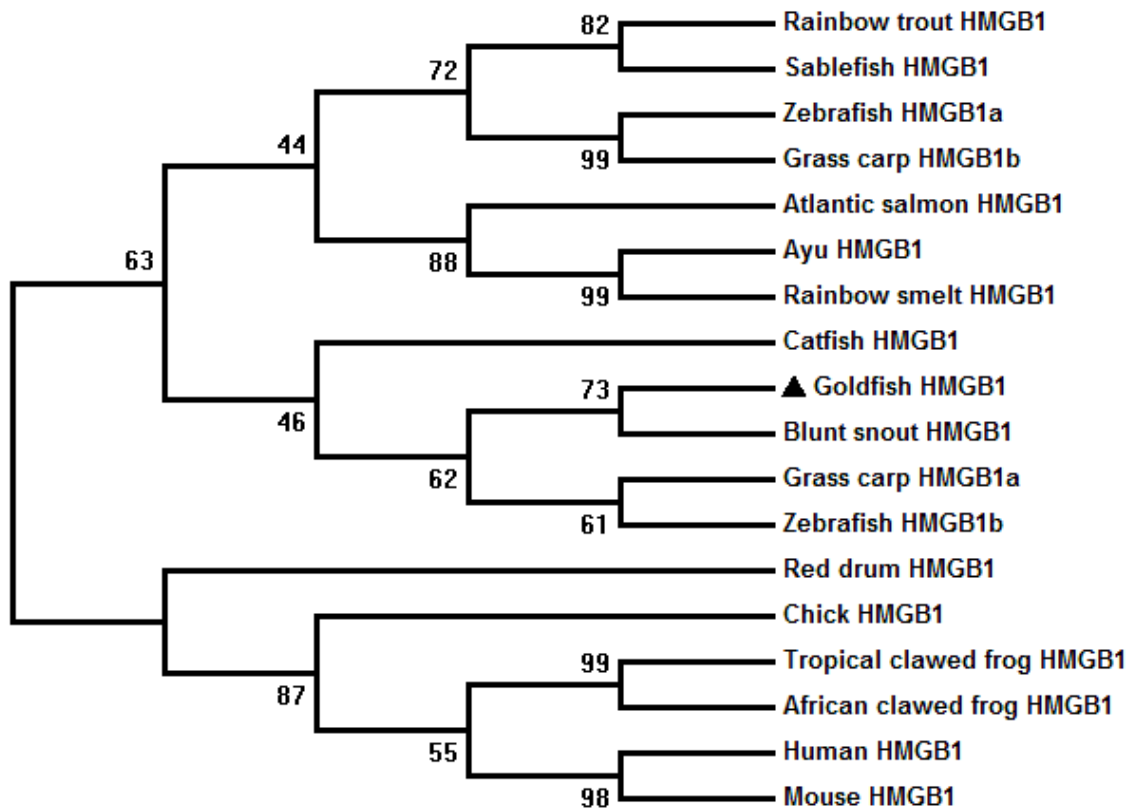


Figure 8.2. Phylogenetic analysis of goldfish HMGB1.

HMGB1 amino acid sequences were aligned by using CLUSTAL-W program and unrooted phylogenetic tree was constructed using the neighbor-joining method of the MEGA 5 program. The tree was bootstrapped 10,000 times. The full length of HMGB1 amino acids sequences used were: Blunt snout bream ACN82089.1, Ayu CBX36444.1, Human AAV38961.1, Mouse AAH91741.1, Rainbow smelt ACO08869.1, Rainbow trout ACO07779.1, Atlantic salmon NP_001133101.1, Chick CAA76978.1, Red drum ADX06860.1, Sablefish ACQ57964.1, Catfish ABD85497.1, Zebrafish (HMGB1a) NP_955849.2, Zebrafish (HMGB1b) NP_001092721.2, African clawed frog NP_001080836.1, Tropical clawed frog NP_989226.1, Grass carp (HMGB1a) AFR33803.1, Grass carp (HMGB1b) AFR33804.1.

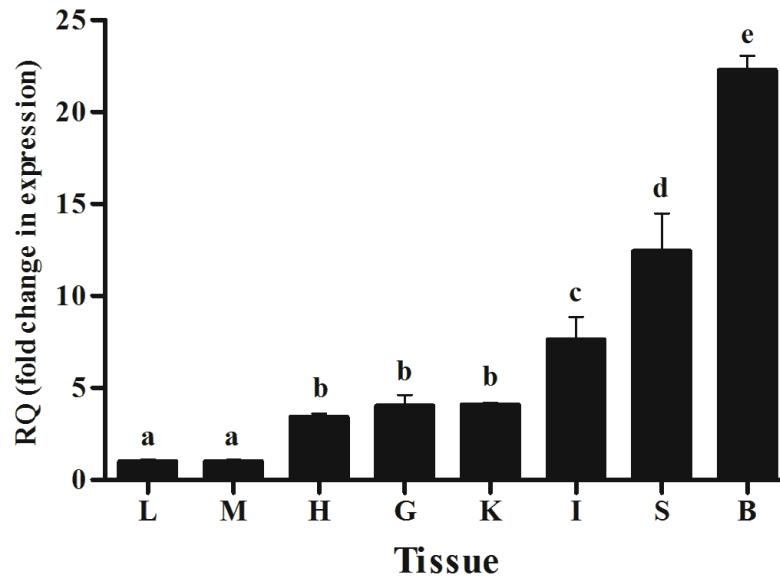


Figure 8.3. Quantitative analysis of goldfish HMGB1 expression in tissues obtained from normal fish.

The goldfish HMGB1 expression was measured relative to endogenous control gene, elongation factor 1 alpha (EF-1 α). Relative tissue expression from 5 individual fish (n = 5), qPCR was done in triplicate for each tissue. All results were normalized against the liver HMGB1 mRNA levels. Statistical analysis was performed using one-way ANOVA and Tukey's post hoc test. Different letters above each bar denote statistically different ($P < 0.05$), and the same letter indicates no statistical differences between groups (L = Liver, M = Muscle, H = Heart, G = Gill, K = Kidney, I = Intestine, S = Spleen, B = brain).

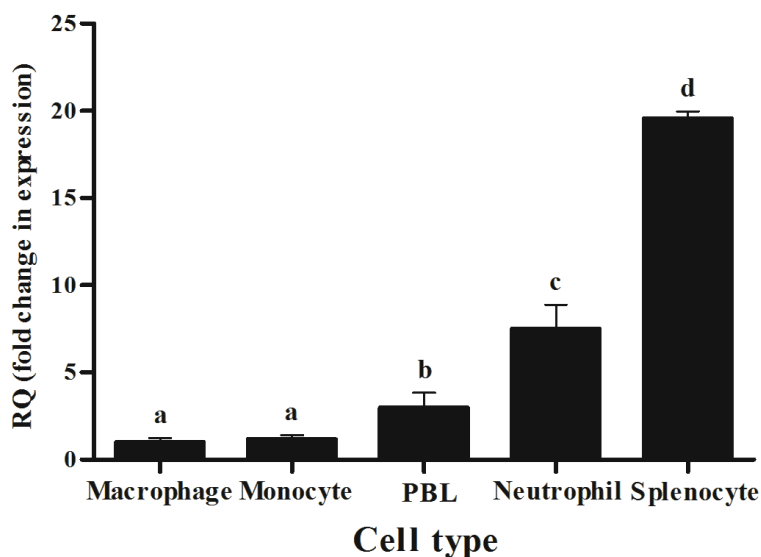


Figure 8.4. Quantitative analysis of goldfish HMGB1 in different immune cell populations of normal fish.

The goldfish HMGB1 expression was measured relative to endogenous control gene, elongation factor 1 alpha (EF-1 α). Analysis of the Relative tissue expression data for immune cell populations isolated from five individual fish ($n = 5$), qPCR was done in triplicate for each immune cell population. All results were normalized against the macrophage HMGB1 mRNA levels. Statistical analysis was performed using one-way ANOVA and Tukey's post hoc test. Different letters above each bar denote statistically different ($P < 0.05$), and the same letter indicates no statistical differences between groups.

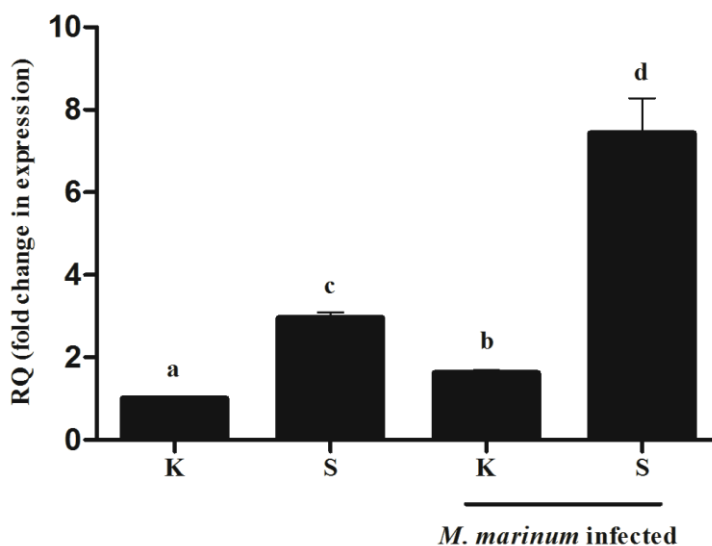


Figure 8.5. Quantitative analysis of goldfish HMGB1 expression kidney and spleen from day-7 *M. marinum* infected goldfish.

The goldfish HMGB1 expression was measured relative to endogenous control gene, elongation factor 1 alpha (EF-1 α). Relative tissue expression from five individual fish ($n = 5$), qPCR was done in triplicate for each tissue. All results were normalized against the normal kidney HMGB1 mRNA levels. Statistical analysis was performed using one-way ANOVA and Tukey's post hoc test. Different letters above each bar denote statistically different ($P < 0.05$), and the same letter indicates no statistical differences between groups (K = Kidney, S = Spleen).

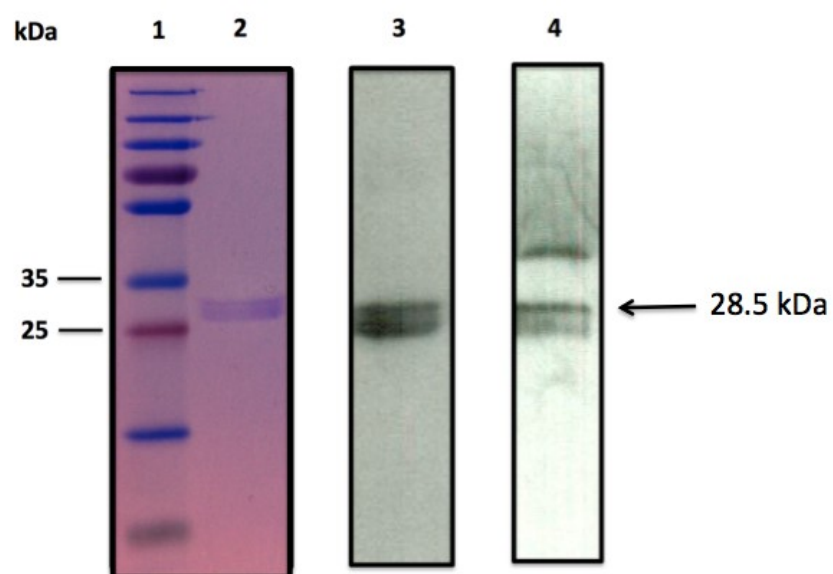


Figure 8.6. SDS-PAGE and Western blot analysis of recombinant HMGB1.

Lane 1: protein ladder; Lane 2: SDS-PAGE analysis of Coomassie blue stained of purified recombinant HMGB1; Lane 3: Western blot of purified recombinant HMGB1 using anti-His antibody; Lane 4: Western blot of purified recombinant HMGB1 using rabbit anti-HMGB1 IgG antibody.

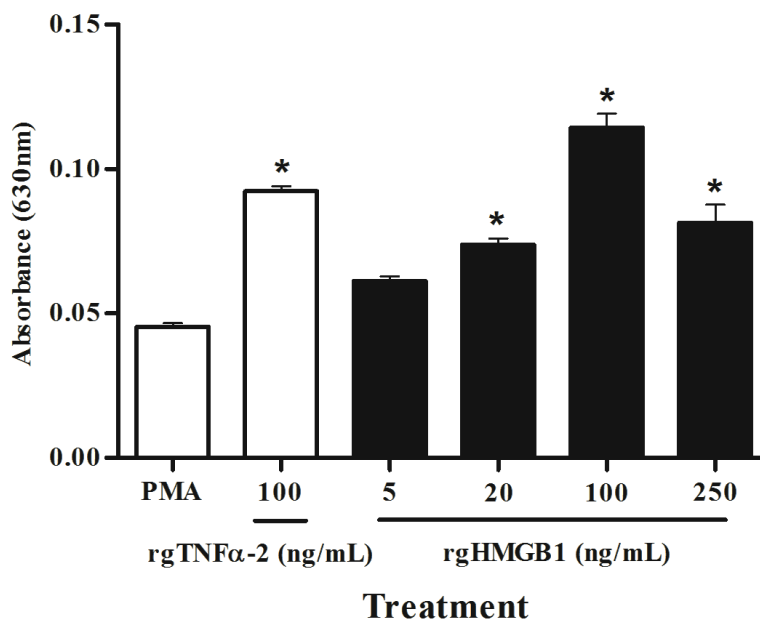


Figure 8.7. Recombinant goldfish HMGB1 (rgHMGB1) primes goldfish monocytes for enhanced respiratory burst response (production of reactive oxygen intermediates; ROI).

The absorbance values of medium-treated controls (no PMA) were subtracted from treatment values to factor in background NBT reduction. Mean \pm S.E.M. of relative reactive oxygen intermediate production by PMA-primed monocytes from three individual fish ($n = 3$). (*) denotes statistically different ($P < 0.05$) compared to 100 ng/mL PMA treated cells.

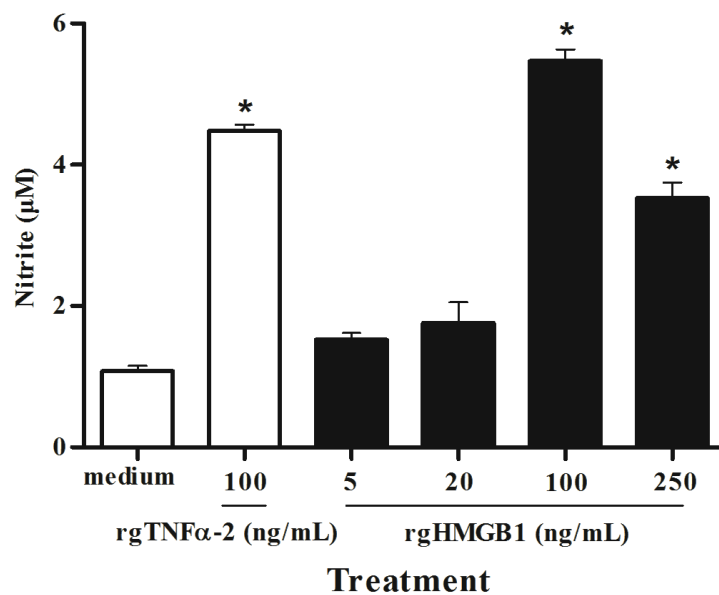


Figure 8.8. Recombinant goldfish HMGB1 enhances nitric oxide response (production of reactive nitrogen intermediates; RNI) of goldfish macrophages.

Nitric oxide production was determined using the Griess reaction and nitrite concentration determined using a nitrite standard curve. The results are mean \pm S.E.M. μ M nitrite in macrophage cultures established from three individual fish ($n = 3$). Statistical analysis was performed using one-way ANOVA. (*) denotes statistically different ($P < 0.05$) from medium control.

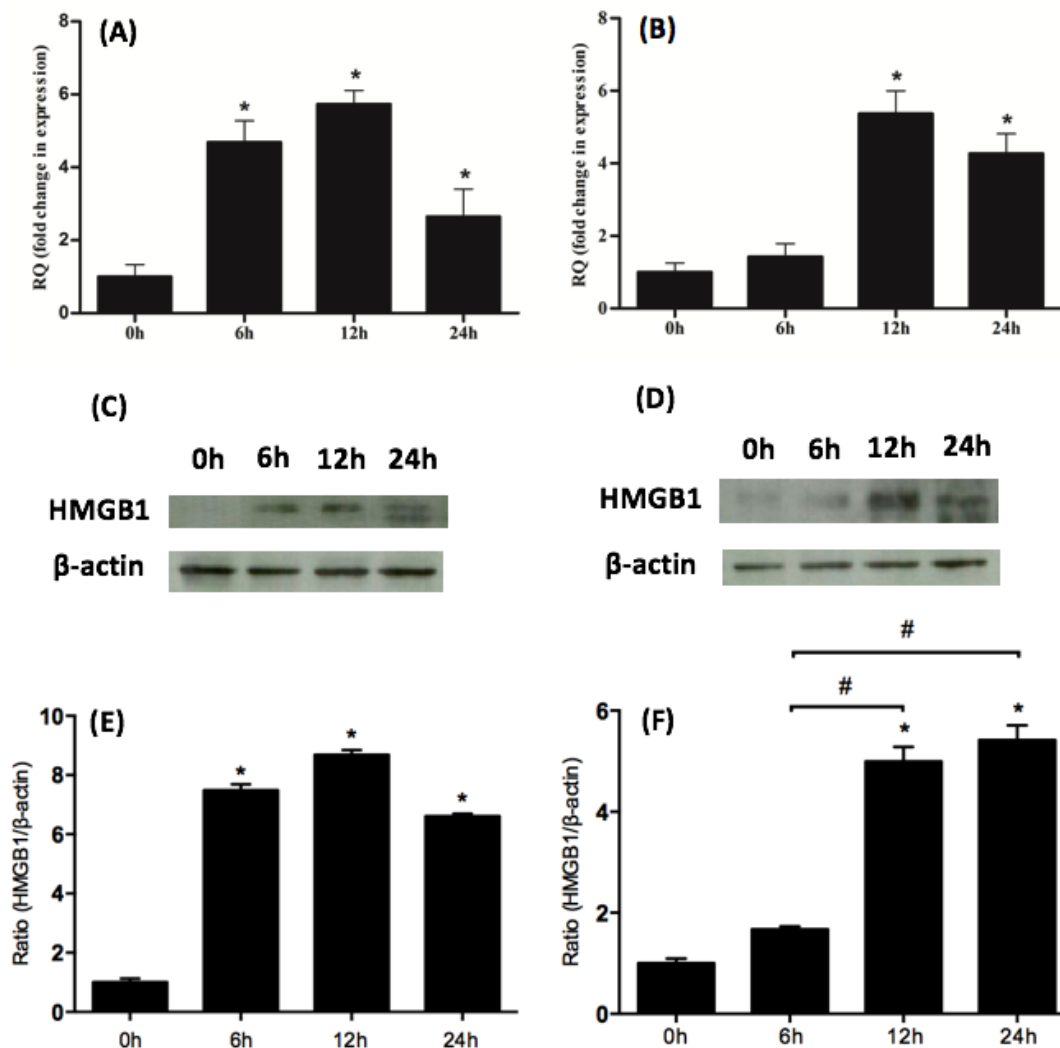


Figure 8.9. Western blot and quantitative expression analysis of goldfish HMGB1 in macrophages treated with heat-killed *M. marinum* (A, C & E) or *A. salmonicida* (B, D & F) for 12 h.

(A and B) The expression of goldfish HMGB1 was examined relative to the endogenous control gene, elongation factor 1 alpha (EF-1 α). The expression values were normalized against those at the 0 h time point. The results are mean \pm S.E.M. of primary macrophage cultures established from three individual fish ($n = 3$). (C and D) Western blot analysis of goldfish HMGB1 was examined relative to β -actin. (E and F) Quantified ratios of HMGB1 protein to β -actin in treated macrophages. The results are shown as the mean \pm SEM of macrophage from cultures established from three individual fish ($n = 3$). (*) denotes significantly different ($P < 0.05$) from the 0 h treated cells. The pound sign (#) indicates the significant difference at $P < 0.05$ between different rgHMGB1 treated groups.

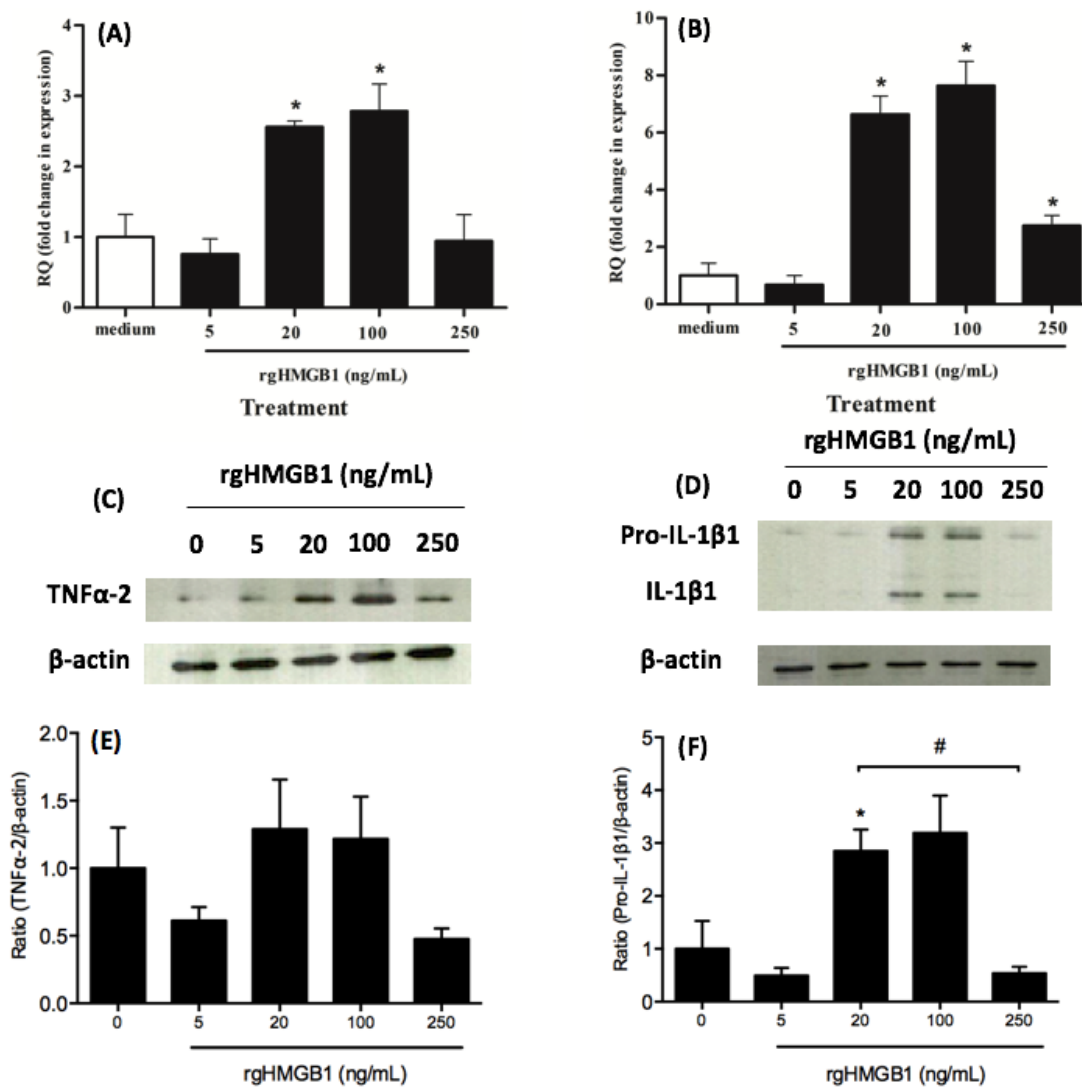


Figure 8.10. Dose-dependent Western blot and quantitative expression analysis of goldfish TNF α -2 (A & C) and IL-1 β 1 (B & D) in macrophages treated with rgHMGB1. The expression of goldfish HMGB1 was examined relative to the endogenous control gene, elongation factor 1 alpha (EF-1 α). The expression values were normalized against those observed in medium treated cells. The results are mean \pm S.E.M. of primary macrophage cultures established from three individual fish ($n = 3$). (E & F) Quantified ratios of TNF α -2 (E) or Pro-IL-1 β 1 (F) protein to β -actin in treated macrophages, compared to medium treated cells. The results are shown as the mean \pm SEM of macrophage from cultures established from three individual fish ($n = 3$). The asterisk (*) indicates the significant difference at $P < 0.05$ compared to the medium treated cells. The pound sign (#) denotes the significant difference at $P < 0.05$ between different rgHMGB1 treated groups.

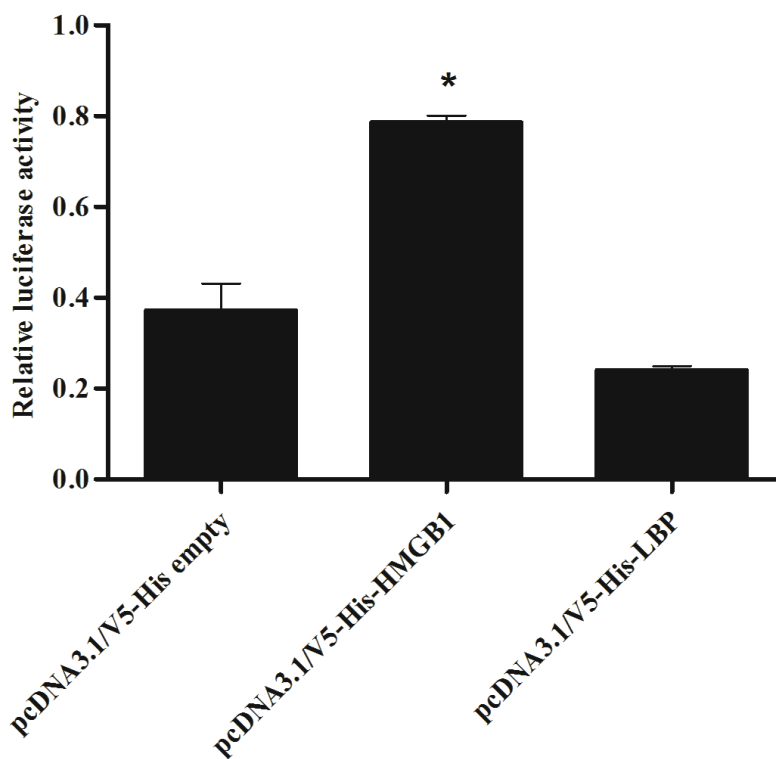


Figure 8.11. Goldfish HMGB1 protein promotes NF- κ B transcriptional activation.

HEK293 cells were transfected with 200 ng of pNF- κ B-Luc, 20 ng of pRL-TK reporter vectors and either 200 ng of pcDNA3.1/V5-His empty vector or the same amount of pcDNA3.1/V5-His-HMGB1 or pcDNA3.1/V5-His-LBP (negative control). At 24 h after transfection, cells were harvested and analyzed using the Dual Luciferase kit. All values represent three independent experiments in triplicates. The asterisk (*) indicates the significant difference at $P < 0.05$ compared to pcDNA3.1/V5-His empty in each group.

CHAPTER IX: GENERAL DISCUSSION

The interest in teleost immune responses is due to at least two reasons: (i) the teleosts are the lower vertebrate class that have functional innate and adaptive immunity, allowing for the assessment of the evolution of immune systems in metazoans; and (ii) crowding and associated stress of fish in aquaculture setting have led to an increase in the prevalence of infectious diseases in farmed fish species. Therefore, knowledge regarding the mechanisms of host defense in fish may allow for optimization of their immune responses against infectious diseases.

Innate immune responses are essential for host defense against infections and are particularly important in lower vertebrates in which the innate immune mechanisms feature prominently in host defense. Lower vertebrates, such as bony fish, have evolved superb innate host defense responses and the central effector cells of the innate immunity are cells called macrophages. The understanding of the regulatory mechanisms of macrophage inflammatory responses, particularly those that play a role in host defense against pathogens is of pivotal importance to augment the ability of bony fish to control infectious diseases.

9.1. OVERVIEW OF FINDINGS

The main goal of my doctoral thesis was to examine the roles of cytosolic PRRs that are involved in the recognition of Gram-negative and Gram-positive bacteria.

Specifically, I focused on the NOD-like receptor (NLRs) expression and functions of NLRs in goldfish macrophages.

To study the role of NLRs in host defense of goldfish, I used the high-throughput sequencing and transcriptome assembly analysis and identified that the NLRs were differentially expressed in goldfish spleen after exposure to *M. marinum* (Appendix A). To my knowledge, this is the first annotated transcriptome database for the goldfish (*C. auratus* L.). The *de novo* assembly of goldfish spleen transcriptome yielded 183,343 unigenes, which was about a 12-fold increase in identified nucleotide sequences compared to what had been deposited to GenBank (as of November 2016). Furthermore, the identified DEGs and signaling pathways between non-infected and *M. marinum*-infected fish will provide a valuable resource for investigation and elucidation of the anti-mycobacterial responses in teleosts (Appendix A).

In the initial group of experiments on the role of NLRs in the antimicrobial responses of goldfish macrophages, I first focused on identifying and characterizing NOD1, NOD2 and NLRX1 following exposure of the cells to various stimuli (Chapter IV, Fig. 9.1). *In silico* analysis of goldfish NOD1, NOD2 and NLRX1 indicated that they shared structural similarity to mammalian NOD1, NOD2 and NLRX1 proteins. Based on the NOD1 and NOD2 expression analyses in normal goldfish tissues and immune cell populations, I concluded that these proteins might be involved in the early detection of fish bacterial pathogens. To understand how these receptors were induced, I examined their expression profiles in response to different PAMPs and Gram-negative and Gram-positive bacteria. The results showed that the mRNA levels of goldfish NOD1 were

primarily upregulated by the Gram-negative bacterial components, such as LPS and PGN, as well as virus mimic structures (Poly I:C) and Gram-negative bacterium *A. salmonicida*. The mRNA levels of goldfish NOD2 and NLRX1 were significantly upregulated after treatment with different bacteria components (LPS, MDP and PGN), and following exposure to, *A. salmonicida* and *M. marinum*. These findings suggested that goldfish NOD-like receptor function is highly conserved and that they play a pivotal role in the recognition of fish pathogens such as *A. salmonicida* and *M. marinum*.

After I characterized goldfish NOD-like receptors and identified their activators in goldfish macrophages, my efforts were directed towards determining whether RIP2 was a critical molecule in NOD1 and NOD2 signaling pathways (Chapter VI, Fig. 9.1). Using co-immunoprecipitation assays, RIP2 was found to associate with NOD1 and NOD2 in eukaryotic cells. Examination of NF- κ B activation using the dual luciferase reporter assay revealed that RIP2 over-expression resulted in the activation of NF- κ B signal pathway. The activation of RIP2 after binding to NOD1 and NOD2 causes the down-stream activation of transcriptional factor NF- κ B, and eventual production of pro-inflammatory cytokines in mammals (100, 101). By employing a specific RIP2 inhibitor (SB203580), I found that RIP2 regulated the production of TNF α -2 and IL-1 β 1 in goldfish macrophages exposed to *M. marinum*. My results indicated that the conserved NOD1/NOD2-RIP2-NF- κ B signaling pathway was present in bony fish, and that it played an important role in antimicrobial responses in goldfish macrophages in response to *M. marinum* (Chapter V).

The *in silico* analysis of the NLRP3rel molecule of the goldfish (Chapter VI, Fig. 9.1), indicated that that it contained most of the important functional domains that

have been identified in mammalian NLRP3. However, the goldfish NLRP3rel molecule structurally differed from its mammalian counterparts because instead of a PYD, it featured a PRY. It has been shown that the PRY domain was functionally similar to the PYD domain in mammals (439, 440). Despite being structurally different to their mammalian counterparts, I postulated that the goldfish NLRP3rel molecule shared similar functions to that reported for the NLRP3 inflammasome of mammals.

To explore the recognition of NLRP3rel molecule in goldfish macrophages, I examined its mRNA and protein levels using Q-PCR and Western blot, respectively, following treatment of macrophages with different PAMPs and two fish pathogens, heat-killed *A. salmonicida* and heat-killed or live *M. marinum* (Chapter VI). The results revealed that gfNLRP3 was activated by nigericin and ATP, indicating that the induction of NLRP3rel molecule was similar between fish and mammals. For example, nigericin was widely used as an activator of NLRP3 inflammasome, and NLRP3-dependent caspase-1 and pro-inflammatory cytokine processing (149, 150). It has been reported that nigericin caused the efflux on intracellular K^+ to activate NLRP3rel molecule inflammasome assembly in mammals (361, 443, 481). In order to investigate signaling pathway of the NLRP3rel molecule in teleost, I also characterized a CARD- and PYD-containing molecule, the ASC, that functions as an adaptor molecule that transduces the intracellular signaling after inflammasome formation in mammals (Chapter VI, Fig. 9.2) (53, 210, 449, 450). I observed that nigericin upregulated the mRNA and protein levels of ASC, and that it also induced LDH release in goldfish macrophages. Given that nigericin-induced LDH release, a critical feature of pyroptosis, was significantly blocked

by the caspase-1 inhibitor, these observations suggested that the nigericin-induced cell death was caspase-1-dependent and was most likely the result of the NLRP3rel inflammasome activation in teleosts.

The confocal microscopy studies indicated that goldfish rgfNLRP3rel molecule associated with ASC forming a unique “ring”-like structures in eukaryotic cells (Chapter VI). The goldfish inflammasome “ring” structure I observed appeared to be distinct from the inflammasome macromolecular complex “ring” structure featured in LPS-primed mammalian THP-1 cells, where NLRP3 formed smaller ring-like structure within the ASC ring, rather than surrounding ASC specks as observed in goldfish macrophages (442). This suggests that the mechanisms of the teleost inflammasome assembly may be different from those of mammals.

The co-IP assays also indicated that goldfish ASC and caspase-1 associated, suggesting that in teleosts, there was the formation of a characteristic NLRP3-ASC-caspase-1 multiprotein complex (Chapter VII). That NLRP3rel molecule signaling pathway was functional in teleosts was confirmed by measuring the protein levels of IL-1 β and HMGB1, produced following treatment of goldfish macrophages with nigericin (Chapter VI).

Unlike teleost IL-1 β , known as a central pro-inflammatory cytokine in teleosts (276, 482–484), there is limited information regarding the effects of HMGB1 on antimicrobial response and cytokine production, as well as its molecular mechanism in fish. It has been shown that HMGB1 acts like a pro-inflammatory cytokine whose production is dependent on inflammasome formation and caspase-1 activation (481).

Recent studies also indicated that during pyroptosis (“inflammatory apoptosis”), there is a translocation of HMGB1 protein from the nucleus into the cell cytoplasm and eventual secretion of HMGB1 by immune cells in response to a variety of exogenous and endogenous danger signals (251, 423). For example, deletion of inflammasome components in mammalian cells severely impaired HMGB1 release during endotoxemia or bacteriemia (251, 423).

In a series of experiments, I demonstrated, for the first time, that goldfish recombinant HMGB1 acted as a critical regulatory cytokine of inflammation and antimicrobial response of the goldfish (Chapter VIII, Fig. 9.1). For example, the recombinant HMGB1 primed respiratory burst in monocytes, as well as induced nitric oxide response and the production of TNF α -2 and IL-1 β 1 in primary goldfish macrophages.

9.2. THE ROLE OF CYTOSOLIC NOD-LIKE RECEPTORS IN THE REGULATION OF THE INNATE IMMUNITY IN TELEOSTS

The antimicrobial innate immune responses are initiated by the recognition of PAMPs through PRRs. Unlike adaptive immune responses, the innate immunity relies primarily on phagocytic cells to “sense” the presence of microbes and initiate mechanisms to eliminate the pathogens. The detection of the highly conserved PAMPs is achieved through PRRs that can be found in the extracellular space, integrated in cellular membranes or in the cytosol. Pattern recognition of non-self molecules or modified endogenous DAMPs is essential for competent innate immune responses. An

expansive repertoire of germ-line encoded PRRs exist in all metazoans, underlining their importance in immune function.

The NLRs are a large family of proteins with diverse functions in the immune system. In addition to NOD-like receptors (NOD1, NOD2 and NLRX1), this family of proteins also contains the subfamily members (NLRP1, NLRP3 and NLRC4), that after PAMPs recognition, form large multiprotein complexes called inflammasomes. In mammals, engagement and oligomerization of inflammasome molecules leads to activation of caspase-1 (148, 450). Caspase-1 activation is achieved through an adaptor molecule, ASC (445, 485), that in turn processes the cytosolic precursors of the pro-inflammatory cytokines IL-1 β and IL-18, allowing for the secretion of biologically active proteins (445, 486).

The NLRP subfamily molecules are large, highly polymorphic molecules in various organisms including *Arabidopsis* spp. (198), zebrafish (27), mouse (199, 200) and humans (201–203). To date there are limited reports on the inflammasomes in teleost fish, although NLRP-like isoforms are present in the National Center for Biotechnology Information (NCBI) database.

In mammals, the ligands of most of the NLRs have been characterized (63, 84). NOD1 and NOD2 recognize different structural core motifs derived from PGN: (i) NOD1 senses the iE-DAP of Gram-negative bacteria and certain Gram-positive bacteria; (ii) NOD2 detects the MDP present in all Gram-negative and Gram-positive bacteria, confirmed by 3D structure analysis between the iE-DAP, MDP and LRR structures of NOD1 and NOD2 (487, 488). Similar to the mammalian NLRs, fish iE-DAP and MDP

activate both NOD1 and NOD2 (50, 51, 53). In addition, the mRNA levels of NOD1 and NOD2 are up-regulated in fish after exposure to various of immune stimuli and pathogens (49–51, 53, 55, 56). Thus, the recognition of bacteria by teleost NOD1 and NOD2 appears to be highly conserved throughout evolution (Figs. 9.1 and 9.2).

The ability of NOD1 and NOD2 to detect viruses, differs between mammals and teleosts. Whereas mammalian NOD1 and NOD2 primarily sense bacterial toxins (97, 476). In contrast, teleost NOD1/NOD2 recognize and respond to the virus mimic Poly I:C and other fish viruses, implying that fish NOD1/NOD2 can efficiently detect viral infections.

In contrast to PAMPs that are recognized by fish NOD1 and NOD2, much less is known about the signaling pathways of NOD1 and NOD2 in teleosts. It has been shown in mammals that once activated, NOD1 and NOD2 receptors oligomerize and recruit RIP2 through CARD-CARD interactions involving their amino-terminal CARD motifs (93, 101). In my doctoral research, I demonstrated, for the first time, that teleost RIP2 plays an essential role in both NOD1 and NOD2 signaling pathways (Fig. 9.1). However, the recruitment mechanisms of NOD1/NOD2-RIP2 association require further investigation. For example, a few members of the inhibitor of apoptosis proteins (IAPs), such as XIAP, cIAP1 and cIAP2 bind and polyubiquitinate RIP2, and promote NOD1/NOD2-RIP2 interaction in mammals (94–96). There are no reported IAPs in teleosts and their function remains largely unknown, let alone their involvement in NOD1/NOD2-RIP2 pathway.

RIP2 interacts with the regulatory NF- κ B subunit NEMO/IKK, triggering I κ B phosphorylation and NF- κ B activation, which leads to production and secretion of pro-inflammatory cytokines and chemokines (93, 100). Previous observations in mammals also suggested that the MAPK kinase family member TAK1 provided the link between RIP2 and NF- κ B activation after NOD1 and NOD2 recognition of specific PAMPs (93, 99–101, 103). Indeed, my results revealed that RIP2 activated NF- κ B and was also involved in the processing of two pro-inflammatory cytokines, TNF α -2 and IL-1 β 1. However, the mechanisms of how NOD1/NOD2-RIP2 complexes trigger the activation of NF- κ B including the degradation of I κ B α , and translocation of NF- κ B subunits, and activation of MAPK such as the phosphorylation of MAPK subunits (JNK, ERK and p38), remain to be fully elucidated in teleosts.

The mammalian NOD1-RIP2 complex has been shown to bind to the TRAF3-TBK1/IKK- ϵ -IRF7 cascade which signals the production of Type I IFN (98). In contrast, NOD2 can also induce Type I IFN production. However, this is achieved through the RIP2-independent MAVS-IRF3 pathway (97). Since TRAF3 and MAVS are the TLR and RLR signaling molecules, respectively, the involvement of these molecules in the NOD1/NOD2 signaling pathway, suggests the existence of a cross-talk between TLR-NLR and RLR-NLR pattern recognition receptors in mammals. The mechanism of the NOD1/NOD2-mediated Type I IFN production, and their relationship to TLR and/or RLR pathways and regulatory machinery remain to be elucidated in teleosts.

As indicated above, a subfamily of the NLRs (NLRP1, NLRP3, NLRC4) are known to form inflammasomes after recognition of PAMPs and/or DAMPs. For example, NLRP1

primarily detects toxins from Gram-negative bacteria (e.g. *Bacillus anthracis*), protozoan parasites (e.g. *Toxoplasma gondii*), as well as muramyl dipeptide (MDP) (137, 434–436). NLRC4, recognizes cytosolic flagellin of Gram-negative bacteria, such as *Salmonella typhimurium*, *Shigella flexneri*, *Pseudomonas aeruginosa* and *Legionella pneumophila* (164–168, 223, 329). In contrast, NLRP3 is more of a “generalist” NLR that recognizes a wide range PAMPs, including bacterial, viral, fungal and protozoan pathogens (164–168, 223, 329). At present, there are no reported NLRPs in teleosts, but several computational predicted NACHT, LRR and PYD domains-containing protein (NLRP) isoforms are featured in the NCBI database, such as NLRP3 (XP_017212365.1), NLRP3X1 (XP_017206752.1), NLRP12 (XP_009299711.1), NLRP12-like (XP_009289652.1) and others. I found that there are many NLRP3 homologues in the assembled goldfish transcriptome (Appendix A). However, the generation of the full NLRP3 sequence would be required for confirmation of its existence in teleosts. In this thesis, I report, for the first time, the full sequence of an “NLRP3rel” molecule in teleosts, because the comparison between mammalian and goldfish NLRP3 sequences revealed that teleost orthologues do not have the PYD domain, which is the central signaling transduction domain of the mammalian NLRP3 inflammasome. Given that goldfish NLRP3rel molecule directly associated with ASC, I postulated that the PYR and SPRY domains may functionally replace the PYD domain in teleosts to initiate the inflammasome pathway, based on the observations that the PYD and SPRY/PYR domains are functionally similar in mammals. The SPRY/PYR domain has been shown to interact with not only NLRP3,

but also caspase-1 to modulate IL-1 β production, suggesting that the SPRY/PYR domain is functionally similar to the PYD domain (439, 440).

To date, there are no reports regarding the characterization of NLRPs and the association of NLRPs and ASC in teleost. In this thesis, I demonstrated that the NLRP3rel molecule of the goldfish associated with ASC, and that this association resulted in IL-1 β and HMGB1 production via the NLRP3/ASC/caspase-1 mediated pathway (Fig. 9.1). Indeed, in contrast to the body of knowledge on the mammalian NLRP3, we know very little about the biology of teleost NLRP3. Future research should focus on whether the SPRY/PYR domain of NLRP3rel directly binds to the PYD domain of ASC in goldfish. In addition, the functional aspects of the activation of ASC and caspase-1-mediated pyroptosis, as well as other inflammasome molecules, their ligands and signaling pathways remain to be characterized in teleosts.

In the chapter VIII, I reported that ASC associated with NLRP3rel and caspase-1, and also associated with RIP2, a CARD-containing molecule of the NOD1/NOD2 signaling pathway. The teleost RIP2-ASC association suggests that there may be a cross-talk between NOD1/NOD2 and inflammasome pathways in bony fish. It has been suggested that RIP2/caspase-1 can associate to mediate NF- κ B activation and generate IL-1 β in mammals (104, 107). Therefore, it is not surprising that teleost CARD-domain-containing molecules may exhibit this homophilic or heterophilic protein interaction that was reported for the mammalian CARD-domain-containing molecules.

In teleost, NLRs and their expression profiles following exposure to immune stimuli and fish pathogens have been examined. However, few studies investigated the

regulation of NLRs and inflammasomes, especially the signaling pathways after exposure to a specific pathogen. I believe that this may be due to several reasons: (i) NLRs are normally very large molecules with a full sequence more than 3000 bp, and are difficult to clone and express; (ii) NLRs are highly polymorphic; (iii) a lack of specific goldfish reagents (primarily antibodies) making it difficult to specifically examine post-transcriptional and phosphorylational regulation of NLR signaling pathways; and (iv) commonly used genetic modification techniques have not been developed and/or validated for most teleost species, except for zebrafish. Further studies on the biology of NLRs must await the development of teleost-specific reagents.

9.3. FUTURE DIRECTIONS

The work presented in this thesis focused on the biology of cytosolic PRRs that recognize bacterial pathogens. I believe that the results of my doctoral thesis research provide a solid basis for future study of innate immune receptors in teleosts. There are, of course, a number of different research areas that I believe should be pursued in the future, some of which are described below.

9.3.1. Understanding the cross-talk between NOD-like receptors and inflammasome pathways

In the proposed NOD1/NOD2 and NLRP3rel inflammasome signaling pathways, there is evidence to indicate that there are cross-talks between these pathways since ASC, RIP2 and caspase-1 were demonstrated to association in goldfish macrophages. In

addition to the direct association between the ASC and both RIP2 and caspase-1, it is also possible that RIP2 and caspase-1 can also associate, with or without the presence of ASC, via the homologous CARD-CARD domains that both molecules possess (206). To investigate the possible association between RIP2 and caspase-1 one could employ confocal microscopy and co-IP analyses. The specific conditions that induce these cross-talks in goldfish macrophages should be examined, especially in response to pathogens, such as *A. salmonicida* and *M. marinum*. This would be of interest since I have demonstrated that *M. marinum* induced NOD2 activation and pro-IL-1 β production, and at the same time down-regulated the NLRP3rel transcriptional activation. I postulated that down-regulation of the NLRP3 inflammasome pathway may be a novel immune evasion strategy evolved by *M. marinum*, in order to protect macrophage integrity, and ensure continued propagation of the bacterium in its host cell.

9.3.2. Pyroptosis

The term pyroptosis was originally introduced to describe inflammatory programmed cell death in macrophages, which is characterized by cell lysis induced by bacterial infection that requires caspase-1 activation and the release of pyrogenic interleukins such as IL-1 β and IL-18 (17, 320). Pyroptosis is also considered as a hallmark of inflammasome-induced caspase-1-dependent processes (312, 313). In teleost, Angosto and colleagues were the first to propose a caspase-dependent pyroptotic cell death in seabream macrophages upon infection of *Salmonella* spp. (197). More recently, Varela and co-workers (319) observed the virus-induced pyroptosis of macrophages

during a viral hemorrhagic infection of zebrafish larvae. However, the distinct cellular morphological changes and biochemical events during pyroptosis have not been fully elucidated in teleosts. I have confirmed that NLRP3, ASC, caspase-1 and IL-1 β , exist in goldfish, and therefore it is probable that bacterially-induced inflammasome-dependent pyroptosis occurs in goldfish macrophages.

The acridine orange/ethidium bromide (AO/EB) staining technique has been used as a simple, rapid and reliable method for the detection of pyroptosis, both qualitatively and quantitatively (489). AO is a cell-permeable, acidophilic green dye that stains lysosomes and nuclei of live cells. EB is a DNA intercalating agent that emits a red fluorescence upon binding to DNA. AO and EB have been used widely in combination to study cell death (489, 490). Therefore, AO/EB staining can be used to examine the pyroptotic cell death using sorted goldfish macrophages in response to *M. marinum* and nigericin.

In addition, ImageStream flow cytometry based Annexin V-FITC/PI staining assay can be used to differentiate between apoptosis and pyroptosis (491, 492). The cells undergoing apoptotic cell death will be FITC positive and PI negative whereas cells undergoing pyroptosis will be positive for both FITC and PI.

To complement the above studies, confocal microscopy can be used to examine the bacterially-induced morphological changes of apoptosis and pyroptosis, especially the chromosomal condensation and cell swelling, to understand the differences between apoptotic and pyroptotic cell death in teleost macrophages. In addition, the

anti-caspase-1 and anti-HMGB1 antibodies that I generated in this thesis could be used for elucidation of biochemical events during pyroptosis.

9.3.3. Using siRNA or CRISPR to mutate target genes to study NLR signaling pathways

The field of fish immunology during the past decade has witnessed tremendous advances to foster the understanding of the fish immune system. However, the examination of teleost immunity still lacks effective research tools. This has hampered the progress in characterization of specific immune mechanisms, such as the ability to produce knockout/knockdown fish (as in zebrafish). Recently, small interfering RNAs (siRNAs), and sequence-specific nuclease tools-based technologies, such as the clustered regularly interspaced short palindromic repeats (CRISPR), have made genome editing possible in lower vertebrates (493–496). It would be worthwhile to apply these technologies to knock down the NLRs, RIP2, ASC or caspase-1 in goldfish macrophages, as well as in whole animals, and then assess the function of NLRs after exposure of fish to different pathogens. Results from such studies would further elucidate the NLR signaling pathways in teleosts.

9.3.4. Functional assessment of PRY/SPRY domain, and other NLR family members and associated signaling molecules, in teleosts

Goldfish NLRP3rel lacks of a PYD domain, while the PRY/SPRY domain has been postulated to function as PYD domain in teleost. To test this hypothesis, one could

generate a truncated NLRP3rel plasmid without the PRY/SPRY domain, and ASC without PYD domain, and then perform the co-IP analyses, as described in Chapter VII.

In addition to NLRP3rel, there may be other candidate molecules in fish that can form inflammasomes, including NLRP1 and NLRC4. For example, in the goldfish spleen transcriptome, there are several NLRP1 transcripts. To evaluate if these can participate in the formation of inflammasomes, one can conduct similar experiments as I described in Chapter VI, to functionally characterize the NLRP1 and to identify the specific inducers of goldfish NLRP1. Similar experiments can be performed to assess the potential functions of other NLRs in goldfish macrophages.

9.3.5. Using the goldfish spleen transcriptome database as a valuable resource to study anti-mycobacterial responses in teleosts

Goldfish serve as useful model organisms in several fields of biology, including neurophysiology (497), immunotoxicity (498–500), endocrinology (501, 502), pharmacology (503) and comparative immunology (53, 117, 194, 504–510). In my thesis research I assembled goldfish spleen transcriptome during the acute *M. marinum* infection (Appendix A). The RNAseq generated 183,343 unigenes (which represents a greater than 12 times increase in identified nucleotide sequences compared to what has been deposited to GenBank, as of November, 2016) and that significantly expanded our knowledge of goldfish transcriptome. In addition, 843 DEGs between non-infected and *M. marinum*-infected fish were identified and 81 of which were immune-related genes. KEGG pathway enrichment analysis of the DEGs identified 19 immune-related pathways

from the enriched 218 pathways. Among these pathways, genes encoding molecules important for both innate and adaptive immunity were identified in goldfish exposed to *M. marinum*, including those involved in the NOD-like receptor signaling pathways, complement and coagulation cascades, FcγR-mediated phagocytosis, chemokine signaling pathway, apoptosis, NF-κB pathway and MAPK signaling pathway. The gene expression results of C-type lectins, complement activation and FcγR-mediated phagocytosis indicated that these immune mechanisms play critical roles in the early host response against *M. marinum* in the goldfish. Based on these observations, the interaction between the NOD-like receptor pathway, complement activation and FcγR-mediated phagocytosis should be investigated to gain a more comprehensive view of the antimycobacterial responses of goldfish macrophages.

9.4. SUMMARY

Fish model systems are being used to study host defense against pathogens because fish represent an essential link between innate and adaptive immunity during early vertebrate evolution, and translocation of organisms from aquatic to terrestrial environments. Although vertebrate immune system appears to be highly conserved, the study of fish immunology could provide insights into the early events in the development of the vertebrate immune system.

In this thesis, I reported on the molecular identification and functional characterization of a number of goldfish NOD-like receptors and their signaling pathway molecules. I believe that the research findings described in this dissertation have

contributed to our knowledge on the function of innate immune receptors of lower vertebrates.

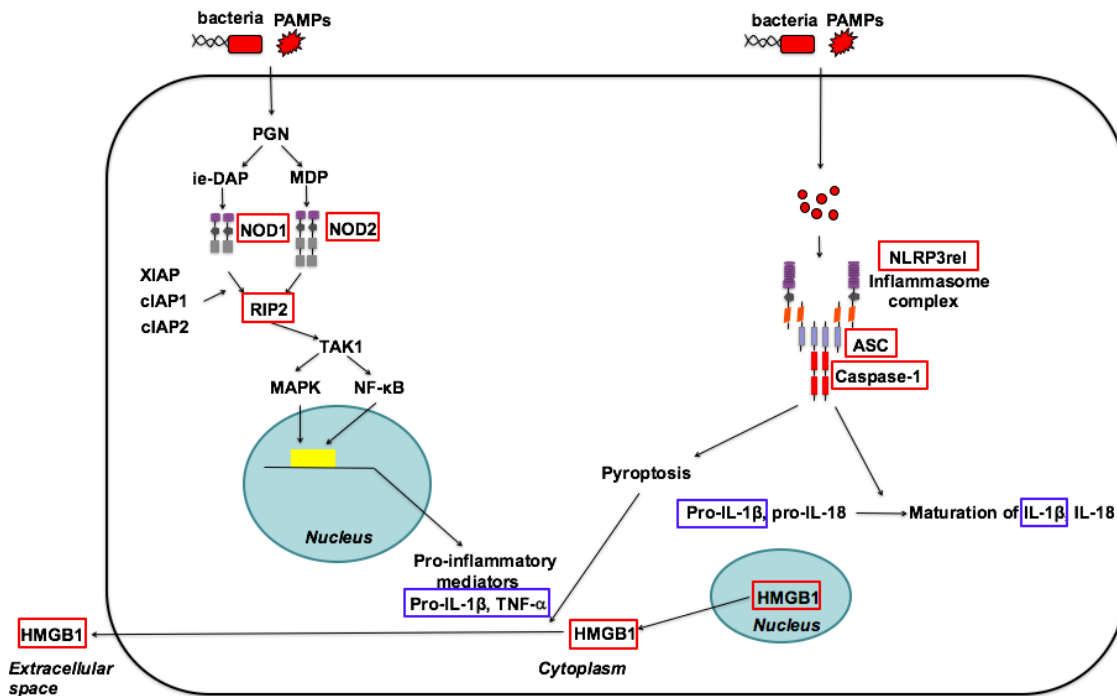


Figure 9.1. Schematic representation of the NOD-like receptors signaling cascades in teleosts.

Upon activation, with effects of XIAP, cIAP1 or cIAP2, NOD1 and NOD2 can recruit with RIP2 to activate NF-κB or MAPK pathway to secrete TNF-α and IL-1β. Similarly, upon activation, the activated NLRP3 inflammasome can associate with ASC and caspase-1 to process IL-1β and IL-18. The red boxes represent genes that were characterized in goldfish in my thesis. The blue boxes represent other goldfish genes that have been studied in our laboratory.

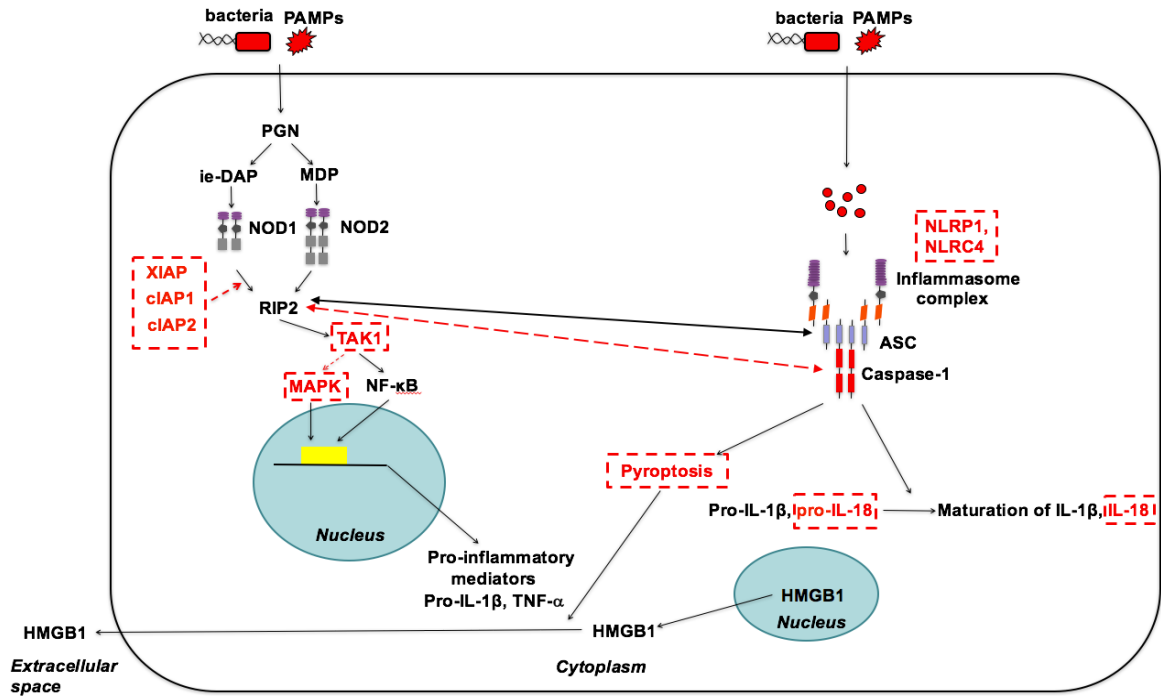


Figure 9.2. Schematic representation of the NOD-like receptors signaling cascades in vertebrates.

Upon activation, NOD1 and NOD2 can recruit with RIP2 to activate NF-κB to secrete TNF-α and IL-1β. The activated NLRP3 inflammasome can interact with ASC and caspase-1 to process IL-1β. The red dotted arrows show the possible associations might be existed in teleost. The red dotted boxes represent the postulated signaling molecules or biochemical events in teleosts.

REFERENCES

1. **Strowig T, Henao-Mejia J, Elinav E, Flavell R.** 2012. Inflammasomes in health and disease. *Nature* **481**:278–286.
2. **Fabbri M.** 2012. TLRs as miRNA Receptors. *Cancer Res* **72**:6333–6337.
3. **Kono DH, Baccala R, Theofilopoulos AN.** 2013. TLRs and interferons: a central paradigm in autoimmunity. *Curr Opin Immunol* **25**:720–727.
4. **Takeda K, Akira S.** 2005. Toll-Like Receptors in Innate Immunity. *Int Immunol* **17**:1–14.
5. **Bird L.** 2010. Inflammation: TLRs find a partner in crime. *Nat Rev Immunol* **10**:82–82.
6. **Palti Y.** 2011. Toll-like receptors in bony fish: From genomics to function. *Dev Comp Immunol* **35**:1263–1272.
7. **Harton JA, Linhoff MW, Zhang J, Ting JP-Y.** 2002. Cutting Edge: CATERPILLER: A Large Family of Mammalian Genes Containing CARD, Pyrin, Nucleotide-Binding, and Leucine-Rich Repeat Domains. *J Immunol* **169**:4088–4093.
8. **Ting JP-Y, Davis BK.** 2005. CATERPILLER: A Novel Gene Family Important in Immunity, Cell Death, and Diseases. *Annu Rev Immunol* **23**:387–414.
9. **Inohara N, Ogura Y, Fontalba A, Gutierrez O, Pons F, Crespo J, Fukase K, Inamura S, Kusumoto S, Hashimoto M, Foster SJ, Moran AP, Fernandez-Luna JL, Nuñez G.** 2003. Host Recognition of Bacterial Muramyl Dipeptide Mediated Through NOD2 Implications For Crohn's Disease. *J Biol Chem* **278**:5509–5512.
10. **Inohara N, Nuñez G.** 2003. NODs: intracellular proteins involved in inflammation and apoptosis. *Nat Rev Immunol* **3**:371–382.
11. **Inohara N, Chamailard M, McDonald C, Nuñez G.** 2005. NOD-LRR PROTEINS: Role in Host-Microbial Interactions and Inflammatory Disease. *Annu Rev Biochem* **74**:355–383.
12. **Martinon F, Tschopp J.** 2004. Inflammatory caspases: linking an intracellular innate immune system to autoinflammatory diseases. *Cell* **117**:561–574.
13. **Fritz JH, Ferrero RL, Philpott DJ, Girardin SE.** 2006. Nod-like proteins in immunity, inflammation and disease. *Nat Immunol* **7**:1250–1257.
14. **Meylan E, Tschopp J, Karin M.** 2006. Intracellular pattern recognition receptors in the host response. *Nature* **442**:39–44.
15. **Carneiro LAM, Travassos LHD.** 2013. The interplay between NLRs and autophagy in immunity and inflammation. *Mol Innate Immun* **4**:361.
16. **Akira S, Takeda K.** 2004. Toll-like receptor signalling. *Nat Rev Immunol* **4**:499–511.
17. **Lamkanfi M, Dixit VM.** 2014. Mechanisms and Functions of Inflammasomes. *Cell* **157**:1013–1022.
18. **Allen IC.** 2014. Non-Inflammasome Forming NLRs in Inflammation and Tumorigenesis. *Front Immunol* **5**.
19. **De Nardo D, De Nardo CM, Latz E.** 2014. New Insights into Mechanisms Controlling the NLRP3 Inflammasome and Its Role in Lung Disease. *Am J Pathol* **184**:42–54.

20. **Neumann S, Burkert K, Kemp R, Rades T, Rod Dunbar P, Hook S.** 2014. Activation of the NLRP3 inflammasome is not a feature of all particulate vaccine adjuvants. *Immunol Cell Biol* **92**:535–542.
21. **Quiniou SMA, Boudinot P, Bengtén E.** 2013. Comprehensive survey and genomic characterization of Toll-like receptors (TLRs) in channel catfish, *Ictalurus punctatus*: identification of novel fish TLRs. *Immunogenetics* **65**:511–530.
22. **Zhu L, Nie L, Zhu G, Xiang L, Shao J.** 2013. Advances in research of fish immune-relevant genes: a comparative overview of innate and adaptive immunity in teleosts. *Dev Comp Immunol* **39**:39–62.
23. **Rajendran KV, Zhang J, Liu S, Peatman E, Kucuktas H, Wang X, Liu H, Wood T, Terhune J, Liu Z.** 2012. Pathogen recognition receptors in channel catfish: II. Identification, phylogeny and expression of retinoic acid-inducible gene I (RIG-I)-like receptors (RLRs). *Dev Comp Immunol* **37**:381–389.
24. **Yang C, Su J, Huang T, Zhang R, Peng L.** 2011. Identification of a retinoic acid-inducible gene I from grass carp (*Ctenopharyngodon idella*) and expression analysis in vivo and in vitro. *Fish Shellfish Immunol* **30**:936–943.
25. **Chang M, Collet B, Nie P, Lester K, Campbell S, Secombes CJ, Zou J.** 2011. Expression and Functional Characterization of the RIG-I-Like Receptors MDA5 and LGP2 in Rainbow Trout (*Oncorhynchus mykiss*). *J Virol* **85**:8403–8412.
26. **Su J, Huang T, Dong J, Heng J, Zhang R, Peng L.** 2010. Molecular cloning and immune responsive expression of MDA5 gene, a pivotal member of the RLR gene family from grass carp *Ctenopharyngodon idella*. *Fish Shellfish Immunol* **28**:712–718.
27. **Laing KJ, Purcell MK, Winton JR, Hansen JD.** 2008. A genomic view of the NOD-like receptor family in teleost fish: identification of a novel NLR subfamily in zebrafish. *BMC Evol Biol* **8**:42.
28. **Rajendran KV, Zhang J, Liu S, Kucuktas H, Wang X, Liu H, Sha Z, Terhune J, Peatman E, Liu Z.** 2012. Pathogen recognition receptors in channel catfish: I. Identification, phylogeny and expression of NOD-like receptors. *Dev Comp Immunol* **37**:77–86.
29. **Zhang H, Robison B, Thorgaard GH, Ristow SS.** 2000. Cloning, mapping and genomic organization of a fish C-type lectin gene from homozygous clones of rainbow trout (*Oncorhynchus mykiss*). *Biochim Biophys Acta BBA - Gene Struct Expr* **1494**:14–22.
30. **Lin A-F, Xiang L-X, Wang Q-L, Dong W-R, Gong Y-F, Shao J-Z.** 2009. The DC-SIGN of Zebrafish: Insights into the Existence of a CD209 Homologue in a Lower Vertebrate and Its Involvement in Adaptive Immunity. *J Immunol* **183**:7398–7410.
31. **Zhang M, Hu Y, Sun L.** 2010. Identification and molecular analysis of a novel C-type lectin from *Scophthalmus maximus*. *Fish Shellfish Immunol* **29**:82–88.
32. **Liu F, Li J, Fu J, Shen Y, Xu X.** 2011. Two novel homologs of simple C-type lectin in grass carp (*Ctenopharyngodon idellus*): Potential role in immune response to bacteria. *Fish Shellfish Immunol* **31**:765–773.
33. **Zhang J, Kong X, Zhou C, Li L, Nie G, Li X.** 2014. Toll-like receptor recognition of bacteria in fish: Ligand specificity and signal pathways. *Fish Shellfish Immunol* **41**:380–388.

34. **Rauta PR, Samanta M, Dash HR, Nayak B, Das S.** 2014. Toll-like receptors (TLRs) in aquatic animals: Signaling pathways, expressions and immune responses. *Immunol Lett* **158**:14–24.
35. **Aoki T, Hikima J, Hwang SD, Jung TS.** 2013. Innate immunity of finfish: Primordial conservation and function of viral RNA sensors in teleosts. *Fish Shellfish Immunol* **35**:1689–1702.
36. **Langevin C, Aleksejeva E, Passoni G, Palha N, Levraud J-P, Boudinot P.** 2013. The Antiviral Innate Immune Response in Fish: Evolution and Conservation of the IFN System. *J Mol Biol* **425**:4904–4920.
37. **Ng TB, Fai Cheung RC, Wing Ng CC, Fang EF, Wong JH.** 2015. A review of fish lectins. *Curr Protein Pept Sci* **16**:337–351.
38. **Baker B, Zambryski P, Staskawicz B, Dinesh-Kumar SP.** 1997. Signaling in Plant-Microbe Interactions. *Science* **276**:726–733.
39. **Cohn J, Sessa G, Martin GB.** 2001. Innate immunity in plants. *Curr Opin Immunol* **13**:55–62.
40. **Bertin J, Nir W-J, Fischer CM, Tayber OV, Errada PR, Grant JR, Keilty JJ, Gosselin ML, Robison KE, Wong GHW, Glucksmann MA, DiStefano PS.** 1999. Human CARD4 Protein Is a Novel CED-4/Apaf-1 Cell Death Family Member That Activates NF- κ B. *J Biol Chem* **274**:12955–12958.
41. **Inohara N, Koseki T, del Peso L, Hu YM, Yee C, Chen S, Carrio R, Merino J, Liu D, Ni J, Nunez G.** 1999. Nod1, an Apaf-1-like activator of caspase-9 and nuclear factor-kappa B. *J Biol Chem* **274**:14560–14567.
42. **Ellis RE, Yuan JY, Horvitz HR.** 1991. Mechanisms and functions of cell death. *Annu Rev Cell Biol* **7**:663–698.
43. **Peter ME, Heufelder AE, Hengartner MO.** 1997. Advances in apoptosis research. *Proc Natl Acad Sci* **94**:12736–12737.
44. **Liu QA, Hengartner MO.** 1999. The Molecular Mechanism of Programmed Cell Death in *C. elegans*. *Ann N Y Acad Sci* **887**:92–104.
45. **Ogura Y, Inohara N, Benito A, Chen FF, Yamaoka S, Núñez G.** 2001. Nod2, a Nod1/Apaf-1 Family Member That Is Restricted to Monocytes and Activates NF- κ B. *J Biol Chem* **276**:4812–4818.
46. **Stein C, Caccamo M, Laird G, Leptin M.** 2007. Conservation and divergence of gene families encoding components of innate immune response systems in zebrafish. *Genome Biol* **8**:R251.
47. **Chen WQ, Xu QQ, Chang MX, Nie P, Peng KM.** 2010. Molecular characterization and expression analysis of nuclear oligomerization domain proteins NOD1 and NOD2 in grass carp *Ctenopharyngodon idella*. *Fish Shellfish Immunol* **28**:18–29.
48. **Chang M, Wang T, Nie P, Zou J, Secombes CJ.** 2011. Cloning of two rainbow trout nucleotide-binding oligomerization domain containing 2 (NOD2) splice variants and functional characterization of the NOD2 effector domains. *Fish Shellfish Immunol* **30**:118–127.

49. **Sha Z, Abernathy JW, Wang S, Li P, Kucuktas H, Liu H, Peatman E, Liu Z.** 2009. NOD-like subfamily of the nucleotide-binding domain and leucine-rich repeat containing family receptors and their expression in channel catfish. *Dev Comp Immunol* **33**:991–999.
50. **Swain B, Basu M, Samanta M.** 2012. Molecular cloning and characterization of nucleotide binding and oligomerization domain-1 (NOD1) receptor in the Indian Major Carp, rohu (*Labeo rohita*), and analysis of its inductive expression and down-stream signalling molecules following ligands exposure and Gram-negative bacterial infections. *Fish Shellfish Immunol* **32**:899–908.
51. **Swain B, Basu M, Sahoo BR, Maiti NK, Routray P, Eknath AE, Samanta M.** 2012. Molecular characterization of nucleotide binding and oligomerization domain (NOD)-2, analysis of its inductive expression and down-stream signaling following ligands exposure and bacterial infection in rohu (*Labeo rohita*). *Dev Comp Immunol* **36**:93–103.
52. **Hou Q-H, Yi S-B, Ding X, Zhang H-X, Sun Y, Zhang Y, Liu X-C, Lu D-Q, Lin H-R.** 2012. Differential expression analysis of nuclear oligomerization domain proteins NOD1 and NOD2 in orange-spotted grouper (*Epinephelus coioides*). *Fish Shellfish Immunol* **33**:1102–1111.
53. **Xie J, Hodgkinson JW, Katzenback BA, Kovacevic N, Belosevic M.** 2013. Characterization of three Nod-like receptors and their role in antimicrobial responses of goldfish (*Carassius auratus* L.) macrophages to *Aeromonas salmonicida* and *Mycobacterium marinum*. *Dev Comp Immunol* **39**:180–187.
54. **Unajak S, Santos MD, Hikima J, Jung T-S, Kondo H, Hirono I, Aoki T.** 2011. Molecular characterization, expression and functional analysis of a nuclear oligomerization domain proteins subfamily C (NLRC) in Japanese flounder (*Paralichthys olivaceus*). *Fish Shellfish Immunol* **31**:202–211.
55. **Park SB, Hikima J, Suzuki Y, Ohtani M, Nho SW, Cha IS, Jang HB, Kondo H, Hirono I, Aoki T, Jung TS.** 2012. Molecular cloning and functional analysis of nucleotide-binding oligomerization domain 1 (NOD1) in olive flounder, *Paralichthys olivaceus*. *Dev Comp Immunol* **36**:680–687.
56. **Li J, Gao Y, Xu T.** 2015. Comparative genomic and evolution of vertebrate NOD1 and NOD2 genes and their immune response in miiuy croaker. *Fish Shellfish Immunol* **46**:387–397.
57. **Biswas G, Bilen S, Kono T, Sakai M, Hikima J.** 2016. Inflammatory immune response by lipopolysaccharide-responsive nucleotide binding oligomerization domain (NOD)-like receptors in the Japanese pufferfish (*Takifugu rubripes*). *Dev Comp Immunol* **55**:21–31.
58. **Dostert C, Meylan E, Tschopp J.** 2008. Intracellular pattern-recognition receptors. *Adv Drug Deliv Rev* **60**:830–840.
59. **Tattoli I, Carneiro LA, Jéhanno M, Magalhaes JG, Shu Y, Philpott DJ, Arnoult D, Girardin SE.** 2008. NLRX1 is a mitochondrial NOD-like receptor that amplifies NF- κ B and JNK pathways by inducing reactive oxygen species production. *EMBO Rep* **9**:293–300.

60. **Magalhaes JG, Lee J, Geddes K, Rubino S, Philpott DJ, Girardin SE.** 2011. Essential role of Rip2 in the modulation of innate and adaptive immunity triggered by Nod1 and Nod2 ligands. *Eur J Immunol* **41**:1445–1455.
61. **Moore CB, Bergstralh DT, Duncan JA, Lei Y, Morrison TE, Zimmermann AG, Accavitti-Loper MA, Madden VJ, Sun L, Ye Z, Lich JD, Heise MT, Chen Z, Ting JP-Y.** 2008. NLRX1 is a regulator of mitochondrial antiviral immunity. *Nature* **451**:573–577.
62. **Franke A, Ruether A, Wedemeyer N, Karlsen TH, Nebel A, Schreiber S.** 2006. No association between the functional CARD4 insertion/deletion polymorphism and inflammatory bowel diseases in the German population. *Gut* **55**:1679–1680.
63. **Franchi L, Warner N, Viani K, Nuñez G.** 2009. Function of Nod-like receptors in microbial recognition and host defense. *Immunol Rev* **227**:106–128.
64. **Paria A, Deepika A, Sreedharan K, Makesh M, Chaudhari A, Purushothaman CS, Thirunavukkarasu AR, Rajendran KV.** 2016. Identification of Nod like receptor C3 (NLRC3) in Asian seabass, *Lates calcarifer*: Characterisation, ontogeny and expression analysis after experimental infection and ligand stimulation. *Fish Shellfish Immunol* **55**:602–612.
65. **Elvitigala DAS, Thulasitha WS, Lee J.** 2016. Characterization of a nucleotide-oligomerization domain (NOD) like receptor C5 (NLRC5) subfamily member from black rockfish (*Sebastes schlegelii*), portraying its transcriptional responses against immune stimulants. *Genes Genomics* **38**:303–310.
66. **Bourhis LL, Benko S, Girardin SE.** 2007. Nod1 and Nod2 in innate immunity and human inflammatory disorders. *Biochem Soc Trans* **35**:1479.
67. **Monie TP, Bryant CE, Gay NJ.** 2009. Activating immunity: lessons from the TLRs and NLRs. *Trends Biochem Sci* **34**:553–561.
68. **Chamaillard M, Hashimoto M, Horie Y, Masumoto J, Qiu S, Saab L, Ogura Y, Kawasaki A, Fukase K, Kusumoto S, Valvano MA, Foster SJ, Mak TW, Nuñez G, Inohara N.** 2003. An essential role for NOD1 in host recognition of bacterial peptidoglycan containing diaminopimelic acid. *Nat Immunol* **4**:702–707.
69. **Girardin SE, Travassos LH, Hervé M, Blanot D, Boneca IG, Philpott DJ, Sansonetti PJ, Mengin-Lecreulx D.** 2003. Peptidoglycan Molecular Requirements Allowing Detection by Nod1 and Nod2. *J Biol Chem* **278**:41702–41708.
70. **Travassos LH, Carneiro LAM, Girardin SE, Boneca IG, Lemos R, Bozza MT, Domingues RCP, Coyle AJ, Bertin J, Philpott DJ, Plotkowski MC.** 2005. Nod1 Participates in the Innate Immune Response to *Pseudomonas aeruginosa*. *J Biol Chem* **280**:36714–36718.
71. **Viala J, Chaput C, Boneca IG, Cardona A, Girardin SE, Moran AP, Athman R, Mémet S, Huerre MR, Coyle AJ, DiStefano PS, Sansonetti PJ, Labigne A, Bertin J, Philpott DJ, Ferrero RL.** 2004. Nod1 responds to peptidoglycan delivered by the *Helicobacter pylori* *cag* pathogenicity island. *Nat Immunol* **5**:1166–1174.
72. **Kim JG, Lee SJ, Kagnoff MF.** 2004. Nod1 Is an Essential Signal Transducer in Intestinal Epithelial Cells Infected with Bacteria That Avoid Recognition by Toll-Like Receptors. *Infect Immun* **72**:1487–1495.

73. **Zilbauer M, Dorrell N, Elmi A, Lindley KJ, Schüller S, Jones HE, Klein NJ, Núñez G, Wren BW, Bajaj-Elliott M.** 2007. A major role for intestinal epithelial nucleotide oligomerization domain 1 (NOD1) in eliciting host bactericidal immune responses to *Campylobacter jejuni*. *Cell Microbiol* **9**:2404–2416.
74. **Girardin SE, Tournebize R, Mavris M, Page A-L, Li X, Stark GR, Bertin J, DiStefano PS, Yaniv M, Sansonetti PJ, Philpott DJ.** 2001. CARD4/Nod1 mediates NF- κ B and JNK activation by invasive *Shigella flexneri*. *EMBO Rep* **2**:736–742.
75. **Carneiro LAM, Travassos LH, Soares F, Tattoli I, Magalhaes JG, Bozza MT, Plotkowski MC, Sansonetti PJ, Molkentin JD, Philpott DJ, Girardin SE.** 2009. *Shigella* Induces Mitochondrial Dysfunction and Cell Death in Nonmyleoid Cells. *Cell Host Microbe* **5**:123–136.
76. **Clarke TB, Davis KM, Lysenko ES, Zhou AY, Yu Y, Weiser JN.** 2010. Recognition of peptidoglycan from the microbiota by Nod1 enhances systemic innate immunity. *Nat Med* **16**:228–231.
77. **Girardin SE, Boneca IG, Viala J, Chamaillard M, Labigne A, Thomas G, Philpott DJ, Sansonetti PJ.** 2003. Nod2 Is a General Sensor of Peptidoglycan Through Muramyl Dipeptide (MDP) Detection. *J Biol Chem* **278**:8869–8872.
78. **Laroui H, Yan Y, Narui Y, Ingersoll SA, Ayyadurai S, Charania MA, Zhou F, Wang B, Salaita K, Sitaraman SV, Merlin D.** 2011. l-Ala- γ -d-Glu-meso-diaminopimelic Acid (DAP) Interacts Directly with Leucine-rich Region Domain of Nucleotide-binding Oligomerization Domain 1, Increasing Phosphorylation Activity of Receptor-interacting Serine/Threonine-protein Kinase 2 and Its Interaction with Nucleotide-binding Oligomerization Domain 1. *J Biol Chem* **286**:31003–31013.
79. **Grimes CL, Ariyananda LDZ, Melnyk JE, O’Shea EK.** 2012. The Innate Immune Protein Nod2 Binds Directly to MDP, a Bacterial Cell Wall Fragment. *J Am Chem Soc* **134**:13535–13537.
80. **Kobayashi KS, Chamaillard M, Ogura Y, Henegariu O, Inohara N, Núñez G, Flavell RA.** 2005. Nod2-Dependent Regulation of Innate and Adaptive Immunity in the Intestinal Tract. *Science* **307**:731–734.
81. **Gandotra S, Jang S, Murray PJ, Salgame P, Ehrt S.** 2007. Nucleotide-Binding Oligomerization Domain Protein 2-Deficient Mice Control Infection with *Mycobacterium Tuberculosis*. *Infect Immun* **75**:5127–5134.
82. **Divangahi M, Mostowy S, Coulombe F, Kozak R, Guillot L, Veyrier F, Kobayashi KS, Flavell RA, Gros P, Behr MA.** 2008. NOD2-Deficient Mice Have Impaired Resistance to *Mycobacterium tuberculosis* Infection through Defective Innate and Adaptive Immunity. *J Immunol* **181**:7157–7165.
83. **Coulombe F, Divangahi M, Veyrier F, De Léséleuc L, Gleason JL, Yang Y, Kelliher MA, Pandey AK, Sassetti CM, Reed MB, Behr MA.** 2009. Increased NOD2-Mediated Recognition of N-Glycolyl Muramyl Dipeptide. *J Exp Med* **206**:1709–1716.
84. **Shaw MH, Reimer T, Kim Y-G, Núñez G.** 2008. NOD-like receptors (NLRs): bona fide intracellular microbial sensors. *Curr Opin Immunol* **20**:377–382.

85. **Silva GK, Gutierrez FRS, Guedes PMM, Horta CV, Cunha LD, Mineo TWP, Santiago-Silva J, Kobayashi KS, Flavell RA, Silva JS, Zamboni DS.** 2010. Cutting Edge: Nucleotide-Binding Oligomerization Domain 1-Dependent Responses Account for Murine Resistance against *Trypanosoma cruzi* Infection. *J Immunol* **184**:1148–1152.
86. **Fritz JH, Girardin SE, Fitting C, Werts C, Mengin-Lecreux D, Caroff M, Cavillon J-M, Philpott DJ, Adib-Conquy M.** 2005. Synergistic stimulation of human monocytes and dendritic cells by Toll-like receptor 4 and NOD1- and NOD2-activating agonists. *Eur J Immunol* **35**:2459–2470.
87. **Enoksson M, Ejendal KFK, McAlpine S, Nilsson G, Lunderius-Andersson C.** 2011. Human Cord Blood-Derived Mast Cells Are Activated by the Nod1 Agonist M-TriDAP to Release Pro-Inflammatory Cytokines and Chemokines. *J Innate Immun* **3**:142–149.
88. **Watanabe T, Kitani A, Murray PJ, Strober W.** 2004. NOD2 is a negative regulator of Toll-like receptor 2-mediated T helper type 1 responses. *Nat Immunol* **5**:800–808.
89. **Tada H, Aiba S, Shibata K-I, Ohteki T, Takada H.** 2005. Synergistic Effect of Nod1 and Nod2 Agonists with Toll-Like Receptor Agonists on Human Dendritic Cells To Generate Interleukin-12 and T Helper Type 1 Cells. *Infect Immun* **73**:7967–7976.
90. **Hisamatsu T, Suzuki M, Reinecker H-C, Nadeau WJ, McCormick BA, Podolsky DK.** 2003. CARD15/NOD2 functions as an antibacterial factor in human intestinal epithelial cells. *Gastroenterology* **124**:993–1000.
91. **Marriott I.** 2004. Osteoblast responses to bacterial pathogens: a previously unappreciated role for bone-forming cells in host defense and disease progression. *Immunol Res* **30**:291–308.
92. **Inohara N, Koseki T, Lin J, Peso L del, Lucas PC, Chen FF, Ogura Y, Núñez G.** 2000. An Induced Proximity Model for NF- κ B Activation in the Nod1/RICK and RIP Signaling Pathways. *J Biol Chem* **275**:27823–27831.
93. **Hasegawa M, Fujimoto Y, Lucas PC, Nakano H, Fukase K, Núñez G, Inohara N.** 2008. A critical role of RICK/RIP2 polyubiquitination in Nod-induced NF- κ B activation. *EMBO J* **27**:373–383.
94. **Bertrand MJM, Doiron K, Labbé K, Korneluk RG, Barker PA, Saleh M.** 2009. Cellular Inhibitors of Apoptosis cIAP1 and cIAP2 Are Required for Innate Immunity Signaling by the Pattern Recognition Receptors NOD1 and NOD2. *Immunity* **30**:789–801.
95. **Krieg A, Correa RG, Garrison JB, Negrate GL, Welsh K, Huang Z, Knoefel WT, Reed JC.** 2009. XIAP mediates NOD signaling via interaction with RIP2. *Proc Natl Acad Sci* **106**:14524–14529.
96. **Damgaard RB, Nachbur U, Yabal M, Wong WW-L, Fiil BK, Kastirr M, Rieser E, Rickard JA, Bankovacki A, Peschel C, Ruland J, Bekker-Jensen S, Mailand N, Kaufmann T, Strasser A, Walczak H, Silke J, Jost PJ, Gyrd-Hansen M.** 2012. The Ubiquitin Ligase XIAP Recruits LUBAC for NOD2 Signaling in Inflammation and Innate Immunity. *Mol Cell* **46**:746–758.
97. **Sabbah A, Chang TH, Harnack R, Frohlich V, Tominaga K, Dube PH, Xiang Y, Bose S.** 2009. Activation of innate immune antiviral responses by Nod2. *Nat Immunol* **10**:1073–1080.

98. **Watanabe T, Asano N, Fichtner-Feigl S, Gorelick PL, Tsuji Y, Matsumoto Y, Chiba T, Fuss IJ, Kitani A, Strober W.** 2010. NOD1 contributes to mouse host defense against *Helicobacter pylori* via induction of type I IFN and activation of the ISGF3 signaling pathway. *J Clin Invest* **120**:1645–1662.
99. **McCarthy JV, Ni J, Dixit VM.** 1998. RIP2 Is a Novel NF- κ B-activating and Cell Death-inducing Kinase. *J Biol Chem* **273**:16968–16975.
100. **Kobayashi K, Inohara N, Hernandez LD, Galán JE, Núñez G, Janeway CA, Medzhitov R, Flavell RA.** 2002. RICK/Rip2/CARDIAK mediates signalling for receptors of the innate and adaptive immune systems. *Nature* **416**:194–199.
101. **Strober W, Murray PJ, Kitani A, Watanabe T.** 2006. Signalling pathways and molecular interactions of NOD1 and NOD2. *Nat Rev Immunol* **6**:9–20.
102. **Park J-H, Kim Y-G, McDonald C, Kanneganti T-D, Hasegawa M, Body-Malapel M, Inohara N, Núñez G.** 2007. RICK/RIP2 Mediates Innate Immune Responses Induced through Nod1 and Nod2 but Not TLRs. *J Immunol* **178**:2380–2386.
103. **Kim J-Y, Omori E, Matsumoto K, Núñez G, Ninomiya-Tsuji J.** 2008. TAK1 Is a Central Mediator of NOD2 Signaling in Epidermal Cells. *J Biol Chem* **283**:137–144.
104. **Sarkar A, Duncan M, Hart J, Hertlein E, Guttridge DC, Wewers MD.** 2006. ASC Directs NF- κ B Activation by Regulating Receptor Interacting Protein-2 (RIP2) Caspase-1 Interactions. *J Immunol* **176**:4979–4986.
105. **Thome M, Hofmann K, Burns K, Martinon F, Bodmer J-L, Mattmann C, Tschopp J.** 1998. Identification of CARDIAK, a RIP-like kinase that associates with caspase-1. *Curr Biol* **8**:885–889.
106. **Humke EW, Shriver SK, Starovasnik MA, Fairbrother WJ, Dixit VM.** 2000. ICEBERG. *Cell* **103**:99–111.
107. **Zhang W-H, Wang X, Narayanan M, Zhang Y, Huo C, Reed JC, Friedlander RM.** 2003. Fundamental role of the Rip2/caspase-1 pathway in hypoxia and ischemia-induced neuronal cell death. *Proc Natl Acad Sci* **100**:16012–16017.
108. **Lupfer C, Thomas PG, Anand PK, Vogel P, Milasta S, Martinez J, Huang G, Green M, Kundu M, Chi H, Xavier RJ, Green DR, Lamkanfi M, Dinarello CA, Doherty PC, Kanneganti T-D.** 2013. Receptor interacting protein kinase 2-mediated mitophagy regulates inflammasome activation during virus infection. *Nat Immunol* **14**:480–488.
109. **Cleveland JL, Ihle JN.** 1995. Contenders in FasL/TNF death signaling. *Cell* **81**:479–482.
110. **Cai X, Du J, Liu Y, Xia W, Liu J, Zou M, Wang Y, Wang M, Su H, Xu D.** 2013. Identification and characterization of receptor-interacting protein 2 as a TNFR-associated factor 3 binding partner. *Gene* **517**:205–211.
111. **Du X, Jiang S, Liu H, Xin X, Li J, Geng M, Jiang H.** 2010. MS80, a novel sulfated polysaccharide, inhibits CD40-NF- κ B pathway via targeting RIP2. *Mol Cell Biochem* **337**:277–285.
112. **Anand PK, Tait SWG, Lamkanfi M, Amer AO, Nunez G, Pagès G, Pouyssegur J, McGargill MA, Green DR, Kanneganti T-D.** 2011. TLR2 and RIP2 Pathways Mediate

Autophagy of *Listeria monocytogenes* via Extracellular Signal-regulated Kinase (ERK) Activation. *J Biol Chem* **286**:42981–42991.

113. **Chin AI, Dempsey PW, Cheng G.** 2005. Rip2: A Key Molecule that Regulates both Innate and Acquired Immunity. *Curr Med Chem - Anti-Inflamm Anti-Allergy Agents* **4**:35–42.
114. **Zou PF, Chang MX, Li Y, Xue NN, Li JH, Chen SN, Nie P.** 2016. NOD2 in zebrafish functions in antibacterial and also antiviral responses via NF- κ B, and also MDA5, RIG-I and MAVS. *Fish Shellfish Immunol* **55**:173–185.
115. **Swain B, Basu M, Samanta M.** 2013. NOD1 and NOD2 receptors in mrigal (*Cirrhinus mrigala*): inductive expression and downstream signalling in ligand stimulation and bacterial infections. *J Biosci* **38**:533–548.
116. **Bilen S, Biswas G, Otsuyama S, Kono T, Sakai M, Hikima J.** 2014. Inflammatory responses in the Japanese pufferfish (*Takifugu rubripes*) head kidney cells stimulated with an inflammasome-inducing agent, nigericin. *Dev Comp Immunol* **46**:222–230.
117. **Xie J, Belosevic M.** 2015. Functional characterization of receptor-interacting serine/threonine kinase 2 (RIP2) of the goldfish (*Carassius auratus* L.). *Dev Comp Immunol* **48**:76–85.
118. **Benko S, Magalhaes JG, Philpott DJ, Girardin SE.** 2010. NLRC5 Limits the Activation of Inflammatory Pathways. *J Immunol* **185**:1681–1691.
119. **Fiorentino L, Stehlik C, Oliveira V, Ariza ME, Godzik A, Reed JC.** 2002. A novel PAAD-containing protein that modulates NF-kappa B induction by cytokines tumor necrosis factor-alpha and interleukin-1beta. *J Biol Chem* **277**:35333–35340.
120. **Schneider M, Zimmermann AG, Roberts RA, Zhang L, Swanson KV, Wen H, Davis BK, Allen IC, Holl EK, Ye Z, Rahman AH, Conti BJ, Eitas TK, Koller BH, Ting JP-Y.** 2012. The innate immune sensor NLRC3 attenuates Toll-like receptor signaling via modification of the signaling adaptor TRAF6 and transcription factor NF- κ B. *Nat Immunol* **13**:823–831.
121. **Zhang L, Mo J, Swanson KV, Wen H, Petrucelli A, Gregory SM, Zhang Z, Schneider M, Jiang Y, Fitzgerald KA, Ouyang S, Liu Z-J, Damania B, Shu H-B, Duncan JA, Ting JP-Y.** 2014. NLRC3, a Member of the NLR Family of Proteins, Is a Negative Regulator of Innate Immune Signaling Induced by the DNA Sensor STING. *Immunity* **40**:329–341.
122. **Cui J, Zhu L, Xia X, Wang HY, Legras X, Hong J, Ji J, Shen P, Zheng S, Chen ZJ, Wang R-F.** 2010. NLRC5 Negatively Regulates the NF- κ B and Type I Interferon Signaling Pathways. *Cell* **141**:483–496.
123. **Davis BK, Roberts RA, Huang MT, Willingham SB, Conti BJ, Brickey WJ, Barker BR, Kwan M, Taxman DJ, Accavitti-Loper M-A, Duncan JA, Ting JP-Y.** 2011. Cutting Edge: NLRC5-Dependent Activation of the Inflammasome. *J Immunol* **186**:1333–1337.
124. **Kobayashi KS, van den Elsen PJ.** 2012. NLRC5: a key regulator of MHC class I-dependent immune responses. *Nat Rev Immunol* **12**:813–820.
125. **Meissner TB, Li A, Biswas A, Lee K-H, Liu Y-J, Bayir E, Iliopoulos D, Elsen PJ van den, Kobayashi KS.** 2010. NLR family member NLRC5 is a transcriptional regulator of MHC class I genes. *Proc Natl Acad Sci* **107**:13794–13799.

126. **Li S, Chen X, Hao G, Geng X, Zhan W, Sun J.** 2016. Identification and characterization of a novel NOD-like receptor family CARD domain containing 3 gene in response to extracellular ATP stimulation and its role in regulating LPS-induced innate immune response in Japanese flounder (*Paralichthys olivaceus*) head kidney macrophages. *Fish Shellfish Immunol* **50**:79–90.
127. **Shimada K, Crother TR, Karlin J, Dagvadorj J, Chiba N, Chen S, Ramanujan VK, Wolf AJ, Vergnes L, Ojcius DM, Rentsendorj A, Vargas M, Guerrero C, Wang Y, Fitzgerald KA, Underhill DM, Town T, Arditi M.** 2012. Oxidized Mitochondrial DNA Activates the NLRP3 Inflammasome during Apoptosis. *Immunity* **36**:401–414.
128. **Arnoult D, Soares F, Tattoli I, Castanier C, Philpott DJ, Girardin SE.** 2009. An N-terminal addressing sequence targets NLRX1 to the mitochondrial matrix. *J Cell Sci* **122**:3161–3168.
129. **Gloire G, Legrand-Poels S, Piette J.** 2006. NF- κ B activation by reactive oxygen species: Fifteen years later. *Biochem Pharmacol* **72**:1493–1505.
130. **Allen IC, Moore CB, Schneider M, Lei Y, Davis BK, Scull MA, Gris D, Roney KE, Zimmermann AG, Bowzard JB, Ranjan P, Monroe KM, Pickles RJ, Sambhara S, Ting JPY.** 2011. NLRX1 Protein Attenuates Inflammatory Responses to Infection by Interfering with the RIG-I-MAVS and TRAF6-NF- κ B Signaling Pathways. *Immunity* **34**:854–865.
131. **Xia X, Cui J, Wang HY, Zhu L, Matsueda S, Wang Q, Yang X, Hong J, Songyang Z, Chen ZJ, Wang R-F.** 2011. NLRX1 Negatively Regulates TLR-Induced NF- κ B Signaling by Targeting TRAF6 and IKK. *Immunity* **34**:843–853.
132. **Hong M, Yoon S, Wilson IA.** 2012. Structure and Functional Characterization of the RNA-Binding Element of the NLRX1 Innate Immune Modulator. *Immunity* **36**:337–347.
133. **Li J, Kong L, Gao Y, Wu C, Xu T.** 2015. Characterization of NLR-A subfamily members in miiuy croaker and comparative genomics revealed NLRX1 underwent duplication and lose in actinopterygii. *Fish Shellfish Immunol* **47**:397–406.
134. **Martinon F, Burns K, Tschopp J.** 2002. The Inflammasome: A Molecular Platform Triggering Activation of Inflammatory Caspases and Processing of proIL- β . *Mol Cell* **10**:417–426.
135. **Kummer JA, Broekhuizen R, Everett H, Agostini L, Kuijk L, Martinon F, Bruggen R van, Tschopp J.** 2007. Inflammasome Components NALP 1 and 3 Show Distinct but Separate Expression Profiles in Human Tissues Suggesting a Site-specific Role in the Inflammatory Response. *J Histochem Cytochem* **55**:443–452.
136. **Chakraborty S, Kaushik DK, Gupta M, Basu A.** 2010. Inflammasome signaling at the heart of central nervous system pathology. *J Neurosci Res* **88**:1615–1631.
137. **Boyden ED, Dietrich WF.** 2006. Nalp1b controls mouse macrophage susceptibility to anthrax lethal toxin. *Nat Genet* **38**:240–244.
138. **Sastalla I, Crown D, Masters SL, McKenzie A, Leppla SH, Moayeri M.** 2013. Transcriptional analysis of the three Nlrp1 paralogs in mice. *BMC Genomics* **14**:188.

139. **Fink SL, Bergsbaken T, Cookson BT.** 2008. Anthrax lethal toxin and *Salmonella* elicit the common cell death pathway of caspase-1-dependent pyroptosis via distinct mechanisms. *Proc Natl Acad Sci* **105**:4312–4317.
140. **Hellmich KA, Levinsohn JL, Fattah R, Newman ZL, Maier N, Sastalla I, Liu S, Leppia SH, Moayeri M.** 2012. Anthrax Lethal Factor Cleaves Mouse Nlrp1b in Both Toxin-Sensitive and Toxin-Resistant Macrophages. *PLOS ONE* **7**:e49741.
141. **Chavarría-Smith J, Vance RE.** 2013. Direct Proteolytic Cleavage of NLRP1B Is Necessary and Sufficient for Inflammasome Activation by Anthrax Lethal Factor. *PLOS Pathog* **9**:e1003452.
142. **Broz P, von Moltke J, Jones JW, Vance RE, Monack DM.** 2010. Differential Requirement for Caspase-1 Autoproteolysis in Pathogen-Induced Cell Death and Cytokine Processing. *Cell Host Microbe* **8**:471–483.
143. **Kovarova M, Hesker PR, Jania L, Nguyen M, Snouwaert JN, Xiang Z, Lommatzsch SE, Huang MT, Ting JP-Y, Koller BH.** 2012. NLRP1-Dependent Pyroptosis Leads to Acute Lung Injury and Morbidity in Mice. *J Immunol* **189**:2006–2016.
144. **Van Opdenbosch N, Gurung P, Vande Walle L, Fossoul A, Kanneganti T-D, Lamkanfi M.** 2014. Activation of the NLRP1b inflammasome independently of ASC-mediated caspase-1 autoproteolysis and speck formation. *Nat Commun* **5**:3209.
145. **Fitzgerald KA.** 2010. NLR-containing inflammasomes: Central mediators of host defense and inflammation. *Eur J Immunol* **40**:595–598.
146. **Rathinam VAK, Vanaja SK, Waggoner L, Sokolovska A, Becker C, Stuart LM, Leong JM, Fitzgerald KA.** 2012. TRIF Licenses Caspase-11-Dependent NLRP3 Inflammasome Activation by Gram-Negative Bacteria. *Cell* **150**:606–619.
147. **Vanaja SK, Rathinam VAK, Fitzgerald KA.** 2015. Mechanisms of inflammasome activation: recent advances and novel insights. *Trends Cell Biol* **25**:308–315.
148. **Lamkanfi M, Dixit VM.** 2011. Modulation of Inflammasome Pathways by Bacterial and Viral Pathogens. *J Immunol* **187**:597–602.
149. **Muñoz-Planillo R, Kuffa P, Martínez-Colón G, Smith BL, Rajendiran TM, Núñez G.** 2013. K⁺ Efflux Is the Common Trigger of NLRP3 Inflammasome Activation by Bacterial Toxins and Particulate Matter. *Immunity* **38**:1142–1153.
150. **Zhou R, Yazdi AS, Menu P, Tschopp J.** 2011. A role for mitochondria in NLRP3 inflammasome activation. *Nature* **469**:221–225.
151. **Hornung V, Bauernfeind F, Halle A, Samstad EO, Kono H, Rock KL, Fitzgerald KA, Latz E.** 2008. Silica crystals and aluminum salts activate the NALP3 inflammasome through phagosomal destabilization. *Nat Immunol* **9**:847–856.
152. **Misawa T, Takahama M, Kozaki T, Lee H, Zou J, Saitoh T, Akira S.** 2013. Microtubule-driven spatial arrangement of mitochondria promotes activation of the NLRP3 inflammasome. *Nat Immunol* **14**:454–460.
153. **Subramanian N, Natarajan K, Clatworthy MR, Wang Z, Germain RN.** 2013. The Adaptor MAVS Promotes NLRP3 Mitochondrial Localization and Inflammasome Activation. *Cell* **153**:348–361.

154. **Ermler ME, Traylor Z, Patel K, Schattgen SA, Vanaja SK, Fitzgerald KA, Hise AG.** 2014. Rift Valley fever virus infection induces activation of the NLRP3 inflammasome. *Virology* **449**:174–180.
155. **Bauernfeind FG, Horvath G, Stutz A, Alnemri ES, MacDonald K, Speert D, Fernandes-Alnemri T, Wu J, Monks BG, Fitzgerald KA, Hornung V, Latz E.** 2009. Cutting Edge: NF- κ B Activating Pattern Recognition and Cytokine Receptors License NLRP3 Inflammasome Activation by Regulating NLRP3 Expression. *J Immunol* **183**:787–791.
156. **Broz P, Monack DM.** 2011. Molecular mechanisms of inflammasome activation during microbial infections. *Immunol Rev* **243**:174–190.
157. **Perregaux D, Gabel CA.** 1994. Interleukin-1 beta maturation and release in response to ATP and nigericin. Evidence that potassium depletion mediated by these agents is a necessary and common feature of their activity. *J Biol Chem* **269**:15195–15203.
158. **Ferrari D, Chiozzi P, Falzoni S, Susino MD, Melchiorri L, Baricordi OR, Virgilio FD.** 1997. Extracellular ATP triggers IL-1 beta release by activating the purinergic P2Z receptor of human macrophages. *J Immunol* **159**:1451–1458.
159. **Kahlenberg JM, Lundberg KC, Kertesz SB, Qu Y, Dubyak GR.** 2005. Potentiation of Caspase-1 Activation by the P2X7 Receptor Is Dependent on TLR Signals and Requires NF- κ B-Driven Protein Synthesis. *J Immunol* **175**:7611–7622.
160. **Juliana C, Fernandes-Alnemri T, Kang S, Farias A, Qin F, Alnemri ES.** 2012. Non-transcriptional Priming and Deubiquitination Regulate NLRP3 Inflammasome Activation. *J Biol Chem* **287**:36617–36622.
161. **Lopez-Castejon G, Luheshi NM, Compan V, High S, Whitehead RC, Flitsch S, Kirov A, Prudovsky I, Swanton E, Brough D.** 2013. Deubiquitinases Regulate the Activity of Caspase-1 and Interleukin-1 β Secretion via Assembly of the Inflammasome. *J Biol Chem* **288**:2721–2733.
162. **Py BF, Kim M-S, Vakifahmetoglu-Norberg H, Yuan J.** 2013. Deubiquitination of NLRP3 by BRCC3 Critically Regulates Inflammasome Activity. *Mol Cell* **49**:331–338.
163. **Pereira MSF, Morgantetti GF, Massis LM, Horta CV, Hori JI, Zamboni DS.** 2011. Activation of NLRC4 by Flagellated Bacteria Triggers Caspase-1–Dependent and –Independent Responses To Restrict *Legionella Pneumophila* Replication in Macrophages and In Vivo. *J Immunol* **187**:6447–6455.
164. **Mariathasan S, Newton K, Monack DM, Vucic D, French DM, Lee WP, Roose-Girma M, Erickson S, Dixit VM.** 2004. Differential activation of the inflammasome by caspase-1 adaptors ASC and Ipaf. *Nature* **430**:213–218.
165. **Amer A, Franchi L, Kanneganti T-D, Body-Malapel M, Özören N, Brady G, Meshinchi S, Jagirdar R, Gewirtz A, Akira S, Núñez G.** 2006. Regulation of *Legionella* Phagosome Maturation and Infection through Flagellin and Host Ipaf. *J Biol Chem* **281**:35217–35223.
166. **Suzuki T, Franchi L, Toma C, Ashida H, Ogawa M, Yoshikawa Y, Mimuro H, Inohara N, Sasakawa C, Nuñez G.** 2007. Differential Regulation of Caspase-1 Activation, Pyroptosis, and Autophagy via Ipaf and ASC in *Shigella* -Infected Macrophages. *PLOS Pathog* **3**:e111.

167. **Galle M, Schotte P, Haegman M, Wullaert A, Yang HJ, Jin S, Beyaert R.** 2008. The *Pseudomonas aeruginosa* Type III secretion system plays a dual role in the regulation of caspase-1 mediated IL-1 β maturation. *J Cell Mol Med* **12**:1767–1776.
168. **Miao EA, Ernst RK, Dors M, Mao DP, Aderem A.** 2008. *Pseudomonas aeruginosa* activates caspase 1 through Ipaf. *Proc Natl Acad Sci* **105**:2562–2567.
169. **Lightfield KL, Persson J, Brubaker SW, Witte CE, von Moltke J, Dunipace EA, Henry T, Sun Y-H, Cado D, Dietrich WF, Monack DM, Tsolis RM, Vance RE.** 2008. Critical function for Naip5 in inflammasome activation by a conserved carboxy-terminal domain of flagellin. *Nat Immunol* **9**:1171–1178.
170. **Miao EA, Leaf IA, Treuting PM, Mao DP, Dors M, Sarkar A, Warren SE, Wewers MD, Aderem A.** 2010. Caspase-1-induced pyroptosis is an innate immune effector mechanism against intracellular bacteria. *Nat Immunol* **11**:1136–1142.
171. **Bonardi V, Tang S, Stallmann A, Roberts M, Cherkis K, Dangl JL.** 2011. Expanded functions for a family of plant intracellular immune receptors beyond specific recognition of pathogen effectors. *Proc Natl Acad Sci* **108**:16463–16468.
172. **Kofoed EM, Vance RE.** 2011. Innate immune recognition of bacterial ligands by NAIPs determines inflammasome specificity. *Nature* **477**:592–595.
173. **Zhao Y, Yang J, Shi J, Gong Y-N, Lu Q, Xu H, Liu L, Shao F.** 2011. The NLRC4 inflammasome receptors for bacterial flagellin and type III secretion apparatus. *Nature* **477**:596–600.
174. **Rayamajhi M, Zhang Y, Miao EA.** 2013. Detection of pyroptosis by measuring released lactate dehydrogenase activity. *Methods Mol Biol Clifton NJ* **1040**:85–90.
175. **Yang J, Zhao Y, Shi J, Shao F.** 2013. Human NAIP and mouse NAIP1 recognize bacterial type III secretion needle protein for inflammasome activation. *Proc Natl Acad Sci* **110**:14408–14413.
176. **Qu Y, Misaghi S, Izrael-Tomasevic A, Newton K, Gilmour LL, Lamkanfi M, Louie S, Kayagaki N, Liu J, Kömüves L, Cupp JE, Arnott D, Monack D, Dixit VM.** 2012. Phosphorylation of NLRC4 is critical for inflammasome activation. *Nature* **490**:539–542.
177. **Grenier JM, Wang L, Manji GA, Huang W-J, Al-Garawi A, Kelly R, Carlson A, Merriam S, Lora JM, Briskin M, DiStefano PS, Bertin J.** 2002. Functional screening of five PYPAF family members identifies PYPAF5 as a novel regulator of NF- κ B and caspase-1. *FEBS Lett* **530**:73–78.
178. **Chen GY, Liu M, Wang F, Bertin J, Núñez G.** 2011. A Functional Role for Nlrp6 in Intestinal Inflammation and Tumorigenesis. *J Immunol* **186**:7187–7194.
179. **Elinav E, Strowig T, Henao-Mejia J, Flavell RA.** 2011. Regulation of the Antimicrobial Response by NLR Proteins. *Immunity* **34**:665–679.
180. **Normand S, Delanoye-Crespin A, Bressenot A, Huot L, Grandjean T, Peyrin-Biroulet L, Lemoine Y, Hot D, Chamaillard M.** 2011. Nod-like receptor pyrin domain-containing protein 6 (NLRP6) controls epithelial self-renewal and colorectal carcinogenesis upon injury. *Proc Natl Acad Sci* **108**:9601–9606.

181. **Anand PK, Malireddi RKS, Lukens JR, Vogel P, Bertin J, Lamkanfi M, Kanneganti T-D.** 2012. NLRP6 negatively regulates innate immunity and host defence against bacterial pathogens. *Nature* **488**:389–393.
182. **Wang L, Manji GA, Grenier JM, Al-Garawi A, Merriam S, Lora JM, Geddes BJ, Briskin M, DiStefano PS, Bertin J.** 2002. PYPAF7, a Novel PYRIN-containing Apaf1-like Protein That Regulates Activation of NF- κ B and Caspase-1-dependent Cytokine Processing. *J Biol Chem* **277**:29874–29880.
183. **Zaki MH, Vogel P, Malireddi RKS, Body-Malapel M, Anand PK, Bertin J, Green DR, Lamkanfi M, Kanneganti T-D.** 2011. The NOD-Like Receptor NLRP12 Attenuates Colon Inflammation and Tumorigenesis. *Cancer Cell* **20**:649–660.
184. **Allen IC, Wilson JE, Schneider M, Lich JD, Roberts RA, Arthur JC, Woodford R-MT, Davis BK, Uronis JM, Herfarth HH, Jobin C, Rogers AB, Ting JP-Y.** 2012. NLRP12 Suppresses Colon Inflammation and Tumorigenesis through the Negative Regulation of Noncanonical NF- κ B Signaling. *Immunity* **36**:742–754.
185. **Vladimer GI, Weng D, Paquette SWM, Vanaja SK, Rathinam VAK, Aune MH, Conlon JE, Burbage JJ, Proulx MK, Liu Q, Reed G, Mecsas JC, Iwakura Y, Bertin J, Goguen JD, Fitzgerald KA, Lien E.** 2012. The NLRP12 Inflammasome Recognizes *Yersinia pestis*. *Immunity* **37**:96–107.
186. **Ataide MA, Andrade WA, Zamboni DS, Wang D, Souza M do C, Franklin BS, Elian S, Martins FS, Pereira D, Reed G, Fitzgerald KA, Golenbock DT, Gazzinelli RT.** 2014. Malaria-Induced NLRP12/NLRP3-Dependent Caspase-1 Activation Mediates Inflammation and Hypersensitivity to Bacterial Superinfection. *PLOS Pathog* **10**:e1003885.
187. **Kayagaki N, Warming S, Lamkanfi M, Walle LV, Louie S, Dong J, Newton K, Qu Y, Liu J, Heldens S, Zhang J, Lee WP, Roose-Girma M, Dixit VM.** 2011. Non-canonical inflammasome activation targets caspase-11. *Nature* **479**:117–121.
188. **Kayagaki N, Wong MT, Stowe IB, Ramani SR, Gonzalez LC, Akashi-Takamura S, Miyake K, Zhang J, Lee WP, Muszyński A, Forsberg LS, Carlson RW, Dixit VM.** 2013. Noncanonical Inflammasome Activation by Intracellular LPS Independent of TLR4. *Science* **341**:1246–1249.
189. **Yang J, Zhao Y, Shao F.** 2015. Non-canonical activation of inflammatory caspases by cytosolic LPS in innate immunity. *Curr Opin Immunol* **32**:78–83.
190. **Shi J, Zhao Y, Wang Y, Gao W, Ding J, Li P, Hu L, Shao F.** 2014. Inflammatory caspases are innate immune receptors for intracellular LPS. *Nature* **514**:187–192.
191. **Moleri S, Cappellano G, Gaudenzi G, Cermenati S, Cotelli F, Horner DS, Beltrame M.** 2011. The HMGB protein gene family in zebrafish: Evolution and embryonic expression patterns. *Gene Expr Patterns* **11**:3–11.
192. **Yang C, Peng L, Su J.** 2013. Two HMGB1 genes from grass carp *Ctenopharyngodon idella* mediate immune responses to viral/bacterial PAMPs and GCRV challenge. *Dev Comp Immunol* **39**:133–146.

193. **Cai J, Xia H, Huang Y, Lu Y, Wu Z, Jian J.** 2014. Molecular cloning and characterization of high mobility group box1 (Ls-HMGB1) from humphead snapper, *Lutjanus sanguineus*. *Fish Shellfish Immunol* **40**:539–544.
194. **Xie J, Hodgkinson JW, Li C, Kovacevic N, Belosevic M.** 2014. Identification and functional characterization of the goldfish (*Carassius auratus* L.) high mobility group box 1 (HMGB1) chromatin-binding protein. *Dev Comp Immunol* **44**:245–253.
195. **van de Veerdonk FL, Netea MG, Dinarello CA, Joosten LAB.** 2011. Inflammasome activation and IL-1 β and IL-18 processing during infection. *Trends Immunol* **32**:110–116.
196. **Hansen JD, Vojtech LN, Laing KJ.** 2011. Sensing disease and danger: A survey of vertebrate PRRs and their origins. *Dev Comp Immunol* **35**:886–897.
197. **Angosto D, López-Castejón G, López-Muñoz A, Sepulcre MP, Arizcun M, Meseguer J, Mulero V.** 2012. Evolution of inflammasome functions in vertebrates: Inflammasome and caspase-1 trigger fish macrophage cell death but are dispensable for the processing of IL-1 β . *Innate Immun* **18**:815–824.
198. **Clark RM, Schweikert G, Toomajian C, Ossowski S, Zeller G, Shinn P, Warthmann N, Hu TT, Fu G, Hinds DA, Chen H, Frazer KA, Huson DH, Schölkopf B, Nordborg M, Räscher G, Ecker JR, Weigel D.** 2007. Common Sequence Polymorphisms Shaping Genetic Diversity in *Arabidopsis thaliana*. *Science* **317**:338–342.
199. **Ogura Y, Saab L, Chen FF, Benito A, Inohara N, Nuñez G.** 2003. Genetic variation and activity of mouse Nod2, a susceptibility gene for Crohn's disease. *Genomics* **81**:369–377.
200. **Wright EK, Goodart SA, Gowney JD, Hadinoto V, Endrizzi MG, Long EM, Sadigh K, Abney AL, Bernstein-Hanley I, Dietrich WF.** 2003. Naip5 affects host susceptibility to the intracellular pathogen *Legionella pneumophila*. *Curr Biol CB* **13**:27–36.
201. **Omi T, Kumada M, Kamesaki T, Okuda H, Munkhtulga L, Yanagisawa Y, Utsumi N, Gotoh T, Hata A, Soma M, Umemura S, Ogihara T, Takahashi N, Tabara Y, Shimada K, Mano H, Kajii E, Miki T, Iwamoto S.** 2006. An intronic variable number of tandem repeat polymorphisms of the cold-induced autoinflammatory syndrome 1 (CIAS1) gene modifies gene expression and is associated with essential hypertension. *Eur J Hum Genet* **14**:1295–1305.
202. **Day TG, Ramanan AV, Hinks A, Lamb R, Packham J, Wise C, Punaro M, Donn RP.** 2008. Autoinflammatory genes and susceptibility to psoriatic juvenile idiopathic arthritis. *Arthritis Rheum* **58**:2142–2146.
203. **Villani A-C, Lemire M, Fortin G, Louis E, Silverberg MS, Collette C, Baba N, Libioulle C, Belaiche J, Bitton A, Gaudet D, Cohen A, Langelier D, Fortin PR, Wither JE, Sarfati M, Rutgeerts P, Rioux JD, Vermeire S, Hudson TJ, Franchimont D.** 2009. Common variants in the NLRP3 region contribute to Crohn's disease susceptibility. *Nat Genet* **41**:71–76.
204. **Ali SR, Karin M, Nizet V.** 2015. Signaling cascades and inflammasome activation in microbial infections. *Inflammasome* **2**.
205. **Conway KE, McConnell BB, Bowring CE, Donald CD, Warren ST, Vertino PM.** 2000. TMS1, a Novel Proapoptotic Caspase Recruitment Domain Protein, Is a Target of

- Methylation-induced Gene Silencing in Human Breast Cancers. *Cancer Res* **60**:6236–6242.
206. **Thornberry NA, Lazebnik Y.** 1998. Caspases: Enemies Within. *Science* **281**:1312–1316.
207. **Hornung V, Ablasser A, Charrel-Dennis M, Bauernfeind F, Horvath G, Caffrey DR, Latz E, Fitzgerald KA.** 2009. AIM2 recognizes cytosolic dsDNA and forms a caspase-1-activating inflammasome with ASC. *Nature* **458**:514–518.
208. **Yamamoto M, Yaginuma K, Tsutsui H, Sagara J, Guan X, Seki E, Yasuda K, Yamamoto M, Akira S, Nakanishi K, Noda T, Taniguchi S.** 2004. ASC is essential for LPS-induced activation of procaspase-1 independently of TLR-associated signal adaptor molecules. *Genes Cells* **9**:1055–1067.
209. **Sutterwala FS, Ogura Y, Szczepanik M, Lara-Tejero M, Lichtenberger GS, Grant EP, Bertin J, Coyle AJ, Galán JE, Askenase PW, Flavell RA.** 2006. Critical Role for NALP3/CIAS1/Cryopyrin in Innate and Adaptive Immunity through Its Regulation of Caspase-1. *Immunity* **24**:317–327.
210. **Fernandes-Alnemri T, Wu J, Yu J-W, Datta P, Miller B, Jankowski W, Rosenberg S, Zhang J, Alnemri ES.** 2007. The pyroptosome: a supramolecular assembly of ASC dimers mediating inflammatory cell death via caspase-1 activation. *Cell Death Differ* **14**:1590–1604.
211. **Franklin BS, Bossaller L, De Nardo D, Ratter JM, Stutz A, Engels G, Brenker C, Nordhoff M, Mirandola SR, Al-Amoudi A, Mangan MS, Zimmer S, Monks BG, Fricke M, Schmidt RE, Espevik T, Jones B, Jarnicki AG, Hansbro PM, Busto P, Marshak-Rothstein A, Hornemann S, Aguzzi A, Kastentmüller W, Latz E.** 2014. The adaptor ASC has extracellular and “prionoid” activities that propagate inflammation. *Nat Immunol* **15**:727–737.
212. **Taxman DJ, Huang MT-H, Ting JP-Y.** 2010. Inflammasome Inhibition as a Pathogenic Stealth Mechanism. *Cell Host Microbe* **8**:7–11.
213. **Manji GA, Wang L, Geddes BJ, Brown M, Merriam S, Al-Garawi A, Mak S, Lora JM, Briskin M, Jurman M, Cao J, DiStefano PS, Bertin J.** 2002. PYPAF1, a PYRIN-containing Apaf1-like Protein That Assembles with ASC and Regulates Activation of NF- κ B. *J Biol Chem* **277**:11570–11575.
214. **Taxman DJ, Lei Y, Zhang S, Holley-Guthrie E, Offenbacher S, Ting JP-Y.** 2012. ASC-dependent RIP2 Kinase Regulates Reduced PGE2 in Production Chronic Periodontitis. *J Dent Res* 0022034512454541.
215. **Sun Y, Wang J, Lao H, Yin Z, He W, Weng S, Yu X, Chan S, He J.** 2008. Molecular cloning and expression analysis of the ASC gene from mandarin fish and its regulation of NF- κ B activation. *Dev Comp Immunol* **32**:391–399.
216. **Li S, Chen X, Peng W, Hao G, Geng X, Zhan W, Sun J.** 2016. Cloning and characterization of apoptosis-associated speck-like protein containing a CARD domain (ASC) gene from Japanese flounder *Paralichthys olivaceus*. *Fish Shellfish Immunol* **54**:294–301.

217. **Cerretti DP, Kozlosky CJ, Mosley B, Nelson N, Ness KV, Greenstreet TA, March CJ, Kronheim, Druck T, Cannizzaro LA, Et A.** 1992. Molecular cloning of the interleukin-1 beta converting enzyme. *Science* **256**:97–100.
218. **Thornberry NA, Bull HG, Calaycay JR, Chapman KT, Howard AD, Kostura MJ, Miller DK, Molineaux SM, Weidner JR, Aunins J, Elliston KO, Ayala JM, Casano FJ, Chin J, Ding GJ-F, Egger LA, Gaffney EP, Limjuco G, Palyha OC, Raju SM, Rolando AM, Salley JP, Yamin T-T, Lee TD, Shively JE, MacCross M, Mumford RA, Schmidt JA, Tocci MJ.** 1992. A novel heterodimeric cysteine protease is required for interleukin-1 β processing in monocytes. *Nature* **356**:768–774.
219. **Ogura Y, Sutterwala FS, Flavell RA.** 2006. The Inflammasome: First Line of the Immune Response to Cell Stress. *Cell* **126**:659–662.
220. **Kuida K, Lippke JA, Ku G, Harding MW, Livingston DJ, Su MS, Flavell RA.** 1995. Altered cytokine export and apoptosis in mice deficient in interleukin-1 beta converting enzyme. *Science* **267**:2000–2003.
221. **Los M, Wesselborg S, Schulze-Osthoff K.** 1999. The Role of Caspases in Development, Immunity, and Apoptotic Signal Transduction: Lessons from Knockout Mice. *Immunity* **10**:629–639.
222. **Johnston JB, Barrett JW, Nazarian SH, Goodwin M, Ricuttio D, Wang G, McFadden G.** 2005. A Poxvirus-Encoded Pyrin Domain Protein Interacts with ASC-1 to Inhibit Host Inflammatory and Apoptotic Responses to Infection. *Immunity* **23**:587–598.
223. **Franchi L, Amer A, Body-Malapel M, Kanneganti T-D, Özören N, Jagirdar R, Inohara N, Vandenabeele P, Bertin J, Coyle A, Grant EP, Núñez G.** 2006. Cytosolic flagellin requires Ipaf for activation of caspase-1 and interleukin 1 β in *salmonella*-infected macrophages. *Nat Immunol* **7**:576–582.
224. **Molofsky AB, Byrne BG, Whitfield NN, Madigan CA, Fuse ET, Tateda K, Swanson MS.** 2006. Cytosolic recognition of flagellin by mouse macrophages restricts *Legionella pneumophila* infection. *J Exp Med* **203**:1093–1104.
225. **Ren T, Zamboni DS, Roy CR, Dietrich WF, Vance RE.** 2006. Flagellin-Deficient *Legionella* Mutants Evade Caspase-1- and Naip5- Mediated Macrophage Immunity. *PLOS Pathog* **2**:e18.
226. **Zamboni DS, Kobayashi KS, Kohlsdorf T, Ogura Y, Long EM, Vance RE, Kuida K, Mariathasan S, Dixit VM, Flavell RA, Dietrich WF, Roy CR.** 2006. The Birc1e cytosolic pattern-recognition receptor contributes to the detection and control of *Legionella pneumophila* infection. *Nat Immunol* **7**:318–325.
227. **Masumoto J, Zhou W, Chen FF, Su F, Kuwada JY, Hidaka E, Katsuyama T, Sagara J, Taniguchi S 'ichiro, Ngo-Hazelett P, Postlethwait JH, Núñez G, Inohara N.** 2003. Caspy, a Zebrafish Caspase, Activated by ASC Oligomerization Is Required for Pharyngeal Arch Development. *J Biol Chem* **278**:4268–4276.
228. **Reis MIR, Vale A do, Pereira PJB, Azevedo JE, Santos NMS dos.** 2012. Caspase-1 and IL-1 β Processing in a Teleost Fish. *PLOS ONE* **7**:e50450.

229. **Vojtech LN, Scharping N, Woodson JC, Hansen JD.** 2012. Roles of Inflammatory Caspases during Processing of Zebrafish Interleukin-1 β in *Francisella noatunensis* Infection. *Infect Immun* **80**:2878–2885.
230. **López-Castejón G, Sepulcre MP, Mulero I, Pelegrín P, Meseguer J, Mulero V.** 2008. Molecular and functional characterization of gilthead seabream *Sparus aurata* caspase-1: The first identification of an inflammatory caspase in fish. *Mol Immunol* **45**:49–57.
231. **Wang S, Miura M, Jung Y, Zhu H, Li E, Yuan J.** 1998. Murine Caspase-11, an ICE-Interacting Protease, Is Essential for the Activation of ICE. *Cell* **92**:501–509.
232. **Kostura MJ, Tocci MJ, Limjuco G, Chin J, Cameron P, Hillman AG, Chartrain NA, Schmidt JA.** 1989. Identification of a monocyte specific pre-interleukin 1 beta convertase activity. *Proc Natl Acad Sci* **86**:5227–5231.
233. **Hagar JA, Powell DA, Aachoui Y, Ernst RK, Miao EA.** 2013. Cytoplasmic LPS Activates Caspase-11: Implications in TLR4-Independent Endotoxic Shock. *Science* **341**:1250–1253.
234. **Bianchi ME, Beltrame M.** 1998. Flexing DNA: HMG-Box Proteins and Their Partners. *Am J Hum Genet* **63**:1573–1577.
235. **Vaccari T, Beltrame M, Ferrari S, Bianchi ME.** 1998. Hmg4,a New Member of theHmg1/2Gene Family. *Genomics* **49**:247–252.
236. **Štros M, Launholt D, Grasser KD.** 2007. The HMG-box: a versatile protein domain occurring in a wide variety of DNA-binding proteins. *Cell Mol Life Sci* **64**:2590–2606.
237. **Catena R, Escoffier E, Caron C, Khochbin S, Martianov I, Davidson I.** 2009. HMGB4, a Novel Member of the HMGB Family, Is Preferentially Expressed in the Mouse Testis and Localizes to the Basal Pole of Elongating Spermatids. *Biol Reprod* **80**:358–366.
238. **Štros M.** 2010. HMGB proteins: Interactions with DNA and chromatin. *Biochim Biophys Acta BBA - Gene Regul Mech* **1799**:101–113.
239. **Sheflin LG, Fucile NW, Spaulding SW.** 1993. The specific interactions of HMG 1 and 2 with negatively supercoiled DNA are modulated by their acidic C-terminal domains and involve cysteine residues in their HMG 1/2 boxes. *Biochemistry (Mosc)* **32**:3238–3248.
240. **Štros M, Štokrová J, Thomas JO.** 1994. DNA looping by the HMG-box domains of HMG1 and modulation of DNA binding by the acidic C-terminal domain. *Nucleic Acids Res* **22**:1044–1051.
241. **Thomas JO, Travers AA.** 2001. HMG1 and 2, and related “architectural” DNA-binding proteins. *Trends Biochem Sci* **26**:167–174.
242. **Knapp S, Müller S, Digilio G, Bonaldi T, Bianchi ME, Musco G.** 2004. The Long Acidic Tail of High Mobility Group Box 1 (HMGB1) Protein Forms an Extended and Flexible Structure That Interacts with Specific Residues within and between the HMG Boxes. *Biochemistry (Mosc)* **43**:11992–11997.
243. **Bianchi ME, Manfredi AA.** 2007. High-mobility group box 1 (HMGB1) protein at the crossroads between innate and adaptive immunity. *Immunol Rev* **220**:35–46.
244. **Goodwin GH, Sanders C, Johns EW.** 1973. A New Group of Chromatin-Associated Proteins with a High Content of Acidic and Basic Amino Acids. *Eur J Biochem* **38**:14–19.

245. **Mosevitsky MI, Novitskaya VA, Iogannsen MG, Zabezhinsky MA.** 1989. Tissue specificity of nucleo-cytoplasmic distribution of HMG1 and HMG2 proteins and their probable functions. *Eur J Biochem* **185**:303–310.
246. **Calogero S, Grassi F, Aguzzi A, Voigtländer T, Ferrier P, Ferrari S, Bianchi ME.** 1999. The lack of chromosomal protein Hmg1 does not disrupt cell growth but causes lethal hypoglycaemia in newborn mice. *Nat Genet* **22**:276–280.
247. **Muller S.** 2001. NEW EMBO MEMBERS' REVIEW: The double life of HMGB1 chromatin protein: architectural factor and extracellular signal. *EMBO J* **20**:4337–4340.
248. **Lotze M, Vernon P, Li G, Liang X.** 2013. High-mobility group box 1 promotes NK and DC function as well as crosstalk: studies of selective knockout in immune cells (P2008). *J Immunol* **190**:214.5.
249. **Wang H, Bloom O, Zhang M, Vishnubhakat JM, Ombrellino M, Che J, Frazier A, Yang H, Ivanova S, Borovikova L, Manogue KR, Faist E, Abraham E, Andersson J, Andersson U, Molina PE, Abumrad NN, Sama A, Tracey KJ.** 1999. HMG-1 as a Late Mediator of Endotoxin Lethality in Mice. *Science* **285**:248–251.
250. **Bustin M, Neihart NK.** 1979. Antibodies against chromosomal HMG proteins stain the cytoplasm of mammalian cells. *Cell* **16**:181–189.
251. **Lamkanfi M, Sarkar A, Walle LV, Vitari AC, Amer AO, Wewers MD, Tracey KJ, Kanneganti T-D, Dixit VM.** 2010. Inflammasome-Dependent Release of the Alarmin HMGB1 in Endotoxemia. *J Immunol* **185**:4385–4392.
252. **Yang H, Hreggvidsdottir HS, Palmblad K, Wang H, Ochani M, Li J, Lu B, Chavan S, Rosas-Ballina M, Al-Abed Y, Akira S, Bierhaus A, Erlandsson-Harris H, Andersson U, Tracey KJ.** 2010. A critical cysteine is required for HMGB1 binding to Toll-like receptor 4 and activation of macrophage cytokine release. *Proc Natl Acad Sci* **107**:11942–11947.
253. **Schlueter C, Weber H, Meyer B, Rogalla P, Röser K, Hauke S, Bullerdiek J.** 2005. Angiogenetic Signaling through Hypoxia: HMGB1: An Angiogenetic Switch Molecule. *Am J Pathol* **166**:1259–1263.
254. **Kim J-B, Choi JS, Yu Y-M, Nam K, Piao C-S, Kim S-W, Lee M-H, Han P-L, Park J, Lee J-K.** 2006. HMGB1, a Novel Cytokine-Like Mediator Linking Acute Neuronal Death and Delayed Neuroinflammation in the Postischemic Brain. *J Neurosci* **26**:6413–6421.
255. **Mishra BB, Mishra PK, Teale JM.** 2006. Expression and distribution of Toll-like receptors in the brain during murine neurocysticercosis. *J Neuroimmunol* **181**:46–56.
256. **Erlandsson Harris H, Andersson U.** 2004. Mini-review: The nuclear protein HMGB1 as a proinflammatory mediator. *Eur J Immunol* **34**:1503–1512.
257. **Lotze MT, Tracey KJ.** 2005. High-mobility group box 1 protein (HMGB1): nuclear weapon in the immune arsenal. *Nat Rev Immunol* **5**:331–342.
258. **Lu B, Nakamura T, Inouye K, Li J, Tang Y, Lundbäck P, Valdes-Ferrer SI, Olofsson PS, Kalb T, Roth J, Zou Y, Erlandsson-Harris H, Yang H, Ting JP-Y, Wang H, Andersson U, Antoine DJ, Chavan SS, Hotamisligil GS, Tracey KJ.** 2012. Novel role of PKR in inflammasome activation and HMGB1 release. *Nature* **488**:670–674.

259. **Zhao X, Kuja-Panula J, Rouhiainen A, Chen Y, Panula P, Rauvala H.** 2011. High Mobility Group Box-1 (HMGB1; Amphoterin) Is Required for Zebrafish Brain Development. *J Biol Chem* **286**:23200–23213.
260. **Fang P, Pan H-C, Lin SL, Zhang W-Q, Rauvala H, Schachner M, Shen Y-Q.** 2013. HMGB1 Contributes to Regeneration After Spinal Cord Injury in Adult Zebrafish. *Mol Neurobiol* **49**:472–483.
261. **Zhao L, Hu Y, Sun J, Sun L.** 2011. The high mobility group box 1 protein of *Sciaenops ocellatus* is a secreted cytokine that stimulates macrophage activation. *Dev Comp Immunol* **35**:1052–1058.
262. **Dinarello CA.** 1996. Biologic basis for interleukin-1 in disease. *Blood* **87**:2095–2147.
263. **Dinarello CA.** 1998. Interleukin-1 β , Interleukin-18, and the Interleukin-1 β Converting Enzyme. *Ann N Y Acad Sci* **856**:1–11.
264. **Dinarello CA.** 2009. Immunological and Inflammatory Functions of the Interleukin-1 Family. *Annu Rev Immunol* **27**:519–550.
265. **Dinarello CA.** 2011. Interleukin-1 in the pathogenesis and treatment of inflammatory diseases. *Blood* **117**:3720–3732.
266. **Hoffman HM, Mueller JL, Broide DH, Wanderer AA, Kolodner RD.** 2001. Mutation of a new gene encoding a putative pyrin-like protein causes familial cold autoinflammatory syndrome and Muckle–Wells syndrome. *Nat Genet* **29**:301–305.
267. **Zou J, Grabowski PS, Cunningham C, Secombes CJ.** 1999. Molecular cloning of interleukin 1 β from rainbow trout *Oncorhynchus mykiss* reveals no evidence of an ice cut site. *Cytokine* **11**:552–560.
268. **Hong S, Zou J, Collet B, Bols NC, Secombes CJ.** 2004. Analysis and characterisation of IL-1 β processing in rainbow trout, *Oncorhynchus mykiss*. *Fish Shellfish Immunol* **16**:453–459.
269. **Fujiki K, Shin D-H, Nakao M, Yano T.** 2000. Molecular cloning and expression analysis of carp (*Cyprinus carpio*) interleukin-1 β , high affinity immunoglobulin E Fc receptor γ subunit and serum amyloid A. *Fish Shellfish Immunol* **10**:229–242.
270. **Wang Y, Wang Q, Baoprasertkul P, Peatman E, Liu Z.** 2006. Genomic organization, gene duplication, and expression analysis of interleukin-1 β in channel catfish (*Ictalurus punctatus*). *Mol Immunol* **43**:1653–1664.
271. **Pelegrín P, García-Castillo J, Mulero V, Meseguer J.** 2001. Interleukin-1 β isolated from a marine fish reveals up-regulated expression in macrophages following activation with lipopolysaccharide and lymphokines. *Cytokine* **16**:67–72.
272. **Buonocore F, Prugnoli D, Falasca C, Secombes CJ, Scapigliati G.** 2003. Peculiar gene organisation and incomplete splicing of sea bass (*Dicentrarchus labrax* L.) interleukin-1 β . *Cytokine* **21**:257–264.
273. **Lee D-S, Hong SH, Lee H-J, Jun LJ, Chung J-K, Kim KH, Jeong HD.** 2006. Molecular cDNA cloning and analysis of the organization and expression of the IL-1 β gene in the Nile tilapia, *Oreochromis niloticus*. *Comp Biochem Physiol A Mol Integr Physiol* **143**:307–314.

274. **Covello JM, Bird S, Morrison RN, Battaglione SC, Secombes CJ, Nowak BF.** 2009. Cloning and expression analysis of three striped trumpeter (*Latris lineata*) pro-inflammatory cytokines, TNF- α , IL-1 β and IL-8, in response to infection by the ectoparasitic, *Chondracanthus goldsmidi*. *Fish Shellfish Immunol* **26**:773–786.
275. **Corripio-Miyar Y, Bird S, Tsamopoulos K, Secombes CJ.** 2007. Cloning and expression analysis of two pro-inflammatory cytokines, IL-1 β and IL-8, in haddock (*Melanogrammus aeglefinus*). *Mol Immunol* **44**:1361–1373.
276. **Seppola M, Larsen AN, Steiro K, Robertsen B, Jensen I.** 2008. Characterisation and expression analysis of the interleukin genes, IL-1 β , IL-8 and IL-10, in Atlantic cod (*Gadus morhua* L.). *Mol Immunol* **45**:887–897.
277. **Emmadi D, Iwahori A, Hirono I, Aoki T.** 2005. cDNA microarray analysis of interleukin-1 β -induced Japanese flounder *Paralichthys olivaceus* kidney cells. *Fish Sci* **71**:519–530.
278. **Øvergård A-C, Nepstad I, Nerland AH, Patel S.** 2011. Characterisation and expression analysis of the Atlantic halibut (*Hippoglossus hippoglossus* L.) cytokines: IL-1 β , IL-6, IL-11, IL-12 β and IFN γ . *Mol Biol Rep* **39**:2201–2213.
279. **Vojtech LN, Scharping N, Hansen JD.** 2012. Processing of zebrafish interleukin-1 beta during *Francisella noatunensis* infection: roles of inflammatory caspases. *Infect Immun* IAI.00543–12.
280. **Okamura H, Tsutsi H, Komatsu T, Yutsudo M, Hakura A, Tanimoto T, Torigoe K, Okura T, Nukada Y, Hattori K.** 1995. Cloning of a new cytokine that induces IFN-gamma production by T cells. *Nature* **378**:88–91.
281. **Gu Y, Kuida K, Tsutsui H, Ku G, Hsiao K, Fleming MA, Hayashi N, Higashino K, Okamura H, Nakanishi K, Kurimoto M, Tanimoto T, Flavell RA, Sato V, Harding MW, Livingston DJ, Su MS.** 1997. Activation of interferon-gamma inducing factor mediated by interleukin-1beta converting enzyme. *Science* **275**:206–209.
282. **Ushio S, Namba M, Okura T, Hattori K, Nukada Y, Akita K, Tanabe F, Konishi K, Micallef M, Fujii M, Torigoe K, Tanimoto T, Fukuda S, Ikeda M, Okamura H, Kurimoto M.** 1996. Cloning of the cDNA for human IFN-gamma-inducing factor, expression in *Escherichia coli*, and studies on the biologic activities of the protein. *J Immunol* **156**:4274–4279.
283. **Zepter K, Häffner A, Soohoo LF, De Luca D, Tang HP, Fisher P, Chavinson J, Elmets CA.** 1997. Induction of biologically active IL-1 beta-converting enzyme and mature IL-1 beta in human keratinocytes by inflammatory and immunologic stimuli. *J Immunol Baltim Md* 1950 **159**:6203–6208.
284. **Horwood NJ, Udagawa N, Elliott J, Grail D, Okamura H, Kurimoto M, Dunn AR, Martin T, Gillespie MT.** 1998. Interleukin 18 inhibits osteoclast formation via T cell production of granulocyte macrophage colony-stimulating factor. *J Clin Invest* **101**:595–603.
285. **Gracie JA, Forsey RJ, Chan WL, Gilmour A, Leung BP, Greer MR, Kennedy K, Carter R, Wei XQ, Xu D, Field M, Foulis A, Liew FY, McInnes IB.** 1999. A proinflammatory role for IL-18 in rheumatoid arthritis. *J Clin Invest* **104**:1393–1401.

286. **Olee T, Hashimoto S, Quach J, Lotz M.** 1999. IL-18 is produced by articular chondrocytes and induces proinflammatory and catabolic responses. *J Immunol Baltim Md* 1950 **162**:1096–1100.
287. **Siegmund B, Lehr H-A, Fantuzzi G, Dinarello CA.** 2001. IL-1 β -converting enzyme (caspase-1) in intestinal inflammation. *Proc Natl Acad Sci* **98**:13249–13254.
288. **Siegmund B, Fantuzzi G, Rieder F, Gamboni-Robertson F, Lehr H-A, Hartmann G, Dinarello CA, Endres S, Eigler A.** 2001. Neutralization of interleukin-18 reduces severity in murine colitis and intestinal IFN- γ and TNF- α production. *Am J Physiol - Regul Integr Comp Physiol* **281**:R1264–R1273.
289. **Tsutsui H, Matsui K, Okamura H, Nakanishi K.** 2000. Pathophysiological roles of interleukin-18 in inflammatory liver diseases. *Immunol Rev* **174**:192–209.
290. **Vidal-Vanaclocha F, Fantuzzi G, Mendoza L, Fuentes AM, Anasagasti MJ, Martín J, Carrascal T, Walsh P, Reznikov LL, Kim S-H, Novick D, Rubinstein M, Dinarello CA.** 2000. IL-18 regulates IL-1 β -dependent hepatic melanoma metastasis via vascular cell adhesion molecule-1. *Proc Natl Acad Sci* **97**:734–739.
291. **Gatti S, Beck J, Fantuzzi G, Bartfai T, Dinarello CA.** 2002. Effect of interleukin-18 on mouse core body temperature. *Am J Physiol - Regul Integr Comp Physiol* **282**:R702–R709.
292. **Li S, Goorha S, Ballou LR, Blatteis CM.** 2003. Intracerebroventricular interleukin-6, macrophage inflammatory protein-1 β and IL-18: pyrogenic and PGE2-mediated? *Brain Res* **992**:76–84.
293. **Kenji Nakanishi, Tomohiro Yoshimoto, Hiroko Tsutsui, Okamura H.** 2001. Interleukin-18 Regulates Both Th1 and Th2 Responses. *Annu Rev Immunol* **19**:423–474.
294. **Hoshino T, Kawase Y, Okamoto M, Yokota K, Yoshino K, Yamamura K, Miyazaki J, Young HA, Oizumi K.** 2001. Cutting Edge: IL-18-Transgenic Mice: In Vivo Evidence of a Broad Role for IL-18 in Modulating Immune Function. *J Immunol* **166**:7014–7018.
295. **Huisling MO, Stet RJM, Savelkoul HFJ, Verburg-van Kemenade BML.** 2004. The molecular evolution of the interleukin-1 family of cytokines; IL-18 in teleost fish. *Dev Comp Immunol* **28**:395–413.
296. **Zou J, Bird S, Truckle J, Bols N, Horne M, Secombes C.** 2004. Identification and expression analysis of an IL-18 homologue and its alternatively spliced form in rainbow trout (*Oncorhynchus mykiss*). *Eur J Biochem* **271**:1913–1923.
297. **Bialik S, Zalckvar E, Ber Y, Rubinstein AD, Kimchi A.** 2010. Systems biology analysis of programmed cell death. *Trends Biochem Sci* **35**:556–564.
298. **Tan ML, Ooi JP, Ismail N, Moad AIH, Muhammad TST.** 2009. Programmed cell death pathways and current antitumor targets. *Pharm Res* **26**:1547–1560.
299. **Kerr JFR, Wyllie AH, Currie AR.** 1972. Apoptosis: A Basic Biological Phenomenon with Wide-ranging Implications in Tissue Kinetics. *Br J Cancer* **26**:239–257.
300. **Horvitz HR.** 1999. Genetic Control of Programmed Cell Death in the Nematode *Caenorhabditis elegans*. *Cancer Res* **59**:1701s–1706s.
301. **Norbury CJ, Hickson and ID.** 2001. Cellular Responses to Dna Damage. *Annu Rev Pharmacol Toxicol* **41**:367–401.

302. **Nishida K, Yamaguchi O, Otsu K.** 2008. Crosstalk between autophagy and apoptosis in heart disease. *Circ Res* **103**:343–351.
303. **Leist M, Jäätelä M.** 2001. Four deaths and a funeral: from caspases to alternative mechanisms. *Nat Rev Mol Cell Biol* **2**:589–598.
304. **McCall K.** 2010. Genetic control of necrosis - another type of programmed cell death. *Curr Opin Cell Biol* **22**:882–888.
305. **Wu W, Liu P, Li J.** 2012. Necroptosis: An emerging form of programmed cell death. *Crit Rev Oncol Hematol* **82**:249–258.
306. **Golstein P, Kroemer G.** 2007. Cell death by necrosis: towards a molecular definition. *Trends Biochem Sci* **32**:37–43.
307. **Galluzzi L, Kroemer G.** 2008. Necroptosis: a specialized pathway of programmed necrosis. *Cell* **135**:1161–1163.
308. **Zychlinsky A, Prevost MC, Sansonetti PJ.** 1992. *Shigella flexneri* induces apoptosis in infected macrophages. *Nature* **358**:167–169.
309. **Chen LM, Kaniga K, Galán JE.** 1996. *Salmonella* spp. are cytotoxic for cultured macrophages. *Mol Microbiol* **21**:1101–1115.
310. **Monack DM, Raupach B, Hromockyj AE, Falkow S.** 1996. *Salmonella typhimurium* invasion induces apoptosis in infected macrophages. *Proc Natl Acad Sci U S A* **93**:9833–9838.
311. **Cookson BT, Brennan MA.** 2001. Pro-inflammatory programmed cell death. *Trends Microbiol* **9**:113–114.
312. **Masters SL, Gerlic M, Metcalf D, Preston S, Pellegrini M, O'Donnell JA, McArthur K, Baldwin TM, Chevrier S, Nowell CJ, Cengia LH, Henley KJ, Collinge JE, Kastner DL, Feigenbaum L, Hilton DJ, Alexander WS, Kile BT, Croker BA.** 2012. NLRP1 Inflammasome Activation Induces Pyroptosis of Hematopoietic Progenitor Cells. *Immunity* **37**:1009–1023.
313. **Sagulenko V, Thygesen SJ, Sester DP, Idris A, Cridland JA, Vajjhala PR, Roberts TL, Schroder K, Vince JE, Hill JM, Silke J, Stacey KJ.** 2013. AIM2 and NLRP3 inflammasomes activate both apoptotic and pyroptotic death pathways via ASC. *Cell Death Differ* **20**:1149–1160.
314. **Aachoui Y, Sagulenko V, Miao EA, Stacey KJ.** 2013. Inflammasome-mediated pyroptotic and apoptotic cell death, and defense against infection. *Curr Opin Microbiol* **16**:319–326.
315. **Sun GW, Lu J, Pervaiz S, Cao WP, Gan Y-H.** 2005. Caspase-1 dependent macrophage death induced by *Burkholderia pseudomallei*. *Cell Microbiol* **7**:1447–1458.
316. **Fink SL, Cookson BT.** 2005. Apoptosis, Pyroptosis, and Necrosis: Mechanistic Description of Dead and Dying Eukaryotic Cells. *Infect Immun* **73**:1907–1916.
317. **Fink SL, Cookson BT.** 2006. Caspase-1-dependent pore formation during pyroptosis leads to osmotic lysis of infected host macrophages. *Cell Microbiol* **8**:1812–1825.

318. **Bergsbaken T, Cookson BT.** 2007. Macrophage Activation Redirects *Yersinia*-Infected Host Cell Death from Apoptosis to Caspase-1-Dependent Pyroptosis. *PLoS Pathog* **3**:e161.
319. **Varela M, Romero A, Dios S, van der Vaart M, Figueras A, Meijer AH, Novoa B.** 2014. Cellular Visualization of Macrophage Pyroptosis and Interleukin-1 β Release in a Viral Hemorrhagic Infection in Zebrafish Larvae. *J Virol* **88**:12026–12040.
320. **Kepp O, Galluzzi L, Zitvogel L, Kroemer G.** 2010. Pyroptosis – a cell death modality of its kind? *Eur J Immunol* **40**:627–630.
321. **Bergsbaken T, Fink SL, Cookson BT.** 2009. Pyroptosis: host cell death and inflammation. *Nat Rev Microbiol* **7**:99–109.
322. **Steimle V, Siegrist CA, Mottet A, Lisowska-Grospierre B, Mach B.** 1994. Regulation of MHC class II expression by interferon-gamma mediated by the transactivator gene CIITA. *Science* **265**:106–109.
323. **Martinon F, Tschopp J.** 2005. NLRs join TLRs as innate sensors of pathogens. *Trends Immunol* **26**:447–454.
324. **Diez E, Yaraghi Z, MacKenzie A, Gros P.** 2000. The neuronal apoptosis inhibitory protein (Naip) is expressed in macrophages and is modulated after phagocytosis and during intracellular infection with *Legionella pneumophila*. *J Immunol Baltim Md 1950* **164**:1470–1477.
325. **Conti BJ, Davis BK, Zhang J, O'Connor W, Williams KL, Ting JP-Y.** 2005. CATERPILLER 16.2 (CLR16.2), a Novel NBD/LRR Family Member That Negatively Regulates T Cell Function. *J Biol Chem* **280**:18375–18385.
326. **Poyet J-L, Srinivasula SM, Tnani M, Razmara M, Fernandes-Alnemri T, Alnemri ES.** 2001. Identification of Ipaf, a Human Caspase-1-activating Protein Related to Apaf-1. *J Biol Chem* **276**:28309–28313.
327. **Geddes BJ, Wang L, Huang WJ, Lavellee M, Manji GA, Brown M, Jurman M, Cao J, Morgenstern J, Merriam S, Glucksmann MA, DiStefano PS, Bertin J.** 2001. Human CARD12 is a novel CED4/Apaf-1 family member that induces apoptosis. *Biochem Biophys Res Commun* **284**:77–82.
328. **Damiano JS, Stehlik C, Pio F, Godzik A, Reed JC.** 2001. CLAN, a novel human CED-4-like gene. *Genomics* **75**:77–83.
329. **Sutterwala FS, Mijares LA, Li L, Ogura Y, Kazmierczak BI, Flavell RA.** 2007. Immune recognition of *Pseudomonas aeruginosa* mediated by the IPAF/NLRC4 inflammasome. *J Exp Med* **204**:3235–3245.
330. **Akhter A, Gavrillin MA, Frantz L, Washington S, Ditty C, Limoli D, Day C, Sarkar A, Newland C, Butchar J, Marsh CB, Wewers MD, Tridandapani S, Kanneganti T-D, Amer AO.** 2009. Caspase-7 Activation by the Nlrc4/Ipaf Inflammasome Restricts *Legionella pneumophila* Infection. *PLOS Pathog* **5**:e1000361.
331. **Dowds TA, Masumoto J, Chen FF, Ogura Y, Inohara N, Núñez G.** 2003. Regulation of cryopyrin/Pypaf1 signaling by pyrin, the familial Mediterranean fever gene product. *Biochem Biophys Res Commun* **302**:575–580.

332. **Lamkanfi M, Kanneganti T-D.** 2012. Regulation of immune pathways by the NOD-like receptor NLRC5. *Immunobiology* **217**:13–16.
333. **Yao Y, Wang Y, Chen F, Huang Y, Zhu S, Leng Q, Wang H, Shi Y, Qian Y.** 2012. NLRC5 regulates MHC class I antigen presentation in host defense against intracellular pathogens. *Cell Res* **22**:836–847.
334. **Kanneganti T-D, Lamkanfi M, Núñez G.** 2007. Intracellular NOD-like Receptors in Host Defense and Disease. *Immunity* **27**:549–559.
335. **Hlaing T, Guo R-F, Dilley KA, Loussia JM, Morrish TA, Shi MM, Vincenz C, Ward PA.** 2001. Molecular Cloning and Characterization of DEFCAP-L and -S, Two Isoforms of a Novel Member of the Mammalian Ced-4 Family of Apoptosis Proteins. *J Biol Chem* **276**:9230–9238.
336. **Levinsohn JL, Newman ZL, Hellmich KA, Fattah R, Getz MA, Liu S, Sastalla I, Leppla SH, Moayeri M.** 2012. Anthrax Lethal Factor Cleavage of Nlrp1 Is Required for Activation of the Inflammasome. *PLOS Pathog* **8**:e1002638.
337. **Zhu X-D, Küster B, Mann M, Petrini JHJ, Lange T de.** 2000. Cell-cycle-regulated association of RAD50/MRE11/NBS1 with TRF2 and human telomeres. *Nat Genet* **25**:347–352.
338. **Bruey JM, Bruey-Sedano N, Newman R, Chandler S, Stehlik C, Reed JC.** 2004. PAN1/NALP2/PYPAF2, an Inducible Inflammatory Mediator That Regulates NF- κ B and Caspase-1 Activation in Macrophages. *J Biol Chem* **279**:51897–51907.
339. **Minkiewicz J, de Rivero Vaccari JP, Keane RW.** 2013. Human astrocytes express a novel NLRP2 inflammasome. *Glia* **61**:1113–1121.
340. **Zhu J, Petersen S, Tessarollo L, Nussenzweig A.** 2001. Targeted disruption of the Nijmegen breakage syndrome gene NBS1 leads to early embryonic lethality in mice. *Curr Biol* **11**:105–109.
341. **Difilippantonio S, Celeste A, Fernandez-Capetillo O, Chen H-T, Martin BRS, Laethem FV, Yang Y-P, Petukhova GV, Eckhaus M, Feigenbaum L, Manova K, Kruhlak M, Camerini-Otero RD, Sharan S, Nussenzweig M, Nussenzweig A.** 2005. Role of Nbs1 in the activation of the Atm kinase revealed in humanized mouse models. *Nat Cell Biol* **7**:675–685.
342. **Peng H, Chang B, Lu C, Su J, Wu Y, Lv P, Wang Y, Liu J, Zhang B, Quan F, Guo Z, Zhang Y.** 2012. Nlrp2, a Maternal Effect Gene Required for Early Embryonic Development in the Mouse. *PLOS ONE* **7**:e30344.
343. **O'Connor W, Harton JA, Zhu X, Linhoff MW, Ting JP-Y.** 2003. Cutting Edge: CIAS1/Cryopyrin/PYPAF1/NALP3/ CATERPILLER 1.1 Is an Inducible Inflammatory Mediator with NF- κ B Suppressive Properties. *J Immunol* **171**:6329–6333.
344. **Kikuchi-Yanoshita R, Taketomi Y, Koga K, Sugiki T, Atsumi Y, Saito T, Ishii S, Hisada M, Suzuki-Nishimura T, Uchida MK, Moon T-C, Chang H-W, Sawada M, Inagaki N, Nagai H, Murakami M, Kudo I.** 2003. Induction of PYPAF1 during *In Vitro* Maturation of Mouse Mast Cells. *J Biochem (Tokyo)* **134**:699–709.

345. **Anderson JP, Mueller JL, Rosengren S, Boyle DL, Schaner P, Cannon SB, Goodyear CS, Hoffman HM.** 2004. Structural, expression, and evolutionary analysis of mouse CIAS1. *Gene* **338**:25–34.
346. **Broz P, Newton K, Lamkanfi M, Mariathasan S, Dixit VM, Monack DM.** 2010. Redundant roles for inflammasome receptors NLRP3 and NLRC4 in host defense against *Salmonella*. *J Exp Med* **207**:1745–1755.
347. **Wree A, Eguchi A, McGeough MD, Pena CA, Johnson CD, Canbay A, Hoffman HM, Feldstein AE.** 2014. NLRP3 inflammasome activation results in hepatocyte pyroptosis, liver inflammation, and fibrosis in mice. *Hepatology* **59**:898–910.
348. **Stehlik C, Fiorentino L, Dorfleutner A, Bruey J-M, Ariza EM, Sagara J, Reed JC.** 2002. The PAAD/PYRIN-Family Protein ASC Is a Dual Regulator of a Conserved Step in Nuclear Factor κ B Activation Pathways. *J Exp Med* **196**:1605–1615.
349. **Belyaeva OV, Kedishvili NY.** 2002. Human pancreas protein 2 (PAN2) has a retinal reductase activity and is ubiquitously expressed in human tissues. *FEBS Lett* **531**:489–493.
350. **Miyamoto T, Hasuike S.** Isolation and Expression Analysis of the Human RNH2 Gene Encoding Ribonuclease Inhibitor 2. *J Assist Reprod Genet* **19**:394–397.
351. **Cui J, Li Y, Zhu L, Liu D, Songyang Z, Wang HY, Wang R-F.** 2012. NLRP4 negatively regulates type I interferon signaling by targeting the kinase TBK1 for degradation via the ubiquitin ligase DTX4. *Nat Immunol* **13**:387–395.
352. **Eibl C, Grigoriu S, Hessenberger M, Wenger J, Puehringer S, Pinheiro AS, Wagner RN, Proell M, Reed JC, Page R, Diederichs K, Peti W.** 2012. Structural and functional analysis of the NLRP4 pyrin domain. *Biochemistry (Mosc)* **51**:7330–7341.
353. **Tian X, Pascal G, Monget P.** 2009. Evolution and functional divergence of NLRPgenes in mammalian reproductive systems. *BMC Evol Biol* **9**:202.
354. **Tschopp J, Martinon F, Burns K.** 2003. NALPs: a novel protein family involved in inflammation. *Nat Rev Mol Cell Biol* **4**:95–104.
355. **Fortier A, Diez E, Gros P.** 2005. Naip5/Birc1e and susceptibility to *Legionella pneumophila*. *Trends Microbiol* **13**:328–335.
356. **Fernandes R, Tsuda C, Perumalsamy AL, Naranian T, Chong J, Acton BM, Tong Z-B, Nelson LM, Jurisicova A.** 2012. NLRP5 Mediates Mitochondrial Function in Mouse Oocytes and Embryos. *Biol Reprod* **86**:138.
357. **Docherty LE, Rezwan FI, Poole RL, Turner CLS, Kivuva E, Maher ER, Smithson SF, Hamilton-Shield JP, Patalan M, Gizewska M, Peregud-Pogorzelski J, Beygo J, Buiting K, Horsthemke B, Soellner L, Begemann M, Eggermann T, Baple E, Mansour S, Temple IK, Mackay DJG.** 2015. Mutations in NLRP5 are associated with reproductive wastage and multilocus imprinting disorders in humans. *Nat Commun* **6**:8086.
358. **Albrecht M, Domingues FS, Schreiber S, Lengauer T.** 2003. Identification of mammalian orthologs associates PYPAF5 with distinct functional roles. *FEBS Lett* **538**:173–177.

359. **Wang Y, Hasegawa M, Imamura R, Kinoshita T, Kondo C, Konaka K, Suda T.** 2004. PYNOD, a novel Apaf-1/CED4-like protein is an inhibitor of ASC and caspase-1. *Int Immunol* **16**:777–786.
360. **Drygin D, Koo S, Perera R, Barone S, Bennett CF.** 2005. Induction of Toll-like Receptors and NALP/PAN/PYPAF Family Members by Modified Oligonucleotides in Lung Epithelial Carcinoma Cells. *Oligonucleotides* **15**:105–118.
361. **Pétrilli V, Dostert C, Muruve DA, Tschopp J.** 2007. The inflammasome: a danger sensing complex triggering innate immunity. *Curr Opin Immunol* **19**:615–622.
362. **Martinon F, Gaide O, Pétrilli V, Mayor A, Tschopp J.** 2007. NALP Inflammasomes: a central role in innate immunity. *Semin Immunopathol* **29**:213.
363. **Liu Y, Meng Y, Wang Q, Sha Z.** 2012. Class II, major histocompatibility complex, transactivator (CIITA) in channel catfish: identification and expression patterns responding to different pathogens. *Mol Biol Rep* **39**:11041–11050.
364. **Oehlers SH, Flores MV, Hall CJ, Swift S, Crosier KE, Crosier PS.** 2011. The inflammatory bowel disease (IBD) susceptibility genes NOD1 and NOD2 have conserved anti-bacterial roles in zebrafish. *Dis Model Mech* **4**:832–841.
365. **Maharana J, Sahoo BR, Bej A, Patra MC, Dehury B, Bhoi GK, Lenka SK, Sahoo JR, Rout AK, Behera BK.** 2014. Structural and functional investigation of zebrafish (*Danio rerio*) NOD1 leucine rich repeat domain and its interaction with iE-DAP. *Mol Biosyst* **10**:2942–2953.
366. **Jang JH, Kim H, Kim YJ, Cho JH.** 2016. Molecular cloning and functional analysis of nucleotide-binding oligomerization domain-containing protein 1 in rainbow trout, *Oncorhynchus mykiss*. *Fish Shellfish Immunol* **51**:53–63.
367. **Hu YW, Yu ZL, Xue NN, Nie P, Chang MX.** 2014. Expression and protective role of two novel NACHT-containing proteins in pathogen infection. *Dev Comp Immunol* **46**:323–332.
368. **Robertson SJ, Rubino SJ, Geddes K, Philpott DJ.** 2012. Examining host–microbial interactions through the lens of NOD: From plants to mammals. *Semin Immunol* **24**:9–16.
369. **Saxena M, Yeretssian G.** 2014. NOD-Like Receptors: Master Regulators of Inflammation and Cancer. *Front Immunol* **5**.
370. **Motta V, Soares F, Sun T, Philpott DJ.** 2015. NOD-Like Receptors: Versatile Cytosolic Sentinels. *Physiol Rev* **95**:149–178.
371. **Latz E, Xiao TS, Stutz A.** 2013. Activation and regulation of the inflammasomes. *Nat Rev Immunol* **13**:397–411.
372. **Franchi L, Muñoz-Planillo R, Núñez G.** 2012. Sensing and reacting to microbes through the inflammasomes. *Nat Immunol* **13**:325–332.
373. **Ozaki E, Campbell M, Doyle SL.** 2015. Targeting the NLRP3 inflammasome in chronic inflammatory diseases: current perspectives. *J Inflamm Res* **8**:15–27.
374. **Neumann NF, Barreda D, Belosevic M.** 1998. Production of a macrophage growth factor(s) by a goldfish macrophage cell line and macrophages derived from goldfish kidney leukocytes. *Dev Comp Immunol* **22**:417–432.

375. **Wang R, Neumann NF, Shen Q, Belosevic M.** 1995. Establishment and characterization of a macrophage cell line from the goldfish. *Fish Shellfish Immunol* **5**:329–346.
376. **Barreda DR, Belosevic M.** 2001. Characterisation of growth enhancing factor production in different phases of *in vitro* fish macrophage development. *Fish Shellfish Immunol* **11**:169–185.
377. **Neumann NF, Barreda DR, Belosevic M.** 2000. Generation and functional analysis of distinct macrophage sub-populations from goldfish (*Carassius auratus* L.) kidney leukocyte cultures. *Fish Shellfish Immunol* **10**:1–20.
378. **Katzenback BA, Belosevic M.** 2009. Molecular and functional characterization of kita and kitla of the goldfish (*Carassius auratus* L.). *Dev Comp Immunol* **33**:1165–1175.
379. **Belosevic M, Hanington PC, Barreda DR.** 2006. Development of goldfish macrophages *in vitro*. *Fish Shellfish Immunol* **20**:152–171.
380. **Grayfer L, Hodgkinson JW, Belosevic M.** 2011. Analysis of the antimicrobial responses of primary phagocytes of the goldfish (*Carassius auratus* L.) against *Mycobacterium marinum*. *Dev Comp Immunol* **35**:1146–1158.
381. **Hodgkinson JW, Ge J-Q, Grayfer L, Stafford J, Belosevic M.** 2012. Analysis of the immune response in infections of the goldfish (*Carassius auratus* L.) with *Mycobacterium marinum*. *Dev Comp Immunol* **38**:456–465.
382. **Tamura K, Peterson D, Peterson N, Stecher G, Nei M, Kumar S.** 2011. MEGA5: Molecular Evolutionary Genetics Analysis Using Maximum Likelihood, Evolutionary Distance, and Maximum Parsimony Methods. *Mol Biol Evol* **28**:2731–2739.
383. **Grayfer L, Belosevic M.** 2009. Molecular characterization of novel interferon gamma receptor 1 isoforms in zebrafish (*Danio rerio*) and goldfish (*Carassius auratus* L.). *Mol Immunol* **46**:3050–3059.
384. **Montgomery BCS, Mewes J, Davidson C, Burshtyn DN, Stafford JL.** 2009. Cell surface expression of channel catfish leukocyte immune-type receptors (IpLITRs) and recruitment of both Src homology 2 domain-containing protein tyrosine phosphatase (SHP)-1 and SHP-2. *Dev Comp Immunol* **33**:570–582.
385. **Godl K, Wissing J, Kurtenbach A, Habenberger P, Blencke S, Gutbrod H, Salassidis K, Stein-Gerlach M, Missio A, Cotten M, Daub H.** 2003. An efficient proteomics method to identify the cellular targets of protein kinase inhibitors. *Proc Natl Acad Sci* **100**:15434–15439.
386. **Windheim M, Lang C, Peggie M, Plater LA, Cohen P.** 2007. Molecular mechanisms involved in the regulation of cytokine production by muramyl dipeptide. *Biochem J* **404**:179–190.
387. **Homer CR, Kabi A, Marina-García N, Sreekumar A, Nesvizhskii AI, Nickerson KP, Chinnaiyan AM, Nuñez G, McDonald C.** 2012. A Dual Role for Receptor-interacting Protein Kinase 2 (RIP2) Kinase Activity in Nucleotide-binding Oligomerization Domain 2 (NOD2)-dependent Autophagy. *J Biol Chem* **287**:25565–25576.
388. **Morchang A, Yasamut U, Netsawang J, Noisakran S, Wongwiwat W, Songprakhon P, Srisawat C, Puttikhunt C, Kasinrerak W, Malasit P, Yenchitsomanus P, Limjindaporn T.**

2011. Cell death gene expression profile: Role of RIPK2 in dengue virus-mediated apoptosis. *Virus Res* **156**:25–34.
389. **Tigno-Aranjuez JT, Asara JM, Abbott DW.** 2010. Inhibition of RIP2's tyrosine kinase activity limits NOD2-driven cytokine responses. *Genes Dev* **24**:2666–2677.
390. **Grayfer L, Walsh JG, Belosevic M.** 2008. Characterization and functional analysis of goldfish (*Carassius auratus* L.) tumor necrosis factor-alpha. *Dev Comp Immunol* **32**:532–543.
391. **Grayfer L, Belosevic M.** 2012. Identification and molecular characterization of the interleukin-10 receptor 1 of the zebrafish (*Danio rerio*) and the goldfish (*Carassius auratus* L.). *Dev Comp Immunol* **36**:408–417.
392. **Katzenback BA, Belosevic M.** 2012. Characterization of granulocyte colony stimulating factor receptor of the goldfish (*Carassius auratus* L.). *Dev Comp Immunol* **36**:199–207.
393. **Uematsu S, Akira S.** 2007. Toll-Like Receptors and Type I Interferons. *J Biol Chem* **282**:15319–15323.
394. **Akira S, Takeda K, Kaisho T.** 2001. Toll-like receptors: critical proteins linking innate and acquired immunity. *Nat Immunol* **2**:675–680.
395. **Iwanaga Y, Davey MP, Martin TM, Planck SR, DePriest ML, Baugh MM, Suing CM, Rosenbaum JT.** Cloning, sequencing and expression analysis of the mouse NOD2/CARD15. *Inflamm Res* **52**:272–276.
396. **Philpott DJ, Girardin SE.** 2004. The role of Toll-like receptors and Nod proteins in bacterial infection. *Mol Immunol* **41**:1099–1108.
397. **Inohara N, Peso L del, Koseki T, Chen S, Núñez G.** 1998. RICK, a Novel Protein Kinase Containing a Caspase Recruitment Domain, Interacts with CLARP and Regulates CD95-mediated Apoptosis. *J Biol Chem* **273**:12296–12300.
398. **Tohno M, Shimazu T, Aso H, Uehara A, Takada H, Kawasaki A, Fujimoto Y, Fukase K, Saito T, Kitazawa H.** 2008. Molecular cloning and functional characterization of porcine nucleotide-binding oligomerization domain-1 (NOD1) recognizing minimum agonists, meso-diaminopimelic acid and meso-lanthionine. *Mol Immunol* **45**:1807–1817.
399. **Li M, Wang Q, Lu Y, Chen S, Li Q, Sha Z.** 2012. Expression profiles of NODs in channel catfish (*Ictalurus punctatus*) after infection with *Edwardsiella tarda*, *Aeromonas hydrophila*, *Streptococcus iniae* and channel catfish hemorrhage reovirus. *Fish Shellfish Immunol* **33**:1033–1041.
400. **Hasegawa M, Yang K, Hashimoto M, Park J-H, Kim Y-G, Fujimoto Y, Nuñez G, Fukase K, Inohara N.** 2006. Differential Release and Distribution of Nod1 and Nod2 Immunostimulatory Molecules among Bacterial Species and Environments. *J Biol Chem* **281**:29054–29063.
401. **Oh H-M, Lee H-J, Seo G-S, Choi E-Y, Kweon S-H, Chun C-H, Han W-C, Lee K-M, Lee M-S, Choi S-C, Jun C-D.** 2005. Induction and localization of NOD2 protein in human endothelial cells. *Cell Immunol* **237**:37–44.

402. **Takahashi Y, Isuzugawa K, Murase Y, Imai M, Yamamoto S, Iizuka M, Akira S, Bahr GM, Momotani E, Hori M, Ozaki H, Imakawa K.** 2006. Up-Regulation of NOD1 and NOD2 through TLR4 and TNF- α in LPS-treated Murine Macrophages. *J Vet Med Sci* **68**:471–478.
403. **Mühlbauer M, Cheely AW, Yenugu S, Jobin C.** 2008. Regulation and functional impact of lipopolysaccharide induced Nod2 gene expression in the murine epididymal epithelial cell line PC1. *Immunology* **124**:256–264.
404. **Kim Y-G, Park J-H, Reimer T, Baker DP, Kawai T, Kumar H, Akira S, Wobus C, Núñez G.** 2011. Viral Infection Augments Nod1/2 Signaling to Potentiate Lethality Associated with Secondary Bacterial Infections. *Cell Host Microbe* **9**:496–507.
405. **Girardin SE, Jéhanno M, Mengin-Lecreulx D, Sansonetti PJ, Alzari PM, Philpott DJ.** 2005. Identification of the Critical Residues Involved in Peptidoglycan Detection by Nod1. *J Biol Chem* **280**:38648–38656.
406. **Brooks MN, Rajaram MVS, Azad AK, Amer AO, Valdivia-Arenas MA, Park J, Nuñez G, Schlesinger LS.** 2011. NOD2 controls the nature of the inflammatory response and subsequent fate of *Mycobacterium tuberculosis* and *M. bovis* BCG in human macrophages. *Cell Microbiol* **13**:402–418.
407. **Cai X, Wang M, Kong H, Liu J, Liu Y, Xia W, Zou M, Wang J, Su H, Xu D.** 2013. Prokaryotic expression, purification and functional characterization of recombinant human RIP2. *Mol Biol Rep* **40**:59–65.
408. **Grayfer L, Hodgkinson JW, Belosevic M.** 2014. Antimicrobial responses of teleost phagocytes and innate immune evasion strategies of intracellular bacteria. *Dev Comp Immunol* **43**:223–242.
409. **Lu B, Wang H, Andersson U, Tracey KJ.** 2013. Regulation of HMGB1 release by inflammasomes. *Protein Cell* **4**:163–167.
410. **Bouchier-Hayes L, Martin SJ.** 2002. CARD games in apoptosis and immunity. *EMBO Rep* **3**:616–621.
411. **Hong G-S, Jung Y-K.** 2002. Caspase recruitment domain (CARD) as a bi-functional switch of caspase regulation and NF-kappaB signals. *J Biochem Mol Biol* **35**:19–23.
412. **Hollenbach E, Neumann M, Vieth M, Roessner A, Malferttheiner P, Naumann M.** 2004. Inhibition of p38 MAP kinase- and RICK/NF-kB-signaling suppresses inflammatory bowel disease. *FASEB J* **18**:1550–1552.
413. **Argast GM, Fausto N, Campbell JS.** 2005. Inhibition of RIP2/RICK/CARDIAK activity by pyridinyl imidazole inhibitors of p38 MAPK. *Mol Cell Biochem* **268**:129–140.
414. **Nembrini C, Kisielow J, Shamshiev AT, Tortola L, Coyle AJ, Kopf M, Marsland BJ.** 2009. The Kinase Activity of Rip2 Determines Its Stability and Consequently Nod1- and Nod2-mediated Immune Responses. *J Biol Chem* **284**:19183–19188.
415. **Madrigal AG, Barth K, Papadopoulos G, Genco CA.** 2012. Pathogen-Mediated Proteolysis of the Cell Death Regulator RIPK1 and the Host Defense Modulator RIPK2 in Human Aortic Endothelial Cells. *PLOS Pathog* **8**:e1002723.

416. **Yang Y, Yin C, Pandey A, Abbott D, Sasseti C, Kelliher MA.** 2007. NOD2 Pathway Activation by MDP or *Mycobacterium Tuberculosis* Infection Involves the Stable Polyubiquitination of Rip2. *J Biol Chem* **282**:36223–36229.
417. **Jing H, Fang L, Wang D, Ding Z, Luo R, Chen H, Xiao S.** 2014. Porcine reproductive and respiratory syndrome virus infection activates NOD2–RIP2 signal pathway in MARC-145 cells. *Virology* **458–459**:162–171.
418. **Pandey AK, Yang Y, Jiang Z, Fortune SM, Coulombe F, Behr MA, Fitzgerald KA, Sasseti CM, Kelliher MA.** 2009. NOD2, RIP2 and IRF5 Play a Critical Role in the Type I Interferon Response to *Mycobacterium tuberculosis*. *PLoS Pathog* **5**.
419. **Uehara A, Yang S, Fujimoto Y, Fukase K, Kusumoto S, Shibata K, Sugawara S, Takada H.** 2005. Muramyl dipeptide and diaminopimelic acid-containing desmuramyl peptides in combination with chemically synthesized Toll-like receptor agonists synergistically induced production of interleukin-8 in a NOD2- and NOD1-dependent manner, respectively, in human monocytic cells in culture. *Cell Microbiol* **7**:53–61.
420. **Uehara A, Fujimoto Y, Fukase K, Takada H.** 2007. Various human epithelial cells express functional Toll-like receptors, NOD1 and NOD2 to produce anti-microbial peptides, but not proinflammatory cytokines. *Mol Immunol* **44**:3100–3111.
421. **Clay H, Volkman HE, Ramakrishnan L.** 2008. Tumor Necrosis Factor Signaling Mediates Resistance to Mycobacteria by Inhibiting Bacterial Growth and Macrophage Death. *Immunity* **29**:283–294.
422. **Mishra BB, Rathinam VAK, Martens GW, Martinot AJ, Kornfeld H, Fitzgerald KA, Sasseti CM.** 2013. Nitric oxide controls the immunopathology of tuberculosis by inhibiting NLRP3 inflammasome-dependent processing of IL-1 β . *Nat Immunol* **14**:52–60.
423. **Willingham SB, Allen IC, Bergstralh DT, Brickey WJ, Huang MT-H, Taxman DJ, Duncan JA, Ting JP-Y.** 2009. NLRP3 (NALP3, Cryopyrin) Facilitates In Vivo Caspase-1 Activation, Necrosis, and HMGB1 Release via Inflammasome-Dependent and -Independent Pathways. *J Immunol* **183**:2008–2015.
424. **Mariathasan S, Weiss DS, Newton K, McBride J, O'Rourke K, Roose-Girma M, Lee WP, Weinrauch Y, Monack DM, Dixit VM.** 2006. Cryopyrin activates the inflammasome in response to toxins and ATP. *Nature* **440**:228–232.
425. **Tschopp J, Schroder K.** 2010. NLRP3 inflammasome activation: the convergence of multiple signalling pathways on ROS production? *Nat Rev Immunol* **10**:210–215.
426. **Kim MS, Lee JA, Kim KH.** 2016. Effects of a broad-spectrum caspase inhibitor, Z-VAD(OMe)-FMK, on viral hemorrhagic septicemia virus (VHSV) infection-mediated apoptosis and viral replication. *Fish Shellfish Immunol* **51**:41–45.
427. **Maekawa T, Kufer TA, Schulze-Lefert P.** 2011. NLR functions in plant and animal immune systems: so far and yet so close. *Nat Immunol* **12**:817–826.
428. **Rast JP, Smith LC, Loza-Coll M, Hibino T, Litman GW.** 2006. Genomic Insights into the Immune System of the Sea Urchin. *Science* **314**:952–956.

429. Li J, Ding J, Zhang W, Zhang Y, Tang P, Chen J-Q, Tian D, Yang S. 2010. Unique evolutionary pattern of numbers of gramineous NBS–LRR genes. *Mol Genet Genomics* **283**:427–438.
430. Meyers BC, Kozik A, Griego A, Kuang H, Michelmore RW. 2003. Genome-Wide Analysis of NBS-LRR–Encoding Genes in Arabidopsis. *Plant Cell* **15**:809–834.
431. Hitomi Y, Ebisawa M, Tomikawa M, Imai T, Komata T, Hirota T, Harada M, Sakashita M, Suzuki Y, Shimojo N, Kohno Y, Fujita K, Miyatake A, Doi S, Enomoto T, Taniguchi M, Higashi N, Nakamura Y, Tamari M. 2009. Associations of functional NLRP3 polymorphisms with susceptibility to food-induced anaphylaxis and aspirin-induced asthma. *J Allergy Clin Immunol* **124**:779–785.e6.
432. Kinose D, Ogawa E, Hirota T, Ito I, Kudo M, Haruna A, Marumo S, Hoshino Y, Muro S, Hirai T, Sakai H, Date H, Tamari M, Mishima M. 2012. A NOD2 gene polymorphism is associated with the prevalence and severity of chronic obstructive pulmonary disease in a Japanese population. *Respirology* **17**:164–171.
433. Neven B, Callebaut I, Prieur A-M, Feldmann J, Bodemer C, Lepore L, Derfalvi B, Benjaponpitak S, Vesely R, Sauvain MJ, Oertle S, Allen R, Morgan G, Borkhardt A, Hill C, Gardner-Medwin J, Fischer A, de Saint Basile G. 2004. Molecular basis of the spectral expression of CIAS1 mutations associated with phagocytic cell-mediated autoinflammatory disorders CINCA/NOMID, MWS, and FCU. *Blood* **103**:2809–2815.
434. Faustin B, Lartigue L, Bruey J-M, Luciano F, Sergienko E, Bailly-Maitre B, Volkmann N, Hanein D, Rouiller I, Reed JC. 2007. Reconstituted NALP1 Inflammasome Reveals Two-Step Mechanism of Caspase-1 Activation. *Mol Cell* **25**:713–724.
435. Newman ZL, Printz MP, Liu S, Crown D, Breen L, Miller-Randolph S, Flodman P, Leppla SH, Moayeri M. 2010. Susceptibility to Anthrax Lethal Toxin-Induced Rat Death Is Controlled by a Single Chromosome 10 Locus That Includes rNlrp1. *PLOS Pathog* **6**:e1000906.
436. Witola WH, Mui E, Hargrave A, Liu S, Hypolite M, Montpetit A, Cavailles P, Bisanz C, Cesbron-Delauw M-F, Fournié GJ, McLeod R. 2011. NALP1 Influences Susceptibility to Human Congenital Toxoplasmosis, Proinflammatory Cytokine Response, and Fate of *Toxoplasma gondii*-Infected Monocytic Cells. *Infect Immun* **79**:756–766.
437. Lamkanfi M, Dixit VM. 2009. The Inflammasomes. *PLOS Pathog* **5**:e1000510.
438. Hise AG, Tomalka J, Ganesan S, Patel K, Hall BA, Brown GD, Fitzgerald KA. 2009. An Essential Role for the NLRP3 Inflammasome in Host Defense against the Human Fungal Pathogen *Candida albicans*. *Cell Host Microbe* **5**:487–497.
439. Chae JJ, Wood G, Masters SL, Richard K, Park G, Smith BJ, Kastner DL. 2006. The B30.2 domain of pyrin, the familial Mediterranean fever protein, interacts directly with caspase-1 to modulate IL-1 β production. *Proc Natl Acad Sci U S A* **103**:9982–9987.
440. Papin S, Cuenin S, Agostini L, Martinon F, Werner S, Beer H-D, Grütter C, Grütter M, Tschopp J. 2007. The SPRY domain of Pyrin, mutated in familial Mediterranean fever patients, interacts with inflammasome components and inhibits proIL-1 β processing. *Cell Death Differ* **14**:1457–1466.

441. **Guarda G, So A.** 2010. Regulation of inflammasome activity. *Immunology* **130**:329–336.
442. **Man SM, Hopkins LJ, Nugent E, Cox S, Glück IM, Tourlomousis P, Wright JA, Cicuta P, Monie TP, Bryant CE.** 2014. Inflammasome activation causes dual recruitment of NLRC4 and NLRP3 to the same macromolecular complex. *Proc Natl Acad Sci* **111**:7403–7408.
443. **Squires RC, Muehlbauer SM, Brojatsch J.** 2007. Proteasomes Control Caspase-1 Activation in Anthrax Lethal Toxin-mediated Cell Killing. *J Biol Chem* **282**:34260–34267.
444. **Wang H, Xing Y, Mao L, Luo Y, Kang L, Meng G.** 2013. Pannexin-1 influences peritoneal cavity cell population but is not involved in NLRP3 inflammasome activation. *Protein Cell* **4**:259–265.
445. **Netea MG, Nold-Petry CA, Nold MF, Joosten LAB, Opitz B, Meer JHM van der, Veerdonk FL van de, Ferwerda G, Heinhuis B, Devesa I, Funk CJ, Mason RJ, Kullberg BJ, Rubartelli A, Meer JWM van der, Dinarello CA.** 2009. Differential requirement for the activation of the inflammasome for processing and release of IL-1 β in monocytes and macrophages. *Blood* **113**:2324–2335.
446. **Smith J, Manoranjan J, Pan M, Bohsali A, Xu J, Liu J, McDonald KL, Szyk A, LaRonde-LeBlanc N, Gao L-Y.** 2008. Evidence for Pore Formation in Host Cell Membranes by ESX-1-Secreted ESAT-6 and Its Role in *Mycobacterium marinum* Escape from the Vacuole. *Infect Immun* **76**:5478–5487.
447. **Koo IC, Wang C, Raghavan S, Morisaki JH, Cox JS, Brown EJ.** 2008. ESX-1-dependent cytolysis in lysosome secretion and inflammasome activation during mycobacterial infection. *Cell Microbiol* **10**:1866–1878.
448. **Abdallah AM, Bestebroer J, Savage ND, Punder K de, Zon M van, Wilson L, Korbee CJ, Sar AM van der, Ottenhoff THM, Wel NN van der, Bitter W, Peters PJ.** 2011. Mycobacterial Secretion Systems ESX-1 and ESX-5 Play Distinct Roles in Host Cell Death and Inflammasome Activation. *J Immunol* **187**:4744–4753.
449. **Stehlik C, Lee SH, Dorfleutner A, Stassinopoulos A, Sagara J, Reed JC.** 2003. Apoptosis-Associated Speck-Like Protein Containing a Caspase Recruitment Domain Is a Regulator of Procaspase-1 Activation. *J Immunol* **171**:6154–6163.
450. **Schroder K, Tschopp J.** 2010. The Inflammasomes. *Cell* **140**:821–832.
451. **Hara H, Tsuchiya K, Kawamura I, Fang R, Hernandez-Cuellar E, Shen Y, Mizuguchi J, Schweighoffer E, Tybulewicz V, Mitsuyama M.** 2013. Phosphorylation of the adaptor ASC acts as a molecular switch that controls the formation of speck-like aggregates and inflammasome activity. *Nat Immunol* **14**:1247–1255.
452. **Masumoto J, Taniguchi S 'ichiro, Nakayama J, Shiohara M, Hidaka E, Katsuyama T, Murase S, Sagara J.** 2001. Expression of Apoptosis-associated Speck-like Protein Containing a Caspase Recruitment Domain, a Pyrin N-terminal Homology Domain-containing Protein, in Normal Human Tissues. *J Histochem Cytochem* **49**:1269–1275.
453. **Martinon F, Hofmann K, Tschopp J.** 2001. The pyrin domain: a possible member of the death domain-fold family implicated in apoptosis and inflammation. *Curr Biol* **11**:R118–R120.

454. **Romberg N, Al Moussawi K, Nelson-Williams C, Stiegler AL, Loring E, Choi M, Overton J, Meffre E, Khokha MK, Huttner AJ, West B, Podoltsev NA, Boggon TJ, Kazmierczak BI, Lifton RP.** 2014. Mutation of NLRC4 causes a syndrome of enterocolitis and autoinflammation. *Nat Genet* **46**:1135–1139.
455. **Centola M, Aksentijevich I, Kastner DL.** 1998. The Hereditary Periodic Fever Syndromes: Molecular Analysis of a New Family of Inflammatory Diseases. *Hum Mol Genet* **7**:1581–1588.
456. **Richards N, Schaner P, Diaz A, Stuckey J, Shelden E, Wadhwa A, Gumucio DL.** 2001. Interaction between Pypin and the Apoptotic Speck Protein (ASC) Modulates ASC-induced Apoptosis. *J Biol Chem* **276**:39320–39329.
457. **Masumoto J, Taniguchi S 'ichiro, Ayukawa K, Sarvotham H, Kishino T, Niikawa N, Hidaka E, Katsuyama T, Higuchi T, Sagara J.** 1999. ASC, a Novel 22-kDa Protein, Aggregates during Apoptosis of Human Promyelocytic Leukemia HL-60 Cells. *J Biol Chem* **274**:33835–33838.
458. **Miao EA, Rajan JV, Aderem A.** 2011. Caspase-1-induced pyroptotic cell death: Caspase-1-induced pyroptotic cell death. *Immunol Rev* **243**:206–214.
459. **Compan V, Martín-Sánchez F, Baroja-Mazo A, López-Castejón G, Gomez AI, Verkhatsky A, Brough D, Pelegrín P.** 2015. Apoptosis-Associated Speck-like Protein Containing a CARD Forms Specks but Does Not Activate Caspase-1 in the Absence of NLRP3 during Macrophage Swelling. *J Immunol* **194**:1261–1273.
460. **Hofmann K, Bucher P, Tschopp J.** 1997. The CARD domain: a new apoptotic signalling motif. *Trends Biochem Sci* **5**:155–156.
461. **Paonessa G, Frank R, Cortese R.** 1987. Nucleotide sequence of rat liver HMG1 cDNA. *Nucleic Acids Res* **15**:9077.
462. **Yotov WV, St-Arnaud R.** 1992. Nucleotide sequence of a mouse cDNA encoding the nonhistone chromosomal high mobility group protein-1 (HMG1). *Nucleic Acids Res* **20**:3516.
463. **Scaffidi P, Misteli T, Bianchi ME.** 2002. Release of chromatin protein HMGB1 by necrotic cells triggers inflammation. *Nature* **418**:191–195.
464. **Medzhitov R, Janeway CJ.** 2000. Innate immune recognition: mechanisms and pathways. *Immunol Rev* **173**:89–97.
465. **Beg AA.** 2002. Endogenous ligands of Toll-like receptors: implications for regulating inflammatory and immune responses. *Trends Immunol* **23**:509–512.
466. **Mogensen TH.** 2009. Pathogen Recognition and Inflammatory Signaling in Innate Immune Defenses. *Clin Microbiol Rev* **22**:240–273.
467. **Shaw MH, Reimer T, Sánchez-Valdepeñas C, Warner N, Kim Y-G, Fresno M, Nuñez G.** 2009. T cell-intrinsic role of Nod2 in promoting type 1 immunity to *Toxoplasma gondii*. *Nat Immunol* **10**:1267–1274.
468. **Akira S, Uematsu S, Takeuchi O.** 2006. Pathogen Recognition and Innate Immunity. *Cell* **124**:783–801.

469. **Tadié J-M, Bae H-B, Banerjee S, Zmijewski JW, Abraham E.** 2012. Differential activation of RAGE by HMGB1 modulates neutrophil-associated NADPH oxidase activity and bacterial killing. *Am J Physiol - Cell Physiol* **302**:C249–C256.
470. **Tadie J-M, Bae H-B, Jiang S, Park DW, Bell CP, Yang H, Pittet J-F, Tracey K, Thannickal VJ, Abraham E, Zmijewski JW.** 2013. HMGB1 promotes neutrophil extracellular trap formation through interactions with Toll-like receptor 4. *Am J Physiol - Lung Cell Mol Physiol* **304**:L342–L349.
471. **Cassatella MA, Della Bianca V, Berton G, Rossi F.** 1985. Activation by gamma interferon of human macrophage capability to produce toxic oxygen molecules is accompanied by decreased km of the superoxide-generating NADPH oxidase. *Biochem Biophys Res Commun* **132**:908–914.
472. **Dragomir A-C, Laskin JD, Laskin DL.** 2011. Macrophage activation by factors released from acetaminophen-injured hepatocytes: Potential role of HMGB1. *Toxicol Appl Pharmacol* **253**:170–177.
473. **Kokkola R, Andersson Å, Mullins G, Östberg T, Treutiger C-J, Arnold B, Nawroth P, Andersson U, Harris RA, Harris HE.** 2005. RAGE is the Major Receptor for the Proinflammatory Activity of HMGB1 in Rodent Macrophages. *Scand J Immunol* **61**:1–9.
474. **Ren D, Sun R, Wang S.** 2006. Role of inducible nitric oxide synthase expressed by alveolar macrophages in High Mobility Group Box 1- induced acute lung injury. *Inflamm Res* **55**:207–215.
475. **Czura CJ, Yang H, Amella CA, Tracey KJ.** 2004. HMGB1 in the Immunology of Sepsis (Not Septic Shock) and Arthritis, p. 181–200. *In Immunology, B-A in (ed.)*, . Academic Press.
476. **Andersson U, Wang H, Palmblad K, Aveberger A-C, Bloom O, Erlandsson-Harris H, Janson A, Kokkola R, Zhang M, Yang H, Tracey KJ.** 2000. High Mobility Group 1 Protein (Hmg-1) Stimulates Proinflammatory Cytokine Synthesis in Human Monocytes. *J Exp Med* **192**:565–570.
477. **Tian J, Avalos AM, Mao S-Y, Chen B, Senthil K, Wu H, Parroche P, Drabic S, Golenbock D, Sirois C, Hua J, An LL, Audoly L, La Rosa G, Bierhaus A, Nawroth P, Marshak-Rothstein A, Crow MK, Fitzgerald KA, Latz E, Kiener PA, Coyle AJ.** 2007. Toll-like receptor 9-dependent activation by DNA-containing immune complexes is mediated by HMGB1 and RAGE. *Nat Immunol* **8**:487–496.
478. **Bonizzi G, Karin M.** 2004. The two NF- κ B activation pathways and their role in innate and adaptive immunity. *Trends Immunol* **25**:280–288.
479. **Bierhaus A, Humpert PM, Morcos M, Wendt T, Chavakis T, Arnold B, Stern DM, Nawroth PP.** 2005. Understanding RAGE, the receptor for advanced glycation end products. *J Mol Med* **83**:876–886.
480. **He Q, You H, Li X-M, Liu T-H, Wang P, Wang B-E.** 2012. HMGB1 promotes the synthesis of pro-IL-1 β and pro-IL-18 by activation of p38 MAPK and NF- κ B through receptors for advanced glycation end-products in macrophages. *Asian Pac J Cancer Prev APJCP* **13**:1365–1370.

481. **Wang Q, Imamura R, Motani K, Kushiya H, Nagata S, Suda T.** 2013. Pyroptotic cells externalize eat-me and release find-me signals and are efficiently engulfed by macrophages. *Int Immunol* **25**:363–372.
482. **Secombes CJ, Bird S, Cunningham C, Zou J.** 1999. Interleukin-1 in fish. *Fish Shellfish Immunol* **9**:335–343.
483. **Bird S, Wang T, Zou J, Cunningham C, Secombes CJ.** 2002. The First Cytokine Sequence Within Cartilaginous Fish: IL-1 β in the Small Spotted Catshark (*Scyliorhinus canicula*). *J Immunol* **168**:3329–3340.
484. **Wang T, Bird S, Koussounadis A, Holland JW, Carrington A, Zou J, Secombes CJ.** 2009. Identification of a Novel IL-1 Cytokine Family Member in Teleost Fish. *J Immunol* **183**:962–974.
485. **Bryan NB, Dorfleutner A, Rojanasakul Y, Stehlik C.** 2009. Activation of Inflammasomes Requires Intracellular Redistribution of the Apoptotic Speck-Like Protein Containing a Caspase Recruitment Domain. *J Immunol* **182**:3173–3182.
486. **Chen KW, Richards AA, Zamoshnikova A, Schroder K.** 2014. Inflammasomes and Inflammation, p. 103–117. *In* Hiraku, Y, Kawanishi, S, Ohshima, H (eds.), *Cancer and Inflammation Mechanisms*. John Wiley & Sons, Inc.
487. **Sahoo BR, Swain B, Dikhit MR, Basu M, Bej A, Jayasankar P, Samanta M.** 2013. Activation of Nucleotide-Binding Oligomerization Domain 1 (NOD1) Receptor Signaling in *Labeo rohita*. *Appl Biochem Biotechnol* **170**:1282–1309.
488. **Maharana J, Patra MC, De BC, Sahoo BR, Behera BK, De S, Pradhan SK.** 2014. Structural insights into the MDP binding and CARD–CARD interaction in zebrafish (*Danio rerio*) NOD2: a molecular dynamics approach. *J Mol Recognit* **27**:260–275.
489. **Lage SL, Amarante-Mendes GP, Bortoluci KR.** 2013. Evaluation of pyroptosis in macrophages using cytosolic delivery of purified flagellin. *Methods* **61**:110–116.
490. **Kasibhatla S, Amarante-Mendes GP, Finucane D, Brunner T, Bossy-Wetzel E, Green DR.** 2006. Acridine Orange/Ethidium Bromide (AO/EB) Staining to Detect Apoptosis. *CSH Protoc* **2006**.
491. **Hersh D, Monack DM, Smith MR, Ghori N, Falkow S, Zychlinsky A.** 1999. The *Salmonella* invasin SipB induces macrophage apoptosis by binding to caspase-1. *Proc Natl Acad Sci U S A* **96**:2396–2401.
492. **Monack DM, Hersh D, Ghori N, Bouley D, Zychlinsky A, Falkow S.** 2000. *Salmonella* exploits caspase-1 to colonize Peyer's patches in a murine typhoid model. *J Exp Med* **192**:249–258.
493. **Schyth BD, Bramsen JB, Pakula MM, Larashati S, Kjems J, Wengel J, Lorenzen N.** 2012. *In vivo* screening of modified siRNAs for non-specific antiviral effect in a small fish model: number and localization in the strands are important. *Nucleic Acids Res* **40**:4653–4665.
494. **He Y-Q, Chen J, Lu X-J, Shi Y-H.** 2013. Characterization of P2X7R and Its Function in the Macrophages of ayu, *Plecoglossus altivelis*. *PLOS ONE* **8**:e57505.
495. **Li M, Li Y, Sun L.** 2015. CD83 is required for the induction of protective immunity by a DNA vaccine in a teleost model. *Dev Comp Immunol* **51**:141–147.

496. **Chakrapani V, Patra SK, Panda RP, Rasal KD, Jayasankar P, Barman HK.** 2016. Establishing targeted carp TLR22 gene disruption via homologous recombination using CRISPR/Cas9. *Dev Comp Immunol* **61**:242–247.
497. **Adeyemo OM, Shapira S, Tombaccini D, Pollard HB, Feuerstein G, Sirén A-L.** 1991. A goldfish model for evaluation of the neurotoxicity of ω -conotoxin GVI A and screening of monoclonal antibodies. *Toxicol Appl Pharmacol* **108**:489–496.
498. **Kerr JL, Guo Z, Smith DW, Goss GG, Belosevic M.** 2008. Use of goldfish to monitor wastewater and reuse water for xenobiotics. *J Environ Eng Sci* **7**:369–383.
499. **Hagen MO, Katzenback BA, Islam MDS, El-Din MG, Belosevic M.** 2014. The Analysis of Goldfish (*Carassius auratus* L.) Innate Immune Responses After Acute and Subchronic Exposures to Oil Sands Process-Affected Water. *Toxicol Sci* **138**:59–68.
500. **Singh A, Havixbeck JJ, Smith MK, Shu Z, Tierney KB, Barreda DR, El-Din MG, Belosevic M.** 2015. UV and hydrogen peroxide treatment restores changes in innate immunity caused by exposure of fish to reuse water. *Water Res* **71**:257–273.
501. **Popescu JT, Martyniuk CJ, Mennigen J, Xiong H, Zhang D, Xia X, Cossins AR, Trudeau VL.** 2008. The goldfish (*Carassius auratus*) as a model for neuroendocrine signaling. *Mol Cell Endocrinol* **293**:43–56.
502. **Chang JP, Johnson JD, Sawisky GR, Grey CL, Mitchell G, Booth M, Volk MM, Parks SK, Thompson E, Goss GG, Klausen C, Habibi HR.** 2009. Signal transduction in multifactorial neuroendocrine control of gonadotropin secretion and synthesis in teleosts—studies on the goldfish model. *Gen Comp Endocrinol* **161**:42–52.
503. **Lathers CM, Mukai C, Smith CM, Schraeder PL.** 2001. A new goldfish model to evaluate pharmacokinetic and pharmacodynamic effects of drugs used for motion sickness in different gravity loads. *Acta Astronaut* **49**:419–440.
504. **Stafford JL, Neumann NF, Belosevic M.** 2002. Macrophage-Mediated Innate Host Defense Against Protozoan Parasites. *Crit Rev Microbiol* **28**:187–248.
505. **Belosevic M, Hanington PC, Barreda DR.** 2006. Development of goldfish macrophages *in vitro*. *Fish Shellfish Immunol* **20**:152–171.
506. **Hanington PC, Barreda DR, Belosevic M.** 2006. A Novel Hematopoietic Granulin Induces Proliferation of Goldfish (*Carassius auratus* L.) Macrophages. *J Biol Chem* **281**:9963–9970.
507. **Hanington PC, Wang T, Secombes CJ, Belosevic M.** 2007. Growth factors of lower vertebrates characterization of goldfish (*Carassius auratus* L.) macrophage colony-stimulating factor-1. *J Biol Chem* **282**:31865–31872.
508. **Oladiran A, Belosevic M.** 2010. *Trypanosoma carassii* calreticulin binds host complement component C1q and inhibits classical complement pathway-mediated lysis. *Dev Comp Immunol* **34**:396–405.
509. **Garcia-Garcia E, Ge JQ, Oladiran A, Montgomery B, El-Din MG, Perez-Estrada LC, Stafford JL, Martin JW, Belosevic M.** 2011. Ozone treatment ameliorates oil sands process water toxicity to the mammalian immune system. *Water Res* **45**:5849–5857.

510. **Rieger AM, Havixbeck JJ, Belosevic M, Barreda DR.** 2015. Teleost soluble CSF-1R modulates cytokine profiles at an inflammatory site, and inhibits neutrophil chemotaxis, phagocytosis, and bacterial killing. *Dev Comp Immunol* **49**:259–266.

**Appendix A: *DE NOVO* ASSEMBLY, TRANSCRIPTOME
SEQUENCING AND DIFFERENTIAL EXPRESSION ANALYSIS OF THE
IMMUNE-RELATED GENES DURING THE ACUTE PHASE OF
INFECTION WITH *Mycobacterium marinum* IN THE GOLDFISH
(*Carassius auratus* L.)**

Paired-end sequencing and *de novo* assembly

With the goal of generating the transcriptome of goldfish infected with *M. marinum*, RNA was extracted from goldfish spleen and sequenced using paired-end sequencing technology. A total of 103,993,458 raw sequencing reads with the length of 100 bp were generated from a 200 bp insert library. According to the overlapping information of high-quality reads, a total of 342,790 contigs were generated with an average length of 314 bp and a N50 of 506 bp, and 11.48% of contigs were greater than 500 bp (Table A1).

The *de novo* assembly of the transcriptome yielded 183,343 unigenes with an average of 898 bp and a total length of 164.67 Mb. The length of assembled unigenes ranged from 200 to 12,444 bp. Among the 183,343 non-redundant unigenes, 110,602 (60.32%) ranged from 200-500 bp in length, 24,990 (13.63%) ranged from 501 to 1,000 bp, and 47,751 (26.04%) were more than 1000 bp in length (Fig. A1). The sequence data were submitted to NCBI Sequence Read Archive under the accession number of SRP059469.

The second round sequencing was performed to identify differentially expressed genes between PBS-sham injected (SI) and *M. marinum*-infected (MI) groups. The raw reads of the second round sequencing had more than 99% clean reads for all of the six sequenced samples (Fig. A2). In addition, the alignment statistics result of the six fish samples showed approximately 70 % mapped reads compared to genes assembled from the first round transcriptome results, suggesting these samples are qualified for DEG identification purpose (Table A2).

Functional annotation by searching public databases

For validation and annotation of the assembled unigenes, sequence similarity search was conducted against the NR database, the COG database, the Swiss-Prot protein databases and the KEGG database with an E-value threshold of 10^{-5} . The results indicated that out of a total of 183,343 unigenes, 75,281 (61.4%), 32,236 (17.6%), 50,597 (27.6%), 21,956 (12.0%) and 45,992 (25.1%) showed significant similarity to known genes that encode proteins in NR, SwissProt, KEGG, COG and GO databases, respectively (Fig. A3). Together, 122,614 (66.9%) unigenes showed similarity to genes that encode known proteins in five databases indicated above. The E-value distribution of the top hits in the NR database revealed that 53.2% of the mapped sequences showed significant homology (less than $1.0E-45$) (Fig. A4A), and 79.8% and 55.8% of the sequences with similarities greater than 60% and 80%, respectively (Fig. A4B).

Functional classification by GO and COG

GO is an international standardized gene functional classification system and covers three domains: biological process, cellular component and molecular function. A total of 45,992 unigenes with BLAST matches to known proteins were assigned to GO classes with 367,469 functional arms. As shown in Fig. A5, the assignments to the biological processes were the most common (214,412; 58.3%), followed by the cellular components (98,019; 26.7%) and molecular function (55,038; 15.0%).

Under the category of biological processes, cellular processes (31,191; 15.0%) were the most common. It was also noteworthy that 12,758 unigenes were involved in response to stimulus and 8,344 unigenes were assigned to signaling (Fig. A5A). Under the classification of cellular components, three categories, cell, cell part, and organelle were approximately 33.85% of cellular components (Fig. A5B). Under the classification of molecular functions, binding (26,205; 14.29%) and catalytic activity (17,136; 9.34%) were the largest categories. Other categories, such as channel regulator activity, chemoattractant activity, chemorepellent activity, metallochaperone activity, protein tag, receptor regulator activity and translation regulator activity, were represented by 104 unigenes (0.0005%) (Fig. A5C).

COGs database was used to identify homologous genes and assign the possible functions to the goldfish unigenes (Fig. A6). Out of 122,343 unigenes with the significant similarity to NR proteins in this chapter, 21,956 sequences were assigned using COG classifications (Fig. A6). Among the 25 COG categories, the cluster for general function prediction only (10,289; 20.3%) was the largest group, followed by replication,

recombination and repair (5,279; 10.4%), transcription (4,646; 9.2%), cell cycle control, cell division, chromosome partitioning (3,243; 6.4%), Signal transduction mechanisms (3,301; 6.5%), translation, ribosomal structure and biogenesis (3,194; 6.3%), posttranslational modification, protein turnover and chaperones (3,123; 6.2%). Only a few unigenes were assigned to extracellular and nuclear structures. In addition, 1,055 unigenes (about 2.1%) were assigned to secondary metabolite biosynthesis, transport and catabolism (Fig. A6).

Functional classification by KEGG

KEGG is a database used for the analysis of gene products during metabolic processes and related gene functions in the cellular processes. This pathway-based analysis enables better understanding of the biological functions and gene interactions. The analysis using KEGG database and BLASTx with an E-value threshold of 10^{-5} , showed that 50,597 (27.6%) unigenes had significant matches in the KEGG database and were assigned to 114 KEGG pathways (Appendix B). Among 5 main categories, metabolism was the largest category (38,702; 76.5%), followed by genetic information processing (9,119; 18.0%), cellular processes (1,650; 3.3%), environmental information processing (675; 1.3%) and organismal systems (455; 0.9%). For genes involved in the metabolic pathways, 9,119 unigenes were related to processes such as transcription, translation, folding, sorting and degrading, replication and repair, and 1,650 unigenes were associated with processes such as transport and catabolism. In addition, the categories

of environmental information processing and organismal systems were represented by 675 and 455 unigenes, respectively (Appendix B).

Analysis of DEGs and immune related DEGs

A total of 843 genes were differentially expressed between the sham and *M. marinum* infected goldfish at 24 h post infection (Figs. A7A and B and Appendix C). Among these DEGs, 81 were identified as immune related DEGs, and of these 46 and 35 genes were up- or down-regulated, respectively (Fig. A7C).

GO and KEGG pathway enrichment analysis of DEGs

GO enrichment analysis provides all GO terms that are significantly enriched in DEGs, and filters the DEGs that correspond to biological functions. In this chapter, 843 DEGs could be categorized into 43 functional groups (Fig. A8). For the three main domains (biological process, cellular component and molecular function) of GO classification, 21, 12 and 10 functional groups were identified, respectively. Among these groups, single-organism process (15.8%), cellular process (13.6%) and metabolic process (13.4%) were dominant in the biological process domain. For the cellular component domain, the major classifications were cell (22.1%), cell part (22.1%) and organelle (15.2%). Most of the genes were classified into binding (47.6%) and catalytic activity (25.6%) of the molecular function category (Fig. A8).

KEGG pathway enrichment analysis identifies significantly enriched metabolic pathways or signal transduction pathways in DEGs. 218 signaling pathways were

identified and further enriched in DEGs between sham-injected control fish and *M. marinum*-exposed goldfish (Appendix D). Of those, 22 pathways were significantly enriched (Q value < 0.05) and genes related to cancer were the most prevalent (Fig. A9). The top 20 KEGG pathways of DEGs are shown in Table A3.

During the acute *M. marinum* infection, 19 pathways identified were related to immune system from the enriched 218 DEG by KEGG analysis (Appendix E), including PI3K-Akt signaling pathway (19 DEGs, ko04151), NF- κ B signaling pathway (12 DEGs, ko04065), chemokine signaling pathway (12 DEGs, ko04062), TNF-signaling pathway (11 DEGs, ko04668), cytokine-cytokine receptor interactions (10 DEGs, ko04060), complement and coagulation cascades (10 DEGs, ko04610), NOD-like receptor signaling pathway (9 DEGs, ko04621), Toll-like receptor signaling pathway (8 DEGs, ko04620), TGF- β signaling pathway (8 DEGs, ko04350), MAPK pathway (8 DEGs, ko04010), natural killer cell mediated cytotoxicity (8 DEGs, ko04650), Jak-STAT signaling pathway (8 DEGs, ko04630), T cell receptor signaling pathway (6 DEGs, ko04660), antigen processing and presentation (6 DEGs, ko04612), apoptosis (5 DEGs, ko04210), B cell receptor signaling pathway (4 DEGs, ko04662), Fc γ R-mediated phagocytosis (4 DEGs, ko04666), p53 signaling pathway (3 DEGs, ko04115) and Fc epsilon RI signaling pathway (2 DEGs, ko04664). The main DEGs involved in these signaling pathways are listed in Appendix E.

Table A1. Statistics of goldfish spleen transcriptome assembly

	Sample	Total Number	Total length (nt)	Mean length (nt)	N50	Total consensus sequences	Distinct Clusters	Distinct singletons
Contig	Goldfish spleen	342,790	107,614,534	314	506	-	-	-
Unigene	Goldfish spleen	183,343	164,679,694	898	2116	183,343	66,182	117,161

Table A2. Alignment statistics result with reference gene for all the second round of sequencing of goldfish spleen transcriptome obtained from PBS-sham injected (SI) and *M. marinum*-infected (MI) fish

Sample	Total reads	Total Base pairs	Total Mapped reads
SI-1	65282512	6528251200	46814230 (71.71%)
SI-2	65108240	6510824000	44867124 (68.91%)
SI-3	61808940	6180894000	42739346 (69.15%)
MI-1	65237628	6523762800	46030400 (70.56%)
MI-2	65264400	6526440000	46060402 (70.58%)
MI-3	66795332	6679533200	48769520 (73.01%)

Table A3. Top 20 KEGG pathway enrichment analysis of all differentially expressed genes

#	Pathway	DEGs with pathway annotation (279)	All genes with pathway annotation (50917)	P value	Q value	Pathway ID
1	Pathway in cancer	29 (10.39%)	2935 (5.76%)	0.001656556	0.022570575	ko05200
2	Metabolic pathways	28 (10.04%)	5648 (11.09%)	0.7405751	0.891994564	ko01100
3	MicroRNAs in cancer	22 (7.89%)	1625 (3.19%)	0.000105075	0.004524739	ko05206
4	Herpes simplex infection	20 (7.17%)	1491 (2.93%)	0.000244072	0.004837063	ko05168
5	PI3K-Akt signaling pathway	19 (6.81%)	2095 (4.11%)	0.02286294	0.14539946	ko04151
6	Epstein-Barr virus infection	17 (6.09%)	1460 (2.87%)	0.003130174	0.034527123	ko05169
7	Platelet activation	16 (5.73%)	1250 (2.45%)	0.001627293	0.022570575	ko04611
8	Influenza A	16 (5.73%)	1598 (3.14%)	0.01581353	0.111204824	ko05164
9	Focal adhesion	16 (5.73%)	1859 (3.65%)	0.05165535	0.256730622	ko04510
10	Tuberculosis	15 (5.38%)	1319 (2.59%)	0.006612899	0.058495426	ko05152
11	Small cell lung cancer	14 (5.02%)	701 (1.38%)	3.91E-05	0.002131324	ko05222
12	HTLV-I infection	14 (5.02%)	1698 (3.33%)	0.08605569	0.312907099	ko05166
13	Leishmaniasis	12 (4.3%)	472 (0.93%)	1.38E-05	0.001587032	ko05140
14	Hematopoietic cell lineage	12 (4.3%)	631 (1.24%)	0.000217302	0.004837063	ko04640
15	NF-kappa B signaling pathway	12 (4.3%)	951 (1.87%)	0.006708191	0.058495426	ko04064
16	Hepatitis B	12 (4.3%)	1137 (2.23%)	0.02401092	0.14539946	ko05161
17	Chemokine signaling pathway	12 (4.3%)	1220 (2.4%)	0.03800845	0.21245749	ko04062
18	ECM-receptor interaction	11 (3.94%)	655 (1.29%)	0.001089521	0.018270429	ko04512
19	TNF-signaling pathway	11 (3.94%)	732 (1.44%)	0.002589224	0.031669272	ko04668
20	Transcriptional misregulation in cancer	11 (3.94%)	1583 (3.11%)	0.2533025	0.57520776	ko05202
	Proteoglycans in cancer	11 (3.94%)	1901 (3.73%)	0.470036	0.746561378	ko05205
	Endocytosis	11 (3.94%)	2051 (4.03%)	0.5716205	0.803956574	ko04144

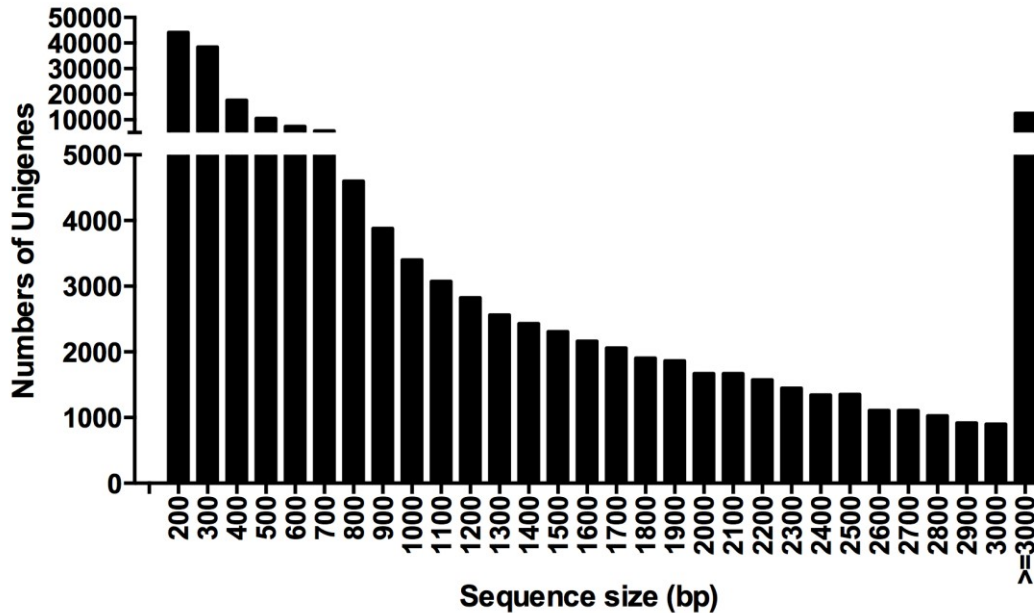


Figure A1. Length distribution of the assembled unigenes in the goldfish transcriptome database.

De novo assembly of transcriptome was carried out using Trinity program. Trinity assembles reads that have overlapping nucleic acid sequences and this analysis results in generation of contigs. To obtain the unigenes, the paired-end reads were realigned to known contigs, present on the corresponding zebrafish transcripts. Subsequently, all contigs in a transcript were assembled by the Trinity program and defined as unigenes. The TIGR Gene Indices clustering tool (TGICL) program was then used to eliminate redundant unigenes and generate single set of non-redundant unigenes. *De novo* transcriptome assembly was performed by the short oligonucleotide alignment (SOAP) *de novo* program.

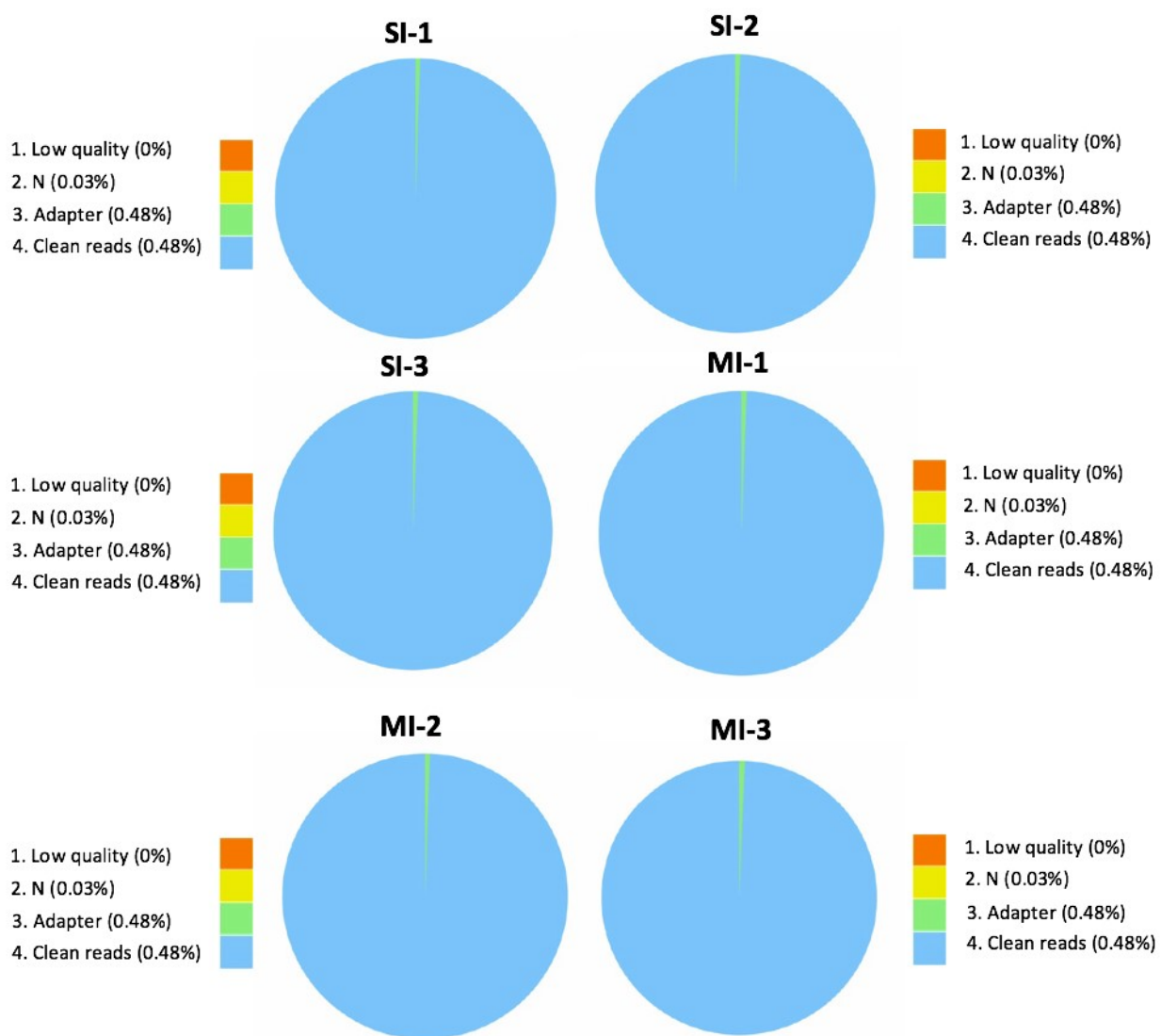


Figure A2. Classification of the raw reads for second round sequencing.

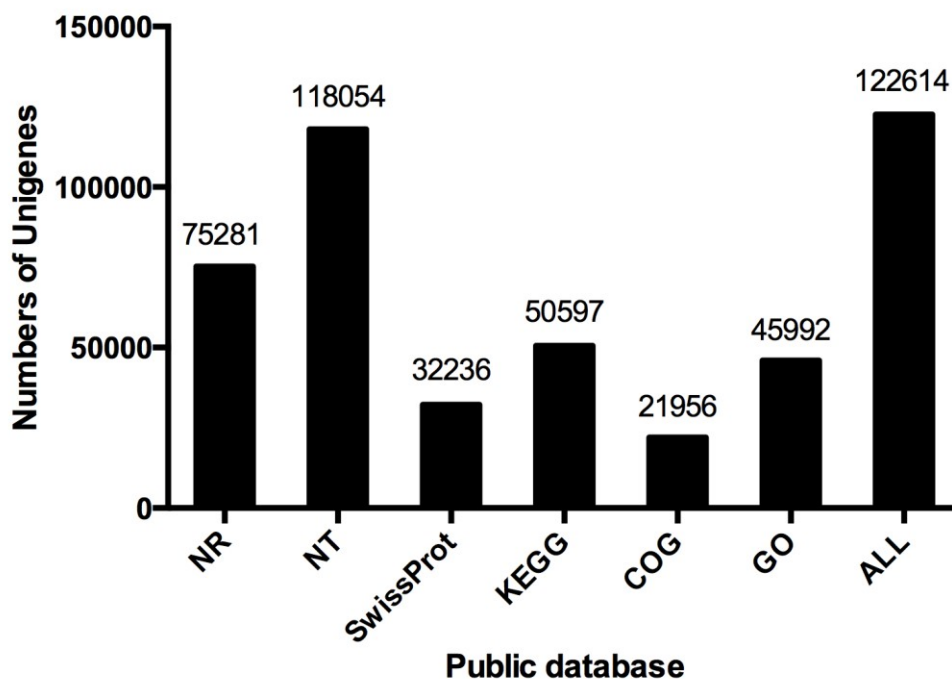


Figure A3. The number of unigenes from goldfish transcriptome database annotated using six public databases.

Unigenes were firstly aligned to protein databases [NR, Swiss-Prot, KEGG and COG (e-value < 0.00001)] by BlastX, and nucleotide database NT (E-value < 0.00001) by BlastN, retrieving proteins with the highest sequence similarity with the given unigenes along with their protein functional annotations. Unigenes were then annotated with the databases of NR, NT, Swiss-Prot, KEGG, COG and GO and the numbers of unigenes annotated with each database were counted.

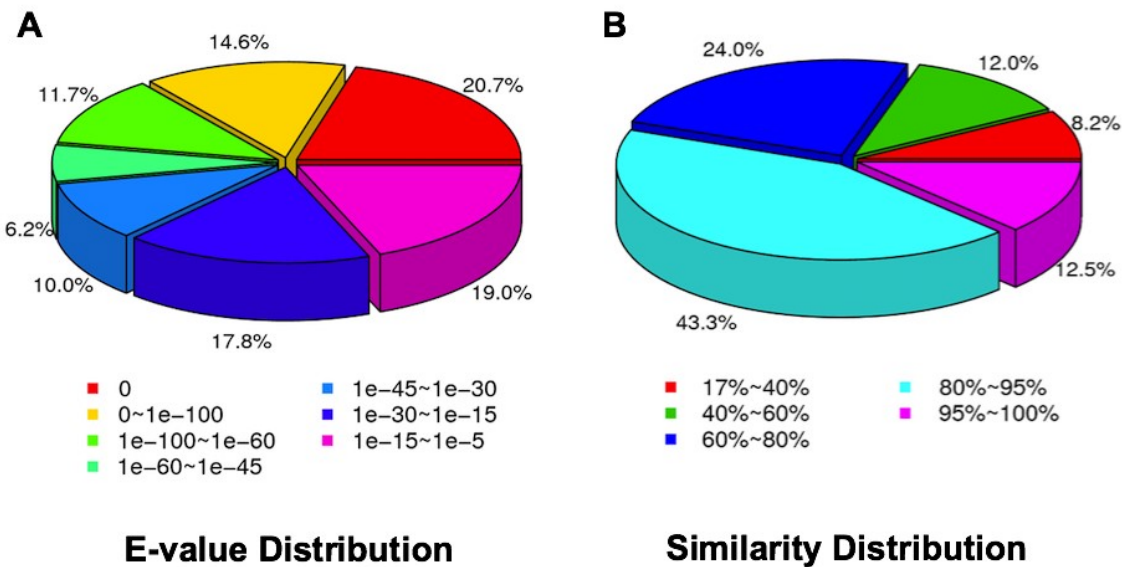
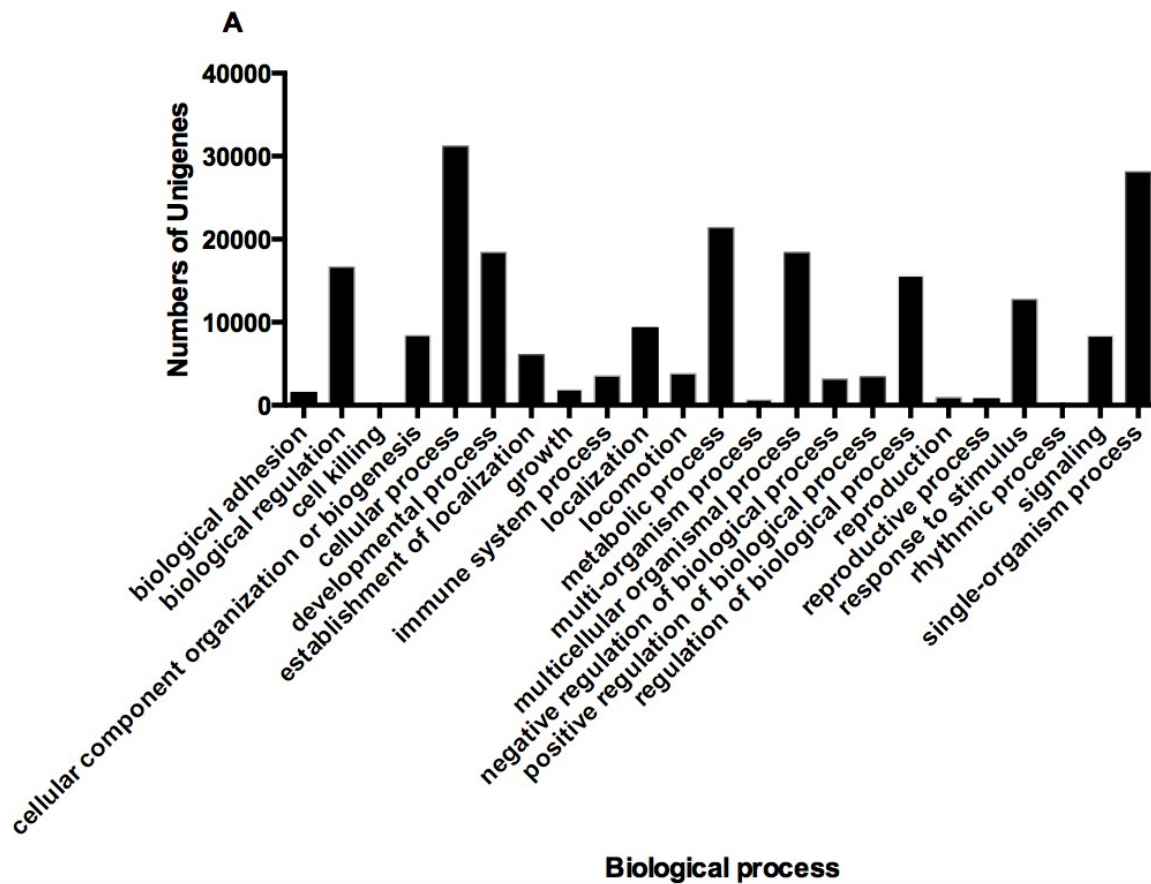
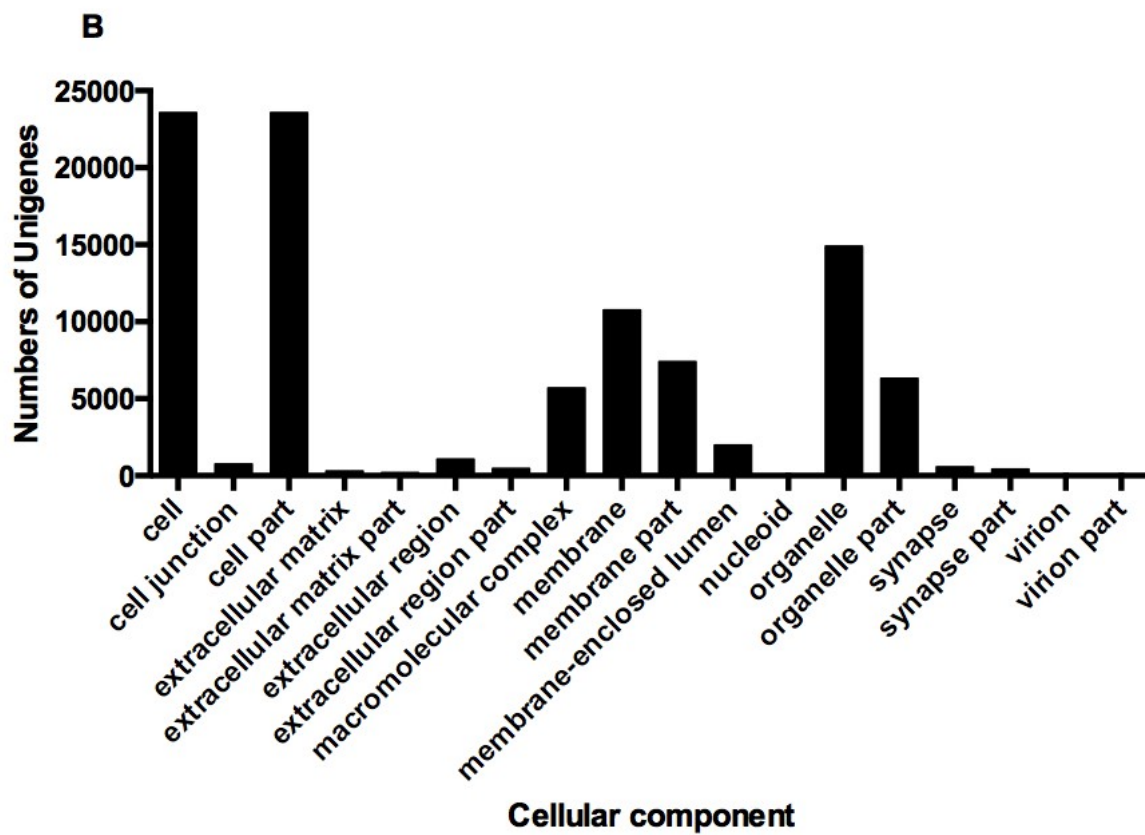


Figure A4. Characteristics of similarity search of unigenes against NR database.
 (A) E-value distribution of BLAST hits for each unigene with a cutoff E-value of 1.0E-5. (B) Similarity distribution of the top BLAST hits for each unigenes in NR database.





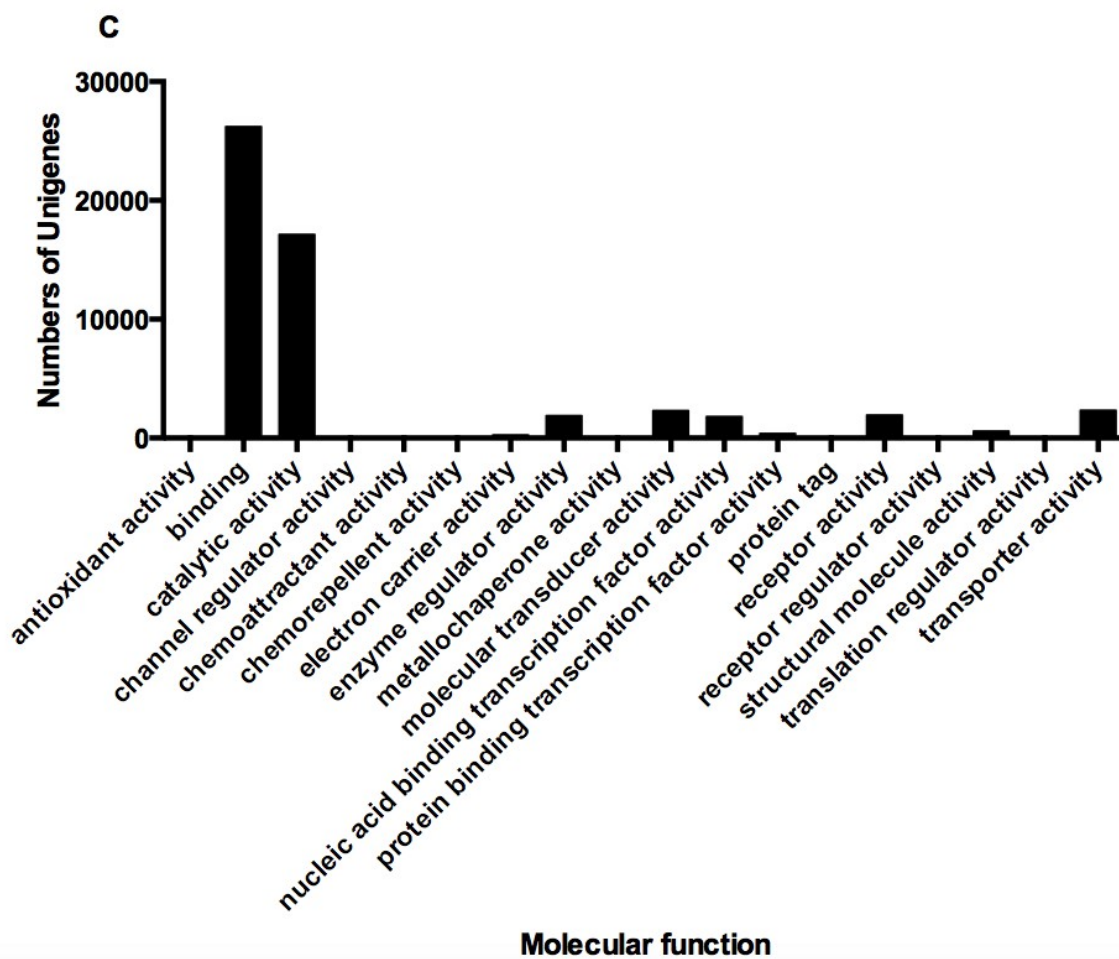


Figure A5. Gene ontology classifications of assembled goldfish transcriptome database unigenes.

The results are summarized in three main categories: (A) Biological process, (B) Cellular component and (C) Molecular function.

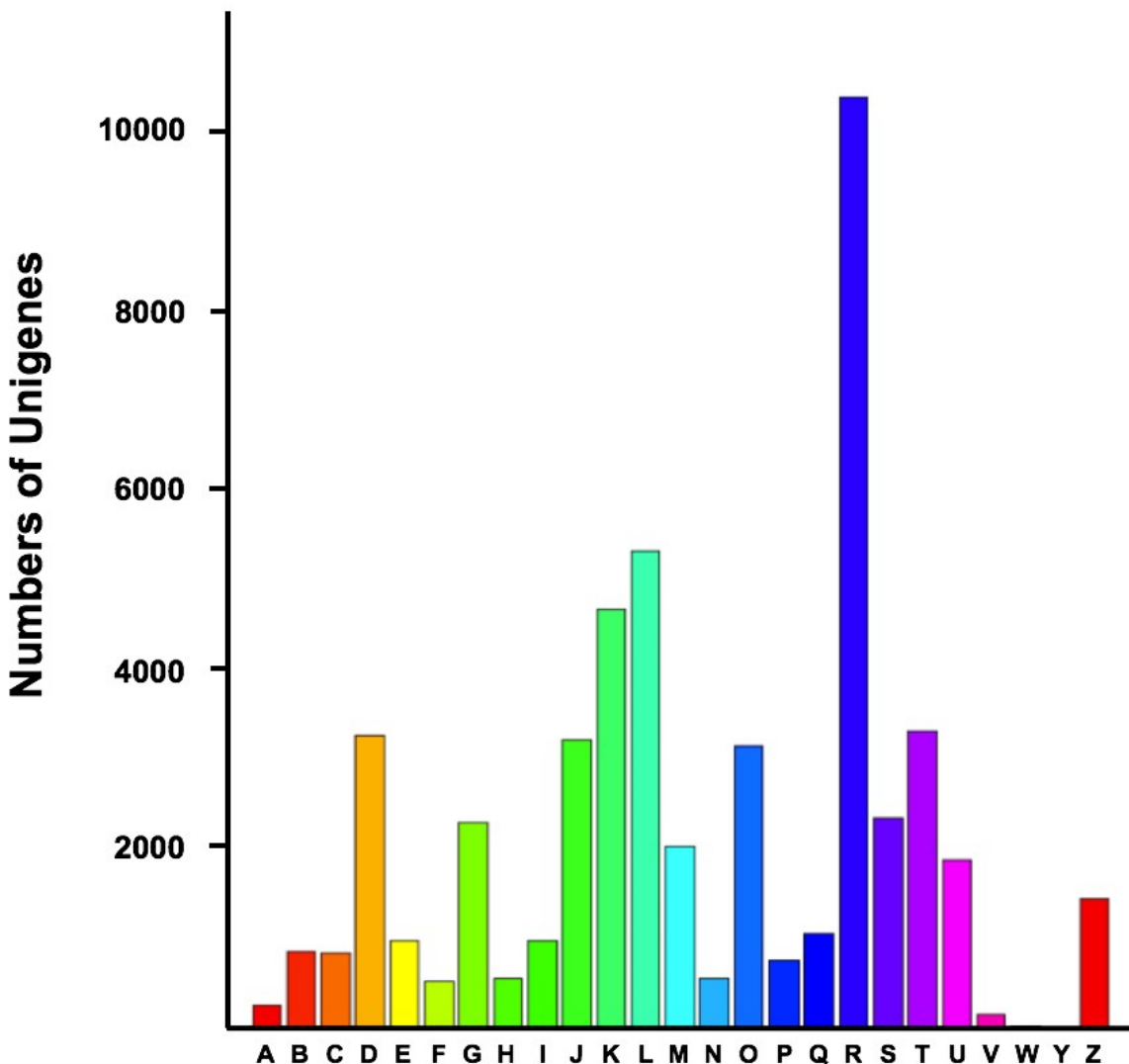


Figure A6. Histogram presentation of clusters of orthologous groups (COG) classification.
 A = RNA processing and modification; B = Chromatin structure and dynamics; C = Energy production and conversion; D = Cell cycle control, cell division, chromosome partitioning; E = Amino acid transport and metabolism; F = Nucleotide transport and metabolism; G = Carbohydrate transport and metabolism; H = Coenzyme transport and metabolism; I = Lipid transport and metabolism; J = Translation, ribosomal structure and biogenesis; K = Transcription; L = Replication, recombination and repair; M = Cell wall/membrane/velop biogenesis; N = Cell motility; O = Posttranslational modification, protein turnover, chaperones; P = Inorganic ion transport and metabolism; Q = Secondary metabolites biosynthesis, transport and catabolism; R = General function prediction only; S = function unknown; T = Signal transduction mechanisms; U = Intracellular trafficking, secretion, and vesicular transport; V = Defense mechanisms; W = Extracellular structures; Y = Nuclear structure; Z = Cytoskeleton;

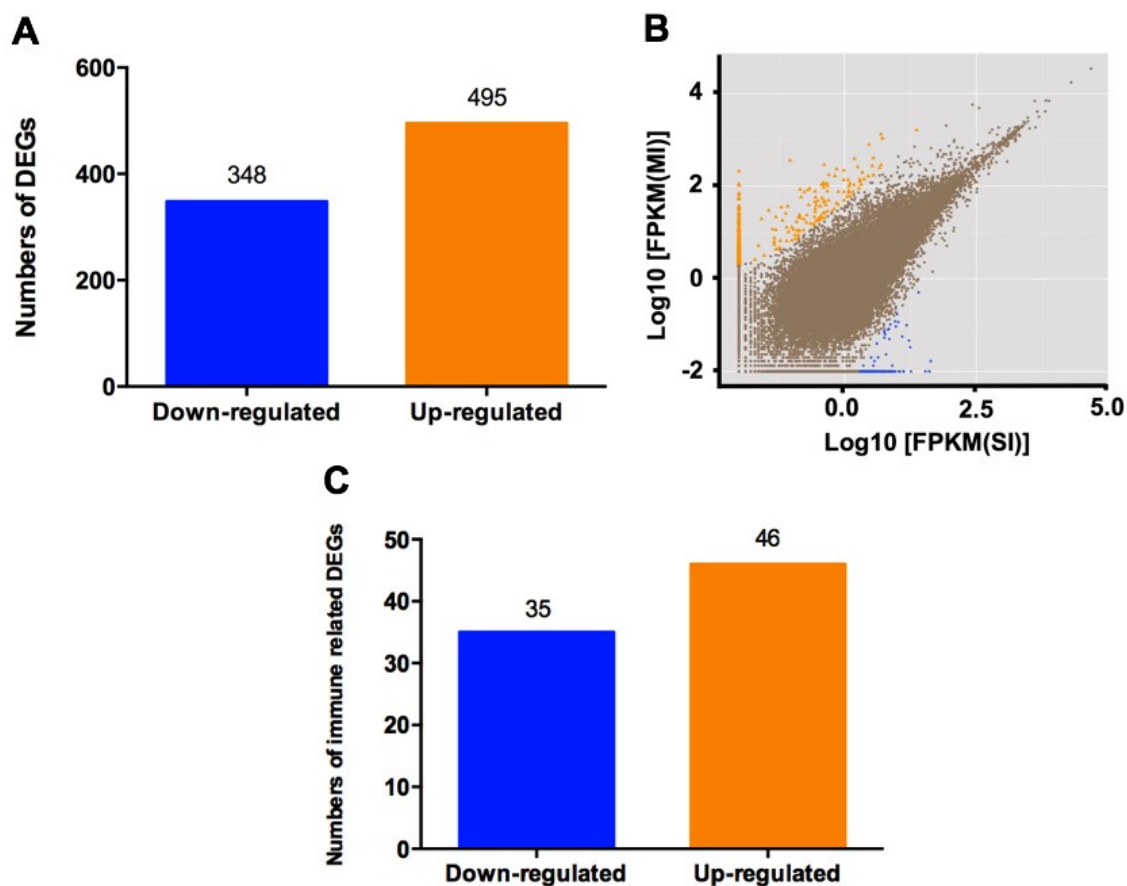
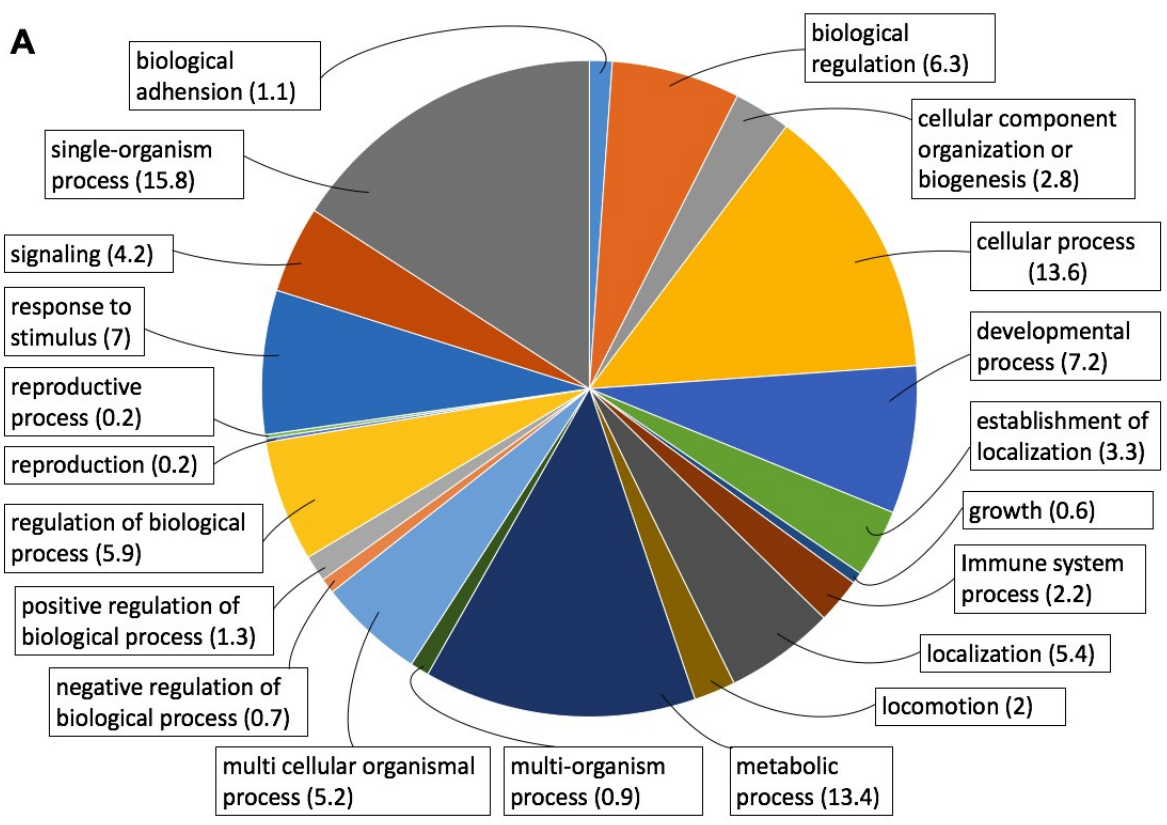
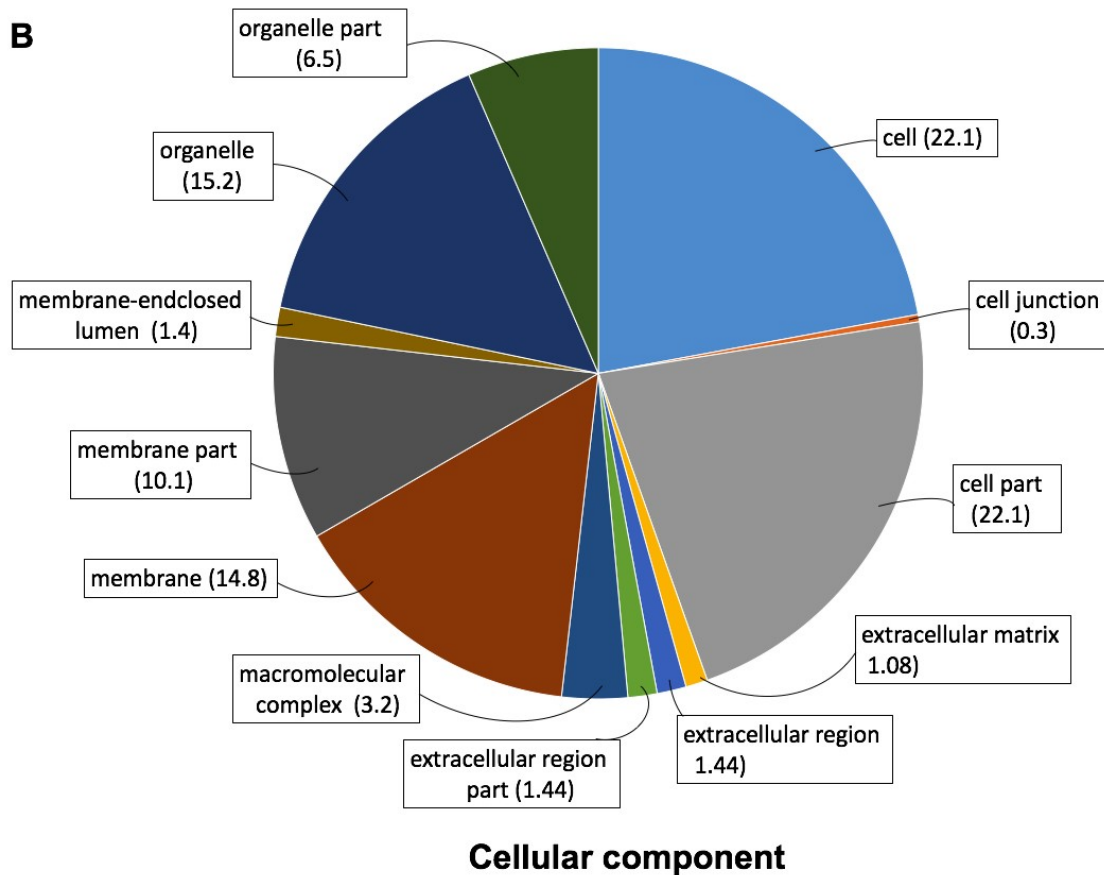


Figure A7. Differentially expressed genes (DEGs) between sham-injected and *M. marinum*-injected goldfish.

(A) The numbers of DEGs. (B) Scattered plot of DEGs. Yellow and blue points represent genes that are significantly up- and down-regulated, respectively (Probability ≥ 0.8 and absolute $\log_2[\text{FPKM}(\text{MI})/\text{FPKM}(\text{SI})] \geq 1$). (C) The numbers of immune related DEGs.



Biological process



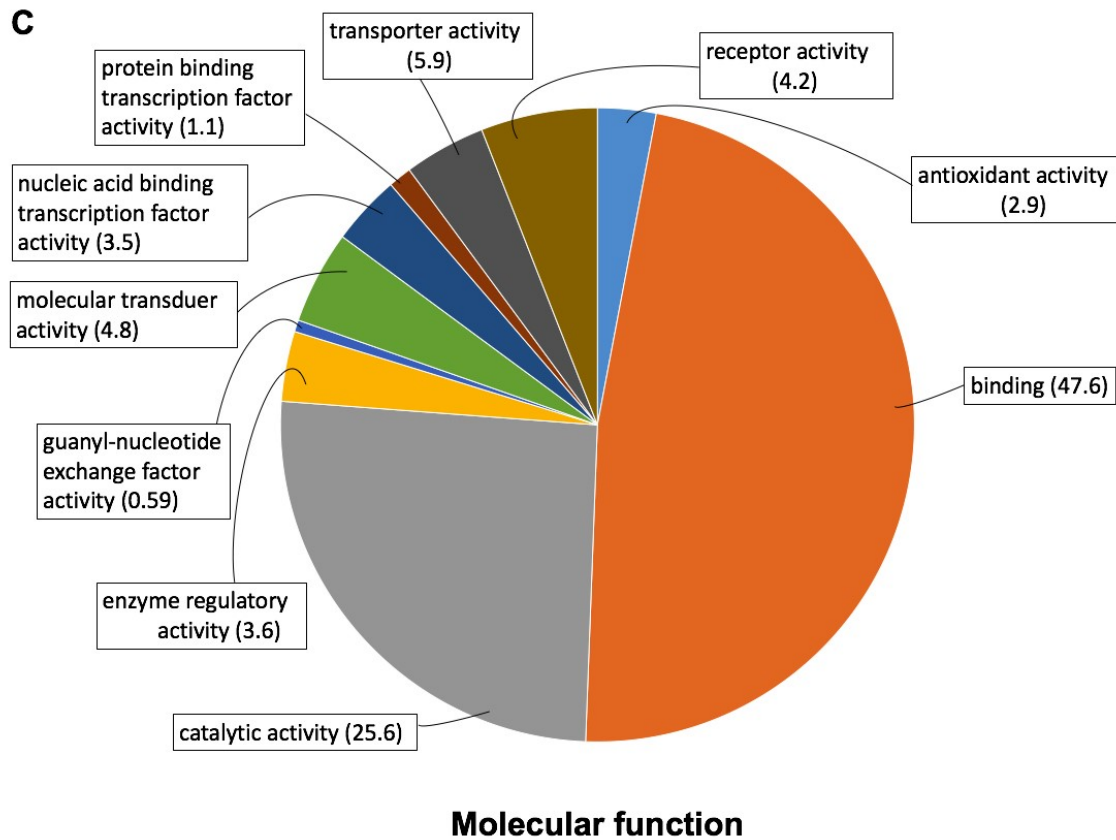


Figure A8. Gene ontology functional classification of differentially expressed genes (DEGs). The results were summarized for three main domains: (A) biological process, (B) cellular component and (C) molecular function. For the three main domains, 21, 12 and 10 functional groups were identified respectively. The numbers in brackets indicate the percentage of probes with each GO annotation.

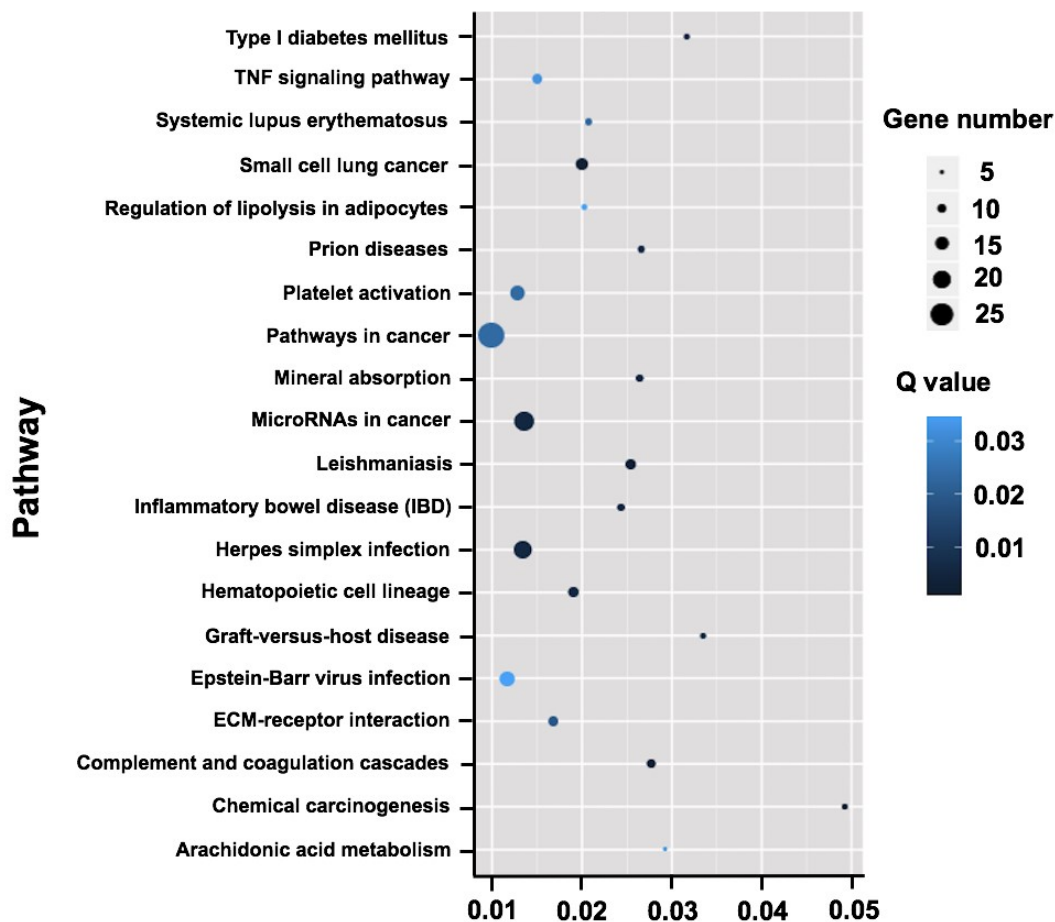


Figure A9. Scatter plot of KEGG pathway enrichment of top 20 statistics.

RichFactor is the ratio of DEG numbers annotated in this pathway term to all gene numbers annotated in this pathway term. Greater RichFactor means great intensiveness. Q-value is corrected P-value ranging from 0-1, and its less value means greater intensiveness. Top 20 enriched pathway terms were displayed.

Appendix B. Goldfish spleen transcriptome KEGG analysis

#	Pathway	All genes with pathway annotation (50597)	Pathway ID	Level 1	Level 2
1	Metabolic pathways	3681 (7.28%)	ko01100	Metabolism	Global map
2	Spliceosome	1695 (3.35%)	ko03040	Genetic Information Processing	Transcription
3	RNA transport	1586 (3.13%)	ko03013	Genetic Information Processing	Translation
4	Biosynthesis of secondary metabolites	1145 (2.26%)	ko01110	Metabolism	Global map
5	Protein processing in endoplasmic reticulum	969 (1.92%)	ko04141	Genetic Information Processing	Folding, sorting and degradation
6	mRNA surveillance pathway	964 (1.91%)	ko03015	Genetic Information Processing	Translation
7	Endocytosis	855 (1.69%)	ko04144	Cellular Processes	Transport and catabolism
8	Ubiquitin mediated proteolysis	807 (1.59%)	ko04120	Genetic Information Processing	Folding, sorting and degradation
9	Purine metabolism	628 (1.24%)	ko00230	Metabolism	Nucleotide metabolism
10	RNA degradation	557 (1.1%)	ko03018	Genetic Information Processing	Folding, sorting and degradation
11	Phosphatidylinositol signaling system	550 (1.09%)	ko04070	Environmental Information Processing	Signal transduction
12	Pyrimidine metabolism	475 (0.94%)	ko00240	Metabolism	Nucleotide metabolism
13	Lysine degradation	441 (0.87%)	ko00310	Metabolism	Amino acid metabolism
14	Inositol phosphate metabolism	426 (0.84%)	ko00562	Metabolism	Carbohydrate metabolism
15	Phagosome	419 (0.83%)	ko04145	Cellular Processes	Transport and catabolism
16	Ribosome biogenesis in eukaryotes	406 (0.8%)	ko03008	Genetic Information Processing	Translation
17	Glycerophospholipid metabolism	399 (0.79%)	ko00564	Metabolism	Lipid metabolism
18	Fructose and mannose metabolism	343 (0.68%)	ko00051	Metabolism	Carbohydrate metabolism
19	Basal transcription factors	308 (0.61%)	ko03022	Genetic Information Processing	Transcription
20	Nucleotide excision repair	288 (0.57%)	ko03420	Genetic Information Processing	Replication and repair
21	Amino sugar and nucleotide sugar metabolism	277 (0.55%)	ko00520	Metabolism	Carbohydrate metabolism
22	Oxidative phosphorylation	263 (0.52%)	ko00190	Metabolism	Energy metabolism
23	Glycolysis / Gluconeogenesis	258 (0.51%)	ko00010	Metabolism	Carbohydrate metabolism
24	Glycerolipid metabolism	258 (0.51%)	ko00561	Metabolism	Lipid metabolism
25	Peroxisome	254 (0.5%)	ko04146	Cellular Processes	Transport and catabolism
26	Base excision repair	240 (0.47%)	ko03410	Genetic Information Processing	Replication and repair

27	Valine, leucine and isoleucine degradation	225 (0.44%)	ko00280	Metabolism	Amino acid metabolism
28	Pyruvate metabolism	215 (0.42%)	ko00620	Metabolism	Carbohydrate metabolism
29	DNA replication	212 (0.42%)	ko03030	Genetic Information Processing	Replication and repair
30	RNA polymerase	208 (0.41%)	ko03020	Genetic Information Processing	Transcription
31	Propanoate metabolism	200 (0.4%)	ko00640	Metabolism	Carbohydrate metabolism
32	Ether lipid metabolism	196 (0.39%)	ko00565	Metabolism	Lipid metabolism
33	Arginine and proline metabolism	195 (0.39%)	ko00330	Metabolism	Amino acid metabolism
34	N-Glycan biosynthesis	175 (0.35%)	ko00510	Metabolism	Glycan biosynthesis and metabolism
35	Fatty acid metabolism	165 (0.33%)	ko00071	Metabolism	Lipid metabolism
36	Natural killer cell mediated cytotoxicity	161 (0.32%)	ko04650	Organismal Systems	Immune system
37	Circadian rhythm - mammal	150 (0.3%)	ko04710	Organismal Systems	Environmental adaptation
38	Glutathione metabolism	150 (0.3%)	ko00480	Metabolism	Metabolism of other amino acids
39	Tryptophan metabolism	149 (0.29%)	ko00380	Metabolism	Amino acid metabolism
40	Aminoacyl-tRNA biosynthesis	141 (0.28%)	ko00970	Genetic Information Processing	Translation
41	Citrate cycle (TCA cycle)	140 (0.28%)	ko00020	Metabolism	Carbohydrate metabolism
42	Cysteine and methionine metabolism	139 (0.27%)	ko00270	Metabolism	Amino acid metabolism
43	Pentose phosphate pathway	137 (0.27%)	ko00030	Metabolism	Carbohydrate metabolism
44	Proteasome	133 (0.26%)	ko03050	Genetic Information Processing	Folding, sorting and degradation
45	beta-Alanine metabolism	131 (0.26%)	ko00410	Metabolism	Metabolism of other amino acids
46	Ribosome	130 (0.26%)	ko03010	Genetic Information Processing	Translation
47	Glycine, serine and threonine metabolism	130 (0.26%)	ko00260	Metabolism	Amino acid metabolism
48	Butanoate metabolism	127 (0.25%)	ko00650	Metabolism	Carbohydrate metabolism
49	ABC transporters	125 (0.25%)	ko02010	Environmental Information Processing	Membrane transport
50	Plant-pathogen interaction	123 (0.24%)	ko04626	Organismal Systems	Environmental adaptation
51	Regulation of autophagy	122 (0.24%)	ko04140	Cellular Processes	Transport and catabolism
52	Homologous recombination	119 (0.24%)	ko03440	Genetic Information Processing	Replication and repair
53	Mismatch repair	118 (0.23%)	ko03430	Genetic Information Processing	Replication and repair
54	Arachidonic acid metabolism	110 (0.22%)	ko00590	Metabolism	Lipid metabolism
55	Galactose metabolism	106 (0.21%)	ko00052	Metabolism	Carbohydrate metabolism
56	Tyrosine metabolism	99 (0.2%)	ko00350	Metabolism	Amino acid metabolism
57	Histidine metabolism	96 (0.19%)	ko00340	Metabolism	Amino acid metabolism
58	Alanine, aspartate and glutamate metabolism	96 (0.19%)	ko00250	Metabolism	Amino acid metabolism

59	Glycosylphosphatidylinositol(GPI)-anchor biosynthesis	94 (0.19%)	ko00563	Metabolism	Glycan biosynthesis and metabolism
60	SNARE interactions in vesicular transport	90 (0.18%)	ko04130	Genetic Information Processing	Folding, sorting and degradation
61	Sphingolipid metabolism	88 (0.17%)	ko00600	Metabolism	Lipid metabolism
62	Glyoxylate and dicarboxylate metabolism	85 (0.17%)	ko00630	Metabolism	Carbohydrate metabolism
63	Carbon fixation in photosynthetic organisms	85 (0.17%)	ko00710	Metabolism	Energy metabolism
64	Pentose and glucuronate interconversions	78 (0.15%)	ko00040	Metabolism	Carbohydrate metabolism
65	Starch and sucrose metabolism	77 (0.15%)	ko00500	Metabolism	Carbohydrate metabolism
66	Porphyrin and chlorophyll metabolism	77 (0.15%)	ko00860	Metabolism	Metabolism of cofactors and vitamins
67	Other types of O-glycan biosynthesis	76 (0.15%)	ko00514	Metabolism	Glycan biosynthesis and metabolism
68	Phenylalanine metabolism	70 (0.14%)	ko00360	Metabolism	Amino acid metabolism
69	Linoleic acid metabolism	68 (0.13%)	ko00591	Metabolism	Lipid metabolism
70	Biosynthesis of unsaturated fatty acids	65 (0.13%)	ko01040	Metabolism	Lipid metabolism
71	alpha-Linolenic acid metabolism	64 (0.13%)	ko00592	Metabolism	Lipid metabolism
72	Protein export	63 (0.12%)	ko03060	Genetic Information Processing	Folding, sorting and degradation
73	Fatty acid elongation	63 (0.12%)	ko00062	Metabolism	Lipid metabolism
74	Terpenoid backbone biosynthesis	61 (0.12%)	ko00900	Metabolism	Metabolism of terpenoids and polyketides
75	Other glycan degradation	61 (0.12%)	ko00511	Metabolism	Glycan biosynthesis and metabolism
76	Non-homologous end-joining	58 (0.11%)	ko03450	Genetic Information Processing	Replication and repair
77	Fatty acid biosynthesis	55 (0.11%)	ko00061	Metabolism	Lipid metabolism
78	Selenocompound metabolism	54 (0.11%)	ko00450	Metabolism	Metabolism of other amino acids
79	Isoquinoline alkaloid biosynthesis	53 (0.1%)	ko00950	Metabolism	Biosynthesis of other secondary metabolites
80	Ascorbate and aldarate metabolism	52 (0.1%)	ko00053	Metabolism	Carbohydrate metabolism
81	Tropine, piperidine and pyridine alkaloid biosynthesis	50 (0.1%)	ko00960	Metabolism	Biosynthesis of other secondary metabolites
82	Limonene and pinene degradation	47 (0.09%)	ko00903	Metabolism	Metabolism of terpenoids and polyketides
83	Pantothenate and CoA biosynthesis	47 (0.09%)	ko00770	Metabolism	Metabolism of cofactors and vitamins
84	Synthesis and degradation of ketone bodies	44 (0.09%)	ko00072	Metabolism	Lipid metabolism
85	Nicotinate and nicotinamide metabolism	41 (0.08%)	ko00760	Metabolism	Metabolism of cofactors and vitamins

86	Ubiquinone and other terpenoid-quinone biosynthesis	40 (0.08%)	ko00130	Metabolism	Metabolism of cofactors and vitamins
87	Steroid biosynthesis	34 (0.07%)	ko00100	Metabolism	Lipid metabolism
88	Vitamin B6 metabolism	32 (0.06%)	ko00750	Metabolism	Metabolism of cofactors and vitamins
89	Glycosaminoglycan degradation	30 (0.06%)	ko00531	Metabolism	Glycan biosynthesis and metabolism
90	Nitrogen metabolism	30 (0.06%)	ko00910	Metabolism	Energy metabolism
91	Sulfur relay system	27 (0.05%)	ko04122	Genetic Information Processing	Folding, sorting and degradation
92	Phenylalanine, tyrosine and tryptophan biosynthesis	24 (0.05%)	ko00400	Metabolism	Amino acid metabolism
93	Glycosphingolipid biosynthesis - ganglio series	22 (0.04%)	ko00604	Metabolism	Glycan biosynthesis and metabolism
94	Taurine and hypotaurine metabolism	22 (0.04%)	ko00430	Metabolism	Metabolism of other amino acids
95	One carbon pool by folate	22 (0.04%)	ko00670	Metabolism	Metabolism of cofactors and vitamins
96	Riboflavin metabolism	21 (0.04%)	ko00740	Metabolism	Metabolism of cofactors and vitamins
97	Sulfur metabolism	21 (0.04%)	ko00920	Metabolism	Energy metabolism
98	Circadian rhythm - plant	21 (0.04%)	ko04712	Organismal Systems	Environmental adaptation
99	Cyanoamino acid metabolism	19 (0.04%)	ko00460	Metabolism	Metabolism of other amino acids
100	Valine, leucine and isoleucine biosynthesis	17 (0.03%)	ko00290	Metabolism	Amino acid metabolism
101	Cutin, suberine and wax biosynthesis	15 (0.03%)	ko00073	Metabolism	Lipid metabolism
102	Glycosphingolipid biosynthesis - globo series	15 (0.03%)	ko00603	Metabolism	Glycan biosynthesis and metabolism
103	Folate biosynthesis	14 (0.03%)	ko00790	Metabolism	Metabolism of cofactors and vitamins
104	Thiamine metabolism	10 (0.02%)	ko00730	Metabolism	Metabolism of cofactors and vitamins
105	Sesquiterpenoid and triterpenoid biosynthesis	9 (0.02%)	ko00909	Metabolism	Metabolism of terpenoids and polyketides
106	Phenylpropanoid biosynthesis	9 (0.02%)	ko00940	Metabolism	Biosynthesis of other secondary metabolites
107	Betalain biosynthesis	8 (0.02%)	ko00965	Metabolism	Biosynthesis of other secondary metabolites
108	Glucosinolate biosynthesis	8 (0.02%)	ko00966	Metabolism	Biosynthesis of other secondary metabolites
109	D-Arginine and D-ornithine metabolism	6 (0.01%)	ko00472	Metabolism	Metabolism of other amino acids
110	Biotin metabolism	6 (0.01%)	ko00780	Metabolism	Metabolism of cofactors and vitamins
111	Zeatin biosynthesis	5 (0.01%)	ko00908	Metabolism	Metabolism of terpenoids and polyketides
112	Lysine biosynthesis	3 (0.01%)	ko00300	Metabolism	Amino acid metabolism
113	Caffeine metabolism	3 (0.01%)	ko00232	Metabolism	Biosynthesis of other secondary metabolites

114	Lipoic acid metabolism	2 (0%)	ko00785	Metabolism	Metabolism of vitamins
-----	------------------------	--------	---------	------------	------------------------

Appendix C. The data of all the differentially expressed genes

#	Gene ID	log2Ratio(MI/SI)	Up-Down-Regulation(MI/SI)	Probability	Blast NR
1	CL8955.Contig3	9.205385996	Up	0.952055092	-
2	Unigene44105	-9.730187062	Down	0.971069056	-
3	CL2844.Contig1	8.13442632	Up	0.872425305	gi 126631572 gb AAI34014.1 /2.48214e-10/LOC553275 protein [<i>Danio rerio</i>]
4	Unigene70905	-7.624490865	Down	0.804937123	-
5	CL18097.Contig5	-7.589963182	Down	0.800433644	-
6	CL16673.Contig2	9.011227255	Up	0.942396258	gi 528515122 ref XP_005161626.1 /4.60361e-12/PREDICTED: uncharacterized protein LOC100034454 isoform X2 [<i>Danio rerio</i>]
7	CL6592.Contig3	-9.21916852	Down	0.966659942	-
8	CL9466.Contig2	8.17990909	Up	0.877322513	-
9	Unigene31781	-9.397318104	Down	0.960145517	gi 120537843 gb AAI29405.1 /7.8236e-10/LOC799852 protein [<i>Danio rerio</i>]
10	Unigene73628	-8.294620749	Down	0.88901507	gi 347360900 ref NP_001229967.1 /1.33256e-25/cyclic AMP-responsive element-binding protein 3-like protein 1 [<i>Danio rerio</i>]
11	Unigene12761	-8.262094845	Down	0.885774128	-
12	CL14099.Contig2	12.36048134	Up	0.997157125	gi 419636307 ref NP_001258699.1 /1.16775e-34/glucagon isoform 1 precursor [<i>Danio rerio</i>]
13	Unigene61370	7.725650281	Up	0.820433557	-
14	Unigene60199	8.479780264	Up	0.905851051	-
15	Unigene73043	9.963859408	Up	0.976980413	gi 326673883 ref XP_001922616.3 /3.97686e-06/PREDICTED: saxitoxin and tetrodotoxin-binding protein 2-like [<i>Danio rerio</i>]
16	Unigene10206	5.691485053	Up	0.813506965	gi 528500654 ref XP_005169681.1 /1.39425e-23/PREDICTED: uncharacterized protein LOC101883159 [<i>Danio rerio</i>]
17	Unigene14435	-8.29615146	Down	0.88901507	-
18	CL4425.Contig20	-9.257387843	Down	0.954417466	gi 528520515 ref XP_005162963.1 /7.65422e-50/PREDICTED: myosin-7 isoform X7 [<i>Danio rerio</i>]
19	CL5562.Contig9	8.801977745	Up	0.929820794	gi 528508455 ref XP_005159286.1 /0/PREDICTED: E3 ubiquitin-protein ligase TRIP12 isoform X5 [<i>Danio rerio</i>]
20	CL4014.Contig11	9.494522283	Up	0.96377585	-
21	CL13597.Contig1	-7.589963182	Down	0.800433644	gi 56693257 ref NP_001008593.1 /4.10369e-11/protein NDRG2 [<i>Danio rerio</i>]
22	Unigene45221	8.855906667	Up	0.933256974	-
23	CL1851.Contig4	-9.844967241	Down	0.97417984	gi 41055500 ref NP_957214.1 /1.85109e-141/phosphatidylinositol transfer protein beta isoform [<i>Danio rerio</i>]
24	Unigene37470	7.098601193	Up	0.928672146	-
25	Unigene11791	-8.159871337	Down	0.875117414	-
26	Unigene30543	10.29462075	Up	0.983134733	gi 528520931 ref XP_003201438.2 /4.22934e-24/PREDICTED: von Willebrand factor A

					domain-containing protein 5A-like [<i>Danio rerio</i>]
27	Unigene9717	7.849631267	Up	0.974421717	-
28	Unigene31408	5.71800997	Up	0.814299846	-
29	Unigene42272	8.062495926	Up	0.864094087	-
30	CL2399.Contig1	-8.22881869	Down	0.88237808	gi 528496592 ref XP_005156444.1 /1.74871e-22/PREDICTED: serine/threonine-protein kinase LMTK1-like isoform X1 [<i>Danio rerio</i>]
31	Unigene34494	8.871391914	Up	0.934236415	-
32	Unigene15025	10.93319886	Up	0.990610161	gi 70907771 emb CAG14936.1 /4.01224e-22/interleukin-11 [<i>Cyprinus carpio</i>]
33	Unigene73962	8.173260714	Up	0.876810557	-
34	Unigene39124	-8.035257325	Down	0.86095944	gi 300810921 gb ADK35755.1 /0/collagen type I alpha 1 [<i>Ctenopharyngodon idella</i>]
35	Unigene3046	-7.660590206	Down	0.810294223	gi 528516429 ref XP_005161827.1 /0/PREDICTED: CREB-binding protein isoform X2 [<i>Danio rerio</i>]
36	Unigene96970	-7.658211483	Down	0.810294223	-
37	CL19534.Contig2	8.266786541	Up	0.886225343	-
38	Unigene63785	7.725650281	Up	0.820433557	gi 528471912 ref XP_005171486.1 /1.39902e-11/PREDICTED: uncharacterized protein LOC101886873 [<i>Danio rerio</i>]
39	CL8181.Contig1	-9.179079717	Down	0.950897767	gi 160693219 gb ABQ86049.2 /2.97723e-155/muscleblind-like protein 1 isoform B [<i>Danio rerio</i>]
40	CL13932.Contig1	8.452584453	Up	0.903487593	gi 528476365 ref XP_005164759.1 /0/PREDICTED: ATP-binding cassette sub-family C member 9 isoform X2 [<i>Danio rerio</i>]
41	Unigene43604	7.607330314	Up	0.802739616	-
42	Unigene31601	8.211442198	Up	0.984007879	gi 187608210 ref NP_001119928.1 /2.10951e-71/immunoresponsive gene 1 [<i>Danio rerio</i>]
43	Unigene41416	-8.118941073	Down	0.870759279	-
44	CL11546.Contig1	7.655828831	Up	0.810294223	-
45	CL12390.Contig1	9.170759653	Up	0.950447636	-
46	Unigene55334	7.334273285	Up	0.939358146	-
47	CL1033.Contig4	7.902877533	Up	0.844362083	-
48	Unigene90766	-7.857980995	Down	0.83873165	-
49	CL2763.Contig17	7.024216237	Up	0.812621888	gi 193248592 dbj BAG50379.1 /2.87114e-73/voltage-sensing phosphoinositide phosphatase [<i>Danio rerio</i>]
50	CL459.Contig1	8.497186541	Up	0.907138534	-
51	CL16221.Contig1	-9.024216237	Down	0.943137076	-
52	CL1013.Contig3	9.844444241	Up	0.974142962	-
53	Unigene50009	-8.048032696	Down	0.862854329	-
54	CL2121.Contig5	-7.658211483	Down	0.810294223	gi 528510305 ref XP_005159743.1 /0/PREDICTED: titin isoform X6 [<i>Danio rerio</i>]
55	CL10425.Contig2	-7.783543961	Down	0.828073852	-
56	Unigene44524	-7.718818247	Down	0.819407476	-
57	CL20380.Contig2	5.942626208	Up	0.838181731	gi 597787387 ref XP_007257135.1 /0/PREDICTED: R3H domain-containing protein 1-like isoform X7 [<i>Astyanax mexicanus</i>]

58	CL1388.Contig7	-8.06608919	Down	0.8646939	gi 269315868 ref NP_001092707.2 /6.29164e-105/eukaryotic translation initiation factor 4Ba [<i>Danio rerio</i>]
59	Unigene12576	-7.948367232	Down	0.850374314	-
60	CL259.Contig15	8.13784503	Up	0.872958955	gi 29540612 gb AAO88245.1 /3.64515e-21/signal transducer and activator of transcription 1 [<i>Carassius auratus</i>]
61	Unigene61992	-8.230420795	Down	0.88237808	-
62	Unigene105269	-9.462161411	Down	0.962602256	-
63	Unigene37507	8.903881846	Up	0.936232176	gi 528509123 ref XP_005159448.1 /0/PREDICTED: uncharacterized protein LOC100006143 isoform X1 [<i>Danio rerio</i>]
64	CL12461.Contig2	5.587431847	Up	0.805138868	gi 189535037 ref XP_001924015.1 /3.508e-39/PREDICTED: uncharacterized protein LOC100148254 isoform X1 [<i>Danio rerio</i>]
65	CL6863.Contig1	7.698125852	Up	0.816427935	-
66	Unigene52490	8.345774837	Up	0.893773442	-
67	Unigene36634	-8.626925794	Down	0.917415619	-
68	Unigene48716	6.452512205	Up	0.878632773	-
69	CL9813.Contig1	8.274572286	Up	0.887045341	-
70	Unigene12880	8.957102042	Up	0.939376585	gi 115529311 ref NP_001070186.1 /8.45746e-33/a disintegrin and metallopeptidase domain 28 precursor [<i>Danio rerio</i>]
71	Unigene57562	-8.022367813	Down	0.859644841	-
72	Unigene28043	-7.807354922	Down	0.831792042	-
73	Unigene47491	-7.992466327	Down	0.856142497	-
74	CL396.Contig9	-6.471559097	Down	0.877848569	gi 319918875 ref NP_001025246.2 /3.25959e-90/serine/arginine repetitive matrix 2 [<i>Danio rerio</i>]
75	Unigene61190	8.419257966	Up	0.900610009	-
76	CL16816.Contig2	10.57805814	Up	0.987068769	-
77	CL2342.Contig11	-7.766626339	Down	0.957364467	gi 49274617 ref NP_957228.2 /2.27001e-44/tropomyosin alpha-1 chain [<i>Danio rerio</i>]
78	CL3732.Contig1	-6.66651991	Down	0.839401966	-
79	CL18879.Contig1	8.375121808	Up	0.987572048	gi 187608210 ref NP_001119928.1 /2.29421e-163/immunoresponsive gene 1 [<i>Danio rerio</i>]
80	Unigene64731	-7.862120725	Down	0.839562494	-
81	CL21530.Contig2	8.515699838	Up	0.90879263	-
82	CL450.Contig6	-8.220781371	Down	0.881382368	gi 190339129 gb AAI63262.1 /1.13431e-13/Btd2 protein [<i>Danio rerio</i>]
83	Unigene81466	7.6794801	Up	0.81339633	gi 136256463 ref NP_001025282.2 /9.60906e-45/follistatin-related protein 3 precursor [<i>Danio rerio</i>]
84	Unigene16550	8.673603533	Up	0.920888678	-
85	Unigene49752	6.315549182	Up	0.823413099	gi 526252896 ref NP_001268280.1 /2.49538e-15/chemokine CXCF1a precursor [<i>Oncorhynchus mykiss</i>]
86	CL15640.Contig1	9.052568051	Up	0.944650167	-
87	Unigene40923	-7.95419631	Down	0.851099946	gi 190338052 gb AAI62633.1 /0/Quo protein [<i>Danio rerio</i>]
88	Unigene13300	7.269905883	Up	0.947481111	-
89	Unigene45101	7.781359714	Up	0.828073852	-

90	Unigene79175	-7.709658248	Down	0.817379175	-
91	Unigene83403	-7.670066069	Down	0.81238001	gi 189027695 sp A8E5C5.1 DS7CA_DANRE /1.56675e-18/RecName: Full=Dehydrogenase/reductase SDR family member 7C-A; Flags: Precursor [<i>Danio rerio</i>]
92	Unigene8681	-7.64625868	Down	0.808135764	gi 528471039 ref XP_005163450.1 /1.37195e-22/PREDICTED: TRAF2 and NCK interacting kinase a isoform X7 [<i>Danio rerio</i>]
93	Unigene3824	8.336878436	Up	0.892978392	gi 617522642 ref XP_007544656.1 /1.29781e-09/PREDICTED: uncharacterized protein LOC103132810, partial [<i>Poecilia formosa</i>]
94	CL12680.Contig2	-7.631783357	Down	0.806007675	gi 125804305 ref XP_697043.2 /0/PREDICTED: alpha-1D adrenergic receptor [<i>Danio rerio</i>]
95	CL2413.Contig1	8.196397213	Up	0.878861635	gi 47214842 emb CAF95748.1 /1.38662e-22/unnamed protein product [<i>Tetraodon nigroviridis</i>]
96	CL1224.Contig2	6.262287956	Up	0.875849554	-
97	Unigene66630	7.8008999	Up	0.83081477	-
98	Unigene26040	11.91818442	Up	0.999448996	gi 536720426 gb AGU42184.1 /1.59035e-23/interleukin-1 beta-1 [<i>Carassius carassius</i>]
99	Unigene20554	6.885225143	Up	0.922661	gi 126632473 emb CAM56444.1 /1.20685e-15/novel protein similar to vertebrate pentaxin-related gene, rapidly induced by IL-1 beta (PTX3) [<i>Danio rerio</i>]
100	Unigene47892	-8.024216237	Down	0.859644841	-
101	CL4087.Contig2	8.506472886	Up	0.908115806	gi 528477272 ref XP_005168114.1 /1.01185e-81/PREDICTED: zinc finger protein 45-like [<i>Danio rerio</i>]
102	CL13054.Contig1	8.311369903	Up	0.890799324	gi 41387132 ref NP_957104.1 /7.94249e-15/protein phosphatase 1, regulatory (inhibitor) subunit 14Ab [<i>Danio rerio</i>]
103	CL9646.Contig2	-8.380821784	Down	0.897115257	-
104	Unigene44547	8.116813665	Up	0.981519685	gi 619325589 gb AHY01350.1 /1.0337e-06/purine nucleoside phosphorylase 5a, partial [<i>Carassius gibelio</i>]
105	Unigene61281	7.695808269	Up	0.815405107	-
106	Unigene62836	5.639194812	Up	0.804401304	gi 597751901 ref XP_007237820.1 /2.6846e-42/PREDICTED: A disintegrin and metalloproteinase with thrombospondin motifs 1 [<i>Astyanax mexicanus</i>]
107	Unigene18167	-9.501837185	Down	0.964019897	gi 528476094 ref XP_005164663.1 /4.57048e-45/PREDICTED: protein-methionine sulfoxide oxidase mical3b isoform X5 [<i>Danio rerio</i>]
108	Unigene18279	8.473029222	Up	0.905208937	-
109	CL1589.Contig1	7.853829352	Up	0.837853082	gi 122114616 ref NP_001073628.1 /3.19808e-112/homeodomain interacting protein kinase 3b [<i>Danio rerio</i>]
110	Unigene36056	7.6794801	Up	0.81339633	-
111	Unigene73266	-7.772589504	Down	0.827073802	-
112	Unigene49316	-8.089229767	Down	0.867158231	-
113	CL3294.Contig10	-8.611024797	Down	0.916330967	gi 528510415 ref XP_005159781.1 /3.29423e-122/PREDICTED: uncharacterized protein LOC100000125 isoform X2 [<i>Danio rerio</i>]
114	Unigene58792	-5.619704532	Down	0.80357046	-
115	Unigene40914	9.73470962	Up	0.971202468	-

116	CL1490.Contig4	-7.928765095	Down	0.848155114	gi 55925399 ref NP_001007454.1 /6.16948e-148/nucleosome assembly protein 1-like 4 [<i>Danio rerio</i>]
117	Unigene30858	7.973458213	Up	0.85327576	gi 326678803 ref XP_003201178.1 /1.26752e-29/PREDICTED: ICOS ligand-like [<i>Danio rerio</i>]
118	CL21474.Contig1	5.780085811	Up	0.816651373	-
119	CL10622.Contig4	-7.745954377	Down	0.823307887	gi 206557842 sp POC7U4.1 C3AR_DANRE/7.4174e-114/RecName: Full=C3a anaphylatoxin chemotactic receptor; Short=C3AR; Short=C3a-R [<i>Danio rerio</i>]
120	Unigene115284	-8.136136688	Down	0.872425305	-
121	CL18916.Contig1	-9.077705875	Down	0.94589101	-
122	Unigene68228	8.233619677	Up	0.882881359	-
123	CL7527.Contig3	-8.024216237	Down	0.859644841	-
124	CL19680.Contig2	-7.754887502	Down	0.824287329	-
125	Unigene53978	-7.619608644	Down	0.804937123	-
126	Unigene18168	-7.705056346	Down	0.817379175	gi 597777652 ref XP_007252478.1 /1.58263e-23/PREDICTED: protein-methionine sulfoxide oxidase mical3b-like [<i>Astyanax mexicanus</i>]
127	Unigene30337	7.768184325	Up	0.826084599	gi 50344880 ref NP_001002112.1 /2.6279e-143/26S proteasome non-ATPase regulatory subunit 4 [<i>Danio rerio</i>]
128	CL8144.Contig3	7.667702932	Up	0.811340913	gi 528519840 ref XP_005162792.1 /0/PREDICTED: probable phospholipid-transporting ATPase IB isoform X2 [<i>Danio rerio</i>]
129	CL79.Contig8	-8.141255659	Down	0.872958955	gi 357575246 gb AET85182.1 /7.22929e-50/TC1-like transposase [<i>Cyprinus carpio</i>]
130	Unigene16322	10.28347426	Up	0.982948173	-
131	Unigene45537	7.906890596	Up	0.84512134	-
132	Unigene402	7.670066069	Up	0.81238001	gi 528516429 ref XP_005161827.1 /0/PREDICTED: CREB-binding protein isoform X2 [<i>Danio rerio</i>]
133	Unigene72143	8.73809226	Up	0.925660065	-
134	CL3011.Contig5	8.06608919	Up	0.8646939	-
135	Unigene93369	8.357552005	Up	0.895035978	-
136	Unigene68729	8.113742166	Up	0.870172481	-
137	Unigene47441	8.784634846	Up	0.928780612	-
138	CL7403.Contig2	7.894817763	Up	0.843535578	gi 2645245 gb AAB87150.1 /1.15671e-124/2',3'-cyclic-nucleotide 3'-phosphodiesterase gRICH70 [<i>Carassius auratus</i>]
139	Unigene45139	11.22901905	Up	0.992761027	-
140	Unigene44154	9.217553864	Up	0.952628873	-
141	Unigene6743	8.581200582	Up	0.914049942	-
142	Unigene26410	8.042571384	Up	0.862280548	-
143	CL6876.Contig4	-9.499845887	Down	0.963959156	-
144	Unigene58512	7.839203788	Up	0.836208748	-
145	Unigene77237	-8.32343012	Down	0.89167247	gi 326679036 ref XP_003201226.1 /3.05638e-22/PREDICTED: leiomodrin-3 [<i>Danio rerio</i>]
146	Unigene94938	-7.684164178	Down	0.81413064	-

147	CL14453.Contig2	6.874281206	Up	0.922934333	-
148	CL2840.Contig3	8.020517017	Up	0.859644841	gi 166158017 ref NP_001107418.1 /3.36754e-59/uncharacterized protein LOC100135258 [<i>Xenopus (Silurana) tropicalis</i>]
149	Unigene54980	-8.060695932	Down	0.864094087	gi 528471942 ref XP_005171495.1 /2.80214e-09/PREDICTED: NACTH, LRR and PYD domains-containing protein 3-like [<i>Danio rerio</i>]
150	Unigene36560	-7.691161905	Down	0.815405107	-
151	Unigene59167	8.765976681	Up	0.927454081	-
152	Unigene109776	-7.636624621	Down	0.807086905	gi 190338070 gb AAI62670.1 /1.09358e-24/Zfp2a protein [<i>Danio rerio</i>]
153	CL8068.Contig4	8.098032083	Up	0.868406667	gi 115313689 gb AAI24376.1 /4.88035e-33/Si:dkey-172m14.1 protein [<i>Danio rerio</i>]
154	CL18234.Contig1	-7.707359132	Down	0.817379175	gi 62205219 gb AAH92938.1 /5.51692e-32/Zgc:110581 [<i>Danio rerio</i>]
155	Unigene103505	7.95419631	Up	0.851099946	-
156	Unigene85624	7.617161323	Up	0.80386874	gi 45709939 gb AAH67712.1 /2.469e-16/LOC407674 protein, partial [<i>Danio rerio</i>]
157	Unigene31962	7.914883386	Up	0.845877343	-
158	Unigene74789	-7.655828831	Down	0.810294223	-
159	Unigene20522	14.35986392	Up	0.999274367	gi 536720426 gb AGU42184.1 /1.8035e-35/interleukin-1 beta-1 [<i>Carassius carassius</i>]
160	CL3790.Contig7	-7.672425342	Down	0.81238001	-
161	Unigene9751	-8.433237678	Down	0.902146962	-
162	CL1266.Contig1	8.376487194	Up	0.896685735	-
163	Unigene93400	6.073391816	Up	0.838554852	-
164	Unigene2510	-6.724513853	Down	0.86739794	-
165	Unigene112829	10.2632692	Up	0.982656402	gi 383282283 gb AFH01333.1 /3.51458e-26/complement component C7-1, partial [<i>Hypophthalmichthys molitrix</i>]
166	CL6411.Contig6	8.985841937	Up	0.941037188	gi 281312212 sp Q2YDQ5.2 FBXL5_DANRE /0/RecName: Full=F-box/LRR-repeat protein 5; AltName: Full=F-box and leucine-rich repeat protein 5 [<i>Danio rerio</i>]
167	Unigene81511	-8.037089319	Down	0.861628671	-
168	Unigene62269	-8.241585987	Down	0.883864054	gi 59933258 ref NP_001012378.1 /1.09601e-24/disks large homolog 2 [<i>Danio rerio</i>]
169	CL6485.Contig21	-10.36522885	Down	0.984259518	gi 40548308 ref NP_954967.1 /0/uncharacterized protein LOC321250 [<i>Danio rerio</i>]
170	Unigene47570	11.74553428	Up	0.99534467	-
171	CL15163.Contig1	-9.580572641	Down	0.966612217	gi 528476578 ref XP_005164839.1 /4.7861e-28/PREDICTED: uncharacterized protein LOC101883282 isoform X1 [<i>Danio rerio</i>]
172	CL4789.Contig5	-7.963859408	Down	0.852425392	gi 82112887 sp Q9DDT5.1 SPT5H_DANRE /0/RecName: Full=Transcription elongation factor SPT5; AltName: Full=DRB sensitivity-inducing factor large subunit; Short=DSIF large subunit; AltName: Full=Protein foggy
173	Unigene36695	7.641449692	Up	0.808135764	-
174	Unigene83091	8.142957954	Up	0.873492604	-
175	Unigene48389	-7.702749879	Down	0.816427935	gi 528518819 ref XP_005162482.1 /3.32196e-16/PREDICTED: uncharacterized protein LOC101884834 [<i>Danio rerio</i>]
176	CL6186.Contig1	-7.135452784	Down	0.907551787	gi 528471942 ref XP_005171495.1 /1.879

					27e-138/PREDICTED: NACHT, LRR and PYD domains-containing protein 3-like [<i>Danio rerio</i>]
177	Unigene9811	5.621711159	Up	0.804462045	gi 115529435 ref NP_001070245.1 /8.71718e-97/major histocompatibility complex class II DBB precursor [<i>Danio rerio</i>]
178	Unigene33912	8.083775799	Up	0.982339683	gi 528504300 ref XP_005158243.1 /5.02446e-67/PREDICTED: uncharacterized protein LOC101883708 [<i>Danio rerio</i>]
179	Unigene7453	7.034523875	Up	0.920143521	-
180	Unigene71109	-8.13784503	Down	0.872958955	-
181	CL9829.Contig2	-8.026062297	Down	0.860310818	gi 33504525 ref NP_878293.1 /1.21621e-180/transforming growth factor, beta 1a precursor [<i>Danio rerio</i>]
182	CL6467.Contig4	8.320424504	Up	0.89167247	gi 41055786 ref NP_956466.1 /9.0441e-157/transcriptional regulator Myc-B [<i>Danio rerio</i>]
183	Unigene103878	7.759333407	Up	0.825171321	gi 189528212 ref XP_001919426.1 /2.07659e-07/PREDICTED: cystine/glutamate transporter-like [<i>Danio rerio</i>]
184	Unigene82415	8.361943774	Up	0.895469839	-
185	CL3111.Contig2	6.825426495	Up	0.912534682	-
186	CL17023.Contig1	7.670066069	Up	0.81238001	gi 375298713 ref NP_001243545.1 /6.50201e-11/SH3-domain GRB2-like endophilin B1 [<i>Danio rerio</i>]
187	Unigene92967	-7.700439718	Down	0.816427935	-
188	CL11992.Contig2	7.658211483	Up	0.810294223	-
189	CL6113.Contig9	-8.007494537	Down	0.857616541	gi 41055454 ref NP_956710.1 /8.3702e-55/transformer-2 protein homolog alpha [<i>Danio rerio</i>]
190	Unigene49248	8.667702932	Up	0.920601245	-
191	CL4726.Contig4	7.973458213	Up	0.85327576	gi 56090164 ref NP_998471.1 /0/phosphatidylinositol-4,5-bisphosphate 3-kinase catalytic subunit gamma isoform [<i>Danio rerio</i>]
192	CL14376.Contig3	9.477083637	Up	0.963192307	-
193	CL30.Contig44	7.807354922	Up	0.831792042	gi 131888307 ref NP_001076466.1 /2.73277e-64/uncharacterized protein LOC100009628 precursor [<i>Danio rerio</i>]
194	Unigene28246	7.609794354	Up	0.802739616	-
195	Unigene109703	8.037089319	Up	0.861628671	-
196	Unigene6188	-7.81164228	Down	0.832666272	gi 528523115 ref XP_005168267.1 /1.12077e-68/PREDICTED: uncharacterized protein LOC101884117 [<i>Danio rerio</i>]
197	CL5158.Contig10	8.836050355	Up	0.932031316	gi 47087291 ref NP_998660.1 /2.85849e-144/cullin-1 [<i>Danio rerio</i>]
198	Unigene78975	8.171593822	Up	0.876259553	-
199	Unigene31414	-7.973458213	Down	0.85327576	-
200	CL13231.Contig2	-7.984893108	Down	0.854749803	gi 47086641 ref NP_997866.1 /7.92124e-122/H2.0-like homeobox protein [<i>Danio rerio</i>]
201	Unigene93475	-8.206200388	Down	0.879854093	-
202	Unigene91776	8.153129759	Up	0.874594611	gi 6009727 dbj BAA85038.1 /1.64157e-12/alpha-2-macroglobulin-1 [<i>Cyprinus carpio</i>]
203	Unigene56272	8.691072405	Up	0.990383468	-

204	Unigene81201	7.882643049	Up	0.842024656	-
205	Unigene33567	7.631783357	Up	0.806007675	gi 289186679 gb ADC91950.1 /2.92406e-86/UDP glucuronosyltransferase 2 family polypeptide a4 isoform 1 [<i>Danio rerio</i>]
206	CL4467.Contig3	8.375039431	Up	0.896685735	-
207	Unigene56478	7.851749041	Up	0.837853082	-
208	Unigene97325	7.609794354	Up	0.802739616	-
209	CL2964.Contig11	-7.928765095	Down	0.848155114	gi 528518412 ref XP_005162410.1 /9.49282e-103/PREDICTED: rap guanine nucleotide exchange factor 3-like [<i>Danio rerio</i>]
210	CL4386.Contig4	-9.171593822	Down	0.950571287	gi 45387529 ref NP_991104.1 /2.70251e-47/dr1-associated corepressor [<i>Danio rerio</i>]
211	Unigene9190	-8.407975835	Down	0.899829059	gi 520689251 gb AGP05313.1 /3.04164e-22/Gpr125 [<i>Danio rerio</i>]
212	Unigene67333	7.892795766	Up	0.843535578	-
213	Unigene59672	-7.982993575	Down	0.854749803	gi 528504018 ref XP_001345180.4 /2.2835e-17/PREDICTED: uncharacterized protein LOC100006440 [<i>Danio rerio</i>]
214	CL6748.Contig4	-8.030667136	Down	0.895168306	-
215	CL9750.Contig1	-7.851749041	Down	0.837853082	gi 528478702 ref XP_005171824.1 /2.14225e-07/PREDICTED: zinc finger BED domain-containing protein 1-like [<i>Danio rerio</i>]
216	Unigene95542	7.902877533	Up	0.844362083	gi 17066696 gb AAL35360.1 AF442732_3/1.63646e-15/reverse transcriptase/ribonuclease H/putative methyltransferase, partial [<i>Tetraodon nigroviridis</i>]
217	CL3076.Contig9	-8.153129759	Down	0.874594611	-
218	CL4377.Contig11	-6.368768349	Down	0.854155413	gi 220678755 emb CAX14794.1 /2.18107e-127/solute carrier family 25, member 28 [<i>Danio rerio</i>]
219	Unigene15870	-8.14635653	Down	0.873492604	-
220	Unigene60218	-8.930737338	Down	0.937840717	gi 528496592 ref XP_005156444.1 /1.94953e-29/PREDICTED: serine/threonine-protein kinase LMTK1-like isoform X1 [<i>Danio rerio</i>]
221	CL18379.Contig3	-8.844444241	Down	0.932604013	gi 50355966 ref NP_001001841.2 /0/v-rel reticuloendotheliosis viral oncogene homolog [<i>Danio rerio</i>]
222	CL8512.Contig11	-7.783980414	Down	0.892831963	gi 390190233 ref NP_998459.2 /4.46218e-70/akirin-2 [<i>Danio rerio</i>]
223	CL868.Contig30	-8.112005026	Down	0.870172481	gi 597733918 ref XP_007229266.1 /9.3858e-30/PREDICTED: antigen WC1.1-like [<i>Astyanax mexicanus</i>]
224	CL5562.Contig8	8.506472886	Up	0.908115806	gi 528508455 ref XP_005159286.1 /0/PREDICTED: E3 ubiquitin-protein ligase TRIP12 isoform X5 [<i>Danio rerio</i>]
225	Unigene66244	7.872418378	Up	0.840426963	gi 66911393 gb AAH97216.1 /2.50132e-08/Si:dkey-78l4.5 protein [<i>Danio rerio</i>]
226	Unigene91527	-8.113742166	Down	0.870172481	-
227	CL10658.Contig7	11.82310182	Up	0.995644034	-
228	Unigene86377	-8.713100067	Down	0.923941975	-
229	Unigene93922	-8.14635653	Down	0.873492604	gi 528504705 ref XP_001921123.3 /6.59918e-17/PREDICTED: neural-cadherin [<i>Danio rerio</i>]
230	Unigene102458	11.33110355	Up	0.993390126	-
231	Unigene98113	-7.626925794	Down	0.806007675	-

232	Unigene45830	8.001877287	Up	0.856922363	-
233	CL3248.Contig1	-8.762658868	Down	0.927249082	-
234	CL16109.Contig2	8.963859408	Up	0.939713912	-
235	CL14020.Contig6	7.660590206	Up	0.810294223	gi 465957657 gb EMP27504.1 /0/Multidrug resistance-associated protein 5 [<i>Chelonia mydas</i>]
236	Unigene2839	-8.230420795	Down	0.88237808	-
237	CL981.Contig8	-9.032504965	Down	0.943613239	-
238	Unigene71670	8.509115185	Up	0.908115806	-
239	Unigene31434	6.129875659	Up	0.862753456	gi 339515652 ref NP_001129727.2 /2.15574e-130/GTP cyclohydrolase 1 [<i>Danio rerio</i>]
240	Unigene95304	9.640244936	Up	0.96844528	gi 189528212 ref XP_001919426.1 /5.58611e-24/PREDICTED: cystine/glutamate transporter-like [<i>Danio rerio</i>]
241	Unigene64243	-7.667702932	Down	0.811340913	gi 292620974 ref XP_002664501.1 /4.53932e-18/PREDICTED: glutaredoxin domain-containing cysteine-rich protein 1-like [<i>Danio rerio</i>]
242	Unigene44663	12.45866293	Up	0.997351278	-
243	CL12752.Contig1	7.672425342	Up	0.81238001	gi 597767263 ref XP_007247490.1 /4.64403e-31/PREDICTED: serine/threonine-protein phosphatase 2A 55 kDa regulatory subunit B beta isoform isoform X2 [<i>Astyanax mexicanus</i>]
244	Unigene98610	7.721099189	Up	0.819407476	-
245	Unigene44281	5.87897051	Up	0.806596641	-
246	CL1716.Contig1	6.471798359	Up	0.894335292	-
247	CL1988.Contig5	-7.702749879	Down	0.816427935	gi 528519901 ref XP_005162811.1 /0/PREDICTED: putative GPI-anchored protein PB15E9.01c-like [<i>Danio rerio</i>]
248	Unigene9005	7.837102265	Up	0.836208748	-
249	Unigene64265	-7.614709844	Down	0.80386874	-
250	Unigene35936	-9.570488231	Down	0.966279229	-
251	Unigene99928	8.706208199	Up	0.92346039	-
252	CL1512.Contig1	8.624490865	Up	0.917381995	gi 34784532 gb AAH56692.1 /3.84935e-153/LOC402865 protein, partial [<i>Danio rerio</i>]
253	CL1056.Contig2	9.022367813	Up	0.942992817	gi 148231201 ref NP_001082847.1 /2.85076e-155/transmembrane protein 63A [<i>Danio rerio</i>]
254	Unigene16464	-8.780266349	Down	0.928570189	-
255	Unigene18966	8.099063845	Up	0.982886348	gi 528475977 ref XP_005164601.1 /1.74745e-85/PREDICTED: uncharacterized protein LOC101882782 [<i>Danio rerio</i>]
256	CL14301.Contig5	-10.33799349	Down	0.983819149	gi 47086711 ref NP_997828.1 /2.74687e-88/CD82 antigen, b [<i>Danio rerio</i>]
257	Unigene15440	8.660590206	Up	0.92008495	gi 47219277 emb CAG11739.1 /6.23209e-15/unnamed protein product [<i>Tetraodon nigroviridis</i>]
258	Unigene96804	10.10678102	Up	0.979920907	gi 383282283 gb AFH01333.1 /6.6787e-22/complement component C7-1, partial [<i>Hypophthalmichthys molitrix</i>]
259	CL672.Contig2	8.06608919	Up	0.8646939	-
260	Unigene17488	-7.592457037	Down	0.800433644	-
261	Unigene3120	6.877330337	Up	0.920027463	gi 38649358 gb AAH63232.1 /1.7511e-

					38/Prostaglandin-endoperoxide synthase 2a [<i>Danio rerio</i>]
262	Unigene60979	7.832890014	Up	0.835361634	-
263	CL20999.Contig3	7.62935662	Up	0.806007675	gi 18157526 dbj BAB83841.1 /1.4218e-12/ReO_6 [<i>Oryzias latipes</i>]
264	CL17015.Contig2	8.089915511	Up	0.981415559	-
265	Unigene59356	-7.612254192	Down	0.80386874	-
266	CL16607.Contig2	8.944468053	Up	0.938723624	-
267	CL18621.Contig1	-6.327926836	Down	0.839174189	gi 528506732 ref XP_005158918.1 /3.36393e-92/PREDICTED: stAR-related lipid transfer protein 9-like isoform X2 [<i>Danio rerio</i>]
268	CL18106.Contig2	-8.335390355	Down	0.892978392	-
269	Unigene16276	-9.024216237	Down	0.943137076	-
270	Unigene114143	9.286172684	Up	0.955617092	-
271	Unigene35948	-7.309855263	Down	0.856573105	-
272	Unigene5664	-7.718818247	Down	0.819407476	-
273	CL1569.Contig1	5.598657291	Up	0.805880771	gi 3769340 dbj BAA33884.1 /1.50907e-125/MHC class I antigen [<i>Cyprinus carpio</i>]
274	CL2602.Contig2	-7.77478706	Down	0.827073802	gi 9082323 gb AAF82808.1 AF282675_1/2.08348e-75/calpain 1 [<i>Danio rerio</i>]
275	CL2013.Contig5	-8.510434522	Down	0.908457472	gi 597786213 ref XP_007256572.1 /1.01173e-76/PREDICTED: uridine phosphorylase 1-like [<i>Astyanax mexicanus</i>]
276	CL15338.Contig1	-8.033423002	Down	0.86095944	-
277	Unigene68162	7.824428435	Up	0.834287828	-
278	Unigene2721	7.686500527	Up	0.81436384	-
279	Unigene64260	8.038918989	Up	0.861628671	gi 528511895 ref XP_683027.5 /3.33352e-21/PREDICTED: androglobin [<i>Danio rerio</i>]
280	Unigene4216	8.785158177	Up	0.988928949	-
281	CL12552.Contig1	-7.665335917	Down	0.811340913	gi 190339184 gb AAI63556.1 /2.78525e-07/Tnc protein [<i>Danio rerio</i>]
282	CL10093.Contig2	7.636624621	Up	0.807086905	gi 53933252 ref NP_001005595.1 /2.08891e-142/protein IMPACT [<i>Danio rerio</i>]
283	CL7047.Contig3	-7.828665428	Down	0.834488489	gi 528518335 ref XP_698367.6 /0/PREDICTED: segment polarity protein dishevelled homolog DVL-1 [<i>Danio rerio</i>]
284	CL2387.Contig10	7.794415866	Up	0.829914508	gi 528501908 ref XP_005157707.1 /3.29085e-50/PREDICTED: coiled-coil domain-containing protein 9 isoform X1 [<i>Danio rerio</i>]
285	CL13720.Contig4	9.136991112	Up	0.948918276	gi 66472650 ref NP_001018387.1 /3.22579e-136/SWI/SNF-related matrix-associated actin-dependent regulator of chromatin subfamily E member 1-related isoform 1 [<i>Danio rerio</i>]
286	Unigene18989	9.314394422	Up	0.95690132	-
287	CL21131.Contig10	-8.665335917	Down	0.920328997	gi 378735269 dbj BAL63124.1 /5.55479e-28/CD2 family receptor [<i>Carassius auratus langsdorfii</i>]
288	Unigene104223	7.938599455	Up	0.848897017	gi 295314918 gb ADF97609.1 /3.46758e-26/fibrinogen B beta polypeptide [<i>Hypophthalmichthys molitrix</i>]
289	CL12039.Contig1	-8.588714636	Down	0.914623723	-
290	Unigene85706	-8.156504486	Down	0.874594611	gi 51571913 ref NP_001004012.1 /4.84525e-60/CMP-N-acetylneuraminate-beta-

					galactosamide-alpha-2,3-sialyltransferase 2 [<i>Danio rerio</i>]
291	CL6313.Contig5	-7.743712427	Down	0.822359901	gi 209152513 gb ACI33116.1 /1.83008e-164/ELAV-like protein 1 [<i>Salmo salar</i>]
292	Unigene73915	-7.732450113	Down	0.82142493	-
293	Unigene82996	-7.74819285	Down	0.823307887	-
294	CL1103.Contig3	-7.950312876	Down	0.850374314	-
295	CL9725.Contig1	-8.103287808	Down	0.868992379	-
296	Unigene35252	8.489178962	Up	0.90651052	gi 153792746 ref NP_001093569.1 /4.57696e-109/uncharacterized protein LOC100006143 [<i>Danio rerio</i>]
297	CL3064.Contig2	8.092757141	Up	0.867816616	-
298	Unigene12129	-8.124121312	Down	0.871352584	-
299	Unigene87234	7.794415866	Up	0.829914508	-
300	CL5719.Contig5	-7.639039173	Down	0.807086905	gi 597770959 ref XP_007249269.1 /2.05756e-07/PREDICTED: uncharacterized protein KIAA0513 homolog isoform X2 [<i>Astyanax mexicanus</i>]
301	Unigene30542	-7.597431853	Down	0.801611577	gi 528520931 ref XP_003201438.2 /3.91156e-27/PREDICTED: von Willebrand factor A domain-containing protein 5A-like [<i>Danio rerio</i>]
302	Unigene22935	6.492106846	Up	0.899063294	gi 38649358 gb AAH63232.1 /2.16042e-80/Prostaglandin-endoperoxide synthase 2a [<i>Danio rerio</i>]
303	Unigene112934	-7.604862058	Down	0.802455437	gi 317418923 emb CBN80961.1 /1.71004e-09/Retrovirus polyprotein [<i>Dicentrarchus labrax</i>]
304	CL8161.Contig1	-6.22828426	Down	0.850752858	gi 528480160 ref XP_005165483.1 /1.36644e-155/PREDICTED: uncharacterized protein LOC101885572 [<i>Danio rerio</i>]
305	CL20610.Contig1	9.57427815	Up	0.966406133	-
306	Unigene7940	-8.464886049	Down	0.904514759	-
307	Unigene18990	12.42031116	Up	0.997275352	-
308	CL2933.Contig40	-7.639039173	Down	0.807086905	gi 23308669 ref NP_694508.1 /0/mucosa associated lymphoid tissue lymphoma translocation gene 1a [<i>Danio rerio</i>]
309	CL4998.Contig2	-7.714245518	Down	0.818344516	gi 256017218 ref NP_001116750.2 /1.21728e-15/Wilms tumor protein 1-interacting protein homolog [<i>Danio rerio</i>]
310	CL20567.Contig4	6.884522783	Up	0.904132961	gi 6573261 gb AAF17609.1 AF206323_1/4.39257e-79/ubiquitin-like protein [<i>Carassius auratus</i>]
311	Unigene76920	8.159871337	Up	0.875117414	-
312	Unigene22630	-8.035257325	Down	0.86095944	gi 528483124 ref XP_690072.5 /2.72077e-39/PREDICTED: SLIT-ROBO Rho GTPase-activating protein 3 isoform X2 [<i>Danio rerio</i>]
313	Unigene57154	8.892795766	Up	0.935539083	-
314	Unigene104476	-7.763765654	Down	0.825171321	-
315	Unigene19491	6.369426105	Up	0.888339331	gi 24119251 ref NP_705943.1 /3.15854e-117/prostaglandin-endoperoxide synthase 2 precursor [<i>Danio rerio</i>]
316	CL1740.Contig3	8.77807713	Up	0.928364105	-
317	Unigene50705	8.99906044	Up	0.941775837	-
318	CL1669.Contig11	10.14380835	Up	0.98063027	gi 74096359 ref NP_001027869.1 /1.04608e-100/alpha3-fucosyltransferase [<i>Takifugu</i>]

					<i>rubripes</i>]
319	CL11738.Contig2	8.220781371	Up	0.881382368	gi 41056185 ref NP_956621.1 /1.36588e-92/uncharacterized protein LOC393297 [<i>Danio rerio</i>]
320	CL13576.Contig2	-8.09978612	Down	0.868406667	gi 41055287 ref NP_956939.1 /1.39688e-142/peroxisomal membrane protein PEX13 [<i>Danio rerio</i>]
321	CL416.Contig1	8.674780763	Up	0.921133809	-
322	CL20939.Contig2	6.855638986	Up	0.922831291	gi 189516081 ref XP_001341582.2 /2.48787e-80/PREDICTED: protein lifeguard 1 isoform X1 [<i>Danio rerio</i>]
323	CL11512.Contig1	8.031586343	Up	0.86095944	-
324	Unigene38845	-6.151712198	Down	0.833697777	gi 528480160 ref XP_005165483.1 /6.73677e-44/PREDICTED: uncharacterized protein LOC101885572 [<i>Danio rerio</i>]
325	Unigene28731	-7.702749879	Down	0.816427935	gi 528478690 ref XP_005171823.1 /1.88124e-57/PREDICTED: zinc transporter ZIP14-like isoform X2 [<i>Danio rerio</i>]
326	Unigene82767	-9.561606175	Down	0.966075314	-
327	Unigene22080	-7.754887502	Down	0.824287329	-
328	CL2763.Contig1	8.233619677	Up	0.882881359	gi 193248592 dbj BAG50379.1 /3.10179e-73/voltage-sensing phosphoinositide phosphatase [<i>Danio rerio</i>]
329	Unigene39742	8.406559345	Up	0.899502578	-
330	Unigene77456	-7.677132345	Down	0.81339633	-
331	Unigene36875	-9.072355949	Down	0.945633947	gi 326664251 ref XP_688463.5 /2.35634e-78/PREDICTED: probable E3 ubiquitin-protein ligase HERC4 isoform X2 [<i>Danio rerio</i>]
332	Unigene6818	8.26052755	Up	0.885774128	-
333	Unigene31599	8.200564274	Up	0.983651028	-
334	CL3572.Contig17	-8.479780264	Down	0.905851051	gi 164523608 gb ABY60839.1 /0/phosphatidylinositol phosphate 5-kinase type III isoform c [<i>Danio rerio</i>]
335	Unigene56266	-7.6794801	Down	0.81339633	-
336	CL4131.Contig2	8.297680549	Up	0.889479302	gi 18859217 ref NP_571687.1 /1.39112e-80/pre-B-cell leukemia transcription factor 2 [<i>Danio rerio</i>]
337	Unigene55728	7.967706597	Up	0.852597852	-
338	Unigene57058	-8.101538026	Down	0.868992379	-
339	CL2767.Contig7	-9.05166212	Down	0.944650167	gi 326665920 ref XP_686514.3 /0/PREDICTED: neurabin-2-like [<i>Danio rerio</i>]
340	CL1347.Contig1	-7.73470962	Down	0.82142493	-
341	Unigene34824	8.585379887	Up	0.988449532	gi 62955445 ref NP_001017734.1 /0/metalloreductase STEAP4 [<i>Danio rerio</i>]
342	CL10947.Contig1	7.540389465	Up	0.960758346	gi 315013535 ref NP_001186649.1 /3.32339e-109/G patch domain containing 4-like [<i>Danio rerio</i>]
343	Unigene35309	7.602389572	Up	0.801611577	gi 632968068 ref XP_007900327.1 /6.57627e-38/PREDICTED: uncharacterized protein LOC103184236 isoform X1 [<i>Callorhinchus milii</i>]
344	CL19877.Contig1	9.120578948	Up	0.990998466	-
345	Unigene16073	7.073495239	Up	0.933362185	-
346	CL4267.Contig16	-7.743712427	Down	0.822359901	gi 121583916 ref NP_001073521.1 /5.72224e-69/eyes absent homolog 3 [<i>Danio rerio</i>]

347	Unigene62735	-7.667702932	Down	0.811340913	gi 554885442 ref XP_005952351.1 /1.41699e-56/PREDICTED: uncharacterized protein LOC102304581 [<i>Haplochromis burtoni</i>]
348	Unigene48287	-7.626925794	Down	0.806007675	gi 528515730 ref XP_005174065.1 /1.22495e-23/PREDICTED: rho guanine nucleotide exchange factor 18 isoform X1 [<i>Danio rerio</i>]
349	Unigene27466	-7.880603904	Down	0.842024656	-
350	Unigene459	-11.97070509	Down	0.99615816	gi 41152379 ref NP_956366.1 /3.43945e-141/lectin, galactoside-binding, soluble, 9 (galectin 9)-like 1 [<i>Danio rerio</i>]
351	Unigene1443	-8.645057935	Down	0.918736727	gi 339895911 ref NP_956573.2 /6.76192e-28/Golgi membrane protein 1-like [<i>Danio rerio</i>]
352	CL16777.Contig1	-7.940558308	Down	0.849630242	gi 242247629 ref NP_001156323.1 /1.07793e-27/glutathione S-transferase M3 (brain) [<i>Danio rerio</i>]
353	CL4078.Contig3	7.803054785	Up	0.83081477	-
354	Unigene15623	7.709658248	Up	0.817379175	-
355	Unigene11405	5.75760715	Up	0.822654926	gi 209733124 gb ACI67431.1 /4.23515e-84/Trans-2-enoyl-CoA reductase, mitochondrial precursor [<i>Salmo salar</i>]
356	CL11110.Contig2	-8.26052755	Down	0.885774128	-
357	Unigene76823	-8.618385502	Down	0.916849431	-
358	CL5198.Contig8	-8.574908836	Down	0.913473991	gi 528502583 ref XP_001919795.3 /9.253e-34/PREDICTED: NACHT, LRR and PYD domains-containing protein 3-like isoform X1 [<i>Danio rerio</i>]
359	Unigene59256	5.933418616	Up	0.836065574	gi 183985554 gb AAI66041.1 /3.96861e-22/LOC560618 protein [<i>Danio rerio</i>]
360	Unigene26499	7.824428435	Up	0.834287828	-
361	Unigene11510	7.16102688	Up	0.942442898	gi 157787137 ref NP_001099167.1 /0/G-protein coupled receptor 84 [<i>Danio rerio</i>]
362	Unigene15574	11.6014613	Up	0.994765466	gi 187607872 ref NP_001120324.1 /5.74189e-21/uncharacterized protein LOC100145387 precursor [<i>Xenopus (Silurana) tropicalis</i>]
363	CL16865.Contig1	8.191470532	Up	0.878333409	-
364	CL5273.Contig1	7.700127451	Up	0.970605909	gi 515019311 gb AGO64769.1 /8.61463e-30/hepcidin [<i>Cyprinus carpio</i>]
365	CL19819.Contig1	8.220781371	Up	0.881382368	-
366	Unigene7615	9.644457188	Up	0.968541814	-
367	CL1292.Contig6	-8.062495926	Down	0.864094087	gi 401663980 dbj BAM36371.1 /5.85588e-102/growth hormone-inducible transmembrane protein [<i>Oplegnathus fasciatus</i>]
368	Unigene14967	6.063103727	Up	0.852644492	gi 54035434 gb AAH83483.1 /3.87471e-83/Adcyap1a protein [<i>Danio rerio</i>]
369	CL6333.Contig2	-7.751544059	Down	0.906609223	gi 432869982 ref XP_004071779.1 /1.07943e-59/PREDICTED: uncharacterized protein LOC101172982 [<i>Oryzias latipes</i>]
370	CL19534.Contig1	8.784634846	Up	0.928780612	-
371	Unigene71547	8.049848549	Up	0.862854329	-
372	CL3470.Contig2	-9.347252251	Down	0.958156264	-
373	Unigene1392	6.740550366	Up	0.911579103	gi 187281105 ref NP_001035333.2 /8.01512e-141/tumor necrosis factor-inducible gene 6 protein precursor [<i>Danio rerio</i>]
374	CL11539.Contig4	8.266786541	Up	0.886225343	gi 573903209 ref XP_006639328.1 /4.00813e-19/PREDICTED: cytidine and dCMP

					deaminase domain-containing protein 1-like [<i>Lepisosteus oculatus</i>]
375	CL13102.Contig2	-7.807354922	Down	0.831792042	-
376	Unigene9605	5.951534511	Up	0.810600095	-
377	Unigene58019	7.79224803	Up	0.829914508	-
378	Unigene91946	8.293088412	Up	0.88901507	gi 425892318 gb AFY09726.1 /3.77865e-41/ceruloplasmin, partial [<i>Labeo rohita</i>]
379	CL1576.Contig3	9.470237255	Up	0.996403291	gi 38143017 emb CAC80551.1 /2.14211e-68/interleukin-1 beta 1 [<i>Carassius auratus</i>]
380	Unigene47959	8.77478706	Up	0.928140666	-
381	Unigene29618	6.010576004	Up	0.848227786	gi 55742482 ref NP_998461.1 /6.07553e-39/tissue inhibitor of metalloproteinase 2b precursor [<i>Danio rerio</i>]
382	CL21075.Contig2	7.695808269	Up	0.815405107	-
383	CL4014.Contig3	8.290018847	Up	0.888541077	-
384	Unigene51717	-8.186526969	Down	0.877827961	-
385	Unigene58139	-7.617161323	Down	0.80386874	gi 528491045 ref XP_005172607.1 /1.23385e-31/PREDICTED: uncharacterized protein LOC101884915 [<i>Danio rerio</i>]
386	CL2646.Contig2	-9.654636029	Down	0.968873718	-
387	CL14147.Contig1	9.675369018	Up	0.969520171	-
388	Unigene41401	-7.803054785	Down	0.83081477	-
389	Unigene44436	8.668884984	Up	0.990038549	gi 29436812 gb AAH49472.1 /2.72902e-15/Matrix metalloproteinase 13 [<i>Danio rerio</i>]
390	Unigene1482	6.062495926	Up	0.817217562	-
391	Unigene78728	7.956134115	Up	0.851099946	-
392	CL1774.Contig16	-6.52438706	Down	0.857766223	gi 59858555 ref NP_001012304.1 /0/RNA-binding protein 39 [<i>Danio rerio</i>]
393	CL18245.Contig2	7.198795806	Up	0.943580699	gi 30231240 ref NP_840079.1 /1.82657e-62/15 kDa selenoprotein precursor [<i>Danio rerio</i>]
394	CL259.Contig16	8.536571017	Up	0.910438048	gi 29540612 gb AAO88245.1 /4.08395e-18/signal transducer and activator of transcription 1 [<i>Carassius auratus</i>]
395	CL14781.Contig1	5.804611633	Up	0.81573918	-
396	Unigene47420	-7.886712714	Down	0.842795844	-
397	CL18279.Contig1	5.586972397	Up	0.806627012	gi 189530404 ref XP_001920566.1 /3.31113e-173/PREDICTED: free fatty acid receptor 2-like [<i>Danio rerio</i>]
398	Unigene68461	-7.607330314	Down	0.802739616	gi 10954052 gb AAG25718.1 AF309416_1/9.4692e-16/ovarian fibroin-like substance-3 [<i>Cyprinus carpio</i>]
399	Unigene78162	-8.611024797	Down	0.916330967	gi 528496592 ref XP_005156444.1 /5.63823e-61/PREDICTED: serine/threonine-protein kinase LMTK1-like isoform X1 [<i>Danio rerio</i>]
400	CL8785.Contig2	-7.597431853	Down	0.801611577	gi 125830338 ref XP_692362.2 /8.42406e-12/PREDICTED: anthrax toxin receptor 1 [<i>Danio rerio</i>]
401	CL7807.Contig2	6.338513555	Up	0.868515132	-
402	Unigene96409	8.087462841	Up	0.867158231	-
403	CL409.Contig24	7.864186145	Up	0.839562494	gi 181330416 ref NP_001116713.1 /7.17489e-101/nuclear receptor subfamily 1, group H, member 5 [<i>Danio rerio</i>]

404	Unigene16146	7.695808269	Up	0.815405107	-
405	Unigene58486	8.772589504	Up	0.927917228	-
406	CL11185.Contig1	-8.224001674	Down	0.881899748	-
407	Unigene76028	-7.651051691	Down	0.809166184	gi 46309481 ref NP_996939.1 /1.24897e-36/phospholipase A1 member A precursor [<i>Danio rerio</i>]
408	CL11090.Contig4	8.118941073	Up	0.870759279	gi 237511645 gb ACQ99544.1 /1.16241e-161/liver X receptor [<i>Cyprinus carpio</i>]
409	CL1933.Contig2	8.082149041	Up	0.866544318	-
410	Unigene94964	-7.828665428	Down	0.834488489	-
411	CL929.Contig3	7.926790153	Up	0.847412127	-
412	CL2302.Contig8	9.038004444	Up	0.943919111	gi 161612143 gb AAI55571.1 /7.20948e-78/LOC559136 protein [<i>Danio rerio</i>]
413	Unigene18061	-8.215937399	Down	0.880891021	gi 528494626 ref XP_005169449.1 /2.51928e-29/PREDICTED: contactin associated protein-like 5 isoform X2 [<i>Danio rerio</i>]
414	CL1512.Contig6	-7.922832139	Down	0.847412127	gi 34784532 gb AAH56692.1 /3.47376e-153/LOC402865 protein, partial [<i>Danio rerio</i>]
415	Unigene49320	-8.09978612	Down	0.868406667	-
416	Unigene38547	-7.651051691	Down	0.809166184	-
417	CL3871.Contig3	8.120669887	Up	0.870759279	gi 50540248 ref NP_001002591.1 /5.6414e-21/rho-related GTP-binding protein RhoE [<i>Danio rerio</i>]
418	Unigene16078	7.732450113	Up	0.82142493	-
419	Unigene44161	6.165691344	Up	0.867461934	-
420	CL6749.Contig1	7.965784285	Up	0.852597852	-
421	CL3516.Contig4	5.86841998	Up	0.833445053	gi 62955445 ref NP_001017734.1 /0/meta lloreductase STEAP4 [<i>Danio rerio</i>]
422	CL9375.Contig4	8.029747343	Up	0.860310818	gi 18859571 ref NP_571121.1 /0/wilms tumor 1a [<i>Danio rerio</i>]
423	CL2464.Contig5	8.122396631	Up	0.871352584	gi 28279226 gb AAH46004.1 /4.23051e-08/Zgc:65788 protein, partial [<i>Danio rerio</i>]
424	CL5857.Contig4	8.820178962	Up	0.931029097	-
425	Unigene84364	8.742050273	Up	0.990639446	gi 488888807 gb AGL08667.1 /6.81193e-22/interleukin-11, partial [<i>Carassius auratus</i>]
426	Unigene11251	-7.994353437	Down	0.856142497	gi 118763931 gb AAI28823.1 /8.96684e-19/Si:ch211-69g19.2 protein [<i>Danio rerio</i>]
427	CL5765.Contig2	8.731319031	Up	0.92517631	-
428	Unigene17618	-8.524868154	Down	0.909485723	-
429	Unigene9628	7.803054785	Up	0.83081477	-
430	Unigene111503	-7.617161323	Down	0.80386874	gi 41054970 ref NP_957345.1 /1.35121e-30/bone morphogenetic protein 5 precursor [<i>Danio rerio</i>]
431	Unigene56556	-8.992466327	Down	0.941332214	-
432	Unigene52459	5.968608024	Up	0.83576621	-
433	CL16918.Contig2	-7.994353437	Down	0.856142497	gi 190339262 gb AAI62500.1 /5.65438e-37/Eph-like kinase 1 [<i>Danio rerio</i>]
434	CL3795.Contig3	-7.920849053	Down	0.846658293	-
435	Unigene17779	7.64385619	Up	0.808135764	-
436	CL5458.Contig8	-7.8008999	Down	0.83081477	-
437	Unigene39267	8.053473413	Up	0.863360862	-

438	Unigene35435	8.382389079	Up	0.981888467	-
439	Unigene36586	-9.092757141	Down	0.946681722	-
440	CL3125.Contig2	-7.614709844	Down	0.80386874	-
441	CL4425.Contig3	-7.655828831	Down	0.810294223	gi 528520507 ref XP_005162959.1 /1.38692e-38/PREDICTED: myosin-7 isoform X3 [<i>Danio rerio</i>]
442	Unigene50251	-7.757112167	Down	0.824287329	-
443	Unigene62941	-7.839203788	Down	0.836208748	-
444	Unigene54572	8.094517599	Up	0.867816616	-
445	Unigene54289	7.882643049	Up	0.842024656	-
446	Unigene48169	8.568589531	Up	0.913181135	gi 134054414 emb CAM73201.1 /2.38332e-19/si:dkey-15j16.3 [<i>Danio rerio</i>]
447	Unigene44991	7.684164178	Up	0.81413064	gi 77403694 dbj BAE46429.1 /1.43524e-53/ORF2-encoded protein [<i>Danio rerio</i>]
448	Unigene77418	9.383704292	Up	0.959632476	-
449	CL8096.Contig18	-8.468187634	Down	0.978519536	gi 528471389 ref XP_005163580.1 /0/PREDICTED: uncharacterized protein LOC101882486 [<i>Danio rerio</i>]
450	Unigene76577	-7.805206455	Down	0.831792042	gi 292610733 ref XP_001337309.3 /6.06125e-39/PREDICTED: carboxypeptidase N subunit 2 [<i>Danio rerio</i>]
451	Unigene33206	-8.54045097	Down	0.910717888	gi 528515420 ref XP_001921427.2 /5.98859e-24/PREDICTED: uncharacterized protein LOC100004641 [<i>Danio rerio</i>]
452	Unigene1243	8.022367813	Up	0.859644841	-
453	Unigene18495	9.206616876	Up	0.994089727	gi 57528839 ref NP_956700.1 /1.48897e-60/uncharacterized protein LOC393377 precursor [<i>Danio rerio</i>]
454	Unigene13585	5.672911311	Up	0.812494983	-
455	Unigene33451	-7.716533694	Down	0.818344516	-
456	Unigene30920	9.729620744	Up	0.971069056	gi 41055766 ref NP_956470.1 /7.56022e-13/trimeric intracellular cation channel type B [<i>Danio rerio</i>]
457	Unigene19	8	Up	0.856922363	gi 597758464 ref XP_007240937.1 /7.88405e-126/PREDICTED: rap guanine nucleotide exchange factor 6-like isoform X3 [<i>Astyanax mexicanus</i>]
458	Unigene59786	9.616548844	Up	0.967747849	-
459	CL10213.Contig2	10.03296406	Up	0.978464218	gi 338176917 gb AEI83864.1 /0/granulocyte colony stimulating factor receptor [<i>Carassius auratus</i>]
460	Unigene97833	-7.843397672	Down	0.836851947	-
461	Unigene49381	5.955548541	Up	0.834066559	-
462	CL4700.Contig2	7.622051819	Up	0.804937123	-
463	CL20263.Contig22	-8.77478706	Down	0.928140666	gi 120537843 gb AAI29405.1 /1.34542e-177/LOC799852 protein [<i>Danio rerio</i>]
464	Unigene56277	7.619608644	Up	0.804937123	-
465	CL1787.Contig6	7.631783357	Up	0.806007675	gi 167963524 ref NP_001108163.1 /5.91483e-44/SH2 domain containing 1A duplicate a [<i>Danio rerio</i>]
466	Unigene49232	11.08170534	Up	0.991783755	-
467	Unigene32768	-7.677132345	Down	0.81339633	gi 432873688 ref XP_004072341.1 /1.59022e-14/PREDICTED: MAP kinase-activated protein kinase 5-like [<i>Oryzias latipes</i>]
468	CL2387.Contig11	8.027905997	Up	0.860310818	gi 528501908 ref XP_005157707.1 /2.853

					99e-64/PREDICTED: coiled-coil domain-containing protein 9 isoform X1 [<i>Danio rerio</i>]
469	Unigene56786	-7.884679317	Down	0.842024656	-
470	Unigene59471	-8.238404739	Down	0.883383553	-
471	Unigene51409	-7.90488546	Down	0.844939118	-
472	Unigene19234	-7.662965013	Down	0.811074088	-
473	Unigene48632	10.23361968	Up	0.982157461	gi 292615091 ref XP_698005.4 /5.44783e-99/PREDICTED: ankyrin repeat domain-containing protein 33B-like [<i>Danio rerio</i>]
474	CL2143.Contig5	-8.058893689	Down	0.864094087	gi 528501806 ref XP_005157655.1 /1.3903e-50/PREDICTED: MAP/microtubule affinity-regulating kinase 4-like isoform X1 [<i>Danio rerio</i>]
475	CL12644.Contig1	7.619608644	Up	0.804937123	gi 215539471 gb AAI71569.1 /1.73526e-79/Unknown (protein for IMAGE:9039285) [<i>Danio rerio</i>]
476	CL20188.Contig2	6.768184325	Up	0.899933185	-
477	Unigene20822	7.727920455	Up	0.820433557	-
478	CL3516.Contig3	7.940487892	Up	0.977560703	gi 62955445 ref NP_001017734.1 /0/meta lloreductase STEAP4 [<i>Danio rerio</i>]
479	CL3530.Contig2	-7.64385619	Down	0.808135764	-
480	Unigene49410	7.830779268	Up	0.835361634	-
481	Unigene51686	7.730187062	Up	0.820433557	-
482	Unigene26790	6.72129453	Up	0.909889214	gi 326381135 ref NP_001191955.1 /3.08992e-14/guanine nucleotide-binding protein G(I)/G(S)/G(O) subunit gamma-10 [<i>Danio rerio</i>]
483	CL1782.Contig7	8.491853096	Up	0.906819646	gi 528513374 ref XP_005161172.1 /6.41118e-25/PREDICTED: ER degradation-enhancing alpha-mannosidase-like protein 3-like isoform X2 [<i>Danio rerio</i>]
484	CL3470.Contig3	-8.027116128	Down	0.939402617	-
485	Unigene103392	10.03479896	Up	0.978501097	gi 351602153 gb AEQ53931.1 /1.03265e-22/complement component C7 [<i>Ctenopharyngodon idella</i>]
486	CL220.Contig17	7.639039173	Up	0.807086905	gi 597778804 ref XP_007253025.1 /1.20657e-41/PREDICTED: YLP motif-containing protein 1-like [<i>Astyanax mexicanus</i>]
487	CL11090.Contig2	10.73781068	Up	0.988802044	gi 62955059 ref NP_001017545.1 /1.58281e-139/oxysterols receptor LXR-alpha [<i>Danio rerio</i>]
488	CL932.Contig3	7.866248611	Up	0.839562494	-
489	CL87.Contig91	8.075033392	Up	0.865893526	gi 528509859 ref XP_005170118.1 /0/PREDICTED: polycystic kidney and hepatic disease 1 (autosomal recessive)-like 1 isoform X1 [<i>Danio rerio</i>]
490	Unigene28571	-7.857980995	Down	0.83873165	-
491	Unigene20546	9.405850578	Up	0.96046332	-
492	Unigene1056	5.925849833	Up	0.840522412	-
493	CL932.Contig6	7.779172154	Up	0.828073852	-
494	CL15463.Contig2	-7.639039173	Down	0.807086905	-
495	Unigene105052	-8.647458426	Down	0.919000297	gi 326679036 ref XP_003201226.1 /2.55586e-13/PREDICTED: leiomodrin-3 [<i>Danio rerio</i>]

496	Unigene84824	8.286942737	Up	0.888071422	-
497	Unigene72855	-8.013089999	Down	0.858326988	gi 317418923 emb CBN80961.1 /9.18118e-27/Retrovirus polyprotein [<i>Dicentrarchus labrax</i>]
498	CL1899.Contig1	-7.691161905	Down	0.815405107	gi 302325339 gb ADL18408.1 /9.66359e-78/Def6-like protein, partial [<i>Danio rerio</i>]
499	CL12864.Contig5	7.714245518	Up	0.818344516	gi 37590396 gb AAH59643.1 /2.11721e-84/Ancient ubiquitous protein 1 [<i>Danio rerio</i>]
500	Unigene42838	-8.330916878	Down	0.8925608	-
501	Unigene72566	7.821880254	Up	0.956997855	gi 545604907 gb AGW43283.1 /2.66477e-92/interleukin-1 receptor 2 [<i>Ctenopharyngodon idella</i>]
502	Unigene32003	10.92357509	Up	0.99053315	-
503	Unigene45886	-8.055282436	Down	0.863478004	-
504	Unigene49426	8.188176706	Up	0.878333409	gi 542261605 ref XP_005465733.1 /1.03814e-06/PREDICTED: uncharacterized protein LOC100698190 [<i>Oreochromis niloticus</i>]
505	CL19408.Contig2	7.403925025	Up	0.951566998	-
506	CL9079.Contig4	9.105908509	Up	0.947320582	gi 308321684 gb ADO27993.1 /7.15433e-79/heme oxygenase [<i>Ictalurus furcatus</i>]
507	Unigene5120	5.982620475	Up	0.839392204	gi 28779299 gb AAO19474.1 /0/toll-like receptor [<i>Carassius auratus</i>]
508	CL517.Contig18	-7.403012024	Down	0.81650386	gi 190337317 gb AAI63305.1 /0/Integrin, alpha 2b (platelet glycoprotein IIb of IIb/IIIa complex, antigen CD41B) [<i>Danio rerio</i>]
509	Unigene68200	8.722238308	Up	0.924440916	-
510	CL5550.Contig9	9.073248982	Up	0.94575109	gi 49618959 gb AAT68064.1 /0/BING4-like [<i>Danio rerio</i>]
511	Unigene93928	10.2227949	Up	0.981963308	gi 326673883 ref XP_001922616.3 /1.17382e-10/PREDICTED: saxitoxin and tetrodotoxin-binding protein 2-like [<i>Danio rerio</i>]
512	Unigene71979	5.814898443	Up	0.820072368	-
513	CL9563.Contig6	8.094517599	Up	0.867816616	gi 559767267 gb AHB12557.1 /1.93327e-116/heat shock transcription factor 2c [<i>Carassius auratus</i>]
514	CL8832.Contig3	-8.65224746	Down	0.919264952	-
515	CL1744.Contig1	9.094517599	Up	0.946785848	-
516	Unigene24012	8.448460501	Up	0.903180636	gi 528508932 ref XP_003200567.2 /9.06691e-64/PREDICTED: NACHT, LRR and PYD domains-containing protein 3-like [<i>Danio rerio</i>]
517	CL15267.Contig2	-8.545608062	Down	0.911348072	-
518	CL10658.Contig6	9.668079144	Up	0.992305473	gi 42542887 gb AAH66390.1 /3.06489e-08/Zgc:65774 [<i>Danio rerio</i>]
519	CL2347.Contig8	-9.024216237	Down	0.943137076	gi 528516862 ref XP_692341.6 /0/PREDICTED: TNF receptor-associated factor 5, partial [<i>Danio rerio</i>]
520	Unigene22417	-7.727920455	Down	0.820433557	-
521	CL3697.Contig1	-8.456696651	Down	0.90382492	gi 292621274 ref XP_002664595.1 /0/PREDICTED: WD repeat-containing protein 62 isoform X3 [<i>Danio rerio</i>]
522	CL1636.Contig2	7.9522559	Up	0.851099946	gi 259089311 ref NP_001158693.1 /9.00082e-53/retinitis pigmentosa 9 (autosomal dominant) [<i>Oncorhynchus mykiss</i>]
523	CL3780.Contig2	-8.277674857	Down	0.887137536	gi 119672903 ref NP_001073305.1 /1.15341e-145/glycoprotein integral membrane protein 1 precursor [<i>Danio rerio</i>]

524	CL10362.Contig8	-7.705056346	Down	0.817379175	gi 37681897 gb AAQ97826.1 /3.64982e-47/poly(A)-specific ribonuclease [<i>Danio rerio</i>]
525	Unigene55272	-7.709658248	Down	0.817379175	-
526	CL12526.Contig2	-11.72266525	Down	0.995264406	gi 47086567 ref NP_997902.1 /0/macrophage expressed 1 precursor [<i>Danio rerio</i>]
527	Unigene51365	8.183221824	Up	0.877827961	-
528	CL2372.Contig2	8.220781371	Up	0.881382368	gi 187608531 ref NP_001119932.1 /2.08249e-34/uncharacterized protein LOC796658 [<i>Danio rerio</i>]
529	CL1328.Contig11	-7.641449692	Down	0.808135764	gi 41053487 ref NP_956984.1 /4.0855e-75/ran-binding protein 3 [<i>Danio rerio</i>]
530	CL5611.Contig2	7.940558308	Up	0.849630242	gi 597751825 ref XP_007237788.1 /2.88047e-08/PREDICTED: uncharacterized protein LOC103033781 [<i>Astyanax mexicanus</i>]
531	CL2229.Contig2	7.196836388	Up	0.945616593	-
532	Unigene98239	-7.73470962	Down	0.82142493	-
533	Unigene47790	7.336729697	Up	0.947208863	-
534	Unigene82099	9.951770389	Up	0.976689726	gi 183985554 gb AAI66041.1 /6.63797e-30/LOC560618 protein [<i>Danio rerio</i>]
535	CL5380.Contig3	7.594946589	Up	0.800433644	-
536	CL6523.Contig5	-9.031494449	Down	0.984542613	gi 32479133 gb AAN12398.1 /1.28779e-161/polyprotein [<i>Tetraodon nigroviridis</i>]
537	Unigene33114	9.594946589	Up	0.967031978	-
538	CL17615.Contig1	-7.589963182	Down	0.800433644	-
539	CL14734.Contig4	7.81164228	Up	0.832666272	gi 51571917 ref NP_001003998.1 /7.74018e-52/BET1-like protein [<i>Danio rerio</i>]
540	CL517.Contig17	-7.602389572	Down	0.801611577	gi 190337317 gb AAI63305.1 /0/Integrin, alpha 2b (platelet glycoprotein IIb of IIb/IIIa complex, antigen CD41B) [<i>Danio rerio</i>]
541	CL3725.Contig10	-8.158188893	Down	0.875117414	-
542	Unigene34823	6.502891368	Up	0.899593689	gi 62955445 ref NP_001017734.1 /0/metalloreductase STEAP4 [<i>Danio rerio</i>]
543	CL4350.Contig1	7.72033396	Up	0.970015858	gi 24119251 ref NP_705943.1 /2.9762e-38/prostaglandin-endoperoxide synthase 2 precursor [<i>Danio rerio</i>]
544	Unigene69076	-7.926790153	Down	0.847412127	-
545	Unigene20260	-7.95806932	Down	0.851831002	-
546	Unigene15828	-7.934673752	Down	0.84871588	-
547	Unigene61375	7.707359132	Up	0.817379175	-
548	CL1763.Contig2	7.73470962	Up	0.82142493	gi 190337632 gb AAI63551.1 /5.96825e-26/Dennd4a protein [<i>Danio rerio</i>]
549	CL1557.Contig2	-7.794415866	Down	0.829914508	-
550	CL7461.Contig3	8.693486957	Up	0.922424546	-
551	CL2518.Contig8	-10.8196469	Down	0.989568894	gi 113671512 ref NP_001038773.1 /4.6951e-14/UPF0471 protein C1orf63 homolog [<i>Danio rerio</i>]
552	Unigene32599	8.227214805	Up	0.88237808	-
553	Unigene50744	9.269126679	Up	0.95495003	-
554	CL5714.Contig1	7.835984585	Up	0.974946689	gi 187608210 ref NP_001119928.1 /1.83685e-60/immunoresponsive gene 1 [<i>Danio rerio</i>]
555	Unigene62024	-7.866248611	Down	0.839562494	-
556	CL1145.Contig1	-7.973458213	Down	0.85327576	-

557	Unigene24850	10.02467797	Up	0.978278743	-
558	CL5155.Contig3	9.445704636	Up	0.961968818	gi 528503831 ref XP_005158140.1 /4.3053e-134/PREDICTED: immunity-related GTPase family, e4 isoform X1 [<i>Danio rerio</i>]
559	CL7082.Contig6	7.837102265	Up	0.836208748	-
560	CL12013.Contig4	10.78053977	Up	0.989200112	gi 41055227 ref NP_956674.1 /1.31732e-95/charged multivesicular body protein 5 [<i>Danio rerio</i>]
561	Unigene79754	7.988684687	Up	0.855498214	gi 528506016 ref XP_001333061.4 /8.91632e-30/PREDICTED: formin-2-like [<i>Danio rerio</i>]
562	Unigene44697	12.68292145	Up	0.997737414	-
563	Unigene6679	8.725650281	Up	0.924650254	-
564	Unigene29619	6.796651365	Up	0.915747423	-
565	CL7242.Contig3	-8.544320516	Down	0.911045453	gi 47087253 ref NP_998681.1 /0/E3 ubiquitin-protein ligase NRDP1 [<i>Danio rerio</i>]
566	Unigene38750	6.415927045	Up	0.883522388	gi 390348052 ref XP_792620.3 /5.42713e-17/PREDICTED: protein SF11 homolog [<i>Strongylocentrotus purpuratus</i>]
567	Unigene2162	-7.787902559	Down	0.829006653	gi 47225388 emb CAG11871.1 /4.53826e-83/unnamed protein product [<i>Tetraodon nigroviridis</i>]
568	CL9090.Contig6	-8.227214805	Down	0.88237808	gi 54400352 ref NP_001005924.1 /5.50029e-40/transmembrane protein 56-B [<i>Danio rerio</i>]
569	Unigene2053	-8.749310785	Down	0.926372682	gi 50540414 ref NP_001002673.1 /0/U4/U6.U5 tri-snRNP-associated protein 1 [<i>Danio rerio</i>]
570	Unigene43087	-8.024216237	Down	0.859644841	-
571	CL3722.Contig1	8.74819285	Up	0.926372682	gi 48734810 gb AAH71412.1 /3.4591e-121/Tmed9 protein [<i>Danio rerio</i>]
572	CL21472.Contig4	-7.752659401	Down	0.824287329	-
573	Unigene54879	7.805206455	Up	0.831792042	gi 188536030 ref NP_001120951.1 /2.6734e-10/bloodthirsty-related gene family, member 6 [<i>Danio rerio</i>]
574	CL1602.Contig8	8.110265791	Up	0.869565076	-
575	Unigene94243	8.816983623	Up	0.93083169	gi 134133234 ref NP_001077028.1 /3.34925e-21/uncharacterized protein LOC566848 [<i>Danio rerio</i>]
576	Unigene59073	8.044394119	Up	0.862280548	-
577	Unigene32971	-7.878561873	Down	0.841231775	-
578	Unigene63656	8.614709844	Up	0.916580437	gi 157954488 ref NP_001103320.1 /2.91654e-17/uncharacterized protein LOC100126122 precursor [<i>Danio rerio</i>]
579	Unigene26300	7.700439718	Up	0.816427935	-
580	CL9347.Contig1	7.992764963	Up	0.97945776	gi 41350992 gb AAH65591.1 /8.87117e-46/Mmp13 protein [<i>Danio rerio</i>]
581	Unigene48604	10.13228551	Up	0.980392731	gi 597753952 ref XP_007238796.1 /8.59428e-49/PREDICTED: disintegrin and metalloproteinase domain-containing protein 28-like [<i>Astyanax mexicanus</i>]
582	Unigene4687	7.617161323	Up	0.80386874	-
583	Unigene41390	-7.908892949	Down	0.84512134	-
584	CL2504.Contig1	-8.701595261	Down	0.922916979	gi 47085979 ref NP_998355.1 /8.16489e-53/tumor necrosis factor receptor superfamily member 1A precursor [<i>Danio rerio</i>]

585	Unigene41545	-7.686500527	Down	0.81436384	-
586	CL6856.Contig1	-8.350202549	Down	0.894178018	gi 113681812 ref NP_001038573.1 /0/unc haracterized protein LOC566573 [<i>Danio rerio</i>]
587	CL2572.Contig7	-7.900866808	Down	0.844362083	gi 194579011 ref NP_001124071.1 /0/USP 6 N-terminal-like protein [<i>Danio rerio</i>]
588	CL5902.Contig1	6.726407402	Up	0.818059252	gi 292614759 ref XP_002662361.1 /4.456 51e-158/PREDICTED: nodal modulator 2 [<i>Danio rerio</i>]
589	Unigene42309	7.8475794	Up	0.837042846	-
590	CL7403.Contig3	-8.486499862	Down	0.90651052	gi 1141708 gb AAA84448.1 /3.30338e- 160/g-RICH [<i>Carassius auratus</i>]
591	CL13201.Contig7	-7.8008999	Down	0.83081477	gi 41056115 ref NP_956858.1 /2.95457e- 109/UV excision repair protein RAD23 homolog B [<i>Danio rerio</i>]
592	CL13720.Contig1	8.536571017	Up	0.910438048	gi 66472650 ref NP_001018387.1 /3.1149 5e-136/SWI/SNF-related matrix-associated actin-dependent regulator of chromatin subfamily E member 1-related isoform 1 [<i>Danio rerio</i>]
593	CL19222.Contig3	-7.918863237	Down	0.846658293	gi 528506766 ref XP_005158923.1 /9.040 07e-06/PREDICTED: kanadaplin isoform X1 [<i>Danio rerio</i>]
594	Unigene26488	8.077616872	Up	0.972656987	-
595	Unigene35683	11.28982678	Up	0.993128724	gi 528477245 ref XP_001920654.4 /7.840 1e-11/PREDICTED: interferon-induced guanylate-binding protein 1 [<i>Danio rerio</i>]
596	CL19711.Contig2	-9.069673528	Down	0.945471249	gi 292626818 ref XP_002666462.1 /3.839 54e-78/PREDICTED: platelet glycoprotein IX [<i>Danio rerio</i>]
597	CL14118.Contig3	-8.193114629	Down	0.878861635	-
598	Unigene33726	6.032872249	Up	0.826031451	-
599	CL377.Contig2	7.660590206	Up	0.810294223	gi 194353931 ref NP_001123874.1 /9.124 3e-122/si:ch211-195h23.3 [<i>Danio rerio</i>]
600	Unigene86069	11.86946532	Up	0.995801309	-
601	CL1141.Contig4	7.772589504	Up	0.827073802	-
602	Unigene32131	6.285402219	Up	0.856775935	-
603	Unigene23810	9.961449694	Up	0.97691425	gi 92096566 gb AAI15346.1 /1.6505e- 20/Zgc:136954 [<i>Danio rerio</i>]
604	CL3516.Contig2	9.528209897	Up	0.988386622	gi 62955445 ref NP_001017734.1 /0/meta lloreductase STEAP4 [<i>Danio rerio</i>]
605	CL20983.Contig2	11.36959735	Up	0.993623326	-
606	Unigene19277	7.589963182	Up	0.800433644	-
607	CL12944.Contig1	-7.938599455	Down	0.848897017	gi 145587648 ref NP_001071069.2 /2.839 76e-165/protein pellino homolog 1 [<i>Danio rerio</i>]
608	CL18715.Contig2	7.34619711	Up	0.924469117	gi 194578843 ref NP_001124059.1 /6.264 01e-21/transmembrane protein 154 precursor [<i>Danio rerio</i>]
609	Unigene14349	-7.714245518	Down	0.818344516	-
610	Unigene36215	6.432959407	Up	0.829731201	-
611	CL6151.Contig2	8.680652546	Up	0.921424496	gi 528474897 ref XP_003198200.2 /0/PRE DICTED: integrator complex subunit 1 isoform 1 [<i>Danio rerio</i>]
612	Unigene71521	8.491853096	Up	0.906819646	-
613	CL517.Contig2	-8.657020649	Down	0.91981921	gi 190337317 gb AAI63305.1 /0/Integrin, alpha 2b (platelet glycoprotein IIb of IIb/IIIa)

					complex, antigen CD41B) [<i>Danio rerio</i>]
614	CL238.Contig1	-7.63420602	Down	0.806796218	gi 528491610 ref XP_003199352.2 /3.10423e-98/PREDICTED: integrin alpha-2-like [<i>Danio rerio</i>]
615	Unigene50583	7.785724906	Up	0.829006653	-
616	Unigene11297	7.985976849	Up	0.97997514	gi 514483113 gb AGO58842.1 /5.74666e-140/C-type lectin, partial [<i>Carassius auratus</i>]
617	CL9460.Contig2	-8.139551352	Down	0.872958955	gi 407728597 ref NP_996973.2 /6.29121e-63/calcium modulating ligand [<i>Danio rerio</i>]
618	Unigene64308	-7.963859408	Down	0.852425392	gi 528501299 ref XP_005157554.1 /2.43451e-24/PREDICTED: uncharacterized protein LOC101885061 [<i>Danio rerio</i>]
619	CL3477.Contig1	-7.631783357	Down	0.806007675	gi 528483515 ref XP_690848.4 /3.82946e-25/PREDICTED: adenosine receptor A3-like isoform X3 [<i>Danio rerio</i>]
620	Unigene5819	8.257387843	Up	0.885309896	-
621	Unigene18342	6.334342265	Up	0.878419097	gi 118734592 gb ABI17540.2 /1.93665e-84/IL-6 family cytokine M17 [<i>Carassius auratus</i>]
622	Unigene18343	9.680066442	Up	0.969615621	gi 118734592 gb ABI17540.2 /5.37425e-19/IL-6 family cytokine M17 [<i>Carassius auratus</i>]
623	CL128.Contig14	8.356085106	Up	0.895035978	-
624	Unigene44363	8.651051691	Up	0.919264952	-
625	Unigene40424	-8.884679317	Down	0.935128	gi 42542887 gb AAH66390.1 /1.38129e-08/Zgc:65774 [<i>Danio rerio</i>]
626	CL698.Contig11	6.86507042	Up	0.875075112	-
627	CL1960.Contig1	-7.700439718	Down	0.816427935	gi 190339262 gb AAI62500.1 /1.50969e-53/Eph-like kinase 1 [<i>Danio rerio</i>]
628	CL12998.Contig11	7.607330314	Up	0.802739616	gi 528490264 ref XP_005167825.1 /0/PREDICTED: interphotoreceptor matrix proteoglycan 2 isoform X1 [<i>Danio rerio</i>]
629	Unigene49201	8.531381461	Up	0.91013326	-
630	CL11294.Contig2	8.576169382	Up	0.913766847	-
631	Unigene86012	7.779172154	Up	0.828073852	-
632	Unigene73111	7.741466986	Up	0.822359901	-
633	CL1482.Contig1	7.130921512	Up	0.933035705	-
634	CL17716.Contig2	10.4767462	Up	0.985851789	-
635	Unigene27407	9.594324604	Up	0.967031978	-
636	Unigene80084	7.969626351	Up	0.85327576	-
637	CL255.Contig13	8.372139541	Up	0.896257297	gi 47086673 ref NP_997849.1 /0/ataxin-2-like protein [<i>Danio rerio</i>]
638	Unigene43384	-10.11504365	Down	0.980089028	gi 224613542 gb ACN60350.1 /7.53118e-13/CD97 antigen precursor [<i>Salmo salar</i>]
639	Unigene61417	7.81164228	Up	0.832666272	-
640	CL9238.Contig1	7.961931959	Up	0.851831002	-
641	CL16860.Contig1	-7.597431853	Down	0.801611577	-
642	Unigene72173	10.48179943	Up	0.985917953	-
643	CL1837.Contig1	8.196397213	Up	0.878861635	gi 125834513 ref XP_694879.2 /5.67003e-80/PREDICTED: ATP-binding cassette sub-family B member 7, mitochondrial [<i>Danio rerio</i>]
644	CL1113.Contig1	6.0726278	Up	0.84487187	-

645	CL18034.Contig4	-7.765976681	Down	0.826084599	-
646	CL7321.Contig4	7.759333407	Up	0.825171321	gi 319803050 ref NP_001188372.1 /1.48846e-20/glucocorticoid modulatory element binding protein 1 [<i>Danio rerio</i>]
647	CL141.Contig1	8.721099189	Up	0.924440916	-
648	Unigene67562	8.571120576	Up	0.913181135	-
649	Unigene44909	-7.973458213	Down	0.85327576	-
650	CL18378.Contig12	-8.922832139	Down	0.93729839	gi 41054287 ref NP_956057.1 /0/RING finger protein 145 [<i>Danio rerio</i>]
651	Unigene101327	-7.839203788	Down	0.836208748	-
652	CL2229.Contig3	5.874439737	Up	0.833069763	-
653	Unigene87712	8.375039431	Up	0.896685735	gi 425892318 gb AFY09726.1 /9.68339e-29/ceruloplasmin, partial [<i>Labeo rohita</i>]
654	CL15853.Contig7	-7.948367232	Down	0.850374314	-
655	CL9525.Contig1	8.494522283	Up	0.907092979	-
656	CL2033.Contig2	-7.849665727	Down	0.837853082	-
657	CL6151.Contig4	10.23561538	Up	0.982199763	gi 528474897 ref XP_003198200.2 /0/PREDICTED: integrator complex subunit 1 isoform 1 [<i>Danio rerio</i>]
658	Unigene43968	8.448102536	Up	0.988325882	gi 317418859 emb CBN80897.1 /3.65265e-53/Cytidine deaminase [<i>Dicentrarchus labrax</i>]
659	CL5377.Contig2	7.684164178	Up	0.81413064	-
660	Unigene65509	7.934673752	Up	0.84871588	-
661	Unigene70859	9.012158928	Up	0.942396258	-
662	CL11091.Contig2	8.761551232	Up	0.927249082	gi 205830387 ref NP_001128615.1 /2.75164e-128/zinc finger protein 831 [<i>Danio rerio</i>]
663	CL15892.Contig2	7.604862058	Up	0.802455437	-
664	CL12852.Contig2	-7.809500194	Down	0.831792042	-
665	Unigene10268	5.733485025	Up	0.818210019	gi 169234882 ref NP_001108541.1 /3.37051e-28/uncharacterized protein LOC100003896 precursor [<i>Danio rerio</i>]
666	Unigene52471	10.06204614	Up	0.979039084	gi 586340943 gb AHJ60479.1 /9.68772e-13/interleukin-11 [<i>Carassius auratus</i>]
667	Unigene114292	7.682911005	Up	0.967479939	-
668	Unigene49034	6.782088163	Up	0.880469091	-
669	CL7104.Contig4	-7.224966365	Down	0.935007603	gi 528471942 ref XP_005171495.1 /0/PREDICTED: NACHT, LRR and PYD domains-containing protein 3-like [<i>Danio rerio</i>]
670	Unigene88011	6.369960791	Up	0.852173753	gi 545604907 gb AGW43283.1 /1.19164e-50/interleukin-1 receptor 2 [<i>Ctenopharyngodon idella</i>]
671	Unigene23916	-8.230420795	Down	0.88237808	-
672	CL18999.Contig4	-7.693486957	Down	0.815405107	gi 542259794 ref XP_005465044.1 /1.63184e-08/PREDICTED: zinc finger BED domain-containing protein 4-like [<i>Oreochromis niloticus</i>]
673	Unigene51158	-7.944468053	Down	0.849630242	-
674	CL19210.Contig2	8.597431853	Up	0.915175811	gi 153792401 ref NP_001093458.1 /1.09208e-107/glycolipid transfer protein [<i>Danio rerio</i>]
675	Unigene33110	7.641449692	Up	0.808135764	gi 50344760 ref NP_001002053.1 /5.74064e-53/splicing factor, arginine/serine-rich 3 [<i>Danio rerio</i>]

676	Unigene39774	-9.256601847	Down	0.954417466	-
677	CL5707.Contig8	7.700439718	Up	0.816427935	gi 291190598 ref NP_001167036.1 /1.62833e-75/cell cycle progression 1 [<i>Salmo salar</i>]
678	CL8076.Contig6	-10.06294557	Down	0.979061862	gi 145587665 ref NP_001076414.2 /9.11147e-71/guanylate binding protein 4 [<i>Danio rerio</i>]
679	CL20876.Contig1	-5.827037288	Down	0.809296342	gi 20196574 emb CAD24458.2 /9.28034e-40/TCR-alpha V segment II-66 [<i>Danio rerio</i>]
680	CL6485.Contig8	-8.497186541	Down	0.907138534	gi 40548308 ref NP_954967.1 /0/uncharacterized protein LOC321250 [<i>Danio rerio</i>]
681	Unigene8508	8.38514339	Up	0.897486209	-
682	CL3294.Contig20	-8.277674857	Down	0.887137536	gi 528510415 ref XP_005159781.1 /3.00534e-139/PREDICTED: uncharacterized protein LOC100000125 isoform X2 [<i>Danio rerio</i>]
683	Unigene6817	7.822305264	Up	0.83360992	-
684	Unigene20062	-7.882643049	Down	0.842024656	gi 542211125 ref XP_005478443.1 /1.04648e-14/PREDICTED: piezo-type mechanosensitive ion channel component 2-like [<i>Oreochromis niloticus</i>]
685	Unigene30921	-8.166581558	Down	0.875694449	gi 41055766 ref NP_956470.1 /5.64092e-34/trimeric intracellular cation channel type B [<i>Danio rerio</i>]
686	Unigene745	8.249508549	Up	0.88434347	gi 528480670 ref XP_005172067.1 /3.24372e-164/PREDICTED: rho guanine nucleotide exchange factor 12 isoform X3 [<i>Danio rerio</i>]
687	CL12823.Contig2	6.931960133	Up	0.921045952	-
688	Unigene52033	7.81164228	Up	0.832666272	gi 115529311 ref NP_001070186.1 /2.00647e-18/a disintegrin and metallopeptidase domain 28 precursor [<i>Danio rerio</i>]
689	CL16968.Contig1	-7.813781191	Down	0.832666272	-
690	Unigene5246	8.011227255	Up	0.858326988	-
691	CL3761.Contig3	8.214319121	Up	0.880891021	gi 62122887 ref NP_001014368.1 /4.49062e-84/sorting nexin-4 [<i>Danio rerio</i>]
692	CL7807.Contig1	7.721099189	Up	0.819407476	-
693	CL14978.Contig2	6.060105529	Up	0.848407838	-
694	CL1266.Contig2	6.358276067	Up	0.889271048	gi 47085913 ref NP_998314.1 /0/peptidyl-prolyl cis-trans isomerase FKBP5 [<i>Danio rerio</i>]
695	CL3516.Contig1	7.371089207	Up	0.954656089	gi 62955445 ref NP_001017734.1 /0/metalloredoxase STEAP4 [<i>Danio rerio</i>]
696	Unigene69212	11.70231701	Up	0.995184142	-
697	Unigene46419	7.589963182	Up	0.800433644	-
698	CL1509.Contig13	8.468963381	Up	0.904864017	-
699	Unigene114626	8.503825738	Up	0.907775225	gi 189528212 ref XP_001919426.1 /7.36102e-24/PREDICTED: cystine/glutamate transporter-like [<i>Danio rerio</i>]
700	CL14419.Contig1	7.084428781	Up	0.8981229	-
701	CL5925.Contig8	-8.344295908	Down	0.893773442	gi 47087415 ref NP_998601.1 /2.06206e-39/pleckstrin homology domain-containing family A member 1 [<i>Danio rerio</i>]
702	CL649.Contig1	8.13784503	Up	0.872958955	-
703	Unigene110029	-7.670066069	Down	0.81238001	-
704	CL19702.Contig1	-7.667702932	Down	0.811340913	-

705	CL17294.Contig1	-7.77478706	Down	0.827073802	-
706	Unigene52523	8.614709844	Up	0.916580437	-
707	Unigene17268	8.7736887	Up	0.928140666	gi 326672602 ref XP_003199701.1 /1.83012e-19/PREDICTED: uncharacterized protein LOC100535892 [<i>Danio rerio</i>]
708	Unigene96986	8.491853096	Up	0.906819646	gi 37695611 gb AAR00337.1 /1.80096e-22/alpha-2-macroglobulin [<i>Ctenopharyngodon idella</i>]
709	Unigene57699	-7.910892526	Down	0.845877343	gi 542230117 ref XP_005453731.1 /1.56957e-41/PREDICTED: uncharacterized protein LOC102078893 [<i>Oreochromis niloticus</i>]
710	CL1756.Contig20	7.597431853	Up	0.801611577	gi 378556115 gb AFC17882.1 /7.53798e-18/cytidine monophosphate sialic acid synthetase 1, partial [<i>Pimephales promelas</i>]
711	Unigene31600	12.78026635	Up	0.997884927	-
712	Unigene54415	-8.716533694	Down	0.924171922	-
713	Unigene42291	8.251087854	Up	0.884833734	-
714	CL6542.Contig2	-7.589963182	Down	0.800433644	-
715	Unigene45206	7.390535994	Up	0.954791671	-
716	CL1205.Contig2	-7.956134115	Down	0.851099946	-
717	Unigene43838	6.151767077	Up	0.86627207	gi 407080643 gb AFS89611.1 /5.41128e-40/interferon-induced transmembrane protein 1 [<i>Cyprinus carpio</i>]
718	CL10768.Contig3	-7.64625868	Down	0.808135764	gi 224495980 ref NP_001139049.1 /1.33545e-33/LIM and calponin homology domains 1a [<i>Danio rerio</i>]
719	Unigene85140	-7.754887502	Down	0.824287329	-
720	Unigene20787	-7.874469118	Down	0.84103003	-
721	CL12583.Contig6	5.960882345	Up	0.837876944	gi 62955133 ref NP_001017578.1 /5.27363e-38/chondrolectin precursor [<i>Danio rerio</i>]
722	CL405.Contig5	8.910892526	Up	0.936584689	gi 161353479 ref NP_998129.3 /2.75994e-23/cannabinoid receptor 2 [<i>Danio rerio</i>]
723	CL15148.Contig2	7.750427854	Up	0.823307887	gi 18858403 ref NP_571912.1 /2.19059e-43/CCAAT/enhancer binding protein (C/EBP) 1 [<i>Danio rerio</i>]
724	CL2309.Contig3	-7.754887502	Down	0.824287329	gi 30231244 ref NP_840081.1 /6.34345e-36/zinc finger protein GL11 [<i>Danio rerio</i>]
725	CL12694.Contig1	-8.299208018	Down	0.889479302	gi 190358874 sp Q7SXG4.2 SAE2_DANRE/3.49046e-61/RecName: Full=SUMO-activating enzyme subunit 2; AltName: Full=Ubiquitin-like 1-activating enzyme E1B; AltName: Full=Ubiquitin-like modifier-activating enzyme 2
726	Unigene2937	-7.589963182	Down	0.800433644	-
727	Unigene30900	8.710806434	Up	0.923700098	gi 157422943 gb AAI53508.1 /3.56839e-176/Eif4a1b protein [<i>Danio rerio</i>]
728	CL259.Contig6	-7.609794354	Down	0.802739616	gi 29540612 gb AAO88245.1 /1.4907e-162/signal transducer and activator of transcription 1 [<i>Carassius auratus</i>]
729	Unigene33201	-7.896836931	Down	0.843535578	gi 158253983 gb AAI53990.1 /8.26704e-33/Zgc:171601 protein [<i>Danio rerio</i>]
730	Unigene48720	-8.279223644	Down	0.88762563	gi 6425168 gb AAC33526.2 /7.94757e-19/pol polyprotein [<i>Takifugu rubripes</i>]
731	Unigene2316	-11.32373034	Down	0.996239509	gi 41055227 ref NP_956674.1 /3.18551e-60/charged multivesicular body protein 5 [<i>Danio rerio</i>]
732	CL7135.Contig8	7.64625868	Up	0.808135764	gi 47087039 ref NP_998533.1 /1.89952e-172/arfaptin-1 [<i>Danio rerio</i>]

733	CL6485.Contig2	-7.807354922	Down	0.831792042	gi 40548308 ref NP_954967.1 /0/uncharacterized protein LOC321250 [<i>Danio rerio</i>]
734	Unigene77833	8.101538026	Up	0.868992379	-
735	Unigene12186	-6.375763494	Down	0.854007901	-
736	CL7286.Contig2	6.633458518	Up	0.905639544	gi 528487971 ref XP_001922678.2 /6.95152e-58/PREDICTED: uncharacterized protein LOC100148399 [<i>Danio rerio</i>]
737	CL5714.Contig2	13.33998915	Up	0.998542227	gi 187608210 ref NP_001119928.1 /3.95646e-30/immunoresponsive gene 1 [<i>Danio rerio</i>]
738	CL1266.Contig3	5.718847845	Up	0.816719706	gi 47085913 ref NP_998314.1 /2.86406e-65/peptidyl-prolyl cis-trans isomerase FKBP5 [<i>Danio rerio</i>]
739	CL1500.Contig2	-7.794415866	Down	0.829914508	gi 117606305 ref NP_001071082.1 /5.20477e-63/phosphatidylcholine:ceramide cholinephosphotransferase 1 [<i>Danio rerio</i>]
740	CL21131.Contig5	-8.303780748	Down	0.889914247	gi 378735269 dbj BAL63124.1 /1.182e-27/CD2 family receptor [<i>Carassius auratus langsdorffii</i>]
741	CL6648.Contig1	7.798741792	Up	0.83081477	-
742	CL18097.Contig3	-8.288481612	Down	0.888541077	-
743	CL4341.Contig1	7.759333407	Up	0.825171321	gi 528483598 ref XP_005166228.1 /8.68549e-24/PREDICTED: DNA-damage-inducible transcript 3 isoform X1 [<i>Danio rerio</i>]
744	CL1636.Contig3	7.597431853	Up	0.801611577	gi 259089311 ref NP_001158693.1 /8.58656e-53/retinitis pigmentosa 9 (autosomal dominant) [<i>Oncorhynchus mykiss</i>]
745	Unigene100800	-8.230420795	Down	0.88237808	-
746	Unigene55750	7.739218046	Up	0.822359901	-
747	Unigene115430	7.81164228	Up	0.832666272	gi 189528212 ref XP_001919426.1 /1.13312e-24/PREDICTED: cystine/glutamate transporter-like [<i>Danio rerio</i>]
748	CL10122.Contig1	8.082558491	Up	0.965329073	gi 432926574 ref XP_004080895.1 /6.28679e-21/PREDICTED: uncharacterized protein LOC101165266 [<i>Oryzias latipes</i>]
749	CL19276.Contig1	9.450523951	Up	0.962204188	-
750	CL437.Contig2	9.986316118	Up	0.977467422	gi 528483252 ref XP_002662570.3 /5.74264e-06/PREDICTED: protein TESPA1-like [<i>Danio rerio</i>]
751	Unigene22638	8.268347055	Up	0.886225343	-
752	Unigene10995	8.193114629	Up	0.878861635	gi 41387132 ref NP_957104.1 /1.63986e-23/protein phosphatase 1, regulatory (inhibitor) subunit 14Ab [<i>Danio rerio</i>]
753	CL2435.Contig2	-8.478432581	Down	0.905851051	gi 12381859 dbj BAB21104.2 /1.57059e-26/SMaf1 [<i>Danio rerio</i>]
754	CL2978.Contig1	8.064293677	Up	0.864573504	-
755	Unigene85237	-7.705056346	Down	0.817379175	-
756	Unigene45864	-7.94641896	Down	0.850374314	-
757	CL1470.Contig1	7.79224803	Up	0.829914508	-
758	CL18103.Contig2	-8.775884583	Down	0.928140666	-
759	Unigene38601	-7.898853277	Down	0.844362083	-
760	CL17731.Contig2	10.15017038	Up	0.980748497	gi 300429859 gb ADK11997.1 /2.97234e-14/MHC class I antigen [<i>Cyprinus carpio 'jian'</i>]
761	CL20263.Contig32	-7.684164178	Down	0.81413064	gi 120537843 gb AAI29405.1 /1.10543e-142/LOC799852 protein [<i>Danio rerio</i>]

762	Unigene82467	-7.794415866	Down	0.829914508	gi 113678254 ref NP_001038341.1 /1.59631e-07/protein NLR3-like [<i>Danio rerio</i>]
763	Unigene2836	8.046214555	Up	0.862280548	gi 548553271 ref XP_005755538.1 /1.35901e-08/PREDICTED: RNA-directed DNA polymerase from mobile element jockey-like [<i>Pundamilia nyererei</i>]
764	Unigene35250	7.874469118	Up	0.84103003	gi 153792746 ref NP_001093569.1 /4.91282e-86/uncharacterized protein LOC100006143 [<i>Danio rerio</i>]
765	CL13034.Contig1	5.626316868	Up	0.809205231	gi 223646097 ref NP_001138714.1 /2.24894e-45/colony stimulating factor 3 (granulocyte) [<i>Danio rerio</i>]
766	Unigene24983	-8.044394119	Down	0.862280548	gi 327239762 gb AEA39725.1 /2.14441e-27/interferon-induced protein 44-like protein [<i>Epinephelus coioides</i>]
767	CL1386.Contig17	-7.730187062	Down	0.820433557	gi 317418898 emb CBN80936.1 /5.69352e-136/Myotubularin-related protein 14 [<i>Dicentrarchus labrax</i>]
768	Unigene64409	8.17990909	Up	0.877322513	-
769	Unigene103345	-7.880603904	Down	0.842024656	-
770	Unigene12475	13.44600631	Up	0.998650692	gi 488888799 gb AGL08666.1 /2.54999e-69/complement component C7-1, partial [<i>Carassius auratus</i>]
771	CL8250.Contig2	9.300733873	Up	0.956319947	-
772	Unigene11665	8.062495926	Up	0.864094087	-
773	Unigene11968	-8.41080465	Down	0.899829059	-
774	Unigene10718	6.626426384	Up	0.906675387	gi 560189337 gb AHB23864.1 /2.15723e-28/purine nucleoside phosphorylase 5a [<i>Carassius auratus</i>]
775	CL14099.Contig3	6.25948174	Up	0.816483252	gi 419636307 ref NP_001258699.1 /5.07729e-32/glucagon isoform 1 precursor [<i>Danio rerio</i>]
776	CL2572.Contig3	9.425565605	Up	0.961295249	gi 194579011 ref NP_001124071.1 /0/USP 6 N-terminal-like protein [<i>Danio rerio</i>]
777	CL10717.Contig3	-8.402301511	Down	0.899109934	gi 213510972 ref NP_001134346.1 /4.21479e-27/neuropeptide-like protein C4orf48 homolog precursor [<i>Salmo salar</i>]
778	CL798.Contig5	9.063395081	Up	0.945194663	gi 528473888 ref XP_685164.4 /0/PREDICTED: serine/threonine-protein kinase WNK4 [<i>Danio rerio</i>]
779	Unigene13658	10.24357071	Up	0.982319074	-
780	Unigene41156	-8.209453366	Down	0.880368218	gi 528503809 ref XP_005169812.1 /0/PREDICTED: SHC-transforming protein 1 isoform X1 [<i>Danio rerio</i>]
781	Unigene66094	7.857980995	Up	0.83873165	-
782	Unigene41128	7.784167425	Up	0.921107778	-
783	CL12864.Contig6	-7.918863237	Down	0.846658293	gi 37590396 gb AAH59643.1 /7.68291e-82/Ancient ubiquitous protein 1 [<i>Danio rerio</i>]
784	Unigene50627	-7.790076931	Down	0.829006653	-
785	CL17731.Contig1	10.67154107	Up	0.988123052	-
786	CL10848.Contig3	-7.809500194	Down	0.831792042	-
787	CL17844.Contig2	-8.018663844	Down	0.859020081	gi 528481551 ref XP_002662317.3 /2.75326e-80/PREDICTED: girdin-like isoform X1 [<i>Danio rerio</i>]
788	CL7927.Contig2	7.90488546	Up	0.844939118	gi 41152014 ref NP_958464.1 /1.15119e-144/nuclear distribution protein nudE-like 1-B [<i>Danio rerio</i>]

789	CL8857.Contig3	-8.176588732	Down	0.876810557	gi 528472160 ref XP_002667428.3 /2.36457e-117/PREDICTED: c-C chemokine receptor type 5-like [<i>Danio rerio</i>]
790	CL5106.Contig3	-7.589963182	Down	0.800433644	gi 542173800 ref XP_005467635.1 /5.19317e-60/PREDICTED: uncharacterized protein LOC102078279 [<i>Oreochromis niloticus</i>]
791	Unigene51072	-8.005624549	Down	0.857616541	gi 315570273 ref NP_001186822.1 /4.18124e-32/actin, gamma-enteric smooth muscle isoform 2 precursor [<i>Homo sapiens</i>]
792	CL416.Contig2	8.335390355	Up	0.892978392	-
793	CL1756.Contig17	8.486499862	Up	0.90651052	gi 390979645 ref NP_001035342.2 /0/N-acetylneuraminase cytidyltransferase [<i>Danio rerio</i>]
794	Unigene12476	10.26678654	Up	0.982706296	gi 383282283 gb AFH01333.1 /6.70814e-22/complement component C7-1, partial [<i>Hypophthalmichthys molitrix</i>]
795	CL9134.Contig1	-9.171593822	Down	0.950571287	gi 305410803 ref NP_001182170.1 /0/potassium voltage-gated channel, Shaw-related subfamily, member 3b [<i>Danio rerio</i>]
796	CL5907.Contig2	8.178249866	Up	0.877322513	gi 229576996 ref NP_001153295.1 /4.45838e-40/LYR motif-containing protein 5A [<i>Danio rerio</i>]
797	CL11789.Contig1	-6.651564285	Down	0.886158095	-
798	Unigene56445	7.672425342	Up	0.81238001	-
799	Unigene73575	11.60130653	Up	0.994765466	-
800	CL7519.Contig3	5.919886741	Up	0.837103587	-
801	CL17514.Contig1	-8.602389572	Down	0.915753931	-
802	CL3929.Contig1	-7.809500194	Down	0.831792042	gi 537142805 gb ERE68650.1 /1.22743e-63/protein yippee-like 5-like protein [<i>Cricetulus griseus</i>]
803	Unigene40016	8.751767197	Up	0.984859331	-
804	CL5155.Contig4	5.839602466	Up	0.818867319	gi 528503831 ref XP_005158140.1 /4.27595e-134/PREDICTED: immunity-related GTPase family, e4 isoform X1 [<i>Danio rerio</i>]
805	Unigene72282	8.14635653	Up	0.873492604	-
806	Unigene17269	8.6783067	Up	0.921424496	-
807	CL8874.Contig5	7.614709844	Up	0.80386874	-
808	CL1707.Contig7	-6.207757075	Down	0.82665838	gi 47551339 ref NP_999980.1 /1.67472e-121/thyroid hormone receptor-associated protein 3 [<i>Danio rerio</i>]
809	Unigene19161	11.78654191	Up	0.995514961	gi 38649358 gb AAH63232.1 /8.3464e-28/Prostaglandin-endoperoxide synthase 2a [<i>Danio rerio</i>]
810	Unigene90123	7.981091537	Up	0.854749803	-
811	Unigene50228	8.302258115	Up	0.889914247	-
812	Unigene75050	7.894817763	Up	0.843535578	gi 18858631 ref NP_571298.1 /9.22291e-27/band 4.1-like protein 4 [<i>Danio rerio</i>]
813	CL6396.Contig1	-7.950312876	Down	0.850374314	-
814	Unigene28146	6.655455288	Up	0.904610208	-
815	Unigene45918	-7.594946589	Down	0.800433644	-
816	Unigene39128	-8.360481336	Down	0.895469839	gi 300810921 gb ADK35755.1 /0/collagen type I alpha 1 [<i>Ctenopharyngodon idella</i>]
817	CL4451.Contig1	-8.113742166	Down	0.870172481	-
818	CL1960.Contig7	-7.872418378	Down	0.840426963	gi 190339262 gb AAI62500.1 /1.17291e-34/Eph-like kinase 1 [<i>Danio rerio</i>]

819	Unigene10588	8.142957954	Up	0.873492604	-
820	CL3917.Contig4	7.990576746	Up	0.855498214	gi 47222682 emb CAG00116.1 /0/unnamed protein product [<i>Tetraodon nigroviridis</i>]
821	Unigene106081	8.793332355	Up	0.929388017	-
822	Unigene64839	8.839203788	Up	0.932238485	gi 528511895 ref XP_683027.5 /4.44089e-58/PREDICTED: androglobin [<i>Danio rerio</i>]
823	Unigene71715	7.894817763	Up	0.843535578	-
824	Unigene31258	9.110265791	Up	0.947600423	-
825	CL7296.Contig1	8.214319121	Up	0.880891021	-
826	Unigene51544	-7.916874684	Down	0.846658293	-
827	Unigene63921	7.839203788	Up	0.836208748	-
828	CL12329.Contig3	-7.604862058	Down	0.802455437	gi 528496194 ref XP_005156361.1 /5.44712e-179/PREDICTED: autism susceptibility gene 2 protein-like isoform X2 [<i>Danio rerio</i>]
829	Unigene44996	8.330916878	Up	0.8925608	-
830	CL11100.Contig1	-8.740342954	Down	0.925914959	gi 51467936 ref NP_001003850.1 /3.31176e-128/RNA-binding protein 42 [<i>Danio rerio</i>]
831	Unigene37922	-9.235216462	Down	0.953505272	-
832	Unigene57835	8.583709617	Up	0.914340629	-
833	CL21131.Contig2	8.997179481	Up	0.941623986	gi 378735269 dbj BAL63124.1 /8.67426e-28/CD2 family receptor [<i>Carassius auratus langsdorfii</i>]
834	CL19980.Contig1	10.88136892	Up	0.990152437	gi 307344647 ref NP_001182542.1 /0/multidrug resistance-associated protein 5 [<i>Danio rerio</i>]
835	CL337.Contig61	5.66492223	Up	0.807860262	gi 63101179 gb AAH95877.1 /2.89553e-120/Zgc:113199 [<i>Danio rerio</i>]
836	CL11696.Contig3	-7.609794354	Down	0.802739616	gi 55250357 gb AAH85577.1 /4.89931e-93/Zgc:158157 protein [<i>Danio rerio</i>]
837	CL5751.Contig1	8.17990909	Up	0.877322513	gi 528505341 ref XP_005169829.1 /7.10485e-16/PREDICTED: nuclear receptor coactivator 7-like isoform X2 [<i>Danio rerio</i>]
838	CL11274.Contig4	-8.338364985	Down	0.893375374	gi 126632493 emb CAM56739.1 /4.79988e-37/novel protein [<i>Danio rerio</i>]
839	CL9568.Contig3	-8.001877287	Down	0.856922363	-
840	CL17775.Contig2	-8.014950341	Down	0.85888233	gi 47221063 emb CAG12757.1 /2.51686e-47/unnamed protein product [<i>Tetraodon nigroviridis</i>]
841	Unigene11958	6.278338826	Up	0.860815182	-
842	Unigene52618	8.66651991	Up	0.920328997	-
843	CL12822.Contig2	-9.626925794	Down	0.968078668	-

Appendix D. KEGG enrichment analysis of all the DEGs

#	Pathway	DEGs with pathway annotation (279)	All genes with pathway annotation (50917)	P value	Q value	Pathway ID
1	Leishmaniasis	12 (4.3%)	472 (0.93%)	1.38219E-05	0.001587032	ko05140
2	Chemical carcinogenesis	7 (2.51%)	142 (0.28%)	1.45599E-05	0.001587032	ko05204
3	Complement and coagulation cascades	10 (3.58%)	361 (0.71%)	3.52328E-05	0.002131324	ko04610
4	Small cell lung cancer	14 (5.02%)	701 (1.38%)	3.91069E-05	0.002131324	ko05222
5	MicroRNAs in cancer	22 (7.89%)	1625 (3.19%)	0.000105075	0.004524739	ko05206
6	Mineral absorption	9 (3.23%)	341 (0.67%)	0.000124534	0.004524739	ko04978
7	Graft-versus-host disease	7 (2.51%)	209 (0.41%)	0.000167647	0.004837063	ko05332
8	Hematopoietic cell lineage	12 (4.3%)	631 (1.24%)	0.000217302	0.004837063	ko04640
9	Inflammatory bowel disease (IBD)	9 (3.23%)	370 (0.73%)	0.000228296	0.004837063	ko05321
10	Type I diabetes mellitus	7 (2.51%)	221 (0.43%)	0.000235745	0.004837063	ko04940
11	Herpes simplex infection	20 (7.17%)	1491 (2.93%)	0.000244072	0.004837063	ko05168
12	Prion diseases	8 (2.87%)	301 (0.59%)	0.000281237	0.005109132	ko05020
13	ECM-receptor interaction	11 (3.94%)	655 (1.29%)	0.001089521	0.018270429	ko04512
14	Systemic lupus erythematosus	8 (2.87%)	386 (0.76%)	0.001413139	0.022004593	ko05322
15	Platelet activation	16 (5.73%)	1250 (2.45%)	0.001627293	0.022570575	ko04611
16	Pathways in cancer	29 (10.39%)	2935 (5.76%)	0.001656556	0.022570575	ko05200
17	TNF signaling pathway	11 (3.94%)	732 (1.44%)	0.002589224	0.031669272	ko04668
18	Arachidonic acid metabolism	5 (1.79%)	171 (0.34%)	0.002614894	0.031669272	ko00590
19	Epstein-Barr virus infection	17 (6.09%)	1460 (2.87%)	0.003130174	0.034527123	ko05169
20	Regulation of lipolysis in adipocytes	7 (2.51%)	346 (0.68%)	0.003167626	0.034527123	ko04923
21	Ovarian steroidogenesis	5 (1.79%)	186 (0.37%)	0.00374512	0.038877912	ko04913
22	Porphyrin and chlorophyll metabolism	4 (1.43%)	123 (0.24%)	0.00480981	0.047660845	ko00860
23	Serotonergic synapse	8 (2.87%)	498 (0.98%)	0.006564802	0.058495426	ko04726
24	Tuberculosis	15 (5.38%)	1319 (2.59%)	0.006612899	0.058495426	ko05152
25	NF-kappa B signaling pathway	12 (4.3%)	951 (1.87%)	0.006708191	0.058495426	ko04064
26	TGF-beta signaling pathway	8 (2.87%)	516 (1.01%)	0.00804286	0.067436288	ko04350
27	Retrograde endocannabinoid signaling	7 (2.51%)	422 (0.83%)	0.009092432	0.073412969	ko04723
28	Antigen processing and presentation	6 (2.15%)	348 (0.68%)	0.01284339	0.09828109	ko04612
29	Pyrimidine metabolism	8 (2.87%)	563 (1.11%)	0.01307409	0.09828109	ko00240
30	Toll-like receptor signaling pathway	8 (2.87%)	571 (1.12%)	0.01411881	0.102596686	ko04620
31	Influenza A	16 (5.73%)	1598 (3.14%)	0.01581353	0.111204824	ko05164
32	ABC transporters	6 (2.15%)	374 (0.73%)	0.01768146	0.118939148	ko02010
33	Allograft rejection	5 (1.79%)	274 (0.54%)	0.01800455	0.118939148	ko05330
34	PI3K-Akt signaling pathway	19 (6.81%)	2095 (4.11%)	0.02286294	0.14539946	ko04151

35	Autoimmune thyroid disease	5 (1.79%)	295 (0.58%)	0.02384432	0.14539946	ko05320
36	Hepatitis B	12 (4.3%)	1137 (2.23%)	0.02401092	0.14539946	ko05161
37	Hypertrophic cardiomyopathy (HCM)	7 (2.51%)	536 (1.05%)	0.02927808	0.172503282	ko05410
38	NOD-like receptor signaling pathway	9 (3.23%)	812 (1.59%)	0.03626686	0.208057249	ko04621
39	Chemokine signaling pathway	12 (4.3%)	1220 (2.4%)	0.03800845	0.21245749	ko04062
40	Phagosome	10 (3.58%)	964 (1.89%)	0.0412217	0.224658265	ko04145
41	RNA polymerase	4 (1.43%)	238 (0.47%)	0.04264327	0.226737387	ko03020
42	Focal adhesion	16 (5.73%)	1859 (3.65%)	0.05165535	0.256730622	ko04510
43	Hepatitis C	9 (3.23%)	871 (1.71%)	0.05219535	0.256730622	ko05160
44	Toxoplasmosis	9 (3.23%)	874 (1.72%)	0.05311064	0.256730622	ko05145
45	Measles	9 (3.23%)	874 (1.72%)	0.05311064	0.256730622	ko05162
46	Dilated cardiomyopathy	7 (2.51%)	617 (1.21%)	0.0548629	0.256730622	ko05414
47	Jak-STAT signaling pathway	8 (2.87%)	748 (1.47%)	0.05535018	0.256730622	ko04630
48	Prolactin signaling pathway	6 (2.15%)	499 (0.98%)	0.05809092	0.259024085	ko04917
49	Cytokine-cytokine receptor interaction	10 (3.58%)	1027 (2.02%)	0.05822101	0.259024085	ko04060
50	VEGF signaling pathway	6 (2.15%)	510 (1%)	0.06314726	0.27082597	ko04370
51	Thiamine metabolism	1 (0.36%)	12 (0.02%)	0.06381486	0.27082597	ko00730
52	Rheumatoid arthritis	5 (1.79%)	390 (0.77%)	0.06460069	0.27082597	ko05323
53	Non-alcoholic fatty liver disease (NAFLD)	9 (3.23%)	922 (1.81%)	0.0691946	0.274136285	ko04932
54	Pertussis	8 (2.87%)	786 (1.54%)	0.06945688	0.274136285	ko05133
55	Chagas disease (American trypanosomiasis)	7 (2.51%)	653 (1.28%)	0.06966661	0.274136285	ko05142
56	Cell adhesion molecules (CAMs)	10 (3.58%)	1065 (2.09%)	0.07042033	0.274136285	ko04514
57	Base excision repair	3 (1.08%)	178 (0.35%)	0.07499507	0.28682325	ko03410
58	Hippo signaling pathway - fly	5 (1.79%)	415 (0.82%)	0.07938499	0.298378066	ko04391
59	HTLV-I infection	14 (5.02%)	1698 (3.33%)	0.08605569	0.312907099	ko05166
60	Drug metabolism - other enzymes	3 (1.08%)	189 (0.37%)	0.08612122	0.312907099	ko00983
61	Morphine addiction	4 (1.43%)	305 (0.6%)	0.08781564	0.313832943	ko05032
62	Amoebiasis	7 (2.51%)	703 (1.38%)	0.09382838	0.329912691	ko05146
63	Drug metabolism - cytochrome P450	2 (0.72%)	100 (0.2%)	0.10454	0.361741587	ko00982
64	Intestinal immune network for IgA production	4 (1.43%)	333 (0.65%)	0.1115439	0.379946409	ko04672
65	Malaria	4 (1.43%)	337 (0.66%)	0.1151459	0.380882017	ko05144
66	Prostate cancer	7 (2.51%)	746 (1.47%)	0.117899	0.380882017	ko05215
67	Steroid hormone biosynthesis	2 (0.72%)	108 (0.21%)	0.1186911	0.380882017	ko00140
68	Insulin secretion	5 (1.79%)	472 (0.93%)	0.1191747	0.380882017	ko04911
69	Natural killer cell mediated cytotoxicity	8 (2.87%)	894 (1.76%)	0.1205544	0.380882017	ko04650
70	Inositol phosphate metabolism	6 (2.15%)	618 (1.21%)	0.1259351	0.382046163	ko00562
71	Viral myocarditis	5 (1.79%)	481 (0.94%)	0.1261852	0.382046163	ko05416
72	Protein processing in endoplasmic reticulum	8 (2.87%)	907 (1.78%)	0.1277794	0.382046163	ko04141

73	Insulin resistance	7 (2.51%)	768 (1.51%)	0.1313453	0.382046163	ko04931
74	Metabolism of xenobiotics by cytochrome P450	2 (0.72%)	115 (0.23%)	0.1314379	0.382046163	ko00980
75	Proteasome	2 (0.72%)	115 (0.23%)	0.1314379	0.382046163	ko03050
76	Sphingolipid signaling pathway	8 (2.87%)	917 (1.8%)	0.1334874	0.382898068	ko04071
77	Osteoclast differentiation	9 (3.23%)	1070 (2.1%)	0.1361248	0.385392291	ko04380
78	Folate biosynthesis	1 (0.36%)	28 (0.05%)	0.1426328	0.39864039	ko00790
79	Estrogen signaling pathway	6 (2.15%)	658 (1.29%)	0.1548506	0.427309251	ko04915
80	Staphylococcus aureus infection	4 (1.43%)	384 (0.75%)	0.1610228	0.43878713	ko05150
81	Apoptosis	5 (1.79%)	527 (1.04%)	0.1647962	0.443525575	ko04210
82	Nitrogen metabolism	1 (0.36%)	34 (0.07%)	0.1704536	0.453157132	ko00910
83	Taste transduction	2 (0.72%)	141 (0.28%)	0.1810577	0.47554914	ko04742
84	Pancreatic cancer	5 (1.79%)	551 (1.08%)	0.1866055	0.484285702	ko05212
85	Hippo signaling pathway	6 (2.15%)	711 (1.4%)	0.1971671	0.505675621	ko04390
86	Axon guidance	9 (3.23%)	1183 (2.32%)	0.2036923	0.516336295	ko04360
87	Arrhythmogenic right ventricular cardiomyopathy (ARVC)	5 (1.79%)	575 (1.13%)	0.2093952	0.521483498	ko05412
88	Sulfur relay system	1 (0.36%)	43 (0.08%)	0.2105071	0.521483498	ko04122
89	Neuroactive ligand-receptor interaction	8 (2.87%)	1049 (2.06%)	0.2199306	0.538706413	ko04080
90	Purine metabolism	7 (2.51%)	899 (1.77%)	0.2252672	0.545647218	ko00230
91	Glycosphingolipid biosynthesis - ganglio series	1 (0.36%)	49 (0.1%)	0.2361329	0.559532307	ko00604
92	Maturity onset diabetes of the young	1 (0.36%)	49 (0.1%)	0.2361329	0.559532307	ko04950
93	Endometrial cancer	4 (1.43%)	455 (0.89%)	0.2401732	0.562986641	ko05213
94	Notch signaling pathway	4 (1.43%)	459 (0.9%)	0.2448887	0.567933368	ko04330
95	Huntington's disease	7 (2.51%)	930 (1.83%)	0.2503442	0.574474059	ko05016
96	Transcriptional misregulation in cancer	11 (3.94%)	1583 (3.11%)	0.2533025	0.57520776	ko05202
97	Asthma	2 (0.72%)	179 (0.35%)	0.2571531	0.577931709	ko05310
98	Glycosaminoglycan biosynthesis - keratan sulfate	1 (0.36%)	56 (0.11%)	0.2649839	0.586502135	ko00533
99	cAMP signaling pathway	9 (3.23%)	1274 (2.5%)	0.2663473	0.586502135	ko04024
100	Nicotinate and nicotinamide metabolism	2 (0.72%)	191 (0.38%)	0.2814473	0.604694538	ko00760
101	Legionellosis	3 (1.08%)	339 (0.67%)	0.2845939	0.604694538	ko05134
102	Dorso-ventral axis formation	2 (0.72%)	193 (0.38%)	0.2854926	0.604694538	ko04320
103	Central carbon metabolism in cancer	4 (1.43%)	493 (0.97%)	0.2857043	0.604694538	ko05230
104	Amino sugar and nucleotide sugar metabolism	3 (1.08%)	347 (0.68%)	0.296483	0.616833445	ko00520
105	Glioma	5 (1.79%)	662 (1.3%)	0.2981379	0.616833445	ko05214
106	Alcoholism	5 (1.79%)	665 (1.31%)	0.3013194	0.616833445	ko05034
107	Oxytocin signaling pathway	7 (2.51%)	992 (1.95%)	0.3027577	0.616833445	ko04921
108	Viral carcinogenesis	10 (3.58%)	1502 (2.95%)	0.3105488	0.623878	ko05203
109	Fatty acid elongation	1 (0.36%)	68 (0.13%)	0.311939	0.623878	ko00062
110	Glycosphingolipid biosynthesis - globo series	1 (0.36%)	69 (0.14%)	0.3157142	0.625688142	ko00603

111	Cytosolic DNA-sensing pathway	2 (0.72%)	210 (0.41%)	0.3197438	0.627965301	ko04623
112	Renin secretion	3 (1.08%)	371 (0.73%)	0.3322768	0.646753057	ko04924
113	mTOR signaling pathway	4 (1.43%)	541 (1.06%)	0.3447216	0.665038131	ko04150
114	Adrenergic signaling in cardiomyocytes	6 (2.15%)	876 (1.72%)	0.348587	0.665909056	ko04261
115	Thyroid hormone signaling pathway	8 (2.87%)	1217 (2.39%)	0.3512823	0.665909056	ko04919
116	Carbohydrate digestion and absorption	3 (1.08%)	391 (0.77%)	0.3620743	0.679331963	ko04973
117	Wnt signaling pathway	6 (2.15%)	897 (1.76%)	0.3689608	0.679331963	ko04310
118	Melanogenesis	4 (1.43%)	562 (1.1%)	0.3707079	0.679331963	ko04916
119	Phosphatidylinositol signaling system	6 (2.15%)	899 (1.77%)	0.3709047	0.679331963	ko04070
120	Melanoma	3 (1.08%)	399 (0.78%)	0.3739442	0.679331963	ko05218
121	Phototransduction	1 (0.36%)	89 (0.17%)	0.3870312	0.69498194	ko04744
122	Mucin type O-Glycan biosynthesis	1 (0.36%)	92 (0.18%)	0.3970701	0.69498194	ko00512
123	African trypanosomiasis	2 (0.72%)	251 (0.49%)	0.4003065	0.69498194	ko05143
124	Ras signaling pathway	9 (3.23%)	1451 (2.85%)	0.4004397	0.69498194	ko04014
125	Glucagon signaling pathway	5 (1.79%)	759 (1.49%)	0.4024907	0.69498194	ko04922
126	PPAR signaling pathway	3 (1.08%)	420 (0.82%)	0.4048748	0.69498194	ko03320
127	Starch and sucrose metabolism	3 (1.08%)	420 (0.82%)	0.4048748	0.69498194	ko00500
128	Chronic myeloid leukemia	5 (1.79%)	766 (1.5%)	0.4100344	0.698339838	ko05220
129	Ascorbate and aldarate metabolism	1 (0.36%)	98 (0.19%)	0.4166589	0.704121242	ko00053
130	p53 signaling pathway	3 (1.08%)	433 (0.85%)	0.4238038	0.707621889	ko04115
131	SNARE interactions in vesicular transport	1 (0.36%)	101 (0.2%)	0.4262142	0.707621889	ko04130
132	Renal cell carcinoma	4 (1.43%)	609 (1.2%)	0.4284683	0.707621889	ko05211
133	Basal cell carcinoma	2 (0.72%)	268 (0.53%)	0.432429	0.708684649	ko05217
134	Primary bile acid biosynthesis	1 (0.36%)	104 (0.2%)	0.4356135	0.708684649	ko00120
135	Cholinergic synapse	4 (1.43%)	634 (1.25%)	0.4586669	0.740662105	ko04725
136	FoxO signaling pathway	6 (2.15%)	994 (1.95%)	0.4628725	0.74195739	ko04068
137	Proteoglycans in cancer	11 (3.94%)	1901 (3.73%)	0.470036	0.746561378	ko05205
138	Olfactory transduction	2 (0.72%)	290 (0.57%)	0.4725939	0.746561378	ko04740
139	Acute myeloid leukemia	3 (1.08%)	472 (0.93%)	0.4792211	0.74949977	ko05221
140	Cell cycle	5 (1.79%)	835 (1.64%)	0.4833289	0.74949977	ko04110
141	Colorectal cancer	3 (1.08%)	476 (0.93%)	0.4847682	0.74949977	ko05210
142	Ubiquitin mediated proteolysis	7 (2.51%)	1213 (2.38%)	0.4979098	0.764396735	ko04120
143	Vasopressin-regulated water reabsorption	4 (1.43%)	678 (1.33%)	0.5103968	0.776179829	ko04962
144	Bile secretion	3 (1.08%)	499 (0.98%)	0.5160973	0.776179829	ko04976
145	Alanine, aspartate and glutamate metabolism	1 (0.36%)	132 (0.26%)	0.5162664	0.776179829	ko00250
146	Long-term potentiation	3 (1.08%)	513 (1.01%)	0.5346628	0.787991956	ko04720
147	Galactose metabolism	2 (0.72%)	328 (0.64%)	0.5377698	0.787991956	ko00052
148	Vitamin digestion and absorption	1 (0.36%)	142 (0.28%)	0.5421963	0.787991956	ko04977
149	Retinol metabolism	1 (0.36%)	142 (0.28%)	0.5421963	0.787991956	ko00830

150	Glycosphingolipid biosynthesis - lacto and neolacto series	1 (0.36%)	142 (0.28%)	0.5421963	0.787991956	ko00601
151	Glutathione metabolism	1 (0.36%)	148 (0.29%)	0.5570845	0.800661281	ko00480
152	T cell receptor signaling pathway	6 (2.15%)	1101 (2.16%)	0.5618505	0.800661281	ko04660
153	Type II diabetes mellitus	2 (0.72%)	343 (0.67%)	0.561932	0.800661281	ko04930
154	Vascular smooth muscle contraction	6 (2.15%)	1111 (2.18%)	0.5706763	0.803956574	ko04270
155	Endocytosis	11 (3.94%)	2051 (4.03%)	0.5716205	0.803956574	ko04144
156	Alzheimer's disease	4 (1.43%)	737 (1.45%)	0.5760088	0.804935374	ko05010
157	GABAergic synapse	2 (0.72%)	360 (0.71%)	0.5882103	0.816750608	ko04727
158	Other types of O-glycan biosynthesis	1 (0.36%)	164 (0.32%)	0.5944696	0.820217549	ko00514
159	Dopaminergic synapse	4 (1.43%)	774 (1.52%)	0.6145301	0.842563282	ko04728
160	Protein digestion and absorption	2 (0.72%)	392 (0.77%)	0.6344655	0.86420031	ko04974
161	Signaling pathways regulating pluripotency of stem cells	4 (1.43%)	798 (1.57%)	0.6383308	0.86420031	ko04550
162	ErbB signaling pathway	4 (1.43%)	802 (1.58%)	0.6422039	0.86420031	ko04012
163	cGMP-PKG signaling pathway	5 (1.79%)	1005 (1.97%)	0.6465358	0.864692052	ko04022
164	Regulation of actin cytoskeleton	10 (3.58%)	1985 (3.9%)	0.6506951	0.864948365	ko04810
165	MAPK signaling pathway	8 (2.87%)	1620 (3.18%)	0.6657533	0.873716978	ko04010
166	Thyroid hormone synthesis	2 (0.72%)	418 (0.82%)	0.668986	0.873716978	ko04918
167	Nucleotide excision repair	1 (0.36%)	201 (0.39%)	0.6693153	0.873716978	ko03420
168	Basal transcription factors	1 (0.36%)	209 (0.41%)	0.6835925	0.879591372	ko03022
169	Pentose and glucuronate interconversions	1 (0.36%)	210 (0.41%)	0.6853334	0.879591372	ko00040
170	Bladder cancer	1 (0.36%)	211 (0.41%)	0.6870648	0.879591372	ko05219
171	Phospholipase D signaling pathway	8 (2.87%)	1657 (3.25%)	0.6899547	0.879591372	ko04072
172	Circadian rhythm	1 (0.36%)	216 (0.42%)	0.6955802	0.881607463	ko04710
173	Rap1 signaling pathway	8 (2.87%)	1686 (3.31%)	0.7081409	0.890280593	ko04015
174	B cell receptor signaling pathway	4 (1.43%)	884 (1.74%)	0.7155336	0.890280593	ko04662
175	Bacterial invasion of epithelial cells	3 (1.08%)	674 (1.32%)	0.7161132	0.890280593	ko05100
176	Salmonella infection	4 (1.43%)	889 (1.75%)	0.719627	0.890280593	ko05132
177	Hedgehog signaling pathway	1 (0.36%)	233 (0.46%)	0.7228425	0.890280593	ko04340
178	Pathogenic Escherichia coli infection	2 (0.72%)	468 (0.92%)	0.7279364	0.891517613	ko05130
179	Metabolic pathways	28 (10.04%)	5648 (11.09%)	0.7405751	0.891994564	ko01100
180	Cocaine addiction	1 (0.36%)	249 (0.49%)	0.7462741	0.891994564	ko05030
181	AMPK signaling pathway	4 (1.43%)	926 (1.82%)	0.7485755	0.891994564	ko04152
182	Lysosome	3 (1.08%)	719 (1.41%)	0.7558187	0.891994564	ko04142
183	Arginine and proline metabolism	1 (0.36%)	257 (0.5%)	0.7572388	0.891994564	ko00330
184	Glutamatergic synapse	2 (0.72%)	501 (0.98%)	0.7617933	0.891994564	ko04724
185	HIF-1 signaling pathway	4 (1.43%)	946 (1.86%)	0.7632487	0.891994564	ko04066
186	Inflammatory mediator regulation of TRP channels	3 (1.08%)	730 (1.43%)	0.7648177	0.891994564	ko04750
187	Sphingolipid metabolism	1 (0.36%)	263 (0.52%)	0.7651513	0.891994564	ko00600

188	Thyroid cancer	1 (0.36%)	280 (0.55%)	0.7862018	0.903163327	ko05216
189	Cardiac muscle contraction	1 (0.36%)	281 (0.55%)	0.7873798	0.903163327	ko04260
190	Fatty acid metabolism	1 (0.36%)	284 (0.56%)	0.7908751	0.903163327	ko01212
191	Shigellosis	2 (0.72%)	536 (1.05%)	0.7936634	0.903163327	ko05131
192	Aldosterone-regulated sodium reabsorption	1 (0.36%)	288 (0.57%)	0.7954466	0.903163327	ko04960
193	Circadian entrainment	2 (0.72%)	547 (1.07%)	0.802875	0.906874352	ko04713
194	Amyotrophic lateral sclerosis (ALS)	1 (0.36%)	318 (0.62%)	0.8267035	0.928976098	ko05014
195	Insulin signaling pathway	4 (1.43%)	1065 (2.09%)	0.8371574	0.935899042	ko04910
196	Leukocyte transendothelial migration	4 (1.43%)	1075 (2.11%)	0.8423882	0.936941978	ko04670
197	Spliceosome	4 (1.43%)	1110 (2.18%)	0.8595995	0.951231934	ko03040
198	Ribosome biogenesis in eukaryotes	1 (0.36%)	389 (0.76%)	0.8830018	0.968043463	ko03008
199	Fc gamma R-mediated phagocytosis	4 (1.43%)	1176 (2.31%)	0.887729	0.968043463	ko04666
200	Primary immunodeficiency	1 (0.36%)	411 (0.81%)	0.8964226	0.968043463	ko05340
201	Amphetamine addiction	1 (0.36%)	411 (0.81%)	0.8964226	0.968043463	ko05031
202	RNA degradation	1 (0.36%)	424 (0.83%)	0.9036201	0.968043463	ko03018
203	Fc epsilon RI signaling pathway	2 (0.72%)	720 (1.41%)	0.9065304	0.968043463	ko04664
204	RNA transport	3 (1.08%)	991 (1.95%)	0.9099749	0.968043463	ko03013
205	Salivary secretion	1 (0.36%)	437 (0.86%)	0.910319	0.968043463	ko04970
206	Choline metabolism in cancer	2 (0.72%)	761 (1.49%)	0.9221882	0.968043463	ko05231
207	Peroxisome	1 (0.36%)	466 (0.92%)	0.9236378	0.968043463	ko04146
208	mRNA surveillance pathway	1 (0.36%)	466 (0.92%)	0.9236378	0.968043463	ko03015
209	Tight junction	4 (1.43%)	1363 (2.68%)	0.9424667	0.9731303	ko04530
210	Adipocytokine signaling pathway	1 (0.36%)	521 (1.02%)	0.9437209	0.9731303	ko04920
211	Neurotrophin signaling pathway	3 (1.08%)	1128 (2.22%)	0.9479049	0.9731303	ko04722
212	Adherens junction	2 (0.72%)	885 (1.74%)	0.9558427	0.9731303	ko04520
213	Calcium signaling pathway	3 (1.08%)	1180 (2.32%)	0.9579337	0.9731303	ko04020
214	Aldosterone synthesis and secretion	1 (0.36%)	585 (1.15%)	0.9605591	0.9731303	ko04925
215	Non-small cell lung cancer	1 (0.36%)	607 (1.19%)	0.9651	0.9731303	ko05223
216	Lysine degradation	1 (0.36%)	619 (1.22%)	0.9673532	0.9731303	ko00310
217	Oocyte meiosis	1 (0.36%)	647 (1.27%)	0.9720628	0.9731303	ko04114
218	Progesterone-mediated oocyte maturation	1 (0.36%)	654 (1.28%)	0.9731303	0.9731303	ko04914

Appendix E. List of immune relevant signaling pathways and involved DEGs in these pathways

Gene ID	log2Ratio(MI/SI)	Up-Down-Regulation(MI/SI)	Probability	Blast NR
PI3K-Akt signaling pathway				
Unigene73628	-8.294620749	Down	0.88901507	gi 347360900 ref NP_001229967.1 /1.33256e-25/cyclic AMP-responsive element-binding protein 3-like protein 1 [<i>Danio rerio</i>]
Unigene39124	-8.035257325	Down	0.86095944	gi 300810921 gb ADK35755.1 /0/collagen type I alpha 1 [<i>Ctenopharyngodon idella</i>]
CL2763.Contig17	7.024216237	Up	0.812621888	gi 193248592 dbj BAG50379.1 /2.87114e-73/voltage-sensing phosphoinositide phosphatase [<i>Danio rerio</i>]
CL1388.Contig7	-8.06608919	Down	0.8646939	gi 269315868 ref NP_001092707.2 /6.29164e-105/eukaryotic translation initiation factor 4Ba [<i>Danio rerio</i>]
CL6467.Contig4	8.320424504	Up	0.89167247	gi 41055786 ref NP_956466.1 /9.0441e-157/transcriptional regulator Myc-B [<i>Danio rerio</i>]
CL4726.Contig4	7.973458213	Up	0.85327576	gi 56090164 ref NP_998471.1 /0/phosphatidylinositol-4,5-bisphosphate 3-kinase catalytic subunit gamma isoform [<i>Danio rerio</i>]
CL6748.Contig4	-8.030667136	Down	0.895168306	-
CL12752.Contig1	7.672425342	Up	0.81238001	gi 597767263 ref XP_007247490.1 /4.64403e-31/PREDICTED: serine/threonine-protein phosphatase 2A 55 kDa regulatory subunit B beta isoform isoform X2 [<i>Astyanax mexicanus</i>]
Unigene35948	-7.309855263	Down	0.856573105	-
CL12552.Contig1	-7.665335917	Down	0.811340913	gi 190339184 gb AAI63556.1 /2.78525e-07/Tnc protein [<i>Danio rerio</i>]
CL2763.Contig1	8.233619677	Up	0.882881359	gi 193248592 dbj BAG50379.1 /3.10179e-73/voltage-sensing phosphoinositide phosphatase [<i>Danio rerio</i>]
CL10213.Contig2	10.03296406	Up	0.978464218	gi 338176917 gb AEI83864.1 /0/granulocyte colony stimulating factor receptor [<i>Carassius auratus</i>]
CL517.Contig18	-7.403012024	Down	0.81650386	gi 190337317 gb AAI63305.1 /0/Integrin, alpha 2b (platelet glycoprotein IIb of IIb/IIIa complex, antigen CD41B) [<i>Danio rerio</i>]
CL517.Contig17	-7.602389572	Down	0.801611577	gi 190337317 gb AAI63305.1 /0/Integrin, alpha 2b (platelet glycoprotein IIb of IIb/IIIa complex, antigen CD41B) [<i>Danio rerio</i>]
Unigene63656	8.614709844	Up	0.916580437	gi 157954488 ref NP_001103320.1 /2.91654e-17/uncharacterized protein LOC100126122 precursor [<i>Danio rerio</i>]
CL517.Contig2	-8.657020649	Down	0.91981921	gi 190337317 gb AAI63305.1 /0/Integrin, alpha 2b (platelet glycoprotein IIb of IIb/IIIa complex, antigen CD41B) [<i>Danio rerio</i>]
CL238.Contig1	-7.63420602	Down	0.806796218	gi 528491610 ref XP_003199352.2 /3.10423e-98/PREDICTED: integrin alpha-2-like [<i>Danio rerio</i>]
Unigene39128	-8.360481336	Down	0.895469839	gi 300810921 gb ADK35755.1 /0/collagen type I alpha 1 [<i>Ctenopharyngodon idella</i>]
NF-κB signaling pathway				

Unigene26040	11.91818442	Up	0.999448996	gi 536720426 gb AGU42184.1 /1.59035e-23/interleukin-1 beta-1 [<i>Carassius carassius</i>]
Unigene3120	6.877330337	Up	0.920027463	gi 38649358 gb AAH63232.1 /1.7511e-38/Prostaglandin-endoperoxide synthase 2a [<i>Danio rerio</i>]
Unigene22935	6.492106846	Up	0.899063294	gi 38649358 gb AAH63232.1 /2.16042e-80/Prostaglandin-endoperoxide synthase 2a [<i>Danio rerio</i>]
CL2933.Contig40	-7.639039173	Down	0.807086905	gi 23308669 ref NP_694508.1 /0/mucosa associated lymphoid tissue lymphoma translocation gene 1a [<i>Danio rerio</i>]
Unigene19491	6.369426105	Up	0.888339331	gi 24119251 ref NP_705943.1 /3.15854e-117/prostaglandin-endoperoxide synthase 2 precursor [<i>Danio rerio</i>]
CL1576.Contig3	9.470237255	Up	0.996403291	gi 38143017 emb CAC80551.1 /2.14211e-68/interleukin-1 beta 1 [<i>Carassius auratus</i>]
CL2347.Contig8	-9.024216237	Down	0.943137076	gi 528516862 ref XP_692341.6 /0/PREDICTED: TNF receptor-associated factor 5, partial [<i>Danio rerio</i>]
CL4350.Contig1	7.72033396	Up	0.970015858	gi 24119251 ref NP_705943.1 /2.9762e-38/prostaglandin-endoperoxide synthase 2 precursor [<i>Danio rerio</i>]
CL2504.Contig1	-8.701595261	Down	0.922916979	gi 47085979 ref NP_998355.1 /8.16489e-53/tumor necrosis factor receptor superfamily member 1A precursor [<i>Danio rerio</i>]
CL255.Contig13	8.372139541	Up	0.896257297	gi 47086673 ref NP_997849.1 /0/ataxin-2-like protein [<i>Danio rerio</i>]
CL20876.Contig1	-5.827037288	Down	0.809296342	gi 20196574 emb CAD24458.2 /9.28034e-40/TCR-alpha V segment II-66 [<i>Danio rerio</i>]
Unigene19161	11.78654191	Up	0.995514961	gi 38649358 gb AAH63232.1 /8.3464e-28/Prostaglandin-endoperoxide synthase 2a [<i>Danio rerio</i>]
Chemokine signaling pathway				
CL6592.Contig3	-9.21916852	Down	0.966659942	-
CL259.Contig15	8.13784503	Up	0.872958955	gi 29540612 gb AAO88245.1 /3.64515e-21/signal transducer and activator of transcription 1 [<i>Carassius auratus</i>]
Unigene49752	6.315549182	Up	0.823413099	gi 526252896 ref NP_001268280.1 /2.49538e-15/chemokine CXCF1a precursor [<i>Oncorhynchus mykiss</i>]
CL4726.Contig4	7.973458213	Up	0.85327576	gi 56090164 ref NP_998471.1 /0/phosphatidylinositol-4,5-bisphosphate 3-kinase catalytic subunit gamma isoform [<i>Danio rerio</i>]
Unigene35948	-7.309855263	Down	0.856573105	-
CL1292.Contig6	-8.062495926	Down	0.864094087	gi 401663980 dbj BAM36371.1 /5.85588e-102/growth hormone-inducible transmembrane protein [<i>Oplegnathus fasciatus</i>]
CL259.Contig16	8.536571017	Up	0.910438048	gi 29540612 gb AAO88245.1 /4.08395e-18/signal transducer and activator of transcription 1 [<i>Carassius auratus</i>]
Unigene26790	6.72129453	Up	0.909889214	gi 326381135 ref NP_001191955.1 /3.08992e-14/guanine nucleotide-binding protein G(I)/G(S)/G(O) subunit gamma-10 [<i>Danio rerio</i>]
Unigene2162	-7.787902559	Down	0.829006653	gi 47225388 emb CAG11871.1 /4.53826e-83/unnamed protein product [<i>Tetraodon nigroviridis</i>]
CL259.Contig6	-7.609794354	Down	0.802739616	gi 29540612 gb AAO88245.1 /1.4907e-162/signal transducer and activator of transcription 1 [<i>Carassius auratus</i>]
Unigene41156	-8.209453366	Down	0.880368218	gi 528503809 ref XP_005169812.1 /0/PREDICTED: SHC-transforming protein 1 isoform X1 [<i>Danio rerio</i>]

CL8857.Contig3	-8.176588732	Down	0.876810557	gi 528472160 ref XP_002667428.3 /2.36457e-117/PREDICTED: c-C chemokine receptor type 5-like [<i>Danio rerio</i>]
TNF signaling pathway				
Unigene73628	-8.294620749	Down	0.88901507	gi 347360900 ref NP_001229967.1 /1.33256e-25/cyclic AMP-responsive element-binding protein 3-like protein 1 [<i>Danio rerio</i>]
Unigene26040	11.91818442	Up	0.999448996	gi 536720426 gb AGU42184.1 /1.59035e-23/interleukin-1 beta-1 [<i>Carassius carassius</i>]
CL4726.Contig4	7.973458213	Up	0.85327576	gi 56090164 ref NP_998471.1 /0/phosphatidylinositol-4,5-bisphosphate 3-kinase catalytic subunit gamma isoform [<i>Danio rerio</i>]
Unigene3120	6.877330337	Up	0.920027463	gi 38649358 gb AAH63232.1 /1.7511e-38/Prostaglandin-endoperoxide synthase 2a [<i>Danio rerio</i>]
Unigene22935	6.492106846	Up	0.899063294	gi 38649358 gb AAH63232.1 /2.16042e-80/Prostaglandin-endoperoxide synthase 2a [<i>Danio rerio</i>]
Unigene19491	6.369426105	Up	0.888339331	gi 24119251 ref NP_705943.1 /3.15854e-117/prostaglandin-endoperoxide synthase 2 precursor [<i>Danio rerio</i>]
CL1576.Contig3	9.470237255	Up	0.996403291	gi 38143017 emb CAC80551.1 /2.14211e-68/interleukin-1 beta 1 [<i>Carassius auratus</i>]
CL2347.Contig8	-9.024216237	Down	0.943137076	gi 528516862 ref XP_692341.6 /0/PREDICTED: TNF receptor-associated factor 5, partial [<i>Danio rerio</i>]
CL4350.Contig1	7.72033396	Up	0.970015858	gi 24119251 ref NP_705943.1 /2.9762e-38/prostaglandin-endoperoxide synthase 2 precursor [<i>Danio rerio</i>]
CL2504.Contig1	-8.701595261	Down	0.922916979	gi 47085979 ref NP_998355.1 /8.16489e-53/tumor necrosis factor receptor superfamily member 1A precursor [<i>Danio rerio</i>]
Unigene19161	11.78654191	Up	0.995514961	gi 38649358 gb AAH63232.1 /8.3464e-28/Prostaglandin-endoperoxide synthase 2a [<i>Danio rerio</i>]
Cytokine-cytokine receptor interaction				
Unigene49752	6.315549182	Up	0.823413099	gi 526252896 ref NP_001268280.1 /2.49538e-15/chemokine CXCF1a precursor [<i>Oncorhynchus mykiss</i>]
Unigene26040	11.91818442	Up	0.999448996	gi 536720426 gb AGU42184.1 /1.59035e-23/interleukin-1 beta-1 [<i>Carassius carassius</i>]
Unigene85624	7.617161323	Up	0.80386874	gi 45709939 gb AAH67712.1 /2.469e-16/LOC407674 protein, partial [<i>Danio rerio</i>]
CL9829.Contig2	-8.026062297	Down	0.860310818	gi 33504525 ref NP_878293.1 /1.21621e-180/transforming growth factor, beta 1a precursor [<i>Danio rerio</i>]
CL30.Contig44	7.807354922	Up	0.831792042	gi 131888307 ref NP_001076466.1 /2.73277e-64/uncharacterized protein LOC100009628 precursor [<i>Danio rerio</i>]
CL1576.Contig3	9.470237255	Up	0.996403291	gi 38143017 emb CAC80551.1 /2.14211e-68/interleukin-1 beta 1 [<i>Carassius auratus</i>]
CL10213.Contig2	10.03296406	Up	0.978464218	gi 338176917 gb AEI83864.1 /0/granulocyte colony stimulating factor receptor [<i>Carassius auratus</i>]
Unigene72566	7.821880254	Up	0.956997855	gi 545604907 gb AGW43283.1 /2.66477e-92/interleukin-1 receptor 2 [<i>Ctenopharyngodon idella</i>]
CL8857.Contig3	-8.176588732	Down	0.876810557	gi 528472160 ref XP_002667428.3 /2.36457e-117/PREDICTED: c-C chemokine receptor type 5-like [<i>Danio rerio</i>]
Complement and coagulation cascades				
CL10622.Contig4	-7.745954377	Down	0.823307887	gi 206557842 sp POC7U4.1 C3AR_DANRE/7.4174e-114/RecName: Full=C3a anaphylatoxin

				chemotactic receptor; Short=C3AR; Short=C3a-R [<i>Danio rerio</i>]
Unigene112829	10.2632692	Up	0.982656402	gi 383282283 gb AFH01333.1 /3.51458e-26/complement component C7-1, partial [<i>Hypophthalmichthys molitrix</i>]
Unigene91776	8.153129759	Up	0.874594611	gi 6009727 dbj BAA85038.1 /1.64157e-12/alpha-2-macroglobulin-1 [<i>Cyprinus carpio</i>]
Unigene96804	10.10678102	Up	0.979920907	gi 383282283 gb AFH01333.1 /6.6787e-22/complement component C7-1, partial [<i>Hypophthalmichthys molitrix</i>]
Unigene104223	7.938599455	Up	0.848897017	gi 295314918 gb ADF97609.1 /3.46758e-26/fibrinogen B beta polypeptide [<i>Hypophthalmichthys molitrix</i>]
CL8161.Contig1	-6.22828426	Down	0.850752858	gi 528480160 ref XP_005165483.1 /1.36644e-155/PREDICTED: uncharacterized protein LOC101885572 [<i>Danio rerio</i>]
Unigene103392	10.03479896	Up	0.978501097	gi 351602153 gb AEQ53931.1 /1.03265e-22/complement component C7 [<i>Ctenopharyngodon idella</i>]
Unigene96986	8.491853096	Up	0.906819646	gi 37695611 gb AAR00337.1 /1.80096e-22/alpha-2-macroglobulin [<i>Ctenopharyngodon idella</i>]
Unigene12475	13.44600631	Up	0.998650692	gi 488888799 gb AGL08666.1 /2.54999e-69/complement component C7-1, partial [<i>Carassius auratus</i>]
Unigene12476	10.26678654	Up	0.982706296	gi 383282283 gb AFH01333.1 /6.70814e-22/complement component C7-1, partial [<i>Hypophthalmichthys molitrix</i>]
NOD-like receptor signaling pathway				
Unigene26040	11.91818442	Up	0.999448996	gi 536720426 gb AGU42184.1 /1.59035e-23/interleukin-1 beta-1 [<i>Carassius carassius</i>]
CL6186.Contig1	-7.135452784	Down	0.907551787	gi 528471942 ref XP_005171495.1 /1.87927e-138/PREDICTED: NACHT, LRR and PYD domains-containing protein 3-like [<i>Danio rerio</i>]
CL3064.Contig2	8.092757141	Up	0.867816616	-
CL5198.Contig8	-8.574908836	Down	0.913473991	gi 528502583 ref XP_001919795.3 /9.253e-34/PREDICTED: NACHT, LRR and PYD domains-containing protein 3-like isoform X1 [<i>Danio rerio</i>]
CL1576.Contig3	9.470237255	Up	0.996403291	gi 38143017 emb CAC80551.1 /2.14211e-68/interleukin-1 beta 1 [<i>Carassius auratus</i>]
Unigene24012	8.448460501	Up	0.903180636	gi 528508932 ref XP_003200567.2 /9.06691e-64/PREDICTED: NACHT, LRR and PYD domains-containing protein 3-like [<i>Danio rerio</i>]
CL377.Contig2	7.660590206	Up	0.810294223	gi 194353931 ref NP_001123874.1 /9.1243e-122/si:ch211-195h23.3 [<i>Danio rerio</i>]
CL7104.Contig4	-7.224966365	Down	0.935007603	gi 528471942 ref XP_005171495.1 /0/PREDICTED: NACHT, LRR and PYD domains-containing protein 3-like [<i>Danio rerio</i>]
CL8076.Contig6	-10.06294557	Down	0.979061862	gi 145587665 ref NP_001076414.2 /9.11147e-71/guanylate binding protein 4 [<i>Danio rerio</i>]
Toll-like receptor pathway				
CL259.Contig15	8.13784503	Up	0.872958955	gi 29540612 gb AAO88245.1 /3.64515e-21/signal transducer and activator of transcription 1 [<i>Carassius auratus</i>]
Unigene49752	6.315549182	Up	0.823413099	gi 526252896 ref NP_001268280.1 /2.49538e-15/chemokine CXCF1a precursor [<i>Oncorhynchus mykiss</i>]
CL4726.Contig4	7.973458213	Up	0.85327576	gi 56090164 ref NP_998471.1 /0/phosphatidylinositol-4,5-bisphosphate 3-kinase catalytic subunit gamma isoform [<i>Danio rerio</i>]
Unigene26040	11.91818442	Up	0.999448996	gi 536720426 gb AGU42184.1 /1.59035e-23/interleukin-1 beta-1 [<i>Carassius carassius</i>]

CL259.Contig16	8.536571017	Up	0.910438048	gi 29540612 gb AAO88245.1 /4.08395e-18/signal transducer and activator of transcription 1 [<i>Carassius auratus</i>]
CL1576.Contig3	9.470237255	Up	0.996403291	gi 38143017 emb CAC80551.1 /2.14211e-68/interleukin-1 beta 1 [<i>Carassius auratus</i>]
Unigene5120	5.982620475	Up	0.839392204	gi 28779299 gb AAO19474.1 /0/toll-like receptor [<i>Carassius auratus</i>]
CL259.Contig6	-7.609794354	Down	0.802739616	gi 29540612 gb AAO88245.1 /1.4907e-162/signal transducer and activator of transcription 1 [<i>Carassius auratus</i>]
TGF-β signaling pathway				
Unigene3046	-7.660590206	Down	0.810294223	gi 528516429 ref XP_005161827.1 /0/PREDICTED: CREB-binding protein isoform X2 [<i>Danio rerio</i>]
Unigene81466	7.6794801	Up	0.81339633	gi 136256463 ref NP_001025282.2 /9.60906e-45/follistatin-related protein 3 precursor [<i>Danio rerio</i>]
Unigene402	7.670066069	Up	0.81238001	gi 528516429 ref XP_005161827.1 /0/PREDICTED: CREB-binding protein isoform X2 [<i>Danio rerio</i>]
CL9829.Contig2	-8.026062297	Down	0.860310818	gi 33504525 ref NP_878293.1 /1.21621e-180/transforming growth factor, beta 1a precursor [<i>Danio rerio</i>]
CL6467.Contig4	8.320424504	Up	0.89167247	gi 41055786 ref NP_956466.1 /9.0441e-157/transcriptional regulator Myc-B [<i>Danio rerio</i>]
CL5158.Contig10	8.836050355	Up	0.932031316	gi 47087291 ref NP_998660.1 /2.85849e-144/cullin-1 [<i>Danio rerio</i>]
CL1292.Contig6	-8.062495926	Down	0.864094087	gi 401663980 dbj BAM36371.1 /5.85588e-102/growth hormone-inducible transmembrane protein [<i>Oplegnathus fasciatus</i>]
Unigene111503	-7.617161323	Down	0.80386874	gi 41054970 ref NP_957345.1 /1.35121e-30/bone morphogenetic protein 5 precursor [<i>Danio rerio</i>]
MAPK signaling pathway				
Unigene26040	11.91818442	Up	0.999448996	gi 536720426 gb AGU42184.1 /1.59035e-23/interleukin-1 beta-1 [<i>Carassius carassius</i>]
CL9829.Contig2	-8.026062297	Down	0.860310818	gi 33504525 ref NP_878293.1 /1.21621e-180/transforming growth factor, beta 1a precursor [<i>Danio rerio</i>]
CL6467.Contig4	8.320424504	Up	0.89167247	gi 41055786 ref NP_956466.1 /9.0441e-157/transcriptional regulator Myc-B [<i>Danio rerio</i>]
CL1576.Contig3	9.470237255	Up	0.996403291	gi 38143017 emb CAC80551.1 /2.14211e-68/interleukin-1 beta 1 [<i>Carassius auratus</i>]
Unigene32768	-7.677132345	Down	0.81339633	gi 432873688 ref XP_004072341.1 /1.59022e-14/PREDICTED: MAP kinase-activated protein kinase 5-like [<i>Oryzias latipes</i>]
Unigene72566	7.821880254	Up	0.956997855	gi 545604907 gb AGW43283.1 /2.66477e-92/interleukin-1 receptor 2 [<i>Ctenopharyngodon idella</i>]
CL2504.Contig1	-8.701595261	Down	0.922916979	gi 47085979 ref NP_998355.1 /8.16489e-53/tumor necrosis factor receptor superfamily member 1A precursor [<i>Danio rerio</i>]
CL4341.Contig1	7.759333407	Up	0.825171321	gi 528483598 ref XP_005166228.1 /8.68549e-24/PREDICTED: DNA-damage-inducible transcript 3 isoform X1 [<i>Danio rerio</i>]
Natural killer cell mediated cytotoxicity				
CL4726.Contig4	7.973458213	Up	0.85327576	gi 56090164 ref NP_998471.1 /0/phosphatidylinositol-4,5-bisphosphate 3-kinase catalytic subunit gamma isoform [<i>Danio rerio</i>]
CL1569.Contig1	5.598657291	Up	0.805880771	gi 3769340 dbj BAA33884.1 /1.50907e-125/MHC class I antigen [<i>Cyprinus carpio</i>]

Unigene18495	9.206616876	Up	0.994089727	gi 57528839 ref NP_956700.1 /1.48897e-60/uncharacterized protein LOC393377 precursor [<i>Danio rerio</i>]
CL1787.Contig6	7.631783357	Up	0.806007675	gi 167963524 ref NP_001108163.1 /5.91483e-44/SH2 domain containing 1A duplicate a [<i>Danio rerio</i>]
Unigene2162	-7.787902559	Down	0.829006653	gi 47225388 emb CAG11871.1 /4.53826e-83/unnamed protein product [<i>Tetraodon nigroviridis</i>]
CL255.Contig13	8.372139541	Up	0.896257297	gi 47086673 ref NP_997849.1 /0/ataxin-2-like protein [<i>Danio rerio</i>]
CL17731.Contig2	10.15017038	Up	0.980748497	gi 300429859 gb ADK11997.1 /2.97234e-14/MHC class I antigen [<i>Cyprinus carpio</i> 'jian']
Unigene41156	-8.209453366	Down	0.880368218	gi 528503809 ref XP_005169812.1 /0/PREDICT ED: SHC-transforming protein 1 isoform X1 [<i>Danio rerio</i>]
Jak-STAT signaling pathway				
Unigene3046	-7.660590206	Down	0.810294223	gi 528516429 ref XP_005161827.1 /0/PREDICT ED: CREB-binding protein isoform X2 [<i>Danio rerio</i>]
CL259.Contig15	8.13784503	Up	0.872958955	gi 29540612 gb AAO88245.1 /3.64515e-21/signal transducer and activator of transcription 1 [<i>Carassius auratus</i>]
Unigene402	7.670066069	Up	0.81238001	gi 528516429 ref XP_005161827.1 /0/PREDICT ED: CREB-binding protein isoform X2 [<i>Danio rerio</i>]
CL6467.Contig4	8.320424504	Up	0.89167247	gi 41055786 ref NP_956466.1 /9.0441e-157/transcriptional regulator Myc-B [<i>Danio rerio</i>]
CL4726.Contig4	7.973458213	Up	0.85327576	gi 56090164 ref NP_998471.1 /0/phosphatidylinositol-4,5-bisphosphate 3-kinase catalytic subunit gamma isoform [<i>Danio rerio</i>]
CL259.Contig16	8.536571017	Up	0.910438048	gi 29540612 gb AAO88245.1 /4.08395e-18/signal transducer and activator of transcription 1 [<i>Carassius auratus</i>]
CL10213.Contig2	10.03296406	Up	0.978464218	gi 338176917 gb AEI83864.1 /0/granulocyte colony stimulating factor receptor [<i>Carassius auratus</i>]
CL259.Contig6	-7.609794354	Down	0.802739616	gi 29540612 gb AAO88245.1 /1.4907e-162/signal transducer and activator of transcription 1 [<i>Carassius auratus</i>]
T cell receptor signaling pathway				
CL6592.Contig3	-9.21916852	Down	0.966659942	-
CL4726.Contig4	7.973458213	Up	0.85327576	gi 56090164 ref NP_998471.1 /0/phosphatidylinositol-4,5-bisphosphate 3-kinase catalytic subunit gamma isoform [<i>Danio rerio</i>]
CL2933.Contig40	-7.639039173	Down	0.807086905	gi 23308669 ref NP_694508.1 /0/mucosa associated lymphoid tissue lymphoma translocation gene 1a [<i>Danio rerio</i>]
CL6523.Contig5	-9.031494449	Down	0.984542613	gi 32479133 gb AAN12398.1 /1.28779e-161/polyprotein [<i>Tetraodon nigroviridis</i>]
CL255.Contig13	8.372139541	Up	0.896257297	gi 47086673 ref NP_997849.1 /0/ataxin-2-like protein [<i>Danio rerio</i>]
CL20876.Contig1	-5.827037288	Down	0.809296342	gi 20196574 emb CAD24458.2 /9.28034e-40/TCR-alpha V segment II-66 [<i>Danio rerio</i>]
Antigen processing and presentation				
Unigene9811	5.621711159	Up	0.804462045	gi 115529435 ref NP_001070245.1 /8.71718e-97/major histocompatibility complex class II DBB precursor [<i>Danio rerio</i>]
CL4386.Contig4	-9.171593822	Down	0.950571287	gi 45387529 ref NP_991104.1 /2.70251e-47/dr1-associated corepressor [<i>Danio rerio</i>]

CL1569.Contig1	5.598657291	Up	0.805880771	gi 3769340 dbj BAA33884.1 /1.50907e-125/MHC class I antigen [<i>Cyprinus carpio</i>]
Unigene18495	9.206616876	Up	0.994089727	gi 57528839 ref NP_956700.1 /1.48897e-60/uncharacterized protein LOC393377 precursor [<i>Danio rerio</i>]
CL20876.Contig1	-5.827037288	Down	0.809296342	gi 20196574 emb CAD24458.2 /9.28034e-40/TCR-alpha V segment II-66 [<i>Danio rerio</i>]
CL17731.Contig2	10.15017038	Up	0.980748497	gi 300429859 gb ADK11997.1 /2.97234e-14/MHC class I antigen [<i>Cyprinus carpio</i> 'jian']
Apoptosis				
Unigene26040	11.91818442	Up	0.999448996	gi 536720426 gb AGU42184.1 /1.59035e-23/interleukin-1 beta-1 [<i>Carassius carassius</i>]
CL4726.Contig4	7.973458213	Up	0.85327576	gi 56090164 ref NP_998471.1 /0/phosphatidylinositol-4,5-bisphosphate 3-kinase catalytic subunit gamma isoform [<i>Danio rerio</i>]
CL2602.Contig2	-7.77478706	Down	0.827073802	gi 9082323 gb AAF82808.1 AF282675_1/2.08348e-75/calpain 1 [<i>Danio rerio</i>]
CL1576.Contig3	9.470237255	Up	0.996403291	gi 38143017 emb CAC80551.1 /2.14211e-68/interleukin-1 beta 1 [<i>Carassius auratus</i>]
CL2504.Contig1	-8.701595261	Down	0.922916979	gi 47085979 ref NP_998355.1 /8.16489e-53/tumor necrosis factor receptor superfamily member 1A precursor [<i>Danio rerio</i>]
B cell receptor signaling pathway				
CL4726.Contig4	7.973458213	Up	0.85327576	gi 56090164 ref NP_998471.1 /0/phosphatidylinositol-4,5-bisphosphate 3-kinase catalytic subunit gamma isoform [<i>Danio rerio</i>]
CL2933.Contig40	-7.639039173	Down	0.807086905	gi 23308669 ref NP_694508.1 /0/mucosa associated lymphoid tissue lymphoma translocation gene 1a [<i>Danio rerio</i>]
Unigene43838	6.151767077	Up	0.86627207	gi 407080643 gb AFS89611.1 /5.41128e-40/interferon-induced transmembrane protein 1 [<i>Cyprinus carpio</i>]
CL337.Contig61	5.66492223	Up	0.807860262	gi 63101179 gb AAH95877.1 /2.89553e-120/Zgc:113199 [<i>Danio rerio</i>]
FcγR-mediated phagocytosis				
Unigene30337	7.768184325	Up	0.826084599	gi 50344880 ref NP_001002112.1 /2.6279e-143/26S proteasome non-ATPase regulatory subunit 4 [<i>Danio rerio</i>]
CL4726.Contig4	7.973458213	Up	0.85327576	gi 56090164 ref NP_998471.1 /0/phosphatidylinositol-4,5-bisphosphate 3-kinase catalytic subunit gamma isoform [<i>Danio rerio</i>]
CL6523.Contig5	-9.031494449	Down	0.984542613	gi 32479133 gb AAN12398.1 /1.28779e-161/polyprotein [<i>Tetraodon nigroviridis</i>]
CL255.Contig13	8.372139541	Up	0.896257297	gi 47086673 ref NP_997849.1 /0/ataxin-2-like protein [<i>Danio rerio</i>]
p53 signaling pathway				
CL2763.Contig17	7.024216237	Up	0.812621888	gi 193248592 dbj BAG50379.1 /2.87114e-73/voltage-sensing phosphoinositide phosphatase [<i>Danio rerio</i>]
CL14301.Contig5	-10.33799349	Down	0.983819149	gi 47086711 ref NP_997828.1 /2.74687e-88/CD82 antigen, b [<i>Danio rerio</i>]
CL2763.Contig1	8.233619677	Up	0.882881359	gi 193248592 dbj BAG50379.1 /3.10179e-73/voltage-sensing phosphoinositide phosphatase [<i>Danio rerio</i>]
Fc epsilon RI signaling pathway				
CL4726.Contig4	7.973458213	Up	0.85327576	gi 56090164 ref NP_998471.1 /0/phosphatidylinositol-4,5-bisphosphate 3-kinase catalytic subunit gamma isoform [<i>Danio rerio</i>]
CL255.Contig13	8.372139541	Up	0.896257297	gi 47086673 ref NP_997849.1 /0/ataxin-2-like protein [<i>Danio rerio</i>]